ISSN: 2456-1878

International Journal of Environment Agriculture and Biotechnology

(IJEAB)

An open access Peer-Reviewed InternationalJournal



DOI: 10.22161/ijeab.115

Vol.- 11 | Issue - 5 | Sep-Oct 2026

editor.ijeab@gmail.com | editor@ijeab.com | https://www.ijeab.com/

International Journal of Environment, Agriculture and Biotechnology

(ISSN: 2456-1878)

DOI: 10.22161/ijeab

Vol-11, Issue-5

September - October, 2026

Editor in Chief

Dr. Pietro Paolo Falciglia

Copyright © 2026 International Journal of Environment, Agriculture and Biotechnology

Publisher

Infogain Publication

Email: editor.ijeab@gmail.com ; editor@ijeab.com

Web: www.ijeab.com

FOREWORD

I am honoured to introduce this latest issue to the International Journal of Environment, Agriculture and Biotechnology (IJEAB). Our journal is dedicated to disseminating high-quality research and innovative findings that contribute to advancing knowledge in these critical fields.

In this issue, we present a collection of papers that exemplify the diversity and depth of contemporary environmental, agriculture, and biotechnology research. The articles include various topics, from sustainable agricultural practices and environmental conservation strategies to cutting-edge biotechnological innovations. Each contribution has undergone a rigorous peer-review process, ensuring the publication of only the most significant and original research.

Our commitment at IJEAB is to provide a robust platform for researchers, academicians, and practitioners to share their work and engage with a global audience. By fostering an interdisciplinary approach, we aim to bridge the gaps between different areas of study and promote holistic understanding and solutions to the challenges we face in these domains.

We are grateful to our dedicated authors, whose hard work and intellectual rigour are the backbone of our journal. We also extend our appreciation to our reviewers and editorial board members, whose expertise and diligence ensure the high standards of our publication. Finally, we thank our readers for their continued support and engagement.

We hope you find the articles insightful and inspiring as you explore this issue. We encourage you to contribute your research to future issues and join us in our mission to advance knowledge and drive positive change in the environment, agriculture, and biotechnology fields.

Sincerely,
Editor-in-Chief
International Journal of Environment, Agriculture and Biotechnology (IJEAB)
NAAS Score Journal
www.ijeab.com

International Editorial Board/ Reviewer Board

- ***Dr. Pietro Paolo Falciglia,*** *Environmental and Sanitary Engineering Group, University of Catania, Italy*
- ***Marcelo Huarte,*** *National Univ. of Mar del Plata. College of Agricultural Sciences, Balcarce, Argentina*
- ***Dr. Mehmet FıratBaran,*** *Department of Energy Systems Engineering, Altinsehir, Adiyaman /Turkey*
- ***Dr. Alexandra D. Solomou,*** *Hellenic Agricultural Organization "DEMETER", Institute of Mediterranean and Forest Ecosystems, Terma Alkmanos, Ilisia, 11528, Athens, Greece.*
- ***Dr. Barbara Molesini,*** *Department of Biotechnology, University of Verona, Italy*
- ***Dr. Krishnakumar Srinivasagam,*** *Vanavarayar Institute of Agriculture, Manakkadavu, Pollachi, Tamil Nadu, India*
- ***Prof.Guoju Xiao,*** *Environmental Ecology, Yinchuan, Ningxia, China*
- ***Dr. Adolf A. Acquaye,*** *University of York, Stockholm Environment Institute, York, United Kingdom*
- ***Dr. R. C. Tiwari,*** *Mizoram University, Tanhril Campus, Mizoram*
- ***Dr. Muhammad Majeed,*** *Kelappaji College of Agricultural Engg. & Technology, Kerala, India*
- ***Jiban Shrestha,*** *National Maize Research Program Rampur, Chitwan, Nepal Agricultural Research Council, Nepal*
- ***Dr. A. Heidari,*** *California South University (CSU), Irvine, California, USA*
- ***Dr. Mukesh Kumar Meena,*** *University of Agricultural Sciences, Raichur, Karnataka, India*
- ***Dr. M. Rajashekhar,*** *Gulbarga University, Gulbarga, Karnataka, India*
- ***Mr. B. A. Gudade,*** *Agronomy Indian Cardamom Research Institute, Tadong, Gangtok, Sikkim, India*
- ***Dr. S. K. Joshi,*** *Krishi Vigyan Kendra (KVK), Ganjam - 1, Orissa University of Agriculture and Technology, Bhanjanagar, Odisha, India*
- ***Heba Mahmoud Mohamed Afify,*** *Biomedical Engineering, Egypt*
- ***Denis Magnus Ken Amara,*** *School of Agriculture, Njala University, Private Mail Bag, Freetown, Sierra Leone.*
- ***Dr. Subha Ganguly,*** *Arawali Veterinary College, Sikar, India*
- ***Shoib A. Baba,*** *Indian institute of integrative medicine, Sanatnagar, Srinagar, India.*
- ***Elias kebede Hailu,*** *Natural Resource Research Directorate, EIAR, Werer , Ethiopia*
- ***Prof. Dr. Mirza Barjees Baig,*** *College of Food and Agriculture Sciences, King Saud University, Kingdom of Saudi Arabia,*
- ***Aliyev Zakir Hussein oglu,*** *Scientific direction: Agricultural sciences Region: Azerbaijan*
- ***Dr. Abd El-Aleem Saad Soliman Desoky,*** *Sohag University, Sohag Governorate, Egypt*
- ***Dr. Ghulam Abbas,*** *PhD (Poultry Nutrition), Riphah College of Veterinary Sciences, Lahore, Pakistan*
- ***Valter Luiz Maciel Júnior,*** *Universidade Estadual do Norte Fluminense, Laboratory of Animal Reproduction and Genetic Improvement – LRMGA, Rio de Janeiro, Brazil*
- ***Shahin Gavanji,*** *Faculty of Advanced Sciences and Technologies, University of Isfahan, Isfahan, Iran.*
- ***Neeraj Khare,*** *Amity Institute of Microbial Technology, Amity University, Jaipur-303002, Rajsthan, India*
- ***Javier Velasco Sarabia,*** *Investigator, National Institute of Fishing and Aquaculture, Avenida México No 190. Col. Del Carmen. CP. 04100. Del. Coyoacán, Ciudad de México.*
- ***Mr. Muhammad Usman,*** *Former Director General of Agricultural Research System, Government of Pakistan*
- ***Jaime Senabre,*** *Director and President of the International Scientific-Professional Committee of the National Symposium on Forest Fires (SINIF), Spain*
- ***Mohamed Ibrahim Mohamed,*** *Central labs, Egypt's Health Ministry, Department. of food bacteriology, zagazig, Egypt*
- ***Professor Jacinta A. Opara,*** *Centre for Health and Environmental Studies, University of Maiduguri, PMB 1069, Maiduguri-Nigeria*
- ***Dr. Josiah Chidiebere Okonkwo,*** *Nnamdi Azikiwe University, PMB 5025, Awka*
- ***Raga Mohamed Elzaki Ali,*** *College of Agricultural and Food Sciences, King Faisal University College of Agricultural and Food Sciences, Saudi Arabia*
- ***Engr. Aliyu Adinoyi,*** *International Crops Research Institute for the Semi-Arid Tropics Kano, Nigeria*
- ***Alireza Haghighi Hasanalideh,*** *Central and West Asian Rice Center (CWARice), Gilan Province, Iran*
- ***Dr. Lalu Prasad Yadav (ARS),*** *ICAR-Central Horticultural Experiment Station (CIAH), Godhra- 389340, Gujarat –India*
- ***Jogendra Singh,*** *Agricultural Research Institute (SKNAU, Jobner), Durgapura-Jaipur, India*
- ***Dr Rakesh Kumar Yadav,*** *Agricultural Research Station, Ummedganj, Agriculture University, Kota, Rajasthan, India.*
- ***Dr. Sanjay Dey,*** *Assistant Professor Department of Zoology, Ananda Mohan College, Kolkata, India*
- ***Dr. Maulin P. Shah,*** *Industrial Wastewater Research Lab, Division of Applied & Environmental Microbiology, Enviro Technology Limited. India*
- ***Dr. Upesh Kumar,*** *Senior Scientist & Head, Krishi Vigyan Kendra, Samoda- Ganwada, Taluka- Siddhpur, District–Patan, Gujarat, India*
- ***Dr. Ashwini Marotirao Charpe,*** *Professor CAS (Pl. Pathology), Dr. Panjabrao Deshmukh Krishi Vidyapith, Akola (MS), India*
- ***Dr Pawan Kumar Poonia,*** *Assistant Professor (forestry), Department of forestry, CCS Haryana, Agricultural University Hisar (HR), India.*

Vol-11, Issue-5, September - October, 2026
(DOI: 10.22161/ijeab.115)

1

Abiotic Stress Tolerance and Breeding Strategies in Rice: A Comprehensive Review

Author(s): Kaustav Biswas, Azubha Pradhan, Wangjuma Tamang, Pranita Subba, Subhas Chandra Roy

DOI: 10.22161/ijeab.115.1

Page No: 001-009

2

Performance assessment of the National Livestock Mission in India using a Composite Performance Index Approach

Author(s): Himanth Raj K N, Devendra Beeraladinni, Vijayachandra Reddy S, D. G. Satihal, Sreedhara J N

Page No: 010-018

3

Basics of Biofilm Architecture and Antimicrobial Resistance

Author(s): Subrat Kumar Barik, Priti Sundar Mohanty, Mugdha Sinha, Shailesh Rout

DOI: 10.22161/ijeab.115.3

Page No: 019-027

4

Profile Characteristics of Extension Personnel and their Relationship with Utilization of a State Agricultural University's Digital Advisory Portal

Author(s): Sankri Karthikeyan, Anand Karthikeyan

DOI: 10.22161/ijeab.115.4

Page No: 028-036

5

Impact of Pradhan Mantri Matsya Sampada Yojana (PMMSY) on Inland Fish Farming Economy in Kalyana Karnataka Region

Author(s): Ninganna, Devendra Beeraladinni, Stephan Raj, Suresh K, Sudhakar A C

DOI: 10.22161/ijeab.115.5

Page No: 037-042

6

Profile Characteristics of Extension Personnel and their Association with Attitude towards ICT Tools and Information Management Patterns

Author(s): Anand Karthikeyan, Sankri Karthikeyan

DOI: 10.22161/ijeab.115.6

Page No: 043-048

7
Environmental Studies: Comprehensive Review of Current Importance and Emerging Horizons
Author(s): Dr. Ranjeeta Soni
DOI: 10.22161/ijeab.115.7

Page No: 049-052

8
In vitro and field evaluation of some sole and combination fungicides against Rhizoctonia solani causing sheath blight disease of rice (Oryza sativa L.) in Eastern Gangetic Plain zone of West Bengal, India
Author(s): Debargha Patra, Birendranath Panja, D. K. Patra, Ashim Midya
DOI: 10.22161/ijeab.115.8

Page No: 053-059

9
A Review on Farmers Expectations from Agricultural Produce Market Committee (APMCs) & e-NAM with Special Reference to Shrirampur APMC, Maharashtra, India
Author(s): Dr. Ganesh S. Shinde, S.S. Temkar, Dattatray Katore
DOI: 10.22161/ijeab.115.9

Page No: 060-065

10
A Study on Physiotherapists' Perceptions Towards Staff Training and Development and Its Impact on Patient Care Quality in Healthcare Settings
Author(s): Dr. Ganesh S. Shinde, S. S. Temkar, S. C. Gujjewar.
DOI: 10.22161/ijeab.115.10

Page No: 066-072

11
Integrated Major Oxide Geochemistry, Contamination Factor and Pollution Load Index for Evaluating Geogenic Enrichment in the Ikole–Itapaji Basement Complex, Southwestern Nigeria
Author(s): Adeleke Ojo
DOI: 10.22161/ijeab.115.11

Page No: 073-113

12
An Assessment of the Sea Buckthorn (Hippophae rhamnoides L.) Value Chain in Uttarakhand and Opportunities for Sustainable Marketing of Himalayan Natural Health Products in India
Author(s): Ambarish Paikaray, Subhashree Priyadarshini, Sandigdha Senapati, Ambarish Ghosh
DOI: 10.22161/ijeab.115.12

Page No: 114-124

13
Analysis of the Physiological Characteristics of 4 Orange Varieties in Kontum (Quang Ngai) and Can Tho, Vietnam
Author(s): Nguyen Trong Phuoc, Bien Anh Khoa, Nguyen Thi Hong Loan, Nguyen Thi Lang
DOI: 10.22161/ijeab.115.13

Page No: 125-133

14
Seasonal Incidence of Natural Enemies Associated with Major Insect Pests in Pearl Millet
Author(s): MP Satpute, DS Mutkule, MK Jadhav, SB Shelke, AP Khating
DOI: 10.22161/ijeab.115.14

Page No: 134-136

15
Effect of Chlorantraniliprole 18.5% SC Applied Through Drone and Knapsack Sprayers on Ladybird Beetle and Spider Populations in Soybean (Glycine max (L.) Merrill)
Author(s): D. K. Thorat, D. S. Mutkule, S. B. Shelke, K. M. Tokhendra, A. P. Khating
DOI: 10.22161/ijeab.115.15

Page No: 137-140

16
Efficacy of Different Botanicals and Insecticide against Chafer Beetles on Jamun (Syzygium cumini L.)
Author(s): A. P. Khating, D. S. Mutkule, S. B. Shelke, K. M. Tokhendra, M. P. Satpute, D. K. Thorat
DOI: 10.22161/ijeab.115.16

Page No: 141-143

17
Economic Study on Targeting Rice Fallow Area (TRFA) Scheme in Kalyana Karnataka Region
Author(s): Aishwarya, Devendra Beeraladinni, Lokesh G.B. Prabhuling Tevari, Sidram Yalwar
DOI: 10.22161/ijeab.115.17

Page No: 144-153

18
Effects of Hevea nitida interstock on the growth and physiology of Hevea brasiliensis
Author(s): Xin-Long Wang, Han-Qi Tu, Jun Wang, Xing-Cheng Yao
DOI: 10.22161/ijeab.115.18

Page No: 154-159

19
Evaluation of Natural Biostimulants for Improving Flowering and Fruiting behaviour in Sweet Orange (Citrus sinensis (L.) Osbeck) var. Nucellar.
Author(s): S. S. Patil, S. G. Patil, R. V. Nainwad, Dr. S. R. Wankhede, Dr. S. V. Pawar
DOI: 10.22161/ijeab.115.19

Page No: 160-163

20
Biomass Partitioning and Root System Development of Acid Lime (Citrus aurantifolia Swingle) Seedlings under Contrasting Growing Media and Nutrient Regimes in a Shade-Net Nursery
Author(s): A. S. Suke, S. G. Patil, R. V. Nainwad, S. R. Wankhede, S. K. Ugile
DOI: 10.22161/ijeab.115.20

Page No: 164-167

21
Ring-like Expansion of Heat Islands and Fragmentation of Cold Islands: Remote Sensing-Based Monitoring and Driving Mechanisms of Thermal Environment Evolution in Wuhan
Author(s): Anqi Bai, Xinrui Gao, Yuxi Yao, Jieting Zhang, Ruei-Yuan Wang
DOI: 10.22161/ijeab.115.21

Page No: 168-189

22
Phytoremediation of Household Air Pollution: A Critical Review of Pollutant Sources, Health Impacts and Plant-Based Mitigation Strategies
Author(s): Dr. Hemant Dnyaneshwar Chandore, Dr. Surnar Laxman Balaji
DOI: 10.22161/ijeab.115.22

Page No: 190-201

23
Evaluation of Mungbean (Vigna radiata L.) genotypes for resistance to Mungbean Yellow Mosaic Virus (MYMV) under natural conditions
Author(s): Lahari Karumuri, V. Satya Priya Lalitha, J. Padmavathi
DOI: 10.22161/ijeab.115.23

Page No: 202-207

24
Parcel-Level Land Cover and Soil Fertility Mapping using Multi-Sensor Satellite Imagery, Cadastral Overlays and Soil Health Card Records in a Semi-Arid Taluka of Saurashtra, Gujarat, India
Author(s): Hardeep Kumar, N. K. Gontia, Pritam Das, P. A. Pandya
DOI: 10.22161/ijeab.115.24

Page No: 208-222

25
Food Consumption, Digestibility and Conversion Efficiency in Bivoltine Silkworm (Bombyx mori L.) Hybrids under Temperate Conditions of Kashmir
Author(s): Gh. Nabi Mir, Aabid Ahmad Bhat, Lubna Altaf, Misara Jaan, Ishfaq Ahmad Malla, M. A. Malik, H. U. Dar
DOI: 10.22161/ijeab.115.25

Page No: 223-231

International Journal of Environment, Agriculture and Biotechnology
Vol-11, Issue-5; Sep-Oct, 2026
Peer-Reviewed International Journal
Journal Home Page Available: https://ijeab.com/
Journal DOI: 10.22161/ijeab

Abiotic Stress Tolerance and Breeding Strategies in Rice: A Comprehensive Review

Kaustav Biswas, Azubha Pradhan, Wangjuma Tamang, Pranita Subba, Subhas Chandra Roy

Plant Genetics & Molecular Breeding Laboratory, Rice Germplasm Conservation & Breeding Center, Department of Botany, University of North Bengal, PO-NBU, Siliguri-734013, Dist-Darjeeling, West Bengal, India

Received: 25 Jul 2026; Received in revised form: 20 Aug 2026; Accepted: 25 Aug 2026; Available online: 04 Sep 2026
©2026 The Author(s). Published by Infogain Publication. This is an open-access article *under* the CC BY license (https://creativecommons.org/licenses/by/4.0/).

Abstract— *Abiotic stresses such as drought, salinity, and temperature extremes, as well as their combinations, often occur during rice production, negatively affecting rice growth, yield, and quality. The impacts include reduced leaf area and photosynthesis, inhibition of spikelet formation and development, and oxidative stress. At the same time, tolerance is determined by the combination of germination capacity, root volume, root number, plant height, and tiller number. The latest research identifies genetic and epigenetic mechanisms of tolerance, including cold tolerance linked to DNA hypomethylation, which underlies acquired and heritable tolerance. The gene pool of wild, weedy, and pre-breed rice varieties can be used to improve cultivated rice's yield potential and tolerance to multiple stresses. Studies on rice's response to salt stress reveal the role of QTL Saltol and mechanisms of ion homeostasis and antioxidant defense that can be harnessed to improve tolerance. The authors conclude that combined physiological, genetic, molecular, epigenetic, and multi-omics approaches, along with the utilization of the wild rice gene pool, speed breeding technologies, genome editing, transgenics, marker-assisted selection, QTL mapping, and GWAS, could be used to develop novel varieties with increased tolerance to multiple stresses, stable yield, and improved grain quality.*

Keywords— ***Rice, abiotic stress, marker-assisted selection, genome-wide association studies, multi-stress tolerance and breeding strategies.***

I. INTRODUCTION

Rice (*Oryza sativa* L.) is a staple crop in which the biotic and abiotic environmental conditions, including high temperatures, drought, and salinity, affect plant growth, yield, and quality. Abiotic stresses are increasingly recognized as critical threats to global food security, given rice productionis high vulnerability to adverse environmental conditions. The growth, yield, and quality of rice are often compromised by unfavorable edaphic and climatic factors. Therefore, rice's response to abiotic stress is critical to investigate to improve stress-resistance breeding and ensure food security and ecosystem services (Sokra *et al*., 2025). Advancements in breeding techniques, such as genetics and genetic engineering, offer novel opportunities to develop crops with improved tolerance and resistance to biotic and abiotic stresses. Genetic breeding can be done in various rice varieties; however, those widely used as wild types for genetic modification include Nipponbare, Zhonghua 11, 9311, and IR64 due to their genome sequence, genetic background, and tissue culture response – attributes ideal for gene function identification and breeding application (Wang *et al*., 2025). Diverse abiotic stresses usually interact in different ways to impair rice productivity. Besides, multiple stresses are often present in the same environment and at the same time or sequentially, and/or one abiotic stressor causes another, for instance, osmotic stress causes salt stress. The interactions of multiple abiotic stresses usually disrupt normal rice growth and development, therefore reducing yield and quality (Yao *et al*., 2025). Generally, abiotic stress tolerance in rice is

determined using germination percentage, root volume, root number, plant height, and tiller number (Yao *et al*., 2025).

II. MECHANISMS OF ABIOTIC STRESS IN RICE

1. Drought Stress

Insufficient rainfall is a major non-biological factor hindering rice cultivation across different geographical regions. The growth and maturation of these plants require a large volume of water, making this cereal crop highly sensitive to changes in environmental moisture (Wang *et al*., 2025). In response to water scarcity, rice biological systems undergo multiple changes to remain alive. As the soil begins to dry, root systems extend deeper and expand their physical reach to collect remaining moisture, but as the dry period continues, these physical changes fail to provide sufficient hydration, and the roots stop growing in length and density (Wang *et al*., 2025). The pores on the surface of the leaves manage the intake of carbon dioxide and the release of water vapor. Under dry conditions, those pores close to prevent water loss, but this also prevents the plant from converting sunlight into energy (Pedrozo *et al*., 2025). To survive the conditions, internal cells increase their concentration of dissolved substances to draw in more water, thereby preserving the physical integrity of the cellular walls. On farms, growers use methods such as periodic flooding, measured water delivery, and precise tubing systems to provide crops with the necessary moisture. By using those strategies, agricultural workers provide sufficient water for rice and use less of the available freshwater supply (Wang *et al*., 2025).

2. Salinity Stress

Worldwide, about 100 million hectares of land are estimated to be salt-affected, representing 7% of the world's land area. Salt (salinity) buildup in the soil results from salts (mainly sodium chloride/NaCl) in the irrigation water and, as a consequence, causes osmotic and ionic stress. At a soil soluble salt concentration of approximately 0.3%, rice production is estimated to fall by more than half on average (Wang *et al*., 2025). Due to climate change and suboptimal irrigation practices, the global habitable area is expected to further expand (Saleem *et al*., 2025).

Salinity stress limits rice growth and yield through osmotic and ionic effects, disrupting water and nutrient uptake and homeostasis. A study in 2026 indicated that shoot biomass and photosynthesis, along with nitrogen, phosphorus, and potassium concentrations, were generally decreased with increasing salinity levels, whilst Na+ concentration in leaves and the Na+/K+ ratio increased. At high salinity, rice yield was also significantly reduced, with a yield penalty of 34.2-54.9%, demonstrating the impact of salt stress. Salinity also had a significant effect on rice during reproductive development, with relative water content, chlorophyll, grain yield, and 1000-seed weight decreasing, while electrolyte leakage and proline increased, illustrating the physiological effects. Molecular studies now indicate oxidative damage caused by increased reactive oxygen species, and the use of antioxidants, osmo-protectants, and transporters, including sodium-hydrogen potassium transporters (HKT) and Na+/H+ antiporters (NHX), helps adapt to salt stress by maintaining cellular water balance and ionic homeostasis. The integration of physiologically based screening strategies and molecular studies is important for improving rice tolerance to salt stress by maintaining ion balance, photosynthesis, and yield (Wei et al., 2026).

3. Temperature Stress

Extreme temperatures, both high and low, limit rice production. High temperatures during flowering reduce pollen viability and, consequently, spikelet fertility. Moreover, prolonged exposure to high temperatures increases respiration and reduces the dry matter available for yield. On the other hand, low temperatures during the establishment phase or at the booting stage slow down plant development and may cause sterility in the panicle. These factors indicate that temperature-tolerant varieties and appropriate growing techniques are critical for rice production (In et al., 2025).

4. Oxidative Stress

In rice, reactive oxygen species (ROS) are primarily produced in response to environmental stresses such as drought, salinity, heat, and pathogen infections. Cell organelles such as chloroplasts, mitochondria, peroxisomes, and the plasma membrane, as well as NADPH oxidases, are the main sites of ROS generation under these stress conditions. Drought stress, for instance, increases photorespiration in chloroplasts and, as a consequence, produces more ROS, which can cause oxidative damage to various biomolecules, including proteins, lipids, and DNA. During drought, peroxisomes also act as ROS generators, worsening oxidative stress. Genes like OsRbohA encode plasma membrane NADPH oxidases, which are induced in response to salt and heat stress, thereby further increasing reactive oxygen species (ROS) activity. Overproduction of ROS may cause cell death, DNA fragmentation, and membrane damage; however, ROS can also act as second messengers to mediate and enhance stress-tolerance mechanisms (Tavu and Redillas, 2025).

Antioxidant Defense Systems in Rice

To eliminate damaging free radicals in plant cells, rice employs an antioxidant defense system that includes both enzymatic and non-enzymatic components. As one of the principal antioxidant enzymes, SOD works by converting O2- into H2O2, which is then broken down into water and oxygen by CAT and/or APX. In addition, the enzymatic action of GPX and GR helps maintain redox homeostasis by reducing H2O2 and hydroxyorganic compounds. These stress-responsive gene-controlled proteins have a preventive role against cellular oxidative injuries (Tavu and Redillas.,2025).

Physiological and Molecular Responses to Abiotic Stress

Osmotic stress occurs very soon after saline stress, whereas ion toxicity from excess Na+ and Cl occurs much later. Excessive accumulation of sodium and chloride ions in intracellular compartments in rice can cause ionic imbalance, also known as toxic ion stress, leading to abnormalities in cellular metabolism and, ultimately, early leaf fall and plant death. Several pathways contribute to Na+ toxicity. Initially, it reduces the rate of enzyme activity and influences metabolism by replacing K+. Excess sodium ions in the cytoplasm also limit the transport and absorption of K+ and macro- and micronutrients such as zinc (Zn2+), calcium (Ca2+), nitrogen (N), and phosphorus (P) (Saleem *et al*., 2025).

Na+ causes plasma membrane depolarization, resulting in K+ efflux into the cytoplasm. This activates endonucleases and caspase-like proteases, leading to cell death and further injury. Toxicity is another major cause of ionic injury, as it can damage N and S accumulated in rice. To cope with ionic disruption, many processes have evolved, including exclusion and tissue tolerance. It has been reported that low-level NaCl (5 mM) improves plant growth by increasing shoot and root dry weights. A NaCl (5 mM) treatment resulted in an increase in K, S, Zn, and Cu levels. These increases could not be observed and were not immune to the NaCl treatments. These resulting increased elements could promote higher processes like photosynthesis and faster cell growth. Noted: S plasma levels were prominent across all studies, with high plasma cysteine levels in high-NaCl treatments. This can be explained by the fact that increased S plasma levels confer considerable growth-promoting effects (Saleem *et al*., 2025).

Plants cope with osmotic stress mainly by accumulating small molecules such as trehalose and proline that help maintain osmotic balance. Key genes involved in osmotic stress response include the trehalose biosynthesis gene OsTrehalose-6-Phosphate Phosphatase 1 (OsTPP1) and the proline synthesis gene OsPyrroline-5-Carboxylate Synthetase (OsP5CS). (Ma *et al*., 2025).

There are many genes responsible for water stress adaptation and rice yield, such as DROT1 RoLe1 ZIP23 MYB ERF/DREB, and NAC, among others. DROT1 is responsible for increased drought tolerance via higher cellulose deposition and retention of cellulose crystallinity. As a result, cellulose wall strengthening and water transport are affected; its expression is drought-response ERF3 and ERF71 dependent. NAC TFs are part of broader stress-response networks, while OsNAC15 boosts OsNCED1, OsNCED2, and OsNCED5 (ABA pathways), thereby regulating the plant's ability to survive drought and salt stress. And it was recently shown that DREB, NAC, and MYB transcription factors, together with ABA signaling and ROS homeostasis, form complex regulatory networks that contribute to osmotic adjustment, antioxidant defense, and drought adaptation in rice. From all of that, it appears that combining drought-tolerant genes with physiological screening and molecular breeding will yield promising results for developing drought-tolerant rice cultivars (Wang *et al*., 2025).

1. Molecular adaptations and breeding implications

At the molecular level, rice regulates kinases, phosphatases, and transcription factors to stabilize ROS levels and enhance stress resilience. Antioxidant defense is modulated by polyamine and proline metabolic pathways, while QTLs such as sub1A are known to contribute to oxidative stress tolerance, particularly in genetically bred varieties for submersion resistance. Many studies have found that more than 50 transcription factors are differentially expressed between resistant and susceptible rice varieties under oxidative stress. These findings support breeding of multi-stress-resistant rice varieties by utilizing the underlying genetic variability (Tavu and Redillas, 2025).

Molecular investigations are pointing more clearly towards Really rice has to be improved on molecular level targeting not single stresses but multiple abiotic stress response pathways. A recent meta-transcriptomic analysis pinpointed the regulatory factors, which are common to drought and iron toxicity, including ROS-related genes and transcription factors like DREB2A, ERF95 and ERF102. These discoveries give an opportunity for molecular breeding of rice plants having tolerance to various stresses.

With the help of recent progress in understanding rice genomics and genome editing, we can say it will become increasingly possible not only to identify the regulatory genes and metabolic pathways but also to pinpoint those genes that will be useful to produce ROS-scavenging proteins, maintain ion balance, and communicate stress signals that will allow for the development of crops with

specific desirable traits. Besides that, the most recent research shows that breeding can be A lot improved when molecular techniques are combined with conventional ones; an example is the manipulation of a rice TPP riboswitch that brought together the benefits of increased yield, higher nitrogen use, better quality of grain nutrition, greater cold adaptability, and better resistance to pests (i.e., blast). Because of this, future rice breeding programs should focus on both stress resistance and nutrient-utilization efficiency, combining them with yield stability and adaptability to changing climates (environmental changes) to develop rice cultivars suited to the changing conditions. Bottom line: a cross-cutting (multidisciplinary) collaboration among genomics, plant physiology, metabolomics, and breeding has great potential to enable climate-smart and environmentally sustainable rice production (Ahmdikhah *et al*., 2025).

III. GENETIC BASIS OF ABIOTIC STRESS TOLERANCE

1. Genetic diversity in wild and weedy rice and its relevance to abiotic stress

Weedy rice (*Oriza sativa* f. spontanea) represents a crop wild relative (CWR) to domesticated rice (*Oriza sativa*) with the same genome type AA (2n = 24). Weedy rice is considered a weed in rice cultivation fields across the globe, primarily in temperate zones and the tropics.1 Due to its reddish color of pericarp, it is popularly named 'red rice'. Although research of this type is progressing, the exact origin of weedy rice remains a major mystery, and as a result, it is often regarded as the clearest case of convergent evolution among rice plants (Roy *et al*., 2023).

Genetic differences between wild and weedy rice varieties are an important source of adaptive traits that increase abiotic stress tolerance in cultivated rice. A broad genomic comparison of 180 wild rice accessions revealed significant genomic differences, including millions of SNPs and InDels, and wild rice being overall more genetically diverse than domesticated rice; meanwhile, some good adaptive alleles might have been lost during the selection of desirable varieties. *Oryza rufipogon* retains genes that enable the plant to survive drought, cold, and salinity stress and to resist diseases, and WRKY67 has proven to be a useful gene for developing salt-resistant rice. In addition, weedy rice exhibits substantial genetic and morphological variation, as well as traits that could aid the study of genotype-environment interactions and the discovery of desirable alleles.

So, the conservation and use of wild and weedy rice materials may expand the genetic base of rice and help create rice varieties that are more resistant to climate change (Tao et al., 2026).

2. Pre-breeding with *Oryza rufipogon* and RIL population

Before one actually begins cross-breeding, parental breeding is required, as it helps develop improvement programs in rice, where several challenges, such as climate change, food security, malnutrition, and sustainability, are being addressed. Through the activation of the latent genetic resources of wild relatives (O. rufipogon), we managed to set up two major large-scale pre-breeding (F8:9) populations, each containing 100 RILs (BWF and CWF), against the background genes of two local indica cultivars, i.e., Badshabhog and Chenga. When the results of an ANOVA test together with an estimate of broad-sense heritability (H percent), the level to which the change of a trait can be passed on through generations, genetic variation, PCA, and Mahalanobis D2 test statistics have been examined, there is a convergence among them that indicates a significant widening of the genetic variation of BWF and CWF RILs which is the combined effect of alien introgression of underutilized wild rice (O. *rufipogon*) with the previously hidden genes (Roy and Shil, 2025).

3. Variation among traditional, modern, and genetically engineered varieties

Different studies have compared how rice cultivars respond to different stress conditions. Traditional, modern, and genetically modified rice cultivars have all demonstrated a difference for how well they tolerate stress. As a traditional variety, Co13 exhibited strong tolerance to oxidative stress - by having efficient photosystem II function and low ion leakage - both suggesting a good maintenance of membrane integrity when under stress. Korgut is a rice variety that contains more unsaturated fatty acids than Jaya, which promotes membrane fluidity and allows it to better tolerate salinity-induced oxidative stress. These features show that local traditional varieties have undergone natural selection and adaptation to their environments and, as a result, are useful in saline or drought-prone areas (Tavu and Redillas, 2025).

Modern Japanese-style rice cultivars like Koshihikari and Indian-type varieties like IR58 have demonstrated a similar level of resistance to oxidative damage, comparable to traditional varieties. This happened mainly because they were bred to select stress-tolerant traits. Such advancements are in line with changes in rice breeding, where the focus has shifted from biotic to abiotic stress resistance to support productivity under varied environmental conditions (Tavu and Redillas, 2025).

Through genetic engineering, we can better harness rice plants' potential against oxidative stress. The technique involves adding genes into rice genome which results in an increase in rice plants' ability to resist the effects of stress through the enhancement of the plants' antioxidant system. The SUB1 gene, which has been introduced into varieties such as Binadhan-11 and BRRI dhan52, increases the abundance of antioxidant enzymes, namely ascorbate peroxidase and peroxidase, so these SUB1 rice varieties are more stress-tolerant than the non-SUB1 varieties. Such modifications allow rice varieties to achieve higher yields even under stress and to show greater resilience to environmental changes (Tavu and Redillas, 2025).

IV. BREEDING STRATEGIES FOR ABIOTIC STRESS TOLERANCE

1. Traditional breeding and selection

Traditional methods of rice plant breeding simply involve identifying rice varieties with desirable traits and then hybridizing them. By using a screen between generations, plants that are better able to resist stress and exhibit other traits have been developed. The main point is to identify genes involved in stress resistance that can be introduced into offspring by crossing parent plants with the trait of interest. For instance, one may cross drought-resistant wild rice varieties with drought-sensitive yet high-yielding cultivated varieties of the plant so that offspring would show both high-yielding and drought-resistant characteristics. Some of the techniques used in traditional plant breeding include family selection, recurrent selection, backcrossing, and induced mutations, to name but a few (Sokra *et al*., 2025).

2. Molecular marker-assisted selection and GWAS

Molecular MAS makes contemporary plant breeding much easier and faster. By identifying molecular markers closely linked to resistance traits to abiotic and biotic stresses, breeders are better equipped to select plants with the desired genes, resulting in higher breeding efficiency and success rates (Wang *et al*., 2025). A thorough study of the abiotic stress response genes will pave the way for the emergence of molecular markers that are closely linked to these genes and, in some cases, virtually interchangeable with them. In rice, such markers enable early screening of breeding materials for resistance to various stresses, allowing breeders to work faster and deliver stress-tolerant varieties on time (Wang *et al*., 2025).

3. Gene Editing Technologies

Current gene-editing technologies enable us to develop varieties of high-yield rice that meet consumer expectations and are highly robust (Wang *et al*., 2025). Using CRISPR/Cas9 technology, which can edit multiple genes simultaneously, researchers induced mutations in the GS3 and GL3.1 genes, which are responsible for determining rice grain shape. The double-mutant gs3 gl3.1 rice they developed had larger, rounder grains, with major benefits in grain appearance, fullness, yield, and stress resistance compared with the single-mutant gs3 rice (Wang *et al*., 2025). Also, deleting the OsPAO5 gene leads to much longer, fatter rice grains and higher grain yields, along with increased stress tolerance and enhanced embryo elongation (In *et al*., 2025).

Adding CRISPR/Cas9 to rice breeding methods opens an avenue for creating new rice varieties with strong, long-lasting resistance (Pedrozo et al., 2025). Since genome-editing techniques target weak points, such as host-susceptibility genes, and build resistance mechanisms, they accelerate the development of high-quality rice varieties and reduce our reliance on pesticides (Pedrozo *et al*., 2025).

Table 1. Quantitative evidence directly relevant to abiotic-stress tolerance and breeding in rice. Values are reported by the cited studies and are not pooled estimates.

Dataset	Stress or breeding context	Rice sample	Important Traits	Breeding implication
Wei *et al.* (2026)	High salinity (HS) vs low salinity (LS)	4 cultivars; 2-year field study	Grain yield reduced 34.2–54.9% at HS	Strong yield penalty supports screening for yield stability and ion-homeostasis traits
Wei *et al.* (2026)	Salinity tolerance comparison	2 tolerant vs 2 susceptible cultivars	Tolerant rice yielded 10.1% more at LS and 27.1% more at HS	Tolerance traits can preserve yield under stronger salinity
2Ma *et al.* (2025)	Modern cultivar genomic/phenomic diversity	6,044 cultivars; 212 datasets	3,131 QTLs linked to 53 phenotypes	Large diversity panels can support breeding-by-design and GWAS
Roy & Shil	Pre-breeding with O. *rufipogon*	100 BWF + 100 CWF RILs	Heritability 74.42–99.87%; first four PCs explained	Wild-rice introgression can broaden selectable variation

(2025)			73.74% in BWF	
Tao *et al.* (2026)	AA-genome wild-rice pan-genomics	180 wild accessions; 5 species	67–224 Mb novel sequence per species	Wild rice contains substantial sequence diversity lost or selected during domestication
Ahmdikhah *et al.* (2025)	Multiple abiotic stresses	Transcriptomic meta-analysis	DREB2A, ERF95 and ERF102 were among shared response factors	Shared regulatory nodes are candidates for multi-stress breeding
Song *et al.* (2025)	Cold stress / epigenetics	Multigenerational cold exposure	Heritable ACT1 promoter hypomethylation associated with acquired cold tolerance	Stable epialleles may complement conventional genetic resources

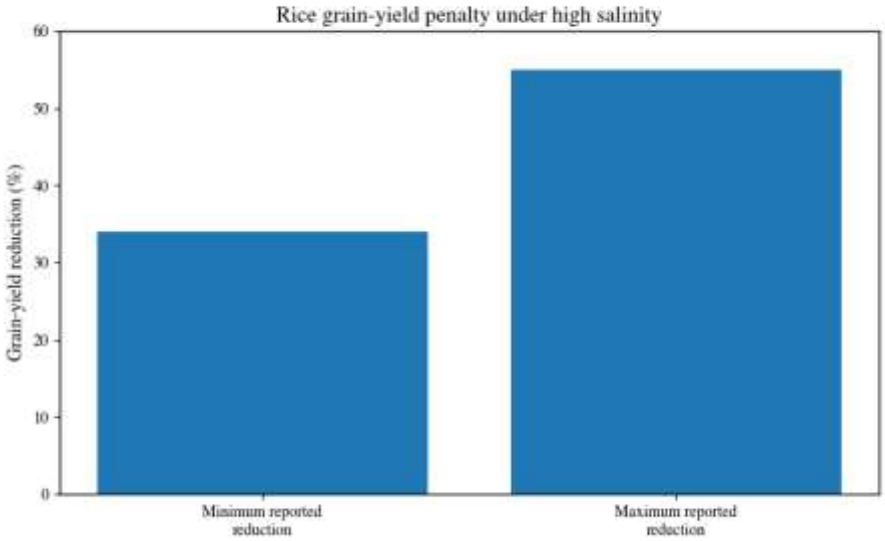


Fig 1. Reported grain-yield reduction of rice under high salinity relative to low salinity in a two-year field study. Source: (Wei et al.,2026).

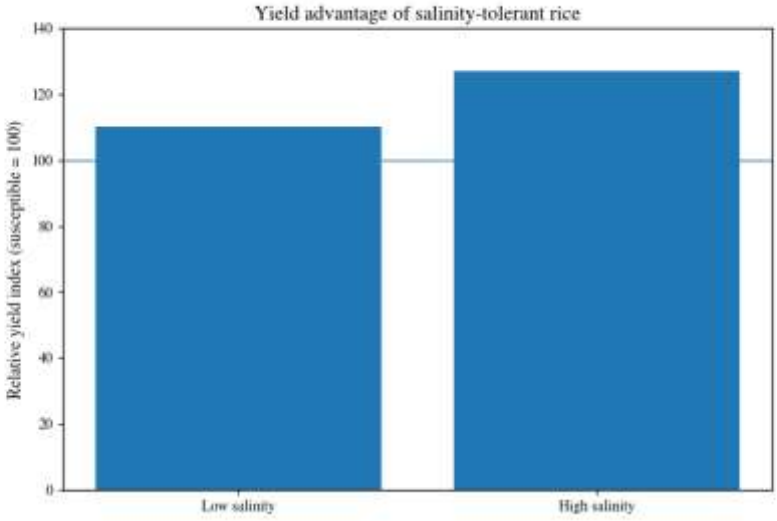


Fig. Relative yield index derived from the reported yield advantage of salinity-tolerant rice over susceptible rice (susceptible = 100). Source: (Wei et al.2026).

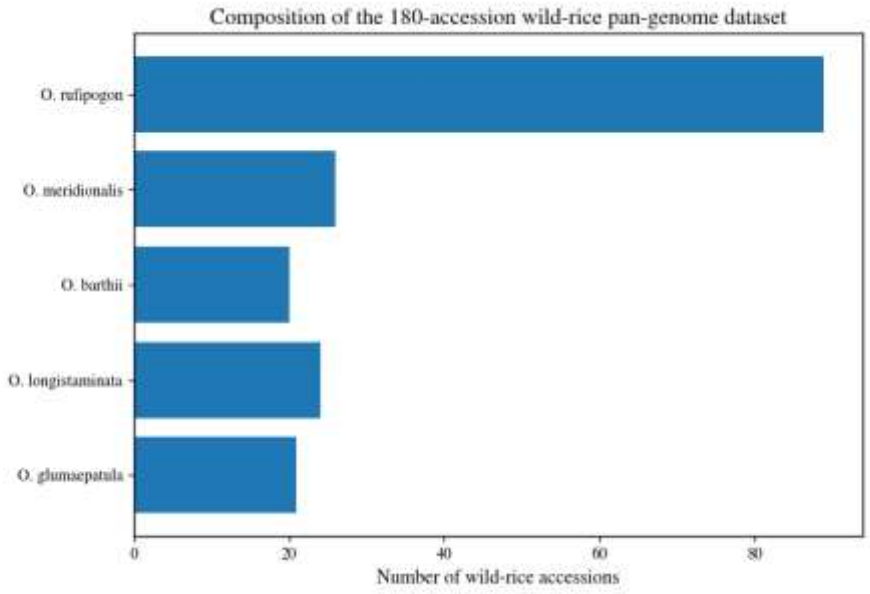


Fig 3. Composition of the 180-accession AA-genome wild-rice dataset used for pan-genome analysis. (Tao et al,.2026).

V. DISCUSSION

The evidence compiled in this review indicates that rice tolerance to abiotic stress should be considered a problem of yield stability rather than merely a physiological trait. Field data under salinity clearly show the scale of the problem: high salinity resulted in a 34.2-54.9% grain yield decrease compared to low salinity, whereas salinity-tolerant cultivars still had a 10.1% yield advantage under low salinity and a 27.1% advantage under high salinity. Notably, tolerant cultivars exhibit lower leaf Na+ and Na+/K+ ratios, along with higher photosynthetic capacity, biomass potassium concentration, and accumulation of N, P, and K, indicating that ionic homeostasis and source-sink maintenance are tightly linked to yield protection (Wei et al., 2026).

The review further illustrates why breeding for a single stressor is not enough. Transcriptome meta-analysis has identified regulatory factors that are common under stress conditions, including DREB2A, ERF95, and ERF102 in drought- and iron-toxicity-related responses. Studies in these fields have shown that salinity combined with drought can be even more detrimental to the crop than either stress alone. These data support a breeding approach that focuses on conserved signaling, ROS regulation, osmotic adjustment, and ion homeostasis while still allowing sufficient growth and reproductive performance (Ahmdikhah et al., 2025).

Another major implication is the use of genetic resources. The 2026 wild-rice pan-genome research work sequenced 180 wild accessions from five AA-genome species and discovered many novel sequences, including, on average, 224 Mb of non-redundant novel sequence per species. Also, the authors pinpointed sequences lost or deliberately selected during domestication and stress-response genes that are located in these regions. For the RIL work using O. *rufipogon*, the results confirm that wild and weedy rice are valuable reservoirs of genetic diversity from which new breeding lines can be developed, mapped, and marker-assisted selection performed (Tao et al., 2026; Roy and Shil, 2025).

Genomic tools of today's data further strengthen this method. An extensive study of 6,044 currently grown rice cultivars identified 3,131 QTLs associated with 53 phenotypes across 212 datasets, illustrating the extent to which genotype, phenotype, and environmental data can be integrated. Such tools can enhance traditional selection by enabling breeders to identify groups of alleles linked to adaptation, productivity traits, and stress responses rather than selecting for stress tolerance alone (Ma et al., 2025).

Epigenetic variability introduces yet another level in the breeding scheme. Song et al. (2025) showed that repeated cold stress caused heritable hypomethylation of the ACT1 promoter, thereby enhancing cold tolerance. This result does not mean that epigenetic variation can substitute for traditional genetic breeding; on the contrary, it suggests that stable epialleles may be another source of adaptive variation to be explored alongside DNA sequence polymorphisms.

Generally, the most logical, scientifically justifiable breeding structure which is backed by evidence points towards a hybrid program: first alter the genetic makeup by introducing genes from wild and weedy rice; testing

under both single and combined realistic environmental stresses; detecting loci, genes, and epigenetic alleles that are consistent; further study the underlying physiological and molecular candidate mechanisms; then integrating mating based on markers, genome-wide association studies genomics targeted gene modification, and traditional breeding. The primary basis for choosing the best one in the end should be high, stable yields across multiple environments, coupled with grain quality and efficient use of resources. This aligns with recent findings that climate, soil, cultivar, and management factors collectively explain rice yield stability, calling for genetic improvement aimed at environmental variability rather than at a single stress treatment (Wang et al., 2025).

VI. CONCLUSION

Rice plant growth and development are controlled by genetic, hormonal, and environmental factors, whereas abiotic stresses like drought, salinity, temperature extremes, and heavy metals severely disrupt growth, yield, and grain quality. These single or combined stress conditions lead to reduced leaf area, altered photosynthesis, impaired spikelet development, oxidative damage, ROS accumulation, and changes in grain composition. Besides cultivated varieties, wild and weedy rice sources such as O. rufipogon have provided not only useful traits for drought, cold, salinity, and other stresses but also the genetic and epigenetic basis of tolerance. Rice's genetic base has been diversified, and new breeding materials with stress tolerance and yield-related traits have been developed through pre-breeding and interspecific hybridization. Besides, epigenetic changes, such as ACT1 promoter hypomethylation, can improve heritable cold tolerance. Mainly for salinity tolerance, integrated approaches including soil and microbial management, genetic resources, marker-assisted introgression of major loci such as Saltol, transgenic approaches, and agronomic practices are required. Today, traditional selection, MAS, GWAS, QTL mapping, genome editing, gene stacking, speed breeding, multi-omics, and systems biology are increasingly combined in modern breeding to produce high-yielding, environmentally adapted rice varieties.

REFERENCES

[1] Ahmdikhah, Asadollah; Safaeizadeh, Mehdi; Tehranian, Alireza S. Responses of rice plant to multiple abiotic stresses revealed by transcriptome meta-analysis and identification of novel genetic factors. Scientific Reports, Volume 15, Issue 1, 2025, Pages 1–12. DOI: 10.1038/s41598-025-92527-2.

[2] Gao, Yujing; Cui, Jinglan; Zhang, Xiuming; Hoogenboom, Gerrit; Wallach, Daniel; Huang, Yuqi; Reis, Stefan; Lin, Tao; Gu, Baojing. Cost-effective adaptations increase rice production while reducing pollution under climate change. Nature Food, Volume 6, Issue 3, 2025, Pages 260–272. DOI: 10.1038/s43016-024-01113-8.

[3] Islam Prova, Nuzhat Noor. Enhancing agricultural research with an Attention-Based Hybrid Model for precise classification of rice varieties. International Journal of Cognitive Computing in Engineering, Volume 6, Issue In progress (December), 2025, Pages 412–430. DOI: 10.1016/j.ijcce.2025.02.002.

[4] Ma, Xiaoding; Wang, Hao; Yan, Shen; Zhou, Chuanqing; Zhou, Kunneng; Zhang, Qiang; Li, Maomao; Yang, Yaolong; Li, Danting; Song, Peng; Tang, Cuifeng; Geng, Leiyue; Sun, Jianchang; Ji, Zhiyuan; Sun, Xianjun; Zhou, Yongli; Zhou, Peng; Cui, Di; Han, Bing; Jing, Xin; He, Qiang; Fang, Wei; Han, Longzhi. Large-scale genomic and phenomic analyses of modern cultivars empower future rice breeding design. Molecular Plant, Volume 18, Issue 4, 2025, Pages 651–668. DOI: 10.1016/j.molp.2025.03.007.

[5] Pedrozo, Rodrigo; Osakina, Aron; Huang, Yixiao; Nicolli, Camila Primieri; Wang, Li; Jia, Yulin. Status on Genetic Resistance to Rice Blast Disease in the Post-Genomic Era. Plants, Volume 14, Issue 5, 2025, Page 807. DOI: 10.3390/plants14050807.

[6] Roy, Subhas Chandra; Shil, Pankaj. Comprehensive genetic diversity revealed in the pre-breeding RILs (O. sativa × O. rufipogon) with enhanced yield and pigmented grain quality. Frontiers in Genetics, Volume 16, Issue not stated, 2025, Article 1659937. DOI: 10.3389/fgene.2025.1659937.

[7] Roy, Subhas Chandra; Singh, Liza; Sarkar, Shukdeb. Agro-Morphological Characteristics of Weedy Rice (Oryza sativa F. spontanea): A Precious Genetic Resource for Rice Improvement. Current Agriculture Research Journal, Volume 11, Issue 2, 2023, Pages 450–467. DOI: 10.12944/CARJ.11.2.08.

[8] Saleem, Muhammad Ahmad; Khan, Ahmad; Tu, Jinji; Huang, Wenkang; Liu, Ying; Feng, Naijie; Zheng, Dianfeng; Xue, Yingbin. Salinity Stress in Rice: Multilayered Approaches for Sustainable Tolerance. International Journal of Molecular Sciences, Volume 26, Issue 13, 2025, Page 6025. DOI: 10.3390/ijms26136025.

[9] Sarkar, S.; Sarkar, J.; Yonzon, B.T.; Limboo, S.; Roy, S.C. Revealing Genetic Diversity in the Rice Breeding Lines (Oryza sativa × O. rufipogon) Based on Whole Genome Sequencing Variants (SNPs/InDels). Research Square, Version 1, 2026, Preprint 8630035. DOI: 10.21203/rs.3.rs-8630035/v1.

[10] Sokra, In; Somaly, Srun; Meta, Horn; Sarun, Horn; Molikoy, Chhaun. Factors Affecting Rice Production: A Systematic Review. Journal of Agriculture and Technology, Volume 2, Issue 1, 2026, Pages 19–46. DOI: 10.6084/m9.figshare.30814034.

[11] Song, Xianwei; Tang, Shanjie; Liu, Hui; Meng, Ying; Luo, Haofei; Wang, Bao; Hou, Xiu-Li; Yan, Bin; Yang, Chao; Guo, Zhenhua; Wang, Lizhi; Jiang, Shukun; Deng, Xian; Cao, Xiaofeng. Inheritance of acquired adaptive cold tolerance in rice through DNA methylation. Cell, Volume

188, Issue 16, 2025, Pages 4213–4224.e12. DOI: 10.1016/j.cell.2025.04.036.

[12] Tao, Huan; Wu, Shuhong; Wu, Guofeng; Chen, Xuan; Sun, Yiqiong; Zhu, Xiangrong; Chen, Lixin; Feng, Changqing; Kabore, Manegdebwaoga Arthur Fabrice; Woldegiorgis, Samuel Tareke; Zhang, Lina; Ai, Yufang; Liu, Wei; He, Huaqin. Pan-genome of wild and cultivated rice uncovers genetic diversity, lost and selected sequences during rice domestication. Rice, Volume 19, Issue 1, 2026, Page 21. DOI: 10.1186/s12284-026-00893-w.

[13] Tavu, Lady Edlenill J.; Redillas, Mark Christian Felipe R. Oxidative Stress in Rice (Oryza sativa): Mechanisms, Impact, and Adaptive Strategies. Plants, Volume 14, Issue 10, 2025, Page 1463. DOI: 10.3390/plants14101463.

[14] Wang, Bo; Zhong, Zhaohui; Wang, Xia; Han, Xiangyan; Yu, Deshui; Wang, Chunguo; Song, Wenqin; Zheng, Xuelian; Chen, Chengbin; Zhang, Yong. Knockout of the OsNAC006 transcription factor causes drought and heat sensitivity in rice. International Journal of Molecular Sciences, Volume 21, Issue 7, 2020, Page 2288. DOI: 10.3390/ijms21072288.

[15] Wang, Siyuan; Liu, Yijiang; Asseng, Senthold; Harrison, Matthew Tom; Tang, Liang; Liu, Bing; Liu, Ke; Luo, Zhongkui; Wang, Enli; Chang, Jinfeng; Qiu, Xiaolei; Liu, Leilei; Zhang, Xiaohu; Cao, Weixing; Zhu, Yan; Xiao, Liujun. Rice yield stability and its determinants across different rice-cropping systems in China. Agricultural and Forest Meteorology, Volume 364, Issue not stated, 2025, Article 110452. DOI: 10.1016/j.agrformet.2025.110452.

[16] Wang, Siyuan; Yao, Yajun; Wang, Jun; Ruan, Bo; Yu, Yiyang. Advancing Stress-Resilient Rice: Mechanisms, Genes, and Breeding Strategies. Agriculture, Volume 15, Issue 7, 2025, Page 721. DOI: 10.3390/agriculture15070721.

[17] Wang, Xiaohui; Liu, Xuelei; Su, Yonglin; Shen, Huaizong. Rice Responses to Abiotic Stress: Key Proteins and Molecular Mechanisms. International Journal of Molecular Sciences, Volume 26, Issue 3, 2025, Page 896. DOI: 10.3390/ijms26030896.

[18] Wei, Huanhe; Jiang, Yue; Ma, Qingqing; Zhu, Jizou; Zhang, Xiang; Chen, Yinglong; Gao, Pinglei; Zhao, Chenchen; Dai, Qigen; Meng, Tianyao. Salinity Effects on Agro-Physiological Characteristics and Yield Formation of Rice Differing in Salinity Tolerance in Saline Lands. Journal of Agronomy and Crop Science, Volume 212, Issue 4, 2026, Pages 1–17. DOI: 10.1111/jac.70216.

[19] Yao, W.; Yang, Y.; Beillouin, D.; Zhao, J.; Olesen, J.E.; Zhou, J.; Smith, P.; Zeng, Z.; Lambers, H.; Rillig, M.C.; Wanger, T.C.; Zang, H. Legume-rice rotations increase rice yields and carbon sequestration potential globally. One Earth, Volume 8, Issue not stated, 2025, Article 101170. DOI: 10.1016/j.oneear.2024.12.006.

International Journal of Environment, Agriculture and Biotechnology
Vol-11, Issue-5; Sep-Oct, 2026
Peer-Reviewed International Journal
Journal Home Page Available: https://ijeab.com/
Journal DOI: 10.22161/ijeab

Performance assessment of the National Livestock Mission in India using a Composite Performance Index Approach

Himanth Raj K N[1*], Devendra Beeraladinni[2], Vijayachandra Reddy S[3], D. G. Satihal[4] and Sreedhara J N[5]

[1]Research Scholar, Department of Agricultural Economics, College of Agriculture, University of Agricultural Sciences, Raichur-584101, Karnataka, India
[2]Associate Professor and Extension Leader, Agricultural Extension Education Centre (AEEC), Devadurga, University of Agricultural Sciences, Raichur-584101, Karnataka, India
[3]Assistant Professor of Agricultural Economics, Office of the Registrar, University of Agricultural Sciences, Raichur, Karnataka, India
[4]Professor and Head, College of Agriculture, Bheemarayanagudi, University of Agricultural Sciences, Raichur, Karnataka, India
[5]Associate Professor of Animal Science, College of Agriculture Engineering, University of Agricultural Sciences, Raichur, Karnataka, India
*Email: himanthrkn16005@uasraichur.edu.in

Received: 03 Aug 2026; Received in revised form: 31 Aug 2026; Accepted: 04 Sep 2026; Available online: 16 Sep 2026
©2026 The Author(s). Published by Infogain Publication. This is an open-access article *under* the CC BY license (https://creativecommons.org/licenses/by/4.0/).

Abstract— *The National Livestock Mission (NLM) is a flagship programme of the Government of India aimed at promoting sustainable livestock development through entrepreneurship development, breed improvement, fodder development and value chain strengthening. Despite substantial financial support, considerable variation exists in the implementation performance of the scheme across Indian States. Therefore, the present study assessed the performance of the National Livestock Mission using a Composite Performance Index (CPI). Secondary data for the period 2021–22 to 2025–26 were compiled from the National Livestock Mission Dashboard of the Department of Animal Husbandry and Dairying, Government of India. Five performance indicators, namely Project Approval Rate, Subsidy Release Rate, Project Cost Utilization Rate, Loan Utilization Rate and Subsidy Utilization Rate, were normalized using the Min–Max normalization technique and aggregated with equal weights to construct the Composite Performance Index. The results revealed considerable inter-state variation in programme implementation. Jharkhand (0.943), Odisha (0.918), Nagaland (0.869), Mizoram (0.865) and Madhya Pradesh (0.802) recorded the highest Composite Performance Index values, whereas Manipur (0.114) and Gujarat (0.365) exhibited relatively poor implementation performance. Based on CPI values, six States were classified under the Excellent category, eighteen under Good, two under Moderate and two under Poor performance. The findings indicate that improving project implementation efficiency, timely subsidy release and financial utilization is essential for enhancing the effectiveness of the National Livestock Mission across States.*

Keywords— ***National Livestock Mission, Composite Performance Index, Programme Performance Evaluation, Livestock Development, Min–Max Normalization, State-wise Performance, Financial Utilization.***

I. INTRODUCTION

The livestock sector is an integral component of the Indian agricultural economy and plays a pivotal role in improving rural livelihoods, ensuring nutritional security and generating employment. Unlike seasonal crop production, livestock provides a regular source of income throughout the year and serves as a sustainable livelihood option, particularly for small and marginal farmers. Besides contributing to household income, the sector supports agricultural diversification through the production of milk, meat, eggs, wool and other livestock products while providing raw materials for allied industries such as dairy

processing, poultry, leather, feed manufacturing and livestock-based enterprises. According to the 20th Livestock Census, India possesses 535.78 million livestock, making it the country with the largest livestock population in the world (DAHD, 2019). Further, the Basic Animal Husbandry Statistics (2024) reported that India produced 239.30 million tonnes of milk during 2023–24, maintaining its position as the world's largest milk producer, while also ranking among the leading producers of eggs and meat. The livestock sector contributes nearly 30 per cent of the Gross Value Added (GVA) of agriculture and allied sectors, highlighting its growing importance in the national economy (DAHD, 2024).

Despite its remarkable contribution, the livestock sector continues to face several production, institutional and infrastructural constraints that limit its overall performance. Low genetic potential of indigenous breeds, inadequate availability of quality fodder and feed resources, disease outbreaks, insufficient veterinary infrastructure, poor market access and limited institutional credit continue to constrain livestock productivity and farmers' income. In addition, fragmented production systems, low adoption of improved technologies and climate-related risks have emerged as major challenges to sustainable livestock development. Addressing these constraints requires well-designed policy interventions that promote productivity enhancement, entrepreneurship development and efficient utilization of financial resources.

Recognizing the strategic importance of livestock in improving farmers' income and ensuring sustainable agricultural growth, the Government of India launched the National Livestock Mission (NLM) during 2014–15. The mission aims to promote sustainable livestock development through entrepreneurship development, breed improvement, fodder development, feed and fodder seed production, value chain strengthening and capacity building. It provides financial assistance for establishing sheep, goat, piggery and poultry enterprises, encourages private investment and generates employment opportunities in rural areas. In recent years, the programme has been restructured to strengthen entrepreneurship-led livestock development, improve programme implementation and enhance the efficiency of financial assistance through improved monitoring and institutional support (Department of Animal Husbandry and Dairying, 2024).

Since its implementation, the National Livestock Mission has supported the establishment of thousands of livestock enterprises across Indian States and Union Territories through financial assistance, subsidy support and institutional credit. Nevertheless, the implementation performance of the programme has varied considerably across States due to differences in administrative efficiency, institutional capacity, beneficiary participation and financial resource utilization. While some States have achieved higher project approval rates, timely subsidy release and efficient utilization of project funds, others have experienced implementation delays, lower subsidy utilization and comparatively weaker programme performance. Such interstate variations highlight the need for a systematic evaluation framework that objectively measures implementation efficiency and identifies areas requiring policy intervention.

Previous studies have primarily focused on livestock production, productivity, value chain development, entrepreneurship promotion and the economic impact of government programmes. However, studies evaluating the implementation performance of the National Livestock Mission remain limited, and most have relied on descriptive indicators rather than integrating multiple dimensions of programme implementation into a single quantitative measure. Consequently, meaningful comparison of programme performance across States has remained difficult, leaving an important research gap in the evaluation of the scheme.

To address this research gap, the Composite Performance Index (CPI) provides a comprehensive and objective framework for integrating multiple implementation indicators into a single standardized measure of programme performance. By combining indicators related to project approval, subsidy release and financial utilization, the CPI facilitates comparison of implementation efficiency across States, identifies high- and low-performing regions and provides evidence for improving programme implementation and resource allocation. Such an approach enables policymakers to assess the overall effectiveness of the National Livestock Mission and formulate targeted strategies for enhancing programme outcomes. Against this background, the present study aims to assess the performance of the National Livestock Mission across Indian States using a Composite Performance Index (CPI) approach by integrating physical and financial performance indicators into a single measure for interstate comparison and policy evaluation.

II. MATERIALS AND METHODS

Data Source

The study utilized secondary data obtained from the National Livestock Mission (NLM) Dashboard maintained by the Department of Animal Husbandry and Dairying (DAHD), Ministry of Fisheries, Animal Husbandry and Dairying, Government of India. State-wise data on the physical and financial performance of the National

Livestock Mission for the period 2021–22 to 2025–26 were compiled for analysis. The dataset included information on recommended projects, approved projects, subsidy-released projects, project cost, loan amount and subsidy amount. States and Union Territories with no eligible projects during the study period were excluded from the analysis.

Selection of Performance Indicators

Five indicators representing the physical and financial dimensions of programme implementation were selected to evaluate the performance of the National Livestock Mission. The selected indicators capture the major stages of programme implementation, namely project approval, subsidy release and financial resource utilization. Since higher values of all indicators represent better programme performance, all indicators were treated as positive indicators.

Table 1. Indicators Used for Construction of Composite Performance Index (CPI)

Code	Indicator	Formula	Nature
PI_1	Project Approval Rate (%)	Approved Projects / Recommended Projects × 100	Positive
PI_2	Subsidy Release Rate (%)	Subsidy Released Projects / Approved Projects × 100	Positive
PI_3	Project Cost Utilization Rate (%)	Released Project Cost / Approved Project Cost × 100	Positive
PI_4	Loan Utilization Rate (%)	Released Loan Amount / Approved Loan Amount × 100	Positive
PI_5	Subsidy Utilization Rate (%)	Released Subsidy Amount / Approved Subsidy Amount × 100	Positive

Normalization of Indicators

The selected performance indicators were measured in percentage terms but differed in their range and magnitude. Therefore, the indicators were normalized using the Min–Max normalization technique to transform all variables into a common scale ranging from 0 to 1.

$$PI_i = (X_i - X_{min}) / (X_{max} - X_{min}) \quad (1)$$

Where: PI_i = normalized value of the i^{th} indicator; X_i = actual value; X_{min} = minimum observed value; X_{max} = maximum observed value.

A normalized value closer to 1 indicates better programme performance, whereas a value closer to 0 indicates relatively poor performance.

Construction of Composite Performance Index

The Composite Performance Index (CPI) was constructed by assigning equal weight to each normalized indicator, assuming that all indicators contribute equally to the overall implementation performance of the National Livestock Mission. The CPI was computed as:

$$CPI = (PI_1 + PI_2 + PI_3 + PI_4 + PI_5) / 5 \quad (2)$$

Where: PI_1 = Project Approval Rate; PI_2 = Subsidy Release Rate; PI_3 = Project Cost Utilization Rate; PI_4 = Loan Utilization Rate; PI_5 = Subsidy Utilization Rate. Higher CPI values indicate better programme implementation performance.

Ranking of States

The participating States were ranked in descending order based on their Composite Performance Index values. The State with the highest CPI was assigned Rank 1, indicating the best overall implementation performance, whereas the State with the lowest CPI received the last rank.

Performance Classification

For interpretation, the participating States were classified into four performance categories based on their Composite Performance Index values.

CPI Range	Performance Category
0.80 – 1.00	Excellent
0.60 – 0.79	Good
0.40 – 0.59	Moderate
Below 0.40	Poor

III. RESULT AND DISCUSSION

The physical performance of the National Livestock Mission during 2021–22 to 2025–26 is presented in Table 2. The number of recommended projects increased from 956 in 2021–22 to 5,420 in 2023–24, showing an increase in the number of projects taken up under the mission. However, the number declined to 4,194 in 2024–25 and 572 in 2025–26. The lower value recorded for 2025–26 is because the data represent the position available up to the date of extraction from the National Livestock Mission Dashboard.

A similar pattern was observed for approved projects and subsidy-released projects. Approved projects increased from 926 in 2021–22 to 4,154 in 2023–24, while subsidy-released projects increased from 804 to 3,362

during the same period. In 2024–25 and 2025–26, both approved projects and subsidy-released projects declined, mainly because the implementation process for these years was still in progress at the time the data were collected.

Table 2. Physical Performance of the National Livestock Mission in India (2021–22 to 2025–26)

Year	Recommended Projects	Approved Projects	Subsidy Released Projects	Approval Rate (%)	Subsidy Release Rate (%)
2021–22	956	926	804	96.86	86.83
2022–23	1,798	1,668	1,456	92.77	87.29
2023–24	5,420	4,154	3,362	76.64	80.93
2024–25	4,194	1,224	660	29.18	53.92
2025–26*	572	126	8	22.03	6.35

**2025–26 represents data available up to the date of extraction from the NLM dashboard.*

The approval rate was highest during 2021–22 (96.86%), followed by 2022–23 (92.77%), but declined to 76.64 per cent in 2023–24. A sharp decline was observed during 2024–25 (29.18%) and 2025–26 (22.03%). Similarly, the subsidy release rate remained above 80 per cent during the first three years of the study period, but declined to 53.92 per cent in 2024–25 and 6.35 per cent in 2025–26.

Overall, the results indicate that the National Livestock Mission expanded considerably during the first three years of the study period. The decline observed during 2024–25 and 2025–26 should be viewed with caution because the figures for these years represent incomplete data available at the time of extraction and may change as programme implementation progresses.

Table 3. Financial Performance of the National Livestock Mission in India (₹ crore) (2021–22 to 2025–26)

Year	Recommended Project Cost	Approved Project Cost	Released Project Cost	Approved Loan	Released Loan	Approved Subsidy	Released Subsidy
2021–22	889.96	860.54	746.60	348.68	304.42	404.94	272.00
2022–23	1,475.78	1,374.22	1,209.44	519.96	456.98	643.92	417.04
2023–24	3,123.98	2,436.60	2,013.34	927.74	761.18	1,151.50	684.12
2024–25	2,334.22	685.20	389.86	285.06	149.78	327.70	88.56
2025–26*	312.10	66.74	5.80	32.96	1.80	31.26	1.98

The financial performance of the National Livestock Mission during 2021–22 to 2025–26 is presented in Table 3. The results show that the financial allocation under the programme increased considerably during the first three years of the study period. The recommended project cost increased from ₹889.96 crore in 2021–22 to ₹3,123.98 crore in 2023–24, indicating expansion in programme implementation. However, it declined during 2024–25 and 2025–26, mainly because the data for 2025–26 are available only up to the date of extraction from the National Livestock Mission Dashboard.

The approved project cost also increased from ₹860.54 crore in 2021–22 to ₹2,436.60 crore in 2023–24, while the released project cost increased from ₹746.60 crore to ₹2,013.34 crore during the same period. Similar trends were observed for the approved and released loan amounts as well as subsidy amounts. Approved loan assistance increased from ₹348.68 crore to ₹927.74 crore, whereas released loan assistance increased from ₹304.42 crore to ₹761.18 crore between 2021–22 and 2023–24. Likewise, approved subsidy increased from ₹404.94 crore to ₹1,151.50 crore, while released subsidy increased from ₹272.00 crore to ₹684.12 crore.

The decline in financial indicators during 2024–25 and 2025–26 should be interpreted with caution because the figures for the latest year represent only the data available at the time of extraction. Overall, the financial performance indicates that the National Livestock Mission expanded substantially during the first three years, with corresponding

increases in project cost, loan assistance and subsidy support.

Table 4. State-wise Physical Performance of the National Livestock Mission (2021–22 to 2025–26)

State	Recommended Projects	Approved Projects	Subsidy Released Projects	Approval Rate (%)	Subsidy Release Rate (%)
Andhra Pradesh	557	321	265	57.63	82.55
Arunachal Pradesh	127	83	47	65.35	56.63
Assam	60	47	37	78.33	78.72
Bihar	9	2	2	22.22	100.00
Chhattisgarh	48	28	21	58.33	75.00
Gujarat	505	245	196	48.51	80.00
Haryana	244	139	111	56.97	79.86
Himachal Pradesh	38	23	18	60.53	78.26
Jammu & Kashmir	42	19	12	45.24	63.16
Jharkhand	6	6	6	100.00	100.00
Karnataka	598	281	224	46.99	79.72
Kerala	466	280	222	60.09	79.29
Madhya Pradesh	659	543	493	82.40	90.79
Maharashtra	1220	553	411	45.33	74.32
Manipur	41	21	15	51.22	71.43
Mizoram	6	6	5	100.00	83.33
Nagaland	26	24	22	92.31	91.67
Odisha	174	143	133	82.18	93.01
Puducherry	5	5	5	100.00	100.00
Punjab	100	88	81	88.00	92.05
Rajasthan	586	266	201	45.39	75.56
Sikkim	16	14	13	87.50	92.86
Tamil Nadu	364	213	158	58.52	74.18
Telangana	246	155	122	63.01	78.71
Tripura	19	10	8	52.63	80.00
Uttar Pradesh	552	222	159	40.22	71.62
Uttarakhand	71	39	33	54.93	84.62
West Bengal	43	18	14	41.86	77.78

The state-wise physical performance of the National Livestock Mission during 2021–22 to 2025–26 is presented in Table 4. Considerable variation was observed among the participating States with respect to recommended projects, approved projects and subsidy-released projects. Maharashtra recorded the highest number of recommended projects (1,220), followed by Madhya Pradesh (659), Karnataka (598), Rajasthan (586) and Andhra Pradesh (557). These States also accounted for a relatively higher number of approved and subsidy-released projects, indicating greater participation under the mission.

The project approval rate also varied across States. Jharkhand, Mizoram and Puducherry recorded a 100 per cent approval rate, followed by Nagaland (92.31%), Punjab (88.00%) and Sikkim (87.50%). In contrast, lower approval rates were observed in Bihar (22.22%), Uttar Pradesh (40.22%), West Bengal (41.86%) and Jammu & Kashmir (45.24%). Similarly, the subsidy release rate was highest in Bihar, Jharkhand and Puducherry (100%), while Odisha (93.01%), Sikkim (92.86%), Punjab (92.05%) and Nagaland (91.67%) also recorded high subsidy release rates.

The observed differences among States may be attributed to variations in project implementation, beneficiary participation and administrative processes. States with higher approval and subsidy release rates indicate relatively better progress in implementing the programme, whereas States with lower rates may require greater attention to improve project approval and subsidy disbursement.

Table 5. Financial Performance Indicators of the National Livestock Mission across Indian States (2021–22 to 2025–26)

State	Project Cost Utilization (%)	Loan Utilization (%)	Subsidy Utilization (%)
Andhra Pradesh	85.81	75.45	28.95
Arunachal Pradesh	61.36	50.15	23.53
Assam	83.23	74.62	13.49
Bihar	100.00	62.07	7.00
Chhattisgarh	75.29	66.72	16.26
Gujarat	64.65	61.48	1.46
Haryana	85.31	71.48	9.53
Himachal Pradesh	80.90	73.11	12.08
Jammu & Kashmir (UT)	83.45	76.73	19.91
Jharkhand	100.00	100.00	33.33
Karnataka	78.76	71.18	19.54
Kerala	58.24	48.71	17.55
Madhya Pradesh	88.88	80.85	22.14
Maharashtra	77.52	71.03	20.56
Manipur	26.12	20.25	0.00
Mizoram	88.96	79.57	28.40
Nagaland	89.61	69.65	31.63
Odisha	100.00	100.00	26.51
Puducherry (UT)	100.00	100.00	0.00
Punjab	88.62	80.78	19.35
Rajasthan	81.80	75.17	20.40
Sikkim	83.33	76.67	24.76
Tamil Nadu	78.64	72.84	18.86
Telangana	82.47	75.34	22.78
Tripura	79.61	74.18	17.24
Uttar Pradesh	67.00	56.46	13.99
Uttarakhand	74.30	64.78	15.03
West Bengal	73.43	74.34	18.18

The state-wise financial performance indicators of the National Livestock Mission during 2021–22 to 2025–26 are presented in Table 5. The financial performance indicators varied across the participating States with respect to project cost utilization, loan utilization and subsidy utilization. Jharkhand, Odisha and Puducherry (UT) recorded 100.00 per cent project cost utilization and loan utilization, indicating complete utilization of the approved project cost and loan amount. High project cost utilization was also observed in Nagaland (89.61%), Mizoram (88.96%), Madhya Pradesh (88.88%) and Punjab (88.62%), indicating better utilization of financial assistance under the mission.

Loan utilization remained above 70 per cent in several States, including Andhra Pradesh, Assam, Himachal Pradesh, Karnataka, Madhya Pradesh, Maharashtra, Punjab, Rajasthan, Tamil Nadu and Telangana, indicating better utilization of the sanctioned loan amount. In contrast, Manipur (20.25%), Kerala (48.71%) and Arunachal Pradesh (50.15%) recorded comparatively lower loan utilization, suggesting that a smaller proportion of the sanctioned loan amount was utilized.

Subsidy utilization also differed across States. Jharkhand (33.33%) recorded the highest subsidy utilization, followed by Nagaland (31.63%), Andhra Pradesh (28.95%), Mizoram (28.40%) and Odisha (26.51%). On the other hand, Puducherry (UT) and Manipur recorded 0.00 per cent subsidy utilization, while Gujarat (1.46%) and Bihar (7.00%) also recorded comparatively lower subsidy utilization. These results show that while several States effectively utilized the approved project cost and loan amount, subsidy utilization varied across the participating States.

Overall, the results indicate that the financial performance of the National Livestock Mission differed across States. Improving the timely release of subsidy and effective utilization of project cost and loan assistance would further strengthen the implementation of the programme.

Table 6. Normalized Performance Indicators and Composite Performance Index (CPI) of the National Livestock Mission across States (2021–22 to 2025–26)

Rank	State	PI_1	PI_2	PI_3	PI_4	PI_5	CPI
1	Jharkhand	1.000	1.000	1.000	1.000	0.714	0.943
2	Odisha	0.679	1.000	1.000	1.000	0.913	0.918
3	Nagaland	0.948	0.856	0.859	0.684	1.000	0.869
4	Mizoram	0.863	0.801	0.851	0.837	0.973	0.865
5	Madhya Pradesh	0.677	0.850	0.850	0.846	0.788	0.802
6	Puducherry (UT)	1.000	1.000	1.000	1.000	0.000	0.800
7	West Bengal	0.697	0.824	0.640	0.694	0.939	0.759
8	Andhra Pradesh	0.455	0.801	0.808	0.799	0.869	0.746
9	Bihar	0.000	1.000	1.000	1.000	0.689	0.738
10	Telangana	0.651	0.752	0.731	0.748	0.773	0.731
11	Karnataka	0.697	0.725	0.713	0.721	0.700	0.711
12	Uttarakhand	0.716	0.718	0.652	0.602	0.852	0.708
13	Assam	0.721	0.757	0.773	0.698	0.567	0.703
14	Sikkim	0.622	0.810	0.763	0.796	0.484	0.695
15	Himachal Pradesh	0.645	0.782	0.741	0.768	0.530	0.694
16	Tripura	0.821	0.629	0.662	0.624	0.643	0.676
17	Punjab	0.378	0.786	0.846	0.829	0.502	0.668
18	Chhattisgarh	0.464	0.714	0.665	0.734	0.754	0.666
19	Tamil Nadu	0.314	0.775	0.766	0.715	0.750	0.664
20	Haryana	0.538	0.771	0.801	0.731	0.464	0.661
21	Jammu & Kashmir (UT)	0.192	0.780	0.776	0.832	0.669	0.650

22	Rajasthan	0.112	0.823	0.754	0.793	0.739	0.644
23	Maharashtra	0.250	0.720	0.696	0.715	0.724	0.621
24	Uttar Pradesh	0.661	0.603	0.553	0.596	0.583	0.599
25	Kerala	0.638	0.503	0.435	0.454	0.661	0.538
26	Arunachal Pradesh	0.555	0.504	0.477	0.450	0.686	0.534
27	Gujarat	0.357	0.314	0.521	0.552	0.079	0.365
28	Manipur	0.571	0.000	0.000	0.000	0.000	0.114

The normalized performance indicators and Composite Performance Index (CPI) of the National Livestock Mission across the participating States are presented in Table 6. The Composite Performance Index was developed by combining five normalized performance indicators, namely project approval rate, subsidy release rate, project cost utilization, loan utilization and subsidy utilization. The CPI values ranged from 0.114 to 0.943, indicating considerable variation in programme performance across the participating States.

Among all the States, Jharkhand recorded the highest Composite Performance Index (0.943) and secured the first rank, followed by Odisha (0.918), Nagaland (0.869), Mizoram (0.865) and Madhya Pradesh (0.802). The higher CPI values of these States indicate better overall performance with respect to project approval, subsidy release and financial utilization under the National Livestock Mission. Puducherry (UT) also recorded a relatively high CPI (0.800) despite lower subsidy utilization, mainly because of complete project approval and financial utilization.

Among the remaining States, West Bengal, Andhra Pradesh, Bihar, Telangana, Karnataka, Uttarakhand, Assam and Sikkim recorded CPI values above 0.69, indicating satisfactory programme performance. In contrast, Kerala (0.538), Arunachal Pradesh (0.534), Gujarat (0.365) and Manipur (0.114) recorded comparatively lower CPI values. The lower index values observed in these States were mainly associated with lower performance in one or more of the selected indicators, particularly subsidy utilization and financial utilization.

The Composite Performance Index provides a comprehensive measure of programme performance by integrating multiple implementation indicators into a single index. The results clearly show that the implementation performance of the National Livestock Mission varied across the participating States, highlighting the need to improve project approval, timely subsidy release and effective utilization of financial assistance in the relatively lower-performing States.

Table 7. Performance Classification of States Based on Composite Performance Index (CPI)

Performance Category	**CPI Range**	**No. of States**	**States**
Excellent	≥ 0.80	6	Jharkhand, Odisha, Nagaland, Mizoram, Madhya Pradesh, Puducherry (UT)
Good	0.60 – 0.79	18	West Bengal, Andhra Pradesh, Bihar, Telangana, Karnataka, Uttarakhand, Assam, Sikkim, Himachal Pradesh, Tripura, Punjab, Chhattisgarh, Tamil Nadu, Haryana, Jammu & Kashmir (UT), Rajasthan, Maharashtra, Uttar Pradesh
Moderate	0.40 – 0.59	2	Kerala, Arunachal Pradesh
Poor	< 0.40	2	Gujarat, Manipur

The classification of the participating States based on the Composite Performance Index (CPI) is presented in Table 7. Based on the CPI values, the States were classified into four categories: Excellent, Good, Moderate and Poor. The classification helps to compare the overall performance of the National Livestock Mission among the participating States.

Out of the 28 participating States, six States/Union Territories were placed under the Excellent category with a CPI value of 0.80 and above. These States recorded higher

performance in most of the selected indicators. Eighteen States were classified under the Good category with CPI values ranging from 0.60 to 0.79, indicating satisfactory implementation of the programme. Kerala and Arunachal Pradesh were placed under the Moderate category, whereas Gujarat and Manipur were classified under the Poor category because of their relatively lower CPI values.

The classification shows that the performance of the National Livestock Mission differed across the participating States. States placed under the Excellent category maintained better overall performance, whereas States under the Moderate and Poor categories require improvement in project approval, subsidy release and financial utilization to enhance the overall performance of the programme.

IV. CONCLUSION

The present study evaluated the performance of the National Livestock Mission across the participating States of India using a Composite Performance Index (CPI) based on five indicators, namely project approval rate, subsidy release rate, project cost utilization, loan utilization and subsidy utilization. The analysis revealed considerable variation in the implementation of the programme across States. The physical and financial performance of the mission improved during the initial years of the study period, indicating increasing participation and expansion of programme activities. However, the decline observed during the later years should be interpreted with caution, as the data for the most recent financial year represent only the progress available up to the date of data extraction.

The Composite Performance Index provided a comprehensive measure for comparing the overall performance of the National Livestock Mission across States. Jharkhand, Odisha, Nagaland, Mizoram and Madhya Pradesh emerged as the best-performing States, reflecting higher project approval, timely subsidy release and better utilization of financial resources. In contrast, Gujarat and Manipur recorded comparatively lower CPI values, indicating the need for improvement in programme implementation. The performance classification further showed that only a few States achieved an excellent level of performance, while the majority of States were placed in the good category, suggesting that there is still scope for improving programme implementation across the country.

The findings of the study highlight that the effectiveness of the National Livestock Mission depends not only on financial allocation but also on the timely approval of projects, prompt release of subsidy and efficient utilization of sanctioned funds. Strengthening administrative coordination, reducing delays in project processing and ensuring timely financial support can further improve the implementation of the programme. Greater attention should also be given to relatively lower-performing States through regular monitoring, capacity building and technical guidance to improve programme outcomes.

The Composite Performance Index developed in the present study provides a simple and systematic framework for evaluating programme performance across States. The methodology can also be applied to assess the performance of other government development programmes involving multiple implementation indicators. Future studies may incorporate additional indicators, district-level analysis and beneficiary-level data to provide a more comprehensive assessment of the National Livestock Mission and its long-term impact on livestock development and rural livelihoods.

REFERENCES

[1] Department of Animal Husbandry and Dairying (DAHD). (2019). 20th Livestock Census. Ministry of Fisheries, Animal Husbandry and Dairying, Government of India, New Delhi.

[2] Department of Animal Husbandry and Dairying (DAHD). (2024). Basic Animal Husbandry Statistics 2024. Ministry of Fisheries, Animal Husbandry and Dairying, Government of India, New Delhi.

[3] Department of Animal Husbandry and Dairying (DAHD). (2024). National Livestock Mission Operational Guidelines. Ministry of Fisheries, Animal Husbandry and Dairying, Government of India, New Delhi.

[4] Department of Animal Husbandry and Dairying (DAHD). (2024). National Livestock Mission Dashboard. Ministry of Fisheries, Animal Husbandry and Dairying, Government of India.

[5] Government of India. (2025). Economic Survey 2024–25. Ministry of Finance, Government of India, New Delhi.

[6] Khandker, S. R., Koolwal, G. B., & Samad, H. A. (2010). Handbook on Impact Evaluation: Quantitative Methods and Practices. World Bank, Washington, DC.

[7] Nardo, M., Saisana, M., Saltelli, A., Tarantola, S., Hoffman, A., & Giovannini, E. (2008). Handbook on Constructing Composite Indicators: Methodology and User Guide. OECD Publishing, Paris.

[8] Organisation for Economic Co-operation and Development (OECD). (2008). Handbook on Constructing Composite Indicators: Methodology and User Guide. OECD Publishing, Paris.

[9] Rossi, P. H., Lipsey, M. W., & Henry, G. T. (2019). Evaluation: A Systematic Approach (8th ed.). Sage Publications, Thousand Oaks, CA.

[10] United Nations Development Programme (UNDP). (2024). Human Development Report 2023/24: Breaking the Gridlock – Reimagining Cooperation in a Polarized World. UNDP, New York.

International Journal of Environment, Agriculture and Biotechnology
Vol-11, Issue-5; Sep-Oct, 2026
Peer-Reviewed International Journal
Journal Home Page Available: https://ijeab.com/
Journal DOI: 10.22161/ijeab

Basics of Biofilm Architecture and Antimicrobial Resistance

Subrat Kumar Barik[1*], Priti Sundar Mohanty[1,2,3], Mugdha Sinha[1], Shailesh Rout[1]

[1]School of Biotechnology, Kalinga Institute of Industrial Technology (KIIT) Deemed to be University, Bhubaneswar 751024, India
[2]School of Chemical Engineering, Kalinga Institute of Industrial Technology (KIIT) Deemed to be University, Bhubaneswar 751024, India
[3]Centre for Soft Matter & Bio-Engineering (CSMBE), Kalinga Institute of Industrial Technology (KIIT) Deemed to be University, Bhubaneswar 751024, India
*Corresponding Author: bariksubratkumar19@gmail.com

Received: 03 Aug 2026; Received in revised form: 31 Aug 2026; Accepted: 04 Sep 2026; Available online: 19 Sep 2026
©2026 The Author(s). Published by Infogain Publication. This is an open-access article *under* the CC BY license (https://creativecommons.org/licenses/by/4.0/).

Abstract— *The most common type of microbial life in nature is found in bacterial biofilms, which are organized colonies attached to surfaces. They are thought to be the cause of up to 80% of human chronic illnesses and over two-thirds of microbiological infections. The global antimicrobial resistance (AMR) epidemic is intimately related to their clinical relevance; in 2021, bacterial AMR was linked to an estimated 4.71 million deaths worldwide. Unlike traditional genetic resistance, biofilm-associated resistance largely stems from the structural and chemical composition of biofilms. The extracellular polymeric substance (EPS) matrix, its three-dimensional organization, and the internal chemical heterogeneity are the main topics of this review, which summarizes the current knowledge on biofilm architecture. It investigates the mechanisms—diffusion limitation, metabolic heterogeneity, efflux pump activity, improved horizontal gene transfer, and quorum-sensing regulation—by which this architecture confers antimicrobial resistance and tolerance.. The clinical impact of biofilm-associated infections in medical devices, chronic wounds, and the airways of cystic fibrosis patients is discussed along with emerging therapeutic strategies targeting biofilms, including quorum-sensing inhibitors, matrix-degrading enzymes, nanotechnology-based delivery systems, and bacteriophage therapy. We conclude that effective management of infections associated with biofilms necessitates strategies that target multiple aspects of biofilm architecture, used in combination with, rather than as a replacement for, conventional antimicrobial therapy.*

Keywords— ***Biofilm, extracellular polymeric substance (EPS), antimicrobial resistance, quorum sensing, persister cells, antibiofilm therapy***

I. INTRODUCTION

Throughout the majority of the twentieth century, bacterial research predominantly focused on free-floating planktonic cells within laboratory cultures. However, it is now well recognized that this does not reflect the natural state of bacteria. Most bacteria exist as biofilms, which are surface-associated, multicellular communities where cells are irreversibly attached to a substratum and to each other, embedded within a self-produced extracellular matrix (1). Researchers and physicians' perspectives on recurrent and persistent infections have been profoundly impacted by this paradigm shift.

Biofilms are increasingly acknowledged as substantial contributors to the global antimicrobial resistance (AMR) crisis, a factor that has been historically underestimated. The magnitude of this crisis is significant. A 2024 study estimated that bacterial AMR was associated with 4.71 million deaths worldwide in 2021, with 1.14 million directly attributable to resistant infections (2). An earlier study attributed 1.27 million deaths in 2019 to antibiotic-resistant infections (3). The World Health Organization's 2024 Bacterial Priority Pathogens List highlights the organisms posing the most significant threat, with Gram-negative bacteria and rifampicin-resistant *Mycobacterium*

tuberculosis identified as critical priorities for research and development (4).

Biofilms are intricately involved in various aspects of clinical practice related to microbial infections. According to estimates by the United States National Institutes of Health, biofilms are implicated in approximately 65% of all microbial infections and up to 80% of chronic human infections (5,6,7). Bacteria residing in a biofilm can tolerate antibiotic concentrations that are significantly higher in some reported cases up to a thousand-fold higher than those required to eliminate genetically identical planktonic cells (8). Importantly, this increased tolerance is usually not due to the acquisition of new resistance genes by biofilm-embedded bacteria. Instead, it is the architecture of the biofilm including its matrix, internal chemistry, and the physiological states it induces in resident cells that actively confers protection. Antimicrobial tolerance is a reversible physiological state that allows cells to withstand drug exposure without changing their genetically determined susceptibility, whereas antimicrobial resistance is a persistent heritable feature encoded by mutation or an acquired resistance gene. (9). Biofilms facilitate this phenomenon. They establish conditions that favour short term tolerance, and, over time, enhance the probability of the emergence and dissemination of true genetic resistance among cells, and even across species (10).

This review initially explores biofilm architecture, focusing on their structural composition. We then delve into the specific mechanisms by which this architecture contributes to antimicrobial resistance and tolerance. Additionally, this review evaluates the clinical burden of biofilm-associated infections and examines novel strategies aimed at directly targeting biofilm architecture directly, rather than relying solely on conventional antibiotics.

II. BIOFILM FORMATION: FROM PLANKTONIC CELLS TO STRUCTURED COMMUNITIES

Biofilm formation is a highly regulated developmental process distinct from bacterial aggregation. Using *Pseudomonas aeruginosa*, the most extensively studied biofilm-forming pathogen, as a model organism, the process is typically divided into five stages (fig.1): reversible attachment, irreversible attachment, maturation I, maturation II, and dispersion (11).

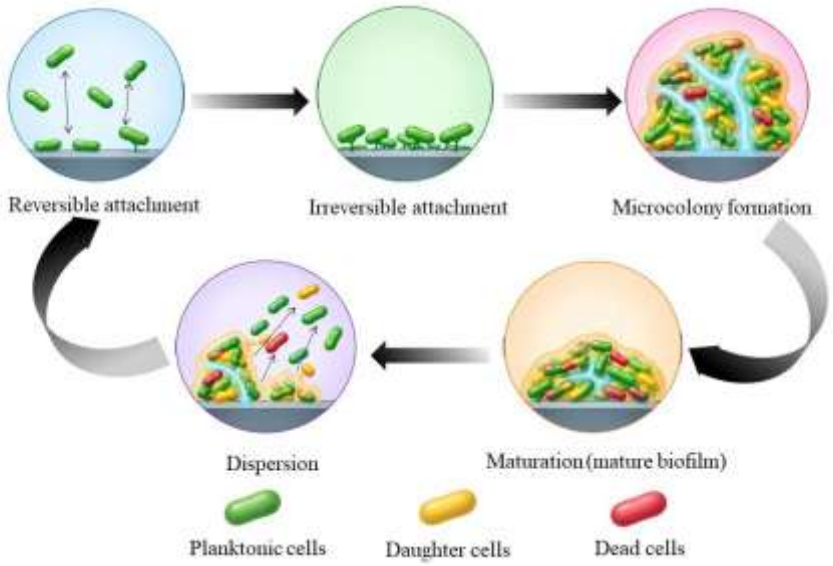


Fig. 1: The Stages of Biofilm Formation (Generated using AI)

Through flagella-mediated movement and general physicochemical interactions, planktonic cells first make weak contact with the surface during the reversible attachment phase. The cells can still separate at this point and return to their free-swimming state (11). The cells move toward irreversible attachment as contact becomes more stable. During this transition, flagellar gene expression is downregulated, type IV pili's surface engagement is increased, and extracellular polymeric substance (EPS) secretion is initiated, all of which help build the biofilm matrix (11). Cyclic di-GMP, an intracellular second messenger, is essential for controlling this transition. While higher amounts promote matrix formation and adherence to a sessile, biofilm-associated lifestyle, low intracellular cyclic di-GMP levels promote mobility and dispersal. Microcolonies are created when cells multiply and attract

more cells after irreversible attachment. During maturation stages I and II (11), these microcolonies develop into distinctive three-dimensional, frequently mushroom-shaped structures of mature biofilms. A subset of cells in the final dispersion stage are prompted by intracellular and environmental cues to change back to a motile planktonic phenotype, which allows them to actively leave the biofilm and colonize new locations. Clinically, dispersion has two sides: while it is essential for the biofilm life cycle and environmental dissemination, it also makes it easier for a persistent, localized biofilm infection to develop into bacteraemia or metastatic infection at distant locations.

III. *ARCHITECTURE OF THE BIOFILM*: THE EXTRACELLULAR MATRIX AND BEYOND

3.1 Composition of the EPS matrix

The matrix of a biofilm is a self-produced, hydrated network of extracellular polymeric substances (EPS) that sets it apart from a bacterial collection. The resident cells, which usually make up the bulk of the biofilm volume, are embedded and connected by this matrix. Flemming and Wingender describe the matrix as aiding adherence to surfaces, offering mechanical stability, and functioning as a "external digestive system." This tactic enables the community to digest biopolymers that would not otherwise be accessible by maintaining extracellular enzymes near to the cells that produce them (12).

The chemical heterogeneity of the matrix is mostly composed of lipids, proteins, extracellular DNA (eDNA), and polysaccharides. Different species, strains, and even growth conditions have very different relative amounts of these components. The most common structural component is often polysaccharides. diverse exopolysaccharides serve diverse purposes in different organisms. For instance, certain adhesins help with initial surface attachment, whereas others provide bulk structural resilience and cohesiveness to the mature biofilm (13). Notable examples include Pel and Psl in Pseudomonas aeruginosa, alginate, bacterial cellulose, and poly-N-acetylglucosamine. Extracellular DNA (eDNA), hitherto believed to be unintentional debris from lysed cells, is now recognized as an essential structural component. It can form stable filamentous networks that interact with other matrix constituents and directly contribute to the overall architecture and mechanical integrity of a strikingly diverse variety of bacterial and fungal biofilms (14). Owing to its structural significance, enzymatic degradation of eDNA is an active target for anti-biofilm therapy, as discussed in Section-7.

3.2 Three-dimensional architecture and spatial heterogeneity

Beyond its chemical composition, the matrix forms a distinct three-dimensional architecture of mushroom- or pillar-shaped microcolonies interspersed with interstitial voids and channels that facilitate the movement of water, nutrients, and metabolic waste. These channel networks are not merely open pathways (Fig. 2). A recent study on *Escherichia coli* biofilm transport channels shows that some are enclosed within thin layers of actively growing cells that maintain distinct internal chemical gradients along the channel, rather than being directly exposed to the external environment (15).

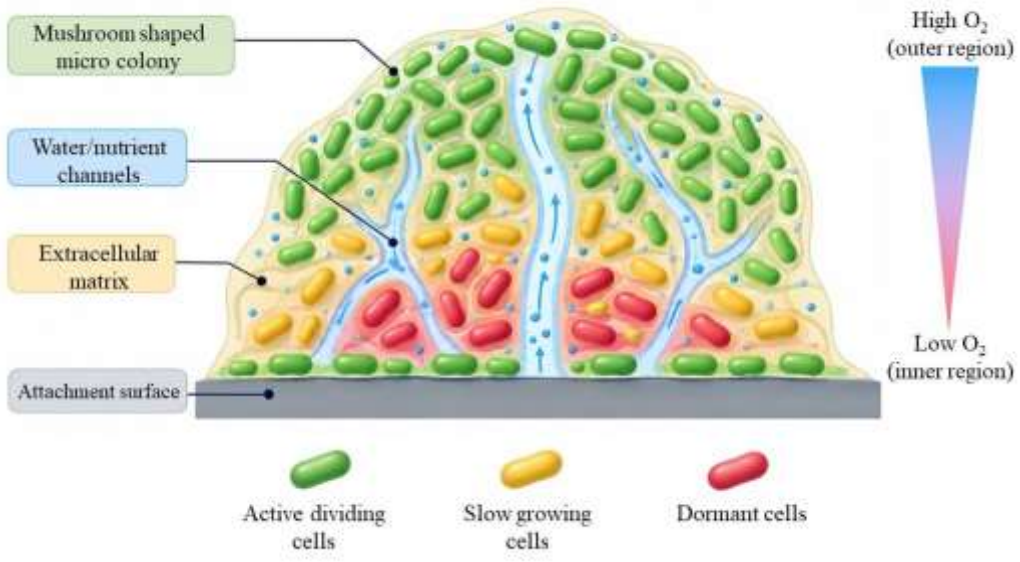


Fig.2: EPS Matrix Architecture & Internal Gradients (Generated using AI)

This architecture introduces significant physicochemical heterogeneity within a single biofilm. Oxygen, nutrients, and antimicrobial agents diffuse inward from the biofilm surface and are gradually consumed or bound as they penetrate deeper, generating steep gradients between an oxygen-abundant, nutrient-rich periphery and an often hypoxic or anoxic, nutrient-depleted core (15). Recent multiscale modelling, which considers the bacterial capsule as a distinct low-diffusivity layer within the bulk matrix, estimates that this fine-scale architecture can decrease local oxygen transfer by approximately 70% compared to a matrix without this structural feature, functioning as a "resistance-in-series" barrier to diffusion (16).

The physiological consequences of this heterogeneity are profound. Various metabolic states are adopted by cells in various micro-regions within the same biofilm because they are exposed to significantly varying local environments. For example, cells in the centre may develop slowly or remain dormant, whereas those near the oxygenated perimeter may divide quickly. This internally produced metabolic variability is one of the key ways that biofilm architecture provides antibiotic tolerance, as covered in Section-5.

IV. TECHNIQUES FOR STUDYING BIOFILM ARCHITECTURE

Understanding biofilm architecture depends heavily on the imaging tools available to study it. Confocal laser scanning microscopy (CLSM) is widely regarded as the single most important technique in the field as it is non-destructive, allowing biofilms to be examined *in situ*, in their native hydrated state, and imaged repeatedly over time (17). Combined with fluorescent- or lectin-conjugated stains specific to individual matrix components, CLSM allows researchers to map the spatial distribution of specific matrix constituents in relation to the cells and to each other (17).

Quantitative analysis of CLSM image stacks, including biomass, thickness, surface roughness, and porosity, is typically performed with dedicated image-analysis software. However, methodological standardization remains a persistent challenge in the field, as automated thresholding procedures may introduce systematic bias unless rigorously validated against the underlying image data. To construct a more comprehensive understanding of biofilm architecture, complementary techniques such as scanning electron microscopy for high-resolution surface topology and microelectrode or optical sensing for the direct measurement of oxygen and pH gradients are often employed alongside CLSM

V. MECHANISMS LINKING BIOFILM ARCHITECTURE TO ANTIMICROBIAL RESISTANCE

Multiple mechanisms contribute to the antimicrobial recalcitrance of biofilms, and no single mechanism provides a complete explanation. Several architecture-dependent mechanisms act in combination, and their relative contribution varies by organism, antimicrobial agent, and biofilm developmental stage (8). It is important to differentiate between these two related yet distinct concepts. Antimicrobial resistance refers to a stable, heritable trait, typically encoded by mutation or an acquired resistance gene. In contrast, antimicrobial tolerance is a reversible physiological state that allows cells to survive drug exposure without altering their genetically determined susceptibility. Both resistance and tolerance are associated with biofilms, and the architecture described in Section 3 is key for understanding these connections.

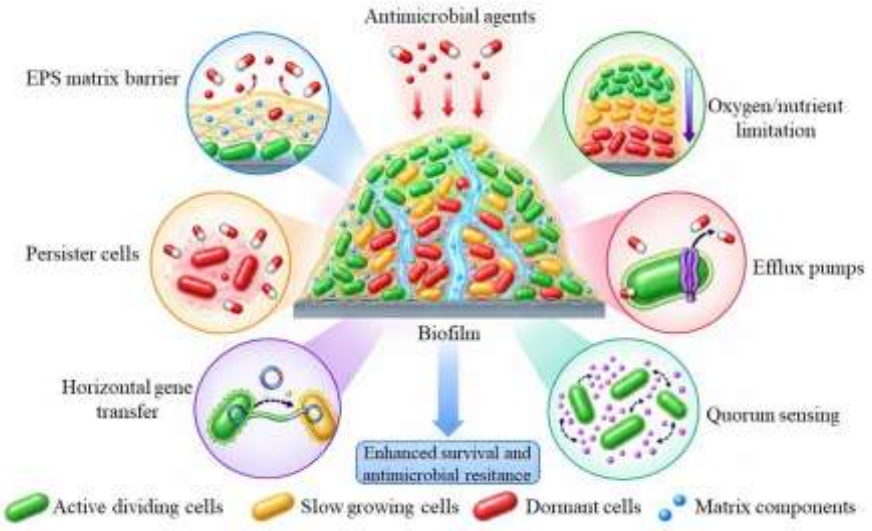


Fig. 3: Mechanism of Antomicrobial resistance in Biofilm (Generated using AI)

5.1 The EPS matrix as a physical and chemical barrier

The simplest and most well-documented mechanism is that the EPS matrix physically prevents antimicrobial drugs from diffusing toward their target cells. The matrix's role as an inert sieving barrier is not the only cause of this process. Instead, antibiotic molecules may interact or chemically bind with matrix components, delaying penetration and lowering the concentration that eventually reaches deeper-lying cells. Furthermore, antibiotics can be actively broken down by matrix-retained enzymes, including released β-lactamases in bacteria like Klebsiella pneumoniae. When these strategies are coupled, they can have a significant therapeutic impact: According to reports, P. aeruginosa biofilms developing on urinary catheters are around a thousand times more resistant to the aminoglycoside tobramycin than genetically identical planktonic cells. It should be noted that matrix-mediated diffusion limitation alone typically does not account for the full extent of biofilm resistance; it should be considered one of several contributing factors rather than the primary explanation (Fig. 3).

5.2 Chemical microenvironment, metabolic heterogeneity, and reduced growth rate

As described in Section 3.2, biofilm architecture induces internal chemical gradients that result in zones with significantly diminished oxygen and nutrient availability, particularly near the biofilm core. Many commonly used antibiotic classes, such as β-lactams, fluoroquinolones, and aminoglycosides, exhibit greater efficacy against actively dividing cells than against slow-growing or non-dividing cells. Consequently, the inherently reduced growth rate of cells within these nutrient- and oxygen-deficient micro-regions imparts a notable degree of antimicrobial tolerance, independent of any genetic change.

5.3 Persister cells and phenotypic tolerance

Persisters are a tiny, unique subpopulation of cells found in biofilms in this varied environment. Genetically similar to their vulnerable neighbours, persister cells go into a temporary, inactive physiological state marked by severely limited macromolecular synthesis and stopped development. Persister cells generally withstand exposure to antibiotics that would otherwise be fatal because the majority of antibiotics target active cellular activities like DNA replication or cell-wall production. This survival is not due to the failure of the drug to reach them but rather because the cellular targets are inactive (9).

Persister cells play a crucial role in the recurrent pattern of biofilm infections, posing significant clinical challenges. Antibiotic treatments can eliminate the metabolically active majority of a biofilm populations while leaving persisters intact, allowing them to repopulate the infection site once treatment is discontinued. Toxin–antitoxin systems, the bacterial stringent response, and SOS DNA-damage response pathways have all been implicated in establishing and maintaining the persister state, although the precise regulatory mechanisms differ across species and remain under investigation.

5.4 Efflux pumps

One well-known resistance mechanism in planktonic bacteria is multidrug efflux pumps, which are transmembrane transporter proteins that actively export antibiotics and other harmful substances from the bacterial cytoplasm. These pumps have been identified as specific genetic determinants of biofilm-associated resistance. The expression of efflux pumps is regulated by quorum-sensing systems in many organisms (Section 5.6). Consequently, enhanced efflux activity within a biofilm is often mechanistically linked to the broader coordination of the biofilm community rather than being independent of it (18).

5.5 Horizontal gene transfer and genetic adaptation within biofilms

In addition to phenotypic tolerance, the biofilm environment actively facilitates the acquisition of genetic resistance. The stabilizing impact of the matrix and the close physical closeness of cells within a biofilm produce favourable circumstances for horizontal gene transfer (HGT) at rates far higher than those usually seen among free-living planktonic bacteria. (10). All three classical HGT mechanisms transformation (uptake of free extracellular DNA), transduction (bacteriophage-mediated gene transfer), and conjugation (direct cell-to-cell transfer via mobile genetic elements such as plasmids and integrative and conjugative elements) have been documented within biofilms, with conjugation considered a particularly important route for the dissemination of antibiotic resistance genes. Recently, membrane vesicles have been identified as an additional route for interspecies gene exchange within biofilm communities.

The clinical significance of this phenomenon is substantial and warrants further investigation. Biofilms function not only as a passive refuge for organisms that are already resistant but also as an active environment capable of generating new resistant strains. Furthermore, they facilitate the dissemination of resistance genes across species boundaries, including between commensal and pathogenic organisms within the same polymicrobial community (19).

5.6 Quorum-sensing regulation of resistance-associated phenotypes

Numerous mechanisms previously described are coordinated rather than incidental, with much of this coordination being facilitated by quorum sensing (QS). QS

is a communication system dependent on cell density, wherein bacteria produce, release, and detect small diffusible signalling molecules to synchronize their collective behaviour across the population[18]. Gram-negative bacteria generally utilize acyl-homoserine lactones (AHLs) for signalling, whereas gram-positive bacteria employ autoinducing peptides (AIPs). Despite the differences in the signalling molecules, both systems result in broadly similar downstream outcomes.

QS regulates transcription of genes governing EPS matrix synthesis, biofilm formation itself, virulence factor production, and, in a number of organisms, efflux pump expression. Given that QS is positioned upstream of many resistance-relevant processes, it has emerged as a promising therapeutic target. Disruption of QS signalling, a strategy referred to as quorum quenching, can reduce EPS production and biofilm formation without directly killing the bacteria. This method may exert less selective pressure for the development of resistance than conventional bactericidal antibiotics. Further, this approach is discussed in Section-7.

5.7 Polymicrobial interactions

Polymicrobial biofilms, rather than single-species communities, are of greater clinical significance, as interactions among co-existing species can enhance antimicrobial resistance in ways that single-species laboratory models cannot replicate. In such biofilms, susceptible species may be shielded physically or chemically by their resistant neighbours. HGT across species can facilitate the exchange of resistance determinants among unrelated organisms within the same matrix. QS signalling can also transcend species boundaries, complicating the diagnosis and treatment of these infections. Polymicrobial dynamics are particularly well- documented in cystic fibrosis lung infections, chronic wound infections, and infections associated with medical devices, where multiple organisms frequently coexist within a single biofilm community.

VI. CLINICAL SIGNIFICANCE OF BIOFILM-ASSOCIATED ANTIMICROBIAL RESISTANCE

The mechanisms previously described are not mere laboratory curiosities; they form the basis of a significant proportion of infections observed in routine clinical practice. Biofilms are involved in approximately 65% of microbial infections and up to 80% of chronic infections in humans (5). They repeatedly appear as central themes across distinct and high-burden clinical contexts (6,7).

Direct biofilm pathology is exemplified by infections linked to medical devices. Catheters, prosthetic joints, heart valves, and pacemakers are examples of devices that provide abiotic surfaces that allow organisms like Staphylococcus epidermidis, Staphylococcus aureus, and other gram-negative bacilli to build biofilms. When antibiotic therapy is not enough to eradicate these infections, the device must often be surgically removed.

Cystic fibrosis (CF) provides one of the best-studied non-device-related examples. Patients with CF produce abnormally viscous airway mucus that predisposes them to infection and provides an environment favouring biofilm formation. This is particularly evident in the mucoid phenotype of *Pseudomonas aeruginosa*, which establishes chronic, biofilm-based lung infection that is rarely eradicated once established (20).

Chronic, non-healing wounds constitute a significant clinical challenge, with biofilm formation increasingly identified as a key factor in the delayed healing. This is distinct from acute wound infections and necessitates different diagnostic and management strategies, such as debridement combined with biofilm-targeted antimicrobial treatments. Biofilms are also heavily implicated in periodontitis, chronic dental plaque-related diseases, chronic rhinosinusitis, otitis media, infective endocarditis and a range of other chronic and recurrent infections.

Given that the six bacterial pathogens contributing most heavily to global AMR mortality; *Escherichia coli*, *Staphylococcus aureus*, *Klebsiella pneumoniae*, *Streptococcus pneumoniae*, *Acinetobacter baumannii*, and *Pseudomonas aeruginosa* are all well-documented biofilm formers (3,4); the overlap between biofilm biology and the broader AMR crisis described in Section 1 is not incidental but structural. When it comes to infections that are the main cause of resistance-associated mortality, strategies that do not take biofilm architecture into account are probably going to be consistently ineffectual.

VII. THERAPEUTIC AND ANTI-BIOFILM STRATEGIES TARGETING BIOFILM ARCHITECTURE

Even when the causal species is categorized as "susceptible" by routine laboratory testing, conventional antibiotics, which were created and tested primarily against planktonic bacteria, frequently show lower efficiency against biofilm-embedded organisms. Due to this restriction, there is now more interest in tactics that specifically target biofilm architecture, either as stand-alone methods or as supplements to antibiotics (21).

7.1 Quorum-sensing inhibitors and quorum quenching

EPS synthesis, biofilm formation, and other resistance-associated phenotypes are all coordinated by QS (Section 5.6). As a result, interfering with QS signalling has become a viable treatment approach (fig.4). In laboratory and early clinical trials, quorum-sensing inhibitors, such as furanones and structural analogues of AHL signalling molecules, have shown the capacity to lower biofilm development and virulence factor expression. QS inhibitors are typically studied in conjunction with traditional antibiotics because they do not directly kill bacteria. Several studies indicate that this strategy can result in a synergistic antibacterial impact while perhaps lowering the antibiotic dose needed for efficacy. (18).

7.2 Matrix-degrading enzymes

Using enzymes that break down particular EPS components, such as DNase (which targets eDNA), glycoside hydrolases (which target exopolysaccharide), and dispersin B, is an architectural technique that directly addresses the physical matrix. These enzymes have the ability to break down or dissolve the matrix, which causes sessile cells to separate (fig.4). This procedure is essential because it increases the accessibility of implanted cells to host immune systems and improves the penetration of co-administered medications (14,21).

7.3 Nanotechnology-based delivery systems

With physicochemical characteristics like small size, tuneable surface charge, and functionalization potential that enable them to more successfully penetrate the EPS matrix than free antibiotic molecules, nanoparticle-based delivery systems have become one of the most active areas of anti-biofilm research (22, 23). While liposomes, polymeric nanoparticles, nanogels, and metal-organic frameworks enable regulated, localized drug release, metal and metal-oxide nanoparticles may also have inherent antibacterial or matrix-degrading catalytic activity (fig.4). Despite this promise, the clinical translation of nanoparticle-based systems is still restricted due to issues with large-scale manufacturing, the lack of established regulatory pathways for many novel formulations, and incomplete characterization of nanoparticle biodistribution and long-term safety in humans. These issues are covered in more detail in Section- 8 (24).

7.4 Bacteriophage therapy and phage-derived enzymes

Bacteriophages, viruses that infect and lyse specific bacterial species and their derived enzymes represent a further architecturally targeted strategy. Antibiotic penetration can be enhanced, biofilm structure can be disrupted, and EPS matrix components can be directly broken down by phage-encoded depolymerases and endolysins. When phages are used in combination with matrix-degrading enzymes or traditional antibiotics, the results are more effective than when each strategy is used alone (25). Phage therapy is of particular interest for infections caused by multidrug-resistant pathogens for which few effective antibiotic options remain, although practical challenges, including bacterial resistance to phages themselves, unresolved regulatory pathways, and the need for rapid phage susceptibility testing, continue to limit routine clinical use (fig.4).

7.5 Combination and multi-targeted strategies

As no single mechanism can entirely explain biofilm-associated resistance, most researchers now prefer combination and multi-targeted strategies over the use of a solitary anti-biofilm agent. For instance, they may pair quorum-sensing inhibitors, efflux pump inhibitors, or matrix-degrading enzymes with conventional antibiotics, or combine nanoparticle carriers with antimicrobial peptides to improve peptide stability in vivo (21,23). This tactical change reflects a more comprehensive realization that biofilm-associated resistance comes from community behaviour and architecture rather than from a particular druggable target. This tactical change reflects a more comprehensive realization that biofilm-associated resistance comes from community behaviour and architecture rather than from a particular druggable target (fig.4).

VIII. CURRENT CHALLENGES AND FUTURE DIRECTIONS

Numerous obstacles still exist in the practical use of antibiofilm methods, despite notable advances in research. First, because biofilm resistance mechanisms differ significantly between species, infection sites, and host immune environments, a strategy that works well against one organism or type of infection may not work well against another. This suggests that customized, infection-specific approaches are preferable to general anti-biofilm solutions (21). Second, the translation of promising laboratory findings into clinical practice is hampered by the absence of standardized, clinically meaningful biofilm models both in vivo and in vitro.

Third, there are still significant translational obstacles, particularly for methods based on nanomedicine. Despite proven laboratory efficacy, clinical adoption is hampered by large-scale, repeatable manufacturing, incomplete characterization of nanoparticle biodistribution and the biomolecular corona that forms on nanoparticle surfaces in vivo, and unresolved regulatory pathways for many novel formulations (24).

Looking forward, several converging directions are likely to shape the field. These include computational and data-

driven approaches aimed to accelerate the discovery of anti-biofilm compounds and optimize combination regimens. Additionally, stimuli-responsive nanotherapeutics are being designed to release their payload in response to the specific pH, enzymatic, or redox conditions found within a biofilm, improving precision and minimizing off-target effects; and continued development of engineered phage and enzyme-based therapeutics tailored to specific pathogens and matrix compositions (23,24,25). Given the close mechanistic relationship between biofilm formation and antimicrobial resistance described throughout this review, integrating biofilm-aware diagnostics and antimicrobial stewardship into routine clinical practice is likely to prove as important as any single new therapeutic agent.

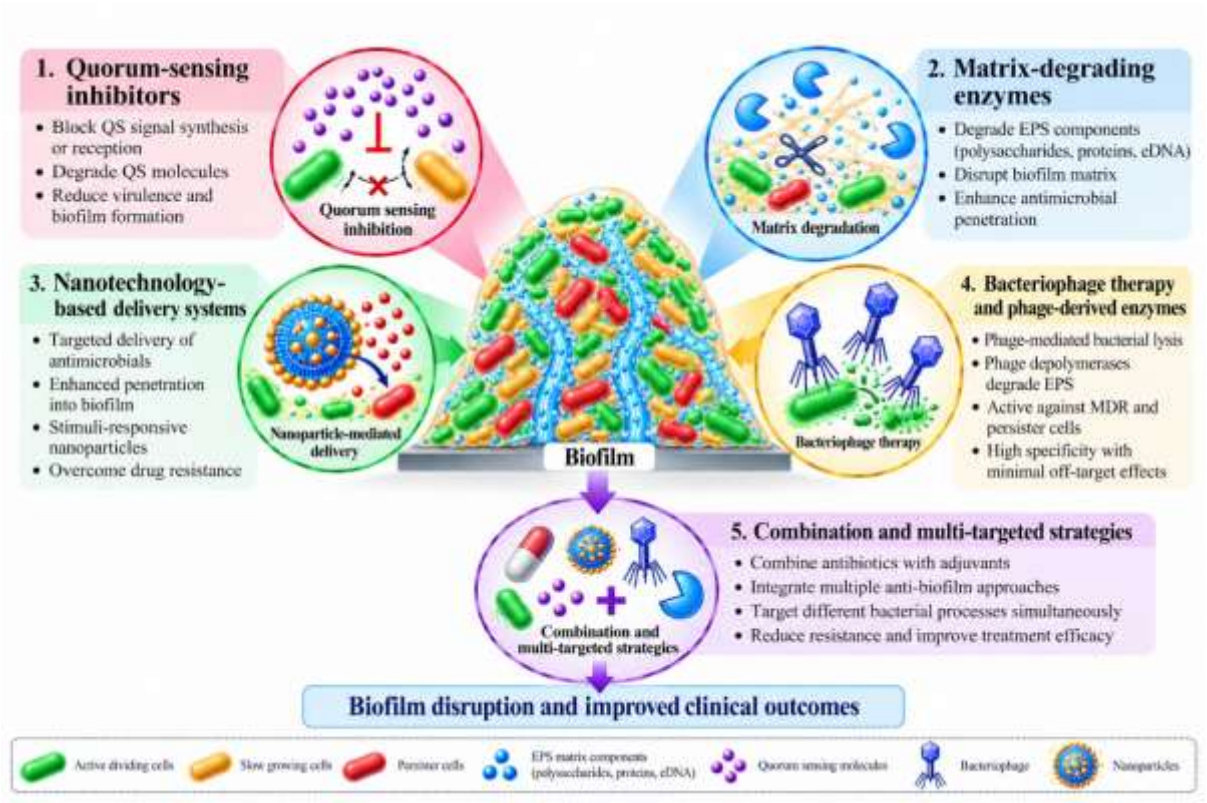


Fig. 4: Anti Biofilm strategies mapped to their targets (Generated using AI)

IX. CONCLUSION

Biofilm architecture is a fundamental and active contributor to antimicrobial resistance and tolerance in chronic bacterial infections, functioning through multiple converging mechanisms rather than singular pathways. The EPS matrix restricts and chemically neutralizes antimicrobial agents. Additionally, the chemical microenvironments generated by these cells induce slow-growing and dormant states, which are inherently challenging to eradicate. Additionally, biofilms' physical proximity speeds up the transfer of resistance genes between cells and even between different species. Therapeutic approaches will probably need to specifically target biofilm architecture because these processes are reliant on structural components rather than specific resistance genes. This strategy could entail providing chemicals that can get past the biofilm's physical defences, upsetting the matrix, or interfering with quorum-sensing coordination. Instead than being used in place of traditional antibiotic therapy, these tactics should be used in conjunction with it. Understanding and directly addressing biofilm architecture will continue to be essential to the larger endeavour to maintain the efficacy of antimicrobial therapy as the burden of antibiotic resistance increases globally.

REFERENCES

[1] Di Martino P. Extracellular polymeric substances, a key element in understanding biofilm phenotype. AIMS Microbiol 2018; 4(2):274-288.

[2] Naghavi M, Vollset SE, Ikuta KS, Swetschinski LR, Gray AP, Wool EE et al. Global burden of bacterial antimicrobial resistance 1990-2021: a systematic analysis with forecasts to 2050. Lancet 2024; 404(10459):1199-1226.

[3] Murray CJL, Ikuta KS, Sharara F, Swetschinski L, Robles Aguilar G, Gray A et al. Global burden of bacterial antimicrobial resistance in 2019: a systematic analysis. Lancet 2022; 399(10325):629-655.

[4] World Health Organization. WHO Bacterial Priority Pathogens List 2024: bacterial pathogens of public health

importance to guide research, development and strategies to prevent and control antimicrobial resistance. Geneva: World Health Organization; 2024.

[5] Davies D. Understanding biofilm resistance to antibacterial agents. Nat Rev Drug Discov 2003; 2(2):114-122.

[6] Mihai MM, Holban AM, Giurcaneanu C, Popa LG, Oanea RM, Lazar V et al. Microbial biofilms: impact on the pathogenesis of periodontitis, cystic fibrosis, chronic wounds and medical device-related infections. Curr Top Med Chem 2015; 15(16):1552-1576.

[7] Vestby LK, Grønseth T, Simm R, Nesse LL. Bacterial biofilm and its role in the pathogenesis of disease. Antibiotics (Basel) 2020; 9(2):59.

[8] Hall CW, Mah TF. Molecular mechanisms of biofilm-based antibiotic resistance and tolerance in pathogenic bacteria. FEMS Microbiol Rev 2017; 41(3):276-301.

[9] Liu HY, Prentice EL, Webber MA. Mechanisms of antimicrobial resistance in biofilms. npj Antimicrob Resist 2024; 2(1):27.

[10] Michaelis C, Grohmann E. Horizontal gene transfer of antibiotic resistance genes in biofilms. Antibiotics (Basel) 2023; 12(2):328.

[11] Wang X, Liu M, Yu C, Li J, Zhou X. Biofilm formation: mechanistic insights and therapeutic targets. Mol Biomed 2023; 4(1):49.

[12] Flemming HC, Wingender J. The biofilm matrix. Nat Rev Microbiol 2010; 8(9):623-633.

[13] Balducci E, Papi F, Capialbi DE, Del Bino L. Polysaccharides' structures and functions in biofilm architecture of antimicrobial-resistant (AMR) pathogens. Int J Mol Sci 2023; 24(4):4030.

[14] Campoccia D, Montanaro L, Arciola CR. Extracellular DNA (eDNA): a major ubiquitous element of the bacterial biofilm architecture. Int J Mol Sci 2021; 22(16):9100.

[15] Bottura B, McConnell G, Florek LC, Smiley MK, Martin R, Foylan S et al. Oxygen microenvironments in Escherichia coli biofilm nutrient transport channels: insights from complementary sensing approaches. Microbiology (Reading) 2025; 171(5):001543.

[16] Moorthy RK, Casey E. Modeling multiscale architecture of biofilm extracellular matrix and its role in oxygen transport. Biotechnology and Bioengineering. 2025 Oct 22.

[17] Reichhardt C, Parsek MR. Confocal laser scanning microscopy for analysis of Pseudomonas aeruginosa biofilm architecture and matrix localization. Front Microbiol 2019; 10:677.

[18] Zhao X, Yu Z, Ding T. Quorum-sensing regulation of antimicrobial resistance in bacteria. Microorganisms 2020; 8(3):425.

[19] Cui S, Kim E. Quorum sensing and antibiotic resistance in polymicrobial infections. Commun Integr Biol 2024; 17(1):2415598.

[20] Høiby N, Ciofu O, Bjarnsholt T. Pseudomonas aeruginosa biofilms in cystic fibrosis. Future Microbiol 2010; 5(11):1663-1674.

[21] Abdelhamid AG, Yousef AE. Combating bacterial biofilms: current and emerging antibiofilm strategies for treating persistent infections. Antibiotics (Basel) 2023; 12(6):1005.

[22] Joshi AA, Patil RH. Nanoparticles targeting biofilms: a new era in combating antimicrobial resistance. Med Microecol 2025; 26:100156.

[23] Xie Y, Liu H, Teng Z, Ma J, Liu G. Nanomaterial-enabled anti-biofilm strategies: new opportunities for treatment of bacterial infections. Nanoscale 2025; 17(10):5605-5628.

[24] Farah H, Kadhim-Abosaoda M, Mohaisen-Mousa H, Renuka Jyothi S, Priyadarshini-Nayak P, Bethanney Janney J, Singh G, Singh-Chauhan A, Kumar-Mishra M. Nanomedicine strategies against biofilm-associated infections: advances, challenges, and translational barriers. MicrobiologyOpen. 2026 Feb;15(1):e70210.

[25] Husain FM, Zahra A, Ali A, Kamthan M, Al-Shabib NA, Farooqui Z et al. Bacteriophages and their enzymes: allies against microbial biofilms. Pharmaceuticals (Basel) 2025; 18(12):1771.

International Journal of Environment, Agriculture and Biotechnology
Vol-11, Issue-5; Sep-Oct, 2026
Peer-Reviewed International Journal
Journal Home Page Available: https://ijeab.com/
Journal DOI: 10.22161/ijeab

Profile Characteristics of Extension Personnel and their Relationship with Utilization of a State Agricultural University's Digital Advisory Portal

Sankri Karthikeyan[1*], Anand Karthikeyan[2]

[1]Assistant Professor (SS), Department of Agricultural Extension and Communication, Vanavarayar Institute of Agriculture, Manakkadavu, Pollachi – 642 103, Coimbatore District, Tamil Nadu, India
[2]Associate Professor and Head, Department of Agricultural Extension and Communication, Vanavarayar Institute of Agriculture, Manakkadavu, Pollachi – 642 103, Coimbatore District, Tamil Nadu, India
*Corresponding author: sankrikarthikeyan@gmail.com

Received: 10 Aug 2026; Received in revised form: 08 Sep 2026; Accepted: 13 Sep 2026; Available online: 20 Sep 2026
©2026 The Author(s). Published by Infogain Publication. This is an open-access article *under* the CC BY license (https://creativecommons.org/licenses/by/4.0/).

Abstract**—** *State agricultural universities (SAUs) in India were early adopters of web-based agricultural advisory portals, and understanding what drives their continued use by front-line extension personnel remains important as the country scales up the Digital Agriculture Mission and its AgriStack farmer-database ecosystem. This study examined the profile characteristics of extension personnel and their relationship with utilization of the TNAU Agritech Portal, one of the pioneering State Agricultural University e-extension platforms in India. An ex-post facto design was adopted among 60 purposively selected Assistant/Deputy Directors and Agricultural/Horticultural Officers drawn from all 12 blocks of Coimbatore district, Tamil Nadu. Data were collected using a pre-tested interview schedule and analysed through percentage analysis, simple correlation and multiple regression. Majority of the respondents were middle-to-old aged graduates with more than fifteen years of service and medium job satisfaction. Training undergone, attitude towards e-media, awareness of agricultural websites, internet usage and portal credibility showed positive and significant correlation with utilization, whereas experience in job showed a significant negative association. The twelve profile characteristics together explained 45.30 per cent of the variance in utilization. The findings identify capacity building and content credibility as priority levers for portal utilization and offer baseline evidence useful for designing the next generation of digital advisory platforms.*

Keywords**— Digital extension, e-Governance, ICT, Utilization pattern, Extension personnel, Agricultural advisory portal, Profile characteristics**

I. INTRODUCTION

Extension personnel constitute the crucial link between the agricultural research system and the farming community, and the effectiveness of technology transfer depends substantially on how well these functionaries themselves access and use the digital knowledge infrastructure placed at their disposal. As information and communication technology (ICT) has moved from the margins to the centre of extension practice, research interest in ICT-based extension and advisory services (EAS) has grown correspondingly: a recent bibliometric analysis of 525 Scopus-indexed publications between 1999 and 2024 shows steady growth in this literature from 2005 onward, with India recording the highest number of publications (446) of any country, even though the highest citation impact still accrues to research from the United States (Mukherjee et al., 2025). Within India, ICTs ranging from radio and Kisan Call Centres to smartphone applications and artificial intelligence-enabled advisories are reported to have substantially reshaped how extension information reaches its users, with platforms such as Kisan Sarathi alone having

registered close to 2.4 crore farmers and 746 institutions (Sharma et al., 2025).

This transformation has accelerated further with the Union Government's Digital Agriculture Mission, which is building an interoperable "India Digital Ecosystem of Agriculture" (IDEA) around AgriStack farmer and land-record databases, and which had generated more than 84 million Farmer IDs by the time of writing. Yet a review of India's e-governance architecture for agriculture cautions that a large number of portals and applications have been launched within a short span, with considerable functional overlap in farmer profiling and market-information services, so that determining which of them are genuinely useful remains a challenge for both functionaries and farmers (Balkrishna et al., 2024). Amid this rapidly expanding national digital layer, the discipline-specific portals built more than a decade ago by individual State Agricultural Universities (SAUs) continue to function as the first point of technical contact for block-level extension officers. Understanding what makes these functionaries actually use such a portal therefore has continuing relevance: it is this frontline usage behaviour, and its determinants, that any newer unified or AI-enabled advisory platform will eventually have to reproduce or improve upon.

Tamil Nadu Agricultural University (TNAU) was among the first SAUs in India to institutionalise this effort, establishing an exclusive e-Extension Centre in 2008 with support from the National Agricultural Development Programme, and launching the TNAU Agritech Portal (agritech.tnau.ac.in) in 2009 as a bilingual repository of more than three-and-a-half lakh web pages spanning agriculture, horticulture, agricultural engineering, forestry, fisheries, animal husbandry, agricultural marketing, sericulture and seed certification. The portal was designed principally for field extension officials located across 385 blocks and district headquarters of the state, and it remains functional today alongside the Centre's other e-governance initiatives.

Although a growing body of recent work has documented constraints and awareness levels around ICT-tool adoption among India's extension workforce (Singh et al., 2026; Singh et al., 2026a) and among extension practitioners elsewhere (Yekinni et al., 2023), the profile-level determinants of utilization of a State Agricultural University's own long-standing digital portal by its extension cadre remain comparatively under-documented, particularly for legacy portals that continue to operate beneath the newer national digital-agriculture layer. Against this background, the present study, drawn from a Master's degree investigation into the reach of the TNAU Agritech Portal among extension officials of Coimbatore district, examines (i) the profile characteristics of extension personnel in the study area, and (ii) the association and relative contribution of these characteristics to utilization of the portal.

II. REVIEW OF LITERATURE

Empirical evidence bearing on the profile determinants of digital-portal utilization by extension personnel is reviewed below under two sub-heads, drawing principally on studies published since 2023 so as to situate the present findings within the current state of the field.

A. Profile characteristics of extension personnel

Singh et al. (2026a), studying 160 KVK-linked progressive farmers in Western Uttar Pradesh, found that education, income and farm size positively influenced ICT-tool adoption, whereas advancing age depressed it, with overall awareness of ICT tools at 69.52 per cent against actual utilization of 62.60 per cent. Sahoo et al. (2025), surveying 248 public extension workers across coastal Odisha, reported that both senior and junior functionaries were comfortable with foundational tools such as computers and mobile phones, but that a hierarchy-linked competence gap persisted for advanced tools such as AI interfaces and drones: junior officers had greater exposure to newer technology yet weaker proficiency in basic digital documentation, while senior officers most needed training in troubleshooting, cybersecurity and common productivity tools. Singh et al. (2026), applying Garrett's ranking technique to 142 Krishi Vigyan Kendra personnel, identified lack of training opportunities as the foremost constraint to ICT-tool adoption, ahead of psychological barriers and insufficient technical knowledge, underscoring how strongly a workforce's training exposure interacts with its demographic profile in shaping digital engagement. Dhillon (2025), in a bibliometric review of 251 publications on digital platforms in rural knowledge transfer (2003–2025), noted that despite India's scale of investment in digital agriculture, India-authored high-impact research specifically profiling the digital competencies of its own extension personnel remains comparatively scarce — a gap the present study addresses for a State Agricultural University cadre.

B. Utilization of digital advisory platforms and its correlates

Mukherjee et al. (2025), in a bibliometric analysis of 525 Scopus-indexed publications (1999–2024) on ICT-based extension and advisory services, identified inclusive service delivery and gender-aware utilization patterns as among the fastest-growing thematic clusters in this literature, with

India contributing the largest share of publications globally. Sharma et al. (2025) found that despite the scale reached by platforms such as Kisan Sarathi, which has registered close to 2.4 crore farmers, the intensity of utilization continues to be constrained more by uneven digital literacy and weak content localisation than by lack of platform availability. Gosavi and Singh (2026), in a systematic review of ICT tools in agricultural extension, concluded that the effectiveness of any given tool is "highly contingent on contextual factors such as infrastructure, digital literacy, and institutional support," and that tools already embedded in existing advisory routines are utilized far more than stand-alone or emerging tools. Balkrishna et al. (2024) further showed that functional overlap among India's many farmer-facing e-governance portals — with several separately performing farmer-profiling and market-information functions — itself works against sustained utilization, since users often cannot tell which of several competing platforms is authoritative for a given purpose.

Taken together, these studies show education, training exposure and institutional/infrastructural context to be recurrent correlates of ICT and digital-portal utilization among extension personnel, even as the platforms themselves have evolved substantially since the TNAU Agritech Portal's 2009 launch. The present analysis extends this literature by quantifying, for a specific State Agricultural University portal, the relative contribution of profile characteristics to utilization through correlation and multiple regression.

III. METHOD

The study was conducted in Coimbatore district of Tamil Nadu, purposively selected for its high penetration of information and communication technologies in agriculture and for hosting the headquarters of Tamil Nadu Agricultural University. All 12 agricultural blocks of the district — Anamalai, Annur, Karamadai, Kinathukadavu, Madhukkarai, Perianaickenpalayam, Pollachi North, Pollachi South, Sarkarsamakulam, Sultanpet, Sulur and Thondamuthur — were covered. An ex-post facto research design was adopted, since the utilization behaviour under study had already occurred and could only be examined after the fact (Singh, 2008). A sample of 60 extension personnel was purposively selected across two functional categories: Assistant/Deputy Directors of Agriculture and Horticulture (ADAs/ADHs, n = 22) and Agricultural/Horticultural Officers (AOs/HOs, n = 38) drawn from the Departments of Agriculture, Horticulture, Seed Certification and Agricultural Marketing. Primary data were collected during 2011–12 using a well-structured, pre-tested interview schedule administered through personal interviews.

Twelve independent variables — age, education, experience in job, job satisfaction, awareness of ICT tools and services, training undergone, possession of modern electronic gadgets, attitude towards e-media, awareness of agricultural websites, internet usage, mobile usage and portal credibility — were studied against utilization pattern of the TNAU Agritech Portal as the dependent variable. Age and education were scored following Asokhan (2006) and Kalaivani (1999) respectively; job satisfaction was measured using a seven-item continuum adapted from Vijayakumar (2009); attitude towards e-media and portal credibility were measured using scales adapted from Nataraju (1991); and the remaining variables were operationalised specifically for the study on multi-point continua. Each variable was summated into a composite score and respondents were classified into low, medium and high categories using the cumulative frequency method. The dependent variable, utilization pattern, was computed from frequency-of-use and purpose-of-use scores and expressed as a Utilization Index, similarly classified into low, medium and high categories. Data were analysed using percentage analysis, cumulative frequency, Karl Pearson's simple correlation and multiple linear regression (ordinary least squares) to determine the association and relative contribution of the independent variables to utilization.

IV. RESULTS

A. Profile characteristics of extension personnel

The distribution of respondents according to their profile characteristics is presented in Table 1.

Table 1: Distribution of extension personnel according to their profile characteristics (n = 60)

Variable	Category	Number	Per cent
Age (years)	Young (≤35)	3	5.00
	Middle (35–45)	29	48.33
	Old (>45)	28	46.67
Education	B.Sc. (Ag.)	45	75.00

Variable	Category	Number	Per cent
	B.Sc. (Ag.) + additional course	4	6.66
	M.Sc. (Ag.)	9	15.00
	M.Sc. (Ag.) + additional course	1	1.67
	Ph.D.	1	1.67
Experience in job	Up to 14 years	17	28.33
	15–20 years	20	33.33
	Above 20 years	23	38.34
Job satisfaction	Low	10	16.70
	Medium	33	55.00
	High	17	28.30
Training undergone – technical	None	7	11.67
	Up to 2 trainings	17	28.33
	More than 2 trainings	36	60.00
Training undergone – computer	None	6	10.00
	Up to 2 trainings	38	63.33
	More than 2 trainings	16	26.67
Possession of electronic gadgets – home	Low	17	28.34
	Medium	27	45.00
	High	16	26.66
Possession of electronic gadgets – office	Low	32	53.33
	Medium	25	41.67
	High	3	5.00
Attitude towards e-media	Less favourable	9	15.00
	Favourable	14	23.33
	Most favourable	37	61.67
Awareness of agricultural websites	Up to 2 websites	7	11.67
	3–5 websites	39	65.00
	More than 5 websites	14	23.33
Utilization of agricultural websites	Up to 2 websites	32	53.33
	3–5 websites	22	36.67
	More than 5 websites	6	10.00
Internet ownership	Office only	12	20.00
	Both office and personal	48	80.00

Variable	Category	Number	Per cent
Portal credibility	Less credible	21	35.00
	Moderately credible	30	50.00
	Highly credible	9	15.00

Extension personnel in the study area were predominantly middle-aged to old (48.33% and 46.67% respectively), graduates at the basic B.Sc. (Agri.) level (75.00%), and experienced, with 38.34 per cent having served for more than 20 years. Job satisfaction was medium for a majority (55.00%). A most-favourable attitude towards e-media was reported by 61.67 per cent, awareness of three to five agricultural websites by 65.00 per cent, and moderate portal credibility by half the respondents (50.00%), with over a third (35.00%) rating the portal as only "less credible".

Awareness and frequency of use of specific ICT tools and services are presented in Table 2.

Table 2: Awareness and frequency of use of ICT tools and services by extension personnel (n = 60)

Particulars	Aware (%)	Daily (%)	Weekly (%)	Monthly (%)	Never (%)
Mobile telephony	100.00	63.33	25.00	3.33	8.33
Websites and portal	100.00	53.33	45.00	1.66	-
e-mail	100.00	60.00	20.00	15.00	3.33
e-courses	13.33	-	-	-	13.33
e-books	18.33	-	-	6.66	11.66
IVRS (Kisan Call Centre)	46.66	-	1.66	5.00	40.00
Video conferencing	51.66	5.00	15.00	16.66	15.00
Touch-screen kiosks	15.00	-	-	3.33	11.66
Social networking tools	35.00	11.66	6.66	10.00	6.66

Note: Frequency of use computed among the aware sub-group; multiple responses obtained; "-" indicates nil response.

All respondents were aware of mobile telephony, websites/portal and e-mail, whereas awareness of e-courses (13.33%), touch-screen kiosks (15.00%) and e-books (18.33%) remained low. Awareness of video conferencing (51.66%), IVRS/Kisan Call Centre (46.66%) and social networking tools (35.00%) was moderate.

B. Utilization pattern of the digital advisory portal

The frequency and purpose of portal use, along with the composite utilization index, are presented in Table 3.

Table 3: Distribution of respondents according to utilization pattern and utilization index of the portal (n = 60)

Particulars	Number	Per cent
Frequency of use		
Regularly	21	35.00
Occasionally	34	56.67
Rarely	5	8.33
Purpose of use (multiple response)		

Particulars	Number	Per cent
Reference and report preparation	12	20.00
Enhancing knowledge	36	60.00
Advice to farmers	42	70.00
Utilization Index		
Low	18	30.00
Medium	34	56.67
High	8	13.33

More than half the respondents (56.67%) used the portal only occasionally, and a similar proportion (56.67%) fell in the medium utilization-index category, with just 13.33 per cent classified as high users. Advising farmers (70.00%) and enhancing personal knowledge (60.00%) were the dominant purposes of use, while report preparation accounted for only 20.00 per cent. The links most frequently consulted, in rank order, are given in Table 4.

Table 4: Frequently accessed portal links in rank order (n = 60)

Link	Number	Per cent	Rank
Dynamic Market Information (DMI)	48	80.00	I
Crop protection	43	71.66	II
Daily newspaper information	36	60.00	III
Special technologies	31	51.66	IV
Crop production	23	38.33	V
Schemes and services	20	33.33	VI
Recent updates	19	31.66	VII
Success stories	12	20.00	VIII
Banking and credit	11	18.33	IX

Dynamic Market Information and crop-protection advisories dominated portal use.

C. Association and contribution of profile characteristics to utilization

Simple correlation coefficients between the twelve independent variables and utilization pattern are presented in Table 5.

Table 5: Correlation of profile characteristics with utilization of the portal (n = 60)

Variable	Correlation "r" value
Age (X1)	-0.176 NS
Education (X2)	0.172 NS
Experience in job (X3)	-0.310*
Job satisfaction (X4)	0.323*
Awareness of ICT tools and services (X5)	0.287*
Training undergone (X6)	0.235**

Variable	Correlation "r" value
Possession of modern electronic gadgets (X7)	0.030 NS
Attitude towards e-media (X8)	0.457**
Awareness of agricultural websites (X9)	0.450**
Internet usage (X10)	0.414**
Mobile usage (X11)	0.076 NS
Portal credibility (X12)	0.225**

**Significant at 5% level; **Significant at 1% level; NS – Non-significant*

Multiple regression analysis was carried out to assess the relative contribution of the twelve variables to utilization pattern; results are presented in Table 6.

Table 6: Multiple regression analysis of profile characteristics with utilization pattern (n = 60)

Variable	Partial regression coefficient	Standard error	't' value
Age (X1)	-0.116	0.043	-1.228 NS
Education (X2)	-0.371	0.231	-1.608 NS
Experience in job (X3)	-0.243	0.678	-0.358 NS
Job satisfaction (X4)	0.107	0.048	2.238*
Awareness of ICT tools and services (X5)	0.704	0.317	2.222*
Training undergone (X6)	0.318	0.127	2.507**
Possession of modern electronic gadgets (X7)	-0.093	0.039	-2.386*
Attitude towards e-media (X8)	-0.407	0.199	-2.048*
Awareness of agricultural websites (X9)	0.236	0.089	2.672**
Internet usage (X10)	-0.167	0.136	0.474**
Mobile usage (X11)	-0.010	0.078	-0.134 NS
Portal credibility (X12)	0.178	0.108	0.225**

*R^2 = 0.453; F = 3.967**; *Significant at 5% level; **Significant at 1% level; NS – Non-significant*

V. DISCUSSION AND CONCLUSION

The age and experience profile recorded here — a predominantly middle-aged to old, experienced workforce — is broadly consistent with the pattern reported more recently for KVK-linked and university-affiliated extension functionaries, where advancing age has continued to depress engagement with newer digital tools even as formal educational qualification improves adoption (Singh et al., 2026a). The moderate-to-low portal credibility reported by over a third of respondents resonates with the broader observation that the proliferation of Indian government digital-agriculture platforms, each launched in quick succession, has made it difficult for users to judge which portals merit sustained trust (Balkrishna et al., 2024). More than a decade after these data were collected, the uneven awareness gradient across ICT-tool types (Table 2) still mirrors what recent NAAS-rated studies of India's extension workforce report: tools already embedded in day-to-day advisory routines are adopted readily, while stand-alone or emerging tools such as AI-based applications and IoT-linked sensors see markedly lower uptake, primarily on account of inadequate training rather than lack of access (Gosavi and Singh, 2026; Singh et al., 2026).

The predominance of occasional over regular use, and the concentration of use around advising farmers and enhancing personal knowledge (Table 3), reflect the heavy administrative workload of ADAs and ADHs and a tendency among older, more experienced officials to

consult only the links relevant to their own charge. The dominance of Dynamic Market Information and crop-protection advisories among frequently accessed links (Table 4) is consistent with contemporary evidence that price-discovery and pest/disease-advisory content remain the most consistently used categories of digital agricultural information even as newer AI-based recommendation layers are introduced (Sharma et al., 2025).

Training undergone, attitude towards e-media, awareness of agricultural websites, internet usage and portal credibility showed positive and highly significant correlation with utilization pattern (Table 5), while job satisfaction and awareness of ICT tools and services were positively and significantly correlated at the five per cent level. Experience in job showed a significant negative association, suggesting that more experienced officials continued to rely on conventional, face-to-face methods of technology dissemination rather than the portal. These directional patterns — favourable attitude and website familiarity reinforcing use, while seniority in service works against it — are consistent with recent regression evidence from KVK-linked users, where education raised, and advancing age depressed, ICT-tool utilization (Singh et al., 2026a), and with the broader finding that training remains the single most decisive lever for closing digital-extension adoption gaps in India (Singh et al., 2026).

The twelve variables together explained 45.30 per cent of the variation in utilization pattern ($R^2 = 0.453$; Table 6), with the overall regression significant at the one per cent level ($F = 3.967^{**}$). Job satisfaction and awareness of ICT tools and services contributed positively and significantly at the five per cent level, while training undergone, awareness of agricultural websites and portal credibility contributed positively and significantly at the one per cent level. Possession of modern electronic gadgets and attitude towards e-media showed a significant negative contribution once other variables were held constant, indicating that these two characteristics operate mainly through their association with other predictors rather than as independent drivers. Practically, this places capacity building (training) and information-source credibility among the strongest, most actionable levers available to portal managers, consistent with more recent, larger-sample evidence that inadequate training is consistently ranked the foremost constraint to ICT-tool adoption among India's extension and KVK personnel (Singh et al., 2026), and with the observation that a fragmented, fast-multiplying set of digital-agriculture platforms makes credibility-building an ongoing institutional task rather than a one-time design choice (Balkrishna et al., 2024).

This analysis of a decade-old but still instructive baseline dataset shows that a predominantly middle-aged, graduate, experienced extension workforce used the TNAU Agritech Portal mainly to advise farmers and update its own knowledge, at a largely medium level of intensity. Training undergone, favourable attitude towards e-media, awareness of agricultural websites, internet usage and portal credibility were the strongest positive correlates of utilization, while seniority in service worked against it; together, the profile variables explained under half the variance in utilization, leaving considerable room for institutional and design-side factors. That training and credibility continue to surface as the dominant levers in more recent, nationally-scaled studies of India's extension cadre (Singh et al., 2026; Gosavi and Singh, 2026) suggests these are structural features of digital-extension adoption rather than artefacts of this particular sample or period, and that they deserve explicit attention as legacy university portals are progressively integrated into the Digital Agriculture Mission's unified digital ecosystem. Because the data reported here are drawn from a single-district, 2011–12 cross-section, they should be read as a historical baseline rather than a current snapshot; replication that captures today's mix of portal, mobile-application and AI-enabled advisory channels would help verify whether these correlates still hold as the digital-extension landscape continues to evolve.

REFERENCES

[1] Asokhan, M. (2006). Empowerment of Rural Women through Self-Help Groups – An Empirical Analysis. Unpublished Ph.D. Thesis, Tamil Nadu Agricultural University, Coimbatore.

[2] Balkrishna, A., Singh, S.K., Pathak, R. and Arya, V. (2024). E-governance paradigm in the Indian agricultural sector. Discover Agriculture, 2(1), 2.

[3] Dhillon, M. (2025). Global research on digital platforms in rural knowledge transfer during 2003–2025: A bibliometric analysis. Indian Journal of Extension Education, 62(1), 135-141.

[4] Gosavi, D.P. and Singh, S.K. (2026). A systematic review of ICT tools in agricultural extension: Trends and challenges. International Journal of Agriculture Extension and Social Development, 9(4), 303-315.

[5] Kalaivani, S. (1999). Managerial Competency, Job Perception and Job Performance of Extension Personnel in Broad Based Extension System. Unpublished Ph.D. Thesis, Tamil Nadu Agricultural University, Coimbatore.

[6] Mukherjee, S., Padaria, R.N., Burman, R.R., Velayudhan, P.K., Mahra, G.S., Aditya, K., Sahu, S., Saini, S., Mallick, S., Quader, S.W., Shravani, K., Ghosh, B. and Bhat, A.G. (2025). Global trends in ICT-based extension and advisory services in agriculture: A bibliometric analysis. Frontiers in Sustainable Food Systems, 9, 1430336.

[7] Nataraju, M.S. (1991). Effectiveness of Farm Magazines – A Component Analysis. Unpublished Ph.D. Thesis, Tamil Nadu Agricultural University, Coimbatore.
[8] Press Information Bureau (PIB). (2024). Digital Agriculture Mission: Tech for Transforming Farmers' Lives. Ministry of Agriculture and Farmers Welfare, Government of India, New Delhi.
[9] Sahoo, S., Parasar, B. and Jayasingh, D.K. (2025). Towards digitally enabled extension services: ICT training directions in coastal Odisha. Indian Journal of Extension Education, 61(4), 66-71.
[10] Sharma, S., Rana, P., Samriti and Sharma, S. (2025). Digital agriculture in India: A review of ICT interventions for sustainable farming. International Journal of Agriculture Extension and Social Development, 8(11).
[11] Singh, A.K. (2008). Tests, Measurements and Research Methods in Behavioural Sciences. Bharati Bhawan Publishers and Distributors, New Delhi.
[12] Singh, S., Doharey, R.K., Meena, N.R., Singh, R. and Singh, A. (2026). Analysis and prioritization of constraints affecting ICT tools adoption among KVK personnel. Indian Journal of Extension Education, 62(3), 305-308.
[13] Singh, S.P., Yadav, R.N., Singh, D.K., Prakash, S. and Tripathi, P. (2026a). Awareness and utilization of ICT tools among KVK-linked progressive farmers in Western Uttar Pradesh. Indian Journal of Extension Education, 62(4), 109.
[14] Vijayakumar, G. (2009). Effect of Stress on Job Performance of Veterinary Teaching Faculty. Unpublished M.V.Sc. Thesis, Madras Veterinary College, Chennai.
[15] Yekinni, O.T., Owolabi, A.O. and Obaniyi, K.S. (2023). Extension practitioners' perception and constraints on ICT use in Southwestern Nigeria. SAGE Open, 13(4).

International Journal of Environment, Agriculture and Biotechnology
Vol-11, Issue-5; Sep-Oct, 2026
Peer-Reviewed International Journal
Journal Home Page Available: https://ijeab.com/
Journal DOI: 10.22161/ijeab

Impact of Pradhan Mantri Matsya Sampada Yojana (PMMSY) on Inland Fish Farming Economy in Kalyana Karnataka Region

Ninganna[1], Devendra Beeraladinni[2]*, Stephan Raj[3], Suresh K[4] and Sudhakar A C[5]

[1]Research Scholar, Department of Agricultural Economics, College of Agriculture, University of Agricultural Sciences, Raichur-584101, Karnataka, India
[2]Associate professor and Extension Leader, Department of Agricultural Economics, UAS, Raichur, Raichur -584104 Karnataka, India
[3]Assisstant Professor, Department of Agricultural Economics, Agriculture College Kalaburagi, UAS, Raichur
[4]Assistant Professor, Department of Agricultural Economics, UAS, Raichur
[5]Professor of Fisheries, MARS, UAS, Raichur
* Corresponding author mail: dbeeraladinnidevendra1975@gmail.com

Received: 16 Aug 2026; Received in revised form: 12 Sep 2026; Accepted: 18 Sep 2026; Available online: 25 Sep 2026
©2026 The Author(s). Published by Infogain Publication. This is an open-access article *under* the CC BY license (https://creativecommons.org/licenses/by/4.0/).

Abstract— *The present study analysed the impact of the Pradhan Mantri Matsya Sampada Yojana (PMMSY) on the inland fish farming economy in Kalyana Karnataka region, with a specific focus on fish production, income and employment of fish farmers. The study was conducted in Raichur and Yadgir districts using a multistage purposive random sampling procedure, covering 80 respondents (40 beneficiaries and 40 non-beneficiaries). Primary data were collected for the years 2020-21 (before PMMSY) and 2023-24 (after PMMSY). Analytical tools such as percentage change and Difference-in-Difference (DiD) technique were employed to measure the scheme impact. A significant increase in fish production, income and employment of beneficiaries compared to non beenficiaries was noticed in the study area due to PMMSY introduction. It was observed that after the introduction of PMMSY, there was about 29.47 per cent increase in fish production among beneficiaries compared to only 0.94 per cent among non-beneficiaries. Similarly, the income of beneficiaries increased significantly by 81.24 per cent compared to 41.34 per cent recorded by non-beneficiaries, the increased in income for non-beneficiaries was mainly attributed to change in price. Employment generation also improved more prominently for beneficiaries, showing an increase of 12.61 per cent compared to only 2.31 per cent among non-beneficiaries. Later the Difference-in-Difference regression results confirmed that with an introduction of PMMSY, fish production increased by 1,151 tonnes per acre, there was an increase in income of beneficiaries by `1,18,549 per acre and employment generation by 22.23 man-days. The findings demonstrate that PMMSY effectively enhanced production, profitability and livelihood opportunities by improving access to quality inputs and technical support. This scheme has played a pivotal role in strengthening the inland fisheries sector and advancing sustainable rural economic development in the Kalyana Karnataka region.*

Keywords— ***Difference-in-Difference, Kalyana Karnataka, Inland fisheries, PMMSY***

I. INTRODUCTION

The world today faces three major interconnected challenges: alleviating poverty, meeting present and future food demands, and managing natural resources to ensure long-term sustainability. Poverty, coupled with population growth, land limitations and the absence of suitable production technologies for agricultural intensification, significantly contributes to environmental degradation in low-income developing nations (Pinstrup & Pandya., 1994). Aquatic resources have been identified as important

for food security and economic development in many developing countries. Aquaculture has emerged as a fast-growing sector for meeting the increased demand for food and it holds immense scope for both horizontal and vertical expansion in the inland fisheries sector (Kumari and Patra., 2014).

The Indian fisheries sector is termed as the "sunrise sector" of the Indian economy, providing livelihoods to around 28 million fishers and fish farmers at the primary level, with many more involved along the value chain. Fish, being an affordable and nutritious source of animal protein, plays a significant role in combating hunger and malnutrition in the country. India's vast freshwater and brackish water resources, combined with its peninsular geography, offer tremendous growth potential for the sector. With an 8% share in global fish production, India is the second-largest producer of fish and aquaculture globally after China. India produced a total of 175.45 lakh tonnes of fish, with 44.32 lakh tonnes from marine fisheries and 131.13 lakh tonnes from inland fisheries (Anon., 2023).

Fisheries is an important sector in the Karnataka state and is blessed with both marine and inland resources offering immense opportunities for fisheries and aquaculture growth. This sector is making valuable contributions to the economic development of the state and has all the potentials to provide livelihood and nutritional security. In India Karnataka ranks third in total fish production with 12.24 lakh tonnes production, fifth in marine fish production with 7.30 lakh tonnes and seventh in inland fish production with 4.94 lakh tonnes (Anon., 2023).

The Pradhan Mantri Matsya Sampada Yojana (PMMSY) is a major scheme introduced to strengthen and modernize the fisheries sector in India. Launched in 2020 as part of the “Atma Nirbhar Bharat” package, the scheme involves an investment of ₹20,050 crore the highest-ever allocation made to the fisheries sector. PMMSY is being implemented across all states and union territories over a five-year period from FY 2020–2021 to FY 2024–2025.

The scheme aims to uplift fish farmers from backwardness by promoting improved farming practices, enhancing income levels and generating employment opportunities across the fisheries value chain.

Hence present study focus on impact of PMMSY on fish farming economy based on pre and post implementation of PMMSY. Therefore, the present study was undertaken in Kalyana Karnataka region with the following specific objectives 1. To analyse the impact of PMMSY on fish production, income and employment of farmers in the study area.

II. MATERIALS AND METHODS

Study area

The study was conducted in two districts of Kalyana Karnataka region *viz.,* Raichur and Yadgir based on their highest levels of inland fish production in Kalyana Karnataka region and the significant number of beneficiaries under the Pradhan Mantri Matsya Sampada Yojana (PMMSY) in Kalyana Karnataka region.

Sampling procedure

The Multistage purposive random sampling procedure was followed for selection of respondents for the study. In total 80 sample constituting 40 beneficiaries, 40 non-beneficiaries of Pradhan Mantri Matsya Sampada Yojana (PMMSY) were selected from the above mentioned districts in which 10 beneficiaries and 10 non-beneficiaries were selected from each taluka.

The primary data were collected on fish production, income and employment for the year 2020-21 to indicate scenario before implementation of PMMSY and for the year 2023-24 to indicate scenario after implementation of PMMSY.

Analytical tools employed

The data collected were presented in tabular form to facilitate easy comparison. The presentation has adopted to compile characteristics of the sample farmers. Data regarding number of beneficiaries involved in the scheme, income and employment of beneficiary farmers under the PMMSY were analysed by average and frequency.

Percentage Change

$$\text{PercentageChange} = \frac{\text{New value - old value}}{\text{old value}} \times 100$$

Difference in Difference (DiD) technique

$$DD = [\frac{1}{P}\sum_{i=1}^{p}(Y_{1ia} - Y_{1ib})] - [\frac{1}{c}\sum_{j=1}^{c}(Y_{oja} - Y_{ojb})]$$

Where,

DD = Income difference between the respondents (beneficiaries and non – beneficiary)

P = number of beneficiary farmers

C = number of individuals in the control group (non – beneficiary farmers)

Y_{1ia} = Income variable of beneficiary after the

PMMSY scheme

Y_{1ib} = Income variable of participant before the PMMSY scheme

$Y_{0\ ja}$ = Income variable of non-beneficiaries after PMMSY scheme

$Y_{0\ jb}$ = Income variable of non-beneficiaries before PMMSY scheme

Difference-in-Difference Regression

$$Y = \beta0 + \beta1 \times D_t + \beta2 \times D_i + \beta3\ (D_i \times D_t) + \varepsilon$$

Where

Y= Production /income /employment

β0 = intercept

D_t (Time) = 1 for 2023-24 (after implementation of PMMSY)

0 for 2020 -21 (before implementation of PMMSY)

D_i (Intervention) = 1 if respondent is beneficiary of PMMSY (treatment)

= 0 if respondent is non-beneficiary of PMMSY (Control)

(D_i x D_t) Interaction = Actual scheme impact (Difference-in-Differences

β1, β2 and β3 are coefficients.

Beneficiary of Pradhan Mantri Matsya Sampada Yojana (PMMSY)

Sample farmers who engaged in inland fish farming and availed the benefit of PMMSY.

Non-beneficiary of PMMSY

Non-beneficiaries are Sample farmers who do not received PMMSY subsidies and still engaged in inland fish farming.

III. RESULTS AND DISCUSSION

Production, income and employment of beneficiary farmers and non- beneficiary farmers of PMMSY.

Production, income and employment of beneficiary farmers and non- beneficiary farmers of PMMSY are presented in Table 1 After the implementation of the scheme beneficiaries increased their fish production from 4038 tonne to 5228 tonne per acre a rise of 29.47 per cent whereas non-beneficiaries showed only a minor increase from 4113 tonne to 4152 tonne a rise is only 0.94 per cent per acre. The higher production among beneficiaries is largely attributed to the use of quality feed and fingerlings provided under a PMMSY subsidy, along with technical guidance from the fish department which ensured proper management practices and efficient input utilization.

Similarly the income of beneficiaries rose significantly increased from ` 3,02,868 to `5,48,940, a rise of 81.24 per cent. Whereas non-beneficiaries income increased only marginally from `3,08,437 to `4,35,960 rise is 41.34 per cent which was mainly attributed to change in price. Employment generation also increased more substantially among beneficiaries from 215.65 to 243.03 12.61 per cent man-days compared to a smaller increase from 222.50 to 227.65 man-days 2.31 per cent for non-beneficiaries. This indicates that PMMSY not only enhanced profitability and productivity but also created additional employment opportunities by promoting better management and adoption of modern fish farming practices. The scheme effectively reduced the financial burden on beneficiaries, improved efficiency and contributed to sustainable inland fish production.

Table 1: Production, income and employment of beneficiary farmers as compared to non- beneficiary farmers of PMMSY

Sl. No.	Particulars	Beneficiary of PMMSY (n=40)		% change	Non- beneficiary (n=40)		% change
		Before PMMSY	After PMMSY		Before	After	
1	Production (tonnes)	4038	5228	29.47	4113	4152	0.94
2	Income (₹)	302868	548940	81.24	308437	435960	41.34
3	Employment (mandays)	215.65	243.03	12.61	222.50	227.65	2.31

Impact of PMMSY on fish production

The double difference estimates of the impact of PMMSY on production as presented in Table 2 indicate a substantial positive effect on beneficiary farmers. Before

the intervention, beneficiaries produced 4,038 tonnes per acre which increased to 5,228 tonnes per acre after the implementation of PMMSY resulting in a mean increase of 1190 tonnes. In contrast non-beneficiaries showed a minimal increase from 4,113 tonnes to 4,152 tonnes per acre with a mean increase of only 39 tonnes.

The estimates of double difference of 1151 tonnes demonstrates that PMMSY had a considerable impact on fish production among beneficiary farmers highlighting the effectiveness of the programme in enhancing productivity. The higher production among beneficiaries is primarily due to the efficient use of resources and the availability of good quality fingerlings and feed through the PMMSY subsidy.

Table 2: Double difference estimates of impact of PMMSY on fish production (n=80)

Sl. No.	Variable	Fish production (tonnes/acre)		Mean Difference	t - statistics
		Before	After		
1	Beneficiary of PMMSY	4038	5228	1190	7.84*
2	Non- beneficiary	4113	4152	39	5.10*
3	Double Difference	-	-	1151	8.85*

Note: * Indicates at 1 per cent level of significance

Impact of PMMSY on income

The double difference estimates of the impact of PMMSY on income, as presented in Table 3 indicate a substantial positive effect for beneficiary farmers. Before the implementation of PMMSY beneficiaries earned `3, 02,868 which increased to `5, 48,940 after participation in the program reflecting a mean income increase of `246072, In contrast non-beneficiaries recorded a smaller rise in income from `3, 08,437 to ` 4, 35,960 with a mean increase of `1, 27,522 which was mainly attributed to change in price.

The estimated double difference of `1, 18,549 demonstrates that PMMSY had a significant impact on the income of beneficiary farmers. This improvement can be largely attributed to the access to high-quality fingerlings and feed under the PMMSY subsidy enabling beneficiaries to invest in better inputs for fish production. Technical guidance from the fisheries department ensured that these inputs were used efficiently optimizing stocking feeding and pond management practices.

Table 3: Double difference estimates of impact of PMMSY on income (n=80)

Sl. No	Variable	Income (`/year)		Mean Difference	t -statistics
		Before	After		
1	Beneficiary of PMMSY	302868	548940	246072	9.10*
2	Non- beneficiary	308437	435960	127522	7.63*
3	Double Difference	-	-	118549	8.13*

Note: * Indicates at 1 per cent level of significance

Impact of PMMSY on employment

Double difference estimates of impact of PMMSY on employment generated from inland fish production presented in Table 4 Beneficiary farmers significantly increased their labour contribution from 215.65 man-days per household before the intervention to 243.03 man-days after reflecting a mean increase of 27.38 man-days which is statistically significant at the 1 per cent level. In contrast non-beneficiary farmers showed only a marginal rise from 222.50 man-days to 227.65 man-days with a mean increase of 5.15 man-days.

The double difference estimate of 22.23 man-days, significant at 1 per cent level, indicates that the observed increase in labor engagement among beneficiaries can be attributed to the PMMSY intervention. The higher employment among beneficiaries is primarily linked to the adoption of improved fish farming practices including optimal stocking regular feeding, and efficient pond management supported by quality fingerlings feed subsidies and technical guidance from the fisheries department.

Table 4: Double difference estimates of impact of PMMSY on employment

(n=80)

Sl. No	Variable	Employment (mandays)		Mean Difference	t -statistics
		Before	After		
1	Beneficiary of PMMSY	215.65	243.03	27.38	8.09*
2	Non- beneficiary	222.50	227.65	5.15	2.33**
3	Double Difference	-	-	22.23	5.56*

Note: * and ** Indicates at 1 and 5 per cent level of significance

Difference–in-Difference regression result for impact of PMMSY on Income, production and employment

The results of the Difference-in-Difference regression result for impact of PMMSY on fish production, income and employment are presented in Table 5 the Difference-in-Difference analysis confirmed a significant positive impact of PMMSY on fish production, income and employment of fish farmer in the study area. The intercept values for all three models were highly significant, indicating the baseline levels of production, income and employment before the programme implementation. The time coefficient (β_1) was positive for all variables, implying a natural growth trend over time even without the programme..

The intervention coefficient (β_2) was negative and significant for all three variables, indicating that prior to the PMMSY implementation, the treatment group (beneficiaries) had lower fish production, income, and employment compared to the non- beneficiary group. This reflects the initial production and economic constraints faced by fish farmers before accessing programme benefits, such as limited technical support, lack of access to quality seed, and financial limitations.

The interaction term (β_3), which represents the DID effect, was positive and highly significant for all variables, demonstrating that PMMSY had a substantial positive impact on beneficiary farmers. After the introduction of the scheme, fish production increased by 1,151 tonnes, income by `1, 18,549 and employment by 22.23 mandays per farmer compared to non-beneficiaries. The high R^2 values for production (0.91) and income (0.98) indicate strong model fit, while employment (0.38) shows moderate explanatory power.

Table 5: Difference–in-Difference regression result for impact of PMMSY on fish production, income, employment in the study area

(Rupees Per acre)

Fish Production (tonnes)					Income (`)			Employment (mandays)		
Sl. No.	**Explanatory Variable**	**Coefficient**	**Std. Error**	**t-value**	**Coefficient**	**Std. Error**	**t-value**	**Coefficient**	**Std. Error**	**t-value**
1	(Intercept)	4 113**	23.45	175.45	3 08 437**	2 006	153.78	222.50**	2.018	110.24
2	Time (β_1) 1= After PMMSY 0= Before PMMSY	38.50	33.16	1.16	1 27 523	2 837	44.96	5.150	2.854	1.80
3	Intervention (β_2) 1= Beneficiary 0= Non-beneficiary	−75.25*	33.16	−2.27	−5 569*	2 837	−1.96	−6.850*	2.854	−2.40
4	Interaction (β_3) (DiD) (time x treatment)	**1 151****	46.89	24.55	**1 18 549****	4 012	29.55	**22.23****	4.037	5.51
5	R^2	**0.91**			**0.98**			**0.38**		
6	F value	581.5**			3421**			33.23**		
7	**Number of**	**160**			**160**			**160**		

	observations			

Note: * and ** Indicates at 1 and 5 per cent level of significance

IV. CONCLUSION

The study concludes that the Pradhan Mantri Matsya Sampada Yojana (PMMSY) has a significant positive impact on the inland fish farming economy in the Kalyana Karnataka region. Beneficiary farmers recorded substantial improvements in fish production, income and employment compared to non-beneficiaries, mainly due to access to quality inputs under subsidies, and technical support provided under the scheme. The double difference and Difference-in-Difference analysis further confirmed that PMMSY increased fish production by 1151 tonnes per acre , income by `1, 18,549 per acre and employment by 22.23 man-days. PMMSY has effectively enhanced productivity, profitability and livelihood security among fish farmers, demonstrating its importance in strengthening the inland fisheries sector and promoting sustainable rural economic development.

ACKNOWLEDGEMENT

This research was a part of M.Sc. (Agri.) thesis and the author greatly appreciate research facilities and support provided from the College of Agriculture, Raichur for conducting this research study. The author is grateful to members of the advisory committee for their engrossing guidance, incessant encouragement, constructive suggestions, propitious assistance, keen and sustained interest, kind and gracious patronage during the entire course of investigation and preparation of this manuscript.

REFERENCES

[1] Anonymous, 2023, Handbook on Fisheries Statistics 2023, Department of fisheries Government of Karnataka.

[2] Anonymous, 2023, Handbook on Fisheries Statistics 2023, Ministry of fisheries animal husbandry and dairying Government of India.

[3] Bhavani G, Sreenivasulu M, Naik R V, Reddy M J M, Darekar A S and Reddy A A, 2022. Impact assessment of seed village programme by using difference in difference (DiD) approach in Telangana, India. *Sustainability*, 14(15): 9543

[4] Kumari M K and Patra S, (2014), Production analysis of inland fish in Angul district of Odisha. *Journal of Economics and Finance*, 3(4): 38-42.

[5] Pinstrup and Pandya-Lorch Rajul, 1994, Alleviating poverty, intensifying agriculture and effectively managing natural resources. Discussion Paper 1.Washington, DC: *International Food Policy Research Institute.*

International Journal of Environment, Agriculture and Biotechnology
Vol-11, Issue-5; Sep-Oct, 2026
Peer-Reviewed International Journal
Journal Home Page Available: https://ijeab.com/
Journal DOI: 10.22161/ijeab

Profile Characteristics of Extension Personnel and their Association with Attitude towards ICT Tools and Information Management Patterns

Anand Karthikeyan[1*] and Sankri Karthikeyan[2]

[1]Associate Professor and Head, Department of Agricultural Extension and Communication, Vanavarayar Institute of Agriculture, Manakkadavu, Pollachi – 642 103, Coimbatore District, Tamil Nadu, India
[2]Assistant Professor, Department of Agricultural Extension and Communication, Vanavarayar Institute of Agriculture, Manakkadavu, Pollachi – 642 103, Coimbatore District, Tamil Nadu, India
*Corresponding Author E-mail: agrianand17@gmail.com

Received: 20 Aug 2026; Received in revised form: 15 Sep 2026; Accepted: 21 Sep 2026; Available online: 28 Sep 2026
©2026 The Author(s). Published by Infogain Publication. This is an open-access article *under* the CC BY license (https://creativecommons.org/licenses/by/4.0/).

Abstract**—** *Extension personnel are increasingly expected to function as information managers, yet the personal and situational factors that shape this capacity remain under-examined for Tamil Nadu's Departments of Agriculture and Horticulture. This study profiled 121 extension personnel (Agricultural/Horticultural Officers, Assistant and Deputy Directors) across Coimbatore, Tiruppur and Erode districts and examined the association and contribution of fifteen profile variables with their attitude towards Information and Communication Technology (ICT) tools and their information management patterns, using correlation and multiple regression analysis. Organizational climate and managerial ability emerged as the only variables contributing significantly to both outcomes, while work experience, value orientation, technical knowledge, job involvement and media talks and publications additionally predicted attitude (R^2 = 0.652, F = 7.182**), and educational status, possession of communication gadgets, achievement motivation and trainings undergone additionally predicted information management patterns (R^2 = 0.724, F = 11.327**). These results indicate that favourable organizational climate and stronger managerial ability are the most consistent, generalisable levers for improving both ICT attitude and information management performance, ahead of variables specific to only one outcome, and provide extension administrators an evidence-based basis for prioritising capacity-building investment.*

Keywords**—Extension personnel, Profile characteristics, ICT attitude, Information management, Multiple regression**

I. INTRODUCTION

Agricultural extension is transitioning from a linear technology-transfer function to a pluralistic, demand-driven advisory system in which extension personnel must acquire, process and disseminate information as a core professional competency rather than an incidental duty. This transition places a premium on identifying which characteristics of extension personnel actually enable stronger engagement with Information and Communication Technology (ICT) tools and better information management, since capacity-building resources are finite and their allocation should be evidence-based rather than uniform. A recent Principal Component Analysis-based assessment of a Digital Competency Index for Indian extension professionals found nearly half of respondents at only a medium level of digital competency, underscoring that competency gaps persist nationally and are not confined to any one state cadre (Mukherjee et al., 2026).

Profile–outcome linkages of this kind have been reported piecemeal in the literature, but rarely as a joint, multivariable regression exercise that isolates which profile characteristics matter once all others are held constant.

Complementary evidence from Krishi Vigyan Kendra personnel shows that the lack of training opportunities remains the single largest constraint to ICT adoption ahead of infrastructural or cost barriers (Singh et al., 2026), while a cadre-wise comparison of extension workers in coastal Odisha found that junior and senior officers differ systematically in which ICT competencies they hold and which they still need, implying that hierarchical position and its correlates (experience, training exposure) are not incidental but structurally linked to ICT-related outcomes (Sahoo et al., 2025). These findings motivate a study that (i) profiles extension personnel on the full set of characteristics plausibly related to information behaviour, and (ii) statistically isolates which of these characteristics independently predict attitude towards ICT tools and information management patterns, so that the two outcomes already reported for this sample (Anand and Ravichandran, 2014a; Anand and Ravichandran, 2014b) can be traced back to their determinants and translated into targeted policy action.

II. METHOD

The study was carried out in Coimbatore, Tiruppur and Erode districts of Tamil Nadu using an ex post facto research design during 2013–14. All blocks in the three districts were covered, and of the 154 extension personnel in the study area, 121 (78.57%) responded to a structured, pre-tested mailed questionnaire and constituted the sample (Agricultural/Horticultural Officers – AO/HO, n=64; Assistant Directors of Agriculture/Horticulture – ADA/ADH, n=33; Deputy Directors of Agriculture/Horticulture – DDA/DDH, n=24). Fifteen profile variables were measured: age (X1), educational status (X2), work experience (X3), organizational climate (X4), managerial ability (X5), value orientation (X6), possession of communication gadgets (X7), workload perception (X8), technical knowledge (X9), achievement motivation (X10), job involvement (X11), job satisfaction (X12), self-confidence (X13), trainings undergone (X14), and media talks and publications (X15). Attitude towards ICT tools was measured using a seven-item scale earlier developed and standardised for this population by the Equal Appearing Interval method (Anand and Ravichandran, 2014a), and information management patterns were measured using a composite Information Management Index integrating information acquisition, processing (evaluation, treatment, storage, transformation) and dissemination, also previously validated for this sample (Anand and Ravichandran, 2014b). The association of the fifteen profile variables with each outcome was tested using Pearson correlation, and their independent contribution was estimated using multiple linear regression, with the two outcome variables entered separately as the dependent variable in each model.

III. RESULTS

Profile characteristics of extension personnel

Table 1 summarises the profile of the 121 extension personnel. Close to half (49.59%) were in the old age category, and a majority held a Bachelor's degree in Agriculture/Horticulture (57.85%), with 39.67% holding a Master's degree. Work experience was bimodal, split between less than 14 years (43.80%) and more than 20 years (41.32%). A large majority perceived organizational climate as more conducive (69.42%) and workload as high (82.64%), and most reported high technical knowledge (68.60%). Possession of communication gadgets at home skewed towards the medium category (51.24%), and two-thirds of respondents (67.77%) had attended more than two trainings.

Table 1. Profile characteristics of extension personnel (n=121)

Profile variable	**Category**	**Percentage**
Age	Young / Middle / Old	31.40 / 19.01 / 49.59
Educational status	B.Sc (Agri./Horti.) / M.Sc (Agri./Horti.) / Ph.D.	57.85 / 39.67 / 2.48
Work experience	≤14 yrs / 15–20 yrs / >20 yrs	43.80 / 14.88 / 41.32
Organizational climate	Moderate / More conducive	30.58 / 69.42
Managerial ability	Self doing / Getting assistance	23.14 / 76.86
Value orientation	Medium / High	33.06 / 66.94
Communication gadgets (home)	Low / Medium / High	19.01 / 51.24 / 29.75

Workload perception	Moderate / High	17.36 / 82.64
Technical knowledge	Low / Moderate / High	0.83 / 30.58 / 68.60
Achievement motivation	Low / Moderate / High	9.09 / 58.68 / 32.23
Job involvement	Less / Moderate / High	9.10 / 40.49 / 50.41
Job satisfaction	Medium / High	60.33 / 39.67
Self-confidence	Moderate / High	52.07 / 47.93
Trainings undergone	None / <2 / >2	5.79 / 26.45 / 67.77
Media talks and publications	Less / Moderate / High	9.10 / 40.49 / 50.41

Note: educational-status and communication-gadget sub-categories condensed for brevity; full cadre-wise breakdowns (AO/HO, ADA/ADH, DDA/DDH) are available from the corresponding author.

Association and contribution of profile variables with attitude towards ICT tools

Correlation analysis showed that work experience, organizational climate, trainings undergone and media talks and publications were positively and significantly associated with attitude towards ICT tools at the 1% level, while achievement motivation, job satisfaction and self-confidence showed no significant association. Multiple regression (Table 2) explained 65.2% of the variance in attitude ($R^2 = 0.652$, $F = 7.182$, $p<0.01$). Seven of the fifteen variables contributed significantly: work experience, organizational climate, managerial ability, value orientation, technical knowledge, job involvement and media talks and publications, each with a positive partial regression coefficient.

Table 2. Association and contribution of profile variables with attitude towards ICT tools

Profile variable	**r**	**b**	**SE**	**t**
Age (X1)	-0.361**	0.610	1.422	0.429 NS
Educational status (X2)	0.324**	-1.062	0.876	-1.212 NS
Work experience (X3)	0.031**	2.964	1.931	1.535**
Organizational climate (X4)	0.098**	0.791	1.200	3.158**
Managerial ability (X5)	0.220	0.588	0.194	2.257*
Value orientation (X6)	0.510**	0.394	2.197	2.910**
Communication gadgets (X7)	0.320**	-1.129	1.952	-0.578 NS
Workload perception (X8)	-0.375**	-3.159	2.379	-1.328 NS
Technical knowledge (X9)	0.364**	0.759	0.344	2.205*
Achievement motivation (X10)	0.172 NS	0.299	0.293	1.022 NS
Job involvement (X11)	-0.047 NS	0.580	0.220	2.635**
Job satisfaction (X12)	-0.206 NS	-1.566	2.341	-0.669 NS
Self-confidence (X13)	0.093 NS	0.289	0.175	1.651 NS
Trainings undergone (X14)	0.465**	0.073	0.335	0.217 NS

Media talks/publications (X15)	0.365**	0.933	0.351	2.661**
Constant = 8.518	*R^2 = 0.652*			*F = 7.182***

** Significant at 5%; ** Significant at 1%; NS – Non-significant; r = simple correlation coefficient; b = partial regression coefficient; SE = standard error of b; t = t-value of b (df = 105).*

Association and contribution of profile variables with information management patterns

For information management patterns, educational status, value orientation, workload perception, technical knowledge and job involvement showed significant positive association at the 1% level, and job satisfaction and self-confidence at the 5% level; managerial ability and achievement motivation showed no significant simple correlation. The regression model (Table 3) explained 72.4% of the variance ($R^2 = 0.724$, $F = 11.327$, $p<0.01$). Six variables contributed significantly: educational status, organizational climate, managerial ability, possession of communication gadgets, achievement motivation and trainings undergone. Possession of communication gadgets, although positively correlated with information management patterns (r = 0.435**), carried a negative partial regression coefficient (b = -2.063) once the other variables were held constant, indicating a suppression effect: gadget ownership per se does not improve information management beyond what is explained by the other profile characteristics.

Table 3. Association and contribution of profile variables with information management patterns

Profile variable	**r**	**b**	**SE**	**t**
Age (X1)	-0.268**	-0.663	0.707	-0.937 NS
Educational status (X2)	0.260**	1.062	0.519	2.048*
Work experience (X3)	0.185**	0.671	0.780	0.860 NS
Organizational climate (X4)	0.031**	1.716	0.600	2.862**
Managerial ability (X5)	0.011 NS	0.549	1.544	3.595**
Value orientation (X6)	0.306**	-2.419	1.372	-1.763 NS
Communication gadgets (X7)	0.435**	-2.063	0.910	-2.267*
Workload perception (X8)	0.306**	2.395	1.226	1.953 NS
Technical knowledge (X9)	0.406**	0.045	0.171	0.262 NS
Achievement motivation (X10)	0.053 NS	0.438	0.194	2.257*
Job involvement (X11)	0.273**	-0.021	0.140	-0.153 NS
Job satisfaction (X12)	0.160*	-1.988	1.289	-1.542 NS
Self-confidence (X13)	0.190*	0.198	0.139	1.423 NS
Trainings undergone (X14)	0.588**	0.529	0.246	2.148*
Media talks/publications (X15)	0.499**	0.191	0.203	0.944 NS
Constant = 18.638	*R^2 = 0.724*			*F = 11.327***

** Significant at 5%; ** Significant at 1%; NS – Non-significant; r = simple correlation coefficient; b = partial regression coefficient; SE = standard error of b; t = t-value of b (df = 105).*

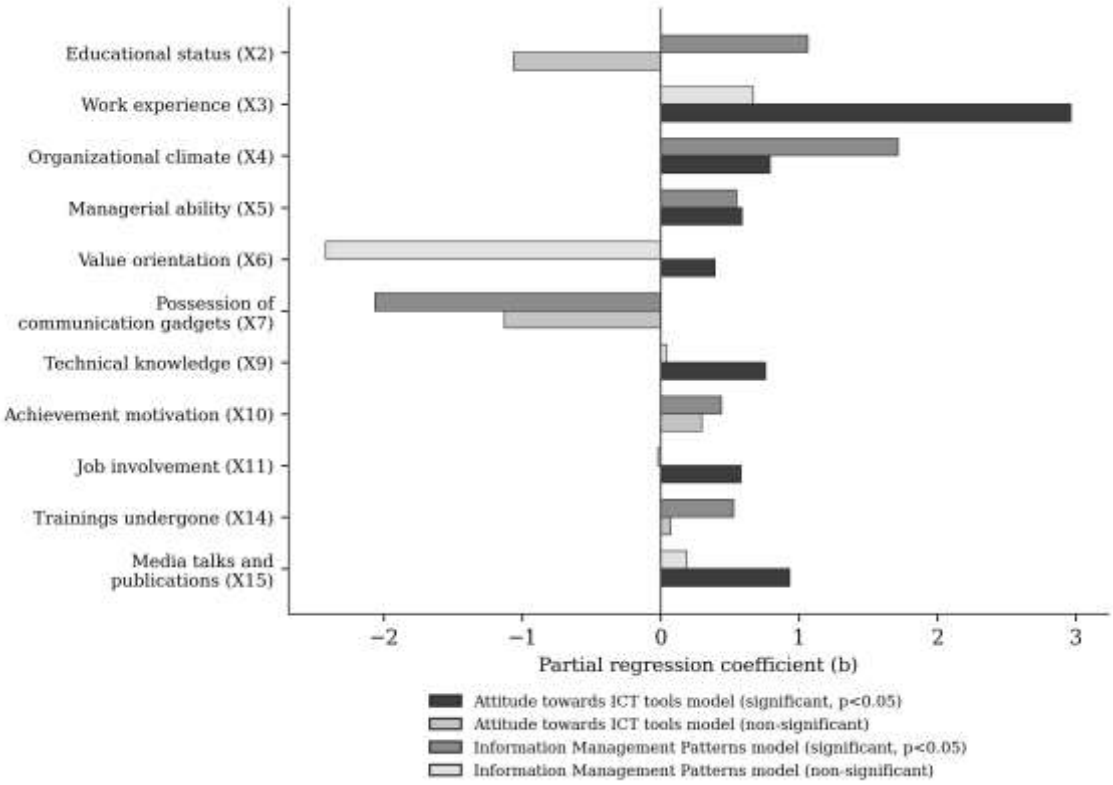


Fig.1: Partial regression coefficients of profile variables on attitude towards ICT tools and on information management patterns (variables non-significant in both models – X1, X8, X12 and X13 – are omitted)

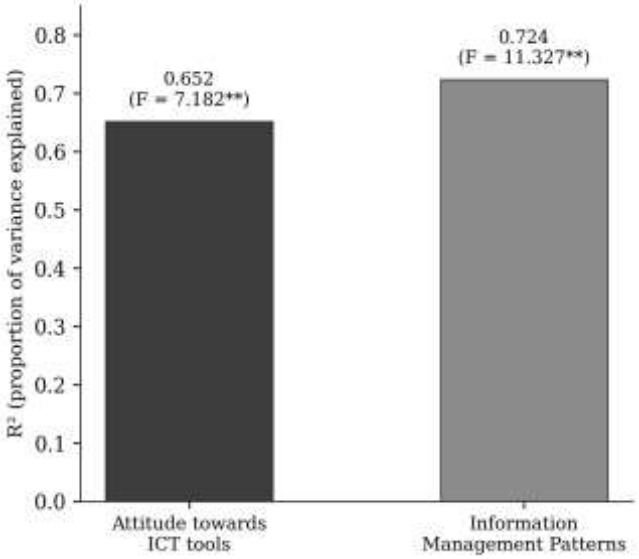


Fig.2: Variance explained (R^2) by the attitude and information-management regression models

IV. DISCUSSION AND CONCLUSION

Work experience, organizational climate and technical knowledge exhibited an expected positive relationship with attitude towards ICT tools: longer service builds the confidence and familiarity needed to engage ICT tools productively, and a conducive organizational climate removes a structural barrier to forming favourable attitudes rather than merely correlating with them. Managerial ability and value orientation also predicted attitude independently, consistent with the view that ICT engagement is as much a managerial and dispositional competency as a technical one. Notably, trainings undergone, although not an

independent predictor of attitude once the other variables were controlled, showed a strong positive simple correlation with it (r = 0.465**). A recent study of KVK personnel found lack of training opportunities to be the single largest constraint to ICT adoption (Singh et al., 2026); the present results suggest that where training has occurred, as in this sample (67.77% attended more than two trainings), it is associated with a more favourable attitude, reinforcing rather than contradicting the constraint-side finding.

Figure 1 makes the comparison across both regression models explicit. Organizational climate and managerial ability are the only two variables that contribute significantly and positively to both outcomes, while the remaining significant predictors are largely outcome-specific: work experience, value orientation, technical knowledge, job involvement and media talks and publications for attitude; and educational status, possession of communication gadgets, achievement motivation and trainings undergone for information management patterns. This pattern is consistent with a recent cadre-wise comparison of extension personnel in coastal Odisha, which found that junior and senior officers diverge in which specific ICT competencies they hold, implying that hierarchy-linked variables such as experience and training operate somewhat differently on attitude formation versus on management behaviour rather than acting as a single undifferentiated 'ICT-readiness' factor (Sahoo et al., 2025). The stronger fit of the information-management model (R^2 = 0.724 against 0.652; Figure 2) further suggests that information management, being a more procedural and habitual set of behaviours, is more fully determined by stable profile characteristics than attitude, which retains a larger unexplained, plausibly dispositional or contextual, component.

Practically, since organizational climate and managerial ability are the only variables that move both outcomes together, they represent the most generalisable and cost-effective entry point for administrative intervention – improving supervisory climate and managerial skill-building would be expected to lift both ICT attitude and information management performance simultaneously, whereas upgrading technical knowledge alone would be expected to improve attitude more than management behaviour, and vice versa for qualification- and training-linked interventions. This distinction directly extends the Digital Competency Index finding that a substantial share of extension professionals remain at only medium digital competency (Mukherjee et al., 2026): the present results indicate that closing that gap requires attention to organizational and managerial conditions, not technical exposure alone.

In conclusion, profiling 121 extension personnel across three Tamil Nadu districts and regressing their previously reported attitude and information-management outcomes on fifteen profile variables identified organizational climate and managerial ability as the sole variables contributing significantly to both, with the remaining significant predictors specific to one outcome or the other. The information-management model explained a materially larger share of variance than the attitude model, indicating that management behaviour is more profile-determined than attitude. These findings offer extension administrators a differentiated, evidence-based basis for capacity building: organizational-climate and managerial-skill interventions for broad-based gains, and outcome-specific interventions (technical-knowledge upgrading and encouragement of media talks and publications for attitude; higher academic qualification and structured training for information management) where a narrower, targeted gain is sought.

ACKNOWLEDGMENT

The authors thank the extension personnel of the Department of Agriculture and Department of Horticulture, Government of Tamil Nadu, in Coimbatore, Tiruppur and Erode districts, for their participation, and the Department of Agricultural Extension and Communication, Vanavarayar Institute of Agriculture, Pollachi, for institutional support.

REFERENCES

[1] Anand, K. and Ravichandran, V. (2014a). A scale to measure the attitude of extension personnel towards the Information and Communication Technology (ICT) tools. Trends in Biosciences, 7(17): 2583-2585.

[2] Anand, K. and Ravichandran, V. (2014b). Assessment of information management pattern among extension personnel. Trends in Biosciences, 7(21): 3402-3404.

[3] Mukherjee, S., Padaria, R.N., Burman, R.R., Nikam, V.R., Velayudhan, P.K., Mahra, G.S., Aditya, K., Chakrabarti, B., Saini, S., Shravani, K. and Ghosh, B. (2026). Development and standardisation of a digital competency index for extension professionals of India: A Principal Component Analysis approach. Agricultural Research, 15(1): 579-586. https://doi.org/10.1007/s40003-025-00865-4

[4] Sahoo, S., Parasar, B. and Jayasingh, D.K. (2025). Towards digitally enabled extension services: ICT training directions in coastal Odisha. Indian Journal of Extension Education, 61(4): 66-71.

[5] Singh, S., Doharey, R.K., Meena, N.R., Singh, R. and Singh, A. (2026). Analysis and prioritization of constraints affecting ICT tools adoption among KVK personnel. Indian Journal of Extension Education, 62(3): 305-308.

International Journal of Environment, Agriculture and Biotechnology
Vol-11, Issue-5; Sep-Oct, 2026
Peer-Reviewed International Journal
Journal Home Page Available: https://ijeab.com/
Journal DOI: 10.22161/ijeab

Environmental Studies: Comprehensive Review of Current Importance and Emerging Horizons

Dr. Ranjeeta Soni

Professor, Environmental Science, Jagannath University, Jaipur, Rajasthan, India
E-mail: ranjeetasoni@gmail.com

Received: 10 Aug 2026; Received in revised form: 13 Sep 2026; Accepted: 17 Sep 2026; Available online: 28 Sep 2026
©2026 The Author(s). Published by Infogain Publication. This is an open-access article *under* the CC BY license (https://creativecommons.org/licenses/by/4.0/).

Abstract**—** *Environmental Studies has evolved from an allied branch of natural sciences into an essential transdisciplinary domain addressing the complex interactions between human systems and the biosphere. In the context of the Anthropogenic—characterized by climate change, accelerating biodiversity loss, and systemic pollution—understanding environmental dynamics is vital for human survival and sustainable development. This review paper examines the core importance of environmental studies, synthesizes its historical and contemporary trajectories, and maps out emerging future scopes. Key areas such as climate modeling, circular economy, ecological economics, environmental justice, and technological integration (AI, GIS, and remote sensing) are highlighted. The paper concludes with a strategic roadmap for research, policy harmonization, and educational reform necessary to achieve long-term ecological balance.*

Keywords**— *Environmental Studies, Planetary Health, Circular Economy, Climate Mitigation, Biodiversity Conservation, Environmental Governance, Sustainable Development.***

I. INTRODUCTION

The Earth system is experiencing unprecedented stress due to rapid urbanization, industrialization, population growth, and unsustainable resource consumption. Human activities have pushed several planetary boundaries—including climate change, ocean acidification, and nitrogen-phosphorus cycles—beyond safe operating zones.

Environmental Studies is an integrative, multi-disciplinary field that bridges the natural sciences, social sciences, humanities, law, and engineering to analyze and address these complex environmental challenges. Unlike traditional siloed disciplines, Environmental Studies analyzes the interconnectedness of biological, physical, chemical, socio-economic, and political dimensions of environmental issues.

The objective of this review paper is to evaluate the crucial role Environmental Studies plays in modern decision-making, explore its foundational importance across key sectors, and delineate the emerging future scopes that will define the field over the coming decades.

II. CORE IMPORTANCE OF ENVIRONMENTAL STUDIES

The significance of environmental studies spans ecological, social, economic, and health dimensions. Its core importance can be categorized into four interconnected domains:

2.1 Preserving Biodiversity and Ecological Services

Ecosystems provide vital services—such as pollination, soil fertility, carbon sequestration, and water purification—that sustain human life. An environmental study provides the framework to assess ecosystem functions, measure species loss, and formulate science-based conservation strategies (e.g., habitat restoration, wildlife corridors, and protected area management).

2.2 Human Health and "Planetary Health"

Environmental degradation directly impairs human health. Air pollution causes millions of premature deaths annually, contaminated water vectors waterborne diseases, and chemical toxins disrupt endocrine systems. Environmental studies links environmental quality to public health, giving rise to the concept of **Planetary**

Health—the understanding that human health relies on the health of Earth's natural systems.

Table 1: Structure of Environmental Studies

ENVIRONMENTAL STUDIES				
Natural Sciences	**Applied Sciences**	**Social Sciences**	**Policy & Law**	**Advanced Tech / Data**
Core Disciplines: Ecology, Biology, Chemistry, Physics. **Focus:** Understanding the physical, chemical, and biological mechanisms of the natural world and ecosystems.	**Core Disciplines:** Engineering, Agronomy, Biomedical Sciences. **Focus:** Practical applications, technological solutions, agricultural management, and human health impacts.	**Core Disciplines:** Economics, Sociology, Ethics. **Focus:** How human societies, behavior, resource allocation, and moral frameworks interact with the environment.	**Core Disciplines:** Legislation, Governance, Treaties. **Focus:** Developing regulations, political frameworks, legal boundaries, and international agreements to protect ecosystems.	**Core Disciplines:** AI, Remote Sensing, GIS (Geographic Information Systems). **Focus:** Utilizing cutting-edge computation, satellite mapping, spatial tracking, and data analysis to monitor and solve environmental challenges.

2.3 Resource Management and Food-Water-Energy Security

The world faces escalating pressure on finite resources. Environmental studies offers tools like Environmental Impact Assessments (EIA), Life Cycle Assessment (LCA), and integrated resource management to ensure that land, water, minerals, and energy are utilized sustainably without exhausting natural stocks.

2.4 Policy, Governance, and Economic Resilience

Environmental degradation carries severe economic consequences through natural disasters, agricultural decline, and health costs. Research in environmental studies informs international treaties (such as the Paris Agreement and the Kunming-Montreal Global Biodiversity Framework), national environmental laws, and economic mechanisms like carbon pricing.

III. COMPARATIVE OVERVIEW: TRADITIONAL VS. EMERGING SCOPES

The scope of environmental studies has broadened from basic pollution control to complex, technology-driven ecosystem management.

Table 2: Comprehensive Overview

Dimension	Traditional Focus	Emerging & Future Horizon
Primary Approach	Reactive (end-of-pipe pollution cleanup)	Proactive (circular design, regenerative systems)
Key Methodologies	Field sampling, physical chemistry	AI modeling, satellite remote sensing, IoT sensor networks
Energy Domain	Fossil fuel conservation & risk mitigation	Renewable systems, green hydrogen, grid decarbonization
Economic Integration	Environmental compliance as a cost center	ESG frameworks, natural capital accounting, carbon markets
Social Focus	General environmental awareness	Climate justice, indigenous knowledge integration, eco-anxiety research

4. Emerging Scopes and Future Research Horizons

As global environmental systems approach critical tipping points, Environmental Studies is branching into several high-priority future domains:

4.1 Climate Adaptation, Resilience, and Decarbonization Technologies

While historical focus was on documenting climate change, the future scope shifts toward operationalzing solutions:

- **Carbon Dioxide Removal (CDR):** Studying direct air capture, enhanced rock weathering, and soil carbon sequestration.
- **Climate Adaptation Engineering:** Designing resilient urban infrastructure, coastal defenses, and heat-resistant agricultural practices.
- **Energy Transition Integration:** Evaluating the ecological land footprints of massive solar, wind, and battery storage projects to minimize local ecological disruption.

4.2 Artificial Intelligence, Remote Sensing, and Big Data Analytics

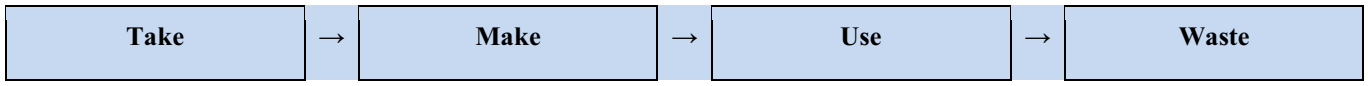
Technological integration represents one of the fastest-growing scopes within environmental science:

- **Earth Observation & GIS:** Satellite imagery combined with deep learning algorithms enables real-time deforestation tracking, illegal fishing monitoring, and precision biodiversity inventorying.
- **Predictive Environmental Modeling:** Machine learning models predict microclimate shifts, extreme weather events, and pollution dispersion patterns with high accuracy.

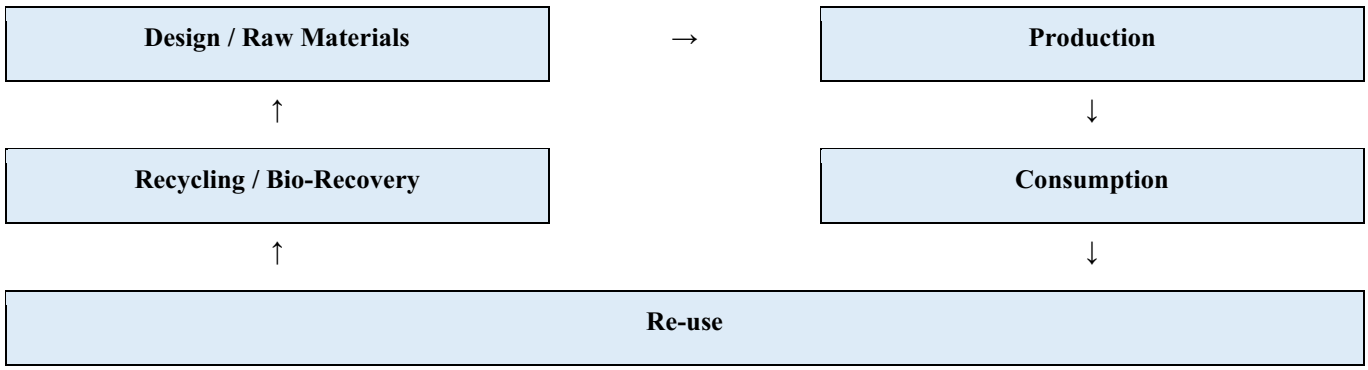
4.3 Circular Economy and Eco-Industrial Systems

The future of waste management lies in eliminating the concept of waste entirely through circular economy models:

- **Bioremediation & Biomimicry:** Engineering microorganisms and plants to detoxify heavy metals, micro plastics, and synthetic chemical pollutants.
- **Material Stewardship:** Designing products for closed-loop recycling, reducing resource extraction dependence, and managing electronic waste (e-waste) streams.
- **Linear Economy:**



- **Circular Economy:**



4.4 Environmental Justice, Governance, and Indigenous Knowledge

Technical solutions alone cannot solve environmental crises without social equity:

- **Environmental Justice:** Investigating the disproportionate exposure of low-income and marginalized communities to environmental hazards and climate impacts.
- **Traditional Ecological Knowledge (TEK):** Integrating indigenous land stewardship practices with modern conservation science to improve ecological management outcomes.

4.5 Corporate Sustainability, ESG, and Green Finance

The private sector increasingly relies on environmental expertise to align with environmental, social, and governance (ESG) expectations:

- **Natural Capital Accounting:** Assigning economic value to ecosystem services so corporations incorporate ecological costs into their balance sheets.
- **Scope 1, 2, and 3 Emissions Auditing:** Developing accurate carbon accounting frameworks across complex global supply chains.

IV. KEY CHALLENGES AND OBSTACLES

Despite its growing relevance, the field faces key structural and operational challenges:

1. **Science-Policy Gap:** Scientific research often struggles to translate into actionable policy due to political resistance, short electoral cycles, and lobby interests.
2. **Data Fragmentation:** In developing regions, critical environmental data—such as baseline biodiversity counts or local hydrologic health—remains incomplete or underfunded.
3. **Transdisciplinary Silos:** Academics in technical fields (such as chemistry or engineering) and social fields (such as policy or ethics) often work in isolation, limiting holistic solutions.

V. CONCLUSION

Environmental Studies is no longer merely an academic exercise in observing natural ecosystems; it is an applied, multi-faceted discipline vital for global stability and human survival. By unifying physical sciences, advanced technologies, economics, and social justice, environmental studies provides the analytical tools required to navigate the Anthropogenic. Moving forward, expanding the scope of environmental research into AI-driven conservation, circular economic models, and equitable governance will be essential to foster a resilient planet.

REFERENCES

[1] Costanzia, R., et al. (2014). *Changes in the global value of ecosystem services*. Global Environmental Change, 26, 152-158.

[2] IPCC (2023). *Climate Change 2023: Synthesis Report. Contribution of Working Groups I, II and III to the Sixth Assessment Report of the Intergovernmental Panel on Climate Change*. IPCC, Geneva, Switzerland.

[3] Rockström, J., et al. (2009). *A safe operating space for humanity*. Nature, 461(7263), 472-475.

[4] Steffen, W., et al. (2015). *Planetary boundaries: Guiding human development on a changing planet*. Science, 347(6223), 1259855.

[5] UNEP (2021). *Making Peace with Nature: A scientific blueprint to tackle the climate, biodiversity and pollution emergencies*. *United Nations Environment Programme, Nairobi.*

[6] World Health Organization (2022). *Ambient (outdoor) air pollution and health*. *WHO Fact Sheets.*

International Journal of Environment, Agriculture and Biotechnology
Vol-11, Issue-5; Sep-Oct, 2026
Peer-Reviewed International Journal
Journal Home Page Available: https://ijeab.com/
Journal DOI: 10.22161/ijeab

In vitro and field evaluation of some sole and combination fungicides against *Rhizoctonia solani* causing sheath blight disease of rice (*Oryza sativa* L.) in Eastern Gangetic Plain zone of West Bengal, India

Debargha Patra[1], Birendranath Panja[1], D. K. Patra[2], Ashim Midya[3,*]

[1]Department of Plant Pathology, Bidhan Chandra Krishi Viswavidyalaya, Mohanpur, 741235, West Bengal, India
[2]Plant Pathology Discipline, Rice Research Station, Chinsurah, Hooghly 712 102 West Bengal, India
[3]Department of Agriculture, Govt. of West Bengal, India
*Corresponding Author: ashimbckv@gmail.com ORCID: 0000-0002-6662-249 X

Received: 23 Aug 2026; Received in revised form: 21 Sep 2026; Accepted: 26 Sep 2026; Available online: 03 Oct 2026
©2026 The Author(s). Published by Infogain Publication. This is an open-access article *under* the CC BY license (https://creativecommons.org/licenses/by/4.0/).

Abstract— *Rhizoctonia solani causing sheath blight disease of rice is one of the most important and prominent fungus in West Bengal as well as other rice growing areas of the world and cause severe yield loss of rice. Due to lack of resistant donor line, a few resistant variety is available for combating the attack of the pathogen and so screening and selection of suitable fungicides is of utmost importance for effective disease management for ensuring sustainable rice production. Due to continuous application of same chemical and global climate crisis, development of resistance is on an increasing trend. Evaluation and screening of new generation fungicide molecules play a pivotal role in Integrated Disease Management for rice sheath blight. Experiment both in vitro and field evaluation, were conducted during the* kharif *(wet) seasons of 2024 and 2025 at Rice Research Station, Chinsurah, West Bengal, India to evaluate the relative efficacy of some new fungicide formulations against sheath blight disease of rice caused by* Rhizoctonia solani. *Two sprays of Mancozeb 50% + Thiophanate-methyl 25% WG @ 3.0 g/L were highly effective in reducing sheath blight disease severity and improving grain yield. Under* in vitro *conditions, the minimum* EC_{50} *value (1.69 ppm) was also recorded for Mancozeb 50% + Thiophanate-methyl 25% WG, indicating that it was the most effective fungicide formulation among those tested and can be effectively recommended for Integrated Disease Management in rice for ensuring sustainable rice production.*

Keywords— ***Rice, Sheath Blight, Rhizoctonia solani, New Fungicide Formulations, Integrated Disease Management, Resistant Development, Field Evaluation, Resistant Donor***

I. INTRODUCTION

Rice (*Oryza sativa* L.), a member of Poaceae, is the staple food for half of the population across the globe and plays a pivotal role in food security and global agricultural economy (Midya, 2025) and feeding more than 9 billion people by 2050 will require doubling of production on sustainable basis (Midya *et al*., 2021)Being the major cultivated cereal of West Bengal, rice has invariably imbued the social and cultural spheres of Bengali culture, performed pivotal role in religious attainment, spiritual liberation and in all aspects became a ubiquitous symbol for the Bengali cultural expression (Samaddar, 2006). West Bengal is the richest reservoir of rice bio-diversity and the rice bowl of the country. Among the biotic stresses, drought, weed infestation, insect pest, disease infestation are the predominantly retardant factors limiting productivity of rice (Midya, 2025), rice is attacked by 36 fungal diseases (11 foliar diseases, 11 stem, leaf sheath and root diseases, 3 seedling diseases and 12 grain and inflorescent diseases), 6 bacterial, 21 viral and mycoplasmal, 6 nematode diseases as well as 4 physiological disorders (Ou, 1985). Among these fungal

diseases sheath blight caused by *Rhizoctonia solani* Kuhn is one of the most important diseases of rice during the *kharif* season in West Bengal as well as in almost all rice growing areas of India (Reddy and Reddy,1986; Biswas, 2000). The disease causes about 11.1- 58 % losses in yield depending on the disease severity and varieties (Chahal *et al*.,2003). There is also strong relationship between disease severity and yield reduction (Marchetti and Bollich, 1991). Presently, due to lack of resistant donor lines, a very few resistant varieties are available to the farmers so management practice with fungicides is the most important practical solution to control the disease. Due to continuous use of same chemical year after year there may develop resistance against the chemicals. Moreover, due to extreme climate variability resulted in ecological intensification, resistance and modification of the behavior of pest and pathogens under the backdrop of global climate crisis (Midya, 2026). So, for the effective management of rice sheath blight disease to ensure sustainable rice production, under the context of ever increasing resistance development and global warming, new generation fungicidal formulations were evaluated accordingly.

II. MATERIALS AND METHODS

2.1, Isolation of *Rhizoctonia solani* from diseased samples:

The disease samples were cut in small pieces and washed in water to remove the soil particles and other dirt materials. During isolation these bits were surface sterilized by 0.1% HgCl2 solution for 40 seconds followed by washing 5-6 times in sterile distilled water. The bits were transferred by using forceps on sterile blotting paper to remove the excess moisture through blotting. Then those bits were transferred on to PDA medium in Petri plates which were placed in BOD incubator for incubation at 28 ± 2° C for 24-72 hours. When the fungal growth was visible, a tiny bit of mycelium was taken from the isolation plate and transferred to PDA containing culture slant and incubated again at 28°C with the objective of having pure culture. The pure culture was maintained and stored in refrigerator at 5ºC for further studies. The fungi were sub cultured at 20 days interval on PDA medium to maintain vigour and vitality.

2.2, Preparation of mass culture of *Rhizoctonia solani* for field inoculation:

Rice leaf sheath was collected and cut it into small pieces of 2 -3 cm. Cut pieces were water soaked 12 hours; excess water was drained out; water-soaked pieces were transferred to open mouth bottles and closed with a cotton wool plug. The bottles with water-soaked straw were sterilized at 15 psi for 20 minutes for two successive days. The six mycelial discs of 9 mm diameter of 3 days old culture of *R. solani* grown on the PDA medium was cut and used to inoculate sterilized water-soaked straw kept in the bottles. The bottles were then incubated at room temperature (28 ± 2°C) for 14 days and the inoculum thus prepared was used for subsequent studies.

2.3, Artificial inoculation of *Rhizoctonia solani* in the field:

R. solani pathogen grown on sterilized straw bits was used as a source of inoculum for artificial inoculation of rice plant under field condition. The tillers to be inoculated with the pathogen were tied using rubber band or piece of rope. At tillering stage, the test entries were inoculated by placing the colonized straw at the centre of the hill just above the water line.

2,4, Fungicide sensitivity analysis:

Five varying concentrations (excluding) of six fungicides viz, Mancozeb 50% + Thiophanate methyl 25% WG, Picoxystrobin 7.05% + Propiconazole 11.7 SC, Azoxystrobin14% + Epoxiconazole 9% SC, Tebuconazole 50% + Trifloxystrobin 25% WG, Propiconazole 25EC and Mancozeb 75 WP were prepared from their respective stock solution. Then the required and calculated volume of each fungicide concentration was poured in sterile Petri plate in triplicate. Then, the molten PDA medium of 20 ml was poured inside the Petriplatewith the help of sterilized micro tips with 200 µ and 1000 µ capacities, mixed thoroughly to obtain the desired concentrations of active ingredients. Control plates were maintained by the addition of same volume of PDA medium in the Petri plates without the addition of any fungicide. Then five mm mycelial discs were cut out from the periphery of 3 days old actively growing cultures with the help of sterilized cork borer and placed at the centre of the Petri plates. Plates were incubated at 28±1^0 C temperature in BOD till the fungal growth covers the entire Petri plate used as control. Radial growth of the fungus on different fungicide concentrations and control was recorded. Extent of inhibition of mycelial growth by each fungicide was calculated by estimating the percent reduction in mean mycelial radial growth over the control (Vincent,1947). Effective concentration for 50% mycelial growth inhibition (EC_{50}) by the fungicides for the fungus was determined by plotting the log values of the fungicide concentration against the probit values of percent inhibition on a log-probit scale (Horsefall, 1956). A regression equation Y = a + bx (Y = antilog of concentration of the fungicide, x = probit value of percent inhibition, b = regression co-efficient/ slope, a = intercept). was worked out and then fitness of the equation was judged comparing the level of significance with the simple

correlation coefficient (r) value at 5% or 1% level. Percent inhibition was measured with the formula, which is given below,

$$\text{Percent inhibition} = \frac{\text{Radial growth in control (C)} - \text{Radial growth in treatment (T)}}{\text{Radial growth in control (C)}} X\ 100$$

2.5, Evaluation of fungicides for the management of sheath blight disease under field condition:

Besides *in vitro* efficacy testing, the fungicides were evaluated under field condition for two consecutive *kharif* (wet) seasons at Rice Research Station, Govt of West Bengal,Chinsurah (Elevation – 8.62 m above mean sea level, latitude- 22° 52´ N, longitude – 88°24´ E), West Bengal. Seven treatments comprising of the said six fungicides with a suitable control were considered, Out of six, four combination fungicides viz, Mancozeb 50% + Thiophanate methyl 25% WG @ 3.0g/L, Picoxystrobin 7.05% + Propiconazole 11.7 SC @2.0 ml /L, Azoxystrobin14% + Epoxiconazole 9% SC @1.5 ml/L, Tebuconazole 50% + Trifloxystrobin 25% WG @0.4 g/L and two sole fungicides viz. Propiconazole 25EC @ 1.0 ml/L and Mancozeb 75 WP @ 1.0 ml/L were evaluated against sheath blight disease of rice. Twenty-five days old seedlings of sheath blight susceptible cultivar Swarna (MTU-7029) were transplanted with 15×15 cm spacing in a randomized complete block design with four replications (plot size 2.1 m× 2.0 m). Uniform fertilizer dose of 120 kg N, 50 kg P_2O_5 and 30 kg K_2O ha^{-1} (both basal and split) was applied in all the trial plots and standard agronomic practices were followed.

All the plants except the border rows were inoculated with ten days old highly virulent culture of the pathogen by the 'straw-bit' plugging method (Rao and Kannaiyan,1973) during the active tillering stage. Fungicides were sprayed twice at an interval of ten days starting from the initial symptom development. After ten days of last spray, final disease incidence was recorded from ten randomly affected plants in each treatment. Plants were assessed individually using SES (0-9) scale (IRRI, 1996).

SES (0-9) scale (1996) for sheath blight disease:

Scale	Description of the scale
0	0 = No infection
1	Vertical spread of the lesions up to 20% of plant height
3	Vertical spread of the lesions up to 21-30%% of plant height
5	Vertical spread of the lesions up to 31%-45% of plant height
7	Vertical spread of the lesions up to 46%-65% of plant height
9	Vertical spread of the lesions up to 66%-100% of plant height

Disease severity was calculated using the following formula:

$$\frac{0(N)_0 + 5(N)_1 + 10(N)_3 + 30(N)_5 + 50(N)_7 + 100(N)_9}{\text{Total no. of tillers of the hill observed}} X\ 100$$

Where, N_0-N_9 = No. of tillers / hill, classified as 0-9 grades respectively, according to SES (0-9) scale for rice. Grain yield recorded on plot basis were converted to kg ha^{-1} for statistical analysis.

III. RESULTS AND DISCUSSION

Determination of effective concentration of fungicides for 50% mycelial growth inhibition (i.e. EC50) of *Rhizoctonia solani*:

Based on regression equation of high correlation value, the effective concentrations of six fungicides for 50% growth inhibition (EC_{50}) of *Rhizoctonia solani* using six concentrations including control were calculated to assess the degrees of its sensitivity towards the fungicides. The EC_{50} values were found to be ranged between 1.23 ppm and 30.19 ppm, with Propiconazole 25% EC being lowest and Mancozeb 75% WP being highest. Among combo products maximum value was noted for Picoxystrobin 7.05% + Propiconazole 11.7 SC (7.07ppm) and minimum value was noted for Mancozeb 50% + Thiophanate methyl 25% WG (1.69 ppm), intermediate values were noted for Tebuconazole 50% + Trifloxystrobin 25% WG (5.75ppm) and Azoxystrobin 14% + Epoxiconazole 9% SC (2.13ppm). Between two sole products Mancozeb75%WP showed the highest EC_{50} value of 30.19 ppm and Propiconazole 25% EC showed the lowest EC_{50} value of 1.23 ppm. The literature on EC_{50} value of all the combo products used at the present experiment against *R. solani* was not available. However, Gong *et al*. (2022) mentioned the EC_{50} range for Epoxiconazole to be between 0.03 and 0.15 µg/mL, with an average EC_{50} value of 0.100 µg/ml and the EC_{50} values for Tebuconazole ranged from 0.02 to 0.23 µg/ml with an average EC_{50} of 0.109 µg/ml. Panja *et al.* (2013) when attempted to determine the EC_{50} value of 10 isolates of *R. solani* using Propiconazole and Mancozeb, they found EC_{50} value within the range of 0.327 to 4.385 and 7.980 to 23.067 ppm respectively.

Table1. Determination of effective concentration of different fungicides (in ppm) for 50% growth inhibition (EC_{50}) of Rhizoctonia solani using regression equation

Name of the chemicals	Regression equations	Simple correlation coefficients (r)	EC_{50} (in ppm)
T1- Mancozeb 50% + Thiophanate methyl 25% WG	Y = 3.3723x + 4.2224	0.829*	1.69
T2- Picoxystrobin 7.05% + Propiconazole 11.7% SC	Y = 4.3151x + 1.3111	0.783	7.07
T3- Azoxystrobin 14% + Epoxiconazole 9% SC	Y = 2.15x + 4.2787	0.721	2.13
T4- Tebuconazole 50% + Trifloxystrobin 25% WG	Y = 5.7446x + 0.6514	0.869*	5.75
T5- Propiconazole 25% EC	Y = 3.3187x + 4.6972	0.885*	1.23
T6-Mancozeb 75% WP	Y = 3.2592x + 0.1525	0.999**	30.19

EC= Effective concentration and ppm = Parts per million; Y = Probit value of percent growth inhibition; x = Log of fungicide concentration; EC_{50}% (ppm) = Antilog of x

WG = Wettable granules,WP = Wettable powder, SC = Soluble concentrate, EC = Emulsifiable concentrates

Table value of simple correlation for 4 df at 5% = 0.811(*) and at 1% = 0.917(**)

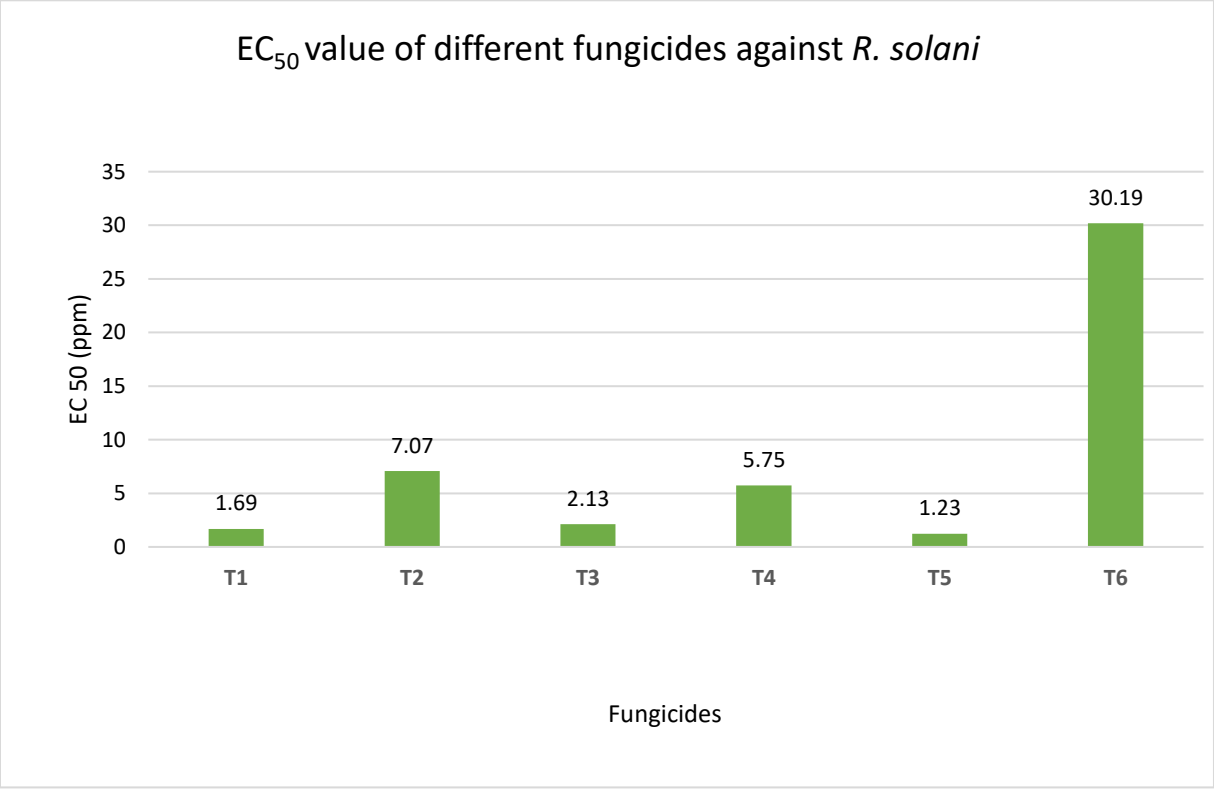
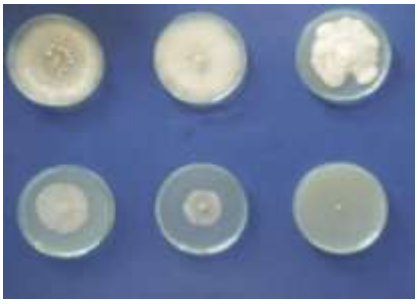
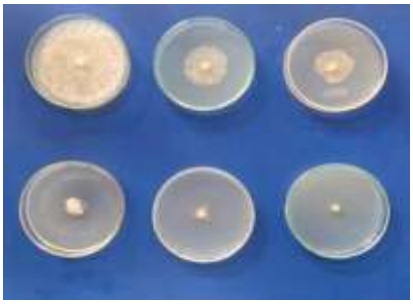


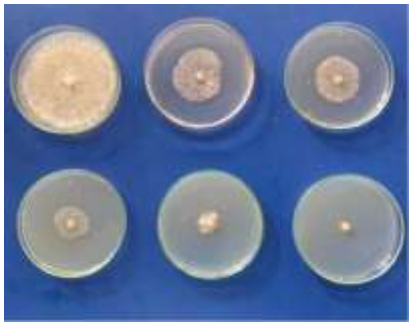
Fig.1: EC_{50} values of different fungicides in laboratory condition against R. solani



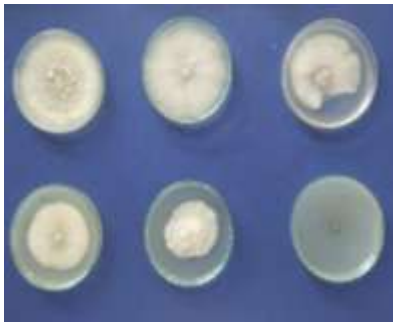
Mancozeb 50% + Thiophanate methyl 25% WG



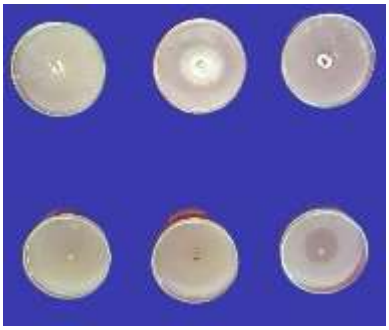
Azoxystrobin14% + Epoxiconazole 9% SC



Picoxystrobin 7.05% + Propiconazole 11.7%SC



Tebuconazole 50% + Trifloxystrobin 25% WG



Propiconazole 25% EC



Mancozeb 75 % WP

Plate 1: In vitro percent mycelial growth inhibition of Rhizoctonia solani by different fungicides at various concentrations

3.2, Management of sheath blight disease by reduction of PDI using fungicides under field condition:

Under field condition the efficacy of seven fungicides e.g. Mancozeb 50% + Thiophanate methyl 25% WG @ 3.0g/L, Picoxystrobin 7.05% + Propiconazole 11.7 SC @ 2.0 ml /L, Azoxystrobin14% + Epoxiconazole 9% SC @1.5 ml/L, Tebuconazole 50% + Trifloxystrobin 25% WG @0.4 g/L and two sole products of fungicides viz. Propiconazole 25% EC @ 1.0 ml /L as systemic fungicide and Mancozeb 75 WP @ 2.5 g /L as non-systemic fungicide was tested against sheath blight disease of rice. Plants were artificially inoculated in the field with *Rhizoctonia solani* at maximum tillering stage of growth by Straw-bit-Plugging method. After emergence of disease symptoms two sprayings of the above said chemicals were given at ten days interval.

All the fungicides significantly reduced the sheath blight infecton over untreated control (Table 2). Mancozeb 50% + Thiophanate methyl 25% WG @ 3.0 g/L was the best effective fungicide in checking sheath blight infection (Mean disease severity 22.75 %) and increasing grain yield by more than 5510 kg ha^{-1} over untreated check. This was followed by Propiconazole 25EC @ 1.0 ml/L and Tebuconazole 50% + Trifloxystrobin 25% WG

@ 0.4 g/L and Azoxystrobin14% + Epoxiconazole 9% SC @ 1.5 ml /L having 26.0, 28.25 and 34.62 percent disease severity respectively.

A maximum increase of 77.73 percent grain yield was achieved with Mancozeb 50% + Thiophanate methyl 25% WG @ 3.0 g/L, followed by by Propiconazole 25EC @ 1.0 ml/L with an increase of 74.32 percent, Tebuconazole 50% + Trifloxystrobin 25% WG @ 0.4 g/L with an increase of 67.25 percent and Azoxystrobin14% + Epoxiconazole 9% SC @ 1.5 ml /L with an increase of 64.52 percent over untreated control.

Table 2: Effect of some commercially available fungicides against sheath blight disease severity and yield of rice during kharif, 2024 &2025

Treatments	Dosages	Mean disease severity (%)	Percentage reduction of disease severity over control	Average grain yield (kg ha^{-1})	Per cent yield increase over control
T1-Mancozeb 50% + Thiophanate methyl 25% WG	3.0g/L	22.75 (28.43)	49.75	5510.5	77.73
T2- Picoxystrobin 7.05% + Propiconazole 11.7 SC	2.0ml/L	37.12 (37.46)	35.38	4795.5	54.69
T3- Azoxystrobin14% + Epoxiconazole 9% SC	1.5ml/L	34.62 (36.00)	37.88	5101.0	64.52
T4- Tebuconazole 50% + Trifloxystrobin 25% WG	0.4g/L	28.25 (32.07)	44.25	5185.5	67.25
T5- Propiconazole 25EC	1.0ml/L	26.0 (30.62)	46.5	5404.75	74.32
T6- Mancozeb 75 WP	2.5g/L	41.88 (40.29)	30.62	4320.0	39.33
T7- Untreated control	--	72.50 (58.41)	00	3100.5	_
SEm(±)		1.88		93.65	
CD(P=0.05)		5.54		275.47	

Figures in parentheses indicate angular transformed values and statics applied to them

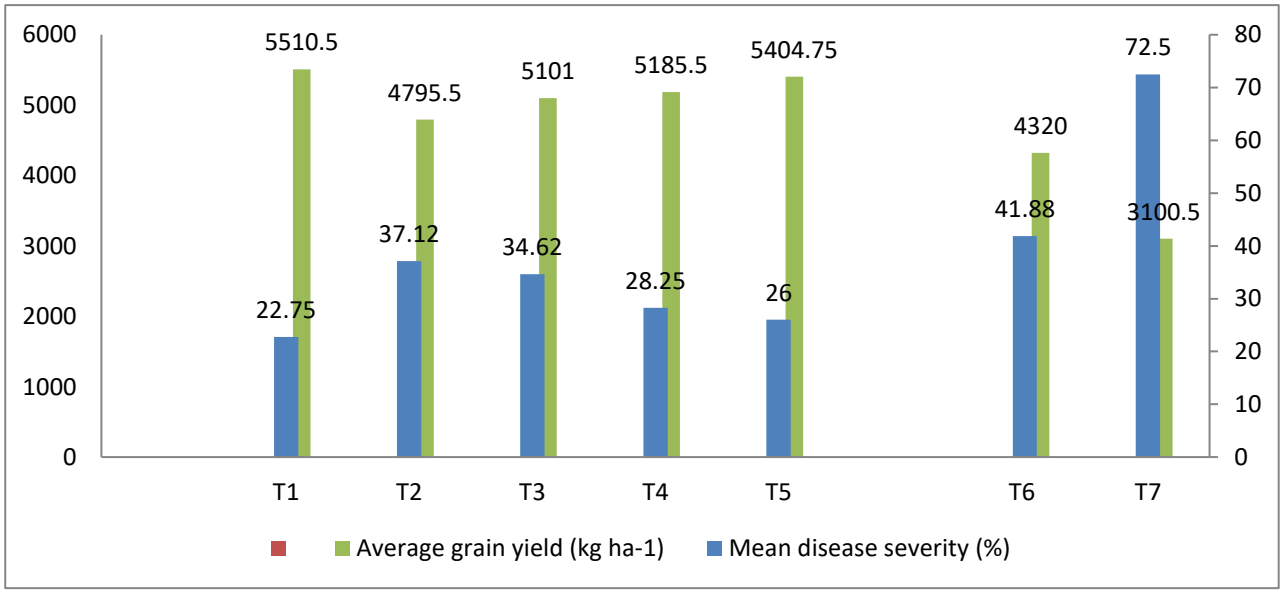


Fig.2: Bar Diagram showing Mean disease severity(%) and average grain yield(kg ha^{-1})

Under AICRIP, Mancozeb 50% + Thiophanate methyl 25% WG @ 3.0 g/L was also tested along with other commercially available fungicides against sheath blight disease of rice during *kharif,* 2023 and 2024 at several locatons. Mancozeb 50% + Thiophanate methyl 25% WGwas also proved highly effective at Chiplima,Moncompu and Rajendranagar (Anonymous, 2024).

IV. CONCLUSION

Two sprays of Mancozeb 50% + Thiophanate-methyl 25% WG @ 3.0 g/L were highly effective in reducing sheath blight disease severity and improving grain yield. Under *in vitro* conditions, the minimum EC_{50} value (1.69 ppm) was also recorded for Mancozeb 50% + Thiophanate-methyl 25% WG, indicating that it was the most effective fungicide formulation among those tested and can be effectively recommended for Integrated Disease Management in rice for ensuring sustainable rice production.

ACKNOWLEDGEMENT

Authors acknowledge the help received from Dr Indrani Dana, Ex- Joint Director of Agriculture (Rice Development), Rice Research Station, Chinsurah, Hooghly.

REFERENCES

[1] Anonymous .(2024). Progress Report 2024, volume – 2, Entomology and Plant Pathology, All India Coordinated Rice Improvement Programme, Directorate of Rice Research (ICAR), Rajendranagar, Hyderabad, India pp. 3.115-3.119.

[2] Biswas, A.(2000). Changing trends of rice diseases in West Bengal, India. *J. Mycopathol.Res.*38(1) pp.33-36.

[3] Chahal, K. S., Sokhi, S. S. and Rattan, G. S. (2003). Investigations on sheath blight of rice in Punjab.*Indian Phytopathology*, 56 pp.22-26.

[4] Gong, C., Liu, M., Liu, D., Wang, Q., Hasnain, A., Zhan, X., Pu, J., Liang, Y., Liu, X. and Wang, X. (2022). Status of fungicide resistance and physiological characterization of tebuconazole resistance in *Rhizoctonia solani* in Sichuan Province, China. *Current Issues in Molecular Biology*, 44(10) pp.4859-4876.

[5] Horsefall, J.G.(1956). Principles of fungicidal action.*Soil Science*, 82(4) pp.348

[6] IRRI, (1996). *Standard Evaluatonsystemfor Rice.*Internatonal Rice Research Institute, Manila, Philippines, pp.25.

[7] Midya, A. (2026). Insect Pest Challenges and Sustainable Management under Climate Resilient Regenerative Agricultural Production System, *NL Journal of Agriculture and Biotechnology* 3(3), pp**.** 01-02.

[8] Midya, A. (2025). Present Research Priority on Aerobic Rice Culture for Sustainable Rice Production under the Backdrop of Shrinking Resource Base: A Review. *Indian Journal of Agricultural Research* 59(3). Pp.339-350

[9] Midya, A., Saren, B. K., Dey, J.K., Maitra, S., Praharaj, S., Gaikwad, , D, J., Gabar, A., Alsanie, W. F., Hossain, A. (2021). Crop Estatablishment Methods and Integrated Nutrient Management improve: Part i: Crop Performance, Water Productivity and Profitability of Rice (*Oryza sativa* L.) in the Lower Indo- Gangetic Plain, India. *Agronomy.* 11, pp. 1860

[10] Midya, A., Saren, B. K., Dey, J.K., Maitra, S., Praharaj, S., Gaikwad, , D, J., Gabar, A., Alsanie, W. F., Hossain, A. (2021). Crop Establishment Methods and Integrated Nutrient Management Improve: Part II. Nutrient Uptake and Use Efficiency and Soil Health in Rice (Oryza sativa L.) Field in the Lower Indo-Gangetic Plain, India. *Agronomy* **11**,pp. 1894. https://doi.org/10.3390/agronomy11091894

[11] Marchetti, M.A. and Bollich, C. N.(1991). Quantification of the relationship between sheath blight severity and yield loss in rice. *Plant Dis*. 75 pp. 773-775.

[12] Ou, S. H.(1985). Rice Disease (2nd ed.) CAB International Mycological Institute, Kew, Surrey, U.K., p.272.

[13] Panja, B. N., Das, A. and Saha, J. (2013). Fungicide tolerance management of isolates of rice sheath blight pathogen (*Rhizoctonia solani*Kűhn), *J. Mycopathological. Res,* **51**(1): 163-168.

[14] Ranjan, C.P.D.(1987). Estimation of yield loss due to sheath blight of rice. *Ind. Phytopath*. 40 ,pp. 174-177.

[15] Rao,A.V. and Kannaiyan, S. (1973). An easy method of screening rice varieties for resistant to sheath blight disease. *Ind. J. Mycol. Pl.Pathol*. 3, pp. 106-107.

[16] Reddy, A.P.K. and Reddy, C.S. (1986). Present status of sheath blight disease and its control. *In Diamond Jubilee Souvenior* , Agri. Rea. Stn., Maruteru, Andhrapradesh, India pp. 118-127.

[17] Samaddar, A. (2006). Traditional and Post traditional: A Study of Agricultural Rituals in Relation to Technological Complexity among Rice Producers in Two Zones of West Bengal, India. Culture Agriculture**,** 28(2), pp 108-121.

[18] Vincent, J,Vincent, J. M. (1947). Distortion of fungal hyphae in the presence of certain inhibitors. *Nature*, 159(4051)pp. 850-850.

International Journal of Environment, Agriculture and Biotechnology
Vol-11, Issue-5; Sep-Oct, 2026
Peer-Reviewed International Journal
Journal Home Page Available: https://ijeab.com/
Journal DOI: 10.22161/ijeab

A Review on Farmers Expectations from Agricultural Produce Market Committee (APMCs) & e-NAM with Special Reference to Shrirampur APMC, Maharashtra, India

Dr. Ganesh S. Shinde, S.S. Temkar, Dattatray Katore

Asst. Professor, Dr. D. Y. Patil Vidyapeeth, Pune (Deemed-to-be University), Centre for Online Learning, Pune - 411018, Maharashtra, India
Email- ganesh.shinde.col@dpu.edu.in

Received: 14 Aug 2026; Received in revised form: 17 Sep 2026; Accepted: 21 Sep 2026; Available online: 03 Oct 2026
©2026 The Author(s). Published by Infogain Publication. This is an open-access article *under* the CC BY license (https://creativecommons.org/licenses/by/4.0/).

Abstract— *This research study focuses on the effectiveness of the Shrirampur Agriculture Produce Market Committee (APMC) and the challenges faced by farmers in participating in the Electronic National Agriculture Market (e-NAM) in India. The findings reveal that the Shrirampur APMC has partially fulfilled the expectations of local farmers in terms of fair pricing, market access, and transparency. While some farmers reported fair pricing and satisfactory market access, others expressed concerns about price manipulation and difficulties in reaching wider buyer bases. Transparency in transactions and information dissemination was also deemed inadequate by a significant number of farmers. The research also highlights the challenges faced by farmers in participating in e-NAM, including limited access to digital infrastructure, technological literacy, lack of awareness, complex registration procedures, and difficulties in navigating the online trading system. Indian farmers have high expectations for fair pricing through APMCs, emphasizing the need for transparent price discovery mechanisms, elimination of intermediaries' exploitative practices, and equitable remuneration. The conclusions drawn from the research suggest that farmers expect APMCs to ensure fair and competitive prices, provide adequate storage and transportation facilities, protect them from exploitative middlemen, assist in accessing credit facilities, and provide market information. Transparency, farmer engagement, communication, and education on e-NAM and technological tools were also highlighted as important factors to address farmers' concerns and promote their well-being and development.*

Keywords— ***Market Committee, Market Yard, Minimum Support Price, MSAMB, e-NAM.***

I. INTRODUCTION

Agricultural Produce Market Committees (APMC) are marketing boards established by state governments to reduce farmer exploitation by middlemen, in which farmers are forced to sell their produce at excessively cheap prices. All agricultural commodities must be brought to market, and transactions are conducted through auction. Mandi, the market place, is put up in various locations around the states. These markets divide the state geographically. Traders are granted license to run in a market. Mall owners, wholesale dealers, and retail traders are not permitted to acquire directly from farmers. Producer-sellers experienced a high marketing cost and suffered from illegal deductions of marketing charges, as well as the prevalence of different malpractices, under the conventional system of agricultural product marketing. Increased negotiating power of producer-sellers was seen as the most significant prerequisite of orderly marketing in order to improve marketing conditions and create fair competitive conditions. The Market Committee's responsibility in the market area is to carry out the

provisions of the Maharashtra Agricultural Produce Marketing (Regulation) Act 1963, as well as any rules and bye-laws made thereunder, and to provide such agricultural produce marketing facilities as the Director may direct from time to time. The Market Committee must also do any other activities necessary for market monitoring, direction, and control, as well as agricultural produce marketing. Market Committees may be created in the state under the terms of the Act. These Market Committees are building market yards for farmers and customers. The Act governs several agricultural output commodities. Currently, there are 306 APMCs, each with 623 market segments.

The exercise of public control over markets, i.e. the formation of regulated marketplaces in the country, has removed most of the flaws and malpractices in the previous agricultural marketing system. The National Agriculture Market (NAM) is a pan-India electronic trading system that connects the existing Agricultural Produce Market Committee (APMC) mandis across the country to develop a unified national market for agricultural commodities. The e-NAM portal provides a one-stop shop for all APMC-related information and services, including: Arrivals and pricing of commodities, Offers to buy and sell Provision for responding to trade offers, as well as other services Even when agricultural produce continues to flow through the mandis, the NAM minimises transaction costs and information irregularity.

National Agriculture Market (e-NAM) Scheme: In 2016, the Government of India established the National Agriculture Market (e-NAM) Scheme to build an online transparent, competitive agriculture market. Competitive bidding system is used to ensure that farmers receive fair rates for their produce. The

Government gives free software and help of 75 lakh per APMC mandi for relevant hardware, including quality assaying equipment and the building of infrastructure such as cleaning, grading, sorting, packaging, compost unit, and so on, under the e-NAM Scheme. More than 1.7 crore farmers and 2.3 lakh dealers had enrolled on the e-NAM portal as of December 31, 2022.

Current Status:

Currently, 1260 markets from 25 states and 3 UTs are connected to the e-NAM network.

The following APMC Act amendments must be made by States (State Agriculture Marketing Boards) interested in integrating their APMCs/mandis with NAM.

A single, state-wide trading licence that is unified

B) State-wide market fees collected in one location;

C) e-auction/e-trading provisions as a method of price discovery.

The market helps exporters and merchants in producing high-quality goods in large quantities at a single location and guarantees fair financial dealings. There are currently 203 commodities on e-NAM, up from 10 recently. Commodities can be found on the e-NAM portal Platform of Platforms (POP), which was introduced as part of the e-NAM (National Agriculture Market) on July 14, 2022, during the National Conference on Agriculture & Horticulture Ministers in Bangalore. Farmers can benefit from the option of receiving a portion of their payment in cash (up to the restrictions imposed by the relevant states) and keeping the remainder in their bank account for e-NAM exchange. This serves to reinforce the prime minister's commitment to the ease of doing business.

The perceived benefits of e-NAM include enhanced price discovery, expanded market reach, reduced transaction costs, improved transparency, reduced market manipulation, and increased competitiveness. However, challenges such as technical glitches, connectivity issues, lack of trust in online transactions, and limited integration of smaller traders were noted as drawbacks.

This research provides valuable insights into the expectations and challenges faced by Indian farmers in the context of APMCs and e-NAM, highlighting the need for policy interventions and support to enhance market access, transparency, and fair pricing for agricultural produce.

Prominent Examples of FPO:

Shrirampur APMC: Located in Ahmednagar district of Maharashtra, Shrirampur APMC is one of the

prominent agricultural produce market committees in the state. It plays a crucial role in facilitating the buying and selling of agricultural commodities in the region.

Vashi APMC: Situated in Navi Mumbai, Vashi APMC is one of the largest and busiest agricultural produce market committees in Maharashtra. It serves as a major hub for the trading of fruits, vegetables, spices, and other agricultural produce.

Pune APMC: Pune APMC, located in the city of Pune, is a significant agricultural market committee in Maharashtra. It handles the trade of various commodities, including fruits, vegetables, grains, and spices.

Nashik APMC: Nashik APMC, situated in the city of Nashik, is known for its thriving trade in onions and grapes. It is one of the largest markets for these commodities in India.

Mumbai APMC: Mumbai APMC, also known as the Vashi Market, is one of the most prominent agricultural produce market committees in Maharashtra. It serves as a

major trading center for fruits, vegetables, and other agricultural commodities in Mumbai and its surrounding areas.

Prominent Examples of APMC in India (outside Maharashtra):

Azadpur Mandi, Delhi: Located in Delhi, Azadpur Mandi is one of the largest wholesale fruit and vegetable markets in India. It is an important APMC that caters to the demands of the national capital region and neighboring states.

Malleshwaram APMC, Bangalore: Malleshwaram APMC is a significant market committee in Bangalore, Karnataka. It facilitates the trade of various agricultural commodities, including fruits, vegetables, and flowers.

Koyambedu Wholesale Market Complex, Chennai: Situated in Chennai, Tamil Nadu, the Koyambedu Wholesale Market Complex is a prominent APMC that handles the trading of fruits, vegetables, and flowers.

Kolkata Municipal Corporation Market, Kolkata: Kolkata Municipal Corporation Market, popularly

known as Burrabazar Market, is a major wholesale market in Kolkata, West Bengal. It caters to the trade

of various agricultural commodities and plays a vital role in the region's economy.

Guntur Market Yard, Andhra Pradesh: Guntur Market Yard is a significant agricultural market committee in Andhra Pradesh. It specializes in the trade of chili peppers and is recognized as one of the largest chili markets in Asia.

Marketing channels adopted by APMC in Maharashtra India:

Auction System: The auction system is a common marketing channel used by APMCs. Farmers bring their produce to the APMC market yards, where it is auctioned to registered buyers. The produce is displayed and bidders participate in a competitive bidding process, with the highest bidder securing the purchase. This system ensures transparency, fair pricing, and market-driven transactions.

Commission Agents: APMCs in Maharashtra often involve commission agents, also known as arhatiyas or adtiyas, who act as intermediaries between farmers and buyers. Commission agents facilitate the selling of produce on behalf of farmers by overseeing the auction process, negotiating prices, and arranging logistics. They charge a commission fee for their services.

Direct Sales: APMCs also provide platforms for farmers to engage in direct sales to buyers. Farmers can negotiate and sell their produce directly to buyers, bypassing the auction system. This marketing channel allows farmers to establish direct relationships with buyers and potentially obtain better prices.

Electronic Trading Platforms: With the advent of technology, APMCs have started adopting electronic trading platforms to enhance efficiency and transparency in the marketing process. Electronic National Agricultural Market (e-NAM) is one such platform implemented by APMCs across Maharashtra. e-NAM facilitates online trading, price discovery, and transparent bidding processes, enabling farmers to access a wider market and buyers to procure produce from different regions.

Wholesale Traders: APMCs act as hubs for wholesale traders who purchase agricultural commodities in bulk and distribute them to retailers, processors, or exporters. These wholesale traders operate within the APMC premises and play a vital role in bridging the gap between farmers and end consumers or industrial buyers.

Grading and Packaging Services: APMCs often provide grading and packaging services to farmers.

Grading involves sorting produce based on quality and size, ensuring consistency in the market. Packaging services help in preserving the quality and extending the shelf life of the produce, making it more marketable.

Storage and Warehousing Facilities: APMCs generally offer storage and warehousing facilities to farmers and traders. These facilities enable farmers to store their produce temporarily, helping them manage market fluctuations and prevent post-harvest losses. Warehousing services also ensure the availability of commodities throughout the year.

II. REVIEW OF LITERATURE

Sharma, R. K.; Kumar, S.; Singh, R.Journal: Agricultural Economics Research

This review examines the role of Agricultural Produce Market Committees (APMCs) and explores the reforms implemented to enhance agricultural marketing channels. The study analyzes the impact of APMC reforms on market efficiency, price discovery, and farmer-beneficial initiatives. It highlights the challenges and opportunities associated with APMC operations and suggests policy measures to improve the functioning of agricultural marketing systems.

Singh, S. P.; Kumar, R.; Singh, A. K. :

This review focuses on the significance of Agricultural Produce Market Committees (APMCs) in agricultural marketing. It explores the regulatory functions performed by APMCs, such as quality control, grading, and dispute resolution. The study examines the challenges faced by

APMCs in ensuring fair pricing and market access for farmers. It suggests strategies for improving APMC operations and strengthening farmer-buyer relationships.

Verma, N.; Srivastava, N. :

This review provides insights into the marketing channels used for agricultural commodities. It discusses various marketing intermediaries involved, such as commission agents, wholesale traders, and electronic

trading platforms. The study highlights the role of these channels in connecting farmers with buyers and examines their impact on price determination and market efficiency. It emphasizes the need for efficient marketing channels to enhance farmers' income and market competitiveness.

Khanna, K.; Tripathi, A.:

This review focuses on electronic trading platforms in agricultural markets, with a specific emphasis on initiatives like the Electronic National Agricultural Market (e-NAM). It examines the advantages and challenges of implementing electronic platforms for agricultural trade. The study evaluates the impact of e-NAM on price discovery, transparency, and market access for farmers. It provides insights into the potential benefits of technology-driven solutions in agricultural marketing.

Pandey, N., Roy, D.:

This critical analysis reviews the Agricultural Produce Market Committee (APMC) system and the Electronic National Agricultural Market (e-NAM) initiative. It examines the objectives, functioning, and challenges of APMCs and evaluates the effectiveness of e-NAM in transforming agricultural marketing. The study discusses the implications of market reforms on farmer welfare, market integration, and price realization. It offers policy recommendations for strengthening the APMC system and leveraging technology for efficient agricultural markets.

OBJECTIVES:

1. To assess the effectiveness of Shrirampur APMC in meeting the expectations of local farmers.
2. To identify the challenges faced by farmers in selling their produce through APMCs and e-NAM.
3. To analyse the expectations of Indian farmers from APMCs in terms of fair pricing, transparency, and market access.
4. To evaluate the impact of e-NAM on the functioning of APMCs and farmers expectations.

RESEARCH QUESTIONS:

1. To what extent does Shrirampur APMC fulfill the expectations of local farmers in terms of fair pricing, market access, and transparency?
2. What specific challenges do farmers face when participating in e-NAM for marketing their agricultural commodities?
3. What are the specific expectations of Indian farmers regarding fair pricing for their agricultural produce through APMCs?
4. What are the perceived benefits and drawbacks of e-NAM from the standpoint of APMC administrators and farmers?
5. To what extent has e-NAM met the expectations of farmers in terms of improving price discovery, transparency, and market access?

III. RESEARCH METHODOLOGY

Secondary data: The different available sources such as research paper, shrirampur taluka farmers opinion, APMC Profiles, farmers interactions, agro own newspaper, times of agriculture e-magazines, journals, articles, reports from MSAMB and case studies were supportive were collected for secondary data.

Scope of the Research:

The scope would include assessing the performance of Shrirampur APMC in meeting farmers' expectations, identifying specific challenges faced by farmers in selling their produce through APMCs and e-NAM, and analysing farmers' expectations regarding fair pricing, transparency, and market access.. The study would focus on evaluating the extent to which e-NAM has met farmers' expectations in terms of improving price discovery, transparency, and market access. The scope of research would likely involve data collection through surveys, interviews, and possibly observations to gather insights and opinions from farmers and stakeholders.

RESEARCH FINDINGS:

1. **Effectiveness of Shrirampur APMC:**

   Shrirampur APMC has partially fulfilled the expectations of local farmers in terms of fair pricing, market access, and transparency. Farmers reported varying levels of satisfaction with the pricing mechanism, with some experiencing fair pricing while others expressing concerns about price manipulation. Market access was found to be satisfactory for some farmers, but others faced challenges in reaching a wider buyer base and accessing distant markets. Transparency in transactions and information dissemination was

deemed inadequate by a significant number of farmers.

2. **Challenges faced by farmers in e-NAM participation:**

   Farmers encountered several challenges when participating in e-NAM for marketing their agricultural commodities. Limited access to digital infrastructure and technological literacy posed significant barriers for farmers to engage effectively with the e-NAM platform. Lack of awareness about the functioning and benefits of e-NAM, complex registration procedures, and difficulties in navigating the online trading system.

3. **Expectations of Indian farmers regarding fair pricing through APMCs:**

   Indian farmers have high expectations for fair pricing of their agricultural produce through APMCs. They expect transparent price discovery mechanisms, elimination of intermediaries' exploitative practices, and equitable remuneration for their efforts and investments. Farmers emphasized the need for price stability, protection against market fluctuations, and fair returns that reflect the quality and market demand for their produce.

4. **Perceived benefits and drawbacks of e-NAM:**

   APMC administrators and farmers acknowledged the potential benefits of e-NAM in terms of enhanced price discovery, expanded market reach, and reduced transaction costs. Improved transparency, reduced market manipulation, and increased competitiveness were seen as positive outcomes of e-NAM implementation. However, challenges such as technical glitches, connectivity issues, lack of trust in online transactions, and limited integration of smaller traders were noted as drawbacks of e-NAM.

5. **Impact of e-NAM on farmers' expectations:**
   While e-NAM has made strides in improving price discovery and transparency, its impact on market access for farmers has been relatively limited. Farmers expressed mixed opinions about the extent to which e-NAM has improved their market access and bargaining power. Some farmers reported positive experiences with expanded buyer options and better prices, while others faced challenges in realizing the full benefits of e-NAM due to infrastructural constraints and limited awareness.

IV. CONCLUSIONS

1. Farmers expect the Agriculture Produce Market Committee (APMC) to ensure that they receive fair and competitive prices for their products. This can be achieved by creating regulated markets and ensuring that farmers are paid appropriately for their produce.
2. The APMC is also responsible for supporting farmers by providing them with adequate storage and transportation facilities. These facilities are crucial in preventing damage to the produce and ensuring that it reaches the market in good condition.
3. Another expectation from farmers is protection from middlemen who exploit them by purchasing their products at low prices and selling them at higher prices. The APMC should safeguard farmers from such practices and ensure that they receive fair prices for their produce.
4. Access to credit facilities is also important for farmers, and they expect the APMC to assist them in this regard. The APMC can help farmers obtain loans from banks and other financial institutions and provide subsidies for agricultural inputs.
5. Farmers rely on the APMC to provide them with market information, including current prices and quality standards. This information enables farmers to make informed decisions and secure the best possible prices for their produce.
6. Displaying price information for incoming commodities in an electronic format or on notice boards at the entrance of the market committee is a necessary step to promote transparency.
7. The Chairperson of the Market Committee should organize farmer meetings on a quarterly basis in each taluka to address their difficulties and concerns.
8. The market committee secretariat should engage with farmers to analyze price fluctuations in agricultural commodities and find suitable solutions.
9. The APMC should arrange meetings to communicate and share the annual expenditure and profit of the market committee with farmers, promoting transparency.
10. Providing information on minimum support prices for agricultural commodities is an important responsibility of the APMC.
11. Farmers expect to receive the correct price for their produce during auctions, ensuring a fair and transparent process.

12. The APMC should conduct auctions in a transparent manner, maintaining fairness and integrity.
13. Preventing farmers from being exploited by traders during the auction process is a key objective for the APMC.
14. Implementing various programs to assist farmers is crucial for their well-being and development.
15. Farmers expect guidance from the APMC in response to price changes, helping them navigate market fluctuations.
16. The APMC should educate farmers on how to check online prices on the Maharashtra State Agricultural Marketing Board (MSAMB) websites.
17. Providing information on e-NAM (Electronic National Agriculture Market) is necessary to ensure farmers can access wider markets.
18. Educating farmers about MSAMB Apps can empower them to leverage technology for their benefit.
19. Establishing suitable warehousing and cold storage facilities is essential to preserve the quality and value of farmers' produce.
20. Farmers expect APMCs to enforce and adhere to strict rules and regulations set by the Maharashtra State Agricultural Marketing Board in each district, ensuring fairness and consistency.

REFERENCES

[1] Sharma, R. K.; Kumar, S.; Singh, R., Agricultural Marketing Channels and APMC Reforms, Agricultural Economics Research Volume 30, Issue 2, Year 2017.
[2] Singh, S. P.; Kumar, R.; Singh, A. K., Role of APMC in Agricultural Marketing, Agricultural Economics Research Review Volume, 33 Issue, 2 Year, 2020.
[3] Kumar, N.; Singh, R.; Sharma, A.Impact of APMC Reforms on Agricultural Marketing Efficiency: A Case Study of Maharashtra, Indian Journal of Agricultural Economics, Volume 74, Issue 1 Year 2019.
[4] Verma, N.; Srivastava, N. Marketing Channels for Agricultural Commodities, Journal of Agri Search, Volume: 3, Issue: 3, Year: 2016.
[5] Joshi, P. K.; Birthal, P. S.; Roy, D., New Directions for Indian Agriculture: Marketing, Farmer Organizations, and Food Processing", Agricultural Economics Research Review, Volume: 32, Issue: 2, Year: 2019.
[6] Sharma, R. K.; Kumar, S.; Singh, R, Agricultural Economics Research Review, Volume: 30 Issue, 2 Year, 2017.
[7] Singh, S. P.; Kumar, R.; Singh, A. K., Role of APMC in Agricultural Marketing: A Review Agricultural Economics Research Review, Volume 33 Issue 2, Year 2020
[8] Verma, N.; Srivastava, N. Journal, Marketing Channels for Agricultural Commodities: A Review, Journal of Agri Search Volume: 3 Issue 3 Year 2016.
[9] Khanna, K. Tripathi, A.International Journal of Scientific Research, Electronic Trading Platforms in Agricultural Markets: A ReviewVolume: 7Issue: 5Year: 2018.
[10] Pandey, N.; Roy, D. Indian Journal of Agricultural Economics, APMC and e-NAM: A Critical Analysis of Agricultural Market ReformsVolume: 73, Issue: 2, Year 2018.
[11] Manju Singh, Shwetank Shukla, Praveen Singh (2023), e-NAM, Times of Agriculture, ISSN : 2582- 6344, Volume 3 , Issue 1.
[12] Dr. Vilas M. Kadrolkar(2012), Role Of Agricultural Produce Marketing Committee (APMC), Department of Studies and Research in Economics, Tumkur University, B. H. Road, TUMKUR - 572 103.
[13] Annapurna (2009) - "Marketing to the Indian Rural Consumers", Marketing Mastermind, Vol. 9(5), May, Pp.35-39.
[14] Ramaswamy, V. S., Marketing Management.
[15] Kadrolkar, V. M., Agricultural Marketing in India: Role of Agricultural Produce Marketing Committee (APMC), 2012.
[16] Acharya, S. S.; Agrawal, N. L., Agriculture Marketing in India, Oxford and IBH Publishing Company, 1987.
[17] Gupta, G. S., Managerial Economics, T. M. H., New Delhi.
[18] Varshney; Maheshwari, Managerial Economics, Sultan Chand and Sons, New Delhi.
[19] Economic Survey Report, 2022–2023.
[20] Economic Budget Report, 2022–2023.
[21] Maharashtra State Agricultural Marketing Board (MSAMB), Available at: www.msamb.com.

International Journal of Environment, Agriculture and Biotechnology
Vol-11, Issue-5; Sep-Oct, 2026
Peer-Reviewed International Journal
Journal Home Page Available: https://ijeab.com/
Journal DOI: 10.22161/ijeab

A Study on Physiotherapists' Perceptions Towards Staff Training and Development and Its Impact on Patient Care Quality in Healthcare Settings

Dr. Ganesh S. Shinde, S. S. Temkar, S. C. Gujjewar.

Asst. Professor, Dr. D. Y. Patil Vidyapeeth, Pune (Deemed-to-be University), Centre for Online Learning, Pune - 411018, Maharashtra, India
Email- ganesh.shinde.col@dpu.edu.in

Received: 11 Aug 2026; Received in revised form: 14 Sep 2026; Accepted: 20 Sep 2026; Available online: 03 Oct 2026
©2026 The Author(s). Published by Infogain Publication. This is an open-access article *under* the CC BY license (https://creativecommons.org/licenses/by/4.0/).

Abstract— *Staff training and development play a vital role in strengthening clinical competency, professional confidence, and the overall quality of healthcare delivery. This study examines physiotherapists' perceptions of staff training and development in healthcare settings, evaluates its perceived impact on patient care quality, and identifies the barriers physiotherapists face in accessing professional development opportunities. A descriptive research design was adopted, and data were collected from 80 practicing physiotherapists working in hospitals, private clinics, rehabilitation centres, and tele-rehabilitation setups through a structured, Google Forms-based questionnaire circulated via WhatsApp, LinkedIn, and physiotherapy professional networks during May 2026. Descriptive statistical methods, including frequencies, percentages, tables, and charts, were used for analysis. The findings reveal an overwhelmingly positive perception of staff training among physiotherapists, with the vast majority agreeing that training enhances clinical knowledge, communication, patient handling, and confidence in clinical decision-making, and that it directly improves patient care quality. Workshops, certification courses, online programmes, and CME sessions emerged as the most common modes of training. However, participation is frequently constrained by lack of time, heavy workload, financial limitations, and limited institutional support. The study concludes that while physiotherapists strongly value continuous professional development, healthcare organisations need to institutionalise regular, practical, and accessible training structures to translate this positive perception into sustained participation and improved patient outcomes.*

Keywords— ***Staff Training, Professional Development, Physiotherapists, Healthcare Quality, Patient Care, Continuing Medical Education***

I. INTRODUCTION

The quality of healthcare services is closely tied to the knowledge, clinical competency, and professional efficiency of healthcare workers. As medical science, rehabilitation techniques, and healthcare technologies continue to advance, healthcare professionals are required to regularly update their skills to deliver safe, effective, and evidence-based care. Staff training and development — encompassing workshops, seminars, continuing medical education (CME), certifications, and hands-on clinical sessions — have therefore become a core organisational function in modern healthcare systems.

Physiotherapists occupy a critical position within this system, contributing to rehabilitation, disability prevention, pain management, and restoration of functional independence across hospitals, private clinics, rehabilitation centres, and increasingly, tele-rehabilitation platforms. The rapid evolution of rehabilitation science, digital health tools, and evidence-based practice standards means physiotherapists must continuously upgrade their

clinical reasoning, patient-handling techniques, and communication skills through structured professional development.

Despite this recognised need, healthcare professionals — physiotherapists included — often encounter practical barriers such as heavy workloads, time constraints, financial limitations, and inconsistent institutional support that restrict their participation in training activities. Understanding how physiotherapists themselves perceive the value of training, and what specifically prevents them from accessing it, is essential for designing development programmes that are both effective and realistic within clinical work environments. This study addresses that gap by directly surveying practising physiotherapists.

1.1 Objectives of the Study :

1. To assess physiotherapists' perceptions on the importance of staff training and development in healthcare settings.
2. To evaluate the perceived impact of staff training on patient care quality delivered by physiotherapists.
3. To identify the challenges faced by physiotherapists in accessing training and development programmes.

1.2 Scope and Purpose of the Study :

The study is confined to practising physiotherapists working across hospital, private clinic, rehabilitation centre, and tele-rehabilitation settings, and examines their perceptions and self-

Reported experiences rather than objective clinical outcome data. Its purpose is to generate evidence-based insight that healthcare organisations can use to design more effective, accessible, and sustained staff development initiatives for physiotherapy professionals.

II. LITERATURE REVIEW

A substantial body of literature supports the link between employee training and both individual and organisational performance.

Aguinis and Kraiger (2009) established that training positively influences work efficiency, professional confidence, and productivity, effects that extend to teams and organisations as a whole. In healthcare specifically, the **World Health Organization (2013)** has argued that strengthening health systems requires continuous competency development so that healthcare workers can meet growing and increasingly complex patient-care demands.

Salas et al. (2012) found that structured training programmes strengthen teamwork, communication, and clinical decision-making — capabilities that are directly relevant to patient safety and care quality.

The **Institute of Medicine (2001)** similarly identified continuous professional learning and improved communication as prerequisites for closing healthcare quality gaps and reducing clinical error.

Within physiotherapy specifically, the **World Confederation for Physical Therapy (2019)** has emphasised lifelong learning as central to maintaining clinical competency and supporting evidence-based rehabilitation practice.

Filipe et al. (2014) noted that ongoing professional development improves not only technical competency but also motivation and adaptability to new healthcare technologies. These effects are particularly relevant given the rapid rise of tele-rehabilitation, digital consultation platforms, and remote patient monitoring — trends that accelerated sharply following the COVID-19 pandemic **(WHO, 2020)** and required physiotherapists to acquire new digital-care competencies quickly.

At the same time, existing research consistently identifies structural barriers to training participation: heavy workload, insufficient staffing, financial constraints, and limited institutional support **(Filipe et al., 2014).**

These barriers appear across healthcare professions generally, but few studies have examined them specifically from the perspective of practising physiotherapists. This gap — physiotherapists' own perceptions of training value, its impact on their patient care, and the obstacles they personally face — forms the basis for the present study.

III. RESEARCH METHODOLOGY

3.1 Research Design

A descriptive research design was adopted, using a questionnaire-based survey method to capture physiotherapists' perceptions in a structured, quantifiable format.

3.2 Population and Sampling

The target population comprised practising physiotherapists working in hospitals, private clinics, rehabilitation centres, and tele-rehabilitation settings. A convenience sampling technique was used. Approximately 400 physiotherapists were approached, of whom 80 responded, forming the final sample for analysis.

3.3 Data Collection Instrument

Data were collected through a structured questionnaire built on Google Forms, comprising two sections. Section A captured demographic details (age, gender, qualification, years of clinical experience, and workplace setting). Section B addressed staff training participation, perceived impact on patient care quality, workplace support, barriers to participation, and satisfaction with existing training opportunities, using a combination of close-ended, multiple-choice, and five-point Likert-scale items (Strongly Agree to Strongly Disagree), along with two open-ended questions for qualitative suggestions.

3.4 Data Collection Procedure

The questionnaire link was circulated through WhatsApp, LinkedIn professional networks, physiotherapy groups, and personal professional contacts. Data collection took place over a four-day period in May 2026. Participation was voluntary, and confidentiality and anonymity were maintained throughout.

3.5 Data Analysis

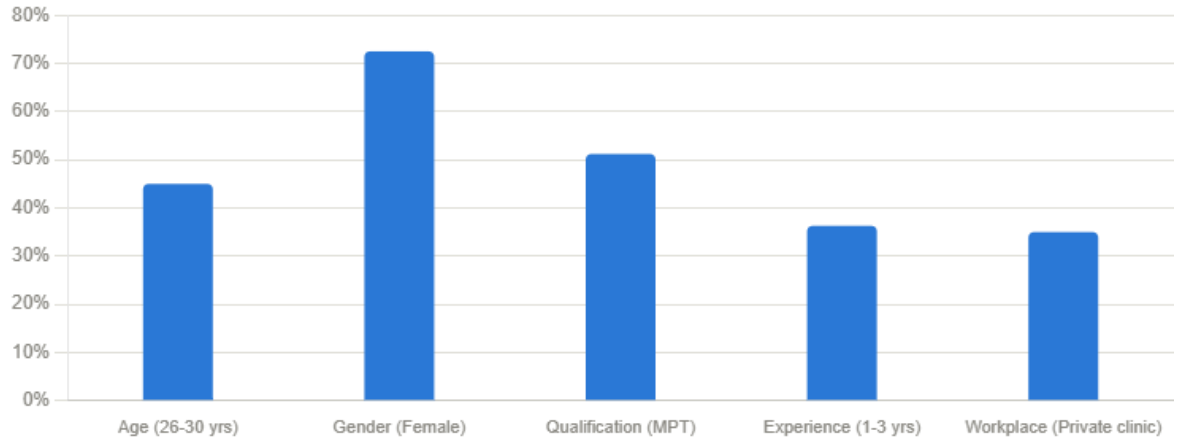
Responses recorded via Google Forms were organised using Google Sheets and Microsoft Excel and analysed using descriptive statistics — frequencies, percentages, tables, pie charts, and bar graphs — to interpret and present the findings.

IV. DATA ANALYSIS AND RESULTS

4.1 Demographic Profile of Respondents

Of the 80 respondents, 45% were aged 26–30 years and 26.3% were aged 21–25 years, indicating that the sample skewed toward early-to-mid-career professionals. Female physiotherapists made up 72.5% of respondents against 27.5% male. In terms of qualification, 51.2% held a Master's in Physiotherapy (MPT) and 41.3% held a Bachelor's (BPT). Regarding clinical experience, 36.3% had 1–3 years, 25% had more than 6 years, 20% had less than 1 year, and 18.8% had 4–6 years. Private clinics (35%) and hospitals (22.5%) were the most common workplace settings, with many respondents reporting affiliations across more than one setting.

Demographic variable	Category	Percentage
Age	26–30 years (largest group)	45.0%
Gender	Female	72.5%
Qualification	MPT	51.2%
Experience	1–3 years (largest group)	36.3%
Workplace	Private clinic (most common)	35.0%



4.2 Perceptions of Staff Training and Development

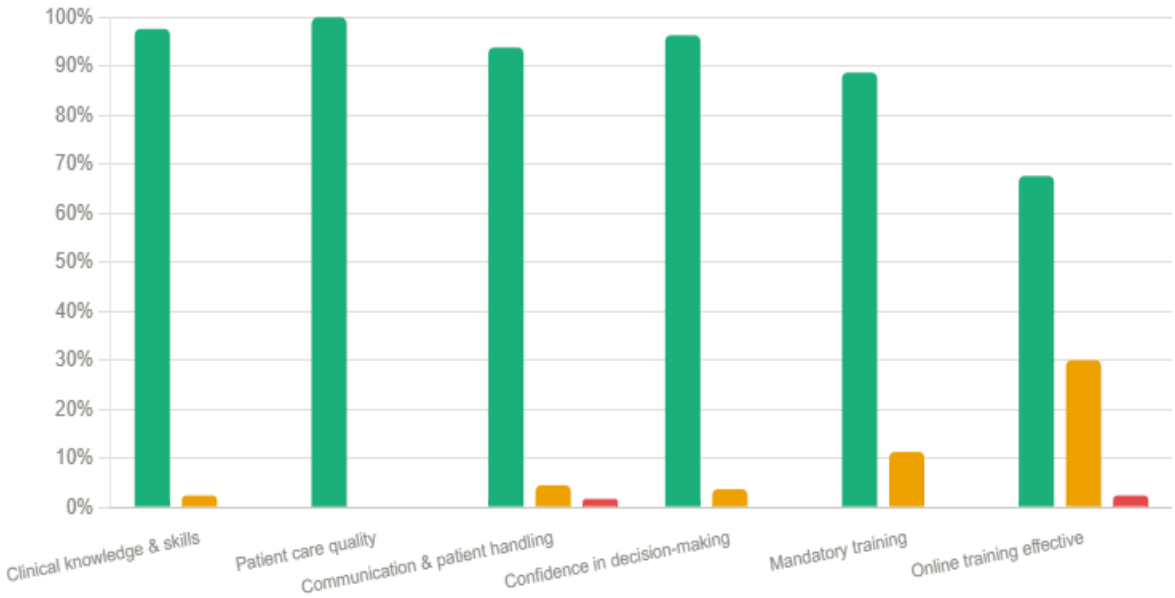
An overwhelming 98.8% of respondents considered staff training and development important in healthcare settings, reflecting near-universal endorsement of continuous learning among physiotherapists. 66.3% had attended a professional training or development programme within the past year, while 33.8% had not. Workshops (68.8%), certification programmes (60%), online courses (58.8%), and CME/seminars (57.5%) were the most commonly attended formats. In terms of frequency, 56.3% participated occasionally, 22.5% frequently, and 20% rarely.

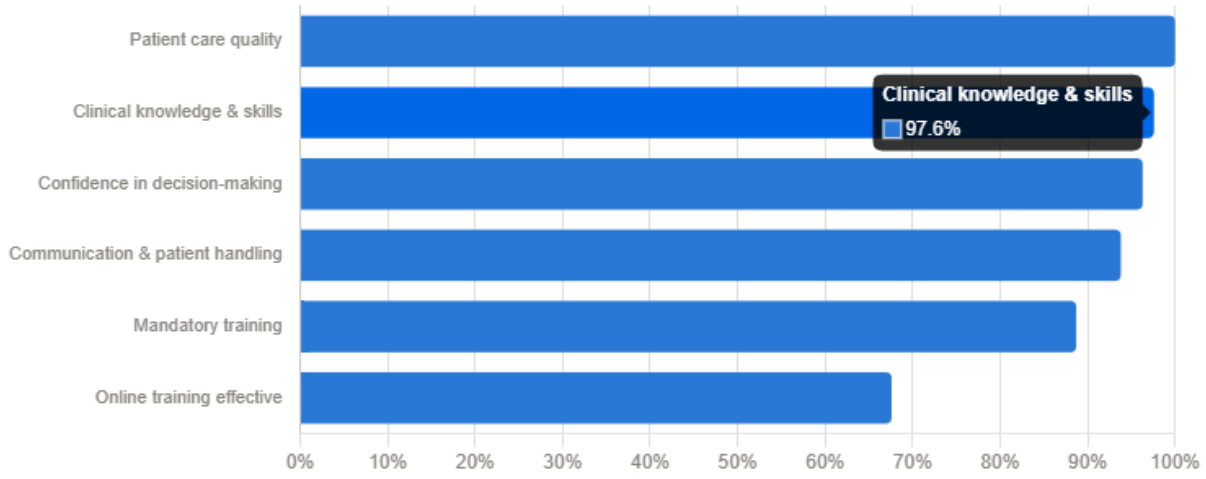
4.3 Perceived Impact on Clinical Competency and Patient Care

Respondents strongly associated training with tangible clinical benefits. 97.6% (56.3% strongly agree + 41.3%

agree) agreed that training improves clinical knowledge and skills, and 100% (66.3% strongly agree + 33.8% agree) agreed that training improves patient care quality, with no respondent disagreeing on either item. Similarly, 93.8% agreed that training improves communication and patient-handling skills, and 96.3% agreed that training builds confidence in clinical decision-making. Online training was also viewed favourably, with 67.6% agreeing it is effective for professional skill development, though 30% remained neutral — suggesting comparatively less certainty about digital formats than about training in general.

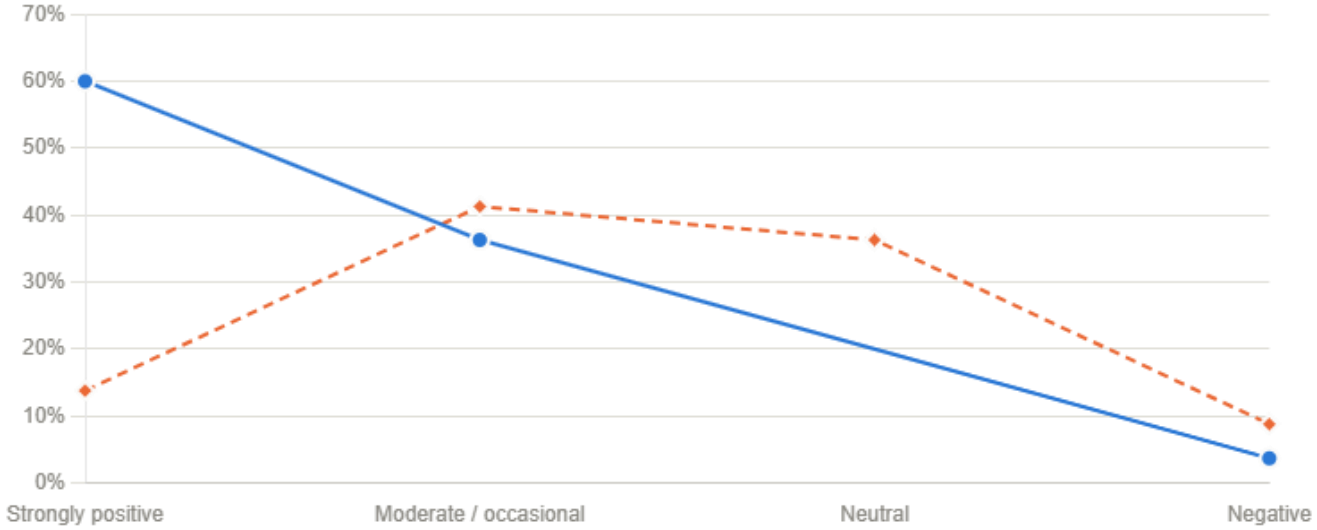
Statement	**Agree / Strongly agree**	**Neutral**	**Disagree / Strongly disagre**	**Statement**	**Agree / Strongly agree**
Training improves clinical knowledge & skills	97.6%	~2.4%	0%	Training improves clinical knowledge & skills	97.6%
Training improves patient care quality	100%	0%	0%	Training improves patient care quality	100%
Training improves communication & patient handling	93.8%	~4–5%	small	Training improves communication & patient handling	93.8%
Training improves confidence in decision-making	96.3%	~3.7%	0%	Training improves confidence in decision-making	96.3%
Regular training should be mandatory	88.7%	11.3%	0%	Regular training should be mandatory	88.7%
Online training is effective	67.6%	30.0%	~2.4%	Online training is effective	67.6%





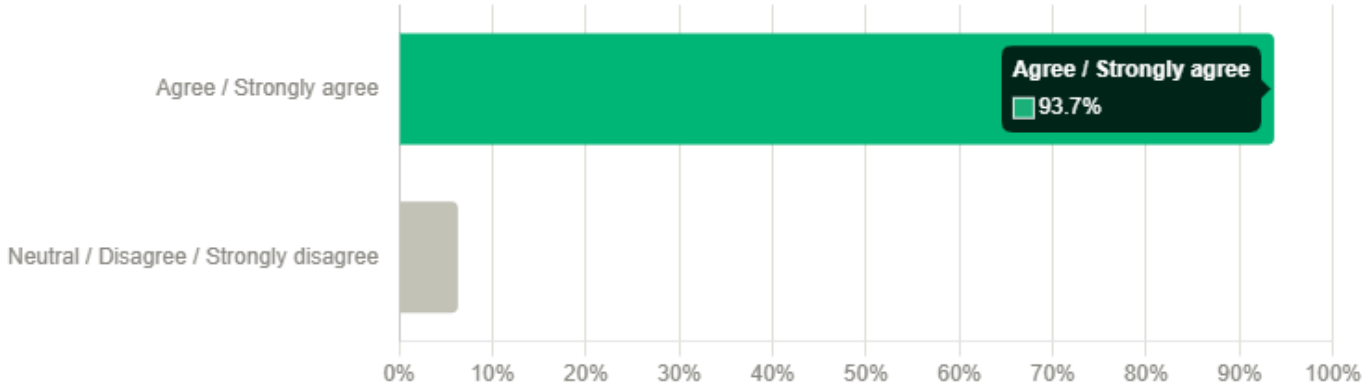
4.4 Workplace Support and Satisfaction

60% of respondents reported that their workplace actively encourages participation in training programmes, and a further 36.3% reported occasional encouragement — indicating that outright lack of support was rare. Satisfaction with available training opportunities was more moderate: 55.1% (41.3% agree + 13.8% strongly agree) expressed satisfaction, while 36.3% remained neutral and 8.8% disagreed, pointing to room for improvement in the quality or accessibility of existing programmes.



4.5 Barriers to Participation

Lack of time was the most frequently cited barrier (65%), followed by heavy workload (43.8%), financial constraints (42.5%), and limited training opportunities (35%); lack of institutional support was cited less often (17.5%). This was corroborated by a separate Likert item, where 93.7% of respondents agreed that lack of time affects their participation in professional development activities — confirming time management as the single most significant obstacle physiotherapist's face.



4.6 Qualitative Insights

Open-ended responses reinforced the quantitative findings. Respondents most frequently called for regular hands-on workshops, evidence-based and practical training sessions, mentorship from experienced clinicians, institutional and financial support, flexible scheduling, and hybrid/online learning options. Communication and soft-skill training, along with interdisciplinary exposure, were also raised as areas for improvement.

V. DISCUSSION

The findings present a clear and internally consistent picture: physiotherapists overwhelmingly value staff training and perceive a strong, direct link between training participation and improved clinical knowledge, communication, decision-making confidence, and — ultimately — patient care quality. This aligns closely with prior literature (Aguinis & Kraiger, 2009; Salas et al., 2012; WCPT, 2019), which similarly links structured professional development to improved competency and care outcomes across healthcare professions.

What distinguishes the present findings is the gap between perception and access. While belief in the value of training is nearly unanimous (98.8%), actual participation in the past year is meaningfully lower (66.3%), and satisfaction with available opportunities is only moderate (55.1%). This gap is explained largely by structural, not attitudinal, barriers — lack of time and heavy workload account for the two most-cited obstacles, consistent with Filipe et al. (2014), who identified similar workload-related constraints across healthcare professions generally. Financial constraints and limited programme availability compound this further, particularly for physiotherapists in private clinics, who may lack the institutional training budgets available in larger hospital systems.

The comparatively lower confidence in online training effectiveness (67.6% agreement, with 30% neutral) is a notable finding given the post-pandemic shift toward digital and tele-rehabilitation practice (WHO, 2020). This suggests that while online formats improve accessibility, physiotherapists may still perceive hands-on, practical training as more valuable for a profession that is fundamentally manual and patient-contact-based — a distinction healthcare organisations should consider when designing blended training models rather than defaulting to purely digital solutions.

VI. KEY FINDINGS

- 98.8% of physiotherapists consider staff training and development important in healthcare settings.
- 66.3% had attended a professional training/development programme in the past year; participation frequency was mostly occasional (56.3%).
- Workshops, certifications, online courses, and CME/seminars were the most commonly attended training formats.
- 100% of respondents who expressed a view agreed that staff training improves patient care quality (66.3% strongly agree, 33.8% agree).
- Training was also strongly associated with improved communication skills, patient handling, and confidence in clinical decision-making.
- 60% of workplaces actively encourage training participation, but satisfaction with available opportunities is only moderately positive (55.1%).
- Lack of time (65%), heavy workload (43.8%), and financial constraints (42.5%) are the leading barriers to participation.
- 88.7% support making regular training programmes mandatory for physiotherapists.
- Respondents favour hands-on, practical, and evidence-based training over purely digital formats, though online/hybrid learning is valued for accessibility.

VII. RECOMMENDATIONS

- Institutionalise regular, mandatory training cycles (workshops, CME, certifications) rather than relying on ad hoc or optional participation.
- Allocate protected time within clinical schedules specifically for training, to directly address the leading barrier of time constraints.
- Provide financial support or subsidised access to certification courses and conferences, particularly for physiotherapists in smaller private-practice settings.
- Prioritise hands-on, practical, evidence-based workshop formats, using online/hybrid learning as a complement rather than a substitute.
- Introduce structured mentorship programmes pairing early-career physiotherapists with experienced clinicians.
- Incorporate communication and soft-skills training alongside clinical/technical content, given its identified link to patient-handling quality.
- Establish periodic feedback and evaluation mechanisms to monitor training effectiveness and satisfaction over time.

VIII. CONCLUSION

This study confirms that physiotherapists hold a strongly positive perception of staff training and development, and consistently associate it with improved clinical competency, communication, decision-making confidence, and patient care quality. However, this positive attitude is not fully matched by consistent access: time constraints, workload pressure, and financial limitations continue to restrict participation for a meaningful proportion of physiotherapists, even where workplace encouragement exists. Closing this perception-to-access gap requires healthcare

organisations to move beyond passive encouragement toward structured, funded, and time-protected training systems — particularly hands-on and mentorship-based formats that physiotherapists themselves identify as most valuable. Doing so would not only support individual professional growth but, based on physiotherapists' own assessment, translate directly into improved patient care quality and healthcare service standards.

REFERENCES

[1] Aguinis, H., & Kraiger, K. (2009). Benefits of training and development for individuals and teams, organizations, and society. Annual Review of Psychology, 60, 451–474.

[2] Filipe, H. P., Silva, E. D., Stulting, A. A., & Golnik, K. C. (2014). Continuing professional development: Best practices. Middle East African Journal of Ophthalmology, 21(2), 134–141.

[3] Institute of Medicine. (2001). Crossing the quality chasm: A new health system for the 21st century. National Academy Press.

[4] Salas, E., Tannenbaum, S. I., Kraiger, K., & Smith-Jentsch, K. A. (2012). The science of training and development in organizations: What matters in practice. Psychological Science in the Public Interest, 13(2), 74–101.

[5] World Confederation for Physical Therapy. (2019). Policy statement on continuing professional development. WCPT.

[6] World Health Organization. (2010). Framework for action on interprofessional education and collaborative practice. WHO.

[7] World Health Organization. (2013). Transforming and scaling up health professionals' education and training. WHO.

[8] World Health Organization. (2020). Maintaining essential health services during COVID-Operational guidance for the COVID-19 context. WHO.

International Journal of Environment, Agriculture and Biotechnology
Vol-11, Issue-5; Sep-Oct, 2026
Peer-Reviewed International Journal
Journal Home Page Available: https://ijeab.com/
Journal DOI: 10.22161/ijeab

Integrated Major Oxide Geochemistry, Contamination Factor and Pollution Load Index for Evaluating Geogenic Enrichment in the Ikole–Itapaji Basement Complex, Southwestern Nigeria

Adeleke Ojo

Department of Geology, Faculty of Physical Sciences, Ekiti State University, Ado Ekiti.
adebolaadeleke2002@gmail.com | ORCID: 0009-0000-3106-2704

Received: 29 Jul 2026; Received in revised form: 22 Aug 2026; Accepted: 27 Aug 2026; Available online: 03 Oct 2026
©2026 The Author(s). Published by Infogain Publication. This is an open-access article *under* the CC BY license (https://creativecommons.org/licenses/by/4.0/).

Abstract— *The Ikole–Itapaji Basement Complex, southwestern Nigeria, comprises diverse crystalline rocks that influence both regional geochemical characteristics and environmental quality. This study integrated major oxide geochemistry, sequential extraction, Contamination Factor (CF), and Pollution Load Index (PLI) to evaluate geogenic enrichment and the environmental behaviour of trace elements within the study area. Geological mapping was conducted, during which thirty-five fresh rock samples representing the major lithological units were collected. Following detailed megascopic examination, twenty representative rock samples were selected for whole-rock major oxide geochemical analyses, while seventeen representative soil/sediment samples were analysed for environmental geochemical assessment. Major oxide analyses were carried out using Inductively Coupled Plasma–Mass Spectrometry (ICP–MS) following lithium metaborate fusion combined with multi-acid digestion ($HCl–HNO_3–HClO_4$), with analytical quality assured through certified reference materials, analytical blanks, duplicate samples, and internal laboratory standards. The soil/sediment samples were subjected to a seven-step modified Tessier sequential extraction procedure to determine trace-element partitioning among water-soluble, exchangeable, carbonate-bound, Fe–Mn oxide-bound, organic-bound, sulfide-bound, and residual fractions. Contamination Factor and Pollution Load Index were subsequently computed using average shale background values to evaluate elemental enrichment and environmental quality. The area is underlain by migmatite, granite gneiss, coarse porphyroblastic gneiss, granite, pegmatite, and charnockite. Major oxide geochemistry indicates predominantly calc-alkaline, magnesian, and metaluminous to weakly peraluminous compositions, reflecting magmatic differentiation and fractional crystallization within the Precambrian Basement Complex. Sequential extraction results reveal that most trace elements are concentrated within the Fe–Mn oxide, sulfide-bound, and residual fractions, indicating strong lithogenic control and generally low environmental mobility. Although CF identifies localized enrichment of Cd and Pb at a few sampling locations, PLI values indicate that most sites remain within the unpolluted to moderately polluted category. Overall, the study demonstrates that the geochemistry of the Ikole–Itapaji Basement Complex is primarily controlled by parent-rock composition, while localized enrichment of Cd and Pb highlights the need for periodic environmental monitoring to safeguard ecosystem integrity and public health.*

Keywords— ***Ikole–Itapaji Basement Complex, major oxide geochemistry, sequential extraction, contamination factor, pollution load index, geogenic enrichment, environmental assessment.***

I. INTRODUCTION

Major oxide geochemistry is one of the most fundamental approaches for characterizing rock composition, classifying lithological units, interpreting magmatic evolution, and understanding crustal differentiation within crystalline basement terrains. The concentrations of major oxides, including SiO_2, Al_2O_3, Fe_2O_3, MgO, CaO, Na_2O, K_2O, TiO_2, MnO, and P_2O_5, provide important information on mineralogical composition, weathering intensity, magma evolution, and tectonic setting (Shand, 1943; Peccerillo & Taylor, 1976; Frost et al., 2001; Frost & Frost, 2011). Consequently, major-oxide geochemistry has become an indispensable tool in geological investigations and mineral exploration, particularly within Precambrian basement complexes, where lithological diversity reflects prolonged tectono-magmatic evolution.

The Nigerian Basement Complex constitutes part of the Pan-African Mobile Belt. It is composed predominantly of migmatite–gneiss complexes, schist belts, Older Granites, charnockitic bodies, and pegmatitic intrusions emplaced during the Pan-African orogeny (Rahaman, 1988; Oyinloye, 2011). These lithological units have experienced multiple episodes of deformation, metamorphism, magmatism, hydrothermal alteration, and tropical weathering, resulting in considerable geochemical variability and natural enrichment of several major and trace elements. As weathering progresses, elements released from crystalline rocks become incorporated into soils and surface materials, where they may influence environmental quality depending on their abundance, mobility, and bioavailability.

Evaluating elemental enrichment within basement terrains requires not only an understanding of their geochemical composition but also an assessment of their environmental significance. Geogenic enrichment, arising from natural geological processes, may produce elevated elemental concentrations comparable to those observed in contaminated environments. Therefore, distinguishing natural geogenic signatures from anthropogenic contamination is essential for environmental assessment, mineral exploration, and sustainable land management (Kabata-Pendias, 2011; Reimann & de Caritat, 2005; Reimann & de Caritat, 2012; Alloway, 2013).

Environmental pollution indices have become widely accepted tools for assessing elemental enrichment in geological materials. The Contamination Factor (CF) quantitatively evaluates the degree of enrichment of individual elements relative to background concentrations, whereas the Pollution Load Index (PLI) provides an integrated measure of the cumulative pollution status of an area (Hakanson, 1980; Birth, 2003). Although originally developed for environmental studies of soils and sediments, these indices have increasingly been applied in geological investigations to differentiate naturally enriched basement terrains from areas affected by anthropogenic pollution and to establish geochemical baseline conditions for environmental monitoring (Förstner & Wittmann, 2012; Wei & Yang, 2010).

While CF and PLI provide valuable information on the degree of elemental enrichment, they do not indicate the chemical forms in which elements occur or their potential mobility within the environment. Sequential extraction techniques complement these pollution indices by partitioning elements into operationally defined geochemical fractions, namely water-soluble, exchangeable, carbonate-bound, Fe–Mn oxide-bound, organic-bound, sulfide/strongly bound, and residual phases. These fractions provide critical information on elemental mobility, bioavailability, and environmental behaviour. Elements occurring within the water-soluble and exchangeable fractions are generally more mobile and readily available for biological uptake, whereas those associated with the residual fraction are strongly incorporated within mineral lattices and therefore exhibit low mobility under natural environmental conditions (Tessier et al., 1979; Filgueiras et al., 2002; Davidson et al., 1998; De Matteis et al., 2023; Çelebi, 2024; Firmino et al., 2025).

The Ikole–Itapaji Basement Complex of southwestern Nigeria consists predominantly of migmatites, granite gneisses, granites, pegmatites, and charnockitic rocks that have undergone prolonged tectono-magmatic evolution and weathering. Previous investigations within the area have largely concentrated on geological mapping, litho-structural characterization, aeromagnetic interpretation, radiometric analysis, and mineral exploration (Ojo et al., 2024; Adetunla et al., 2025; Ogah & Abubakar, 2024; Salako et al., 2024). Although these studies have significantly improved the understanding of the geological framework and mineral potential of the area, little attention has been given to integrating major oxide geochemistry with environmental pollution indices and sequential extraction techniques to evaluate geogenic enrichment, elemental mobility, and their environmental implications. Such integration provides a more comprehensive understanding of whether elevated elemental concentrations reflect natural geological processes or constitute potential environmental concerns.

This study therefore integrates major oxide geochemistry, sequential extraction, Contamination Factor (CF), and Pollution Load Index (PLI) to evaluate geogenic enrichment, elemental partitioning, and the environmental implications of naturally occurring elements within the

Ikole–Itapaji Basement Complex, Southwestern Nigeria. The study establishes baseline geochemical conditions, assesses elemental mobility through sequential extraction, and provides valuable information for sustainable mineral exploration, environmental monitoring, and future land-use planning within the study area.

This study aims to integrate major oxide geochemistry, sequential extraction, Contamination Factor (CF), and Pollution Load Index (PLI) to evaluate geogenic enrichment, elemental mobility, and their environmental implications within the Ikole–Itapaji Basement Complex, Southwestern Nigeria.

To achieve this aim, the study seeks to:

1. Determine the major oxide composition of the basement rocks within the study area.
2. Evaluate the geochemical characteristics and petrogenetic affinities of the rocks using major oxide data.
3. Characterize the partitioning of elements into water-soluble, exchangeable, carbonate-bound, Fe–Mn oxide-bound, organic-bound, sulfide/strongly bound, and residual fractions using sequential extraction.
4. Calculate the Contamination Factor (CF) of the investigated elements to assess their degree of geogenic enrichment.
5. Determine the Pollution Load Index (PLI) to evaluate the overall geochemical enrichment status of the study area.
6. Assess elemental mobility, bioavailability, and potential environmental implications by integrating sequential extraction results with CF and PLI.
7. Distinguish between natural geogenic enrichment and possible environmental contamination and establish a baseline for future environmental monitoring and sustainable mineral exploration.

1.1 Study Area

Figure 1 illustrates the geographical location of the Ikole–Itapaji study area within Ekiti State, southwestern Nigeria. The inset map of Nigeria shows the position of Ekiti State in the southwestern region of the country, while the highlighted rectangle delineates the study area. The area lies within the Precambrian Basement Complex of southwestern Nigeria, which forms part of the Pan-African Mobile Belt. The Basement Complex is composed predominantly of migmatite–gneiss complexes, Older Granites, charnockitic bodies, pegmatites, and minor metasedimentary rocks that were emplaced and reworked during the Pan-African orogeny through multiple episodes of magmatism, metamorphism, deformation, and hydrothermal activity (Rahaman, 1988; Oyinloye, 2011).

The enlarged topographic map indicates that the study area extends approximately between latitudes 7°47′N and 8°05′N and longitudes 5°26′E and 5°34′E, covering an estimated surface area of about 590 km². The terrain is rugged and undulating, consisting of numerous hills, ridges, valleys, and lowlands that are characteristic of crystalline basement environments. Closely spaced contour lines represent areas of steep slopes and resistant rock units, whereas widely spaced contours indicate relatively gentle terrain. These geomorphological variations are primarily controlled by differences in lithology, structural deformation, and the differential weathering of basement rocks (Ojo et al., 2024).

The drainage pattern is predominantly dendritic, indicating that stream development is mainly influenced by the regional topographic gradient and the relatively homogeneous crystalline basement. However, local changes in drainage orientation reflect the influence of fractures, joints, faults, and other structural discontinuities that serve as zones of weakness within the Basement Complex. These structures enhance weathering, groundwater circulation, and the migration of dissolved elements released during rock alteration, thereby influencing the geochemical evolution of soils and surface materials (Adetunla et al., 2025).

The study area is readily accessible through a network of major and minor roads linking Ikole-Ekiti and Itapaji, thereby facilitating geological mapping, structural measurements, and representative rock-sample collection. The abundance of fresh outcrops, combined with rugged topography and an extensive drainage network, provides favourable conditions for major oxide geochemical investigations, sequential extraction studies, and the assessment of geogenic elemental enrichment and environmental quality within the Basement Complex (Ogah & Abubakar, 2024; Salako et al., 2024).

Overall, the geological and physiographic characteristics of the Ikole–Itapaji area typify the crystalline Basement Complex of southwestern Nigeria. The combination of diverse lithological units, pronounced topographic relief, structural complexity, and active weathering processes provides an ideal natural laboratory for investigating major oxide geochemistry, elemental partitioning through sequential extraction into water-soluble, exchangeable, carbonate-bound, Fe–Mn oxide-bound, organic-bound, sulfide/strongly bound, and residual fractions, as well as evaluating geogenic enrichment using Contamination Factor (CF) and Pollution Load Index (PLI). This

integrated approach provides valuable insight into elemental mobility, environmental behaviour, and the natural geochemical baseline of the study area.

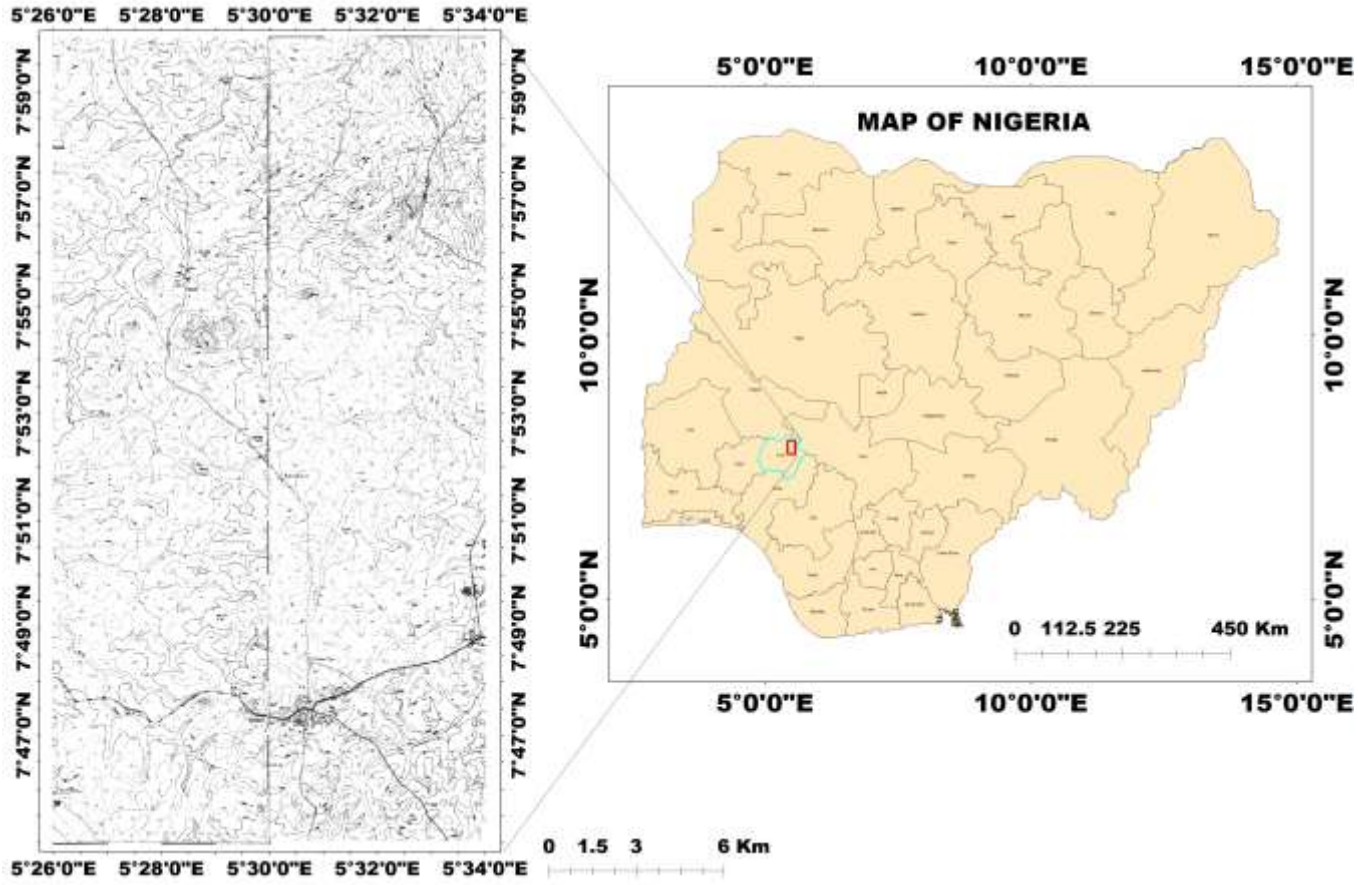


Fig.1. Location and topographic map of the Ikole–Itapaji area, Ekiti State, southwestern Nigeria, illustrating the geographical extent, drainage network, road accessibility, and topographic relief of the study area.

II. GEOLOGICAL SETTING

The study area is situated within the Precambrian Basement Complex of southwestern Nigeria, which forms part of the Pan-African Mobile Belt between the West African and Congo Cratons. This crystalline basement terrain is composed predominantly of ancient metamorphic and igneous rocks that contrast sharply with the surrounding sedimentary basins of Nigeria. The Basement Complex evolved through several tectono-magmatic events, including the Liberian, Eburnean, and Pan-African orogenies, which collectively produced extensive deformation, regional metamorphism, migmatization, granitic magmatism, and hydrothermal activity (Rahaman, 1988; Oyinloye, 2011). These geological processes resulted in the formation of the major lithological assemblages that characterize the Nigerian Basement Complex, including the migmatite–gneiss complex, Older Granites, charnockitic bodies, pegmatites, and minor metasedimentary rocks.

The Ikole–Itapaji area is underlain predominantly by migmatites, granite gneisses, granites, pegmatites, and charnockitic rocks that exhibit varying degrees of deformation and weathering. These lithological units display distinct mineralogical and geochemical characteristics that influence their major oxide composition and the natural distribution of chemical elements released during weathering. The contrasting mineral assemblages and weathering behaviours of these rocks contribute significantly to geogenic elemental enrichment and the chemical composition of the overlying soils and regolith (Kabata-Pendias, 2011; Reimann & de Caritat, 2012).

Structurally, the study area is characterized by well-developed foliations, joints, fractures, faults, and shear zones, which predominantly trend NE–SW and NW–SE in response to Pan-African tectonic deformation. These structural features have influenced magmatic emplacement, fluid circulation, weathering, and mineralization within the Basement Complex. They also enhance rock permeability, thereby promoting

groundwater movement and accelerating geochemical alteration processes that influence elemental redistribution during weathering (Adetunla et al., 2025; Ogah & Abubakar, 2024).

The occurrence of pegmatitic intrusions, quartz veins, and structurally controlled granitic bodies further reflects the prolonged tectono-magmatic evolution of the area. These lithological and structural features contribute to the natural enrichment of major and trace elements and provide favourable conditions for the development of geogenic geochemical anomalies. Recent integrated geological and geophysical investigations have demonstrated that the Ikole–Itapaji Basement Complex possesses considerable mineral resource potential associated with structurally controlled crystalline rocks (Ojo et al., 2024; Salako et al., 2024).

The geological framework of the study area therefore represents a complex interaction between lithology, tectonic deformation, magmatism, weathering, and hydrothermal processes. This complexity makes the Ikole–Itapaji Basement Complex an ideal environment for investigating major oxide geochemistry, sequential extraction of geochemical fractions, and the application of Contamination Factor (CF) and Pollution Load Index (PLI) to distinguish natural geogenic enrichment from potential environmental contamination (Fig. 2).

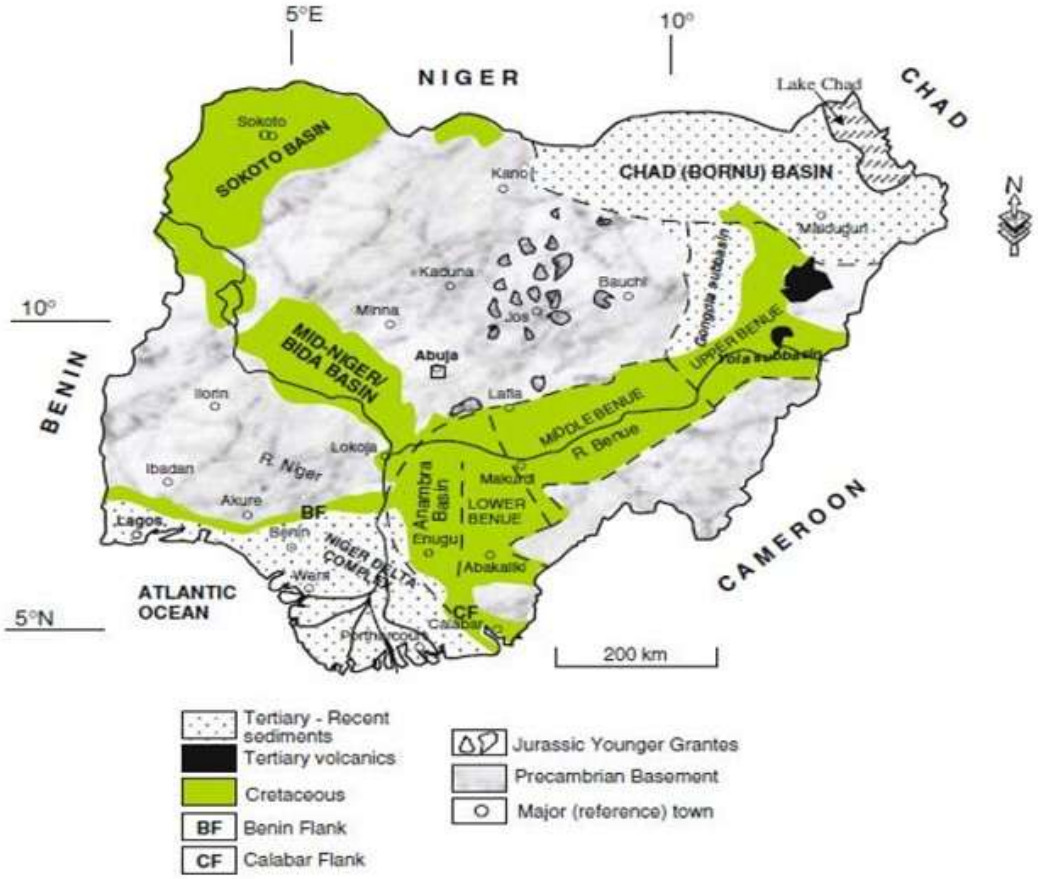


Fig.2: Geological map of Nigeria showing the distribution of major lithological units, including the Precambrian Basement Complex and surrounding sedimentary basins (Sokoto, Chad, Bida, and Benue Trough). The study area (Ikole–Itapaji, southwestern Nigeria) is located within the Basement Complex.

The topographic map (Figure 3) illustrates the spatial distribution of geological sampling locations across the Ikole–Itapaji–Bolorunduro–Odo Oro area. The sampling points are systematically distributed from the southern sector around Ikole and Odo Oro through Bolorunduro to the northern part around Itapaji, ensuring adequate representation of the major lithological units within the study area. This broad spatial coverage provides a reliable framework for major oxide geochemical analysis, sequential extraction, and the assessment of geogenic enrichment using Contamination Factor (CF) and Pollution Load Index (PLI) (Ogah & Abubakar, 2024).

Sampling density is relatively higher around Itapaji and Bolorunduro, where rugged topography and elevated terrain provide abundant exposures of fresh crystalline basement rocks suitable for representative sampling. In contrast, fewer sampling locations occur around Odo Oro and parts of Ikole, where gentle relief, thicker weathered overburden, and vegetation locally limit rock exposure. Nevertheless, the sampling strategy ensured adequate coverage of all major lithological units and geomorphological settings within the study area (Ojo et al., 2024).

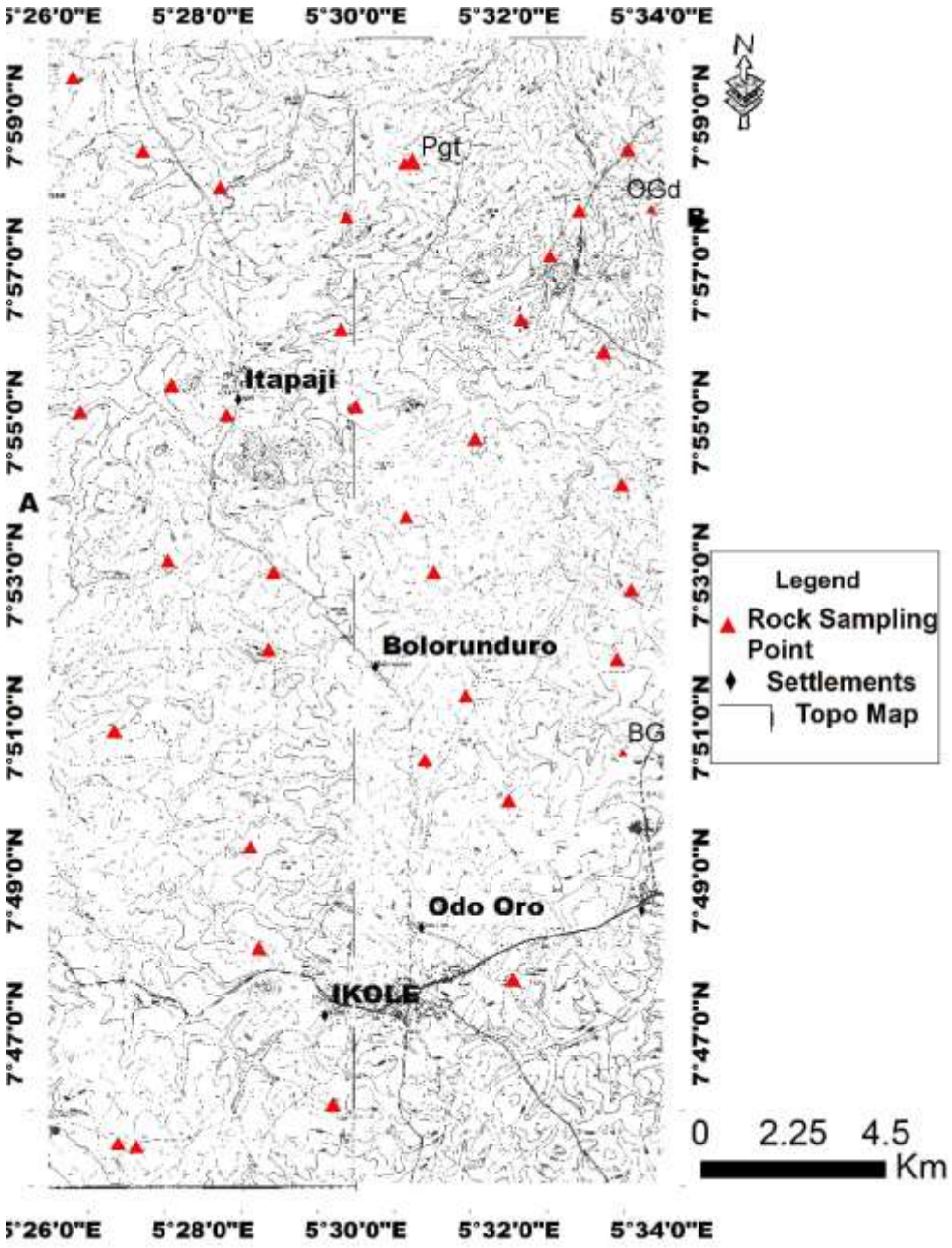


Fig.3. Topographic map of the Ikole–Itapaji–Ake-Ako area, Southwestern Nigeria, showing the distribution of geological sampling points used for geological mapping, structural measurements, and petrographic investigations. The sampling locations provide representative coverage of the major basement rock units across the study area.

The sampling locations extend across hills, ridges, valleys, and gently undulating terrains, thereby minimizing spatial bias and capturing the effects of lithology, weathering, and topography on the geochemical characteristics of the basement rocks. This representative distribution enhances the reliability of major oxide analyses and provides an appropriate basis for evaluating natural geogenic enrichment and elemental mobility through sequential extraction studies (Kabata-Pendias, 2011; Reimann & de Caritat, 2012).

Furthermore, the sampling programme encompasses the principal crystalline rock units, including migmatite, granite gneiss, coarse porphyroblastic gneiss, granite, pegmatite, and charnockite, ensuring that the geochemical dataset adequately reflects the lithological diversity of the Ikole–Itapaji Basement Complex. This comprehensive coverage provides a robust basis for interpreting major oxide variations, calculating Contamination Factor (CF) and Pollution Load Index (PLI), evaluating elemental partitioning into water-soluble, exchangeable, carbonate-bound, Fe–Mn oxide-bound, organic-bound, sulfide/strongly bound, and residual fractions, and establishing the natural geochemical baseline of the study area (Adetunla et al., 2025).

Overall, the systematic distribution of sampling locations provides a representative dataset for evaluating the geochemistry of the crystalline basement rocks and their environmental significance. The combination of extensive spatial coverage, lithological representation, and varying topographic settings establishes a sound foundation for investigating petrogenesis, geogenic elemental enrichment, elemental mobility, and the environmental implications of naturally occurring chemical constituents within the Ikole–Itapaji Basement Complex.

The geological map and accompanying cross-section (Figure 4) reveal that the Ikole–Itapaji–Ake-Ako area is underlain predominantly by rocks of the Precambrian Basement Complex comprising migmatite (Mg), granite gneiss (GG), charnockite (Ch), granodiorite (OGd), and minor pegmatite intrusions. The spatial distribution of these lithologies indicates a complex geological history involving high-grade metamorphism, partial melting, magmatic emplacement, and crustal reworking during the Pan-African tectonothermal event (Rahaman, 1988; Oyinloye, 2011).

The geological map shows that granite gneiss constitutes the dominant lithological unit, occupying a large proportion of the central and northern parts of the study area. This unit extends continuously from Itapaji through Bolorunduro towards the northeastern portion of the map, suggesting that granite gneiss forms the principal basement framework of the area. Field observations and petrographic characteristics indicate that the granite gneiss is composed predominantly of quartz, feldspar, biotite, and muscovite, reflecting amphibolite- to granulite-facies metamorphic conditions typical of the Nigerian Basement Complex (Rahaman, 1988; Oyinloye, 2011).

Migmatite occurs extensively in the southern portion of the study area around Ikole and Odo Oro. Its widespread distribution reflects extensive partial melting and anatexis within the basement rocks. The gradational contact observed between migmatite and granite gneiss suggests a shared tectonometamorphic history, with the migmatites representing zones of more intense metamorphic reworking and crustal melting during the Pan-African orogeny (Rahaman, 1988; Oyinloye, 2011).

The charnockite body exposed in the southwestern portion of the map occurs as a relatively restricted lithological unit enclosed within the surrounding granite gneiss. Its limited areal extent suggests emplacement or preservation as an isolated deep-crustal body. Charnockitic rocks are generally associated with high-temperature metamorphism and deep crustal processes, indicating that parts of the study area experienced elevated thermal conditions during crustal evolution (Rahaman, 1988; Adetunla et al., 2025).

The granodiorite body located in the northeastern section of the map forms a discrete intrusive mass. The geological cross-section demonstrates that the granodiorite extends to depth, confirming its emplacement as a plutonic intrusion within the surrounding granite gneiss. Pegmatite veins associated with the granodiorite represent late-stage magmatic differentiates formed from residual silica-rich melts during the final stages of crystallization, reflecting continued magmatic evolution of the basement complex (Rahaman, 1988; Oyinloye, 2011).

The geological cross-section along A–B (Figure 4) illustrates the subsurface relationships between the major lithological units. Granite gneiss occupies much of the intermediate crustal section and overlies a broad migmatitic basement. The irregular contact between the granite gneiss and migmatite reflects differential melting, metamorphic segregation, and prolonged crustal evolution. The continuity of the migmatite beneath most of the profile indicates that it represents one of the oldest exposed basement units within the study area (Rahaman, 1988).

The cross-section further demonstrates that the granodiorite intrusion cuts across the surrounding granite gneiss in the northeastern segment of the profile, confirming that the granodiorite is younger than its host rock. The pegmatite body emplaced within the granodiorite represents a younger magmatic phase produced through crystallization of residual melts enriched in incompatible elements. Such pegmatitic intrusions commonly record the final stages of granitic differentiation and may locally concentrate economically important elements (Oyinloye, 2011; Adetunla et al., 2025).

From a geological evolution perspective, the study area records multiple episodes of crustal development. The migmatites represent the oldest basement components formed through high-grade metamorphism and partial melting. These rocks were subsequently reworked into

granite gneiss during regional tectonometamorphic events. Charnockitic bodies developed under high-temperature crustal conditions, whereas granodioritic intrusions and pegmatites represent younger magmatic phases associated with crustal melting and magmatic differentiation during the Pan-African orogeny (Rahaman, 1988; Oyinloye, 2011). These lithological variations provide the geochemical framework controlling the distribution of major oxides and the natural geogenic enrichment evaluated using Contamination Factor (CF) and Pollution Load Index (PLI).

The geological architecture depicted by the map and cross-section demonstrates that the Ikole–Itapaji–Ake-Ako area forms part of a deeply reworked Precambrian basement terrane characterized by extensive migmatization, granitoid emplacement, and localized charnockitic development. The intimate association of these lithologies records repeated episodes of metamorphism, partial melting, magmatism, and crustal stabilization, which collectively govern the present-day distribution of major oxide compositions and the geogenic elemental enrichment within the study area (Rahaman, 1988; Oyinloye, 2011; Adetunla et al., 2025).

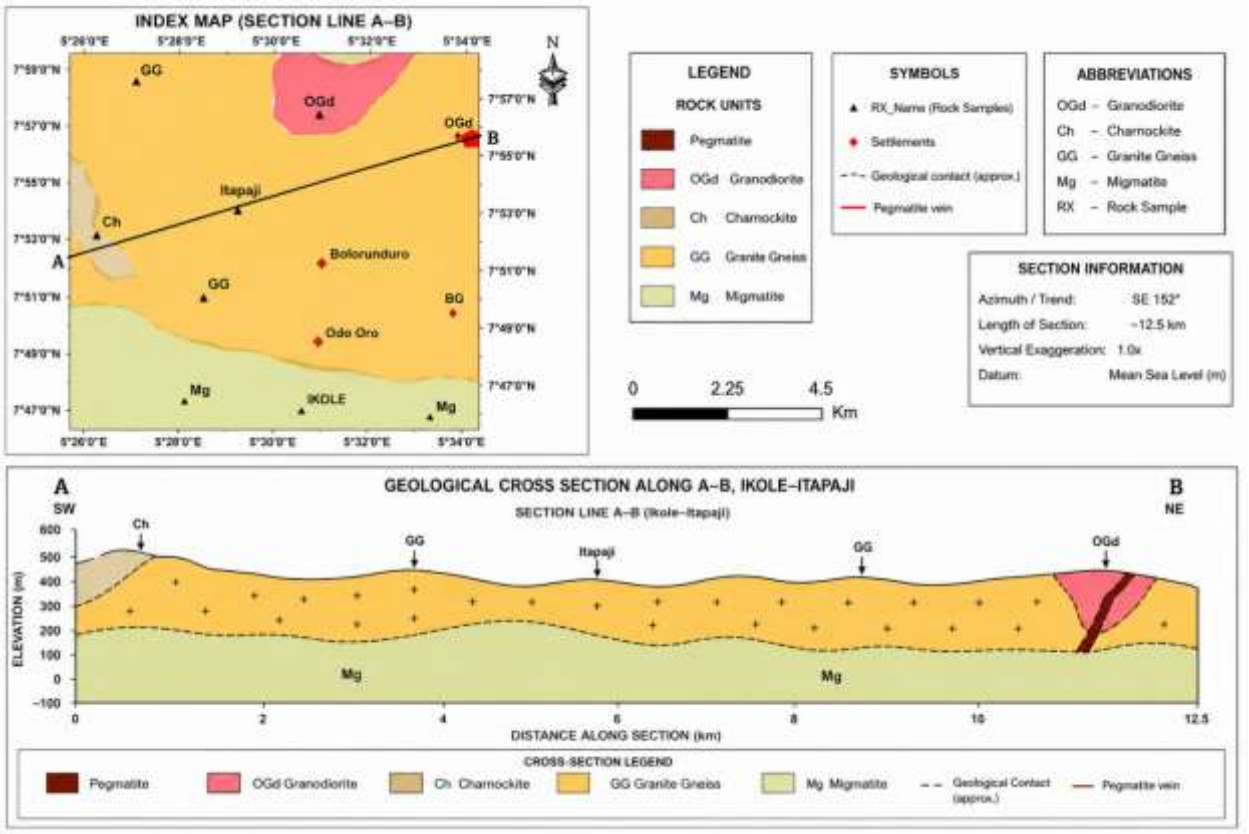


Fig.4. Geological cross-section along A–B across the Ikole-Itapaji area, showing the subsurface relationships between migmatite, granite gneiss, charnockite, granodiorite, and pegmatite units. The section reveals a migmatitic basement overlain by granite gneiss and intruded by younger granodiorite and pegmatite bodies. The geometry of the rock units reflects prolonged crustal evolution involving metamorphism, partial melting, and magmatic emplacement within the Precambrian Basement Complex.

III. MATERIALS AND METHODS

3.1 Materials

The materials used for this study comprised field and laboratory equipment required for geological mapping, rock and soil/sediment sample collection, whole-rock major oxide geochemical analyses, and geogenic enrichment assessment. Field equipment included a 1:25,000-scale topographic map of the Ikole–Itapaji–Ake-Ako area, a Brunton compass clinometer, a Garmin GPSMAP 64s handheld Global Positioning System (GPS), geological hammer, chisel, hand lens, measuring tape, sample bags, permanent markers, field notebook, digital camera, and personal protective equipment comprising safety boots, reflective jacket, hand gloves, and safety helmet. These materials facilitated geological mapping, structural observations, accurate location referencing, documentation of field observations, and the collection of representative rock and soil/sediment samples.

Laboratory equipment comprised a diamond rock-cutting machine, jaw crusher, pulverizing machine, analytical weighing balance, drying oven, laboratory sieves, and computer software for geochemical data processing, statistical analysis, and graphical presentation. Whole-rock major oxide and soil/sediment geochemical analyses were carried out at ACME Analytical Laboratories (Bureau Veritas Commodities Canada Ltd.), Vancouver, Canada, using Inductively Coupled Plasma–Mass Spectrometry (ICP–MS).

3.2 Geological Mapping and Sample Collection

The investigation commenced with a reconnaissance survey using a 1:25,000-scale topographic map to obtain preliminary information on accessibility, drainage pattern, topography, and distribution of rock exposures within the Ikole–Itapaji–Ake-Ako area. The reconnaissance survey formed the basis for planning detailed geological traverses and ensuring adequate spatial coverage during field investigations.

Detailed geological mapping was subsequently carried out along accessible roads, footpaths, stream channels, farm tracks, and exposed rock outcrops. Lithological characteristics including colour, grain size, texture, mineral composition, weathering characteristics, and field relationships were carefully observed and documented. Structural features such as foliations, joints, fractures, folds, quartz veins, mineral lineations, and shear zones were identified, while their strike and dip were measured using a Brunton compass clinometer. Geographic coordinates and elevations were recorded using a Garmin GPSMAP 64s handheld GPS receiver, and representative field photographs were taken to document significant geological features. The geological observations formed the basis for the geological map and subsequent geochemical interpretations.

A total of thirty-five (35) fresh rock samples representing the major lithological units encountered during geological mapping, including migmatite, granite gneiss, coarse porphyroblastic gneiss, granite, pegmatite, and charnockite, were collected from different locations across the study area. Following detailed megascopic examination, twenty (20) representative rock samples were selected for whole-rock major oxide geochemical analyses based on the following criteria:

1. Representation of all the major lithological units identified during geological mapping.
2. Freshness of the rock samples, with preference given to fresh, unweathered, and minimally altered specimens.
3. Lithological and mineralogical diversity to ensure adequate representation of the compositional variability of the different rock units within the study area.
4. Megascopic textural variability, including differences in grain size, mineral fabric, and weathering characteristics.
5. Structural characteristics, particularly representative foliations, mineral banding, folds, quartz veins, fractures, and shear fabrics.
6. Spatial distribution to ensure adequate geographical representation of the different lithological units across the study area.
7. Elimination of duplicate samples exhibiting similar lithological, mineralogical, and structural characteristics from the same locality to avoid analytical redundancy while maintaining representative coverage.

This selection procedure ensured that the analysed rock samples adequately represented the lithological, structural, and compositional variability of the crystalline basement rocks within the study area.

In addition, seventeen (17) representative soil/sediment samples were collected from selected locations across the study area to evaluate the degree of geogenic enrichment using Contamination Factor (CF) and Pollution Load Index (PLI). The samples were collected from the near-surface horizon after removing organic debris and other surface contaminants. The collected samples were air-dried at room temperature, gently disaggregated, homogenized, and sieved through a 63 µm mesh to obtain the fine-grained fraction suitable for geochemical analysis.

3.3 Sample Preparation and Geochemical Analysis

Fresh portions of the selected rock samples were cleaned to remove weathered surfaces before being reduced to smaller fragments using a jaw crusher and subsequently pulverized into fine homogeneous powders. The prepared soil/sediment samples were similarly homogenized after drying and sieving to obtain representative analytical aliquots. Both rock and soil/sediment samples were packaged and submitted to ACME Analytical Laboratories (Bureau Veritas Commodities Canada Ltd.), Vancouver, Canada, for geochemical analysis.

Major oxide analyses were carried out using Inductively Coupled Plasma–Mass Spectrometry (ICP–MS) following partial multi-acid digestion with hydrochloric acid (HCl), nitric acid (HNO_3), and perchloric acid ($HClO_4$), combined with lithium metaborate fusion. The lithium metaborate fusion technique ensured complete dissolution of refractory silicate minerals, while the acid digestion

enhanced the extraction and determination of the major rock-forming oxides. Quality assurance and quality control (QA/QC) procedures included the analysis of certified reference materials, analytical blanks, duplicate samples, and internal laboratory standards to ensure the accuracy, precision, and reliability of the analytical results.

3.4 Major Oxide Geochemical Evaluation

Whole-rock major oxide data obtained from the twenty representative rock samples were evaluated to characterize the chemical composition, magmatic affinity, and geochemical evolution of the basement rocks. Major oxide variation diagrams (Harker plots) were employed to evaluate compositional trends and magmatic differentiation among the investigated lithologies. The degree of alumina saturation was assessed using the A/CNK–A/NK diagram after Shand (1943), while magmatic affinity was evaluated using the Fe-number [FeOt/(FeOt + MgO)] versus SiO_2 discrimination diagram proposed by Frost et al. (2001). These geochemical evaluations provided the basis for interpreting petrogenesis and crustal evolution within the study area.

3.5 Contamination Factor (CF)

The Contamination Factor (CF) was employed to evaluate the degree of geogenic enrichment in the analysed soil/sediment samples relative to average shale background concentrations following Hakanson (1980). The contamination factor was calculated as:

- $CF = Csample / Cbackground$ (1)

where:

- Csample is the measured concentration of the investigated major oxide in the soil/sediment sample.
- Cbackground is the corresponding average shale background concentration (Turekian & Wedepohl, 1961).

The calculated CF values were interpreted as follows:

- CF < 1: Low contamination
- 1 ≤ CF < 3: Moderate contamination
- 3 ≤ CF < 6: Considerable contamination
- CF ≥ 6: Very high contamination

3.6 Pollution Load Index (PLI)

The Pollution Load Index (PLI) was used to evaluate the overall degree of geogenic enrichment within the study area based on the analysed soil/sediment samples. The index was calculated as:

- $PLI = (CF1 \times CF2 \times CF3 \times \ldots \times CFn)^{(1/n)}$ (2)

where:

- CF_1–CF_n represent the contamination factors of the investigated major oxides.
- n is the total number of investigated oxides.

The calculated PLI values were interpreted as follows:

- PLI < 1: Background or unpolluted condition.
- PLI = 1: Baseline geochemical condition.
- PLI > 1: Progressive geogenic enrichment above background concentrations.

Table 1. Average shale values used as background concentrations for Contamination Factor (CF) and Pollution Load Index (PLI) calculations (after Turekian and Wedepohl, 1961).

S/N	Element	Average shale value (mg/kg)
1	Fe	47,200
2	Mn	850
3	Pb	20
4	Cu	45
5	Zn	95
6	Ni	68
7	Co	19
8	Cr	90
9	Cd	0.30

IV. RESULTS AND DISCUSSION

4.1 Sequential extraction techniques

4.1.1 Water-soluble Phase

The water-soluble phase represents the most mobile and readily bioavailable fraction of metals in soils and weathered rocks. In natural environments, this fraction is generally very low because most metals remain strongly bound within mineral lattices or secondary mineral phases (Kabata-Pendias, 2011; Alloway, 2013; Filgueiras et al., 2002).

Results in Table 2a show consistently low concentrations of all analysed metals across samples (SQ1–SQ17), indicating limited metal dissolution and mobility. Iron (Fe) records the highest concentrations (2.873–7.427 mg/kg), followed by Mn (1.742–3.128 mg/kg), reflecting their natural abundance in the basement rocks. Copper, Zn, Pb, Ni, Co, Cr, and Cd occur at comparatively low

concentrations, suggesting that their distribution is primarily controlled by natural weathering rather than anthropogenic contamination (Reimann & de Caritat, 2005).

The statistical summary in Table 2b confirms this trend, with mean concentrations following the order Fe > Mn > Cu ≈ Zn > Pb > Co ≈ Ni > Cr > Cd. Similarly, Figure 5 shows a uniform spatial distribution of the analysed metals, with no pronounced enrichment or pollution hotspots across the study area.

From an environmental perspective, the low concentrations in the water-soluble fraction indicate limited metal mobility and bioavailability, suggesting minimal immediate risk to groundwater, agricultural soils, and the local population. Overall, the water-soluble phase reflects predominantly geogenic metal occurrence and indicates that the study area presently poses low environmental and human health risk under existing conditions (De Matteis et al., 2023; Wei & Yang, 2010).

Table 2a. Heavy metals concentration in the water-soluble phase (mg/kg) of sediments/soils from the Ikole–Itapaji area, Southwestern Nigeria. This fraction represents the most mobile and immediately bioavailable portion of trace metals, reflecting their potential short-term environmental availability and mobility in the near-surface environment.

Samples	Fe (mg/Kg)	Mn (mg/Kg)	Pb (mg/Kg)	Cu (mg/Kg)	Zn (mg/Kg)	Ni (mg/Kg)	Co (mg/Kg)	Cr (mg/Kg)	Cd (mg/Kg)
SQ 1	6.321	2.087	0.077	0.681	0.572	0.054	0.062	0.023	0.004
SQ 2	6.128	2.063	0.072	0.631	0.509	0.059	0.063	0.021	0.003
SQ 3	7.427	3.108	0.083	0.724	0.592	0.063	0.069	0.028	0.005
SQ 4	7.129	3.099	0.081	0.711	0.579	0.061	0.066	0.025	0.005
SQ 6	5.873	2.145	0.094	0.742	0.582	0.063	0.067	0.029	0.006
SQ7	4.568	1.958	0.064	0.465	0.368	0.043	0.048	0.016	0.003
SQ 8	6.409	2.056	0.076	0.641	0.539	0.052	0.063	0.022	0.004
SQ 10	2.873	1.742	0.049	0.163	0.126	0.034	0.037	0.013	0.002
SQ 11	3.208	1.839	0.056	0.218	0.189	0.041	0.045	0.015	0.003
SQ 12	5.175	2.094	0.086	0.598	0.565	0.061	0.057	0.024	0.005
SQ 13	5.387	2.109	0.087	0.605	0.591	0.063	0.054	0.026	0.005
SQ 14	6.125	2.135	0.092	0.676	0.608	0.067	0.061	0.029	0.006
SQ 15	7.105	3.128	0.091	0.624	0.573	0.056	0.054	0.031	0.006
SQ 16	5.891	2.207	0.095	0.673	0.606	0.065	0.059	0.034	0.007
SQ 17	5.006	1.876	0.098	0.659	0.627	0.064	0.062	0.033	0.007

Table 2b. Statistical summary of the heavy metals concentration in the water-soluble phase (mg/kg). This table presents the minimum, maximum, and mean concentrations of the selected metals across all samples in the study area. It provides a simplified statistical overview of metal distribution and mobility within the most labile geochemical fraction of the soil–sediment system.

Metal	**Fe**	**Mn**	**Pb**	**Cu**	**Zn**	**Ni**	**Co**	**Cr**	**Cd**
Min	2.873	1.742	0.049	0.163	0.126	0.034	0.037	0.013	0.002
Max	7.427	3.128	0.098	0.742	0.627	0.067	0.069	0.034	0.007
Mean	5.642	2.243	0.080	0.587	0.508	0.056	0.058	0.025	0.005

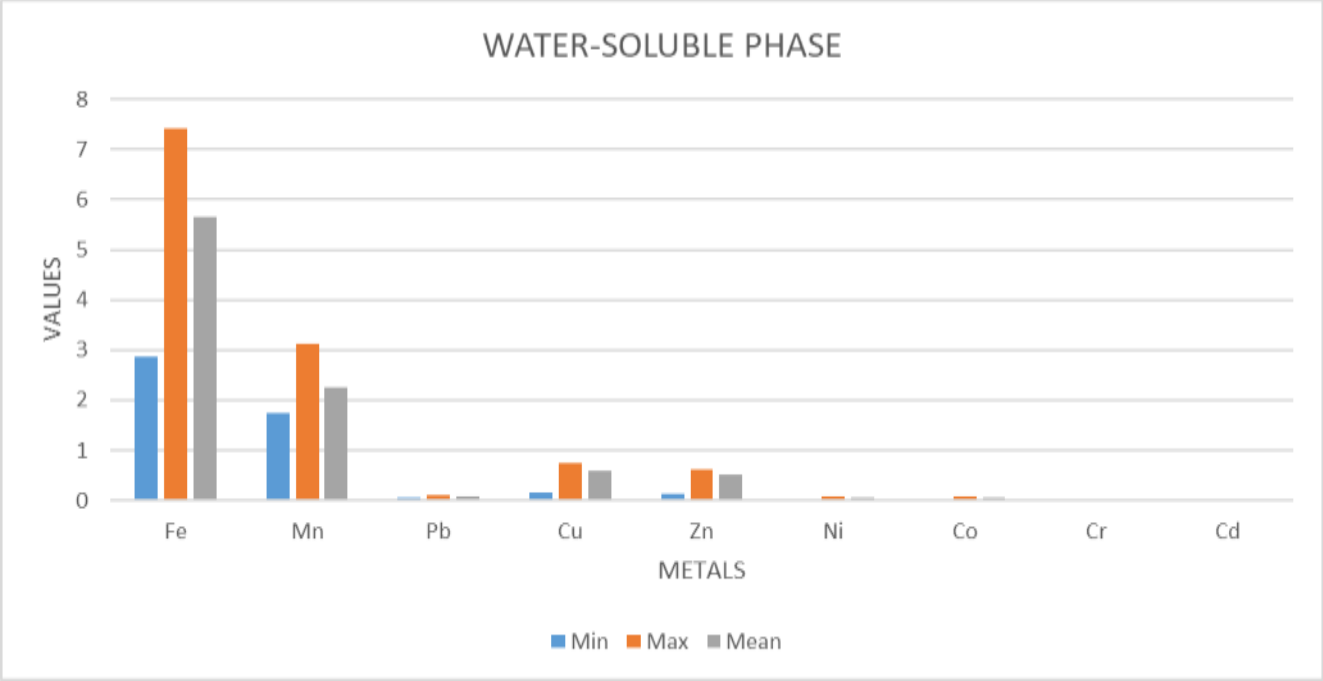


Fig.5. Cluster column chart of heavy metal concentrations in the water-soluble phase (mg/kg). The figure illustrates the comparative distribution of selected metals across all samples, highlighting variations in their mobility and relative abundance within the most labile geochemical fraction.

4.1.2 The Exchangeable Phase

The exchangeable phase contains metals weakly adsorbed onto soil particles and represents a potentially mobile fraction that can be released under changes in pH or ionic conditions (Kabata-Pendias, 2011; Alloway, 2013). Table 3a shows higher metal concentrations than the water-soluble phase, indicating greater but reversible metal retention. Iron (5.731–10.742 mg/kg) and Mn (1.342–3.127 mg/kg) dominate, while Cu and Zn occur in moderate concentrations. Pb and Cd remain low but exhibit slight enrichment, whereas Ni, Co, and Cr are consistently low.

The statistical summary Table 3b confirms the abundance order of Fe > Mn > Cu > Zn > Pb > Ni > Co > Cr > Cd, reflecting strong lithological control. Figure 6 similarly shows the dominance of Fe and Mn with moderate Cu and Zn enrichment, while the remaining metals display relatively uniform distributions across the sampling locations.

Overall, the exchangeable phase indicates limited metal mobility and low environmental risk under present conditions. However, the slight enrichment of Pb and Cd suggests that future soil acidification or environmental disturbance could enhance their mobility, posing potential risks to groundwater quality, agricultural soils, and the health of residents through long-term exposure (Reimann & de Caritat, 2005; Alloway, 2013).

Table 3a: Exchangeable phase of the heavy metal concentrations in soil samples (mg/kg). The table presents the distribution of Fe, Mn, Pb, Cu, Zn, Ni, Co, Cr, and Cd across all sampling locations, reflecting metals weakly bound to soil exchange sites and their potential environmental mobility.

Samples	Fe (mg/Kg)	Mn (mg/Kg)	Pb (mg/Kg)	Cu (mg/Kg)	Zn **(mg/Kg)**	Ni (mg/Kg)	Co (mg/Kg)	Cr (mg/Kg)	Cd (mg/Kg)
SQ 1	8.084	1.875	0.098	0.789	0.701	0.072	0.071	0.031	0.007
SQ 2	8.005	1.802	0.097	0.712	0.685	0.073	0.069	0.032	0.005
SQ 3	10.742	2.085	0.102	0.826	0.732	0.081	0.075	0.037	0.029
SQ 4	10.488	2.016	0.108	0.813	0.735	0.085	0.076	0.037	0.028
SQ 6	6.402	2.073	0.112	0.839	0.784	0.082	0.073	0.042	0.009
SQ7	6.023	1.762	0.082	0.619	0.586	0.065	0.059	0.025	0.005

SQ 8	8.787	1.904	0.126	0.804	0.721	0.075	0.073	0.034	0.026
SQ 10	5.731	1.342	0.085	0.279	0.261	0.067	0.072	0.026	0.004
SQ 11	6.174	1.563	0.096	0.351	0.31	0.071	0.072	0.029	0.005
SQ 12	7.787	2.012	0.113	0.801	0.721	0.094	0.087	0.038	0.009
SQ 13	7.819	2.105	0.109	0.799	0.726	0.097	0.085	0.042	0.01
SQ 14	8.534	3.083	0.138	0.902	0.846	0.102	0.095	0.051	0.017
SQ 15	10.231	3.127	0.146	0.927	0.872	0.117	0.102	0.054	0.021
SQ 16	7.118	2.105	0.128	0.942	0.839	0.112	0.11	0.059	0.028
SQ 17	6.104	2.098	0.131	0.967	0.886	0.132	0.121	0.061	0.026

*Table 3b: Statistical summary of the heavy metals concentration in the exchangeable phase (mg/kg**). This table presents the minimum, maximum, and mean concentrations of selected metals across all samples in the exchangeable fraction. It highlights the variability and relative mobility of metals weakly bound to soil exchange sites, which are potentially available for environmental release.*

Metal	Fe	Mn	Pb	Cu	Zn	Ni	Co	Cr	Cd
Min	5.731	1.342	0.082	0.279	0.261	0.065	0.059	0.025	0.004
Max	10.742	3.127	0.146	0.967	0.886	0.132	0.121	0.061	0.029
Mean	7.869	2.064	0.111	0.758	0.694	0.088	0.083	0.040	0.015

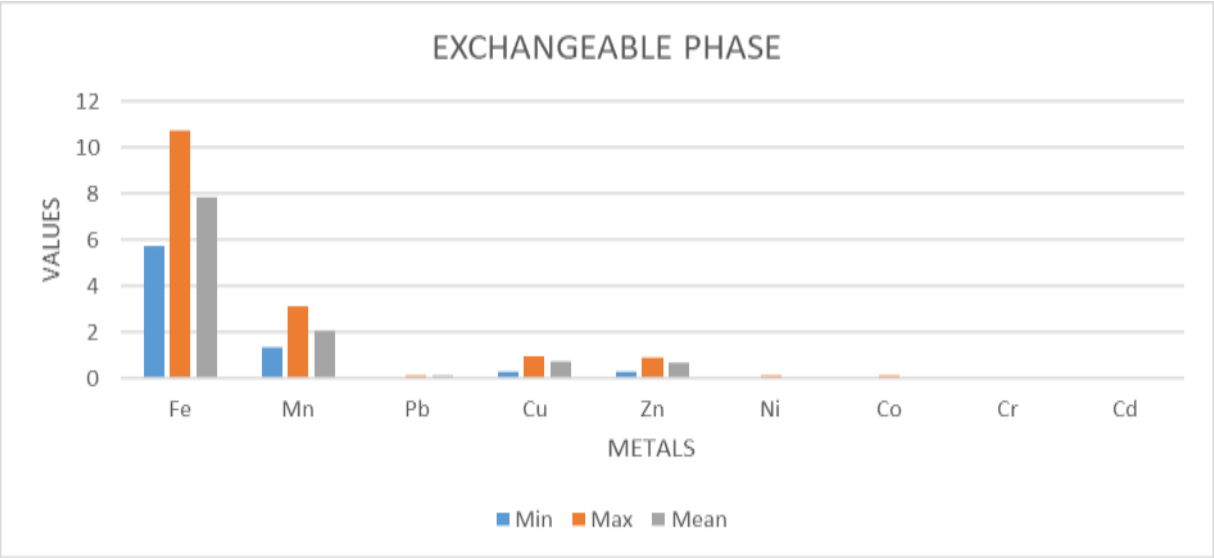


Fig.6. Cluster column chart of heavy metal concentrations in the exchangeable phase (mg/kg). The figure illustrates the comparative distribution of metals across all samples in the exchangeable fraction, highlighting variations in their relative mobility and binding strength to soil exchange sites.

4.1.3 The carbonate-bound phase

The carbonate-bound phase consists of metals associated with carbonate minerals and is susceptible to release under acidic conditions due to carbonate dissolution (Kabata-Pendias, 2011; Alloway, 2013). Table 4a shows a marked increase in metal concentrations compared to the previous fractions, indicating stronger incorporation into carbonate phases. Iron (36.325–66.488 mg/kg) and Mn (23.728–38.019 mg/kg) are the dominant metals, followed by Zn and Cu, while Pb exhibits moderate enrichment. Nickel, Co, Cr, and Cd occur at comparatively lower concentrations.

The statistical summary in Table 4b confirms the abundance order of Fe > Mn > Zn > Pb > Cu > Ni > Co >

Cr > Cd, reflecting the natural geochemical composition of the basement rocks. Figure 7 also shows higher concentrations around samples SQ3, SQ4, and SQ15, with lower values at SQ10, indicating lithological variation rather than anthropogenic contamination.

Overall, the carbonate-bound phase represents a relatively stable metal reservoir under existing environmental conditions. However, increased soil acidity could enhance the release of carbonate-bound metals, potentially affecting soil quality and groundwater. The current distribution nevertheless suggests predominantly geogenic enrichment with low environmental and human health risk to residents of the study area.

Table 4a. Heavy metal concentrations in the carbonate-bound phase (mg/kg). The table shows the distribution of metals associated with carbonate minerals across all samples, reflecting their relative stability and potential release under acidic environmental conditions.

Samples	Fe (mg/Kg)	Mn (mg/Kg)	Pb (mg/Kg)	Cu (mg/Kg)	Zn (mg/Kg)	Ni (mg/Kg)	Co (mg/Kg)	Cr (mg/Kg)	Cd (mg/Kg)
SQ 1	40.129	25.207	2.279	2.439	13.226	2.147	1.701	0.531	0.069
SQ 2	41.052	25.422	2.142	2.197	13.055	2.132	1.626	0.625	0.065
SQ 3	65.246	37.529	3.217	2.826	18.614	2.704	2.002	0.954	0.089
SQ 4	66.488	38.019	3.832	3.213	18.901	3.125	2.106	1.005	0.103
SQ 6	38.615	24.234	1.715	2.327	13.178	2.362	1.448	0.603	0.059
SQ7	38.247	24.127	1.665	2.401	13.218	2.295	1.353	0.616	0.055
SQ 8	41.271	25.431	3.102	2.424	13.286	2.149	1.747	1.103	0.072
SQ 10	36.325	23.728	1.025	1.112	12.521	1.891	0.829	0.518	0.054
SQ 11	37.623	24.061	2.611	2.103	12.101	2.047	1.521	0.556	0.055
SQ 12	39.114	25.716	3.112	2.518	12.224	2.104	1.687	0.738	0.069
SQ 13	38.864	24.612	3.109	2.429	12.138	2.049	1.716	0.742	0.071
SQ 14	41.451	26.128	2.234	2.657	13.441	2.162	1.392	0.671	0.077
SQ 15	46.539	37.423	3.627	2.985	19.807	3.127	2.108	1.054	0.121
SQ 16	41.318	25.035	2.512	2.548	13.033	2.102	1.711	1.005	0.098
SQ 17	38.712	24.291	2.271	2.462	12.987	1.937	1.491	0.657	0.097

Table 4b. Statistical summary of the heavy metals in the carbonate-bound phase (mg/kg). The table presents the minimum, maximum, and mean concentrations of metals associated with carbonate fractions, highlighting their relative enrichment and stability within this geochemical phase.

Metal	**Fe**	**Mn**	**Pb**	**Cu**	**Zn**	**Ni**	**Co**	**Cr**	**Cd**
Min	36.325	23.728	1.025	1.112	12.101	1.891	0.829	0.518	0.054
Max	66.488	38.019	3.832	3.213	19.807	3.127	2.108	1.103	0.121
Mean	43.580	26.998	2.630	2.450	13.915	2.235	1.629	0.758	0.078

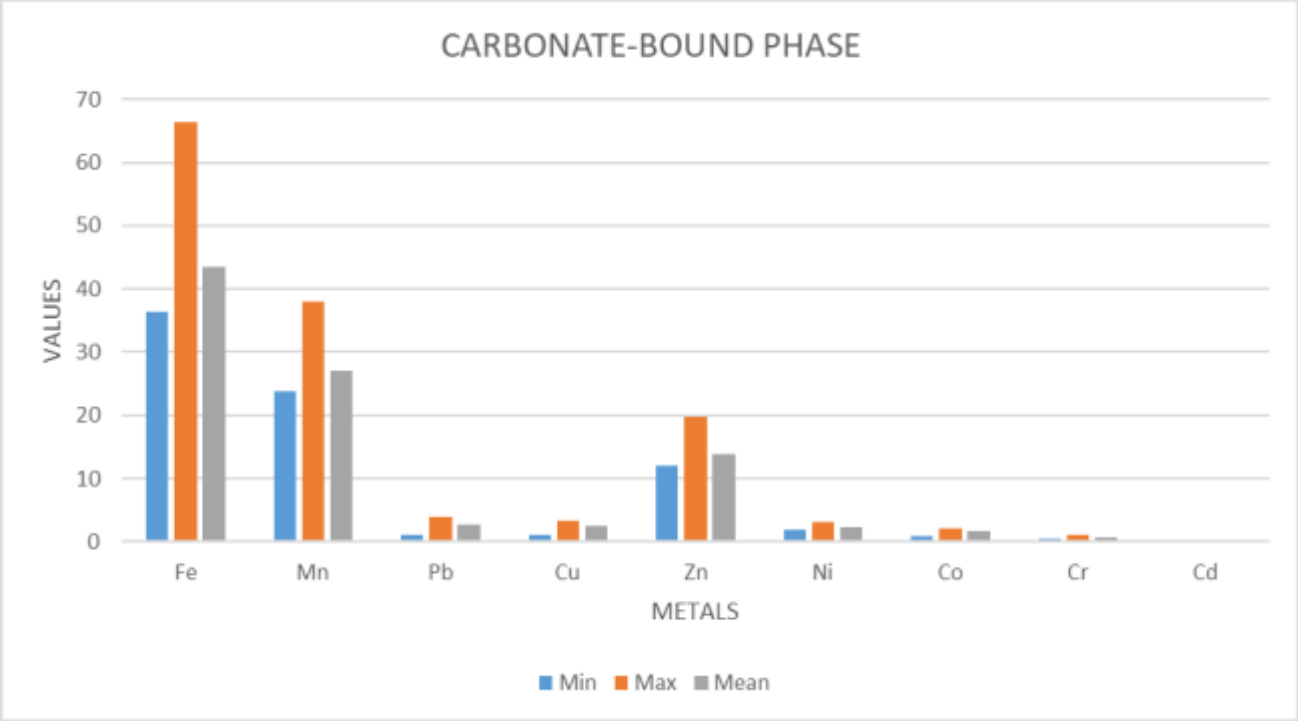


Fig.7. Cluster column chart of the heavy metal concentrations in the carbonate-bound phase (mg/kg). The figure illustrates the comparative distribution of metals across all samples, highlighting their relative enrichment and association with carbonate minerals within this geochemical fraction.

4.1.4 The Fe–Mn oxide phase

The Fe–Mn oxide phase represents an important metal-binding fraction because iron and manganese oxides possess high adsorption capacities and effectively retain trace metals within soils (Kabata-Pendias, 2011; Alloway, 2013). Tables 5a and 5b show that Fe (303.187–476.031 mg/kg) and Mn (139.204–267.163 mg/kg) dominate this fraction, indicating that Fe–Mn oxides are the principal sinks for trace metals in the study area. Zinc, Pb, Cu, and Ni also occur at relatively higher concentrations, whereas Co, Cr, and Cd are comparatively lower.

The statistical summary confirms the abundance order of Fe > Mn > Zn > Pb > Cu > Ni > Co > Cr > Cd, while samples SQ3, SQ4, and SQ15 exhibit relatively higher concentrations than SQ10, reflecting lithological variation and natural adsorption processes. The strong association of these metals with Fe–Mn oxides indicates efficient immobilization under the prevailing environmental conditions (Tessier et al., 1979).

Overall, the Fe–Mn oxide phase serves as a major geochemical reservoir that limits metal mobility and reduces their immediate availability to plants and groundwater. However, changes in redox conditions could release these adsorbed metals into the environment. Under the current conditions, the results suggest predominantly geogenic enrichment and a generally low environmental and human health risk to the local population.

Table 5a: Heavy metal concentrations in the Fe–Mn oxide phase (mg/kg). The table presents the distribution of metals associated with iron and manganese oxides across all samples, reflecting their strong adsorption capacity and role as key geochemical sinks for trace elements.

Samples	Fe (mg/Kg)	Mn (mg/Kg)	Pb (mg/Kg)	Cu (mg/Kg)	Zn **(mg/Kg)**	Ni (mg/Kg)	Co (mg/Kg)	Cr (mg/Kg)	Cd (mg/Kg)
SQ 1	354.813	152.227	25.711	13.403	63.866	19.181	10.271	6.361	0.621
SQ 2	361.558	175.129	22.019	15.019	63.545	20.196	11.287	6.185	0.657
SQ 3	435.209	237.214	33.277	20.236	74.091	22.573	14.263	9.159	1.872
SQ 4	446.513	241.116	35.332	21.873	77.129	26.103	14.742	10.015	1.983
SQ 6	362.145	154.434	26.072	12.615	63.071	20.032	10.481	5.235	0.598

SQ7	358.903	149.828	21.612	13.211	63.242	18.269	9.593	6.062	0.615
SQ 8	371.874	185.401	26.128	14.029	70.008	20.542	11.792	8.187	1.328
SQ 10	303.187	139.204	16.623	11.197	54.584	16.352	6.282	4.815	0.574
SQ 11	337.217	144.436	18.217	12.018	58.611	19.142	8.027	5.251	0.591
SQ 12	349.812	147.164	23.712	16.182	62.202	20.017	10.019	6.131	0.691
SQ 13	345.875	147.119	23.389	16.429	62.138	20.049	9.948	5.782	0.711
SQ 14	360.158	176.524	25.304	15.173	63.493	21.366	11.097	7.176	0.877
SQ 15	476.031	267.163	36.125	22.957	75.937	25.183	13.162	10.254	2.021
SQ 16	361.521	155.003	22.574	14.348	64.113	19.179	11.201	7.012	0.798
SQ 17	338.019	142.401	17.753	12.967	59.285	18.331	10.096	8.954	0.917

Table 5b: Statistical summary of the heavy metals concentration in the Fe–Mn oxide phase (mg/kg). The table shows the minimum, maximum, and mean concentrations of metals bound to Fe–Mn oxides, highlighting their significant enrichment and strong affinity for adsorption within this geochemical fraction.

Metal	Fe	Mn	Pb	Cu	Zn	Ni	Co	Cr	Cd
Min	303.187	139.204	16.623	11.197	54.584	16.352	6.282	4.815	0.574
Max	476.031	267.163	36.125	22.957	77.129	26.103	14.742	10.254	2.021
Mean	370.456	173.958	24.790	15.977	65.554	20.454	10.751	7.122	0.923

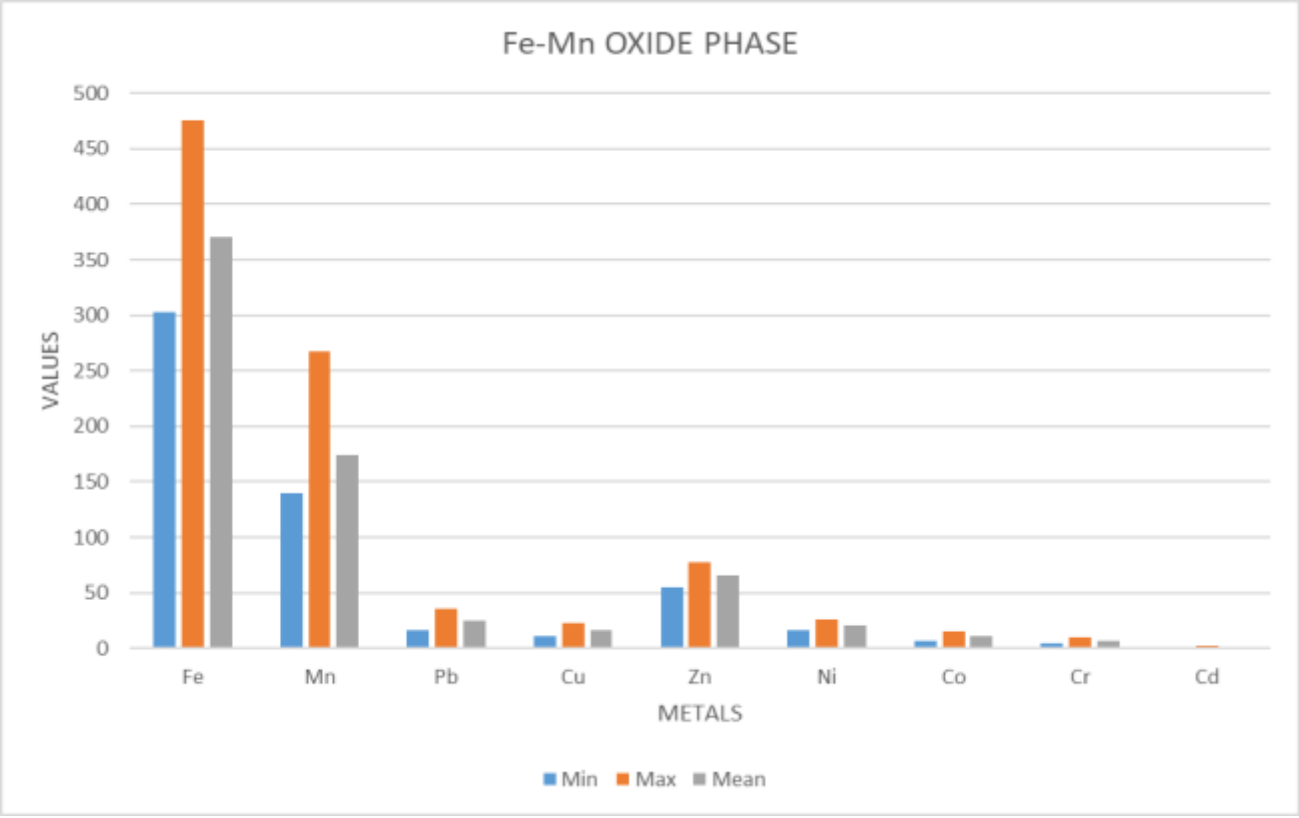


Figure 8. Cluster column chart of the heavy metal concentrations in the Fe–Mn oxide phase (mg/kg). The figure illustrates the comparative distribution of metals across all samples, highlighting strong enrichment and adsorption of trace elements onto Fe–Mn oxide phases within the study area.

4.1.5 The organic matter–bound phase

The organic matter–bound phase comprises metals complexed with organic materials such as humic substances and decomposed plant residues, serving as an important reservoir that regulates metal retention and release during organic matter decomposition (Kaiser & Kalbitz, 2012; Liu et al., 2022). Table 6a shows that Fe (148.854–356.163 mg/kg) and Mn (55.772–89.112 mg/kg) dominate this fraction, while Zn and Cu exhibit relatively high concentrations due to their strong affinity for organic compounds. Lead, Ni, Co, Cr, and Cd occur at comparatively lower concentrations.

The statistical summary in Table 6b indicates the abundance order of Fe > Mn > Zn > Cu > Ni ≈ Pb > Co > Cr > Cd, with relatively higher concentrations recorded in samples SQ3, SQ4, and SQ15. Figure 9 also demonstrates the dominance of Fe and Mn, reflecting the important role of organic matter in retaining trace metals within the soil.

Overall, the organic matter–bound phase indicates effective metal stabilization under current environmental conditions. However, decomposition of organic matter or changes in redox conditions could remobilize some metals into the soil solution. The present distribution suggests predominantly geogenic enrichment with low environmental and human health risk to residents of the study area (Alloway, 2013; Kaiser & Kalbitz, 2012).

Table 6a: Heavy metals concentrations in the organic matter–bound phase (mg/kg). The table shows the distribution of metals associated with organic matter across all samples, reflecting their affinity for organic complexation and potential release during organic matter decomposition.

Samples	Fe (mg/Kg)	Mn (mg/Kg)	Pb (mg/Kg)	Cu (mg/Kg)	Zn (mg/Kg)	Ni (mg/Kg)	Co (mg/Kg)	Cr (mg/Kg)	Cd (mg/Kg)
SQ 1	182.012	75.224	12.172	20.032	33.213	12.817	6.915	5.503	0.453
SQ 2	181.654	78.127	13.181	20.215	33.158	13.102	6.429	6.232	0.485
SQ 3	335.147	87.225	14.137	22.864	37.685	16.214	8.105	6.954	0.981
SQ 4	341.401	89.112	16.562	23.509	40.021	18.121	9.012	7.051	1.128
SQ 6	164.319	64.435	10.345	15.861	27.183	10.129	4.971	4.672	0.429
SQ7	168.247	64.247	10.631	15.539	28.011	10.216	5.056	4.956	0.433
SQ 8	189.074	81.236	13.123	20.421	33.786	13.014	6.747	6.143	0.472
SQ 10	148.854	55.772	9.926	14.158	24.128	8.997	4.635	4.329	0.414
SQ 11	152.627	57.201	10.011	15.141	25.091	9.089	4.921	4.457	0.425
SQ 12	169.612	65.236	11.162	16.214	25.274	10.176	5.068	4.781	0.446
SQ 13	169.881	64.837	11.134	16.452	25.181	10.089	5.112	8.714	0.451
SQ 14	180.575	76.294	12.634	21.052	32.846	12.763	6.557	5.773	0.472
SQ 15	356.163	87.826	15.663	24.486	40.372	18.522	9.138	7.074	1.221
SQ 16	185.052	75.135	12.246	20.415	33.325	13.012	6.751	6.028	0.482
SQ 17	168.176	65.095	10.773	15.404	28.197	10.332	6.904	6.193	0.462

Table 6b: Statistical summary of the heavy metals in the organic matter–bound phase (mg/kg). The table presents the minimum, maximum, and mean concentrations of metals associated with organic matter, indicating their degree of complexation and relative stability within this geochemical fraction.

Metal	Fe	Mn	Pb	Cu	Zn	Ni	Co	Cr	Cd
Min	148.854	55.772	9.926	14.158	24.128	8.997	4.635	4.329	0.414
Max	356.163	89.112	16.562	24.486	40.372	18.522	9.138	8.714	1.221
Mean	206.186	72.467	12.247	18.784	31.165	12.440	6.421	5.924	0.584

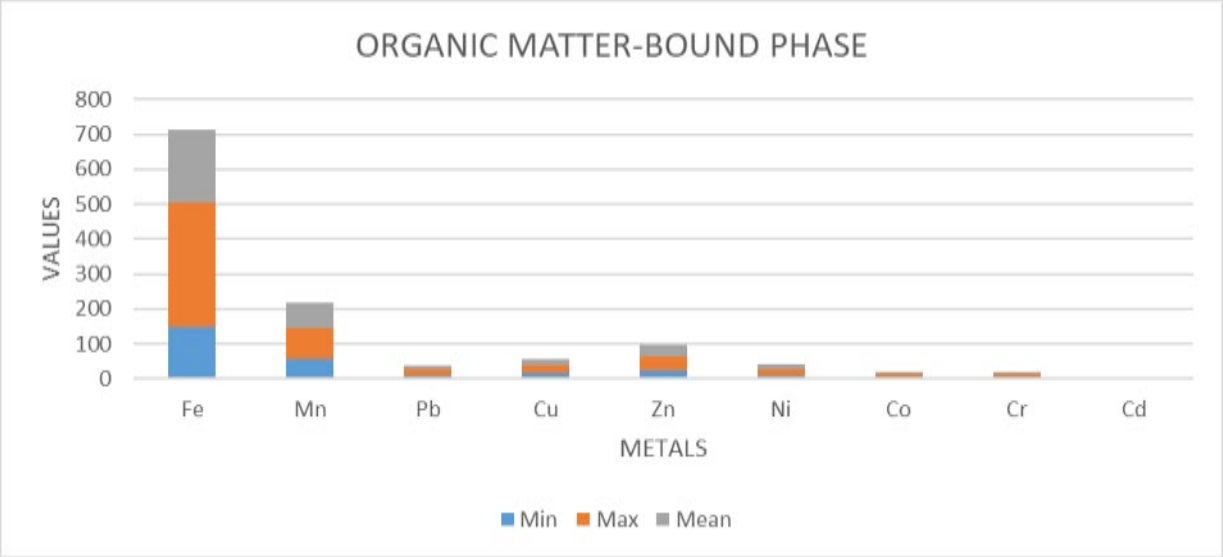


Fig.9. Cluster column chart of the heavy metal concentrations in the organic matter–bound phase (mg/kg). The figure illustrates the distribution of metals across all samples, highlighting their association with organic matter and relative enrichment through complexation with organic ligands.

4.1.6 The sulfide/strongly bound phase

The sulfide/strongly bound phase represents metals incorporated into sulfide minerals and resistant mineral lattices, making it one of the most stable and least mobile geochemical fractions (Tessier et al., 1979; Davidson et al., 1998). Table 7a shows that Fe (184.382–353.506 mg/kg) and Mn (75.148–150.084 mg/kg) dominate this phase, while Zn, Cu, and Pb exhibit moderate enrichment, indicating their affinity for sulfide-bearing minerals. Nickel, Co, Cr, and Cd occur at comparatively lower concentrations.

The statistical summary in Table 7b confirms the abundance order of Fe > Mn > Zn > Cu > Pb > Ni > Co > Cr > Cd. Higher concentrations recorded in samples SQ3, SQ4, and SQ15 suggest localized sulfide enrichment related to lithological variations rather than anthropogenic inputs. Figure 10 similarly highlights the dominance of Fe and Mn across the study area.

Overall, the sulfide/strongly bound phase represents a stable geochemical reservoir with very low metal mobility under present conditions. Although oxidation could release some of these metals into the environment, the current distribution indicates predominantly geogenic enrichment and poses minimal environmental and human health risk to the local population (Hakanson, 1980; Davidson et al., 1998).

Table 7a: Heavy metal concentrations in the sulfide/strongly bound phase (mg/kg). The table shows metals strongly associated with sulfide minerals and resistant phases, reflecting their low mobility and long-term geochemical stability within the soil matrix.

Samples	Fe (mg/Kg)	Mn (mg/Kg)	Pb (mg/Kg)	Cu (mg/Kg)	Zn (mg/Kg)	Ni (mg/Kg)	Co (mg/Kg)	Cr (mg/Kg)	Cd (mg/Kg)
SQ 1	251.118	105.746	18.723	14.103	31.411	11.652	6.342	5.126	0.343
SQ 2	252.049	108.224	17.916	14.321	30.782	11.761	6.226	5.472	0.345
SQ 3	345.371	147.602	24.432	20.438	35.255	15.004	7.752	6.159	0.798
SQ 4	352.217	147.916	25.543	20.825	36.126	15.243	8.116	6.458	1.128
SQ 6	184.382	83.239	12.621	13.127	26.134	9.827	4.279	4.174	0.312
SQ7	186.641	84.043	12.584	13.312	26.187	10.022	4.853	4.956	0.331
SQ 8	262.248	115.741	19.251	14.329	31.732	12.021	6.349	5.765	0.372
SQ 10	201.508	75.148	11.016	12.503	22.101	8.217	4.251	4.329	0.314
SQ 11	205.421	77.713	11.172	13.008	23.061	8.734	4.584	4.457	0.325

SQ 12	216.142	85.062	11.729	13.543	27.658	10.964	5.866	4.586	0.337
SQ 13	217.618	84.927	11.972	13.729	27.851	11.492	5.982	8.148	0.421
SQ 14	250.354	106.109	18.649	15.021	30.496	12.035	6.264	5.228	0.432
SQ 15	353.506	150.084	25.791	22.129	37.022	15.232	8.335	6.784	1.147
SQ 16	253.127	107.732	18.069	16.011	32.029	12.022	6.016	5.822	0.441
SQ 17	184.783	85.106	11.967	12.938	25.867	10.112	5.241	5.013	0.437

Table 7b: Statistical summary of the heavy metals concentration in the sulfide/strongly bound phase (mg/kg). This table presents the minimum, maximum, and mean concentrations of metals strongly bound within sulfide and resistant mineral phases, indicating their low mobility and high geochemical stability.

Metal	Fe	Mn	Pb	Cu	Zn	Ni	Co	Cr	Cd
Min	184.382	75.148	11.016	12.503	22.101	8.217	4.251	4.174	0.312
Max	353.506	150.084	25.791	22.129	37.022	15.243	8.335	8.148	1.147
Mean	247.766	104.293	16.762	15.289	29.581	11.623	6.030	5.498	0.499

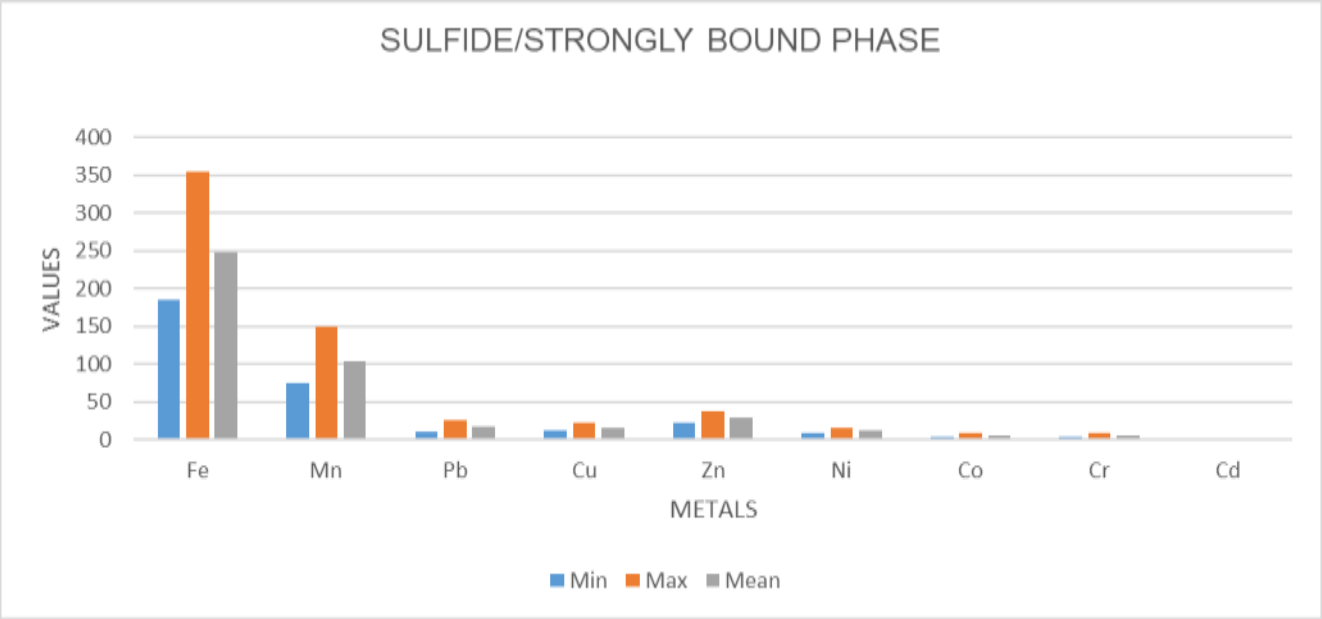


Fig.10. Cluster column chart of the heavy metal concentrations in the sulfide/strongly bound phase (mg/kg). The figure illustrates the distribution of metals strongly bound to sulfide and resistant mineral phases across all samples, highlighting their relative stability and low mobility in the geochemical system.

4.1.7 The residual phase

The residual phase represents metals incorporated within primary and secondary mineral lattices and is regarded as the most stable and least mobile fraction under natural environmental conditions (Tessier et al., 1979; Kabata-Pendias, 2011). Table 8a shows that Fe (12,532.459–16,416.143 mg/kg) and Mn (769.814–946.516 mg/kg) dominate this fraction, confirming strong lithogenic control. Zinc, Cr, Cu, Ni, Co, and Pb also occur at relatively higher concentrations, reflecting structural incorporation within silicate minerals, whereas Cd remains consistently low.

The statistical summary in Table 8b indicates the abundance order of Fe > Mn > Zn > Cr > Cu > Ni > Co > Pb > Cd. Higher concentrations observed in samples SQ3, SQ4, SQ14, and SQ15 reflect variations in parent rock composition, while lower values in SQ6, SQ10, and SQ13 are consistent with more felsic lithologies. Figure 11

further confirms the dominance of Fe and Mn and the stable distribution of the remaining metals.

Overall, the residual phase represents a long-term geochemical reservoir with negligible metal mobility under present conditions. The predominance of metals in this fraction indicates that their distribution is controlled mainly by the natural composition of the basement rocks, posing minimal environmental and human health risk to residents of the study area (Alloway, 2013).

Table 8a: Heavy metal concentrations in the residual phase (mg/kg). The table shows metals strongly locked within primary and secondary mineral lattices, representing the most stable and least mobile geochemical fraction in the soil system.

Samples	Fe (mg/Kg)	Mn (mg/Kg)	Pb (mg/Kg)	Cu (mg/Kg)	Zn **(mg/Kg)**	Ni (mg/Kg)	Co (mg/Kg)	Cr (mg/Kg)	Cd (mg/Kg)
SQ 1	13124.153	851.125	37.231	51.609	86.332	31.861	18.715	66.322	0.597
SQ 2	13231.582	862.197	35.793	52.096	84.809	32.168	19.207	66.188	0.553
SQ 3	16265.625	946.516	40.714	62.631	95.119	42.732	23.061	78.751	1.177
SQ 4	16416.143	941.849	42.028	61.979	97.151	43.833	23.146	80.015	1.185
SQ 6	15693.198	874.034	38.624	56.235	93.009	40.635	21.081	72.231	0.682
SQ7	12758.903	780.623	32.627	53.018	66.745	30.561	13.196	57.592	0.414
SQ 8	14753.727	865.106	36.942	54.723	88.126	34.642	20.731	68.685	1.127
SQ 10	12593.684	789.702	30.574	51.052	65.905	29.364	14.211	55.885	0.534
SQ 11	12682.363	776.937	31.077	51.031	68.016	29.902	13.723	55.759	0.511
SQ 12	14723.794	867.369	38.362	56.387	86.972	34.558	20.148	69.101	0.746
SQ 13	12532.459	769.814	30.984	52.125	68.132	32.092	13.741	55.704	0.642
SQ 14	15562.525	876.614	39.072	58.521	90.165	38.965	22.094	73.672	0.779
SQ 15	15469.538	872.607	40.729	57.985	92.007	39.018	21.628	71.961	1.302
SQ 16	13063.523	856.735	35.071	53.081	84.717	35.109	18.591	67.412	0.698
SQ 17	13274.221	842.699	34.866	52.983	85.458	35.238	18.793	66.923	0.602

Table 8b: Statistical summary of heavy metals in the residual phase (mg/kg). This table presents the minimum, maximum, and mean concentrations of metals retained in the residual fraction, representing the most stable and structurally bound geochemical pool in the soil matrix.

Metal	**Fe**	**Mn**	**Pb**	**Cu**	**Zn**	**Ni**	**Co**	**Cr**	**Cd**
Min	12532.459	769.814	30.574	51.031	65.905	29.364	13.196	55.704	0.414
Max	16416.143	946.516	42.028	62.631	97.151	43.833	23.146	80.015	1.302
Mean	14143.029	851.595	36.313	55.030	83.511	35.379	18.804	67.080	0.770

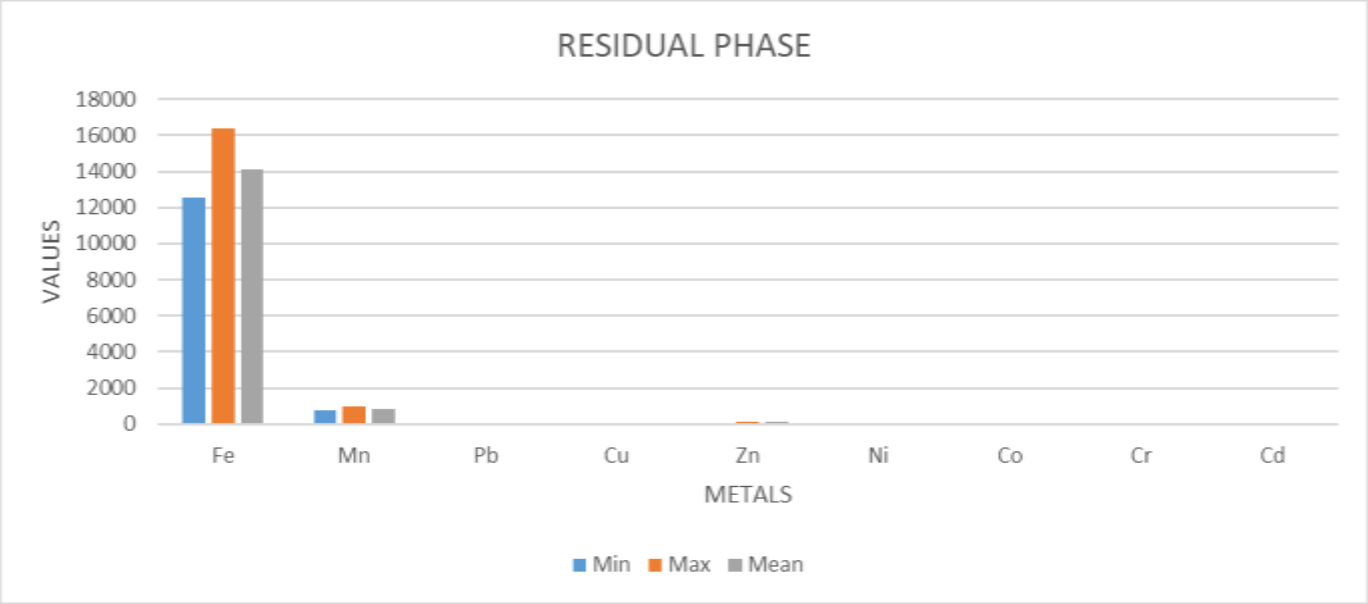


Fig.11. Cluster column chart of the heavy metal concentrations in the residual phase (mg/kg). The figure illustrates the distribution of metals in the residual fraction, highlighting their strong lithogenic control and dominance within primary mineral structures across all samples.

4.2 Contamination factor (CF) of heavy metals in soils of the study area

The Contamination Factor (CF) values presented in Table 9 and Figure 12 indicate varying degrees of heavy metal enrichment across the 17 sampling locations (SQ1–SQ17). Cadmium (Cd) records the highest CF values, with severe contamination at SQ3 (5.92), SQ4 (6.08), and SQ15 (6.20), while Pb also exhibits considerable contamination, with CF values ranging from 2.42 to 4.20. These patterns suggest localized metal enrichment within the study area.

Comparison with the geological setting indicates that samples collected from migmatite and granite gneiss terrains generally exhibit higher Cd concentrations, reflecting the influence of parent rock composition. However, the elevated CF values for Cd and Pb also suggest localized anthropogenic contributions, particularly around settlements and cultivated areas, where agricultural practices and other human activities may enhance metal accumulation (Reimann & de Caritat, 2005; Förstner & Wittmann, 2012).

Overall, Cd and Pb constitute the principal contaminants within the study area, whereas Fe remains largely within natural background levels. Although the observed contamination is localized, prolonged exposure to elevated Cd and Pb concentrations through soil, crops, or groundwater may pose potential environmental and human health risks, highlighting the need for periodic monitoring and sustainable land-use practices.

Table 9. Contamination factor (CF) of heavy metals in soils of the study area, indicating the degree of metal enrichment relative to background concentrations and providing an assessment of the level of soil contamination across the sampled locations.

Sample	Fe	Mn	Pb	Cu	Zn	Ni	Co	Cr	Cd
SQ1	0.315	1.34	3.29	2.13	2.04	1.06	1.17	0.88	3.31
SQ2	0.318	1.37	3.20	2.17	2.02	1.09	1.19	0.91	3.17
SQ3	0.396	1.67	4.03	2.64	2.38	1.29	1.39	1.17	5.92
SQ4	0.401	1.68	4.20	2.67	2.43	1.35	1.42	1.21	6.08
SQ6	0.324	1.33	3.38	2.25	2.22	1.17	1.13	1.01	3.79
SQ7	0.290	1.18	2.82	2.02	1.85	0.97	0.92	0.83	2.68
SQ8	0.351	1.47	3.66	2.31	2.23	1.18	1.22	1.09	5.03

Sample	Fe	Mn	Pb	Cu	Zn	Ni	Co	Cr	Cd
SQ10	0.273	1.06	2.42	1.73	1.57	0.86	0.74	0.76	2.21
SQ11	0.281	1.10	2.57	1.84	1.66	0.91	0.81	0.79	2.36
SQ12	0.338	1.34	3.41	2.22	2.19	1.14	1.13	1.03	3.88
SQ13	0.339	1.33	3.39	2.23	2.23	1.16	1.11	1.08	4.05
SQ14	0.372	1.60	3.73	2.46	2.33	1.24	1.20	1.13	4.32
SQ15	0.395	1.71	4.10	2.61	2.41	1.31	1.21	1.22	6.20
SQ16	0.342	1.36	3.27	2.30	2.22	1.19	1.18	1.12	4.51
SQ17	0.319	1.29	3.18	2.19	2.17	1.16	1.17	1.10	4.36

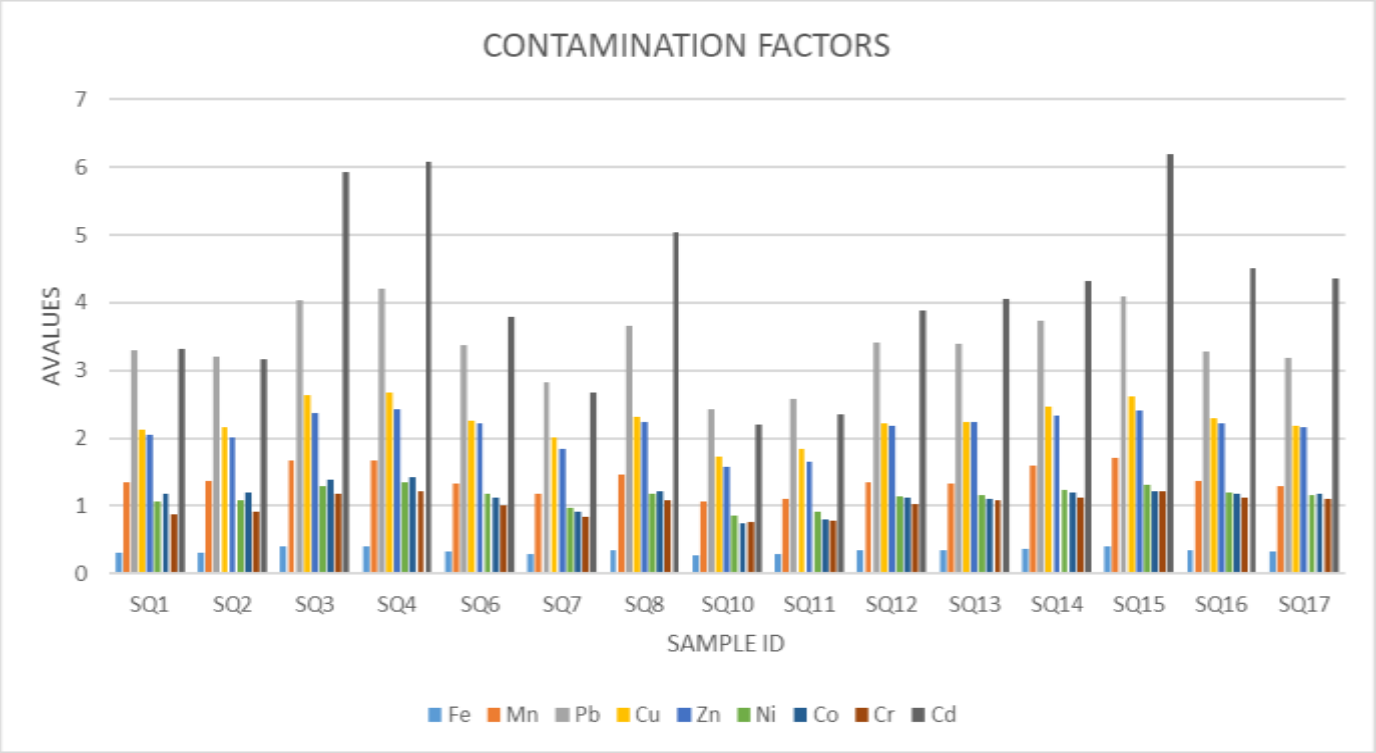


Fig.12: Clustered column chart showing the contamination factor of heavy metals in soil of the study area

4.3 Pollution Load Index (PLI) of heavy metals in soils from the study area

The Pollution Load Index (PLI) provides an integrated assessment of overall heavy metal contamination by combining the contributions of all analyzed elements at each sampling location. From Table 10 and Figure 13, the spatial variation of soil quality across the study area can be effectively evaluated.

In general, the PLI interpretation follows the standard classification where PLI = 1 indicates baseline conditions, PLI > 1 reflects progressive soil deterioration due to pollution, and PLI < 1 suggests unpolluted or near-pristine conditions (Tessier et al., 1979; Förstner & Wittmann, 2012). Based on Table 10, most sampling points exhibit PLI values greater than 1, indicating widespread deterioration of soil quality and confirming the presence of significant heavy metal stress across the study area (Hakanson, (1980).

Spatially, Figure 13 reveals distinct contamination hotspots, with the highest PLI values recorded at SQ15 (1.45), SQ4 (1.41), and SQ3 (1.38). These locations coincide with areas of more intense human activity and possible lithological influence from Migmatite–Gneiss transitions, which may enhance metal retention and accumulation (Reimann & de Caritat, 2005). In contrast,

lower PLI values at SQ9 (0.85), SQ10 (0.86), and SQ11 (0.90) suggest relatively unpolluted conditions, likely reflecting reduced anthropogenic disturbance or more effective natural dispersion mechanisms.

The combined interpretation of Table 10 and Figure 13 shows that soil contamination in the study area is spatially variable but generally elevated, with clear evidence of localized hotspots. This pattern reflects the combined influence of geogenic background variability and anthropogenic inputs, consistent with established soil geochemical behavior in complex terrains (Reimann & de Caritat, 2005; Förstner & Wittmann, 2012).

Table 10. Pollution Load Index (PLI) of heavy metals in soils from the study area, providing an integrated assessment of the overall level of soil contamination based on the combined contribution of all analyzed heavy metals across the sampled locations.

Sample	PLI
SQ1	1.12
SQ2	1.11
SQ3	1.38
SQ4	1.41
SQ6	1.15
SQ7	0.98
SQ8	1.27
SQ9	0.85
SQ10	0.86
SQ11	0.90
SQ12	1.18
SQ13	1.20
SQ14	1.31
SQ15	1.45
SQ16	1.29
SQ17	1.22

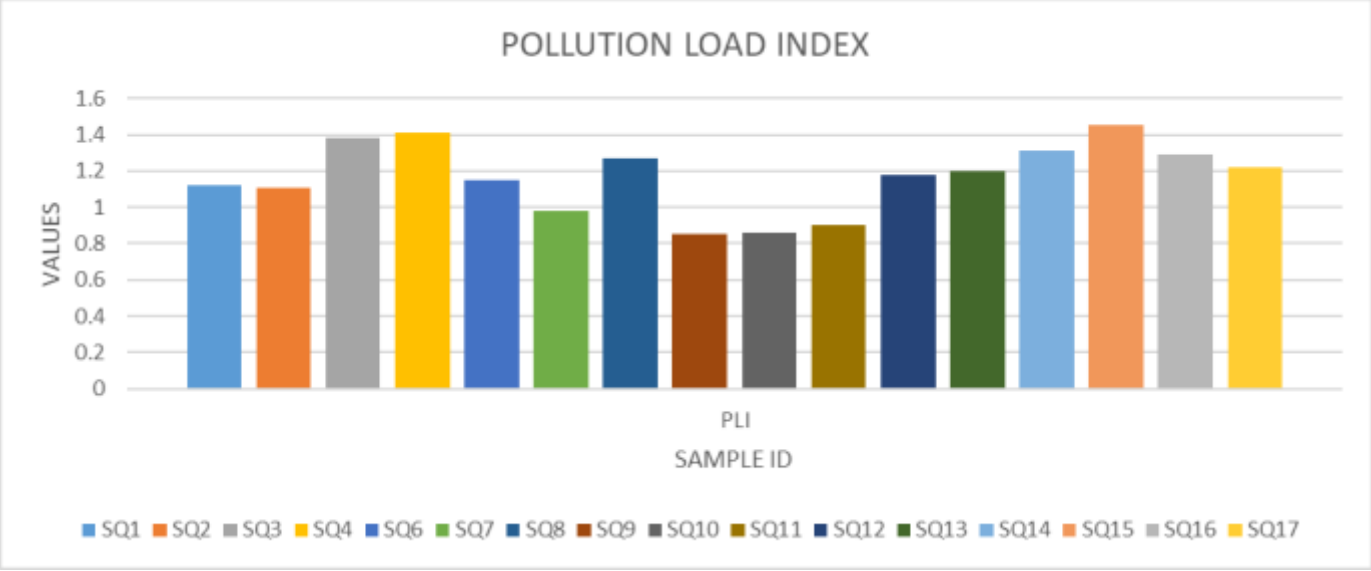


Fig.13: Clustered column chart showing the pollution load index of heavy metals in soil of the study area.

4.4 Major oxides geochemistry (Charnockite)

The Harker variation diagrams (Figure 14) illustrate the relationship between SiO_2 and the major oxides (Al_2O_3, MgO, CaO, Na_2O, K_2O, TiO_2, P_2O_5, and FeOt) for the charnockitic rocks from the Ikole–Itapaji–Ake-Ako area. Although only a few samples were analysed, the diagrams display coherent geochemical trends that provide insight into the magmatic evolution of the rocks.

MgO, CaO, TiO_2, and FeOt decrease with increasing SiO_2, indicating progressive depletion of ferromagnesian components during magmatic differentiation. This trend is consistent with fractional crystallization involving the early removal of pyroxene, amphibole, biotite, Fe–Ti oxides, and calcic plagioclase from the evolving magma. The decline in CaO further reflects continuous plagioclase fractionation, while the decrease in TiO_2 and FeOt suggests crystallization of Fe–Ti oxide minerals (Frost et al., 2001).

Conversely, K_2O, Na_2O, Al_2O_3, and P_2O_5 show positive correlations with increasing SiO_2. The enrichment of K_2O and Na_2O indicates increasing concentrations of alkali feldspars during the later stages of magmatic evolution, whereas the slight increase in Al_2O_3 reflects the dominance of feldspar-rich felsic assemblages. The progressive increase in P_2O_5 is attributed to the delayed crystallization of apatite, allowing phosphorus to accumulate in the residual melt before saturation (Frost & Frost, 2011).

Overall, the Harker variation patterns indicate that the charnockitic rocks evolved through fractional crystallization of a common parental magma, producing progressively silica-rich and compositionally evolved rocks. These trends are consistent with the magmatic evolution of granitoid suites within the Pan-African Basement Complex of southwestern Nigeria (Rahaman, 1988; Oyinloye, 2011).

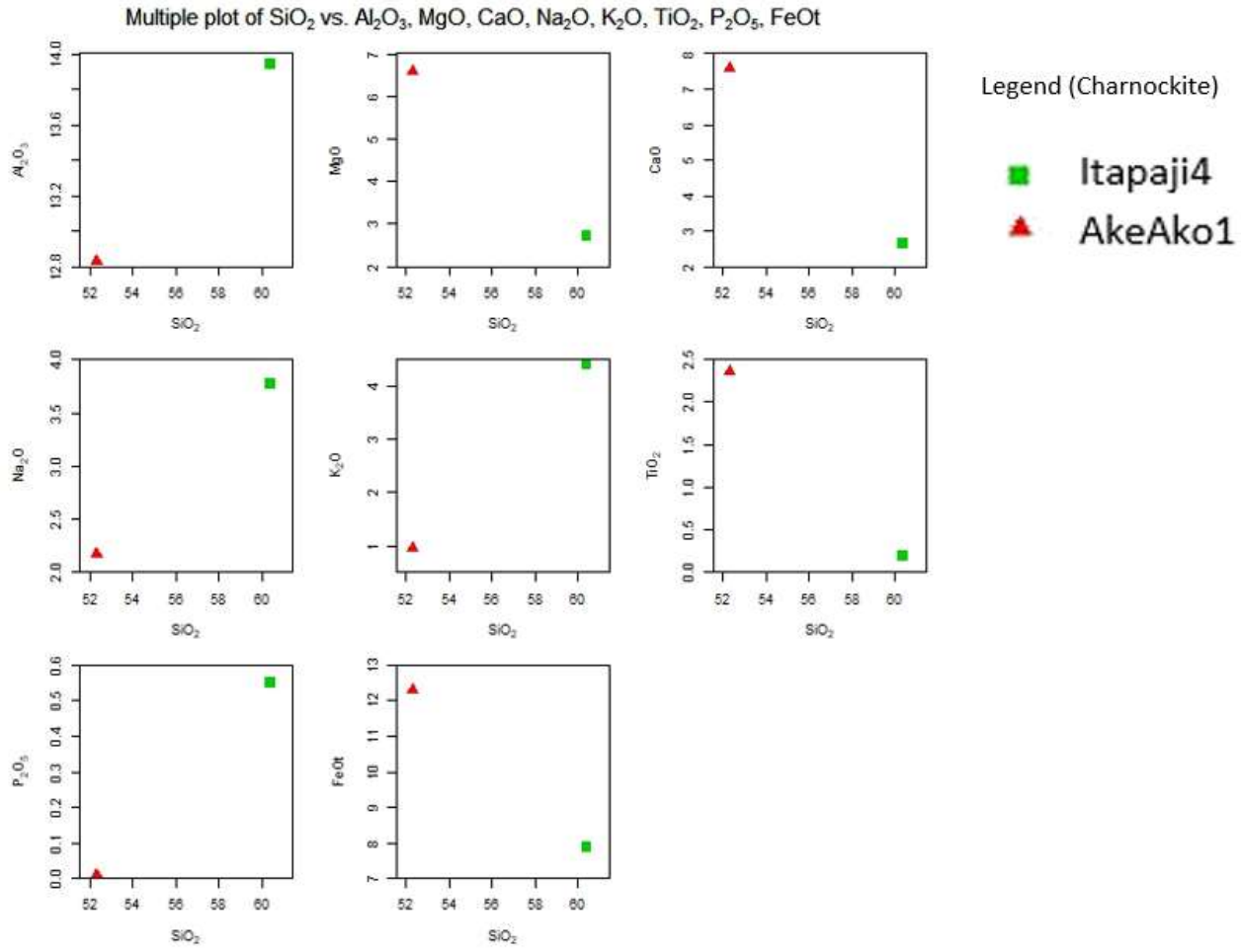


Fig.14. Harker variation diagrams showing the relationships between SiO_2 and the major oxides (Al_2O_3, MgO, CaO, Na_2O, K_2O, TiO_2, P_2O_5, and FeOt) for the charnockitic rocks from the Ikole–Itapaji–Ake-Ako area. The diagrams indicate systematic geochemical variations consistent with fractional crystallization and progressive magmatic differentiation (after Peccerillo & Taylor, 1976).

The A/CNK–A/NK diagram (Figure 15), proposed by Shand (1943), is widely used to classify granitoids according to their alumina saturation characteristics. The diagram distinguishes peralkaline, metaluminous, and peraluminous rocks based on the molecular proportions of Al_2O_3, CaO, Na_2O, and K_2O. The two analysed charnockitic samples from the Ikole–Itapaji–Ake-Ako area plot within the metaluminous field, indicating that the rocks contain sufficient Ca, Na, and K relative to Al to accommodate aluminium within feldspars and ferromagnesian minerals without forming peraluminous phases (Shand, 1943).

The Itapaji4 sample plots close to the boundary between the metaluminous and peralkaline fields (A/CNK ≈ 0.88), whereas the AkeAko1 sample lies more centrally within the metaluminous field (A/CNK ≈ 0.70). Both samples have A/CNK values below 1.0, confirming their metaluminous character. Such compositions are typically associated with granitoids dominated by plagioclase, hornblende, biotite, and pyroxene, reflecting magmas derived from mantle or lower crustal sources with limited crustal contamination (Frost et al., 2001).

The absence of peraluminous compositions indicates that the parental magma was not significantly enriched in aluminium through extensive crustal melting or sedimentary assimilation. Instead, the metaluminous nature of the charnockites suggests evolution through fractional crystallization of feldspars and ferromagnesian minerals. This interpretation is consistent with the evolution of Pan-African granitoids within the southwestern Nigerian Basement Complex (Rahaman, 1988; Oyinloye, 2011; Frost & Frost, 2011).

Overall, the clustering of both samples within the metaluminous field indicates a common magmatic affinity and supports their derivation from a genetically related parental magma that evolved primarily through fractional crystallization.

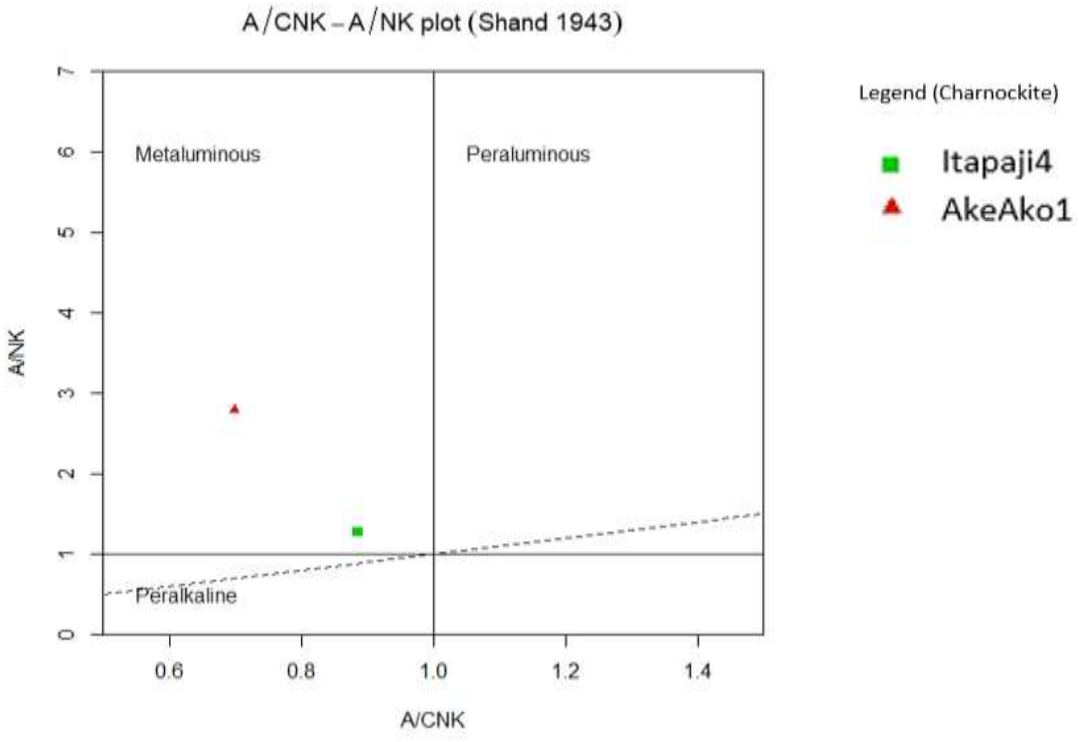


Fig.15. A/CNK–A/NK alumina saturation diagram after Shand (1943) showing that the analyzed charnockitic samples from the Ikole–Itapaji–Ake-Ako area plot within the metaluminous field, indicating crystallization from mantle-influenced magmas with limited crustal contamination.

The Fe-number versus SiO_2 diagram (Figure 16), proposed by Frost et al. (2001), classifies granitoid rocks into ferroan and magnesian series based on the ratio FeOt/(FeOt + MgO). This classification provides important information on magma evolution, oxidation state, and tectonic affinity. The analysed charnockitic samples from the Ikole–Itapaji–Ake-Ako area plot on opposite sides of the discrimination boundary, indicating subtle variations in their magmatic evolution (Frost et al., 2001).

The Itapaji4 sample plots within the ferroan field, indicating enrichment of total iron relative to magnesium. Ferroan granitoids are generally associated with iron-rich magmas that evolve through extensive fractional crystallization under relatively reduced conditions. Such granitoids commonly occur in post-collisional or within-plate tectonic environments where prolonged magmatic differentiation favours iron enrichment in the residual melt (Frost & Frost, 2011).

In contrast, the AkeAko1 sample plots within the magnesian field, indicating relatively higher magnesium contents compared to total iron. Magnesian granitoids are typically derived from relatively oxidized magmatic systems in which early crystallization of Fe–Ti oxides restricts iron enrichment while preserving higher Mg contents. These granitoids are commonly associated with calc-alkaline magmatic suites formed in convergent margin settings (Peccerillo & Taylor, 1976; Frost et al., 2001).

The close proximity of both samples to the ferroan–magnesian boundary suggests that the charnockitic suite exhibits transitional geochemical characteristics rather than representing two distinct magma series. The observed variation is most likely related to differences in fractional crystallization, oxidation conditions, or minor compositional heterogeneity within a common parental magma. This interpretation is consistent with the Pan-African evolution of granitoids within the southwestern Nigerian Basement Complex (Rahaman, 1988; Oyinloye, 2011).

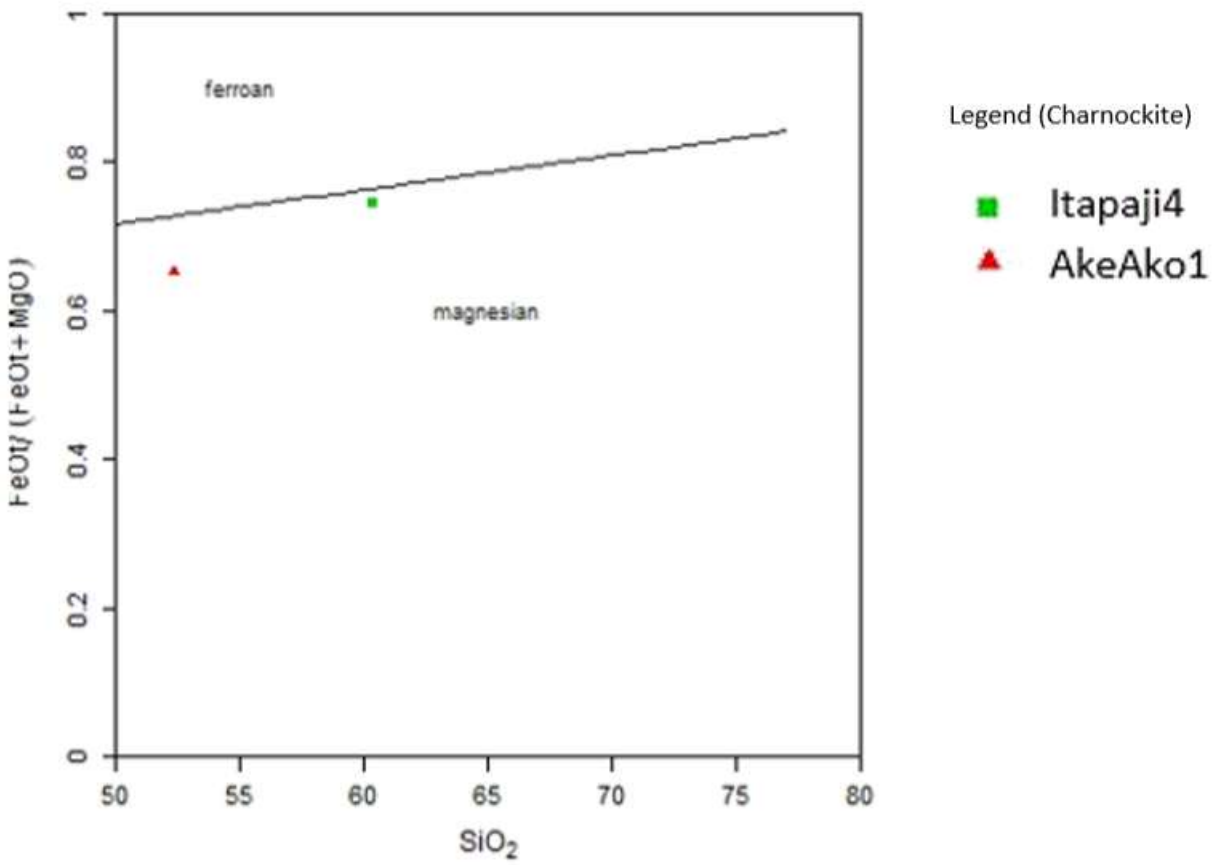


Fig.16. Fe-number (FeOt/ (FeOt + MgO)) versus SiO_2 discrimination diagram after Frost et al. (2001) showing that the charnockitic samples from the Ikole–Itapaji–Ake-Ako area exhibit both ferroan and magnesian affinities, indicating variations in iron enrichment during magmatic differentiation.

4.5 Major oxide geochemistry (Granite)

The Harker variation diagrams (Figure 17) show the relationships between SiO_2 and the major oxides (Al_2O_3, MgO, CaO, Na_2O, K_2O, TiO_2, P_2O_5, and FeOt) for the Igbona–Ikole granite samples. The sample with higher SiO_2 (Igbona–Ikole 2) exhibits lower Al_2O_3 and FeOt contents, indicating progressive depletion of ferromagnesian minerals and feldspars during fractional crystallization. These trends are consistent with magmatic differentiation commonly observed in felsic granitoids (Frost et al., 2001; Frost & Frost, 2011).

In contrast, Igbona–Ikole 2 shows slightly higher MgO, CaO, K_2O, TiO_2, and P_2O_5 contents than Igbona–Ikole 1. Considering the limited number of analysed samples, these variations likely reflect local compositional differences rather than systematic magmatic trends. The high silica contents (68–72 wt.% SiO_2) indicate that both samples represent evolved felsic granites derived from a common calc-alkaline magma (Rahaman, 1988; Oyinloye, 2011).

Overall, the Harker variation patterns support the results of the AFM, TAS, A/CNK–A/NK, and Fe-number classification diagrams, indicating that the Igbona–Ikole granites evolved through fractional crystallization and belong to a calc-alkaline granitoid suite emplaced during the Pan-African tectono-magmatic event (Peccerillo & Taylor, 1976; Frost et al., 2001).

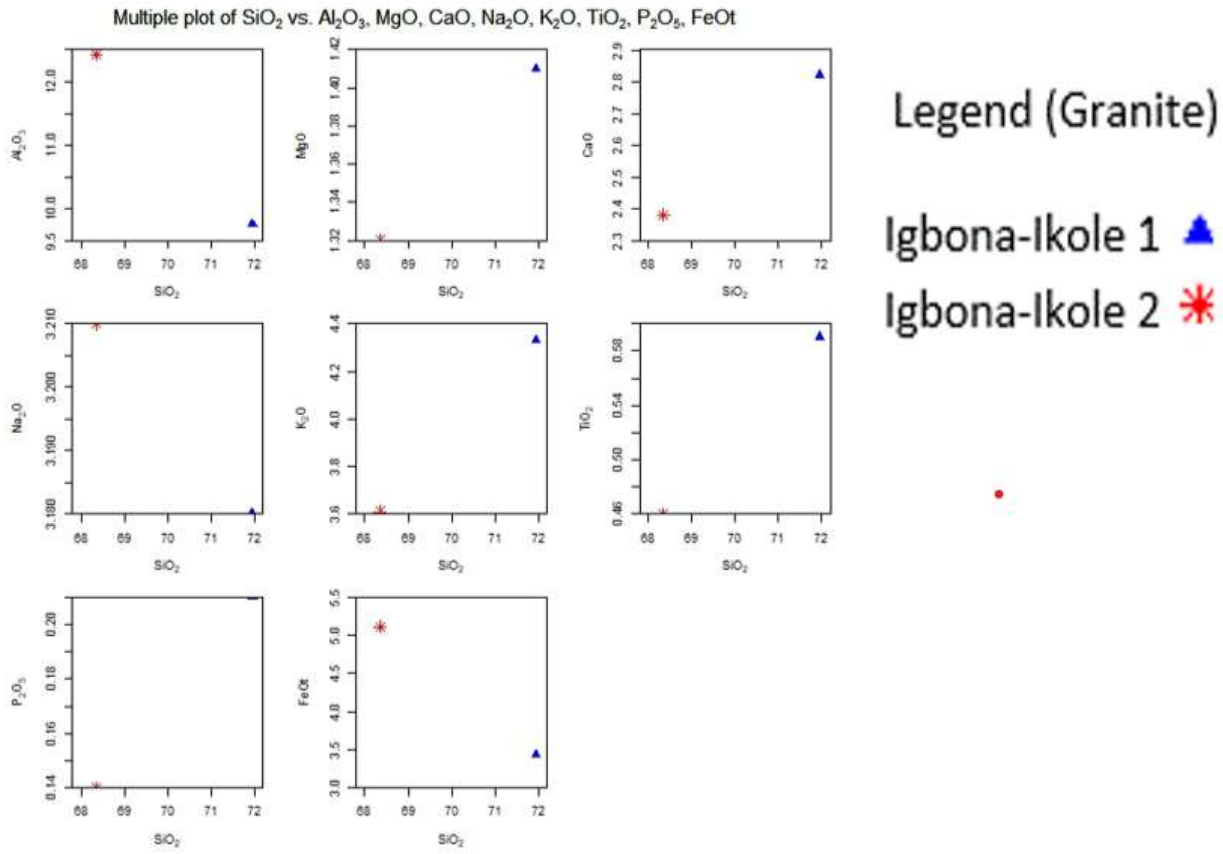


Fig.17. Harker variation diagrams showing the relationships between SiO_2 and the major oxides (Al_2O_3, MgO, CaO, Na_2O, K_2O, TiO_2, P_2O_5, and FeOt) for the granitic rocks from the Ikole–Itapaji–Ake-Ako area. The observed geochemical variations suggest progressive fractional crystallization and magmatic differentiation (after Peccerillo & Taylor, 1976).

The A/CNK–A/NK diagram (Figure 18), after Shand (1943), classifies the granite samples according to their alumina saturation characteristics using the molecular proportions of Al_2O_3, CaO, Na_2O, and K_2O. The two analyzed granite samples exhibit slight compositional variation, plotting within the metaluminous and weakly peraluminous fields.

The Igbona–Ikole 2 sample plots within the metaluminous field (A/CNK < 1.0), indicating that aluminium is balanced by Ca, Na, and K and is mainly hosted in feldspars and ferromagnesian minerals. In contrast, the

Igbona–Ikole 1 sample plots within the weakly peraluminous field, suggesting a slight excess of aluminium that may reflect limited crustal assimilation or partial melting of aluminous crustal materials during magma evolution. These characteristics are consistent with progressive fractional crystallization accompanied by minor crustal interaction in granitoid magmas (Shand, 1943; Frost et al., 2001; Frost & Frost, 2011).

The close proximity of the two samples indicates that the granites are genetically related and most likely evolved from a common parental magma, with the observed variation reflecting different degrees of magmatic differentiation rather than distinct magma sources (Peccerillo & Taylor, 1976; Frost & Frost, 2011).

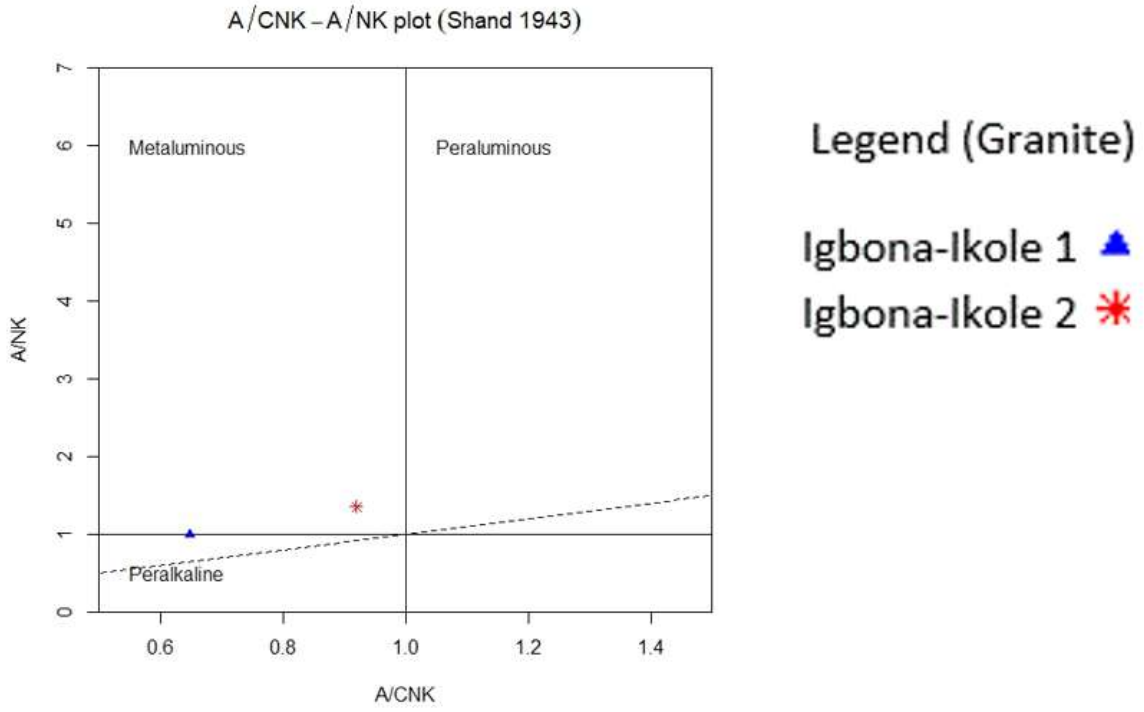


Fig.18. A/CNK–A/NK alumina saturation diagram showing the alumina saturation characteristics of the granitic rocks from the Ikole–Itapaji–Ake-Ako area. The samples plot within the metaluminous and weakly peraluminous fields, indicating evolution through fractional crystallization with limited crustal contamination (after Shand, 1943).

The Fe-number versus SiO_2 diagram (Figure 19), after Frost et al. (2001), classifies the granite samples according to their FeOt/(FeOt + MgO) ratios. Both Igbona–Ikole 1 and Igbona–Ikole 2 plot within the magnesian field, indicating that the granitic suite possesses a magnesian affinity typical of calc-alkaline granitoids (Frost et al., 2001; Frost & Frost, 2011).

Igbona–Ikole 2 plots well within the magnesian field, whereas Igbona–Ikole 1 lies close to the ferroan–magnesian boundary but remains magnesian. This slight variation suggests minor differences in iron enrichment during magma evolution while indicating that both samples are genetically related and evolved through progressive fractional crystallization.

The magnesian affinity implies crystallization under relatively oxidizing conditions, where early removal of Fe–Ti oxides limited iron enrichment in the residual magma. This interpretation is consistent with the calc-alkaline nature of the granites and supports emplacement within a convergent to post-collisional tectonic setting (Frost et al., 2001; Frost & Frost, 2011; Shand, 1943).

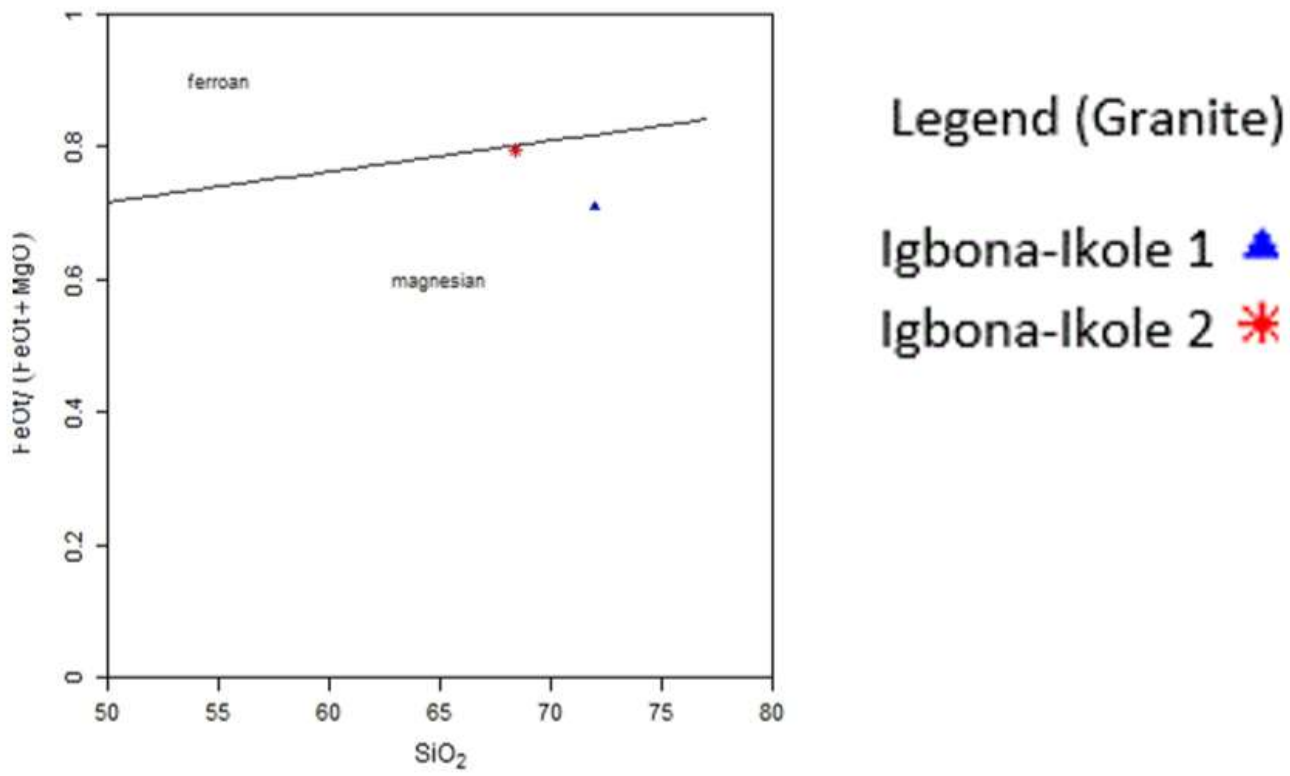


Fig.19. Fe-number (FeOt/(FeOt + MgO)) versus SiO_2 discrimination diagram after Frost et al. (2001) showing that the granitic rocks from the Ikole–Itapaji–Ake-Ako area plot within the magnesian field, indicating evolution under relatively oxidizing conditions through fractional crystallization.

4.6 Major oxide geochemistry (Granite Gneiss)

The Harker variation diagrams (Figure 20) illustrate the relationships between SiO_2 and the major oxides for the granite gneiss samples from the Ikole–Itapaji–Ake-Ako area. Most major oxides (Al_2O_3, MgO, CaO, Na_2O, K_2O, TiO_2, P_2O_5, and FeOt) generally decrease with increasing SiO_2, indicating progressive magmatic differentiation. Samples with lower silica contents contain higher MgO, CaO, and FeOt, whereas the high-silica samples are depleted in these oxides, reflecting fractional crystallization of ferromagnesian minerals, plagioclase, Fe–Ti oxides, and apatite (Frost et al., 2001; Frost & Frost, 2011).

Although slight scatter is observed for Na_2O and K_2O, the overall geochemical trends indicate evolution from a common calc-alkaline parental magma. Minor deviations are expected because the samples were collected from different outcrops that have experienced varying degrees of deformation and metamorphic overprinting within the Pan-African Basement Complex (Rahaman, 1988; Oyinloye, 2011).

Overall, the Harker variation patterns indicate that the granite gneiss represents differentiated felsic magmas that evolved through progressive fractional crystallization before regional metamorphism. This interpretation agrees with the AFM, TAS, A/CNK–A/NK, and Fe-number classification diagrams, which collectively indicate calc-alkaline affinity and predominantly metaluminous to weakly peraluminous compositions (Peccerillo & Taylor, 1976; Frost et al., 2001).

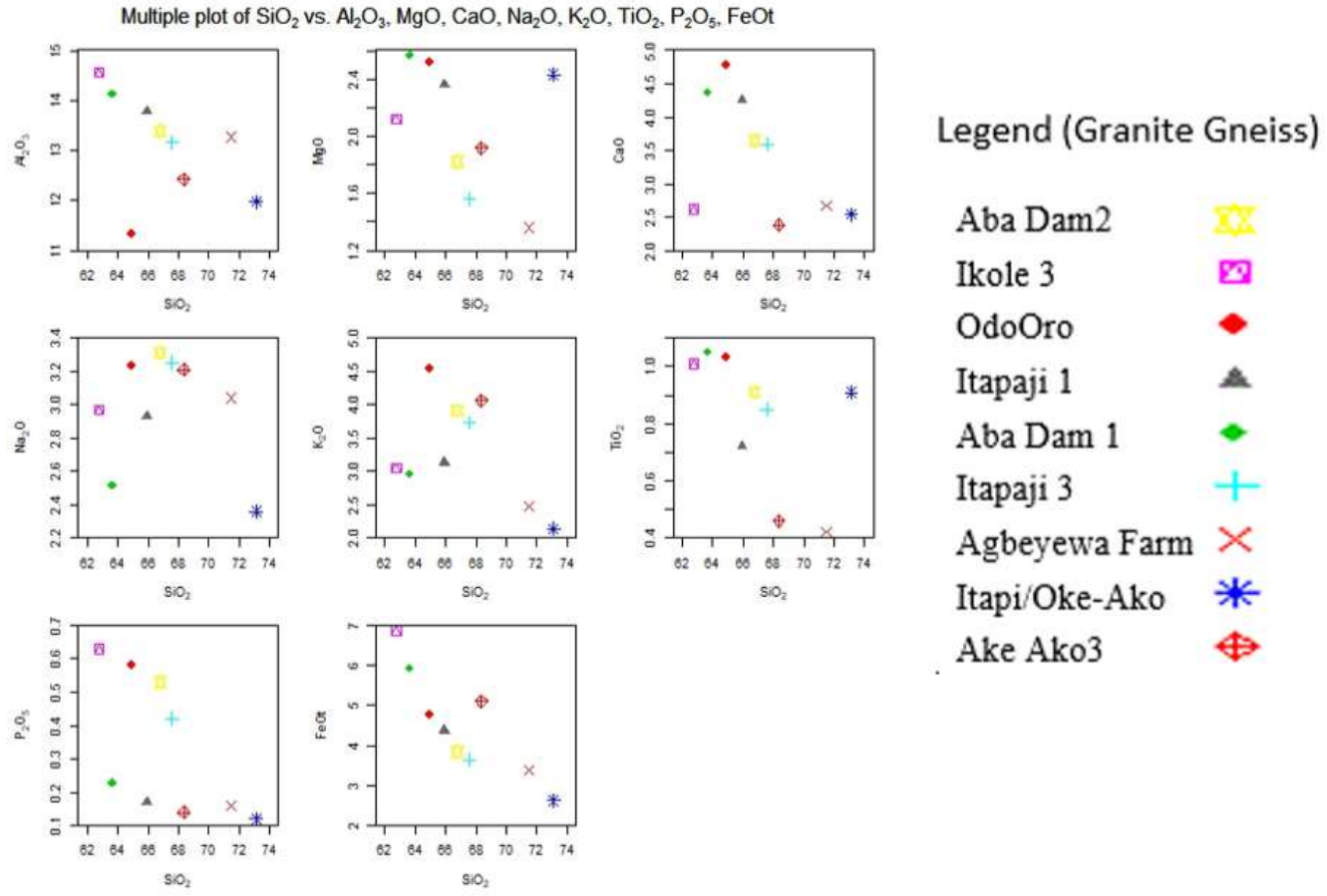


Fig.20. Harker variation diagrams showing the relationships between SiO_2 and the major oxides (Al_2O_3, MgO, CaO, Na_2O, K_2O, TiO_2, P_2O_5, and FeOt) for the granite gneisses from the Ikole–Itapaji–Ake-Ako area. The diagrams indicate systematic geochemical variations consistent with progressive fractional crystallization and magmatic differentiation (after Peccerillo & Taylor, 1976).

The A/CNK–A/NK diagram (Figure 21), after Shand (1943), classifies the granite gneiss samples according to their alumina saturation characteristics. The samples are distributed within both the metaluminous and weakly peraluminous fields, indicating slight compositional variation during magma evolution. Most samples plot within the metaluminous field (A/CNK < 1.0), suggesting that aluminium is mainly accommodated within feldspars and ferromagnesian minerals, a characteristic of I-type granitoids (Shand, 1943; Frost et al., 2001).

The Ayewagba and Itapi/OkeA samples plot within the weakly peraluminous field (A/CNK > 1.0), indicating a slight excess of aluminium that may reflect advanced fractional crystallization and limited crustal assimilation. Such compositions are commonly associated with evolved granitoid magmas emplaced during the Pan-African orogeny (Rahaman, 1988; Oyinloye, 2011).

Overall, the clustering of samples near the A/CNK = 1.0 boundary suggests that the granite gneisses evolved from a common parental magma, with the observed variation resulting from progressive differentiation and minor crustal interaction rather than distinct magma sources (Frost & Frost, 2011; Peccerillo & Taylor, 1976).

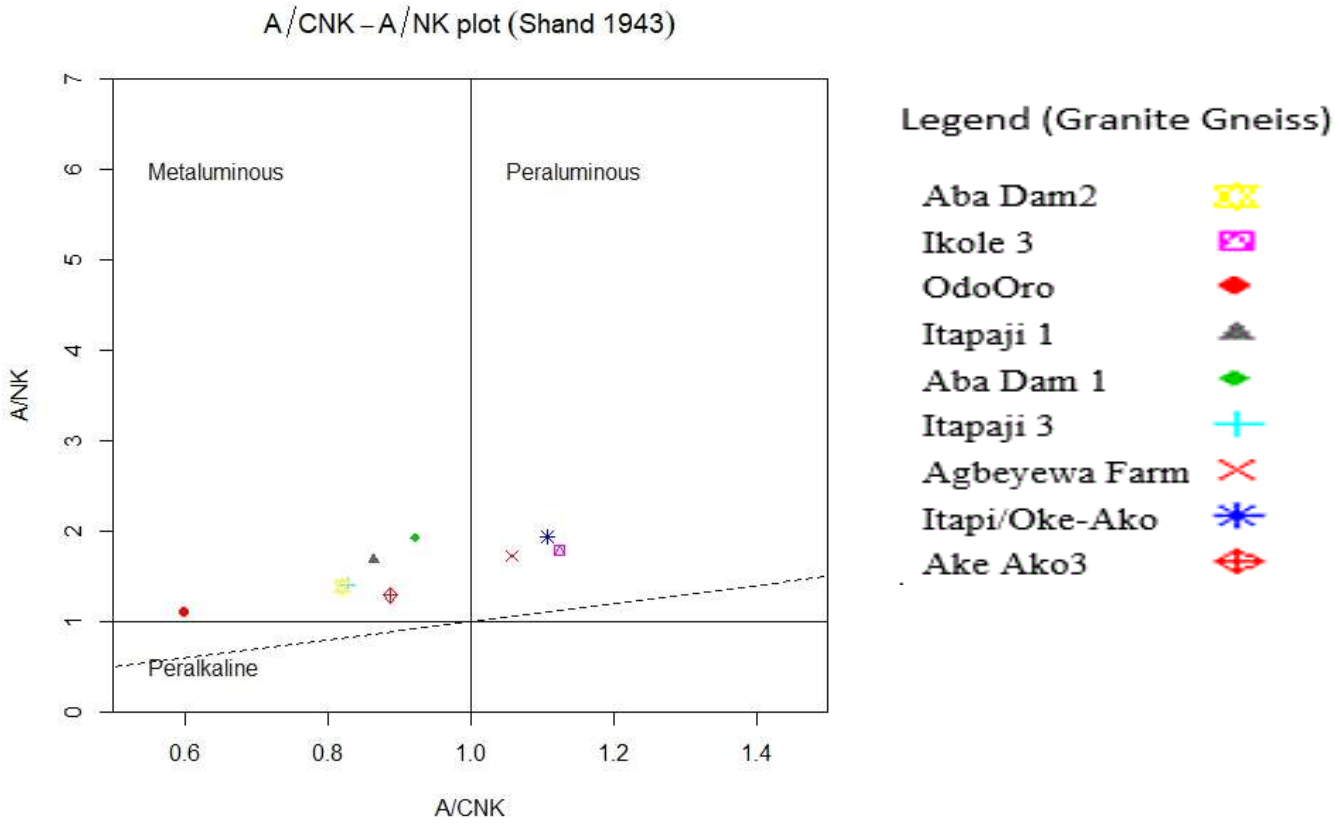


Fig.21. A/CNK–A/NK alumina saturation diagram showing that the granite gneisses from the Ikole–Itapaji–Ake-Ako area are predominantly metaluminous with a few weakly peraluminous samples, indicating evolution through fractional crystallization with minor crustal contamination (after Shand, 1943).

The Fe-number versus SiO_2 diagram (Figure 22), after Frost et al. (2001), classifies the granite gneiss samples into ferroan and magnesian series. Most of the samples plot within the magnesian field, indicating limited iron enrichment during magma evolution. This suggests crystallization under relatively oxidizing conditions typical of calc-alkaline granitoid suites (Frost et al., 2001; Frost & Frost, 2011).

The Ikole 3 sample plots close to the ferroan–magnesian boundary but remains within the magnesian field, indicating only slight iron enrichment relative to the other samples. This variation is interpreted as the result of progressive fractional crystallization rather than evidence for a separate magma series (Rahaman, 1988; Oyinloye, 2011).

Overall, the predominance of magnesian compositions supports the Harker and A/CNK–A/NK interpretations, indicating that the granite gneisses evolved from a common calc-alkaline parental magma through fractional crystallization with only limited crustal contamination (Peccerillo & Taylor, 1976; Frost et al., 2001).

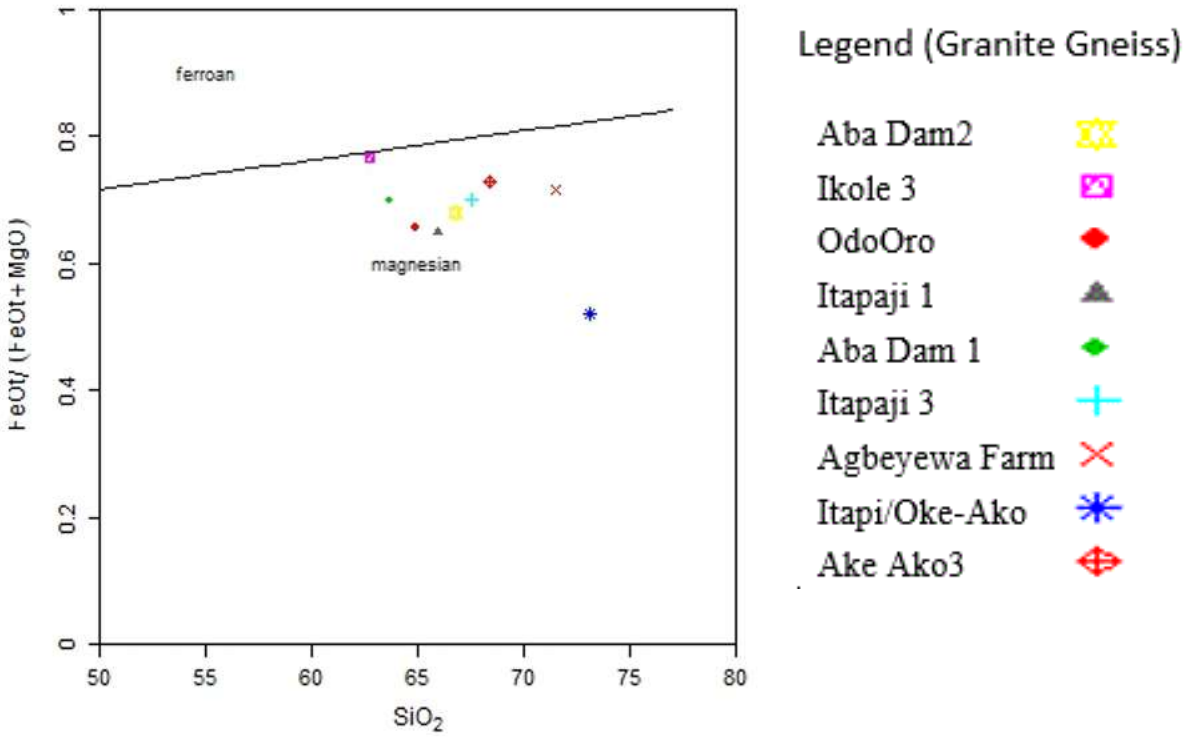


Fig.22. Fe-number (FeOt/ (FeOt + MgO)) versus SiO_2 discrimination diagram after Frost et al. (2001) showing that the granite gneisses from the Ikole–Itapaji–Ake-Ako area are predominantly magnesian, indicating evolution under relatively oxidizing conditions through progressive fractional crystallization

4.7 Major oxide geochemistry (Migmatite)

The Harker variation diagrams (Figure 23) illustrate the relationships between SiO_2 and the major oxides for the migmatite samples from the Ikole–Itapaji–Ake-Ako area. The diagrams show systematic geochemical trends typical of differentiated felsic magmas. The Ikole 4 sample, with the lowest SiO_2 content, contains the highest concentrations of Al_2O_3, MgO, CaO, Na_2O, TiO_2, and FeOt, indicating a relatively primitive composition enriched in ferromagnesian minerals and calcic plagioclase (Rahaman, 1988; Oyinloye, 2011).

In contrast, the Ikole 1 and Ikole 2 samples show higher SiO_2 contents accompanied by decreases in MgO, CaO, TiO_2, and FeOt, reflecting progressive fractional crystallization of amphibole, biotite, plagioclase, and Fe–Ti oxides. Al_2O_3 and Na_2O also decrease slightly with increasing silica, whereas K_2O increases, indicating enrichment of K-feldspar during the later stages of magma evolution (Frost et al., 2001; Frost & Frost, 2011).

Overall, the Harker variation patterns indicate that the migmatites evolved through progressive fractional crystallization from a common felsic parental magma, consistent with the prolonged magmatic evolution and crustal reworking associated with the Pan-African Basement Complex (Peccerillo & Taylor, 1976; Rahaman, 1988).

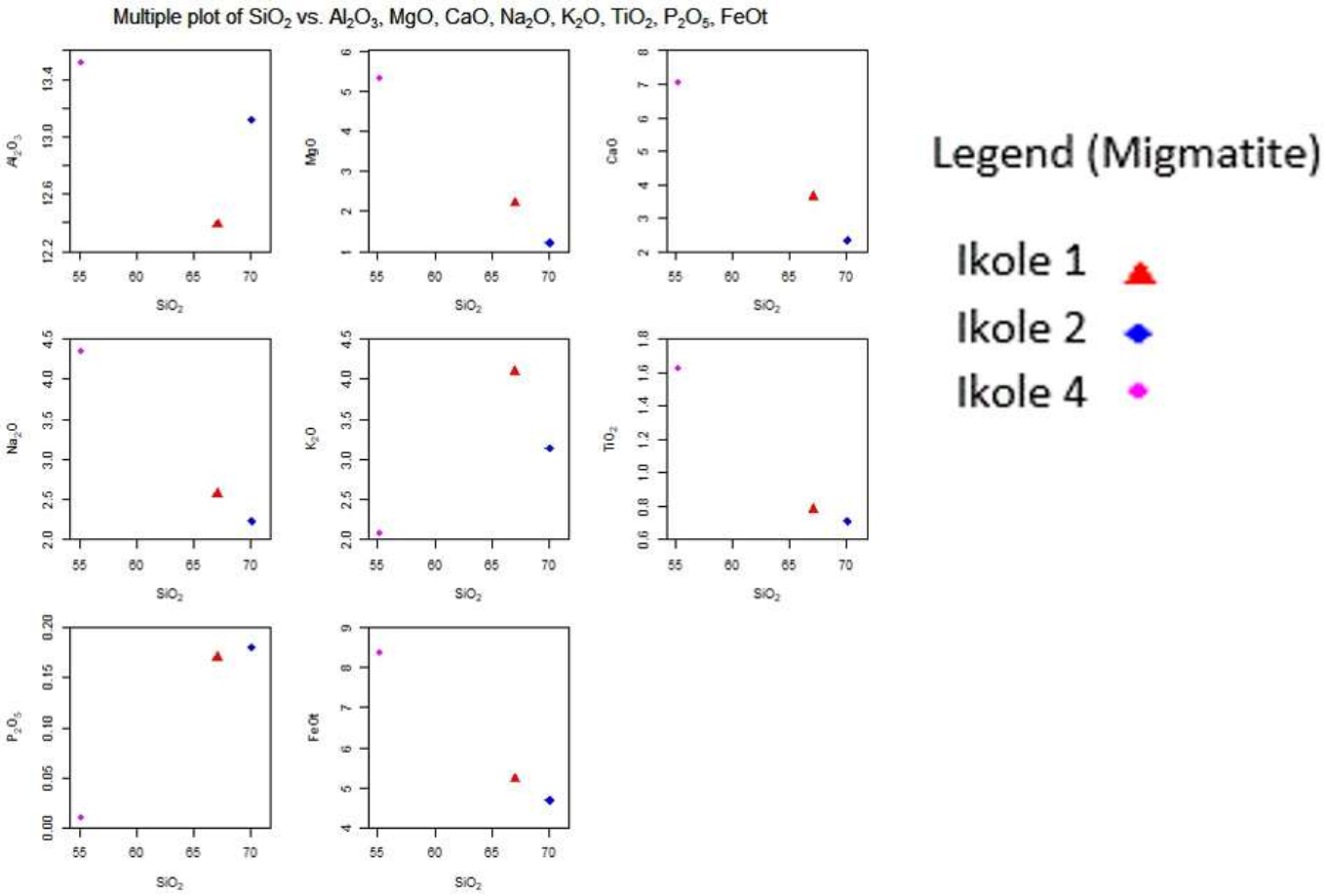


Fig.23. Harker variation diagrams showing the relationships between SiO_2 and the major oxides (Al_2O_3, MgO, CaO, Na_2O, K_2O, TiO_2, P_2O_5, and FeOt) for the migmatites from the Ikole–Itapaji–Ake-Ako area. The observed geochemical variations indicate progressive fractional crystallization and magmatic differentiation (after Peccerillo & Taylor, 1976).

The A/CNK–A/NK diagram (Figure 24), after Shand (1943), classifies the migmatite samples according to their alumina saturation characteristics. The samples plot within both the metaluminous and weakly peraluminous fields, indicating slight compositional variation during magma evolution. Ikole 1 and Ikole 4 are metaluminous (A/CNK < 1.0), suggesting that aluminium is mainly accommodated within feldspars and ferromagnesian minerals, whereas Ikole 2 is weakly peraluminous (A/CNK > 1.0), indicating a slight excess of aluminium (Shand, 1943; Frost et al., 2001).

The weakly peraluminous nature of the Ikole 2 sample suggests limited crustal contribution through partial melting or minor crustal assimilation during magmatic evolution, while the metaluminous samples reflect evolution dominated by fractional crystallization. These characteristics are consistent with granitoid magmatism within the Pan-African Basement Complex (Rahaman, 1988; Oyinloye, 2011).

Overall, the close distribution of the samples around the metaluminous–peraluminous boundary indicates that the migmatites evolved from a common parental magma, with the observed variations reflecting progressive differentiation and localized crustal reworking rather than distinct magma sources (Frost & Frost, 2011; Peccerillo & Taylor, 1976).

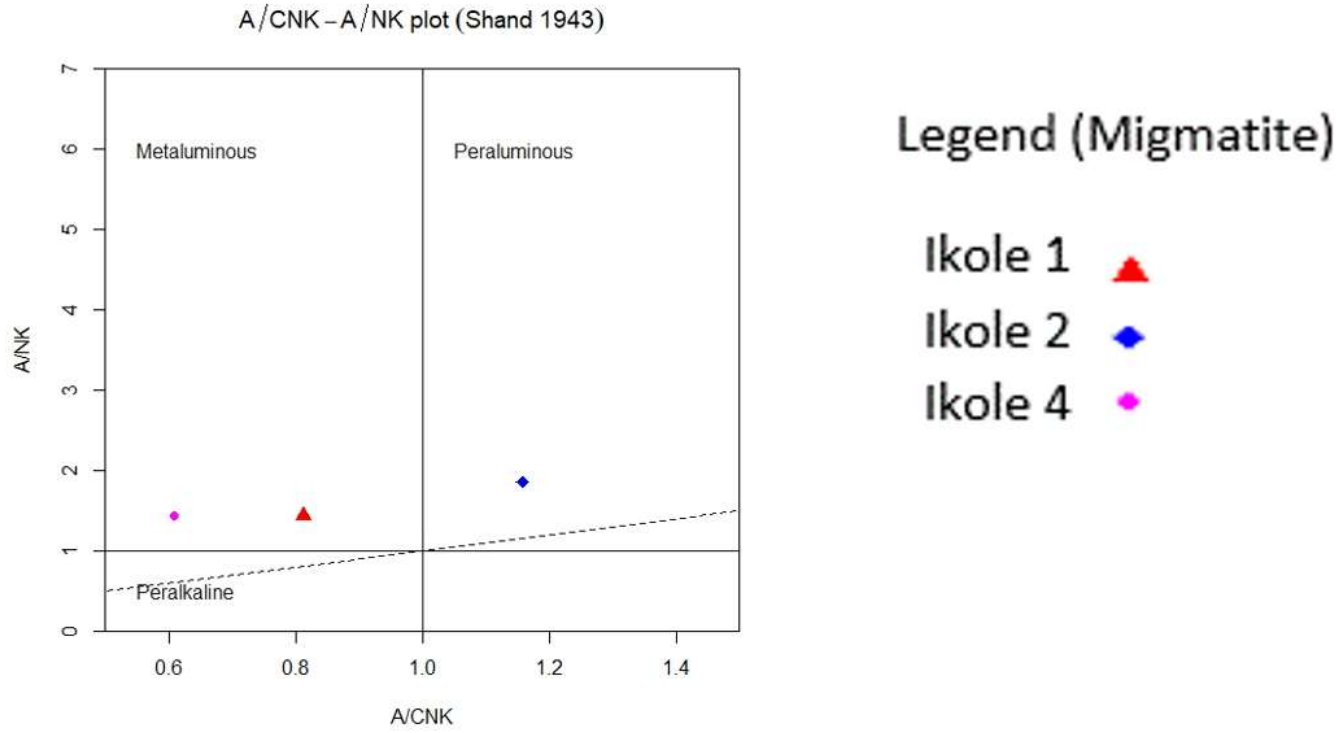


Fig.24. A/CNK–A/NK alumina saturation diagram showing that the migmatites from the Ikole–Itapaji–Ake-Ako area are predominantly metaluminous with one weakly peraluminous sample, indicating evolution through fractional crystallization accompanied by limited crustal contamination (after Shand, 1943).

The Fe-number versus SiO_2 diagram (Figure 25), after Frost et al. (2001), classifies the migmatite samples into ferroan and magnesian series. All the analyzed samples plot within the magnesian field, indicating a consistent magnesian affinity and limited iron enrichment during magma evolution. Although Ikole 2 plots close to the ferroan–magnesian boundary, it remains within the magnesian field, reflecting only minor compositional variation (Frost et al., 2001; Frost & Frost, 2011).

The predominance of magnesian compositions suggests that the parental magma evolved under relatively oxidizing conditions, where early crystallization of Fe–Ti oxides restricted iron enrichment in the residual melt. This geochemical signature is typical of calc-alkaline granitoids emplaced during the Pan-African tectono-magmatic evolution of the Nigerian Basement Complex (Rahaman, 1988; Oyinloye, 2011).

Overall, the close clustering of the samples within the magnesian field supports derivation from a common parental magma and agrees with the Harker and A/CNK–A/NK diagrams, which indicate progressive fractional crystallization with only minor crustal interaction (Peccerillo & Taylor, 1976; Frost et al., 2001).

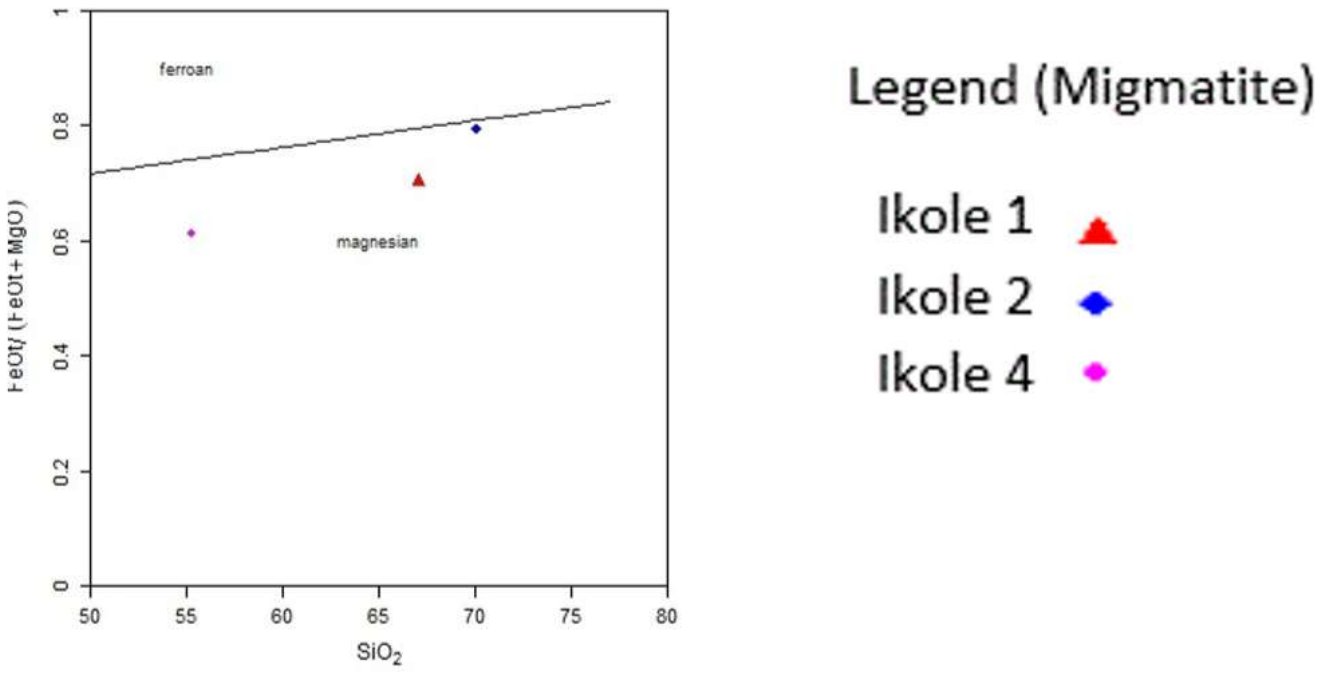


Fig.25. Fe-number (FeOt/(FeOt + MgO)) versus SiO_2 discrimination diagram after Frost et al. (2001) showing that the migmatites from the Ikole–Itapaji–Ake-Ako area plot within the magnesian field, indicating evolution under relatively oxidizing conditions through progressive fractional crystallization.

4.8 Major oxide geochemistry (Pegmatite)

The Harker variation diagrams (Figure 26) illustrate the relationships between SiO_2 and the major oxides for the pegmatite samples from the Ikole–Itapaji–Ake-Ako area. The diagrams show systematic geochemical trends characteristic of highly differentiated felsic magmas. The Omu sample, with the lowest SiO_2 content, contains the highest concentrations of MgO, CaO, TiO_2, and FeOt, indicating a relatively less evolved composition. In contrast, the Aba Farm Itapaji sample, with the highest SiO_2 content, is depleted in these oxides, reflecting advanced fractional crystallization (Rahaman, 1988; Oyinloye, 2011).

The general decrease in MgO, CaO, TiO_2, and FeOt with increasing SiO_2 indicates progressive removal of ferromagnesian minerals, calcic plagioclase, and Fe–Ti oxides during magma evolution. Al_2O_3 and Na_2O also show slight decreases, whereas K_2O remains consistently high, reflecting the abundance of K-feldspar and the highly evolved nature of the pegmatitic melt (Frost et al., 2001; Frost & Frost, 2011).

Overall, the Harker variation patterns indicate that the pegmatites represent highly evolved felsic melts produced through advanced fractional crystallization, consistent with the late-stage magmatic evolution of the Pan-African Basement Complex (Peccerillo & Taylor, 1976; Rahaman, 1988).

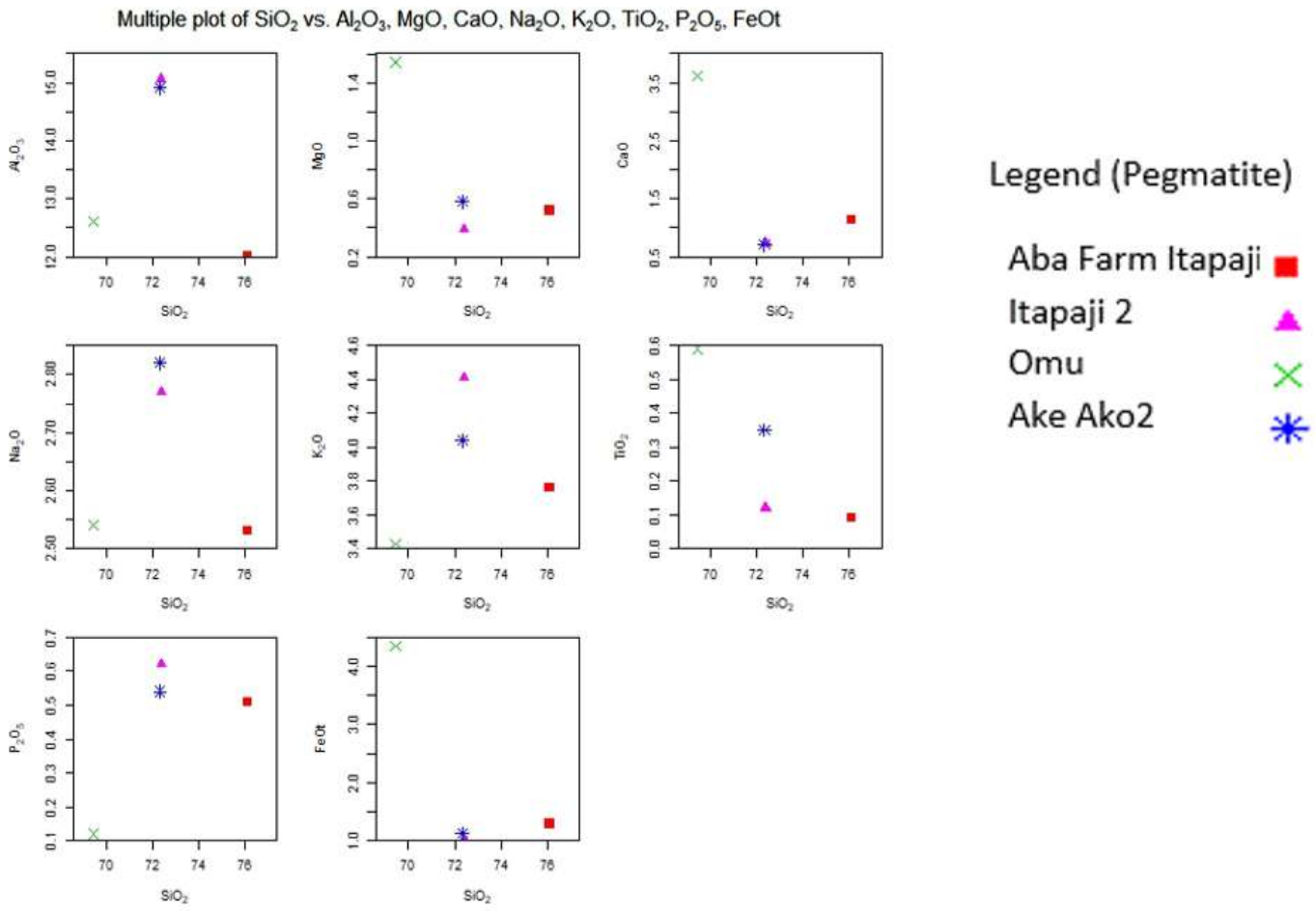


Fig.26. Harker variation diagrams showing the relationships between SiO_2 and the major oxides (Al_2O_3, MgO, CaO, Na_2O, K_2O, TiO_2, P_2O_5, and FeOt) for the pegmatites from the Ikole–Itapaji–Ake-Ako area. The geochemical trends indicate advanced fractional crystallization and the evolution of highly differentiated felsic magmas (after Peccerillo & Taylor, 1976).

The A/CNK–A/NK diagram (Figure 27), after Shand (1943), classifies the pegmatite samples according to their alumina saturation characteristics. The samples are predominantly peraluminous, with only the Omu sample plotting within the metaluminous field. The metaluminous composition of Omu (A/CNK < 1.0) suggests crystallization from a relatively less evolved felsic magma, whereas the other samples (A/CNK > 1.0) indicate increasing aluminium enrichment during magma evolution (Shand, 1943; Frost et al., 2001).

The Aba Farm Itapaji, Itapaji 2, and Ake Ako 2 samples exhibit weakly to strongly peraluminous compositions, reflecting advanced fractional crystallization and the evolution of highly differentiated pegmatitic melts. The higher A/CNK value of the Ake Ako 2 sample suggests the greatest degree of aluminium saturation within the suite (Rahaman, 1988; Oyinloye, 2011).

Overall, the predominance of peraluminous compositions and the absence of peralkaline samples indicate that the pegmatites evolved from highly fractionated calc-alkaline granitic magmas emplaced during the late stages of the Pan-African tectono-magmatic evolution of the Nigerian Basement Complex (Frost & Frost, 2011; Peccerillo & Taylor, 1976).

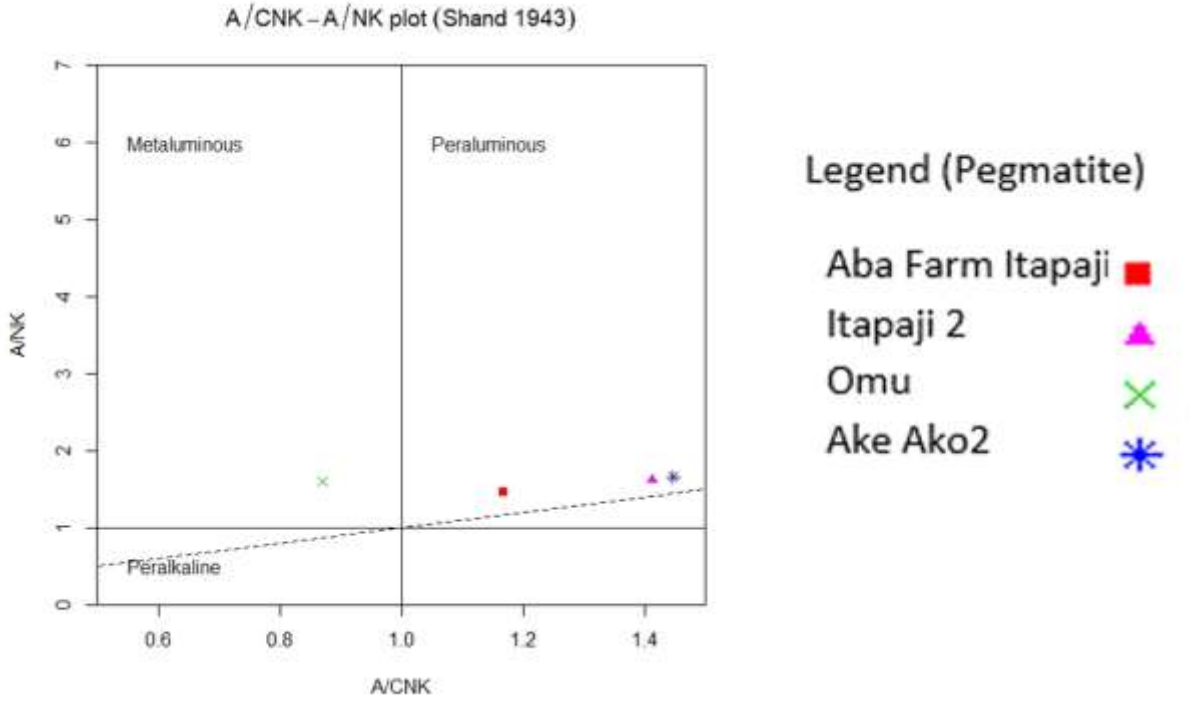


Fig.27. A/CNK–A/NK alumina saturation diagram showing that the pegmatites from the Ikole–Itapaji–Ake-Ako area are predominantly peraluminous, with one metaluminous sample, indicating derivation from highly evolved felsic magmas through extensive fractional crystallization and crustal interaction (after Shand, 1943).

4.9 Integrated Major Oxide Geochemistry, Contamination Factor and Pollution Load Index

The integration of the major oxide geochemistry with the Contamination Factor (CF) and Pollution Load Index (PLI) demonstrates that the geochemical characteristics of the Ikole–Itapaji area are controlled predominantly by the composition of the Precambrian Basement Complex rather than widespread anthropogenic contamination. The major oxide classification diagrams indicate that the crystalline rocks evolved mainly through fractional crystallization, producing predominantly calc-alkaline, magnesian, and metaluminous to weakly peraluminous granitoids that constitute the principal source of the major and trace elements observed in the soils (Rahaman, 1988; Oyinloye, 2011).

The sequential extraction results further show that most trace metals occur within the Fe–Mn oxide, sulfide/strongly bound, and residual fractions, indicating strong mineralogical control inherited from the parent rocks. This interpretation is consistent with the residual phase, where Fe and Mn dominate the geochemical composition, confirming that weathering of ferromagnesian and silicate minerals is the principal source of these elements. The relatively low concentrations observed in the water-soluble and exchangeable fractions indicate limited metal mobility under present environmental conditions.

The Contamination Factor results, however, reveal localized enrichment of Cd and Pb at a few sampling locations, while most other metals exhibit low to moderate contamination levels. Although the elevated Cd and Pb values may partly reflect localized anthropogenic inputs, their distribution does not alter the overall lithogenic signature established by the major oxide geochemistry. Similarly, the Pollution Load Index indicates that most sampling locations remain within acceptable to moderately polluted conditions, suggesting that natural geological processes exert a stronger influence on soil chemistry than human activities.

Overall, the integrated geochemical evidence indicates that the elemental composition of the study area is largely controlled by the evolution and weathering of calc-alkaline Pan-African granitoids, with only localized enrichment of environmentally sensitive metals. The combined application of major oxide geochemistry, sequential extraction, Contamination Factor, and Pollution Load Index therefore provides a comprehensive framework for distinguishing natural geogenic signatures from localized environmental contamination within the Ikole–Itapaji

Basement Complex (Peccerillo & Taylor, 1976; Frost et al., 2001).

4.10 Study Limitation

The present study provides a comprehensive assessment of the geochemical characteristics of the Ikole–Itapaji area; however, certain limitations should be acknowledged. The major oxide geochemical interpretation was based on a limited number of representative rock samples for each lithological unit, which, although adequate for lithological characterization, may not fully capture the complete geochemical variability of the entire Basement Complex.

The sequential extraction and pollution assessment were restricted to selected soil samples collected from representative locations within the study area. Consequently, localized variations in trace metal distribution associated with seasonal changes, land-use practices, or small-scale anthropogenic activities may not have been fully represented. In addition, the Contamination Factor (CF) and Pollution Load Index (PLI) were calculated using average shale values as background concentrations, which may differ slightly from the natural local geochemical background of the study area.

Furthermore, this study focused primarily on major oxide geochemistry and trace metal partitioning without incorporating isotopic analyses or geochronological investigations that could provide additional constraints on magma sources, timing of emplacement, and crustal evolution. Future studies integrating isotopic techniques, mineral chemistry, and a larger geochemical dataset would provide a more detailed understanding of the petrogenesis, tectonic evolution, and environmental geochemistry of the Ikole–Itapaji Basement Complex.

V. CONCLUSION

This study integrated geological mapping, major oxide geochemistry, sequential extraction, Contamination Factor (CF), and Pollution Load Index (PLI) to evaluate the petrogenesis of the crystalline basement rocks and the environmental status of soils within the Ikole–Itapaji area, Southwestern Nigeria. Geological mapping revealed that the area is underlain predominantly by migmatite, granite gneiss, granite, pegmatite, and charnockite, reflecting a complex Precambrian geological history involving high-grade metamorphism, partial melting, granitoid emplacement, and Pan-African tectonic reworking.

Major oxide geochemistry indicates that the granitoids evolved mainly through fractional crystallization, producing calc-alkaline, predominantly magnesian, and metaluminous to weakly peraluminous compositions. The Harker variation diagrams, A/CNK–A/NK plots, and Fe-number classifications collectively suggest that the rocks were derived from genetically related magmas with only minor crustal contamination, consistent with Pan-African granitoid evolution within the Nigerian Basement Complex.

Sequential extraction demonstrates that most trace metals are concentrated in the Fe–Mn oxide, sulfide/strongly bound, and residual fractions, indicating strong lithogenic control and limited mobility under present environmental conditions. The low proportions of metals in the water-soluble and exchangeable fractions further suggest that the majority of trace metals remain strongly retained within the soil matrix and are not readily available for migration or biological uptake.

The Contamination Factor and Pollution Load Index reveal that, although the overall geochemical signature is dominated by natural weathering of the basement rocks, localized enrichment of cadmium (Cd) and lead (Pb) occurs at some sampling locations. These elevated values indicate moderate to considerable contamination in specific areas and suggest that localized anthropogenic activities may have contributed to metal accumulation. While the present environmental risk is generally low because most metals are retained within relatively stable geochemical fractions, changes in soil pH, redox conditions, or prolonged weathering could enhance the release and mobility of Cd and Pb. Such mobilization may result in soil and groundwater contamination**,** uptake by food crops**,** bioaccumulation through the food chain**,** and ecotoxicological impacts on soil microorganisms and vegetation**.** Prolonged human exposure, particularly to cadmium and lead, may increase the risk of kidney dysfunction, neurological disorders, developmental impairment in children, skeletal damage, and other chronic health effects, underscoring the need for continuous environmental monitoring and sustainable land-use management.

Overall, the study establishes that the geochemistry of the Ikole–Itapaji area is controlled primarily by the composition and evolution of the underlying Precambrian Basement Complex. Nevertheless, the localized enrichment of potentially toxic metals highlights the need for periodic environmental monitoring, particularly in agricultural and residential areas, to prevent future ecological degradation and possible human exposure. The integrated approach adopted in this study provides a reliable framework for understanding basement rock petrogenesis, evaluating trace metal behaviour, and supporting sustainable environmental management and future mineral exploration within the study area.

5.1 Recommendations

Based on the findings of this study, the following recommendations are made:

1. Periodic environmental monitoring of soils within the Ikole–Itapaji area should be undertaken to track changes in trace metal concentrations, particularly cadmium (Cd) and lead (Pb), which exhibited localized enrichment in the Contamination Factor analysis.
2. Agricultural activities should be accompanied by routine soil quality assessments to ensure that trace metal concentrations remain within acceptable limits for sustainable crop production and to minimize the potential transfer of toxic metals into the food chain.
3. Anthropogenic activities capable of introducing heavy metals into the environment, such as indiscriminate waste disposal, excessive agrochemical application, and poorly managed artisanal activities, should be properly regulated to prevent further metal accumulation in soils.
4. Public awareness programmes should be implemented to educate local communities on the potential environmental and health implications of heavy metal contamination and the importance of adopting environmentally sustainable land-use practices.
5. Future studies should incorporate larger sample populations, seasonal sampling, groundwater and surface water analyses, and biological assessments to provide a more comprehensive evaluation of trace metal mobility, bioavailability, and ecological risk within the study area.
6. Advanced geochemical techniques, including isotope geochemistry, mineral chemistry, and geochronological analyses, are recommended to further constrain the petrogenesis, magma sources, and tectonic evolution of the granitoids within the Ikole–Itapaji Basement Complex.
7. The integrated geological and geochemical information generated in this study should be utilized as baseline data for future mineral exploration, environmental impact assessments, and land-use planning within the Ikole–Itapaji–Ake-Ako area and other parts of the Nigerian Basement Complex.

Declaration of competing interests

Ethical Approval

This study did not involve human participants, animals, or any form of clinical or ethical experimentation. Therefore, formal ethical approval was **not required.**

Declaration of generative AI and AI-assisted technologies in the manuscript preparation process

During the preparation of this work, the authors used ChatGPT (GPT-5-mini) to assist with language editing and content organization. After using this tool, the authors reviewed, revised, and verified all content to ensure accuracy, originality, and authenticity, and take full responsibility for the content of the published article.

Consent to Participate

As no human participants were involved in this research, obtaining consent for participation was **not applicable.** All research activities adhered to standard field and laboratory protocols without the involvement of people.

Consent to Publish

This study does not include any personal, sensitive, or identifiable information. Consequently, consent to publish was **not applicable**. All data presented are **scientific observations and analyses**, fully anonymized, and pose no ethical concerns.

Availability of Data and Materials:

The datasets used and analyzed during this study are available from the corresponding author upon reasonable request.

Authors' Contributions

Adeleke Ojo conceived and designed the study, conducted the geological field investigations, collected the rock and soil samples, carried out the laboratory investigations, performed the major oxide geochemical, sequential extraction, and environmental risk analyses, interpreted the results, prepared the figures and tables, and wrote, revised, and approved the final manuscript.

REFERENCES

[1] Abule, E. C., & Ekpete, O. A. (2025). Geochemical speciation and environmental implications of heavy metal mobility. https://doi.org/10.63561/fnas-jsi.v6i3.955

[2] Adetunla, F. R., Ayodele, O. S., Asowata, I. T., & Olususi, J. (2025). Integrated geological, aeromagnetic and remote sensing datasets in litho-structural mapping of basement rocks in southwestern Nigeria. *Asian Journal of Geological Research, 8*(3), 523–553. https://doi.org/10.9734/ajoger/2025/v8i3213

[3] Adriano, D. C. (2001). *Trace Elements in Terrestrial Environments: Biogeochemistry, Bioavailability, and Risks*

of Metals. Springer, New York. https://link.springer.com/book/10.1007/978-0-387-21510-5

[4] Alloway, B. J. (2013). *Heavy Metals in Soils: Trace Metals and Metalloids in Soils and Their Bioavailability* (3rd ed.). Springer. https://doi.org/10.1007/978-94-007-4470-7

[5] Birth, G. (2003). A scheme for assessing human impacts on coastal aquatic environments using sediments. https://doi.org/10.1007/978-3-662-05950-8_7

[6] Bouazizi, N., Baraud, F., Lemoine, M., & Leleyter, L. (2023). Shortened sequential extraction procedure: An effective and time-saving determination of trace metals in sediments. *Soil and Sediment Contamination.* https://doi.org/10.1080/15320383.2023.2293879

[7] Çelebi, E. E. (2024). Determination of metal fractions and rare earth anomalies using modified sequential extraction. *Environmental Earth Sciences, 83*, 93. https://doi.org/10.1007/s12665-023-11409-w

[8] Davidson, C. M., Duncan, A. L., Littlejohn, D., Ure, A. M., & Garden, L. M. (1998). A critical evaluation of the three-stage BCR sequential extraction procedure to assess the potential mobility and toxicity of heavy metals in industrially contaminated land. *Analytica Chimica Acta, 363*(1–2), 45–55. https://doi.org/10.1016/S0003-2670(98)00057-9

[9] De Matteis, C., Mantovani, L., Tribaudino, M., et al. (2023). Sequential extraction procedure of municipal solid waste incineration bottom ash targeting grain size and amorphous fraction. *Frontiers in Environmental Science, 11*, 1254205. https://doi.org/10.3389/fenvs.2023.1254205

[10] Delina, R. E. G. (2024). Partitioning and mobility of chromium using sequential extraction. *Environmental Science & Technology.* https://doi.org/10.1021/acs.est.3c10774

[11] Doi, T., Hamasaki, S., Yamamoto, H., et al. (2023). Dynamic sequential extraction procedure for extracting mercury from soil samples. *Analytical Sciences, 39*(5), 739–748. https://doi.org/10.1007/s44211-023-00313-9

[12] Filgueiras, A. V., Lavilla, I., & Bendicho, C. (2002). Chemical sequential extraction for metal partitioning in environmental solid samples. *Journal of Environmental Monitoring, 4*, 823–857. https://doi.org/10.1039/B207574C

[13] Firmino, F. H. T., et al. (2025). Efficiency of sequential extraction schemes in partitioning toxic elements. *European Journal of Soil Science.* https://doi.org/10.1111/ejss.70090

[14] Förstner, U., & Wittmann, G. T. W. (2012). *Metal Pollution in the Aquatic Environment.* Springer. https://doi.org/10.1007/978-3-642-69385-4

[15] Frost, B. R., Barnes, C. G., Collins, W. J., Arculus, R. J., Ellis, D. J., & Frost, C. D. (2001). A geochemical classification for granitic rocks. *Journal of Petrology, 42*(11), 2033–2048. https://doi.org/10.1093/petrology/42.11.2033

[16] Frost, C. D., & Frost, B. R. (2011). On ferroan (A-type) granites: Their compositional variability and modes of origin. *Journal of Petrology, 52*(1), 39–53. https://doi.org/10.1093/petrology/egq070

[17] Hakanson, L. (1980). An ecological risk index for aquatic pollution control: A sedimentological approach. *Water Research, 14*(8), 975–1001. https://doi.org/10.1016/0043-1354(80)90143-8

[18] Ibrahim, R., et al. (2024). Sequential extraction of heavy metals in soils. https://doi.org/10.33003/fjs-2024-0803-2451

[19] Kabata-Pendias, A. (2011). *Trace Elements in Soils and Plants* (4th ed.). CRC Press. https://doi.org/10.1201/b10158

[20] Kaiser, K., & Kalbitz, K. (2012). Cycling downwards—Dissolved organic matter in soils. *Soil Biology and Biochemistry, 52*, 29–32. https://doi.org/10.1016/j.soilbio.2012.04.002

[21] Liu, J., et al. (2022). Speciation of heavy metals in soils and their immobilization at micro-scale interfaces among soil components. *Science of the Total Environment, 825*, 153862. https://doi.org/10.1016/j.scitotenv.2022.153862

[22] Müller, G. (1969). Index of geoaccumulation in sediments of the Rhine River. *GeoJournal, 2*(3), 108–118. https://www.semanticscholar.org/paper/INDEX-OF-GEOACCUMULATION-IN-SEDIMENTS-OF-THE-RHINE-Muller/03688e2c0b4cabea9023db05e6b9a33281f0ea06

[23] Nigerian Geological Survey Agency (NGSA). (2006). *Geophysical Mapping of Nigeria: Airborne Radiometric and Magnetic Survey Data, 2006.* https://ngsa.gov.ng

[24] Ogah, A. J., & Abubakar, F. (2024). Solid mineral potential evaluation using integrated aeromagnetic and aeroradiometric datasets. *Scientific Reports, 14*, 1637. https://doi.org/10.1038/s41598-024-52270-6

[25] Ojo, O. F., Osazuwa, B. I., Chiemeke, C. C., Osumeje, O. J., Oyedele, A. A., Adagunodo, T. A., Oyeyemi, K. D., & Ejiga, E. G. (2024). Classification of the basement complex using aeromagnetic and remote sensing data analyses: Case study of Ekiti State, southwestern Nigeria. *Earth Sciences Malaysia, 8*(2), 158–162. https://doi.org/10.26480/esmy.02.2024.158.162

[26] Oyinloye, A. O. (2011). Geology and geotectonic setting of the Basement Complex rocks in Southwestern Nigeria: Implications on provenance and evolution. https://doi.org/10.5772/26990

[27] Peccerillo, A., & Taylor, S. R. (1976). Geochemistry of Eocene calc-alkaline volcanic rocks from the Kastamonu area, northern Turkey. *Contributions to Mineralogy and Petrology, 58*(1), 63–81. https://doi.org/10.1007/BF00384745

[28] Rahaman, M. A. (1988). Recent advances in the study of the Basement Complex of Nigeria. In *Precambrian Geology of Nigeria* (pp. 11–41). Geological Survey of Nigeria, Kaduna. https://www.scirp.org/reference/referencespapers?referenceid=1712445

[29] Reimann, C., & de Caritat, P. (2005). Distinguishing between natural and anthropogenic sources for elements in the environment. *Science of the Total Environment, 337*, 91–107. https://doi.org/10.1016/j.scitotenv.2004.06.011

[30] Reimann, C., & de Caritat, P. (2012). *Chemical Elements in the Environment: Factsheets for the Geochemist and Environmental Scientist.* Springer. https://doi.org/10.1007/978-3-642-72016-1

[31] Salako, K. A., Adetona, A. A., Rafiu, A. A., Augie, A. I., Jimoh, M. O., Alkali, A., Muriana, R. A., & Lawrence, J. O.

(2024). Integrated geophysical investigation for gold mineralization potential over the southern parts of Kebbi State, northwestern Nigeria. *Heliyon, 10*(14), e34093. https://doi.org/10.1016/j.heliyon.2024.e34093

[32] Shand, S. J. (1943). *Eruptive Rocks: Their Genesis, Composition, Classification, and Their Relation to Ore Deposits* (2nd rev. ed.). London: Thomas Murby & Co.

[33] Souza, J. P. R., Garnier, J., Quintarelli, J. M., et al. (2024). Adapted sequential extraction protocol for mercury speciation in mining environments. *Toxics, 12*(5), 326. https://doi.org/10.3390/toxics12050326

[34] Tessier, A., Campbell, P. G. C., & Bisson, M. (1979). Sequential extraction procedure for the speciation of particulate trace metals. *Analytical Chemistry, 51*, 844–851. https://doi.org/10.1021/ac50043a017

[35] Turekian, K. K., & Wedepohl, K. H. (1961). Distribution of the elements in some major units of the Earth's crust. *Geological Society of America Bulletin, 72*(2), 175–192. https://doi.org/10.1130/0016-7606(1961)72[175:DOTEIS]2.0.CO;2

[36] Wei, B., & Yang, L. (2010). A review of heavy metal contaminations in urban soils, urban road dusts and agricultural soils from China. *Microchemical Journal, 94*(2), 99–107. https://doi.org/10.1016/j.microc.2009.09.014

International Journal of Environment, Agriculture and Biotechnology
Vol-11, Issue-5; Sep-Oct, 2026
Peer-Reviewed International Journal
Journal Home Page Available: https://ijeab.com/
Journal DOI: 10.22161/ijeab

An Assessment of the Sea Buckthorn (*Hippophae rhamnoides L.)* Value Chain in Uttarakhand and Opportunities for Sustainable Marketing of Himalayan Natural Health Products in India

Ambarish Paikaray[1*], Subhashree Priyadarshini[2], Sandigdha Senapati[3] and Ambarish Ghosh[4]

[1,4]Faculty of Management Studies, The ICFAI University, Raipur, Bhilai Road, Kumhari, Durg-490042, Chhattisgarh, India
[2]The Department of Commerce and Management Studies, Andhra University, Visakhapatnam-530003, Andhra Pradesh, India
[3]Department F & ARD, Veterinary Officers' Training Institute, Laxmisagar, Bhubaneswar-751009, Odisha, India
*Email ID: ambarish.raipur@gmail.com

Received: 27 Aug 2026; Received in revised form: 23 Sep 2026; Accepted: 28 Sep 2026; Available online: 08 Oct 2026
©2026 The Author(s). Published by Infogain Publication. This is an open-access article *under* the CC BY license (https://creativecommons.org/licenses/by/4.0/).

Abstract— *Sea Buckthorn (Hippophae spp.) is a climate-resilient Himalayan resource with significant nutritional, ecological and value-addition potential. This study assesses the Sea Buckthorn value chain in Uttarakhand, focusing on Chamoli, Pithoragarh, Bageshwar and Uttarkashi. A participatory mixed-methods approach was adopted using field observations, FGDs, KIIs, stakeholder consultations and secondary data. The study examines collection, aggregation, processing, value addition, marketing and income distribution across the value chain. Findings indicate substantial potential for products such as juice, pulp, squash, herbal tea, dried berries and oils; however, the sector faces constraints related to difficult terrain, high harvesting and transportation costs, limited processing and storage infrastructure, weak market linkages and inadequate branding. The study proposes decentralized processing, sustainable sourcing, traceability, product diversification, stronger SHG/CLF/FPO participation and market linkages through House of Himalaya, tourism, institutional and digital channels.*

Keywords— ***Sea Buckthorn, Value Chain, Value Addition, Sustainable Marketing, Himalayan Products.***

I. INTRODUCTION

Sea Buckthorn (*Hippophae rhamnoides L)* is a high-altitude, climate-resilient and multipurpose shrub associated with the Himalayan and other temperate mountain ecosystems. The genus is valued for its ecological adaptability, nutritional richness and wide range of food, nutraceutical, cosmetic and medicinal applications. Sea buckthorn berries contain substantial quantities of Vitamin C, carotenoids, flavonoids, phenolic compounds, tocopherols, fatty acids and other bioactive constituents, which provide a strong scientific basis for their utilisation in functional foods and value-added products (Bal *et al.,* 2011; Olas, 2018; Sytar *et al.,* 2020). In India, Sea Buckthorn occurs primarily in high-altitude Himalayan environments, including Ladakh, Himachal Pradesh, Uttarakhand and parts of the North-Eastern Himalayan region. In Uttarakhand, different *Hippophae* species have been documented from high-altitude areas of districts including Bageshwar, Chamoli, Uttarkashi, Pithoragarh and adjoining Himalayan landscapes, particularly along river valleys, riverbanks and exposed slopes at approximately 2,000–3,600 m above sea level (Singh *et al.,* 2005; Naithani & Bist, 2009). Recent studies further emphasise the ecological, ethnobotanical and livelihood significance of *Hippophae* resources in the Indian Himalayas, while highlighting the need for sustainable harvesting and conservation-oriented utilization (Singh *et al.,* 2026).

Despite its considerable biological and nutritional potential, the commercial utilization of Sea Buckthorn in Himalayan regions remains constrained by the remoteness and dispersed nature of natural populations, difficult terrain, limited post-harvest infrastructure and weak market linkages. The collection stage is therefore a critical component of the value chain. Research on Uttarakhand has documented traditional utilization of Sea buckthorn berries in products such as chutney, pickle, squash and juice, indicating an existing foundation for local value addition (Naithani & Bist, 2009). Scientific and sustainable harvesting practices, primary sorting, appropriate containers, aggregation at collection points and rapid movement of harvested berries can help maintain raw-material quality and reduce post-harvest deterioration. This is particularly important because Sea buckthorn berries have high moisture content and are highly susceptible to deterioration after harvesting; consequently, freezing, drying and other preservation technologies are important for extending shelf life and facilitating transportation (Li & Beveridge, 2003; Bal *et al*., 2011; Yao *et al.,* 2023).

An organised collection and aggregation system can therefore provide an important linkage between dispersed production areas and downstream processors. Local collection centres equipped with basic facilities for sorting, grading, weighing and temporary storage can improve procurement efficiency while enabling better traceability and quality management. At the same time, harvesting systems should be designed around ecological sustainability because uncontrolled extraction from natural populations may adversely affect regeneration and long-term resource availability. Recent literature on the Indian Himalayan region identifies overexploitation, habitat degradation, weak regeneration and climate-related pressures among the major challenges affecting sustainable utilisation of *Hippophae* resources (Singh *et al*., 2026).

From a value-addition perspective, the major opportunity lies in moving beyond the traditional **"collect and sell"** model towards an integrated **"collect, process, brand and market"** approach. Fresh Sea Buckthorn berries have limited shelf life and are difficult to transport over long distances, making local or cluster-based processing particularly relevant. Processing technologies can convert berries into juice, pulp, squash, syrup, jam, dried berries, powder, concentrates and other food products, while seed and pulp fractions can be utilised for oil extraction. Reviews of Sea Buckthorn processing demonstrate considerable potential for beverages, freeze-dried powders, oils and other functional food products, while improved drying and preservation technologies can enhance product quality and shelf stability (Yao *et al*., 2023).

The utilisation of processing residues also offers an opportunity to develop a more resource-efficient and circular value chain. Sea Buckthorn pomace and other by-products contain residual polyphenols, carotenoids, fatty acids and dietary fibre and can potentially be converted into powders, extracts, functional food ingredients and other higher-value products (Jiang *et al.,* 2026). Such comprehensive utilisation can increase resource efficiency, reduce processing waste and generate additional revenue streams for enterprises. The nutritional and functional characteristics of Sea buckthorn also support its potential application in functional foods and wellness-oriented products, although specific health claims require appropriate scientific substantiation and regulatory compliance (Olas, 2018; Chen *et al.,* 2023).

From a marketing perspective, Sea buckthorn can be positioned as a premium Himalayan-origin natural product by emphasizing its geographical provenance, high-altitude production environment, distinctive nutritional composition, traceability and sustainable sourcing. Branding, attractive packaging, quality assurance, batch-level traceability and QR-enabled product information can strengthen product differentiation and consumer confidence. The expanding interest in functional foods and naturally derived ingredients creates opportunities for Sea buckthorn products in specialised food, wellness and premium consumer segments (Chen *et al.,* 2023). Tourism and hospitality markets may provide additional opportunities through hotels, resorts, homestays, wellness centres, tourist destinations and specialty stores, particularly where products are linked with the broader Himalayan identity. Digital marketing, e-commerce and direct-to-consumer channels can further connect Himalayan producers and processors with urban and geographically dispersed consumers.

Overall, the literature indicates that the commercial development of Sea buckthorn requires an integrated collection–aggregation–processing–quality control–value addition–branding–marketing system rather than an isolated focus on berry production. Such a value-chain approach can reduce post-harvest losses, improve shelf life, facilitate product diversification, strengthen market connectivity and increase value retention within Himalayan production communities. The combination of sustainable resource management, decentralized aggregation, appropriate processing technologies, by-product utilization and premium market positioning can provide a scientific and commercially relevant pathway for developing Sea buckthorn as a distinctive Himalayan natural-product sector.

Target Area of the Study

The study focuses on the major Sea Buckthorn-growing regions of Uttarakhand, particularly the high-altitude and cold-arid areas where Sea Buckthorn *(Hippophae rhamnoides L.)* is naturally distributed. The study will cover selected districts such as Bageshwar, Chamoli, Pithoragarh and Uttarkashi, representing important production and collection areas. These regions possess favourable agro-climatic conditions for Sea Buckthorn and have considerable potential for sustainable harvesting, primary processing, value addition, and development of Himalayan-origin health and wellness products. The study will examine the existing value chain from collection and aggregation to processing, packaging, branding, marketing, and end-market linkages, with particular emphasis on the prospects for sustainable commercialization in India.

Objectives

1. To assess the Sea Buckthorn value chain in Uttarakhand, from production and collection to processing and marketing.
2. To identify key value-chain actors, linkages, and major constraints affecting Sea Buckthorn development.
3. To assess value-addition and product development opportunities for Sea Buckthorn-based natural health products.
4. To examine market potential and consumer-oriented opportunities for Himalayan Sea Buckthorn products in India.
5. To propose sustainable marketing strategies for the commercialization of Sea Buckthorn-based Himalayan natural health products.

II. MATERIALS AND METHODS

The present study adopted a participatory mixed-methods research approach to assess the Sea Buckthorn (*Hippophae rhamnoides L.*) value chain in Uttarakhand. The approach integrated quantitative and qualitative information to examine the major stages of the value chain, including natural resource availability, collection, aggregation, primary processing, value addition, packaging, marketing, and consumption. The methodology also assessed the major constraints, market opportunities, stakeholder relationships, and prospects for developing Sea Buckthorn as a premium Himalayan-origin natural health product.

Study Area and Field Visits

The study was conducted in selected high-altitude and Himalayan regions of Uttarakhand where Sea Buckthorn occurs naturally or has potential for organized collection and commercial utilization. Chamoli, Pithoragarh, Bageshwar, and Uttarkashi were considered important study areas based on the occurrence of Sea Buckthorn, availability of collection resources, existing utilization practices, processing potential, and market linkages.

Detailed field visits and stakeholder consultations were undertaken to understand the existing value-chain structure and identify key actors involved in collection, aggregation, processing, value addition, trading, and marketing. Particular attention was given to remote and high-altitude production areas where geographical conditions, accessibility, seasonal availability, and limited market connectivity influence the commercialization of Sea Buckthorn.

Data Collection

Both primary and secondary data were used for the study. Primary data were collected through field observations, household interactions, Focus Group Discussions (FGDs), Key Informant Interviews (KIIs), trader and processor consultations, and stakeholder discussions**.** Information was collected from local collectors, farmers and community members, traders, aggregators, processors, retailers, entrepreneurs, and other stakeholders associated with Sea Buckthorn-based products.

FGDs were conducted to understand traditional collection and utilization practices, harvesting methods, post-harvest handling, seasonal availability, local marketing practices, price realization, constraints, and opportunities for value addition. KIIs were conducted with relevant officials, researchers, extension personnel, market actors, processors, entrepreneurs, and other knowledgeable stakeholders to assess production-resource availability, processing technologies, market demand, institutional support, and commercialization prospects.

The study also examined the value distribution and market linkages across different stages of the Sea Buckthorn value chain, from collection of berries to processing and final marketing. Particular emphasis was placed on identifying value-chain gaps related to collection efficiency, aggregation, transportation, cold-chain or storage requirements, processing capacity, product development, quality standards, packaging, branding, and access to domestic markets.

Secondary Data

Secondary data were collected from government reports, departmental records, scientific publications, research papers, market reports, policy documents, institutional databases, and available literature on Sea Buckthorn. Information relating to geographical distribution, resource

availability, collection and production potential, processing technologies, nutritional and functional properties, value-added products, market trends, and commercialization opportunities was compiled and reviewed.

Published literature on Sea Buckthorn from the Himalayan region and other relevant production areas was also examined to understand existing research, identify knowledge gaps, and compare different approaches to sustainable utilization and value-chain development.

III. SEA BUCKTHORN IN INDIA

The sea buckthorn (*Hippophae rhamnoides L.)* is a perennial, woody, economically important thorny shrub with yellow or orange berries also referred to as 'Wonder Plant', 'Golden Bush' or 'Gold Mine' because every component of this plant has historically been utilized for therapeutic purposes, as a dietary supplement and to preserve soil and moisture. It is a member of the Elaeagnaceae family that grows naturally in large areas of temperate parts of the world. Around 3.0 million hectares of land are believed to be covered by Sea Buckthorn worldwide (both in its natural state and in cultivation) and 90% of its total distribution is found in China, Mongolia, Russia, Northern Europe and Canada. This fruit is high in Vitamin C (300-2400 mg/100g), Vitamin A, E and K, protein, organic acids, carotenoids, flavonoids and steroids and has been utilized in the manufacturing of many drugs, cosmetics and food items. The leaf extract exhibited strong anti-dengue activity, and its seed oil contains Vitamin K which promotes blood coagulation.

Table: Sea Buckthorn Producing States in India (Area in '000 Hectares)

State / UT	2020–21	2021–22	2022–23	2023–24	2024–25	Share of India (%)
Ladakh (UT)	4.2	4.5	4.9	5.3	5.7	36.8
Himachal Pradesh	2.1	2.3	2.5	2.8	3.0	19.5
Uttarakhand	1.6	1.7	1.9	2.1	2.3	14.9
Arunachal Pradesh	0.9	1.0	1.1	1.3	1.4	9.1
Sikkim	0.7	0.8	0.9	1.0	1.1	7.1
Jammu & Kashmir	0.6	0.7	0.8	0.9	1.0	6.5
Other Himalayan States	0.5	0.6	0.7	0.8	0.9	5.8
All India	10.6	11.6	12.8	14.2	15.4	100.0

Source: (DIHAR, 2024-25)

Over the past 25 years, researchers in India have documented the significance and prevalence of Sea Buckthorn in the chilled deserts of Ladakh (Jammu and Kashmir) and Lahaul and Spiti (H.P), Uttarakhand, Sikkim and Arunachal Pradesh. The Sea Buckthorn production in India, rising from 10.6 units in 2020–21 to 14.2 units in 2023–24, with production projected at 15.4 units in 2024–25. Ladakh remains the leading contributor (36.8%), followed by Himachal Pradesh (19.4%) and Uttarakhand (14.6%). Uttarakhand also shows consistent growth from 1.6 to to reach 2.3 units in 2024–25, indicating increasing potential for value addition, processing, and sustainable commercialization.

IV. SEA BUCKTHORN IN UTTARAKHAND

Hippophae salicifolia L , commonly known as Sea Buckthorn, is an important wild plant native to the Uttarakhand Himalayas, valued for its nutritious fruits with significant medicinal and pharmaceutical properties. In India, three species of *Hippophae* are reported: *H. rhamnoides* and *H. salicifolia* are common, while *H. tibetana* grows in limited patches at very high altitudes. Among these, *H. salicifolia* remains relatively understudied despite its high medicinal value. It differs from *H. rhamnoides* in two keyways.

H. salicifolia is a shrub that can grow into a tree up to 4–10 meters tall and is restricted to the central and Northern Himalayas at elevations of 1,500–3,200 meters. In contrast, *H. rhamnoides* is a bushy tree widely distributed across Asia and Europe's higher altitudes, including regions like Tibet, Bhutan, Nepal, and the Himalayan hills of India. Within India, *H. rhamnoides* is found at high altitudes in Himachal Pradesh, Jammu and Kashmir, Sikkim, and Uttarakhand.

In Uttarakhand, ***H. salicifolia*** is abundant in the higher hills of *Chamoli* and *Uttarkash*i districts, though comprehensive biodiversity studies on this species are lacking. To address this, the *Defense Institute of Bio-Energy Research in Haldwani* conducted a systematic study of the plant's

biodiversity in Chamoli district. Traditionally, regional communities in the Central Himalayas use *Hippophae salicifolia* for diverse purposes, including animal feed, cosmetics, food, fuel, medicine, veterinary care, and bio-fencing.



Fig.1: Sea Buckthorn (Hippophae salicifolia) in district Pithoragarh, Uttrakhand

Table 1 : Types of species available in Uttarakhand

Species	Uttarakhand Districts / Locations	Ecology & Utilization
Hippophae salicifolia	**Chamoli:** Harsil, Tambara-Kali, Yamunotri, Gangotri, Badrinath, Gori & Niti Valleys. **Uttarkashi:** Budhi, Darm, Gaurikund, Lachen, Dormang, Zema & Lachung	Predominant species at **1,500–3,200 m**. Used for medicinal, nutritional, fodder and soil-conservation purposes; important for ecological restoration and local livelihoods.
Hippophae tibetana	Niti Valley, Ranimani, Nelong, Gomukh, Shinla & Milam	Occurs in **high-altitude areas (>3,000 m)** under extreme alpine conditions. Important for ecosystem restoration and specialized traditional uses.
Hippophae rhamnoides	Scattered/less documented; reported or potentially occurring in remote high-altitude areas of **Pithoragarh and Champawat**	Occurs mainly in patches. Fruits are **vitamin-rich** and have potential for nutritional, medicinal, cosmetic and industrial applications.

Table 2:Basic Features of Sea buckthorn species found in India

Species	Growing Elevation (m)	Plant Height (m)	Flowering Time	Ripening Time
Hippophae rhamnoides	600–4,200	5.0	May	August–September
Hippophae salicifolia	2,700–3,700	3.0	June	September–October
Hippophae tibetana	3,000–5,200	0.8–1.2	May	October

Among the many useful species of the high Himalaya, Sea Buckthorn (*Hippophae salicifolia* and *Hippophae tibetana*) holds ecological, nutritional, and socio-cultural significance. These dioecious, nitrogen-fixing shrubs are naturally distributed across the upper Himalayan valleys of ***Chamoli, Uttarkashi, Bageshwar***, and ***Pithoragarh*** districts, where they thrive at elevations of 2200–3300 m. Key habitats include the *Niti–Mana valleys (Chamoli), Gangotri–Yamunotri catchments (Uttarkashi), Munsyari–Dharchula regions (Pithoragarh),* and the *Sundar Dunga–Pinder valley (Bageshwar).* These areas are characterized by extreme environmental conditions such as low atmospheric pressure, high UV radiation, steep temperature

gradients, and short growing season conditions to which Sea Buckthorn is physiologically well adapted.

Table 3:Sea Buckthorn Production in Major Districts of Uttarakhand

S. No.	District	Production MT			% of total UK (2023–24)
		2021–22	2022–23	2023–24	
1	Chamoli	1399	1315	1250	**24.29%**
2	Bageshwar	800	973	885	**16.29%**
3	Pithoragarh	1540	1510	1495	**27.86%**
4	Uttarkashi	1750	1690	1710	**31.56%**
	Total	5489	5488	5340	**100%**

Source: Primary level Data from field study

From an ecological perspective, Sea Buckthorn plays a vital role in soil stabilization, slope protection, and the improvement of nutrient-poor substrates due to its extensive root system and symbiotic nitrogen-fixing nodules. It acts as a pioneer species in degraded alpine and glacial landscapes, facilitating ecological succession and enhancing habitat quality for other plant and animal species.

Traditionally, the Bhotiya and other high-altitude communities of Uttarakhand have utilized the fruits, juice, and various parts of Sea Buckthorn for their medicinal, nutritional, and adaptogenic benefits. The berries are exceptionally rich in vitamin C, vitamin E, carotenoids, flavonoids, essential fatty acids (including Omega 3, 6, 7, and 9), and a diverse range of bioactive antioxidants, making them valuable in preventing nutrient deficiencies and enhancing resilience against cold stress, fatigue, and altitude-related health issues. Decoctions, pastes, and fermented preparations made from the fruits and leaves are integral to traditional healthcare practices, commonly used to treat respiratory problems, digestive disorders, and inflammation.

Table 4: Nutritional composition per 100 g of sea buckthorn fruit is

S.No.	Nutrient	Amount (%) or (mg)
1	Moisture (%)	98.3
2	Protein (g)	12.1
3	Fat (g)	12.3
4	Carbohydrates (g)	9.4
5	Calcium (mg)	50
6	Phosphorus (mg)	150
7	Iron (mg)	116
8	Ascorbic acid (mg)	20

Table 5: Major phytochemicals present in Sea buckthorn and their medicinal values

Phytoconstituents	Medicinal Properties	Reference
Tocopherols	Act as antioxidants; minimize lipid oxidation; help to relieve pain	Kallio *et al.* 2002
Carotenoids	Act as antioxidants; help in collagen synthesis and epithelialization	Andersson *et al.* 2009
Vitamin K	Prevents bleeding; promotes wound healing; shows anti-ulcer effects	Jamyansan and Badgaa 2005
Vitamin C	Acts as an antioxidant; sustains cell membrane integrity; accelerates collagen synthesis	Kallio *et al.* 2002
Vitamin B complex	Stimulates cell repair and nerve regeneration	Jamyansan and Badgaa 2005
Phytosterols	Improve microcirculation in the skin; show anti-ulcer, anti-atherogenic and anti-cancer effects; regulate inflammatory processes	Yang and Kallio 2001

Polyphenolic compounds	Show antioxidant, cytoprotective and cardioprotective effects; promote wound healing	Upadhyay *et al*. 2010
Polyunsaturated fatty acids (PUFA)	Immunomodulatory, neuroprotective and anti-tumor activity	Yang and Kallio 2001
Organic acids	Lower the risk of heart attack and stroke; show anti-ulcer effects; promote wound healing; anti-arthritic	Yang and Kallio 2001
Coumarins and triterpenes	Control of appetite; promote sleep, memory, and learning	Grey *et al*. 2009
Zinc	Strengthens blood circulation; aids in cell proliferation; reveals anti-tumor effects; acts as a cofactor for enzymes; enhances utilization of vitamin A	Gupta and Singh 2005

V. VALUE CHAIN MAPPING

Insights from stakeholder consultations were used to create process-flow diagrams depicting the journey of Sea Buckthorn—from collection and aggregation to primary processing, value addition, and final market distribution. The mapping also included key support institutions, research organizations, community groups (SHGs/CLFs), extension services, and the overall enabling environment shaping Sea Buckthorn development in high-altitude Uttarakhand. Data gathered from multiple primary sources—including individual stakeholder interviews, surveys of processors and traders, Focus Group Discussions (FGDs), and relevant secondary information—was thoroughly cross-checked and compared to ensure accuracy and internal consistency. Any discrepancies or inconsistencies were addressed through follow-up discussions with respondents, consultations with local community representatives, and verification with extension staff and subject matter experts. This rigorous data validation process strengthened the reliability, transparency, and overall credibility of the primary research conducted in the hill and high-altitude regions of Uttarakhand.

Cost calculation of Sea Buckthorn Production

In the high-altitude collection zones of Uttarakhand, particularly Niti Valley (Chamoli), Pinder Valley (Bageshwar), Yamunotri and Gangotri Valleys (Uttarkashi), and Dharchula and Munsiyari (Pithoragarh), Sea Buckthorn collection involves negligible cultivation-input costs. Consequently, harvesting and transportation constitute the major operational costs.

Harvesting Cost

Sea Buckthorn harvesting is labour-intensive because of dense thorny shrubs, steep terrain, and riverbank locations, requiring manual berry plucking or branch cutting. Labour charges generally range from ₹200–₹300 per person per day, depending on terrain, remoteness, and local labour availability. A labour typically collects 5–10 kg of fresh berries per day, resulting in an estimated harvesting cost of ₹20–₹25/kg under normal accessibility conditions. In remote areas such as upper Niti Valley and Dharchula, lower collection productivity and higher labour requirements may increase harvesting costs to ₹30–₹35/kg. In some villages, on-site juice extraction is practiced to reduce bulk during transportation, although this involves additional minor handling costs.

Transportation Cost

Transportation costs vary according to terrain, distance, road accessibility, and the number of handling points between the collection site, village aggregation point, road head, and processing unit. Headload and mule transport generally costs ₹3–₹6/kg for short distances (2–5 km), while jeep or pick-up transport costs approximately ₹4–₹8/kg. In remote areas of Chamoli and Pithoragarh with limited motorable access, transportation costs may increase to ₹8–₹12/kg, particularly where multiple handling and transfer points are required**.**

Distribution of Income among Actors in the Sea Buckthorn Value Chain

The Sea Buckthorn value chain shows a progressive increase in value and profitability from primary harvesting to retail marketing. Although primary collectors undertake labour-intensive harvesting under difficult high-altitude conditions, their income remains relatively low because of limited value addition and weak bargaining power. In contrast, processing and retail actors capture substantially higher margins through product transformation, packaging, branding, and market access.

Table 6: Distribution of Income among Actors in the Sea Buckthorn Value Chain

Actor	Product	Major Activity	Qty. (kg)	Selling Price (₹/kg)	Purchase/Collection Cost (₹/kg)	Gross Margin (₹/kg)	Operational Cost (₹/kg)	Net Margin (₹/kg)	Net Profit (%)
Collector (Primary)	Fresh Sea Buckthorn berries	Wild harvesting	1	80	50	30	5	25	31.25
Village Aggregator/ Primary Processor	Filtered juice (fresh-equivalent)	Aggregation, basic filtration and transport	1	120	80	40	10	30	25.00
Secondary Processor	Processed juice/pulp	Processing and packaging	1	250	120	130	12	118	47.20
Retailer	Branded Sea Buckthorn juice	Retail marketing	1	800	250	550	8	542	67.75

The analysis indicates a substantial disparity in income distribution across the value chain. Primary collectors receive ₹80/kg for fresh berries, with a net margin of ₹25/kg and a net profit margin of 31.25%. The village aggregator/primary processor earns a net margin of ₹30/kg, while the secondary processor generates a considerably higher net margin of ₹118/kg through processing and packaging. The retailer captures the highest absolute margin, with a net margin of ₹542/kg and a reported net profit margin of 67.75%.

Thus, although collectors perform the most labour-intensive activity, their share of the final consumer value is limited. A substantial proportion of value is created and captured at downstream stages through processing, packaging, branding and retail marketing. Strengthening decentralized processing facilities, improving aggregation and cold-chain/logistics systems, developing a credible "Himalayan Sea Buckthorn" brand, and establishing direct market linkages could enable producer groups and collectors to retain a greater share of the value generated from Sea Buckthorn products.

VI. VALUE ADDED PRODUCTS



Fig.2:Sea Buckthorn based commercialized products

Field visits toChamoli, Pithoragarh, and Bageshwar documented several locally processed Sea Buckthorn (*Hippophae rhamnoides*) products, including juice/RTS beverages, squash and syrup, pulp, herbal tea, dried berries, and oil. These products are prepared through SHGs, CLFs, and rural enterprises. Local processing improves value

realization over raw berry sales, creates rural employment—particularly for women—and supports livelihood diversification in remote high-altitude areas of Uttarakhand.

Table 7: Various Sea buckthorn-based products

Category	Products / Uses	Raw Materials
Food Products	Tea, juice, jam, pickle, fermented products, powder	Leaves, berries, pulp
Oils & Extracts	Pulp oil, seed oil, concentrates, extracts	Pulp, seeds, berries
Medicinal	Ulcer, burn and radiation-damage preparations	Extracts, oils
Defence Nutrition	Multivitamin beverages for high-altitude troops	Juice, fruit extracts
Cosmetics	Creams, sunscreen, face wash, serums	Oils, extracts
Beverages	Juice, squash, syrup, herbal tea, wine and sparkling drinks	Juice, pulp, concentrates

VII. GAP ANALYSIS OF SEA BUCKTHORN

The gap analysis of Uttarakhand's Sea Buckthorn value chain reveals that the crop is primarily viewed as a wild or semi-wild resource rather than a fully developed commercial horticultural product. Despite its significant nutraceutical, cosmetic, and pharmaceutical potential, the sector remains underdeveloped due to inadequate institutional support, limited processing facilities, and weak market connections

Table 8: Gap Analysis on the Research Study

S. No.	Stage	Key Gaps
1	Production & Collection	• Poor resource mapping and organized cultivation. • Unsustainable harvesting and limited regeneration. • Difficult terrain, high labour costs and scattered resources. • Inadequate collection centres, grading and cold chain. • Unclear harvesting rights and certification mechanisms.
2	Processing	• Limited pulping, processing and cold-storage facilities. • Low technical capacity and inefficient processing methods. • Gaps in product development, hygiene, FSSAI compliance and packaging.
3	Marketing	• No assured procurement or buy-back system. • Informal marketing and low price realization. • High logistics costs and fragmented volumes. • Weak branding, market intelligence and digital/urban market linkages.
4	Policy & Institutional Support	• Limited integration with horticulture, AYUSH and livelihood programmes. • Weak inter-departmental convergence. • Limited R&D, extension and financial support. • No dedicated cluster-based development strategy.

VIII. MARKETING STRATEGY

A phased marketing strategy is proposed to promote Sea Buckthorn as a value-added Himalayan natural product. Initially, fresh berries, pulp, juice and other minimally processed products can be marketed through SHGs, CLFs, FPOs, local markets, fairs and institutional outlets. In the next phase, products such as RTD beverages, dried berries, herbal teas and jams can be introduced in urban, tourism and wellness markets. In the long term, linkages with organized retailers, nutraceutical and cosmetic companies, e-commerce platforms and institutional buyers can support wider market access and stable demand.

Positioning under "Brand House of Himalaya

Sea Buckthorn can be positioned as a premium Himalayan natural product under the "Brand House of Himalaya" umbrella, highlighting its Himalayan origin, nutritional attributes, quality and sustainable sourcing. House of Himalaya can support branding, product promotion, retailing and market linkage, while private partners can contribute to product development, packaging, distribution and market expansion.

Product Diversification and Value Addition

The product portfolio may include juice, pulp, RTD beverages, squash, dried berries, herbal teas, jams, seed oil and selected wellness/cosmetic products. Product development should focus on shelf life, consumer preference, standardized quality and commercial viability.

Tourism and Institutional Markets

Tourism provides an important market opportunity for Sea Buckthorn. Products can be promoted through hotels, homestays, restaurants, tourist centers, fairs and House of

Himalaya outlets. Institutional and bulk buyers can provide relatively stable demand and improve market predictability.

Private-Sector Partnerships

A public–community–private partnership can be developed involving Government/project institutions, SHGs, CLFs/FPOs, House of Himalaya and private enterprises. Private partners can support processing, product innovation, packaging, branding, distribution, e-commerce and national market expansion, while community organizations undertake aggregation and primary processing.

Product Authentication and Traceability

A traceability system should ensure quality, food safety, origin verification and consumer confidence from collection to final sale. Each batch should be assigned a unique identification number linked to collection, processing, testing and packaging records.

Chemical Traceability

Products should be tested through appropriate/accredited laboratories for relevant nutritional, bioactive, microbiological, heavy-metal and chemical-residue parameters, as applicable. Verified results can support product information and legitimate quality claims.

Physical and Digital Traceability

QR/barcodes can provide information on producer organization, village/district, harvest season, batch number, processing unit, testing and certification details. A simple digital database can maintain batch-wise records.

Organic and Quality Certification

Eligible clusters may be promoted under organic certification or PGS, where technically and economically feasible. Appropriate food-safety and quality certifications can improve product credibility and facilitate access to premium and institutional markets.

Sustainable Sourcing

Commercialization should be supported by resource mapping, sustainable harvesting protocols, regeneration measures and community-based resource management to ensure long-term availability of Sea Buckthorn without over-exploitation.

Branding and Promotion

Promotion should focus on Himalayan origin, verified nutritional attributes, quality, traceability and community sourcing. Product tasting, exhibitions, tourism events, digital campaigns and social-media promotion can improve consumer awareness.

E-Commerce and Digital Marketing

Shelf-stable Sea Buckthorn products can be promoted through House of Himalaya's digital channels, e-commerce platforms, private brand partners and social-commerce channels, supported by standardized product information and consumer feedback mechanisms.

Market-Linkage Model

Collectors/Producers → SHGs/CLFs/FPOs → Aggregation & Processing → Quality Testing & Traceability → House of Himalaya/Private Partners → Retail/Tourism/Institutional/E-commerce Markets → Consumers



Fig.3: Marketing Strategy of Sea Buckthorn Value Chain

IX. CONCLUSION

The study establishes that Sea Buckthorn has considerable potential for sustainable value-chain development and livelihood enhancement in Uttarakhand, particularly in high-altitude regions. However, the sector remains constrained by fragmented collection, difficult terrain, limited processing and storage infrastructure, weak market linkages, and inadequate institutional support. The value-chain assessment indicates that greater value is captured at downstream stages through processing, packaging,

branding, and retailing, while primary collectors receive a relatively limited share.

The study therefore highlights the need for organized aggregation, decentralized processing, sustainable harvesting, quality assurance, traceability, product diversification, and stronger market linkages. A coordinated community–government–private-sector approach, supported by branding through House of Himalaya and access to tourism, institutional, retail, and digital markets, will improve value realization for producer groups. Overall, integrating sustainable sourcing with authentication, value addition, branding and market development will strengthen the commercialization of Sea Buckthorn while supporting rural livelihoods and long-term resource conservation in Uttarakhand.

REFERENCES

[1] Andersson, S. C., Olsson, M. E., Johansson, E., & Rumpunen, K. (2009). Carotenoids in sea buckthorn (*Hippophae rhamnoides* L.) berries during ripening and use of pheophytin a as a maturity marker. *Journal of Agricultural and Food Chemistry, 57*(1), 250–258. https://doi.org/10.1021/jf802599f

[2] Bal, L. M., Meda, V., Naik, S. N., & Satya, S. (2011). Sea buckthorn berries: A potential source of valuable nutrients for nutraceuticals and cosmoceuticals. *Food Research International, 44*(7), 1718–1727. https://doi.org/10.1016/j.foodres.2011.03.002

[3] Chen, A., Feng, X., Dorjsuren, B., Chimedtseren, C., Damda, T.-A., & Zhang, C. (2023). Traditional food, modern food and nutritional value of sea buckthorn (*Hippophae rhamnoides* L.): A review. *Journal of Future Foods, 3*(3), 191–205. https://doi.org/10.1016/j.jfutfo.2023.02.001

[4] Chen, Y., Cai, Y., Wang, K., & Wang, Y. (2023). Bioactive compounds in sea buckthorn and their efficacy in preventing and treating metabolic syndrome. *Foods, 12*(10), 1985. https://doi.org/10.3390/foods12101985

[5] Grey, C., Widén, C., Adlercreutz, P., Rumpunen, K., & Duan, R.-D. (2010). Antiproliferative effects of sea buckthorn (*Hippophae rhamnoides* L.) extracts on human colon and liver cancer cell lines. *Food Chemistry, 120*(4), 1004–1010. https://doi.org/10.1016/j.foodchem.2009.11.039

[6] Gupta, R. K., & Singh, V. (2005). Mineral composition of sea buckthorn (*Hippophae* L.). In V. Singh (Ed.), *Seabuckthorn (Hippophae L.): A multipurpose wonder plant* (Vol. 2, pp. 272–284). Daya Publishing House.

[7] Jamyansan, Y., & Badgaa, D. (2005). Bioactive substances of Mongolian seabuckthorn (*Hippophae rhamnoides* L.). In V. Singh (Ed.), *Seabuckthorn (Hippophae L.): A multipurpose wonder plant* (Vol. 2, pp. 145–150). Daya Publishing House

[8] Jiang, X., Sun, M., Deng, W., Zhu, M., Wang, L., Zheng, L., Xing, J., & Hong, J. (2026). From nutritional profile to circular bioeconomy: A review of sea buckthorn oil and by-product valorization. *Foods, 15*(11), 1873. https://doi.org/10.3390/foods15111873

[9] Kallio, H., Yang, B., & Peippo, P. (2002). Effects of different origins and harvesting time on vitamin C, tocopherols, and tocotrienols in sea buckthorn (*Hippophaë rhamnoides*) berries. *Journal of Agricultural and Food Chemistry, 50*(21), 6136–6142. https://doi.org/10.1021/jf020421v

[10] Li, T. S. C., & Beveridge, T. H. J. (2003). *Sea buckthorn (Hippophae rhamnoides L.): Production and utilization*. National Research Council Canada.

[11] Naithani, H. B., & Bist, N. S. (2009). Seabuckthorn in Uttarakhand. In S. K. Dwivedi, T. Parimelazhagan, S. B. Singh, & Z. Ahmed (Eds.), *Seabuckthorn: Hippophae spp.: The golden bush*. Satish Serial Publishing House.

[12] Negi, S., Bhandari, A., Chauhan, A., Kumar, A., Singh, S., & Singh, Y. (2026). *Hippophae* spp. (sea buckthorn) value addition for sustainable livelihood generation in the Uttarakhand Himalayan region. *Journal of Applied Biology and Biotechnology, 14*(5), 35–45. https://doi.org/10.7324/JABB.2026.274527

[13] Olas, B. (2018). The beneficial health aspects of Sea buckthorn (*Hippophae rhamnoides* L.) in human nutrition. *Journal of Functional Foods, 46*, 274–279.

[14] Olas, B. (2018). The beneficial health aspects of Sea Buckthorn (*Elaeagnus rhamnoides* (L.) A. Nelson) oil. *Journal of Ethnopharmacology, 213*, 183–190. https://doi.org/10.1016/j.jep.2017.11.022

[15] Singh, K., Sharma, U., Sharma, S., Bussmann, R. W., et al. (2026). Sea buckthorn (*Hippophae* spp.) in the Indian Himalayas: Integrating ethnobotanical knowledge, phytomedicinal potential, and conservation strategies. *Ethnobotany Research and Applications, 35*.

[16] Sytařová, I., Orsavová, J., Snopek, L., Mlček, J., Byczyński, Ł., & Mišurcová, L. (2020). Impact of phenolic compounds and vitamins C and E on antioxidant activity of sea buckthorn (*Hippophaë rhamnoides* L.) berries and leaves of diverse ripening times. *Food Chemistry, 310*, 125784. https://doi.org/10.1016/j.foodchem.2019.125784

[17] Yang, B., & Kallio, H. P. (2001). Fatty acid composition of lipids in sea buckthorn (*Hippophaë rhamnoides* L.) berries of different origins. *Journal of Agricultural and Food Chemistry, 49*(4), 1939–1947. https://doi.org/10.1021/jf001059s

[18] Yang, B., Karlsson, R. M., Oksman, P. H., & Kallio, H. P. (2001). Phytosterols in sea buckthorn (*Hippophaë rhamnoides* L.) berries: Identification and effects of different origins and harvesting times. *Journal of Agricultural and Food Chemistry, 49*(11), 5620–5629. https://doi.org/10.1021/jf010813m

[19] Yao, et al. (2023). Sea buckthorn pretreatment, drying, and processing of high-quality products: Current status and trends. *Foods, 12*(23), 4255

International Journal of Environment, Agriculture and Biotechnology
Vol-11, Issue-5; Sep-Oct, 2026
Peer-Reviewed International Journal
Journal Home Page Available: https://ijeab.com/
Journal DOI: 10.22161/ijeab

Analysis of the Physiological Characteristics of 4 Orange Varieties in Kontum (Quang Ngai) and Can Tho, Vietnam

Nguyen Trong Phuoc, Bien Anh Khoa, Nguyen Thi Hong Loan, Nguyen Thi Lang

High Agricultural Technology Research Institute for Mekong Delta
Web: hatri.org
*Corresponding author's email: ntlang.prof@gmail.com

Received: 24 Jul 2026; Received in revised form: 25 Aug 2026; Accepted: 25 Sep 2026; Available online: 08 Oct 2026
©2026 The Author(s). Published by Infogain Publication. This is an open-access article *under* the CC BY license (https://creativecommons.org/licenses/by/4.0/).

Abstracts— *Studies on the characteristics and evaluation of genetic resources regarding physicochemical and morphological properties are necessary for selecting good orange varieties for Kon Tum (Quang Ngai). A selection and evaluation study was conducted at the Orange Research Program in Kon Tum (Quang Ngai) and Can Tho (as a control). The evaluation of citrus species regarding various quantitative and qualitative characteristics related to leaf, fruit, and seed morphology at the phenotypic level, yield, and yield composition of four different orange varieties was performed growing at KonTum (Quang Ngai). Juice content showed a maximum positive correlation with flesh weight, followed by fruit weight. The CT 36 orange had a thin peel, high firmness, and juice content (67.17%) was determined in Măng Đen; reducing sugar content (7.52%) and 7.35% at Đăk Pxi). The Sanh orange. thick peel, poor hardness, sugar content (2.16-2.44%) and sourness (1.75-2.3%) were reported in Kon Tum; while sugar content (6.55-7.35%) was recorded in Honey oranges. High sensory value was reported in site Đăk Mar, fruit with high flavor, sweetness and overall juice impression. The existence of wide variation in morphological characteristics with the highest yield prospects was confirmed in Sanh oranges (35.72) followed by Honey oranges (34.62). Therefore, morphology is an effective tool for successfully establishing different citrus varieties. This review will emphasize the evaluation of organges gene resources through the analysis of growth and yield-related traits as well as various physicochemical properties at four different locations of the plants at KonTum (Quang Ngai) and CanTho.*

Keywords— ***Morphological characteristics, Oranges, qualitative characteristics.***

I. INTRODUCTION

Quang Ngai province (KonTum) is strategically located in the central part of Vietnam This area grows a lot of oranges for export.Morphological characteristics and morphological methods on various agronomic traits related to the leaves, flowers, and fruits of citrus trees. Standardized morphology provides a practical and reliable means of distinguishing closely related crop varieties, especially in diverse agricultural climates of highlands and lowlands. Morphological characteristics play an important role in assessing genetic diversity, crop variety identification and improvement programs. Important characteristics such as plant shape, leaf morphology, fruit shape, peel texture, flesh characteristics and seed characteristics serve as reliable markers for distinguishing crop varieties (Jaskani et al., 2006; Khan et al., 2008). These morphological differences facilitate field-level identification and provide a valuable resource for germplasm conservation and breeding programmes aimed at citrus improvement under subtropical conditions(Shivali Chauhan et la.2025). Furthermore, sex selection is not always feasible because some of the plant varieties used in hybrids are incompatible, sterile, or dabrionic (Talon and Gmitter, 2008). Orange Varieties in Vietnam. In Vietnam, many orange varieties are widely grown and developed, including:

- Mandarin oranges: grown in the mountainous regions of Northern Vietnam and the Mekong Delta. Mandarin oranges are a popular choice for refreshing juice.

- Citrus oranges: mainly grown in Central and Southern Vietnam. Citrus oranges have a characteristic sweet and sour flavor and are often used to make jam.

- Lemon oranges: grown in the mountainous regions of Central and Southern Vietnam. Lemon oranges have a slightly sour flavor and are often used to make refreshing drinks and juices.

- Xoan oranges: Xoan oranges have a sweet, fragrant taste.

- Sugar oranges: grown in the Western and Southern regions. Sugar oranges have a rich, sweet taste.

- Honey orange

- Canh orange: concentrated in the North

In addition, there are many other orange varieties grown in Vietnam such as Sanh orange.

Sanh orange is a fruit tree variety belonging to the Citrus genus (Citrus reticulata x maxima) with fruit almost like an orange, originating from Vietnam. Sanh oranges are easily recognizable by their thick, rough peel resembling the surface of pottery shards and are usually light green (turning orange when ripe), with orange flesh segments and rough skin. Subsequently, the development of yield and quality components of fruit grown at four different locations in Kon Tum was investigated. The aim is to produce high-quality citrus fruits (in terms of size, sugar and acidity balance, juice yield, and seedlessness), that are healthy and rich in antioxidant compounds, tolerant to or resistant to various abiotic and biotic threats, and with high yields. Conventional citrus breeding is a lengthy and expensive process; long periods and resources are required to obtain offspring and to evaluate their traits.This study allows us to clarify whether different fruit quality and environmental parameters at these four locations can lead to specific changes in seedless or seeded oranges, as well as their yields.

II. MATERIALS AND METHODS

Four orange varieties were grown at three locations in Quang Ngai (*1: Đăk Mar, 2: Đăk Pxi, 3: Măng Đen)* and one location in Can Tho (control group).

Morphological characteristics of leaves, flowers, pollen, and fruit.

Morphological characteristics of leaves (leaf blade size, leaf weight per unit, guard cell size, and stomatal density),

Flowers (size of flower buds, petals, pistils, and ovules, and number of petals, stamens, and ovules) and pollen grains. Fully opened leaves and flowers just before blooming were collected in mid-July and mid-December of the following year, respectively.

Fruit height (mm): Measured from the bottom to the top of the fruit using calipers.

Fruit diameter (mm): Measured at the widest point of the fruit.

Peel thickness (mm): Averaged the peel thickness at 3 representative points.

Indentation diameter (mm): Measured the representative diameter of the indentation.

Yield and yield components

Yield: Number of fruits/plant: Count all fruits on the plant at harvest.

Yield: Weigh all fruits at harvest.

Yield Components

Section Weight: Separate the orange segments and weigh them using a TANITA technical balance manufactured in Japan.

Number of Segments: Count the total number of segments in the fruit.

Fruit Quality Analysis

Fruit quality was assessed over two years (before and after the investigation). Twenty fruits were used for quality testing.Total Dissolved Solids (TSS) Content:

Extract the fruit juice and measure the Brix (%) of the juice using an ATAGO refractometer manufactured in Japan. The measurement range is 0-32%. The juice is dropped directly onto the prism of the refractometer and the results are recorded.

TSS (%) = 0 Brix * (1 + V/W)

Where:

V: Volume of dissolved water (ml)

W: Sample weight (g)

Titrant Acidity (TA): Grind 2g of sample with distilled water to make 25ml. Take 2ml of the extract and add 2ml of 5% PEG (polyethylene glycol 5%). Centrifuge at 3000 rpm for 5 minutes. Then, take 0.5ml of the extract and add 9.5ml of distilled water for titration. Add 2-3 drops of phenolphthalein (1%), shake well, and titrate with 0.01 M NaOH until a stable pale pink color is obtained. Simultaneously, perform a blank test with the 5% PEG solution by taking 0.5ml of PEG, adding 0.5ml of distilled water, then taking 0.5ml of the mixture and adding 9.5ml of distilled water for titration, similar to the real sample.

The results are calculated as follows:

TA(%) = ((V_f - V_0) × 0.01 × K × 100) / ([W / (W + V_n)] × V_m)

Where:

V_f: Volume of actual titrating NaOH solution (ml)

V_0: Volume of blank titrating NaOH solution (ml)

V_n: Total volume of sample solution (ml)

V_m: Volume of diluted solution used for titration (ml)

W: Mass of sample (g)

0.01: Concentration of NaOH used for titration

K: Characteristic coefficient for citric acid 0.064

The peel color is evaluated using a color chart (FUJIHIRA INDUSTRY Co. Ltd., Tokyo, Japan). The degree of peel swelling is assessed using a scale from 0 (no swelling) to 3 (severe swelling) upon touch.

Vitamin C analysis: Ascorbic acid was determined by titrimetric method as described by Ranganna (1995).Vitamin C (mg/100g): Quantitative determination of vitamin C by titration with 2,6-dichlorophenol indophenol (Murin, 1990).Weigh approximately 5g of sample into a porcelain mortar with 20ml of 1% HCl and crush the sample. Then, add 100ml to a volume of 1% oxalic acid, shake well, and let the solution stand for 10 minutes. Next, take a 10ml sample and titrate it with 0.001N 2,6-dichlorophenol indophenol solution until a persistent pink color appears after one minute, then stop the titration. Read the volume of 0.001N 2,6-dichlorophenol indophenol solution used. Repeat the analysis 3 times. The control sample was titrated with 2ml of 1% HCl and 8ml of 1% oxalic acid as described above.

The vitamin C content in 100g of fresh sample was calculated using the formula:

X = ((a-b) × 0.088 × V_1) / (V_2 × m) × 100

Where:

a: Average number of ml when titrating the sample.

b: Average number of ml when titrating the control sample.

V_1: Initial volume of extraction solution (100ml).

V_2: Volume of extraction solution for titration (10ml).

0.088: Number of mg of ascorbic acid equivalent to 1ml of 2,6-dichlorophenol indophenol titration solution.

m: Initial sample weight (g).

The sugar and organic acid content of the juice was determined according to the method of Mukai et al., (1996). Sugar content was calculated using sucrose, fructose, and glucose. For organic acid content, citric and malic acids were measured. Ten types of fruit were used for analysis.The determination and quantification of carotenoids in fruit juices were carried out according to the methods (Kato et al., 2004).

III. RESULTS AND DISCUSSION

3.1 Analysis of Honey Oranges (Cam Mat)

In the third year, honey orange trees began to fruit, although the quantity was very small, 120.7 fruits per tree at *Đăk Mar* site.

The trees developed very well, and began to flower in July 2025. The number of flowers was very large. The level of male infertility (pollen) varied among orange varieties. Planting density often leads to seedless or few-seeded fruit when planted without cross-pollination (Yamamoto et al., 1995). This phenomenon has been observed in honey orange varieties. The number of flowers was very large, but the pollination rate was low.



Fig.1. Honey orange tree beginning to flower at Đăk Mar (Phuoc 2025)

Meanwhile, the orange fruit contains essential oils. The outer peel of the fruit turns orange or yellow when ripe, while the inner peel is odorless, spongy, and white. An orange usually consists of about 12 separate wedge-shaped compartments. Each compartment may contain at least 2 to 4 irregular white seeds. The flesh of a ripe fruit may be yellow.

This is a type with pale yellow flesh, low acidity ranging from 0.76 to 0.87%, not harsh or sour when eaten, only a refreshing sweetness. They have very few seeds and are difficult to peel. In addition, their flesh has a juicy flavor ranging from 72.38 to 79.51%, averaging 76.93%, making them an excellent choice for fresh consumption. Vitamin C content varies from 64.7 to 73.38%.



Fig.2. Honey oranges harvested at 3 experimental sites in the third year (Lang 2025)

Table 1. Analysis and evaluation of yield, yield components and quality of Honey oranges in the third year

sites	Hight (m)	Number fruit/ tree	Weight of fruit (gram)	number of segments in an orange	Numbers seeds (seed/ fruit)	yield/ ha	sweet	juicy flesh (%)	Suger	Vitamin C (mg/g)	sour (%)
1	2.6c	120.7c	11.8b	360b	1.9b	33.4b	2.2a	79.51a	6.67b	73.38a	0.82a
2	2.53d	140.4a	12a	342c	3.2a	32.2c	1.9b	72.38d	7.35a	67.16b	0.87a
3	2.8a	130.5b	11.7b	250d	3.3a	30.1d	2a	78.95b	6.55b	64.7b	0.76b
4	2.7b	140a	12a	420a	3a	42.8a	2.5a	75.6c	6.85b	69.1b	0.7b
mean	2.65	130.65	11.87	343	2.85	34.62	2.15	76.61	6.85	68.68	0.78

Note : 1: Đăk Mar, 2: Đăk Pxi, 3: Măng Đen, 4: Can Tho

3.2. Analysis of Sanh Oranges

This analysis of Sanh oranges is characterized by the formation of a rough-skinned fruit – a berry with a tough, oily peel surrounding swollen, juicy sacs inside. Citrus trees are perennial evergreens, maintaining a complex tree structure with one to three distinct annual vegetative growth cycles. Sanh oranges flower and bear fruit annually in subtropical conditions, with flowering in spring, largely dependent on rainfall or adequate water supply. Fruit yield varies from 130.2 to 140.4 fruits per tree in the third year. Sanh oranges are easily recognizable by their thick, rough peel resembling the surface of pottery shards, usually light green (turning orange-yellow when ripe), with orange-yellow flesh and rough skin. A single orange typically contains about 12 distinct wedge-shaped compartments. Each compartment may contain at least 3 to 4 irregular white seeds, with some fruits having 5 seeds. The flesh of ripe oranges can be yellow, easy to peel, and the juicy flavor varies from 85.79 to 88.49%, averaging 86.96%, making them excellent for refreshing juice. Vitamin C content is very high, varying by region from 74.26 to 77.57 mg/g, averaging 75.42 mg/g. Sweetness is low, acidity is high, varying from 1.75 to 2.3%. The aroma is easily recognizable thanks to the flavor of the peel, which contains many essential oils.

Analysis of seedless orange varieties on Sanh oranges. Seeds play an important role as a source of phytohormones necessary for fruit development, including regulating fruit size (Balaguera et al., 2020). In addition, fruit size significantly affects the marketability of oranges

(Bons et al., 2015). Generally, seedless fruits, due to mutations preventing seed formation, tend to be smaller than seeded fruits. Seedless Sanh oranges are smaller than seeded varieties (Figure 3.). Plant hormone status, including auxin and gibberellin concentrations, may influence early fruit development in seedless citrus fruits (Mesejo et al., 2016). Hypothesized, hormonal changes and regulatory processes during the seedless fruiting (parthenocarpic) stage may have contributed to its increased fruit size. This unique characteristic, combined with the absence of seeds, further enhances the commercial value of the Sanh orange variety.



Fig.3. Harvested Sanh oranges at 3 experimental sites in the third year (Lang 2025)

Table 2. Analysis and evaluation of yield, yield composition, and quality of Sanh oranges in the third year

sites	Hight (Cm)	Number fruit/ tree	Weight of fruit (gram)	number of segments in an orange	Numbers seeds (seed/ fruit)	yield/ ha	sweet	juicy flesh (%)	Suger	Vitamine C (mg/g)	sour (%)
1	3.01a	130.2c	12.1a	3.7b	350b	33.5b	0.05	85.79c	2.16a	77.57a	1.75b
2	2.94b	140.4b	12a	3.2b	320c	32.4c	0	86.68b	2.44a	74.44c	1.92b
3	3.04a	130.4c	12a	3.9b	300d	31.5d	0.1	88.49a	2.18a	74.26c	2.3a
4	3.25a	250a	12.0a	4a	410a	45.5a	0.05	86.96b	2.26a	76.2b	2a
mean	3.06	160.5	12.03	3.7	345.0	35.72	0.05	86.98	2.26a	75.61	1.99

Note : 1: Đăk Mar, 2: Đăk Pxi, 3: Măng Đen, 4: Can Tho

3.3 Analysis of CT36 Oranges

CT36 oranges are high-yielding, sweet-tasting varieties with a slight hint of sourness (low acidity of 0.41-0.47%). They are easily recognizable by their deep orange color. The flesh is very juicy, with a water content ranging from 69.26% to 71.42%. The vitamin C content is very high, varying by region from 57.62 to 65.4 mg/g. The sweetness level is high (grade 3). Harvesting takes place from December to February, with the peak season in January



Fig.4. A mature orange flower and its various parts connected to the bud via the flower stalk on Sanh orange variety at Đăk Mar (Phuoc 2025)



Fig.5. Harvested CT36 oranges at 3 experimental sites in the third year (Khoa.2025)

ISSN: 2456-1878 (Int. J. Environ. Agric. Biotech.)
https://dx.doi.org/10.22161/ijeab.115.13

Table 3. Analysis and evaluation of yield, yield composition, and quality of CT36 oranges in the third year

sites	Hight (Cm)	Number fruit/ tree	Weight of fruit (gram)	number of segments in an orange	Numbers seeds (seed/ fruit)	yield/ ha	sweet	juicy flesh (%)	Suger	Vitamin C (mg/g)	sour (%)
1	2.21b	50.6s	11.5b	220a	0.7b	32.5b	2.0	69.26b	7.48a	65.4a	0.47b
2	2.19c	70c	11.3b	200b	0.5c	31.2c	2.0	71.42a	7.35a	58.16c	0.41b
3	2.36a	80b	11.3b	195b	0.3d	30.7d	2.0	67.17c	7.52a	57.62d	0.43b
4	2.25b	100a	12a	150c	1a	35.1a	1.5	65.2d	7.45a	61.2b	0.5a
mean	2.25	70.65	11.52	191.25	0.62	32.37	1.5	68.2	7.45	60.59	0.45

Note : 1: Đăk Mar, 2: Đăk Pxi, 3: Măng Đen, 4: Can Tho



Fig.6. The CT36 orange tree was planted at the experimental site Đăk Pxi (Phuoc 2025).

3.4. Analysis of V2 Oranges

Short-stemmed trees

This variety has a mildly sweet taste. They are easily recognizable by their deep orange color and juicy flesh, varying from 70.3% to 74.31%. The vitamin C content is very high, varying by region from 59.02% to 62.65 mg/g. The sweetness level is high (1.5).

Table 4. Analysis and evaluation of yield, yield components, and quality of V2 oranges in the third year.

sites	Hight (Cm)	Number fruit/ tree	Weight of fruit (gram)	number of segments in an orange	Numbers seeds (seed/ fruit)	yield/ ha	sweet	juicy flesh (%)	Suger	Vitamin C (mg/g)
1	1.43a	50.4c	210a	10.3a	1	28.7a	1.5	73.45b	7.45b	62.43
2	1.35b	120.5b	200b	10a	1	25.2b	1.5	70.3c	7.83a	59.02
3	1.31b	140.8a	200b	10a	2	20.8c	1.5	74.31a	7.47b	62.65
mean	1.63	100.9	203 .3	10.1	1.5	24.9	1.5	72.68	7.58	61.36

Note: 1: Đăk Mar, 2: Đăk Pxi, 3: Măng Đen, 4: Can Tho

IV. DISCUSSION

The high water content of Sanh oranges makes them suitable for juice processing. Oranges have been shown to contain high levels of minerals, low moisture, low ash content, and crude fiber (Wall et al., 2006), and are a source of sugar, vitamins A, C, and B, protein, and low lipids (Ogbonna et al., 2013). Juices are non-alcoholic liquid products with a certain clarity and viscosity obtained by pressing or crushing the fruit with or without added sugar or carbon dioxide (Costescu et al., 2006). Mật oranges are large, about 2-3 fruits/kg. Sanh oranges are of similar size, about 2 fruits/kg. CT36 oranges are medium-sized, about 3-4 fruits/kg. V2 oranges are small, about 4-5 fruits/kg.Oranges are a distinct fresh fruit, widely consumed and especially valued for their delicious flavor. Fruits and their juices constitute one of the most important foods for humans. Regular consumption maintains health and compensates for dietary deficiencies. The Sanh orange variety adapts well to the conditions at *Đăk Mar* and *Măng Đen* locations. The table shows that Sanh oranges have the highest juice content at 86.96%, while other orange varieties show 69.28% for CT 36 oranges, 72.68% for V2 oranges, and 76.94% for Mat oranges.Oranges are an excellent source of vitamin C. The different orange varieties in the experiment showed varying vitamin C content, with Sành oranges providing the highest levels (7.26–77.57 mg/g), followed by Mat oranges (64.7–73.38 mg/g). Oranges CT36 (57.62-65.4 mg/g) and V2 (59.02-62.43 mg/g) are rich in vitamin C. Besides vitamin C content, orange juice is also rich in folic acid, potassium, and is an excellent source of secondary compounds with high antioxidant activity, making them important commercial commodities in most countries (Vasavada et al., 2003).

The CT 36 orange has a thin peel, high firmness, and juice content (%) determined in *Măng Đen*; reducing sugar content (7.52%) and 7.35% at *Đăk Pxi*. The Sanh orange has a thick peel, low firmness, sugar content (2.16-2.44%) and sourness (1.75-2.3%) reported in Kon Tum;

while the sugar content (6.55-7.35%) was recorded in the Mat orange. High sensory value was reported in the *Đăk Mar* fruit with high flavor, sweetness, and overall juice impression. The existence of wide variation in morphological characteristics confirms the highest yield potential in the Sanh orange variety (35.72), followed by the Mat orange (34.62).Seedlessness in oranges usually arises from a combination of factors rather than a single cause. The external environment, in addition to common infertile types, also has a significant impact on flower development and seed formation in the fruit. Seedlessness can be achieved by combining pollination without fertilization with factors that inhibit normal fertilization (Varoquaux et al., 2000). Several environmental factors, such as low or high temperatures, chromosomal abnormalities, and certain chemical treatments, can cause seedlessness (Ali et al., 2013). Irregular seed and fruit formation is particularly pronounced when plants are exposed to suboptimal or superoptimal temperatures during the flowering stage (Hedhly et al., 2011). Exposure to varying temperatures during bud development alters the expression of the autoincompatibility response (Distefano et al., 2018). This is consistent with the results in Kon Tum (Quang Ngai) where climate changes during the flowering stage.

V. CONCLUSION

In terms of fruit yield per hectare, the Sanh orange variety yielded the highest at 35.72, followed by the Mat orange variety (34.62%), and the V2 orange variety had the lowest yield (24.9).Regarding sweetness, the Mat orange was the sweetest, followed by the CT orange at 36. The Sanh orange variety showed the highest juice content. Juicy flesh of Sanh orange was 86.98%. Juice content showed a

maximum positive correlation with flesh weight, followed by fruit weight. The CT 36 orange had a thin peel, high firmness, and juice content (67.17%) was determined in Dak Ha; reducing sugar content (7.52%) and 7.35% at *Đăk Pxi*). The Sanh orange. thick peel, poor hardness, sugar content (2.16-2.44%) and sourness (1.75-2.3%) were reported in Kon Tum(Quang Ngai) ; while sugar content (6.55-7.35%) was recorded in Honey oranges.

ACKNOWLEDGEMENTS

This paper presents findings from" Selection of disease-free, seedless, high-yielding, high-quality, ripe orange varieties for production development in Kon Tum (Quang Ngai) province 'project'. We thanks Quang Ngai People's Committees and Department of Science and Technology for supported this project and We also acknowledge the support of and gene bank of the plant breeding and genetic division at HATRI.

REFERENCES

[1] Ali, S.; Khan, A.S.; Raza, S.A.; Rehman, R.N.U. Innovative breeding methods to develop seedless citrus cultivars. *Int. J. Biosci.* **2013**, *3*, 191–201.

[2] Balaguera-López, H.E.; Fischer, G.; Magnitskiy, S. Seed-fruit relationships in fleshy fruit: Role of hormones. A review. *Rev. Colomb. Cienc. Hortícolas* **2020**, *14*, 90–103.

[3] Bons, H.; Nirmaljit, K.; Rattanpal, H. Quality and Quantity Improvement of Citrus: Role of Plant Growth Regulators. *Int. J. Agric. Environ. Biotechnol.* **2015**, *8*, 433.

[4] Costescu C, Parvu D and Rivis A (2006). The determination of some physico-chemical characteristics for orange, grapefruit and tomato juices. Journal of Agro Alimentary Processes and Technologies, 12(2), 429-432.

[5] Distefano, G.; Gentile, A.; Hedhly, A.; La Malfa, S. Temperatures during flower bud development affect pollen germination, self-incompatibility reaction and early fruit development of clementine (*Citrus clementina* Hort. ex Tan.). *Plant Biol.* **2018**, *20*, 191–198.

[6] Jaskani MJ, Abbas H, Khan MM, Shahzad U, Hussain Z. Morphological description of three potential citrus rootstocks. Pak J Bot. 2006;38:311-317.

[7] Hedhly, A. Sensitivity of flowering plant gametophytes to temperature fluctuations. *Environ. Exp. Bot.* **2011**, *74*, 9–16.

[8] Khan MM, Mumtaz S, Ahmad S, Abbas M, Khan IA. Some studies on the morphology of Kinnow mandarin and Feutrell's early. Pak J Agric Sci. 2008;45:424-431.

[9] Mesejo, C.; Yuste, R.; Reig, C.; Martínez-Fuentes, A.; Iglesias, D.J.; Munoz-Fambuena, N. Gibberellin reactivates and maintains ovary-wall cell division causing fruit set in parthenocarpic Citrus species. *Plant Sci.* **2016**, *247*, 13–24.

[10] Ogbonna A.C, Abuajah C.I and Ekpe G.E (2013). A comparative study of the nutritive factors and sensory acceptance of juices from selected Nigerian fruits. Croatian Journal of Food Technology, Biotechnology and Nutrition, 8(1-2), 47-51.

[11] Shivali Chauhan. Vikas Kumar Sharma, Lakesh Rahi, Rupam Nehta, MA Kuchay and Sanjeev 2025. Morphological characterization of citrus cultivars in the subtropical region of Himachal Pradesh International Journal of Advanced Biochemistry Research 2025; 9(6): 988-992

[12] Talon, M., Gmitter, F. G. (2008). Citrus genomics. Int. J. Plant Genomics, 1–17. doi: 10.1155/2008/528361

[13] Varoquaux, F.; Blanvillain, R.; Delseny, M.; Gallois, P. Less is better: New approaches for seedless fruit production. *Trends Biotechnol.* **2000**, *18*, 233–242.

[14] Vasavada P.C (2003). Microbiology of Fruit Juice and Beverage. In: Foster T and Vasada P.C (eds). Beverage Quality and Safety, pp. 95-123.

[15] Wall M.M (2006). Ascorbic acid, vitamin C and mineral composition of banana (Musa spp.) and papaya (Carica papaya) cultivars grown in Hawaii. Journal of Food Composition and Analysis, 19(5), 234-445.

[16] Yamamoto, M.; Matsumoto, R.; Yamada, Y. Relationship between sterility and seedlessness in citrus. *J. Jpn. Soc. Hortic. Sci.* **1995**, *64*, 23–29.

International Journal of Environment, Agriculture and Biotechnology
Vol-11, Issue-5; Sep-Oct, 2026
Peer-Reviewed International Journal
Journal Home Page Available: https://ijeab.com/
Journal DOI: 10.22161/ijeab

Seasonal Incidence of Natural Enemies Associated with Major Insect Pests in Pearl Millet

MP Satpute, DS Mutkule, MK Jadhav, SB Shelke, AP Khating

College of Agriculture, Badnapur, Vasantrao Naik Marathwada Krishi Vidyapeeth, Parbhani, Maharashtra, India

Received: 03 Sep 2026; Received in revised form: 03 Oct 2026; Accepted: 07 Oct 2026; Available online: 15 Oct 2026
©2026 The Author(s). Published by Infogain Publication. This is an open-access article *under* the CC BY license (https://creativecommons.org/licenses/by/4.0/).

Abstract— *A field investigation was conducted during Kharif 2025 at the Research Farm of the National Agricultural Research Project (NARP), Chhatrapati Sambhajinagar, Maharashtra, to record the seasonal occurrence of natural enemies in pearl millet. Ladybird beetles (LBB) and chrysopids were observed at weekly intervals from the 29th to the 38th standard meteorological week (SMW), alongside major insect pests. Ladybird beetle abundance ranged from 0.0 to 1.5 per observation, with the maximum value of 1.5 recorded during the 36th SMW. Chrysopid abundance ranged from 0.0 to 1.2, reaching its maximum during the 38th SMW. Ladybird beetles were not recorded during the 32nd SMW, while chrysopids were absent during the 31st SMW. Both groups were recorded during several crop-growth stages, indicating that natural enemies were present in the pearl millet ecosystem during the observation period. The findings highlight the importance of regular field monitoring and conservation of beneficial arthropods as components of integrated pest management. The study records seasonal occurrence only; further replicated studies are required to establish the role of these natural enemies in suppressing particular pests.*

Keywords— ***Pearl millet, natural enemies, ladybird beetles, chrysopids, seasonal incidence, Kharif 2025***

I. INTRODUCTION

Pearl millet is an important cereal crop grown under rainfed and semi-arid conditions, and its crop ecosystem supports both insect pests and beneficial arthropods. Conservation of natural enemies is recognised as one component of integrated pest management in millet crops (Gahukar and Reddy, 2019). Ladybird beetles (*coccinellids*), green lacewings and spiders have been recorded as natural enemies associated with insect pests in pearl millet fields (Savithri and Prakash, 2023).

Information on the seasonal presence of beneficial insects can help describe their occurrence during crop growth and support decisions about conserving natural enemies in the field. Savithri and Prakash (2023) reported seasonal activity of coccinellids and green lacewings in a pearl millet ecosystem at Vijayapura. Patange et al. (2024) also recorded ladybird beetles and chrysopids while studying biotic factors associated with seasonal pest incidence in pearl millet. Therefore, the present study documented the weekly incidence of ladybird beetles and chrysopids associated with pearl millet during Kharif 2025 at Chhatrapati Sambhajinagar, Maharashtra.

II. MATERIALS AND METHODS

The field observations were recorded during *Kharif* 2025 at the Research Farm of the National Agricultural Research Project (NARP), Chhatrapati Sambhajinagar, Maharashtra, on pearl millet hybrid ABH 1200. Weekly observations were made from the 29th to the 38th standard meteorological week (SMW). Ladybird beetles (LBB) and *chrysopids* were recorded as associated natural enemies along with observations on major insect pests. The values presented here are reproduced from the seasonal-incidence dataset in the supplied Chapter 4. The original table does not specify the unit or sampling denominator for the natural-enemy values; therefore, the values are reported as recorded and are not re-labelled as insects per plant.

III. RESULTS AND DISCUSSION

3.1 Seasonal occurrence of ladybird beetles

The recorded data showed that ladybird beetles were observed during most of the monitoring period. The recorded values were 0.8 during the 29th SMW, 0.6 during the 30th SMW, and 0.5 during the 31st SMW. No ladybird beetles were recorded in the 32nd SMW. Their occurrence was again recorded during the 33rd and 34th SMW at 0.6 and 1.0, respectively. The value decreased to 0.5 during the 35th SMW, then increased to the maximum recorded value of 1.5 during the 36th SMW. Values of 1.0 and 0.8 were recorded during the 37th and 38th SMW, respectively. This pattern indicates variation in ladybird beetle occurrence across the crop season.

3.2 Seasonal occurrence of chrysopids

Chrysopids were recorded at 1.0 during the 29th SMW and 0.6 during the 30th SMW, but were not recorded during the 31st SMW. Their recorded value was 0.4 during the 32nd SMW and 0.6 during the 33rd SMW. A value of 1.0 was recorded during the 34th SMW, followed by 0.4 during the 35th SMW. Chrysopid values were 1.0 during both the 36th and 37th SMW and reached the maximum recorded value of 1.2 during the 38th SMW. Thus, chrysopids remained detectable during most of the observation period, with their highest recorded occurrence at the final observation.

3.3 Implications for integrated pest management

The seasonal records confirm the presence of ladybird beetles and chrysopids in the pearl millet field during *Kharif* 2025, although their recorded values fluctuated among weeks. Similar seasonal occurrence of coccinellids and green lacewings in pearl millet was reported by Savithri and Prakash (2023). These observations support including beneficial insects in routine crop monitoring. However, the present dataset describes occurrence and does not by itself demonstrate the amount of pest suppression provided by either group. Future studies should record sampling units consistently, use replicated plots, and examine relationships between natural-enemy abundance and pest populations before drawing conclusions about biological-control effectiveness.

Table 1. Weekly occurrence of natural enemies in pearl millet during Kharif 2025

SMW	Ladybird beetles (LBB)	Chrysopids
29	0.8	1.0
30	0.6	0.6
31	0.5	0.0
32	0.0	0.4
33	0.6	0.6
34	1.0	1.0
35	0.5	0.4
36	1.5	1.0
37	1.0	1.0
38	0.8	1.2

.

IV. CONCLUSION

Ladybird beetles and chrysopids were recorded during the Kharif 2025 pearl millet season, with fluctuations in their weekly occurrence. The highest recorded LBB value was 1.5 during the 36th SMW, while chrysopids reached 1.2 during the 38th SMW. These observations indicate that beneficial insects were present in the crop ecosystem and should be included in field surveillance and conservation-oriented pest management. Since the available data do not quantify their direct effect on pest populations, additional studies are needed to evaluate their biological control contribution.

REFERENCES

[1] Gahukar, R. T. (1981). Biological control of insect pests of sorghum and pearl millet in West Africa. In: Biological Control of Pests: Its Potential in West Africa, Dakar, Senegal, 9–13 February 1981. International Crops Research Institute for the Semi-Arid Tropics (ICRISAT).

[2] Gurr, G. M., Wratten, S. D., Landis, D. A., and You, M. (2012). Habitat management to suppress pest populations: Progress and prospects. Annual Review of Entomology, 57, 239–259. https://doi.org/10.1146/annurev-ento-120710-100632

[3] Juneja, R. P., Jaba, J., Mohammed, R., Sharma, R., Perumal, R., Prasad, P. V. V., Satyavathi, C. T., Govindaraj, M., and Tenkouano, A. (2024). Pearl millet: Pest management. In: Pearl Millet: A Resilient Cereal Crop for Food, Nutrition, and Climate Security. Agronomy Monographs, 1, 393–416. American Society of Agronomy, Crop Science Society of America, and Soil Science Society of America.

[4] Landis, D. A., Wratten, S. D., and Gurr, G. M. (2000). Habitat management to conserve natural enemies of arthropod pests in agriculture. Annual Review of Entomology, 45, 175–201. https://doi.org/10.1146/annurev.ento.45.1.175

[5] Nwanze, K. F., and Harris, K. M. (1992). Insect pests of pearl millet in West Africa. Review of Agricultural Entomology, 80(12), 1132–1155.

[6] Obrycki, J. J., Harwood, J. D., Kring, T. J., and O'Neil, R. J. (2009). Aphidophagy by Coccinellidae: Application of biological control in agroecosystems. Biological Control, 51(2), 244–254. https://doi.org/10.1016/j.biocontrol.2009.05.009

[7] Reddy, K. V. S., and Davies, J. C. (1979). Pests of sorghum and pearl millet, and their parasites and predators, recorded at ICRISAT Center, India up to August 1979. Cereal

Entomology Progress Report No. 2. ICRISAT, Patancheru, India.

[8] Savithri, K. S., and Prakash, H. T. (2023). Population dynamics of insect pests and their natural enemies in pearl millet ecosystem. Journal of Farm Sciences, 36(4), 364–368. https://doi.org/10.61475/JFS.2023.v36i4.08

[9] Sharma, H. C., and Davies, J. C. (1988). Insect and Other Animal Pests of Millets. International Crops Research Institute for the Semi-Arid Tropics (ICRISAT), Patancheru, India.

[10] Snyder, W. E. (2019). Give predators a complement: Conserving natural enemy biodiversity to improve biocontrol. Biological Control, 135, 73–82. https://doi.org/10.1016/j.biocontrol.2019.04.017

[11] Symondson, W. O. C., Sunderland, K. D., and Greenstone, M. H. (2002). Can generalist predators be effective biocontrol agents? Annual Review of Entomology, 47, 561–594. https://doi.org/10.1146/annurev.ento.47.091201.145240

International Journal of Environment, Agriculture and Biotechnology
Vol-11, Issue-5; Sep-Oct, 2026
Peer-Reviewed International Journal
Journal Home Page Available: https://ijeab.com/
Journal DOI: 10.22161/ijeab

Effect of Chlorantraniliprole 18.5% SC Applied Through Drone and Knapsack Sprayers on Ladybird Beetle and Spider Populations in Soybean (*Glycine max* (L.) Merrill)

D. K. Thorat[1], D. S. Mutkule[2], S. B. Shelke[3], K. M. Tokhendra[4], A. P. Khating[5]

[1]MSc Research Scholar, Department of Entomology, College of Agriculture, Badnapur, Maharashtra, India.
[2]Professor (CAS), Department of Entomology, NARP, Chh. Sambhajinagar, Maharashtra, India.
[3]Senior Research Fellow, National Agricultural Research Project Chh. Sambhajinagar, Maharashtra, India
[4]Ph.D Research Scholar, Department of Entomology, VNMKV, Parbhani, Maharashtra, India
[5]MSc Research Scholar, Department of Entomology, College of Agriculture, Badnapur, Maharashtra, India.

Received: 07 Sep 2026; Received in revised form: 01 Oct 2026; Accepted: 05 Oct 2026; Available online: 15 Oct 2026
©2026 The Author(s). Published by Infogain Publication. This is an open-access article *under* the CC BY license (https://creativecommons.org/licenses/by/4.0/).

Abstract— *The field experiment was conducted during Kharif 2025 at the research farm of the National Agriculture Research Project (NARP), Chhatrapati Sambhajinagar, Maharashtra, to evaluate the effect of drone and conventional knapsack application of chlorantraniliprole 18.5% SC on natural enemies associated with soybean, Glycine max (L.) Merrill. The experiment included different doses of chlorantraniliprole applied through a drone, a conventional knapsack sprayer, and an untreated control. Populations of spiders and ladybird beetles were recorded before and after each spray. Following the first spray, the untreated control (T_5) recorded the highest mean populations of spiders (1.86 spiders/mrl) and ladybird beetles (1.88 beetles/mrl), whereas T_3 (chlorantraniliprole 18.5% SC @ 187.5 ml/ha through drone) recorded the lowest populations of spiders (1.51 spiders/mrl) and ladybird beetles (1.42 beetles/mrl). Similarly, after the second spray, the highest populations of spiders (1.95 spiders/mrl) and ladybird beetles (1.93 beetles/mrl) were recorded in T_5, while the lowest populations of spiders (1.43 spiders/mrl) and ladybird beetles (1.41 beetles/mrl) were observed in T_3. However, differences among treatments were statistically non-significant for both natural enemies. These findings indicate that the tested chlorantraniliprole 18.5 SC treatments did not produce statistically significant changes in spider and ladybird beetle populations under the experimental conditions.*

Keywords— ***Soybean, Glycine max, Chlorantraniliprole 18.5% SC, Drone application, Ladybird beetle, Spider.***

I. INTRODUCTION

Soybean (*Glycine max* (L.) Merrill) is an important legume and oilseed crop cultivated extensively in Maharashtra, particularly in the Marathwada region. Sustainable soybean production requires effective insect pest management along with the conservation of beneficial arthropods. Ladybird beetles (Coccinellidae) and spiders are important natural enemies that contribute to the suppression of insect pest populations and help maintain ecological balance in soybean agroecosystems. Chemical insecticides are widely used to manage insect pests in soybean; however, their effects on beneficial arthropods need to be evaluated to support environmentally sustainable pest management practices. Drone-based pesticide application is emerging as an alternative to conventional spraying methods because of its operational efficiency and lower spray volume requirements. Nevertheless, the effects of insecticides applied through drones on beneficial arthropod populations under field conditions require further investigation. In view of these considerations, the present investigation was undertaken during the *kharif* season of 2025 at the NARP research farm, Chhatrapati Sambhajinagar, Maharashtra, to evaluate the effects of different doses of chlorantraniliprole

18.5% SC applied through a drone sprayer, in comparison with a conventional knapsack sprayer, on ladybird beetle and spider populations in soybean.

II. MATERIALS AND METHOD

The experiment was conducted during *kharif* 2025 at the research farm of National Agriculture Research Project (NARP), Chh. Sambhajinagar, to evaluate the efficacy of Chlorantraniliprole 18.5% SC against major defoliator insect pests of soybean through drone application under field conditions. The experimental field was prepared by ploughing followed by harrowing and levelling. The field experiment was laid out in Randomized Block Design (RBD) with five treatments replicated four times. Soybean variety MAUS 71 was sown at a spacing of 45 × 5 cm following the recommended package of practices.

Table 1. Experimental Details

Sr. No.	Particulars	Details
1	Design	RBD
2	Treatments	05
3	Replications	04
4	Spacing	45 × 5 cm
5	Plot size	500 m²
6	Variety	MAUS 71
7	Season	*Kharif* 2025
8	Date of sowing	04 July 2025
9	Number of sprays	02
10	Spray interval	15 days
11	Drone spray volume	25 L/ha
12	Knapsack spray volume	500 L/ha

Table 2. Treatment Details :

Sr. No.	Treatments	Dose (ml ha^{-1})	Method of application	Spray volume
1	T_1 – Chlorantraniliprole 18.5% SC	112.5 (0.75X)	Drone	25 L/ha
2	T_2 – Chlorantraniliprole 18.5% SC	150.0 (1X)	Drone	25 L/ha
3	T_3 – Chlorantraniliprole 18.5% SC	187.5 (1.25X)	Drone	25 L/ha
4	T_4 – Chlorantraniliprole 18.5% SC	150.0 (1X)	Knapsack sprayer	500 L/ha
5	T_5 – Untreated control	–	–	–

Imposition of Treatments

The first spray was applied on 25 August 2025, followed by the second spray on 10 September 2025. Treatments T1 (112.5 ml/ha), T2 (150 ml/ha) and T3 (187.5 ml/ha) were applied using a drone sprayer at 25 L/ha, while T4 (150 ml/ha) was applied using a knapsack sprayer at 500 L/ha. T5 was maintained as an untreated control. Ladybird beetle and spider populations were recorded before and after spraying.

Method of recording Observations

Observations were recorded on the total number of natural enemies *viz*., Ladybird Beetles and spider. per metre row length from three selected places per replication before spray and at 1, 3, 7 and 10 days after the 1st and 2nd sprays.

The collected data were subjected to Analysis of Variance (ANOVA) suitable for a Randomized Block Design (RBD), as described by Gomez and Gomez (1984). Treatment means were compared using the Critical Difference (CD) test at a 5% level of significance ($P = 0.05$).

Table 3. Population of spider after spray. (1st and 2nd Spray)

Tr. No	Treatments	Method	Dosage ml/ha	Average spiders / mrl.										
				1st Spraying						2nd Spraying				
				1 DBS	1 DAS	3 DAS	7 DAS	10 DAS	Mean	1 DAS	3 DAS	7 DAS	10 DAS	Mean
T_1	Chlorantraniliprole 18.5 SC	Drone	112.5	1.87 (1.54)	1.75 (1.50)	1.69 (1.48)	1.55 (1.43)	1.63 (1.46)	1.70 (1.48)	1.72 (1.49)	1.67 (1.47)	1.59 (1.45)	1.63 (1.46)	1.64 (1.47)
T_2	Chlorantraniliprole 18.5 SC	Drone	150	1.85 (1.53)	1.67 (1.47)	1.53 (1.42)	1.49 (1.41)	1.55 (1.43)	1.60 (1.46)	1.63 (1.46)	1.54 (1.43)	1.50 (1.41)	1.51 (1.42)	1.55 (1.43)
T_3	Chlorantraniliprole	Drone	187.5	1.86	1.62	1.35	1.30	1.40	1.51	1.57	1.44	1.32	1.38	1.43

	18.5 SC			(1.54)	(1.46)	(1.36)	(1.34)	(1.38)	(1.41)	(1.44)	(1.39)	(1.35)	(1.37)	(1.38)
T_4	Chlorantraniliprole 18.5 SC	Knapsack sprayer	150	1.86 (1.54)	1.65 (1.47)	1.56 (1.44)	1.48 (1.41)	1.58 (1.44)	1.62 (1.45)	1.69 (1.48)	1.59 (1.45)	1.39 (1.37)	1.49 (1.41)	1.54 (1.43)
T_5	Untreated (Control)	-	-	1.80 (1.52)	1.82 (1.52)	1.85 (1.53)	1.90 (1.55)	1.95 (1.57)	1.86 (1.54)	1.82 (1.52)	1.92 (1.56)	2.00 (1.58)	2.07 (1.60)	1.95 (1.57)
	S.E.(m) ±			0.07	0.06	0.06	0.07	0.06	0.07	0.07	0.08	0.06	0.07	0.07
	C.D. at 5%			NS	NS	NS	NS	NS	NS	NS	NS	NS	NS	NS
	C.V.			12.50	11.94	11.21	12.64	12.73	12.20	11.42	12.02	11.53	12.93	11.98

(Figures in the parentheses are √ x + 0.5 transformed values)

Population of Spiders After First Spray

The data presented in Table 3 indicated that the mean spider population was highest in the untreated control (T_5) (1.86 spiders/mrl), followed by T_1 (1.70), T_4 (1.62), T_2 (1.60) and T_3 (1.51 spiders/mrl). Treatment T_3, chlorantraniliprole 18.5 SC @ 187.5 ml/ha applied through a drone, recorded the lowest population. However, differences among treatments were statistically non-significant.

Population of Spiders After Second Spray

As presented in Table 3, the highest mean spider population was recorded in the untreated control (T_5) (1.95 spiders/mrl), while the lowest was observed in T_3 (1.43 spiders/mrl), chlorantraniliprole 18.5 SC @ 187.5 ml/ha applied through a drone .The differences among treatments were statistically non-significant, indicating no significant adverse effect on spider populations.

Reddy *et al.* (2024) observed no significant adverse effect of chlorantraniliprole 18.5% SC on spider populations under field conditions. Nadagoud *et al.* (2024) also reported no significant adverse impact on spiders following chlorantraniliprole application. Biradar *et al.* (2023) and Liyas *et al.* (2015) reported comparatively lower toxicity of chlorantraniliprole to beneficial arthropods, including spiders, than broad-spectrum insecticides. Similarly, Natikar *et al.* (2015) found chlorantraniliprole 18.5% SC to be comparatively safer to spiders under field conditions. These findings are in agreement with the present study, in which differences in spider populations among treatments were statistically non-significant.

Table 4 Population of ladybird beetle after spray. (1st and 2nd Spray)

Tr. No	Treatments	Method	Dosage ml/ha	Average ladybird beetle / mrl.										
				1st Spraying						2nd Spraying				
				1 DBS	1 DAS	3 DAS	7 DAS	10 DAS	Mean	1 DAS	3 DAS	7 DAS	10 DAS	Mean
T_1	Chlorantraniliprole 18.5 SC	Drone	112.5	1.79 (1.51)	1.75 (1.50)	1.59 (1.45)	1.50 (1.41)	1.67 (1.47)	1.66 (1.46)	1.70 (1.48)	1.56 (1.43)	1.47 (1.40)	1.60 (1.45)	1.58 (1.44)
T_2	Chlorantraniliprole 18.5 SC	Drone	150	1.84 (1.53)	1.67 (1.47)	1.42 (1.38)	1.33 (1.35)	1.45 (1.39)	1.54 (1.43)	1.65 (1.46)	1.52 (1.42)	1.43 (1.39)	1.49 (1.41)	1.53 (1.43)
T_3	Chlorantraniliprole 18.5 SC	Drone	187.5	1.84 (1.53)	1.50 (1.41)	1.25 (1.32)	1.17 (1.29)	1.33 (1.35)	1.42 (1.39)	1.56 (1.43)	1.40 (1.38)	1.29 (1.34)	1.38 (1.37)	1.41 (1.38)
T_4	Chlorantraniliprole 18.5 SC	Knapsack sprayer	150	1.89 (1.54)	1.75 (1.50)	1.47 (1.40)	1.42 (1.38)	1.50 (1.41)	1.61 (1.45)	1.68 (1.47)	1.52 (1.42)	1.46 (1.40)	1.52 (1.42)	1.55 (1.43)
T_5	Untreated (Control)	-	-	1.80 (1.52)	1.82 (1.52)	1.86 (1.54)	1.91 (1.55)	1.98 (1.57)	1.88 (1.54)	1.85 (1.53)	1.90 (1.55)	1.96 (1.57)	2.01 (1.58)	1.93 (1.56)
	S.E.(m) ±			0.06	0.05	0.06	0.07	0.06	0.06	0.07	0.06	0.05	0.07	0.06
	C.D. at 5%			NS	NS	NS	NS	NS	NS	NS	NS	NS	NS	NS
	C.V.			11.89	12.82	11.86	12.71	12.62	11.93	12.16	12.53	11.31	11.92	11.23

Population of Ladybird Beetle After First Spray

The data presented in Table 4 indicated that the mean ladybird beetle population was highest in the untreated control (T_5) (1.88 beetles/mrl), followed by T_1 (1.66), T_2 (1.54), T_4 (1.51) and T_3 (1.42 beetles/mrl). Treatment T_3, comprising chlorantraniliprole 18.5 SC @ 187.5 ml/ha applied using a drone, recorded the lowest mean population. However, the differences among treatments were statistically non-significant.

Population of Ladybird Beetle After Second Spray

The data presented in Table 4 revealed that the highest mean ladybird beetle population was recorded in the untreated control (T_5) (1.93 beetles/mrl), followed by T_1 (1.58), T_4 (1.55), T_2 (1.53) and T_3 (1.41 beetles/mrl). Treatment T_3, comprising chlorantraniliprole 18.5 SC @ 187.5 ml/ha applied using a drone, recorded the lowest mean population. However, the differences among treatments were statistically non-significant, indicating no significant adverse effect on ladybird beetle populations under the experimental conditions.

Nadagoud *et al.* (2024) also observed no significant adverse impact of chlorantraniliprole on coccinellids and spiders. In soybean ecosystem, Biradar *et al.* (2023) and Liyas *et al.* (2015) reported that selective molecules like chlorantraniliprole 18.5 SC exhibited lower toxicity and were comparatively safer to natural enemies than broad spectrum insecticides. Cong *et al*. (2023) demonstrated that chlorantraniliprole cause a low risk and hazard quotient to the predatory ladybird beetle (*Coccinella septempunctata*) compared with other diamides. Earlier, Natikar *et al*. (2015) observed chlorantraniliprole 18.5 SC to be safer to coccinellids, while He *et al.* (2019) confirmed its low contact toxicity at recommended field rates. These findings corroborate the present study, indicating the relative safety of drone applied chlorantraniliprole towards predatory ladybird beetles.

III. CONCLUSION

The mean populations of spiders and ladybird beetles were numerically highest in the untreated control (T_5) and lowest in T_3 (chlorantraniliprole 18.5 SC @ 187.5 ml/ha applied through a drone) after both sprays. However, the differences among treatments were statistically non-significant. Thus, although T_3 recorded comparatively lower populations of these beneficial arthropods, the observed reductions were not statistically significant and did not demonstrate a significant adverse effect under the experimental conditions. These findings are consistent with previous studies reporting the relative safety of chlorantraniliprole to spiders and predatory ladybird beetles.

REFERENCES

[1] Biradar, S. G., Mahale, A. S., Wagh, V. P., Rane, P. S., Akhade, S. H., Kabre, G. B., Nandre, D. R., & Shivagaje, A. J. (2023). Impact of different insecticides on natural enemies in soybean (*Glycine max L). Pharma Innovation Journal* **12**(1): 2059–2063.

[2] Cong, Y., Chen, J., Xie, Y., Wang, Y., & Cheng, C. (2023). Toxicity and sublethal effects of diamide insecticides on key non-target natural predators, the larvae of *Coccinella septempunctata* L.(Coleoptera: Coccinellidae). *Toxics*, **11**(3), 270.

[3] Gomez, K. A., & Gomez, A. A. (1984). Statistical procedures for agricultural research. John wiley & sons.

[4] He, F., Sun, S., Tan, H., Sun, X., Shang, D., Yao, C.,& Jiang, X. (2019). Compatibility of chlorantraniliprole with the generalist predator *Coccinella septempunctata* L.(Coleoptera: Coccinellidae) based toxicity, life-cycle development and population parameters in laboratory microcosms. *Chemosphere*, *225*, 182-190.

[5] Liyas, M.D., Patil, R.R., and Dhere, D.A., (2015). Effect of some insecticides on population of natural enemies and yield of soybean. *J. Ent. Res.* **39**(2): 149-151.

[6] Nadagoud, S., Kalmath, B. S., Gouda, S., Srinivas, A. G., Hadimani, D. K., & Sajjanar, S. (2024). Field efficacy of chlorantraniliprole 600 g/L SC against American bollworm (*Helicoverpa armigera*) and tobacco caterpillar (*Spodoptera litura*) in cotton ecosystem. *International Journal of Advanced Biochemistry Research,* **8**(6S), 782–786.

[7] Natikar, Prashant K., (2015) . "Effect of newer insecticides on population of natural enemies and yield of soybean." *Journal of Experimental Zoology India*, vol. **18**, no. 2.

[8] Reddy, T. R., Sudhakar, C., Sudha Rani, C., Babu, T. K., Varma, N. R. G., Minnie, C. M., Rahman, S. J., Umadevi, G., & Jagadeeshwar, R. (2024). *Standard operating protocols (SOPs) for Drone-based pesticide application in safflower* (Publication No. 22/SP/PJTAU/2024). Professor Jayashankar Telangana Agricultural University.

International Journal of Environment, Agriculture and Biotechnology
Vol-11, Issue-5; Sep-Oct, 2026
Peer-Reviewed International Journal
Journal Home Page Available: https://ijeab.com/
Journal DOI: 10.22161/ijeab

Economic Study on Targeting Rice Fallow Area (TRFA) Scheme in Kalyana Karnataka Region

Aishwarya[1], Devendra Beeraladinni[2]*, Lokesh G.B[3]. Prabhuling Tevari[4], Sidram Yalwar[5]

[1]Research Scholar, Department of Agricultural Economics, College of Agriculture, University of Agricultural Sciences, Raichur, Karnataka, India
[2]Associate Professor and Extension Leader, Department of Agricultural Economics, UAS, Raichur, Karnataka, India
[3] Professor and Head, Department of Agricultural Economics, UAS, Raichur
[4] Professor, Department of Agricultural Economics, Agriculture College Dharwad, UAS, Dharwad, Karnataka, India
[5] Professor of Agricultural Extension Education, College of Agriculture, Kalaburagi, UAS, Raichur
* Corresponding author mail: beeraladinnidevendra1975@gmail.com

Received: 06 Sep 2026; Received in revised form: 04 Oct 2026; Accepted: 09 Oct 2026; Available online: 16 Oct 2026
©2026 The Author(s). Published by Infogain Publication. This is an open-access article *under* the CC BY license (https://creativecommons.org/licenses/by/4.0/).

Abstract— *Rice is a major staple crop cultivated extensively in Karnataka; however, a substantial portion of the rice area remains fallow during the rabi season due to moisture stress, inadequate irrigation facilities and limited awareness regarding suitable crop diversification options. These rice fallow areas offer considerable scope for enhancing agricultural production, farm income and employment through the cultivation of short-duration pulses and oilseeds. In this background, the present study analyses the impact of the Targeting Rice Fallow Areas (TRFA) scheme on area utilization, production performance, income and employment of farmers in Karnataka, with special emphasis on the Kalyana Karnataka region. The study was conducted in Raichur and Ballari districts of Kalyana Karnataka using a multistage random sampling technique. Primary data were collected from 120 sample farmers, comprising 60 TRFA beneficiary farmers and 60 non-beneficiary farmers. In addition, data were collected from 10 government officials of the Department of Agriculture to identify the major constraints in the implementation of the TRFA scheme. Secondary data on area, production and productivity of pulses and oilseeds were collected for the period 2008-09 to 2023-24. The analytical tools employed included compound annual growth rate (CAG) and Difference-in-Difference (DiD) technique. The results revealed that in Kalyana Karnataka, the area under pulses increased marginally by 0.46 per cent during the post-TRFA period, while production and productivity declined by 3.95 per cent and 4.39 per cent, respectively. In contrast, oilseeds showed better performance with an increase in area (2.56%), production (8.80%) and productivity (6.44%), indicating a stronger positive impact of the TRFA scheme. At the state level, oilseeds recorded higher growth in production (5.62%) compared to pulses. The extent of utilization of rice fallow areas was significantly higher among TRFA beneficiary farmers, contributing to improved cropping intensity. The Difference-in-Difference analysis indicated that TRFA beneficiary farmers experienced a significant increase in annual farm income ranging from Rs.27419 per farm and generated additional employment of about 38 man-days per annum compared to non-beneficiaries. The study recommends timely fund release, development and promotion of short-duration, drought-tolerant pulse varieties suitable for rice fallow conditions and adoption of crop replacement strategies such as promoting sunflower in place of poorly performing crops like mustard. Further, advance identification and mapping of suitable rice fallow areas, intensive pre-season awareness programmes and strengthening of monitoring and evaluation mechanisms are essential to enhance the effectiveness and sustainability of the TRFA scheme.*

Keywords— ***Employment, Farm income, Kalyana Karnataka, Rice fallow, TRFA scheme.***

I. INTRODUCTION

Paddy is the principal crop during kharif season in India. The crop occupies an area of over 40 million ha. This area is not fully utilized for crop production in the subsequent rabi season; about 12 million ha remains fallow (Subbarao et al., 2001). This unutilized area offers enormous opportunities to overcome the problem of food and nutritional insecurity. Accomplishing household food security remains the primary concern though at the national level India has piled up a huge stock (about 60 million tonnes) of food grains, mainly rice and wheat. Food crops such as pulses and oilseeds are critical to food security. Nutritional security is equally important; about 30 per-cent of the population suffer from malnutrition in India (Joshi et al., 2002). A majority of Indian population is vegetarian, deriving its protein requirement from pulses and other vegetarian sources. The per capita availability of pulses has been declining. India is deficit in pulses and edible oils and imports huge quantities of these commodities to meet the domestic demand.

About 30 per-cent (11.7 m ha) of the area under paddy production during kharif season in India remain fallow in the subsequent rabi due to number of biotic, abiotic and socioeconomic constrains. Despite of ample opportunities rice fallow systems have been bypassed in the research and developments for a number of constraints. Major rice fallow area (82%) is concentrated in eastern parts of the country. States with larger area of rice- fallows are Chhattisgarh, Madhya Pradesh, Jharkhand, Bihar, West Bengal and Orissa the remaining 18 per-cent area is in the states like Tamil Nadu, Karnataka and Andhra Pradesh and there exists a large scope for expansion of area under pulse crops. Short duration pulses are ideal crops for their cultivation in such areas (Joshi et al., 2002).

Pulses are required to grow not only for nutritional security but also for sustainability of any system. To cope up with the increasing demand of pulses in the country pulses should be included as an integral part in rice fallow areas with a dual advantage of crop diversification for sustainable production and increasing the area under pulses. To exploit these rice fallow areas with pulses, location specific and economically viable technology for better performances of pulses are required to be standardized through proper understanding of the system ecology and constraints study. This effort should have strong research support to deliver appropriate varieties and matching crop management technology suited to rice fallows cultivation. The existing rice fallow area (11.7 m ha) in India is almost equivalent to the net sown area of Punjab, Haryana and western Uttar Pradesh. If this area is brought under cultivation, it may usher another green revolution in India benefiting millions of farmers. Promotion of pulses crops in the existing paddy fallow area would also improve sustainability of the rice production system besides enhancing production and augmenting farmers income. It should be considered appropriate to identify abiotic, biotic and socio- economic constraints to rabi cropping that can be addressed through technological and policy intervention.

After the harvest of kharif rice, climatic conditions of rice fallow lands in many areas are suitable for growing cool and warm season pulses profitably. The residual moisture left in the soil at the time of rice harvest is often sufficient to raise short-season crops. Further, by use of short-duration and high-yielding varieties of rice allowing to vacate fields during September-October, the traditional rice fallows can be converted into productive lands. Introduction of cool and warm season pulses such as lentil, mungbean, urdbean, lathyrus, peas etc. Rice fallows can increase the productivity as well as sustainability of rice. The small-seeded varieties of these pulses may find prominence under utera cultivation (relay cropping) in the states of Chhattisgarh, Jharkhand, Bihar, West Bengal and Assam. This practice can be made more effective by using short- duration and high-yielding varieties of rice, as rice crop will vacate the field in September-October. In low land areas with excessive soil moisture, lentil is more suitable and assured than chickpea. Consequently, the rice-lentil system can be made more popular in the low lands of eastern Uttar Pradesh, Bihar, Jharkhand and West Bengal.

Introduction of groundnut in rice fallows can be a profitable proposition in Char area of Bihar and eastern Uttar Pradesh, Mahananda of Odisha, Brahmaputra valley of Tripura, Assam, Meghalaya, Manipur and coastal Andhra Pradesh. Under zero-till, mustard in eastern Uttar Pradesh has good scope besides traditional urdbean and mungbean. Of late, rabi sorghum has also been successfully introduced in the rice fallows of coastal Andhra Pradesh (Mishra et al., 2013). This unutilized area offers enormous opportunities to overcome the problem of food and nutritional insecurity. The rice fallows have a great potential for cultivation of short-duration pulses and oilseeds. However, very little efforts have been made to efficiently utilize these rice fallow with appropriate technical and developmental back-up. It is expected that nearly 3.0-million-hectare area of rice fallows can be brought under cultivation, which can provide about 1.5-2.0 million tonnes of additional food grain production (Anon, 2018) and help in meeting the increasing demands of pulses and oilseeds. Development and popularization of improved varieties of pulses and oilseeds suiting to rice fallows of different agro-ecological regions coupled with improved agro- technology will boost production and thus

improve income and livelihood security as well as nutritional security of farming community. Most pronounced effect of climate change is a drastic change in the rainfall pattern in the form of delayed monsoon, early withdrawal or inadequate precipitation with poor distribution leading to either drought or waterlogged conditions, particularly in rain fed ecosystem. Therefore, timing of rice transplanting plays an important role in getting higher yield of rice and sowing of succeeding dry season crops mainly pulses or oilseeds. Kalyana Karnataka, a region located in the northern part of Karnataka, is an agriculturally significant area, where rice is a major crop during the kharif season. However, a substantial portion of the region's rice fields remain fallow during the rabi (post-monsoon) season due to factors such as water scarcity, inadequate irrigation infrastructure and limited crop diversification. This fallow period not only results in underutilization of valuable agricultural land but also restricts the earning potential of farmers, contributing to economic vulnerabilities in the region.

Targeting Rice Fallow Areas (TRFA) Scheme

Recognizing the potential of rice fallow areas for crop diversification and productivity enhancement, the Department of Agriculture & Farmers Welfare (DA&FW), Ministry of Agriculture and Farmers Welfare, Government of India, launched the Targeting Rice Fallow Areas (TRFA) Scheme during 2016–17 under the umbrella of the National Food Security Mission (NFSM). The scheme was initially implemented in six eastern states Assam, Bihar, Chhattisgarh, Jharkhand, Odisha and West Bengal where the rice fallow problem was most prominent. Following its initial success, the program was expanded in 2018-19 and 2019-20 to include additional states such as Madhya Pradesh, Maharashtra, Gujarat, Tamil Nadu and Karnataka which also have significant rice fallow. The TRFA operates through cluster-based demonstrations, seed and input support, awareness creation and convergence with ICAR institutions, State Agricultural Universities (SAUs) and Krishi Vigyan Kendras (KVKs) to promote sustainable intensification in rice-based systems.

II. MATERIALS AND METHODS

Selection of the districts

The two districts *viz*., Raichur and Ballari districts of Kalyana Karnataka were purposively selected as beneficiaries under TRFA scheme is relatively higher in two districts of the region. Kalyana Karnataka region contributes about 49.07 per cent to the total pulses production and 53.56 per cent to the total oilseeds production of the state.

Selection of the taluks and villages

Two taluks were selected from each selected district and these taluks chosen based on the highest number of beneficiaries. Further, villages in all 4 taluks were selected in consultation with agriculture officer (AO) of respective taluks.

The list of beneficiary farmers under the TRFA Scheme was obtained from the district agriculture office and the multistage random sampling technique was used for selection of sample farmers. In the first stage Raichur and Ballari districts were chosen based on highest number of TRFA beneficiaries in the Kalyana Karnataka region. In the second stage, two taluks *viz*., Raichur and Manvi were selected from Raichur districts, Ballari and Siruguppa from Ballari district were chosen for the study. Accordingly, four taluks were selected based on highest number of beneficiaries and area under pulses and oilseeds cultivation in rice fallow area to obtain the required number of sample farmers. In the third stage, two villages from each of the chosen taluks were selected randomly. Finally, 15 beneficiary farmers and 15 non-beneficiary farmers were chosen from eight villages of each taluk. Thus, a total of 120 sample farmers constituting 60 beneficiaries (TRFA) and 60 Non-beneficiaries (non-TRFA) were chosen from 8 villages across 4 taluks in 2 districts (Table 3.4). In addition, 10 government officials from agricultural department were consulted to gather the information on constraints faced by them in implementation of TRFA scheme.

Under the TRFA scheme, beneficiary farmers in Ballari and Raichur districts received various inputs and technical support to promote the cultivation of pulses and oilseeds, particularly Bengal gram and mustard in rice fallow lands. The scheme aimed to enhance input use efficiency, ensure timely availability of quality resources, and improve productivity under residual soil moisture conditions. For evaluating the objectives of the study, the required data was collected through personal interview method with the help of a well-structured and pre-tested schedule. The collected data pertained to the agricultural year 2023-24. The data relating to the size of holding, general information of farmers, labour and input use in pulse and oilseed production, availing benefits under the TRFA scheme and constraints faced in adopting the scheme were collected from the sample farmers.

Secondary data pertaining to area,production and productivity of pulses and oilseeds of the study districts, Kalyana Karnataka region as a whole and Karnataka for the year 2008-09 to 2023-24 from the Directorate of Economics and Statistics, Bangalore. However, for better understanding of growth and development of pulses and

oilseeds, their growth rate in area, production and productivity were compared for period from 2008-09 to 2023-24 which was further divided in to two periods: i) the first period ranging from 2008-09 to 2015-16 (before TRFA) and ii) the period ranging from 2016-17 to 2023-24 (After-TRFA).The year 2016 was considered as a cut-off point because of implementation of "Targeting rice fallow area" to promote pulse and oilseeds production in India where in Karnataka state also covered.

Compound Annual Growth Rate (CAGR) analysis

For analysing the growth trend in area, production and productivity of pulses and oilseeds in Karnataka and the study districts of Kalyana Karnataka region, compound growth rates were computed using the following form of relationship. Before calculating the growth rate, the exponential function of area, production and yield has to be estimated i.e.

$$Y_t = ab^t u_t \quad \text{.....(01)}$$

Where,

Yt: Dependent variable of which growth rate is estimated (area, production and productivity of pulses and oilseeds).

a: Intercept (constant)

b: Regression coefficient

t: Years which take values, 1, 2, 3,……,n.

u_t: Disturbance term for the year t

The compound growth rate was obtained from the logarithmic form of the equation (1) as below

$$\ln Y = \ln a + t \ln b$$

The per cent compound growth rate was derived using the relationship

CAGR = (Anti log of ln b – 1) *100

Difference in Difference (DiD) technique

Difference-in-Differences (DiD) is a quantitative method was used to estimate and compare change in income and employment before and after scheme for beneficiary and non-beneficiary farmers. The advantage of using the double difference method is that it nets out the effects of additive factors that have fixed (time-invariant) impacts on income indicator, or that reflect common trends affecting beneficiary and non-beneficiary equally such as changes in prices (Ravallion *et al.* 2005). The Double-Difference method, which is also known as Difference-in-Difference method has the following formula:

$$DD = \left[\frac{1}{P}\sum_{i=1}^{P}(Y_{1ia} - Y_{1ib})\right] - \left[\frac{1}{C}\sum_{j=1}^{c}(Y_{0ja} - Y_{0jb})\right]$$

Where,

DD = Income difference between the respondents

P = Number of beneficiary farmers

C = Number of individuals in the control group (non – beneficiary farmers)

Y_{1ia} = Income variable of beneficiary after the TRFA scheme (2024)

Y_{1ib} = Income variable of participant before the TRFA scheme (2015)

$Y_{0\,ja}$ = Income variable of non-beneficiaries after TRFA scheme (2024)

$Y_{0\,jb}$ = Income variable of non-beneficiaries before TRFA scheme (2015)

Difference-in-Differences Regression

The Difference-in-Difference (DiD) approach was used to compare the beneficiaries with non-beneficiaries in terms of income and employment. DiD is a quasi-experimental design that makes use of longitudinal data from treatment (beneficiaries) and control (non-beneficiaries) groups to obtain an appropriate counterfactual to estimate a causal effect of Targeting Rice Fallow Area (TRFA) Scheme. DiD is typically used to estimate the effect of a specific intervention or treatment (implementation of TRFA) by comparing the changes in outcomes (income and employment) over time between beneficiaries of TRFA (the treatment group) and non-beneficiary farmers (the control group). In the DiD approach, the interaction term between time and treatment group dummy variables shows the impact of the treatment after the introduction of the TRFA Scheme. In this β3 indicates the increase in the income and employment of beneficiary farmers when compared to the non-beneficiary farmers after discounting for initial differences in profitability. We have used data for 2015 (before TRFA Scheme) and 2024 (after TRFA Scheme). The study uses robust standard errors to account for autocorrelation between before and after while running regression

$$Y_t = \alpha + \beta_1 D_{1i} + \beta_2 D_t + \beta_3 (D_{1i} * D_t) + u_t$$

Where,

α = Intercept

D_{1i} = 1 for Beneficiary of TRFA

0 for Non-beneficiary of TRFA

D_t = 1 for income / employment before TRFA (2015)

0 for income / employment after TRFA (2024)

D_{1i}*D_t = Interaction term (DiD)

β_1, β_2 and β_3 are coefficients

u_t = error term

III. RESULTS AND DISCUSSION

Cropping pattern and extent utilization of rice fallow area by sample farmers

The data presented in Table 1 Illustrate cropping pattern and extent of utilization of rice fallow areas among TRFA and Non-TRFA farmers in the study region. The analysis depicted how effectively the rice fallow lands were brought under cultivation during the *rabi* season, highlighted differences in the extent of area utilized, crop composition and cropping intensity between the two categories of farmers.

During the *kharif* season, paddy was found to be the major crop cultivated by all the sample farmers, covering 332 acres among TRFA farmers and 280 acres among Non-TRFA farmers, accounting for 100 percent of the cropped area in both cases. This indicated that paddy continued to dominate the agricultural landscape of the study area as the principal *kharif* crop due to its suitability to local agro-climatic conditions and the availability of monsoon rainfall.

In the *rabi* season, the rice fallow lands were partially utilized for growing pulses and oilseeds, reflecting the extent to which farmers were able to convert fallow lands into productive use. Among TRFA farmers, 268 acres (80.72%) of the total 332 acres were utilized, while 64 acres (19.28%) remained unutilized. In contrast, Non-TRFA farmers utilized 207 acres (73.92%) of their 280 acres, with 73 acres (26.08%) remaining fallow. This showed that TRFA farmers had achieved a higher utilization rate, mainly due to the awareness and guidance provided under the TRFA scheme, which targeted the promotion of secondary crops in rice fallow lands.

Among the crops grown in rice fallow areas, Bengal gram emerged as the dominant crop cultivated by both groups. It occupied 132 acres (39.75%) among TRFA farmers and 126 acres (45.00%) among Non-TRFA farmers. Farmers preferred Bengal gram due to its short duration, ability to thrive under residual soil moisture conditions and higher market price. The crop also helped in enriching soil fertility through biological nitrogen fixation, making it an ideal choice for inclusion in rice-based cropping systems.

Mustard was the next important crop grown in the rice fallow areas, covering 90 acres (27.10%) among TRFA farmers and 41 acres (14.64%) among Non-TRFA farmers. The relatively higher share of mustard cultivation among TRFA farmers indicated that they were more exposed to demonstrations and technical support provided under the TRFA scheme, which encouraged diversification towards oilseeds. Mustard was valued for its adaptability to low-moisture conditions and its potential as a cash crop, thereby generating additional income for farmers during the *rabi* season.

Green gram accounted for 9.03 per cent (32 acres) of the rice fallow area among TRFA farmers and 10.00 per cent (28 acres) among Non-TRFA farmers. Farmers cultivated green gram mainly because of its short growing period and low input requirements. The crop also contributed to improving soil structure and fertility, which benefited the subsequent paddy crop. Similarly, black gram occupied a smaller share of the rice fallow area, covering 14 acres (4.21%) and 12 acres (4.28%) among TRFA and Non-TRFA farmers, respectively.

Table 1. Cropping pattern and extent utilization of rice fallow area by sample farmers

SI. No	Particulars	TRFA farmers (n=60)		Non-TRFA farmers (n=60)	
		Area (acre)	%	Area (acre)	%
A	**Kharif**				
1	Paddy	332	100.00	280	100.00
B	**Rabi (Rice fallow)**				
1	Bengal gram	132	39.75	126	45.00
2	Mustard	90	27.10	41	14.64
3	Green gram	32	9.03	28	10.00
4	Black gram	14	4.21	12	4.28
5	**Utilized area (a)**	**268**	**80.72**	**207**	**73.92**

6	**Unutilized area (b)**	**64**	**19.28**	**73**	**26.08**
7	**Grand Total (a+b)**	**332**	**100.00**	**280**	**100.00**
8	**Gross cropped area**	**600**		**487**	
9	**Net sown area**	**332**		**280**	
10	**Cropping Intensity (%)**	**180.72**		**173.92**	

Note: TRFA-Targeting Rice Fallow Area

Although the area under black gram was limited, it played an important role in providing household nutrition and enhancing soil fertility.

The gross cropped area was recorded as 600 acres for TRFA farmers and 487 acres for non-TRFA farmers, while the net sown area stood at 332 acres and 280 acres, respectively. The cropping intensity was higher among TRFA farmers (180.72%) compared to Non-TRFA farmers (173.92%). This indicated that TRFA beneficiaries were able to achieve better land-use efficiency by adopting pulse and oilseed cultivation in rice fallows, primarily due to the awareness, input support and training they received under the scheme.

It was concluded that during the *kharif* season, paddy continued to be the predominant crop cultivated by all farmers, while during the *rabi* season, a significant proportion of the rice fallow lands was converted into productive use by TRFA farmers through the cultivation of pulses and oilseeds such as Bengal gram and mustard. The TRFA farmers exhibited a higher level of rice fallow utilization and cropping intensity compared to Non-TRFA farmers, reflecting the positive impact of the TRFA scheme on land-use efficiency and diversification.

However, a considerable portion of the rice fallow area among Non-TRFA farmers remained unutilized due to lack of awareness, inadequate information and limited exposure to the TRFA scheme targeting rice fallow areas. Insufficient irrigation facilities, unavailability of short-duration crop varieties, and lack of institutional support further constrained the adoption of *rabi* crops among Non-beneficiary farmers. Therefore, strengthening extension activities, improving awareness about the TRFA programme and promoting water-saving technologies could play a crucial role in enhancing the productive use of rice fallow lands and increasing cropping intensity in the region.

Income and employment of the farmer before and after implementation of TRFA

The average farm household income and employment level of sample farmers before and after implementation of TRFA scheme summarized in Tables 2 and 3. The total annual income of TRFA farmers increased from Rs.92,900 before the implementation of TRFA scheme to Rs.1,51,183 after implementation, showing a remarkable gain of Rs.58,283 per farmer. Meanwhile, Non-TRFA farmers experienced a smaller increase from Rs.78,508 to Rs.1,09,647, with a gain of Rs.31,139. Improvement among beneficiaries can be attributed to the adoption of improved technologies, access to quality seeds and better input management practices facilitated under TRFA scheme. These interventions helped reduce production costs and increase productivity, thereby enhancing net returns.

A detailed examination of seasonal income revealed that during the *kharif* season, TRFA farmers income raised from Rs.83,666 to Rs.1,16,867, while Non-beneficiaries' income increased from Rs.71,166 to Rs.95,283. In the *rabi* season, where Bengal gram and mustard was the major crop promoted under TRFA scheme, the income of beneficiaries more than tripled from Rs.9,233 to Rs.34,316 compared to a smaller rise among Non-beneficiaries i.e., Rs.7,341 to Rs.14,363. This clearly demonstrates that TRFA played a pivotal role in promoting profitable crop diversification in rice fallows, transforming an otherwise idle period into a productive and income-generating season.

The total employment increased from 202 to 264 man-days per household, a gain of 62 man-days, whereas Non-beneficiaries recorded a smaller increase from 194.57 to 218.74 man-days (24 man-days gain). Seasonal data shows that in the *rabi* season, employment among TRFA farmers nearly doubled from 60 to 116 man-days indicating that the introduction of pulse and oilseeds such as Bengal gram and mustard in rice fallows significantly expanded rural employment opportunities. The increase in labour use during this season reflects the adoption of improved crop management practices and the shift from fallow to productive cultivation, leading to higher on-farm labour demand.

Overall, it can be concluded that the TRFA scheme positively impacted farmers' socio-economic conditions, boosting both income and employment through the promotion of pulse and oilseed-based intensification in rice fallows. The findings align closely with those of

Mankar *et al.* (2013) who found that 74.16 per cent of National Horticultural Mission (NHM) beneficiaries income increased by 50.69 per cent (from Rs. 1.65 to Rs. 2.49 lakhs), employment days rose by 41.12 per cent

Table 2. Farm household income of the sample farmer before and after implementation of TRFA

Season	Income (₹/year)			
	TRFA farmer (Beneficiary)		Non-TRFA farmer (Non-Beneficiary)	
	Before TRFA (2015)	After TRFA (2024)	Before TRFA (2015)	After TRFA (2024)
Kharif	83666	116867	71166	95283
Rabi	9233	34316	7341	14363
Total	**92900**	**151183**	**78508**	**109647**

Table 3. Farm household employment of the sample farmer before and after implementation of TRFA

Season	Employment (mandays/year)			
	TRFA farmer (Beneficiary)		Non-TRFA farmer (Non-Beneficiary)	
	Before TRFA (2015)	After TRFA (2024)	Before TRFA (2015)	After TRFA (2024)
Kharif	142	148	137.16	135.58
Rabi	60	116	57.41	83.16
Total	**202**	**264**	**194.57**	**218.74**

Impact of TRFA on income and employment of respondents

The results presented in Table 4 clearly indicate that the TRFA scheme had a significant positive impact on both income and employment of the beneficiary farmers. The average annual income of beneficiaries increased from Rs.92,900 before participation to Rs.1,51,183 after, registering a mean difference of Rs.58,283, which was statistically significant at the 1% level (t = 19.76*). In comparison, Non-beneficiaries recorded a smaller increase in income from Rs.78,508 to Rs.1,09,647 with a mean difference of Rs.31,439 (t = 13.82*). The double difference estimate of Rs.26,844 signifies that TRFA beneficiaries experienced a substantially higher gain in income due to improved access to inputs, training, and technology provided under the scheme.

In terms of employment generation, a similar trend was observed. The average employment days for TRFA beneficiaries increased from 202.16 before implementation of TRFA scheme to 264.75 man-days per year after implementation of TRFA, reflecting a mean difference of 62.58 man-days (t = 14*). Non-beneficiaries showed a smaller increase from 194.57 before TRFA to 218.74 man-days after TRFA with a mean difference of 24.16 man-days (t = 3.11*). The double difference value of 38.41 man-days demonstrates that TRFA farmers benefited more in terms of labour engagement and farm employment opportunities, likely due to the adoption of improved crop management and resource utilization practices encouraged by the TRFA interventions.

These findings suggest that TRFA has not only enhanced the economic status of farmers but also contributed to labour absorption in rural areas, reducing underemployment during the *rabi* season. The increase in income can be attributed to higher productivity, better input use efficiency and cost-effective technologies promoted under TRFA. Similarly, increased employment reflects the expansion of area under Bengal gram and mustard cultivation in rice fallows and the adoption of labour-intensive but remunerative practices such as integrated nutrient and pest management.

Overall, the TRFA programme proved to be an effective institutional intervention in improving the socio-economic conditions of pulse growers in rice-fallow areas. The double difference estimates confirmed that TRFA beneficiaries experienced greater economic gains and

employment growth than their Non-beneficiary counterparts. The present findings are in close agreement with those of Manjunatha *et al.* (2019), who evaluated the impact of the National Food Security Mission (NFSM) across major rice- and wheat-growing states of India. Their study revealed that NFSM farmers earned on average 40 per cent higher annual income (Rs.2,25,463 per household) compared to Non-NFSM farmers (Rs.1,60,621 per household), primarily due to increased productivity and cost reduction. Similarly, the programme also led to higher employment generation through better access to inputs and mechanization. These findings support the current study's observation that institutional programmes like TRFA play a vital role in raising farm income and employment levels by improving technology adoption, resource efficiency and capacity building among farmers.

Table 4. Double difference estimates on impact of TRFA on income and employment of respondents

Variables	Income (₹/year)			
	Before	After	Mean Difference	t-Statistics
Beneficiary	92900	151183	58283	19.76*
Non-Beneficiary	78508	109647	31439	13.82*
Double Difference	-	-	26844	7.38*
Variables	**Employment (mandays/year)**			
	Before	**After**	**Mean Difference**	**t-Statistics**
Beneficiary	202.16	264.75	62.58	14*
Non-Beneficiary	194.57	218.74	24.16	3.11*
Double Difference	-	-	38.41	4.11*

Note: * Indicates significant at 5%

Impact of TRFA scheme on income and employment in the study area

The results in Table 5 revealed that the intercept for income was Rs.78,508 with a standard error of 6551 and a t-value of 11.985, which was significant at 1% level. The coefficient for time (β_1) was Rs.31,138 and highly significant, indicating a positive increase in income over time. The coefficient for the intervention (β_2) was Rs.14,392 but was not statistically significant, whereas the interaction term (Time × Intervention, β_3) had a positive and significant coefficient of Rs.27,419, showing that the programme brought about a significant improvement in farmers' income due to the intervention. The R^2 value of 0.2268 indicated that about 22.68% of the variation in income was explained by the model. In terms of employment, the intercept coefficient was 194.583 mandays, the time coefficient (β_1) was 24.167, and the interaction term (β_3) was highly significant with 38.497 mandays, suggesting that the intervention led to a substantial increase in employment opportunities. The R^2 value for employment was 0.3833, explaining 38.33% of variation. The F-values were 22.97 and 48.68 respectively, confirming the overall significance of both models, and the number of observations used was 240.

Table 5. Difference-in-Differences Regression results for income and employment in the study area

SI. No.	Explanatory variables	Income (₹/year)			Employment (mandays)		
		Coefficient	Std. Error	t-value	Coefficient	Std. Error	t-value
1	Intercept (α)	78508**	6551	11.985	194.583**	4.488	43.356
2	Time (β_1) 1 for Beneficiary of TRFA and 0 for Non-beneficiary of TRFA	31138**	9264	3.361	24.167**	6.347	3.808
3	Intervention (β_2) 1 for income / employment before TRFA (2015)and 0 for income / employment after	14392	9264	1.553	7.583**	6.347	1.195

	TRFA (2024)						
4	Interaction (Time ×intervention) (β_3) (DiD)	**27419***	13129	2.088	**38.497****	8.995	4.280
5	R^2	**0.2268**			**0.3833**		
6	F value	22.97			48.68		
7	Number of observations	**240**			**240**		

Note: * and ** indicates significant at 5% and 1%

Dependent variable: Income and employment

The increase in income and employment might have occurred due to the implementation of the Targeted Rice Fallow Area (TRFA) scheme, which enabled farmers to cultivate short duration pulse and oilseeds rice fallow lands and adopt improved management practices. The programme also provided input subsidies and technical guidance, resulting in better productivity and higher labour demand. The positive and significant interaction term indicated that farmers under the scheme experienced greater gains compared to non-beneficiaries due to enhanced access to inputs, extension support, and efficient use of land that was previously uncultivated. The intervention not only increased farm income but also generated additional employment days within the agricultural sector.

Overall, the difference-in-differences regression results clearly showed that the TRFA scheme had a favourable and statistically significant impact on both income and employment of the farmers in the study area. The results are consistent with the findings of Bhavani *et al*. (2022) reported a significant rise in profitability among seed-growing farmers due to the intervention of seed village programme Using Difference-in-Difference Approach in Telangana.

IV. CONCLUSION

The introduction of short-duration and drought-tolerant crops like black gram, green gram, horse gram, and chickpea in rice fallows offers a promising opportunity to enhance cropping intensity, soil fertility and overall farm productivity. The utilization of rice fallows for pulses not only ensures efficient land use but also aligns with sustainable agricultural goals and improves nutritional security for rural communities. Recognizing the importance of these fallow lands, the Government of India launched the Targeting Rice Fallow Areas (TRFA) Scheme in 2016–17 under the National Food Security Mission (NFSM). Apart from enhancing the area and production of pulses and oilseeds, the broader objectives of the TRFA scheme include improving soil fertility and land productivity at the individual farm level, creating additional employment opportunities and strengthening the economic stability of farming households. The scheme also aims to restore farmers' confidence by promoting sustainable agricultural practices through crop diversification and efficient utilization of rice fallow lands. These efforts contribute to the long-term goals of achieving food and nutritional security, reducing dependency on imports of pulses and oilseeds and ensuring livelihood resilience among small and marginal farmers. To address the decline in pulse area and productivity after TRFA, there is a need to develop short-duration greengram and blackgram varieties which are suitable to the study area. These targeted measures could help revive and enhance pulse cultivation in rice fallow areas. There is a consistent negative growth in the area, production and productivity of mustard after the implementation of the TRFA scheme in the study area, introducing a crop replacement strategy (sunflower in place of mustard) could be considered. Promoting more suitable and climate-resilient crop such as sunflower may be promoted in rice fallow areas.

REFERENCES

[1] Anonymous, 2018-19, Operational guidelines of Targeting Rice Fallow Area in Eastern India for Pulses and Oilseeds, Department of Agriculture and Farmer Welfare. Government of India, pp.1-8.

[2] Bhavani G Sreenivasulu M, Naik R V, Reddy M J M, Darekar A S and Reddy A A, 2022, Impact Assessment of Seed Village Programme by Using Difference in Difference (DiD) Approach in Telangana, India. *Sustainability*, 14(15): 9543.

[3] Joshi P K, Birthal P S and Bourai V A, 2002, Socioeconomic constraints and opportunities in rainfed rabi cropping in rice fallow areas of India. *International Crops Research Institute for the Semi-Arid Tropics,* Patancheru, 50(4): 68-72.

[4] Manjunatha A V, Kumar P and Preethika D T, 2019, Impact of National Food Security Mission on Input Use, Yield and Income. *Indian Journal of Agricultural Economics*, 74(4): 562-575.

[5] Mankar D M, Wahkhade P P and Shambharkar Y B, 2013. Impact of national horticultural mission on its beneficiaries. *International Journal of Extension Education*, 9(4): 72-80.

[6] Mishra J S, Chapke R R, Subbarayudu B, Hariprasanna K and Patil J V, 2013, Response of sorghum (*Sorghum bicolor*) hybrids to nitrogen under zero tillage in rice-fallows of Coastal Andhra Pradesh. *The Indian Journal of Agricultural Sciences*, 83(3): 359-361.

[7] Subbarao G V, Kumar R, Kumar J, Johansen C, Deb U K, Ahmed I and Harris D, 2001, Spatial distribution and quantification of rice-fallows in South Asia: potential for legumes. ICRISAT, India. Pp. 315-319.

International Journal of Environment, Agriculture and Biotechnology
Vol-11, Issue-5; Sep-Oct, 2026
Peer-Reviewed International Journal
Journal Home Page Available: https://ijeab.com/
Journal DOI: 10.22161/ijeab

Effects of *Hevea nitida* interstock on the growth and physiology of *Hevea brasiliensis*

Xin-Long Wang[1,2], Han-Qi Tu[1], Jun Wang[1,2], Xing-Cheng Yao[1,2]*

[1]Rubber Research Institute, Chinese Academy of Tropical Agricultural Sciences (CATAS), Haikou 571101, China
[2]Haikou Key Laboratory of Innovation of Seedlings of Tropical Plants, Haikou
*: corresponding author

Received: 07 Sep 2026; Received in revised form: 05 Oct 2026; Accepted: 10 Oct 2026; Available online: 17 Oct 2026
©2026 The Author(s). Published by Infogain Publication. This is an open-access article *under* the CC BY license (https://creativecommons.org/licenses/by/4.0/).

Abstract— *This study aimed to evaluate the effects of* Hevea nitida *as an interstock on* Hevea brasiliensis. *The* H. nitida *interstock was set at 10 and 30 cm (H. nitida-10 and H. nitida-30). Growth indices, leaf stomatal traits, mineral element contents, carbohydrate contents, and rubber particle size were measured. The* H. nitida *interstock significantly reduced plant height and scion diameter, and the inhibitory effect increased with interstock length. H. nitida-10 showed larger scion and interstock diameters than H. nitida-30. The* H. nitida *interstock did not affect scion stomatal size or density. The interstock did not affect N or P contents, but reduced Ca and Mg contents. Soluble sugar and starch contents were significantly higher in H. nitida-10 and H. nitida-30 than in CK, but did not differ between the two interstock lengths. The average rubber particle size of* H. nitida *was smaller than that of* H. brasiliensis*, but* H. nitida *interstock did not affect rubber particle size in the scion. These results indicate that* H. nitida *interstock causes dwarfing and alters mineral and carbohydrate status in the scion, with effects dependent on interstock length, but does not affect leaf stomatal traits or rubber particle size.*

Keywords— ***Hevea brasiliensis, Hevea nitida, interstock, stock-scion interaction***

I. INTRODUCTION

The interstock is a segment of a tree trunk grafted between the rootstock and the scion. Interstocks were initially studied as a means to overcome interspecific incompatibility between rootstocks and scions (Rogers et al, 2003). For instance, 'Hongmian miyou' is incompatible with trifoliate orange rootstocks such as *Poncirus trifoliata*, therefore, an interstock of 'Guanxi miyou' (compatible with *Poncirus trifoliata*) was commonly used between the scion ('Hongmian miyou') and the rootstock (*Poncirus trifoliata*) (He et al, 2018). Heretofore, interstocks have been used in persimmon (Shen et al, 2019), lemon (Gil-Izquierdo et al, 2004), apple (Seleznyova et al,2008), and other fruit trees to regulate tree size (Calderón et al, 2021), improve fruit yield and quality, and delay tree aging (Gil-Izquierdo et al, 2004). The rational use of a combination of citrus rootstocks and interstocks can enhance disease resistance (Shokrollah et al, 2011, Elias-Roman et al 2019), promote tree dwarfing (Seleznyova et al, 2008), and improve citrus fruit quality (Almqvist et al, 2013, Rebolledo-Martínez et al, 2019).

Rubber trees (*Hevea brasiliensis*), which produce natural rubber, are important economic crops in tropical regions. Cultivated rubber trees are propagated by grafting high-yielding clones onto seedling rootstocks. Studies have

shown that both rootstocks and interstocks can affect the growth of rubber tree scions (Yao et al., 2017; Bastiah Ahmad et al., 1996). Leong and Yoon (1978) reported that interstocks with reduced growth potential, such as *H. spruceana*, could substantially reduce scion growth. Rubber trees planted in Hainan Province are frequently damaged by typhoons. Reducing tree height is an effective means of mitigating typhoon damage. *H. nidita*, which is small to medium in size, dwarfed the tree when used as a crown scion in a three-part tree (Lin et al., 1995). However, the effect of *H. nidita* as an interstock on rubber tree growth remains unknown. In the present study, *H. nidita* was used as an interstock, and its effect on tree growth and physiology was investigated.

II. MATERIALS AND METHODS

Experimental materials

H. nitida was grafted onto *H. brasiliensis* seedlings, and then the *H. brasiliensis* clone CATAS 73397 was grafted onto *H. nitida* as the scion. The *H. nitida* interstock was set to lengths of 10 and 30 cm (plants designated as H. nitida-10 and H. nitida-30, respectively). For the control treatments, both the interstock and the scion were the clone CATAS 73397, and the interstock length was also set to 10 and 30 cm (designated as CK-10 and CK-30, respectively). In addition, *H. nitida* grafted onto *H. brasiliensis* rootstock was prepared and used as a control.

Measurement of plant growth index

The diameter of the scion stem was measured at 20 cm above the graft union between the scion and the interstock every two months after planting. The diameter of the interstock was also measured at its midpoint at 12 and 24 months after planting.

Leaf stomatal analysis

A thin layer of epidermis from the lower surface was peeled off and stained with I_2-KI on a slide. Stomatal images were captured using a light microscope equipped with a digital camera (Leica, DFC550). Stomatal length, width, and density were measured using the free software ImageJ 1.5.

Determination of physiological parameters

Leaves from H. nitida-10 and H. nitida-30 were collected separately, while leaves from CK-10 and CK-30 were mixed to form one treatment, designated CK. The collected leaves were immediately oven-dried at 110 °C for 30 min and then dried at 60 °C for 24 h. The dried leaf samples were ground into powder and then used for the determination of mineral elements and carbohydrates. Total nitrogen content was determined by Nessler's colorimetric method, total phosphorus content by the molybdenum–antimony–ascorbic acid colorimetric method, and the contents of potassium (K) and calcium (Ca) by flame atomic absorption spectrometry (Bao, 2000). Soluble sugar content was determined by the anthrone–sulfuric acid method. Starch content was determined by polarimetry.

Rubber particle size analysis

Latex from the primary laticifers was collected from scion leaves of H. nitida-30, CATAS 73397 (CK), and *H. nitida*, and transferred into a tube containing ice-cold buffer (10 mM Tris-HCl, 100 mM sucrose, pH 7.5). The particle size of the rubber particles was determined using an LA-960 laser scattering particle size distribution analyzer according to the manufacturer's instructions.

III. RESULTS

Effect of *H.nitida* interstock on the plant growth

The effect of the *H. nitida* interstock on plant height is shown in Table 1. The *H. nitida* interstock resulted in shorter plants. The inhibitory effect of the *H. nitida* interstock on plant height became more evident with age, as illustrated in Figure 1. Scion diameter was also affected by the *H. nitida* interstock. The inhibitory effect on scion diameter was similar to that observed for plant height. The *H. nitida* interstock reduced scion diameter growth, and this reduction was more pronounced during the rainy seasons (July to December, 8 to 14 months after planting; Figure 1).

The effect of the *H. nitida* interstock on scion growth was associated with interstock length, as illustrated in Figures 1 and 2. Plant height and scion diameter in H. nitida-30 were lower and smaller, respectively, than those in H. nitida-10, indicating that the longer the *H. nitida* interstock, the stronger the inhibitory effect on plant growth.

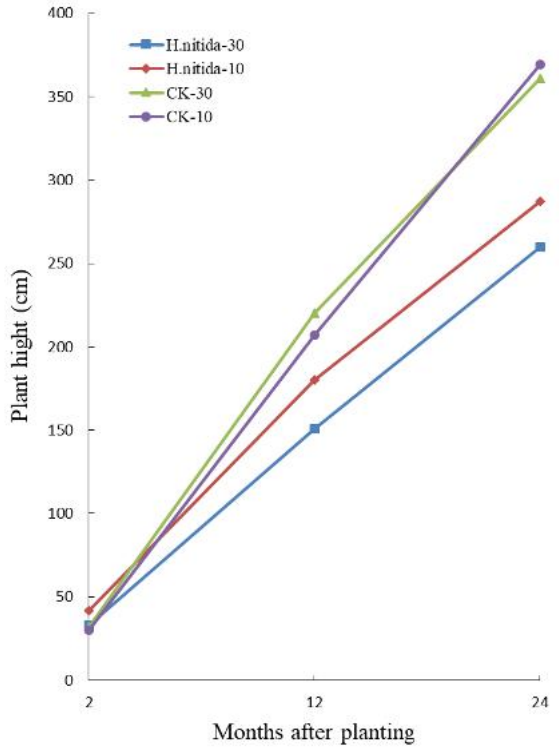


Fig.1 Effect of interstock on the plant height

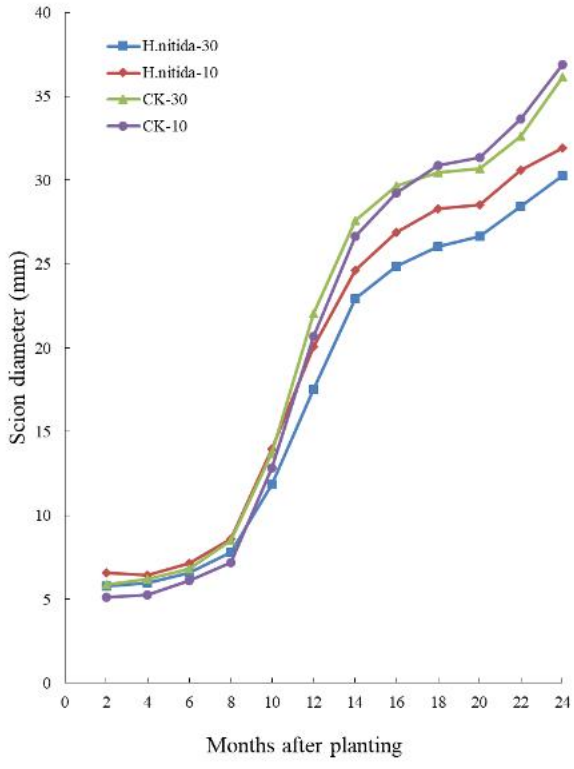


Fig.2 Effect of interstock on scion diameter

H. nitida exhibited a lower diameter growth rate than *H. brasiliensis* (0.68 vs. 1.05 mm/month; clone CATAS 73397). Therefore, when used as an interstock, *H. nitida* had a smaller diameter than CK-10 and CK-30 (Figure 3). The scion and interstock diameters of CK-10 were comparable to those of CK-30; however, the scion and interstock diameters of H. nitida-10 were larger than those of H. nitida-30. This indicated that the scion also affected interstock growth; the more vigorous scion growth in H. nitida-10 therefore resulted in a larger interstock diameter.

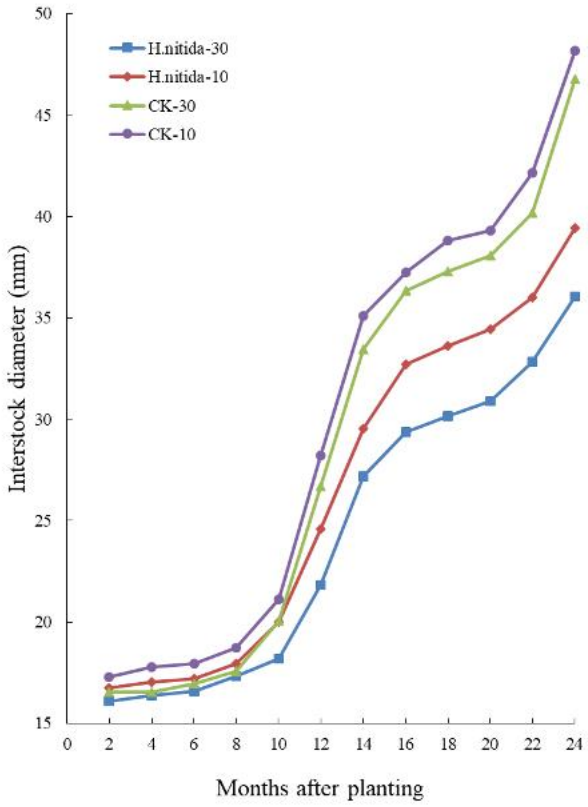


Fig.3 Effect of interstock on the interstock diameter

Effect of *H.nitida* interstock on leaf stomata

Leaf stomata are related to water utilization and further affect plant growth. The stomatal characteristics of *H. nitida* differ from those of *H. brasiliensis* (CK, viz. CATAS 73397). Stomatal density did not differ between *H. nitida* and *H. brasiliensis* (CK, viz. CATAS 73397) (514 vs. 499/mm²). Stomatal length and width of *H. nitida* were 16.42 and 11.52 µm, respectively, significantly different from those of CK (24.51 and 15.58 µm, respectively). Stomatal length and width of H. nitida-30 and H. nitida-10 were similar to those of CK-10 and CK-30.

Effect of *H.nitida* interstock on leaf mineral element content

The leaves were analyzed for mineral element content. The *H. nitida* interstock did not affect the macronutrients N and P (Figure 4). The macronutrient K content of H. nitida-30 was comparable to that of H. nitida-10 but significantly lower than that of CK. The *H. nitida* interstock significantly reduced Ca and Mg contents in H. nitida-30 and H. nitida-10. The length of the *H. nitida* interstock did not affect Ca and Mg contents.

Effect of *H.nitida* interstock on carbohydrate content

Soluble sugar content in H. nitida-30 and H. nitida-10 was significantly higher than that in CK (Figure 5). Starch content in H. nitida-30 and H. nitida-10 was also significantly higher than that in CK. However, the length of the *H. nitida* interstock did not affect the contents of soluble sugar and starch, as both were comparable between H. nitida-30 and H. nitida-10.

Effect of *H.nitida* interstock on rubber particle size

The average rubber particle size of *H. nitida* from primary laticifers was smaller than that of *H. brasiliensis* (clone CATAS 73397; 0.32 vs. 0.35 μm). The average rubber particle size of H. nitida-30 was similar to that of CK (0.35 μm). The particle size frequency curves of *H. nitida*, CK, and H. nitida-30 illustrated in Figure 6 showed the difference between *H. nitida* and *H. brasiliensis* (CK), and the similarity between CK and H. nitida-30. Therefore, the *H. nitida* interstock did not affect rubber particle size in the scion.

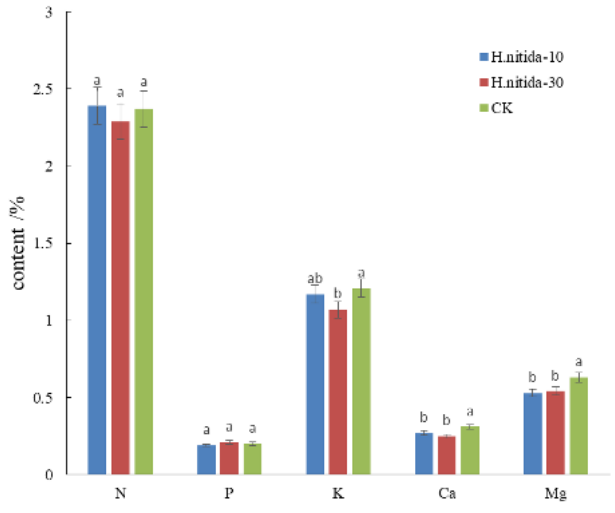


Fig.4 Effect of interstock on mineral element content

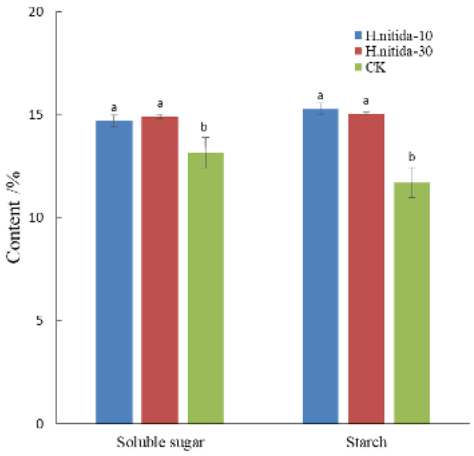


Fig.5 Effect of interstock on soluble sugar and starch contents

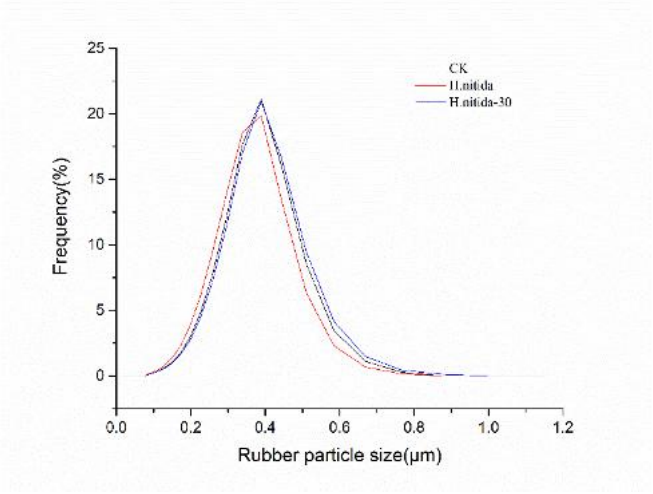


Fig.6 Comparison of the size of rubber particles

IV. DISCUSSION

Using low-vigor species as interstocks can suppress scion growth. Low-vigor *Hevea* species, such as *H. spruceana* and dwarf H. brasiliensis varieties, have also been shown to inhibit growth when used as interstocks (Leong and Yoon, 1978; Bastiah Ahmad et al., 1996). In this study, *H. nitida* exhibited low growth vigor and consequently reduced scion growth. *H. nitida* not only shortened the height of the composite plant but also retarded scion stem growth. Together with earlier findings (Leong and Yoon, 1978; Bastiah Ahmad et al., 1996), these results suggest that low-vigor *Hevea* species share similar characteristics when used as interstocks. By reducing plant height, *H. nitida* interstock has the potential to enhance typhoon resistance.

The dwarfing effect of interstock length is commonly

observed across different tree species: the longer the interstock, the shorter the plant height (Jiang et al., 2010). In this study, a longer *H. nitida* interstock produced a stronger dwarfing effect, which is consistent with the findings of Leong and Yoon (1978) for *H. spruceana* interstock. For *H. nitida* interstock, the stem growth rate was expected to be similar between H. nitida-30 and H. nitida-10. However, the *H. nitida* interstock in H. nitida-10 was larger than that in H. nitida-30. This was probably due to the scion effect: H. nitida-10 grew faster than H. nitida-30 and therefore produced more dry matter, resulting in more dry matter being allocated to the *H. nitida* interstock in H. nitida-10.

Although the leaf stomata of *H. nitida* were smaller than those of *H. brasiliensis* (CK), the stomatal size and density in H. nitida-30 and H. nitida-10 were similar to those in the CK, indicating that *H. nitida* interstock did not affect the leaf stomata of the scion. This result differs from the findings of Bastiah Ahmad (1990), which showed that *Hevea* interstock affected stomatal density and size. *H. nitida* interstock also did not affect the size of rubber particles in the primary laticifers of the leaf, suggesting that it would not affect rubber synthesis and, consequently, rubber production in the scion. Bastiah Ahmad's study demonstrated that rubber production in scions depended largely on the genotype of the scion clone and rarely on that of the interstock clone. However, this conclusion was based on *H. brasiliensis* species; the effect of other species used as interstock on rubber production has not yet been reported.

The effect of interstock on leaf mineral element contents in fruit trees has been widely reported (Jiang et al., 2010; He et al., 2018; Li et al., 2023). In this study, the *H. nitida* interstock did not affect N or P contents, but it reduced Ca and Mg contents. In addition, K content was found to be affected by interstock length. These results suggest that *H. nitida* interstock may influence the distribution and/or transport of K, Ca, and Mg.

Plant growth is closely associated with carbohydrate status. Soluble sugar and starch are the main carbohydrate components, and their contents are closely related to plant growth. The contents of soluble sugar and starch in H. nitida-30 and H. nitida-10 were significantly higher than those in the CK. This suggests that the *H. nitida* interstock may reduce sink strength, restrict carbohydrate export from the leaves, and decrease carbohydrate consumption, thereby leading to greater carbohydrate accumulation in the leaves.

ACKNOWLEDGEMENT

This study was financially supported by Hainan Provincial Natural Science Foundation of China (No.325MS134).

REFERENCES

[1] Almqvist, C. (2013). Interstock effects on topgraft vitality and strobili production after topgrafting in *Pinus sylvestris*. Can J For Res, 43: 584–588.

[2] Bao, S.D. (2000). Soil and agricultural chemistry analysis (3rd Edition) [M]. Beijing: China Agriculture Press.

[3] Bastiah B. Ahmad, Wan, C.K., Mohd Ahib Mohd Yusoff. (1996). Effect of interstock on dry matter production and growth analysis of Hevea brasiliensis (Muell. Arg.) J Nat Rubb Res, 11(4): 265–296.

[4] Bastiah B. Ahmad. (1990). Effect of interstock on growth and yield of Hevea brasiliensis (Muell. Arg). [D] Universiti Putra Malaysia.

[5] Calderón, F., Weibel, A.M., Trentacoste, E.R. (2021). Effects of different interstock length on vegetative growth and flowering in peach cv. Pavie Catherine. Sci Hortic, 285: 110174.

[6] Elias-Roman, R.D., Calderon-Zavala, G., Guzman-Mendoza, R., et al. (2019). 'Mondragon': a clonal plum rootstock to enhance management of Armillaria root disease in peach orchards of Mexico. Crop Prot, 121: 89–95.

[7] Gil-Izquierdo, A., Riquelme, M.T., Porras, I., et al. (2004). Effect of the rootstock and Interstock grafted in lemon tree (*Citruslimon* (L.) *Burm*.) on the flavonoid content of lemon juice. J Agric Food Chem, 52: 324–331.

[8] He, P., Li, L.G., Wang, H.B., et al. (2018). Effects of five dwarfing interstocks on shoot growth, fruiting and accumulation of mineral elements in leaves of Yishui red Fuji apple. Scientia Agricultura Sinica, 51(4):750–757.

[9] He, W., Wang, Y., Chen, Q., et al. (2018). Dissection of the mechanism for compatible and incompatible graft combinations of *Citrus grandis* (L.) Osbeck ('Hongmian Miyou'). Int J Mol Sci, 19: 505.

[10] Jiang, S.L., Jia, J.X., Wang, F., et al. (2010). The dwarfing effect of three pear dwarfing intermediate stocks on grafting trees. Scientia Agricultura Sinica, 43(23): 4886–4892.

[11] Leong, W., Yoon, P.K. (1978). Effect of interstock on growth o Hevea. J Rubb Res Inst Malaysia, 26(3): 99–104.

[12] Li, S., Chen, H.W., Zhang, Y.H., et al. (2023). Effects of Jizhen 1 interstock on mineral nutrition and endogenous hormone contents in

leaves of 'Tianhong 2'. J Hebei Agric University, 46(2): 28–34.

[13] Lin, W.F., Huang, S. F. (1995). Dwarf three-part trees of *Hevea brasiliensis*. Chinese J Tropical Crops, 16(1): 1–9.

[14] Luo, J., Wang, F., Han., M.Y, et al. (2013) Anatomical mechanism of two apple dwarf interstocks. J Northwest Agri Forest University, 41(6): 124–132.

[15] Rebolledo-Martínez, A., Peralta-Antonio, N., Rebolledo-Martínez, L., et al. (2019). Effect of rootstock in tree growth, dry matter, flowering, yield and quality of 'Manila' mango. Sci. Hortic, 251: 155–161.

[16] Rogers, W.S., Beakbane, A.B. (2003). Stock and scion relations. Annu. Rev. Plant Physiol, 8: 217–236.

[17] Seleznyova, A.N., Tustin, D.S., Thorp, T.G. (2008). Apple dwarfing rootstocks and interstocks affect the type of growth units produced during the annual growth cycle: Precocious transition to flowering affects the composition and vigour of annual shoots. Ann Bot, 101: 679–687.

[18] Shen, Y., Zhuang, W., Tu, X., et al. (2019). Transcriptomic analysis of interstock-induced dwarfism in sweet persimmon (*Diospyros kaki Thunb*.). Hortic Res, 6: 1086–1102.

[19] Shokrollah, H., Abdullah, T.L., Sijam, K., et al. (2011). Potential use of selected citrus rootstocks and interstocks against HLB disease in Malaysia. Crop Prot, 30: 521–525.

[20] Yao, X., Chen, X., Wang, J., et al. (2017). Effect of clonal rootstocks on the growth and yield of hevea rubber. Journal of Rubber Research, 20(3): 203–212.

International Journal of Environment, Agriculture and Biotechnology
Vol-11, Issue-5; Sep-Oct, 2026
Peer-Reviewed International Journal
Journal Home Page Available: https://ijeab.com/
Journal DOI: 10.22161/ijeab

Evaluation of Natural Biostimulants for Improving Flowering and Fruiting behaviour in Sweet Orange (Citrus sinensis (L.) Osbeck) var. Nucellar.

S. S. Patil[1], S. G. Patil[2], R. V. Nainwad[3], Dr. S. R. Wankhede[4], Dr. S. V. Pawar[5]

[1]M.Sc. (Hort.) student, Department of Horticulture, College of Agriculture, Badnapur, Vasantrao Naik Marathwada Krishi, Vidyapeeth, Parbhani, Maharashtra, India
[2]O/I Fruit Research Station, Chhatrapati Sambhajinagar, Maharashtra, India
[3]Assistant Horticulturist, Fruit Research Station, Chhatrapati Sambhajinagar, Maharashtra, India
[4]Assistant Professor, Horticulture, College of Agriculture, Badnapur, VNMKV, Parbhani, Maharashtra, India
[5]Assistant Professor, Plant Pathology, College of Agriculture, Badnapur, Maharashtra, India

Received: 18 Sep 2026; Received in revised form: 10 Oct 2026; Accepted: 16 Oct 2026; Available online: 24 Oct 2026
©2026 The Author(s). Published by Infogain Publication. This is an open-access article *under* the CC BY license (https://creativecommons.org/licenses/by/4.0/).

Abstract— *The present investigation was conducted during the Ambe Bahar season of 2024–25 at the Sweet Orange Research Station, Badnapur, Tq. Badnapur, Dist. Jalna, Maharashtra, to evaluate the influence of natural biostimulants on flowering and fruiting behaviour of nucellar sweet orange (Citrus sinensis (L.) Osbeck). The experiment was laid out in a Randomized Block Design (RBD) comprising seven treatments replicated thrice. The treatments consisted of brassinolide @ 10, 15 and 20 ppm and yeast extract @ 1000, 1500 and 2000 ppm, along with an untreated control. The biostimulants were applied as foliar sprays at full bloom and again 30 days after full bloom. Observations were recorded on days required for flowering, number of flowers, days required from fruit set to fruit maturity, fruit set, fruit drop and fruit retention. Significant variation was observed among the treatments for flowering and fruiting parameters. Brassinolide @ 20 ppm (T3) recorded superior performance with respect to flowering and fruiting attributes, followed by brassinolide @ 15 ppm (T2), while yeast extract @ 2000 ppm (T6) performed comparatively better among the yeast extract treatments. The application of biostimulants favourably influenced fruit set and fruit retention while reducing fruit drop compared with the untreated control. Overall, foliar application of brassinolide @ 20 ppm and yeast extract @ 2000 ppm showed a positive influence on flowering and fruiting behaviour of nucellar sweet orange under the agro-climatic conditions of the Marathwada region.*

Keywords— ***Sweet orange, Citrus sinensis, natural biostimulants, brassinolide, yeast extract, flowering, fruit set, fruit drop, fruit retention, fruit maturity.***

I. INTRODUCTION

Sweet orange (*Citrus sinensis* (L.) Osbeck) is an important citrus fruit crop widely cultivated in tropical and subtropical regions for its nutritional and economic importance. In India, it is mainly grown in Andhra Pradesh, Maharashtra and Telangana, while Jalna, Chh. Sambhajinagar, Nanded and Parbhani are major sweet orange-growing regions of Maharashtra. sweet orange (Nucellar Mosambi) is widely cultivated in the Jalna region due to its good yield potential and desirable fruit quality (Thorat *et al*.,2018).

Flowering and fruiting are important phases in sweet orange production and are closely associated with fruit set, fruit retention and final crop productivity. Plant biostimulants have gained importance for their potential to improve plant growth, flowering, fruit set and crop productivity. Rouphael and Colla (2020) reported that biostimulants can enhance flowering, fruit set and crop productivity through various physiological mechanisms.

Brassinolide, a biologically active brassinosteroid, regulates important processes such as cell division, cell elongation and plant development. Bishop and Yokota (2002) described the role of brassinosteroid signaling in plant developmental processes, while Manghwar *et al*. (2022) reported its role in regulating plant growth and development.

Yeast extract is a natural biostimulant rich in amino acids, vitamins, polypeptides and minerals, and its nutrient-rich composition supports plant growth and physiological activity (Tao *et al*., 2022). El Ghit (2020) reported that foliar application of yeast extract improved plant growth and fruit number. Considering the importance of flowering and fruiting in crop productivity, the present investigation was undertaken to study the effect of foliar application of brassinolide and yeast extract on flowering and fruiting parameters of nucellar sweet orange.

II. MATERIALS AND METHODS

The study was undertaken during the 2024–25 season at the Sweet Orange Research Station, Badnapur, District Jalna, Maharashtra. The experiment was performed on 16-year-old nucellar sweet orange trees, for which 42 healthy and uniform trees were selected. The trial was arranged in a Randomized Block Design (RBD) consisting of seven treatments, each replicated three times, with two plants representing each treatment within a replication. The treatment schedule included brassinolide at 10, 15 and 20 ppm and yeast extract at 1000, 1500 and 2000 ppm, along with an untreated control. All treatments were administered through foliar application at the full bloom stage, followed by a second application one month after the first spray.

Table 1: Treatments Details

Sr. No	Treatment	Treatments Details
1	T1	Brassinolide @ 10 ppm
2	T2	Brassinolide @ 15 ppm
3	T3	Brassinolide @ 20 ppm
4	T4	Yeast extract @ 1000 ppm
5	T5	Yeast extract @ 1500 ppm
6	T6	Yeast extract @ 2000 ppm
7	T7	Control

Flowering Parameters:

Number of flowers per plant: The number of flowers per plant was recorded by manually counting the flowers on each experimental tree.

Days required for flowering: The number of days required for flowering was recorded from the initiation of flowering to full bloom and expressed in days.

Days required from fruit set to maturity: The number of days required for fruit maturity was recorded from fruit set to harvest for each tree and expressed in days.

Fruiting Parameters:

Fruit set (%): Fruit set was recorded by determining the number of fruits successfully established from the tagged flowers after full bloom and expressed as percentage.

Fruit drop (%): The set fruit from above tagged flowers were used for studying the intensity of fruit drop up to the time of harvesting and percentage were worked out.

$$Fruit\ drop\ (\%) = \frac{\text{Total number of fruit set} - \text{No. of fruits at harvest time}}{Total\ no.of\ fruit\ set} X\ 100$$

Fruit retension (%): At the time of harvest, we counted the total number of fruits that remained on the tagged flowers. The percentage of fruit retention was then calculated based on the number of fruits initially present at the fruit set stage.

$$Fruit\ retention\ (\%) = \frac{\text{Number of fruits as harvest}}{Total\ no.of\ fruit\ set} X\ 100$$

Statistical Analysis: The experimental data were statistically analysed as per the methods described by Panse and Sukhatme (1985). The standard error (S.E.) and critical difference (C.D.) at the 5% level of significance were calculated wherever applicable.

III. RESULT AND DISCUSSION

The effect of biostimulants on flowering parameters:

Table 2.: Effect of Brassinolide and Yeast extract treatments on Days required for flowering, days required for fruit set to fruit maturity and Number of flowers.

Treatment	Treatments Detail	Days required for flowering	Days required from fruit set to fruit maturity	Number of flowers (Per tree)
T1	Brassinolide @ 10 ppm	17.69	243.81	8076.97
T2	Brassinolide @ 15 ppm	16.83	239.05	8223.73
T3	Brassinolide @ 20 ppm	15.46	220.60	8806.11
T4	Yeast extract @ 1000 ppm	18.09	244.00	7761.96
T5	Yeast extract @ 1500 ppm	16.93	235.74	7930.35
T6	Yeast extract @ 2000 ppm	15.97	232.23	8616.11
T7	Control	18.98	255.29	7567.01

Biostimulant application significantly influenced flowering behaviour of sweet orange (Table 1). The number of flowers per tree was highest with T_3 (brassinolide @ 20 ppm; 8806.11), which was at par with T_6 (8616.11) and T_2 (8223.73), whereas the lowest number was recorded in T_7 (7567.01). The time required for flowering was shortest under T_3 (15.46 days), at par with T_6 (15.97), T_2 (16.83) and T_5 (16.93), while T_7 required the maximum period (18.98 days). Similarly, the minimum duration from fruit set to fruit maturity was recorded with T_3 (220.60 days), statistically at par with T_6 (232.23 days), whereas the maximum duration was observed in T_7 (255.29 days).

The earlier flowering and reduced time to fruit maturity under T_3 indicate a favourable response of brassinolide, while T_6 showed a comparatively better response among yeast extract treatments. The response may be associated with the reported role of brassinolide in promoting flowering, whereas yeast extract may improve nutrient uptake and thereby support flowering and subsequent development.

These findings are consistent with Tepkaew *et a*l. (2022) and Al-Ealayawi and Al-Dulaimy (2023) for brassinolide-induced flowering, and with Faten and Bakry (2004) and El-Desouky *et al*. (2011) for the beneficial effect of yeast extract on flowering.

The effect of biostimulants on Fruiting parameters:

Table 3.: Effect of Brassinolide and Yeast extract treatments on Fruit set (%), Fruit drop (%) and Fruit retension(%).

Treatment	Treatments Detail	Fruit set (%)	Fruit drop (%)	Fruit retention (%)
T1	Brassinolide @ 10 ppm	21.83	82.25	17.75
T2	Brassinolide @ 15 ppm	25.70	80.16	19.84
T3	Brassinolide @ 20 ppm	27.32	79.30	20.70
T4	Yeast extract @ 1000 ppm	17.42	84.92	15.08
T5	Yeast extract @ 1500 ppm	19.93	83.38	16.62
T6	Yeast extract @ 2000 ppm	23.35	82.53	17.46
T7	Control	16.43	86.82	13.17

Biostimulant application significantly affected fruit set, fruit drop and fruit retention (Table 2). Fruit set was highest with T_3 (27.32%), followed by T_2 (25.70%) and T_6 (23.35%), compared with 16.43% in the control. Fruit drop was lowest under T_3 (79.30%), at par with T_2 (80.16%) and T_1 (82.25%), whereas the control recorded the highest drop (86.82%). Conversely, fruit retention was highest with T_3 (20.70%), statistically at par with T_2 (19.84%) and T_6 (17.46%), while the lowest retention (13.17%) was recorded in T_7.

The higher fruit set and retention and lower fruit drop under T_3 indicate a favourable effect of brassinolide on fruit establishment and retention. Among yeast extract treatments, T_6 (2000 ppm) showed a comparatively better

response. The improved fruit set with yeast extract was attributed in the source to enhanced nutrient uptake, while the reduction in fruit drop and increase in fruit retention were associated with biostimulant application.

The present findings are in agreement with Mostafa and Kotb (2018), Ali *et al*. (2019) and Sharma (2021) for improved fruit set, and with Ali *et al*. (2019), Kumari et al. (2019) and El-Boray *et al*. (2015) for reduced fruit drop. The improvement in fruit retention is also supported by Mostafa and Kotb (2018) and Kumari *et al*. (2019).

IV. CONCLUSION

Biostimulant application significantly influenced the flowering and fruiting performance of sweet orange. Brassinolide @ 20 ppm (T_3) emerged as the most effective treatment, promoting early flowering and fruit maturity and increasing the number of flowers per plant. It also enhanced fruit set and fruit retention while reducing fruit drop compared with the control. Overall, brassinolide @ 20 ppm demonstrated the most favourable effect on flowering and fruiting performance of sweet orange.

REFERENCES

[1] Al-Ealayawi, Z. A., & Al-Dulaimy, A. F. (2023, December). Response of Strawberry saplings Cv. Albion to spraying with Seaweed Extract, Arginine and Brassinolide. *In IOP Conference Series: Earth and Environmental Science* (*Vol. 1262*, No. 4, p. 042065). IOP Publishing.

[2] Ali, M. A., Ezz, T. M., Abd El-Megeed, N., & Ismail, M. (2019). Foliar Application of Kelpak, Brassinolide and Boron in Relation to Fruit Set, Drop, Yield and Fruit Quality of'Canino'Apricot Trees. *Journal of the Advances in Agricultural Researches, 24*(2), 194-211.

[3] Bishop, G. J., & Yokota, T. (2002). Brassinosteroids and plant steroid hormone biosynthesis signaling. *Plant Physiology, 130*(1), 1–7.

[4] El-Boray, M. S., Mostafa, M. F. M., Salem, S. E., & El-Sawwah, O. A. O. (2015). Improving yield and fruit quality of Washington navel orange using foliar applications of some natural biostimulants. *Journal of Plant Production, 6*(8), 1317–1332.

[5] El-Desouky, S. A., Ismaeil, F. H., Wanas, A. L., Fathy, E. S. L., Abd El-All, M. M., & Abd, M. M. (2011). Effect of yeast extract, amino acids and citric acid on physioanatomical aspects and productivity of tomato plants grown in late summer season. *Minufiya J. Agric. Res, 36*(4), 859-884.

[6] El Ghit, H. M. A. (2020). Effect of application of yeast extract on hydroponic tomato plants grown in a soilless culture system.

[7] Faten, H. M., & Bakry, K. H. (2004). Response of papaya plants to some chemical substances and yeast extract treatments. *Proceedings the American society of Horticultural sciences, 75*, 244-252.

[8] Kumari, S., Yeptho, K. Y., Pande, K. K., Roshan, R. K., & Debbarma, A. (2019) Crosstalk effect of brassinosteroids and gibberelic acid affects plant phenology, yield and fruit quality traits in sugar apple (*Annona squamosa* L.) cv. Balanagar.

[9] Manghwar, H., Hussain, A., Ali, U., Shoukat, A., Ali, M., Shabbir, M. A., & Wang, G. (2022). Brassinosteroids role in plant development and stress responses: A review. *Frontiers in Plant Science, 12*, 8835148.

[10] Mostafa, L. Y., & Kotb, H. R. (2018). Effect of brassinosteroids and gibberellic acid on parthenocarpic fruit formation and fruit quality of sugar apple *Annona squamosa* L. *Middle East J, 7*(4), 1341-1351.

[11] Panse, V.G., Sukhatme, P.V. and Sable. (1995). *Statistical method for Agriculture*. workers Pub. I.C.A.R. New Delhi.

[12] Rouphael, Y., & Colla, G. (2020). Biostimulants in agriculture. *Frontiers in plant science*, *11*,40.

[13] Sharma, S. K. (2021). Brassinosteroids application responses in fruit crops-a review. *International Journal of Agriculture, Environment and Biotechnology, 14*(2), 123-140.

[14] Tao, Z., Yuan, H., Liu, M., Liu, Q., Zhang, S., Liu, H., ... & Wang, T. (2022). Yeast extract: characteristics, production, applications and future perspectives. *Journal of microbiology and biotechnology*, *33*(2), 151.

[15] Tepkaew, T., Khamsuk, O., Chumpookam, J., Sonjaroon, W., & Jutamanee, K. (2022). Exogenous brassinosteroids regulate mango fruit set through inflorescence development and pollen fertility. *Horticultural Science and Technology, 40*(5), 481-495.

[16] Thorat MA, Patil MB, Patil SG and Deshpande DP (2018). Effect of soil and foliar application of zinc on quality parameters of sweet orange Var. Nucellar (*Citrus sinensis* L. Osbeck). *Journal of Pharmacognosy and Phytochemistry.* 7(5), 737-740.

International Journal of Environment, Agriculture and Biotechnology
Vol-11, Issue-5; Sep-Oct, 2026
Peer-Reviewed International Journal
Journal Home Page Available: https://ijeab.com/
Journal DOI: 10.22161/ijeab

Biomass Partitioning and Root System Development of Acid Lime (Citrus aurantifolia Swingle) Seedlings under Contrasting Growing Media and Nutrient Regimes in a Shade-Net Nursery

A. S. Suke[1], S. G. Patil[2], R. V. Nainwad[3], S. R. Wankhede[4], S. K. Ugile[5]

[1]M.Sc. (Hort.) student, Department of Horticulture, College of Agriculture, Badnapur, Vasantrao Naik Marathwada Krishi, Vidyapeeth, Parbhani, Maharashtra, India
[2]O/I Fruit Research Station, Chhatrapati Sambhajinagar, Maharashtra, India
[3]Assistant Horticulturist, Fruit Research Station, Chhatrapati Sambhajinagar, Maharashtra, India
[4]Assistant Professor, Horticulture, College of Agriculture, Badnapur, Maharashtra, India
[5]Principal, ATS Latur and Assistant Professor, Dept. of Soil Science, College of Agriculture, Latur, Maharashtra, India

Received: 15 Sep 2026; Received in revised form: 14 Oct 2026; Accepted: 18 Oct 2026; Available online: 24 Oct 2026
©2026 The Author(s). Published by Infogain Publication. This is an open-access article *under* the CC BY license (https://creativecommons.org/licenses/by/4.0/).

Abstract— *The quality of citrus nursery stock depends not only on shoot growth but also on the development and proportional allocation of root and shoot biomass. A secondary analysis was undertaken using the root and biomass observations from an acid lime (Citrus aurantifolia Swingle) cv. Sai Sharbati nursery experiment conducted during 2025–26 at Sweet Orange Research Station, Badnapur. The original experiment comprised seven media–nutrition treatments in a Completely Randomized Design with three replications. The present manuscript focuses specifically on root biomass, shoot biomass, root volume and biomass partitioning rather than the germination and general growth response reported in the associated publication. The integrated potting mixture + cocopeat medium supplied with 20:10:10 g NPK seedling^{-1} (T7) produced the highest root fresh weight (3.45 g), root dry weight (0.68 g), shoot fresh weight (16.55 g), shoot dry weight (4.19 g) and root volume (3.89 cm³). Potting mixture + cocopeat with 40:25:25 NPK (T6) and potting mixture with 40:25:25 NPK (T3) were the next strongest treatments for biomass production. Although the sole cocopeat treatment with 60:25:25 NPK (T4) showed the highest root:shoot dry ratio (0.59), its absolute root and shoot biomass were very low, demonstrating that a high ratio alone is not an indicator of superior seedling quality. T7 combined substantial absolute root development with markedly greater shoot biomass and therefore showed the most favourable overall biomass architecture. The findings highlight the importance of evaluating absolute root traits together with biomass allocation when selecting acid lime seedlings for nursery transplanting.*

Keywords— ***acid lime, root biomass, shoot biomass, root volume, biomass partitioning, cocopeat, nursery substrate***

I. INTRODUCTION

High-quality nursery plants are essential for successful establishment of perennial citrus orchards. While conventional nursery assessments commonly emphasize height, leaf number and survival, the root system is equally important because it determines anchorage, water acquisition, nutrient absorption and the ability of a seedling to establish after transplanting. A seedling with a large shoot but weak roots may suffer transplant shock, whereas a seedling with a high root:shoot ratio but very small absolute biomass may simply be under severe growth restriction.

Growing media strongly influence root-zone aeration, water availability, bulk density and nutrient retention. Cocopeat has high porosity and water-holding capacity and

can improve physical conditions when appropriately blended with mineral and organic media. However, the response of seedlings to a substrate cannot be interpreted independently of nutrient supply. Moderate fertilization in a physically favourable substrate may stimulate both root exploration and shoot biomass, whereas an excessive nutrient concentration in a poorly buffered substrate can restrict growth.

The associated acid lime nursery experiment compared conventional potting mixture, cocopeat and a blended medium under different NPK regimes. The published analysis emphasized germination, survival, vegetative growth and overall seedling vigour. The present secondary analysis addresses a different question: how do these media–nutrition combinations modify absolute root and shoot biomass, root volume and the partitioning of dry matter between roots and shoots? Such an analysis is useful for nursery quality assessment because biomass allocation provides information that cannot be obtained from shoot growth measurements alone.

II. OBJECTIVES

- To evaluate the effect of contrasting growing media and NPK regimes on root fresh and dry biomass of acid lime seedlings.
- To quantify treatment effects on shoot fresh and dry biomass and root volume.
- To interpret root:shoot dry biomass allocation together with absolute root and shoot development for nursery seedling quality assessment.

III. MATERIALS AND METHODS

The secondary analysis used observations from the original shade-net nursery experiment conducted at Sweet Orange Research Station, Badnapur during 2025–26 on acid lime cv. Sai Sharbati. The original experiment followed a Completely Randomized Design with seven treatments and three replications, with six seedlings per treatment unit. Seedlings were raised in 40 × 30 × 10 cm trays. The media consisted of conventional potting mixture, cocopeat and a 1:1 blend of potting mixture and cocopeat, with NPK regimes imposed according to the original treatment structure.

Table 1. Treatment structure used in the original experiment.

Treatment	Media and nutrient regime
T1	Potting mixture 2:1:1 (Sand:Soil:FYM)
T2	Potting mixture + 60:25:25 NPK g seedling^{-1}
T3	Potting mixture + 40:25:25 NPK g seedling^{-1}
T4	Cocopeat + 60:25:25 NPK g seedling^{-1}
T5	Cocopeat + 40:25:25 NPK g seedling^{-1}
T6	Potting mixture + cocopeat + 40:25:25 NPK g seedling^{-1}
T7	Potting mixture + cocopeat + 20:10:10 NPK g seedling^{-1}

Root fresh weight was measured after uprooting and washing the root system. Root dry weight was determined after oven drying at 65 ± 2 °C to constant weight. Shoot fresh weight was measured after separation from the root system, and shoot dry weight was obtained after drying under the same conditions. Root volume was determined by water displacement. Root:shoot ratio was calculated from dry root weight divided by dry shoot weight.

For the present secondary analysis, two descriptive biomass-allocation indicators were additionally calculated from treatment means: root dry matter percentage = root dry weight/(root dry weight + shoot dry weight) × 100; and shoot:root dry biomass ratio = shoot dry weight/root dry weight. These derived indicators are used for interpretation only and do not replace the statistical analyses reported in the original thesis.

IV. RESULTS AND DISCUSSION

4.1 Root biomass response

Marked treatment differences were observed in root biomass. T7 produced the highest root fresh weight (3.45 g) and root dry weight (0.68 g), followed by T3 (3.07 and 0.61 g) and T1/T6 (0.56 g root dry weight each). T4 produced the lowest root fresh weight (0.74 g) and root dry weight (0.15 g). Thus, the treatment with the highest root:shoot ratio was not the treatment with the largest root system. The results demonstrate the importance of considering absolute root biomass when judging nursery quality.

Table 2. Root-system characteristics under different media–nutrition combinations.

Parameter	T1	T2	T3	T4	T5	T6	T7
Root fresh weight (g)	2.82	2.35	3.07	0.74	1.10	2.77	3.45
Root dry weight (g)	0.56	0.48	0.61	0.15	0.23	0.56	0.68
Root volume (cm³)	3.36	2.61	3.50	0.94	1.42	3.07	3.89

4.2 Shoot biomass response

Shoot biomass showed a strong response to the interaction between growing medium and nutrient regime. T7 produced 16.55 g shoot fresh weight and 4.19 g shoot dry weight, the highest values among all treatments. T3 recorded 14.01 and 3.43 g, while T6 recorded 13.11 and 3.17 g, respectively. In contrast, T4 recorded only 1.29 g shoot fresh weight and 0.27 g shoot dry weight. The large difference indicates that substrate suitability, rather than nutrient dose alone, was critical for converting available nutrients into structural biomass.

Table 3. Shoot biomass under different media–nutrition combinations.

Parameter	T1	T2	T3	T4	T5	T6	T7
Shoot fresh weight (g)	12.55	8.56	14.01	1.29	2.77	13.11	16.55
Shoot dry weight (g)	3.10	1.93	3.43	0.27	0.60	3.17	4.19

4.3 Biomass partitioning and root:shoot relationships

The conventional root:shoot dry ratio provides a relative measure of biomass allocation but can be misleading if interpreted without absolute biomass. T4 had the highest ratio (0.59), followed by T5 (0.40) and T2 (0.25), whereas T7 had the lowest ratio (0.16). However, T4 had only 0.15 g root dry weight and 0.27 g shoot dry weight, while T7 had 0.68 g root dry weight and 4.19 g shoot dry weight. Consequently, the high ratio in T4 reflected severe restriction of shoot growth rather than superior root development.

On a treatment-mean basis, T7 allocated approximately 14.0% of total dry biomass to roots and 86.0% to shoots, whereas T4 allocated approximately 35.7% to roots and 64.3% to shoots. The shoot:root dry biomass ratio was approximately 6.16 under T7 compared with 1.80 under T4. This contrast indicates that T7 produced a much larger and more productive shoot system while retaining substantial absolute root biomass. For nursery purposes, this combination is more meaningful than a high root:shoot ratio produced by severely stunted seedlings.

Table 4. Derived biomass-allocation indicators based on treatment means.

Indicator	T1	T2	T3	T4	T5	T6	T7
Total dry biomass (g)	3.66	2.41	4.04	0.42	0.83	3.73	4.87
Root dry matter (%)	15.30	19.92	15.10	35.71	27.71	15.01	13.96
Shoot dry matter (%)	84.70	80.08	84.90	64.29	72.29	84.99	86.04
Shoot:root dry ratio	5.54	4.02	5.62	1.80	2.61	5.66	6.16

4.4 Root volume as an indicator of transplantable root-zone development

Root volume provides a complementary measure of the three-dimensional extent of the root system. T7 recorded the maximum root volume (3.89 cm³), followed by T3 (3.50 cm³) and T1 (3.36 cm³), while T4 recorded only 0.94 cm³. The simultaneous increase in root dry weight and root volume under T7 suggests that the treatment promoted both root mass accumulation and spatial development. The close performance of T3 indicates that conventional potting mixture supplied with an intermediate nutrient dose can also produce a substantial root system when cocopeat is unavailable.

The contrast between T7 and T4 is particularly relevant to nursery management. Both treatments contained NPK, but their substrate environments differed substantially. The blended substrate in T7 likely provided a more favourable balance between water retention and aeration, while the sole-cocopeat treatment with the higher nutrient dose was associated with restricted root and shoot development. Therefore, nutrient concentration should be optimized in

relation to substrate physical properties rather than considered independently.

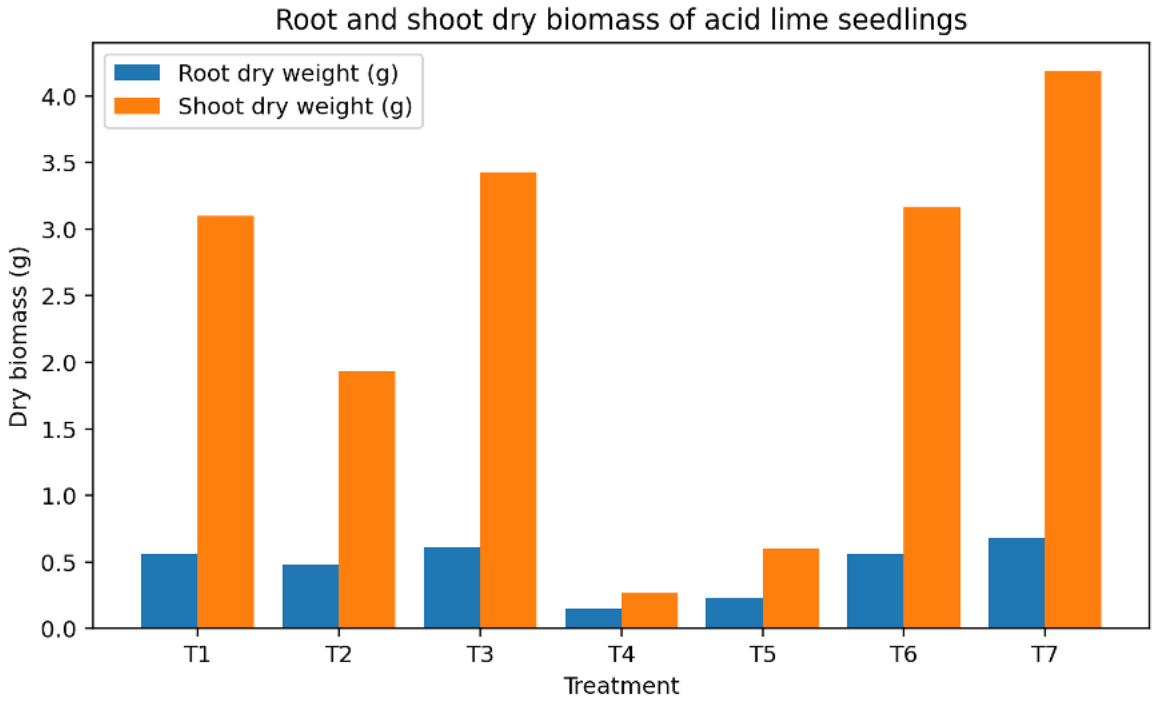


Fig.1. Comparative root and shoot dry biomass under the seven media–nutrition treatments.

V. CONCLUSION

The secondary analysis demonstrates that the best nursery treatment should not be identified from root:shoot ratio alone. Potting mixture + cocopeat supplemented with 20:10:10 g NPK seedling^{-1} (T7) produced the greatest absolute root fresh and dry biomass, shoot biomass and root volume, while maintaining a comparatively low root:shoot ratio because of strong canopy development. The poor-performing sole-cocopeat treatment T4 showed the highest root:shoot ratio but had extremely low absolute root and shoot biomass, confirming that the ratio represented growth restriction rather than superior seedling quality.

From a nursery-quality perspective, T7 provided the most favourable combination of root-system size, shoot biomass and overall biomass accumulation. T3 was the strongest alternative among the conventional potting-mixture treatments. Future work should validate whether these biomass and root traits translate into faster transplant establishment, greater field survival and improved early growth after planting in the orchard.

REFERENCES

[1] Marathe, R.A., Murkute, A.A., Ladaniya, M.S., Sonkar, R.K. and Kolwadkar, J. (2020). Standardization of potting media and nutrition protocol for raising acid lime seedling in containerized nursery. Indian Journal of Horticulture, 77(2): 261–266.

[2] Parmar, M., Pandey, S.K., Pandey, C.S., Singh, P. and Ravi, A. (2019). Effect of growing media and GA3 on seed germination and seedling growth of acid lime (Citrus aurantifolia Swingle) cv. Vikram. International Journal of Current Microbiology and Applied Sciences, 8(8): 1260–1271.

[3] Yadav, R.K., Jain, M.C. and Jhakar, R.P. (2012). Effect of media on growth and development of acid lime (Citrus aurantifolia Swingle) seedling with or without Azotobacter. African Journal of Agricultural Research, 7(48): 6421–6426.

[4] Abbas, M., Aftab, M., Zafar-ul-Hye, M., Iqbal, Q., Hussain, M. and Khan, M.M. (2015). Effect of organically amended growing substrates on the growth and physiological attributes of citrus plants. Communications in Soil Science and Plant Analysis, 46(15): 1863–1880.

[5] Aishwarya and Bahadur, V. (2024). Effect of different growing media and varying levels of gibberellic acid on seed germination and vigour of acid lime (Citrus aurantifolia Swingle) cv. Kagzi lime. Journal of Advances in Biology & Biotechnology, 27(8): 91–96.

International Journal of Environment, Agriculture and Biotechnology
Vol-11, Issue-5; Sep-Oct, 2026
Peer-Reviewed International Journal
Journal Home Page Available: https://ijeab.com/
Journal DOI: 10.22161/ijeab

Ring-like Expansion of Heat Islands and Fragmentation of Cold Islands: Remote Sensing-Based Monitoring and Driving Mechanisms of Thermal Environment Evolution in Wuhan

Anqi Bai, Xinrui Gao, Yuxi Yao, Jieting Zhang, Ruei-Yuan Wang*

School of Sciences, Guangdong University of Petrochem Technology (GDUPT), Maoming 525000, China

Received: 18 Sep 2026; Received in revised form: 16 Oct 2026; Accepted: 22 Oct 2026; Available online: 28 Oct 2026
©2026 The Author(s). Published by Infogain Publication. This is an open-access article *under* the CC BY license (https://creativecommons.org/licenses/by/4.0/).

Abstract— *The urban heat island (UHI) effect is a typical eco-environmental problem during urbanization, significantly affecting urban ecosystems and residents' quality of life. Using Wuhan City as the study area, we employed Landsat images from 2013, 2018, and 2024, along with multi-source data including DEM, population density, and land use types. Land surface temperature (LST) was retrieved using the mono-window algorithm. By combining the mean–standard deviation classification method with the geographical detector model, we systematically analyzed the spatiotemporal evolution characteristics and driving mechanisms of the UHI effect. The results show that: (1) From 2013 to 2024, the proportion of heat islands in Wuhan increased from 43.98% to 54.17%, while the proportion of cold islands decreased from 24.81% to 19.96%. Heat islands expanded outward in a concentric pattern with continuously increasing intensity, whereas cold islands shrank globally and their fragmentation intensified. (2) The spatial pattern exhibited a stable dual-circle structure of "strong heat islands in the center—shrinking cold islands in the periphery." The Yangtze River and Han River acted as natural "cold corridors," serving as spatial barriers that segmented heat islands. (3) The geographical detector revealed that NDBI and NDVI were the long-term dominant independent driving factors, and their interaction yielded the highest explanatory power ($q = 0.771$). The superimposed effect of construction land expansion and vegetation degradation constituted the core mechanism of heat island formation. All factor interactions exhibited a two-factor enhancement effect, and the driving intensity dominated by human activities displayed a dynamic fluctuation pattern: high in 2013, decline in 2018, and rebound in 2024, corresponding to different stages of urban development. (4) The risk detector indicated that NDBI, population density, and land surface temperature were significantly and positively correlated with heat island intensity, while NDVI and elevation were significantly negatively correlated. The warming effect of positive factors was stronger in high-risk areas. This study provides a quantitative scientific basis for optimizing the thermal environment and guiding ecological regulation in Wuhan.*

Keywords— ***Heat Island Effect (UIE), Land Surface Temperature (LST) Inversion, RS and GIS, GeoDetector, Wuhan City***

I. INTRODUCTION

With accelerating urbanization and industrialization, the urban heat island (UHI) effect has increasingly affected urban ecosystems and residents' daily lives, becoming a major concern in urban environmental research (Liang et al., 2010). Meteorologists have recognized that the UHI effect not only influences local meteorological conditions and climate but also contributes to broader climate change in the context of urbanization (Li, 2013). Wuhan, located in the middle and lower reaches of the Yangtze River, experiences prolonged periods of hot weather in summer, when the western Pacific subtropical high frequently dominates regional atmospheric conditions, resulting in abundant sunshine, high temperatures, limited rainfall, and intense solar radiation. When combined with the UHI effect, these climatic conditions can exacerbate the intensity and duration of summer heat, contributing to Wuhan's reputation as a typical "furnace city." In addition, Wuhan is characterized by a dense network of rivers and lakes, diverse land-use types, and heterogeneous underlying surfaces, including plains, hills, built-up areas, woodlands, and water bodies. These characteristics contribute to pronounced spatial variations in the urban thermal environment, making Wuhan a suitable case study for investigating the UHI effect in a large city under specific climatic conditions.

Accordingly, this study investigates Wuhan using remote sensing (RS) and geographic information system (GIS) technologies, integrating Landsat imagery from 2013, 2018, and 2024 with multisource datasets to examine the spatiotemporal patterns and driving mechanisms of the urban thermal environment. Specifically, this study aims to characterize the temporal trends and spatial distribution of LST, assess differences in thermal environmental effects among land-use types, and identify key driving factors using the Geodetector method. By examining both the individual effects of these factors and their interactions, this study seeks to clarify the mechanisms underlying spatial variations in the urban thermal environment and provide a scientific basis for thermal environment assessment and optimization in Wuhan.

II. STUDY AREA AND DATA SOURCES

2.1 Overview of the Study Area

Wuhan is located in eastern Hubei Province, in the middle reaches of the Yangtze River, between 29°58′ and 31°22′ N and 113°41′ and 115°05′ E. The city comprises 13 administrative districts and covers an area of approximately 8,569 km². Located in the eastern Jianghan Plain, Wuhan is characterized by predominantly low-lying, flat terrain, interspersed with a small number of low mountains and hills (Figure 1). The Yangtze River and the Han River flow through the city, which also contains numerous lakes. Water bodies account for approximately one-quarter of the city's total area, earning Wuhan its reputation as the "City of a Hundred Lakes" in China.

Wuhan has a subtropical monsoon climate, with summers frequently influenced by the subtropical high-pressure system, resulting in prolonged periods of high temperatures and hot, humid weather. The annual mean temperature is approximately 16.8°C, while extreme summer temperatures can exceed 40°C and extreme winter temperatures can fall to approximately −10°C. Annual precipitation averages approximately 1,200 mm and is concentrated mainly in summer. As of 2024, Wuhan had a permanent resident population of approximately 13.8 million, with an urbanization rate exceeding 80%. As a major economic, cultural, and transportation hub in central China, Wuhan has experienced rapid urban development in recent years. The continuous expansion of built-up areas, together with the concentration of population and industrial activities in the central urban area, has increased pressure on the urban thermal environment and potentially intensified the urban heat island effect.

International Journal of Environment, Agriculture and Biotechnology
Vol-11, Issue-5; Sep-Oct, 2026
Peer-Reviewed International Journal
Journal Home Page Available: https://ijeab.com/
Journal DOI: 10.22161/ijeab

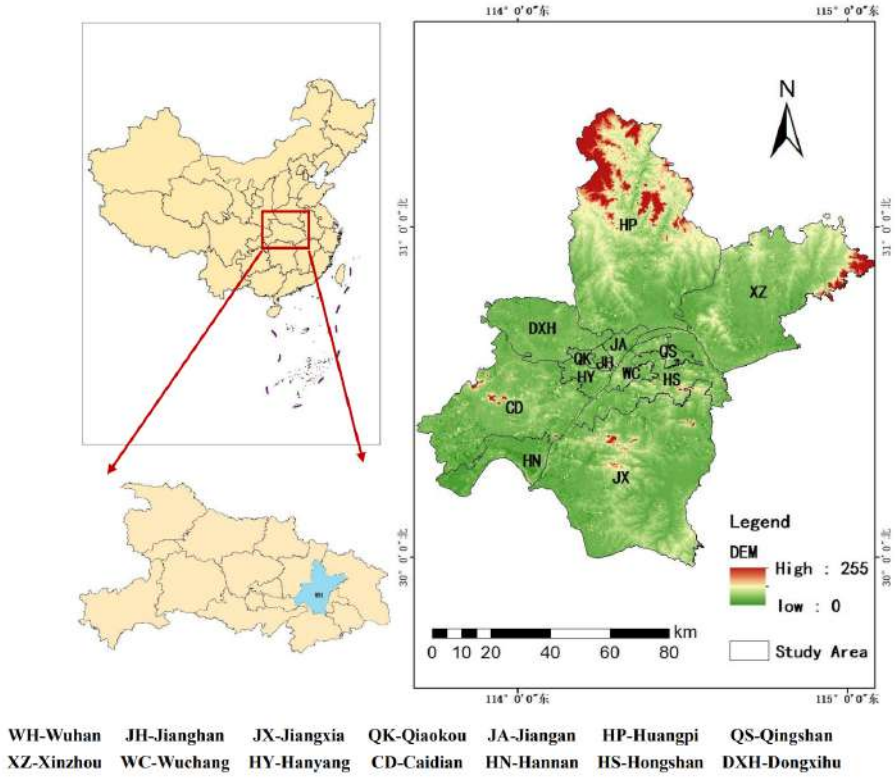


Fig.1 Location and topographic elevation map of Wuhan City

2.2 Data Sources

This study uses multisource datasets for Wuhan for 2013, 2018, and 2024. The data sources and associated preprocessing procedures are described below and summarized in Table 1.

(1) **Administrative boundary data.** Vector data delineating the administrative boundaries of Wuhan's districts were obtained from the National Geomatics Information Public Service Platform. These boundaries define the study area and serve as the spatial reference for data clipping and subsequent spatial analyses.

(2) **Land surface temperature (LST) data.** Landsat Collection 2 Level-2 imagery covering the study area during the summer period (May–August) was obtained through Google Earth Engine (GEE). Cloud-contaminated pixels were masked using the QA_PIXEL quality assessment band, and the appropriate scale factors were applied to convert the original pixel values into physically meaningful measurements. Median compositing was then performed to generate representative imagery for each study year. Where necessary, residual data gaps were filled using observations from adjacent months. The resulting imagery was clipped to the study area boundary, and the thermal and optical bands were exported separately for subsequent analyses.

(3) **Digital elevation model (DEM) data.** DEM data at a spatial resolution of 30 m were obtained from the ASTER Global Digital Elevation Model (ASTER GDEM) dataset through the Geospatial Data Cloud platform. The raster data were clipped to the study area boundary, and the resulting DEM was used for terrain-related analyses.

(4) **Population density (PD) data.** Population density data were obtained from WorldPop's gridded population distribution dataset for China, with a spatial resolution of 1

km. The raster data were clipped to the study area boundary to characterize the spatial distribution of population density and investigate its relationship with the urban thermal environment. Owing to the delayed availability of updated, high-resolution population datasets, a 1-km-resolution population raster based on the latest available census benchmarks was not available for 2024. According to the Wuhan Statistical Yearbook, the city's permanent resident population increased from 12.4477 million in 2020 to 13.8091 million in 2024, while the reported population density increased from 1,453 to 1,611 persons/km². This represents an increase of approximately 10.94% in the total permanent resident population. At the district level, central urban districts, including Jianghan (24,415 persons/km²), Qiaokou (18,727 persons/km²), and Wuchang (13,202 persons/km²), continued to exhibit relatively high population densities, whereas peripheral districts, such as Jiangxia (728 persons/km²) and Xinzhou (640 persons/km²), had substantially lower densities. These figures suggest that the broad spatial contrast between densely populated central districts and less densely populated peripheral districts remained evident during the study period. Accordingly, the 2020 population raster was used as an approximate proxy for the 2024 population distribution. This substitution allows the analysis to retain a spatially explicit representation of population density, although it may not capture population redistribution between 2020 and 2024.

(5) **Vegetation and built-up indices.** The Normalized Difference Vegetation Index (NDVI) and Normalized Difference Built-up Index (NDBI) were derived from Landsat imagery obtained through GEE. These indices were used to characterize vegetation cover and built-up surfaces, respectively, and to examine their relationships with the urban thermal environment.

(6) **Land-use data.** Land-use data were obtained from the China Land Use/Cover Change (CNLUCC) dataset developed by the Resource and Environment Science and Data Center of the Chinese Academy of Sciences. Raster data at a spatial resolution of 1 km were selected to investigate the relationship between land-use patterns and the urban thermal environment. Because data for 2024 were not available in the dataset at the time of analysis, the 2023 land-use dataset was used as a proxy for the 2024 land-surface conditions. This substitution was based on the assumption that broad-scale land-use patterns generally change gradually, although localized changes associated with urban expansion and vegetation loss may occur over shorter periods. The CNLUCC dataset was developed through visual interpretation of Landsat imagery and provides spatial information on major land-use categories, including built-up land, woodland, and water bodies. The 2023 dataset therefore provides a basis for examining the broad spatial relationships between land use and the urban thermal environment near the end of the study period, while potential discrepancies between the 2023 land-use patterns and actual conditions in 2024 should be acknowledged.

Table 1 Data Sources

Number	Data Name	Source and Description
1	Administrative area vector boundary data	Sourced from the National Geomatics Information Public Service Platform （https://www.tianditu.gov.cn）
2	LST	The data is sourced from the Google Earth Engine (GEE) platform. Landsat Level-2 images covering Wuhan City during the summer (May–August) were selected. （https://earthengine.google.com）
3	DEM	From the Geospatial Data Cloud Platform (https://www.gscloud.cn)
4	Population density (PD)	From the WorldPop platform (https://hub.worldpop.org)

5	NDVI	Generated from Landsat image data calculated on the GEE platform (https://earthengine.google.com)
6	NDBI	Generated from Landsat image data calculated on the GEE platform (https://earthengine.google.com)
7	Land use type	Excerpted from the China's Multi-Period Land Use Land Cover Remote Sensing Monitoring Dataset (CNLUCC) data (https://www.resdc.cn/)

III. RESEARCH METHODS

3.1 Technical Workflow

Using Landsat imagery, DEM data, population density data, land-use data, and other relevant datasets for Wuhan, this study follows the technical workflow illustrated in Figure 2. The main procedures are described below.

Step 1. Data Collection and Preprocessing

Multisource datasets for 2013, 2018, and 2024 were collected and preprocessed, including coordinate system transformation, spatial clipping, and cloud masking, as appropriate for each dataset. These procedures ensured a consistent spatial extent and compatible data formats for subsequent analyses. Landsat 8 Collection 2 Level-2 imagery was selected as the primary remote sensing data source. This product provides atmospherically corrected surface reflectance and surface temperature data, subject to the quality and availability of the respective bands.

Step 2. LST Retrieval and Cold- and Hot-Island Classification

The Landsat imagery was processed in ENVI 6.2, including clipping to the study area, application of a vector mask, and the required band-specific preprocessing. The NDVI was calculated from the red and near-infrared bands. Fractional vegetation cover and land surface emissivity were then estimated using the specified methods. LST was retrieved using the single-window algorithm, after which the resulting LST values were classified into cold- and hot-island categories according to the established classification criteria. Spatiotemporal analyses were subsequently conducted at both the city-wide and district levels to examine changes in the proportions of the different thermal categories and identify spatial variations in Wuhan's thermal environment.

Step 3. Extraction of Driving Factors

Five categories of explanatory variables were derived to investigate the factors associated with Wuhan's urban thermal environment: terrain elevation, population density, NDVI, the NDBI, and reclassified land-use categories. These variables represent topographic conditions, human activity intensity, vegetation conditions, built-up surface characteristics, and land-use patterns, respectively.

Step 4. GeoDetector Analysis

The selected explanatory variables were incorporated into the GeoDetector framework to investigate the factors associated with the spatial variation in LST. The factor detector was used to quantify the explanatory power of individual factors, while the interaction detector was applied to assess whether combinations of factors enhanced or weakened their explanatory power. The ecological detector was used to examine whether the effects of different factors differed significantly, and the risk detector was employed to identify differences in LST across the strata of each explanatory variable and to locate areas associated with relatively high temperatures. Together, these analyses were used to identify the dominant factors and their potential interactions in shaping Wuhan's urban thermal environment.

Step 5. Integration of Results

The spatiotemporal patterns of the thermal categories were integrated with the GeoDetector results to characterize the evolution of Wuhan's urban thermal environment and examine its associated driving factors. Based on these findings, targeted recommendations were

formulated to support urban thermal environment management and planning.

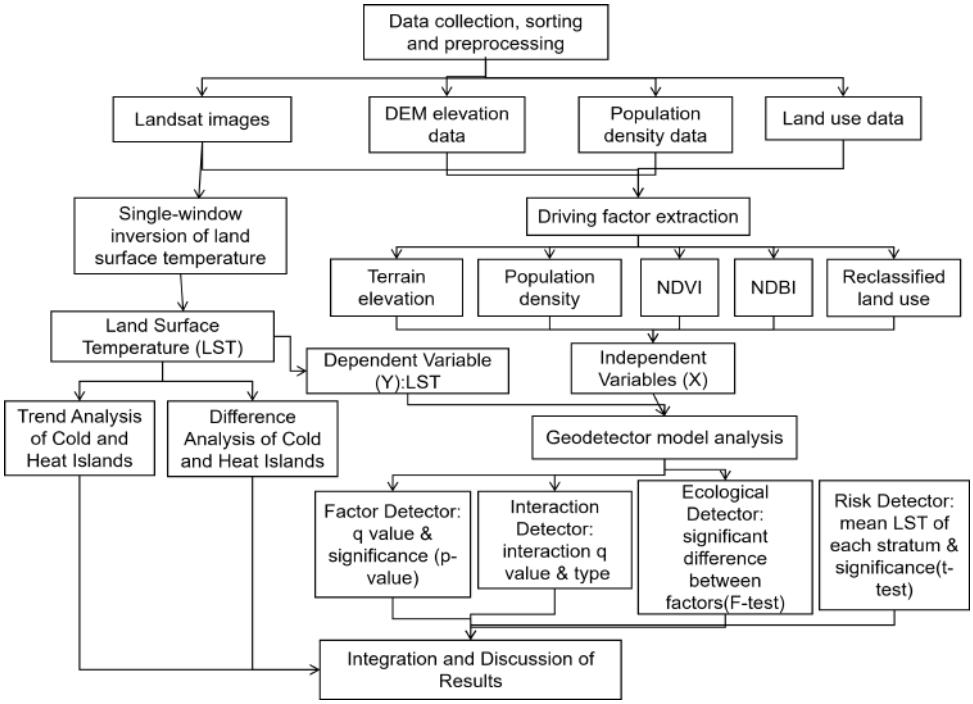


Fig.2 Technical Flowchart

3.2 Heat Island Effect Analysis

3.2.1 Normalized Difference Vegetation Index (NDVI）

NDVI can effectively reflect the surface vegetation coverage, serving as a core indicator to characterize the ecological conditions of the urban underlying surface, and also as the basis for estimating the surface emissivity. The calculation method is as follows in Formula (1):

$$\mathrm{NDVI} = \frac{\rho_{\mathrm{NIR}} - \rho_{\mathrm{RED}}}{\rho_{\mathrm{NIR}} + \rho_{\mathrm{RED}}} \qquad (1)$$

In Equation (1): ρ_{NIR} is the surface reflectance of the near-infrared band of the Landsat L2 product; ρ_{RED} is the surface reflectance of the red band. The NDVI value ranges from [-1, 1], and higher values indicate greater vegetation coverage.

3.2.2 Fractional Vegetation Cover（FVC）

FVC refers to the proportion of the vertical projection area of ground vegetation leaves to the total calculated area (Zhao et al., 2023). The calculation formula for vegetation cover degree (FVC) is constructed based on the pixel binary model and NDVI index (Sheng et al., 2023), as shown in Formula (2):

$$FVC = \frac{NDVI - NDVI_{soil}}{NDVI_{veg} - NDVI_{soil}} \qquad (2)$$

In Equation (2): $NDVI_{soil}$ is the NDVI value of bare soil areas; $NDVI_{veg}$ is the NDVI value of pure vegetation pixels. In this study, cumulative frequencies of 5% and 95% were used as the confidence interval for value selection.

3.2.3 Calculation of Surface Emissivity

Surface emissivity (ε). There is a certain mathematical relationship between surface emissivity and NDVI. When 0.157 ≤ NDVI ≤ 0.727, the calculation process of surface emissivity is as shown in Equation (3).

$$\varepsilon = 1.0094 + 0.047 \times ln(NDVI) \qquad (3)$$

If NDVI > 0.727, the corresponding land surface area is classified as 'fully vegetated area' or 'high-density vegetation area', with ε = 0.986. If NDVI < 0.157, it is either impervious surface or bare soil, which can be further distinguished using the Modified Normalized Difference

Water Index (MNDWI) as shown in Equation (4). A positive result indicates water bodies (ε = 0.995), while a negative result indicates constructed land (ε = 0.970).

$$MNDWI = \frac{p(gre) - p(swir1)}{p(gre) + p(swir1)} \quad (4)$$

In Equation (4), p(gre) represents the reflectance of the green band, and p(swir1) represents the reflectance of the middle infrared band.

This estimation method is the vegetation coverage method for extracting land surface emissivity as a accessories scheme for the single-window algorithm by Sobrino et al. (2004), which is widely used in the study of land surface temperature inversion from Landsat series satellite imagery.

3.2.4 Land Surface Temperature (LST) Retrieval

The land surface temperature (Ts) was retrieved using the single-channel method, and the retrieved results were converted from Kelvin to Celsius (Zhou et al., 2026). Formula (5) is as follows:

$$T_s = \frac{K_2}{\ln\left(\frac{K_1}{L_\lambda} + 1\right)} \quad (5)$$

$$T(℃) = T_S - 273.15$$

In Equation (5): Ts is the surface temperature (K); K_1 and K_2 are satellite calibration constants (Landsat8: K_1=774.89, K_2=1321.08).

3.2.5 Heat Island Classification

To eliminate differences in remote sensing images and land surface temperatures across different times and seasons, enhance comparability between datasets, and avoid the subjective maximum-minimum equal-interval classification method, the mean-standard deviation equal-interval method was adopted (Sui et al., 2024).

$$\bar{T} = \frac{1}{n}\sum_{i=1}^{n} T_i \quad (6)$$

$$\sigma = \sqrt{\frac{1}{n}\sum_{i=1}^{n}(T_i - \bar{T})^2} \quad (7)$$

In Equation (6): $\bar{T}$ is the average land surface temperature of the study area; n is the total number of valid land surface temperature pixels; T*i* is the land surface temperature value of the i-th pixel. In Equation (7): σ is the standard deviation of land surface temperature, representing the degree of spatial dispersion and variation of land surface temperature in the study area.

Based on the land surface temperature inversion results of three periods (2013, 2018, and 2024), the mean and standard deviation of land surface temperature for each year were calculated: in 2013, the mean $\bar{T}$=36.59∘Cand the standard deviation σ=3.54∘C; in 2018, the mean $\bar{T}$=37.60∘C and the standard deviation σ=4.48∘C; in 2024, the mean $\bar{T}$=37.89∘C and the standard deviation σ=4.29∘C. To ensure consistency for interannual comparison, the data from the three periods were integrated and calculated to obtain the overall average $\bar{T}$=37.36∘C and overall standard deviation σ=4.16∘C for the entire study period. Based on this, a unified classification standard was established to divide the study area into five temperature zones (Wang, 2025):

Strong Cold Island Zone：$T < \bar{T} - 1.5\sigma$

Cold Island Zone：$\bar{T} - 1.5\sigma \le T < \bar{T} - 0.5\sigma$

Normal Temperature Zone：$\bar{T} - 0.5\sigma \le T < \bar{T} + 0.5\sigma$

Heat Island Zone：$\bar{T} + 0.5\sigma \le T < \bar{T} + 1.5\sigma$

Strong Heat Island Zone：$T \ge \bar{T} + 1.5\sigma$

3.3 GeoDetector

GeoDetector is a spatial statistical method widely used to investigate spatial stratified heterogeneity and identify factors associated with geographical differentiation. It has two major advantages: first, it can accommodate both numerical and categorical explanatory variables, subject to appropriate data processing; second, it can assess the interaction effects of two factors on a dependent variable (Ma and Ding, 2025). The q-statistic quantifies the extent to which an explanatory variable

accounts for the spatial stratified heterogeneity of the dependent variable. Its underlying principle is based on stratification: the study area is divided into several strata according to the categories or discretized values of an explanatory variable. When the within-stratum variation is lower than the overall variation, the dependent variable exhibits spatial stratified heterogeneity. If the spatial distributions of two variables exhibit a degree of correspondence, their spatial association can be further investigated using GeoDetector.

GeoDetector comprises four components: the factor detector, interaction detector, risk detector, and ecological detector.

1. Factor detector

The factor detector quantifies the spatial stratified heterogeneity of the dependent variable Y and evaluates the explanatory power of an explanatory variable X. It produces a q-statistic, with statistical significance assessed where applicable. A larger q-value indicates that the spatial stratification defined by X accounts for a greater proportion of the spatial stratified heterogeneity of Y. For example, (q = 0.75) indicates that the stratification associated with X accounts for 75% of the spatial stratified heterogeneity of Y, according to the GeoDetector formulation.

2. Interaction detector

The interaction detector assesses whether the combined effect of two explanatory variables, X1 and X2, enhances or weakens their individual explanatory power with respect to Y. Specifically, it calculates the individual q-statistics, q(X1) and q(X2)), and the q-statistic for the overlay strata formed by X1 and X2, denoted as X1∩X2. The interaction type is then identified by comparing the combined q-statistic with the individual q-statistics and their sum.

The five commonly used interaction types are defined as follows:

(1)Nonlinear weakening: q(X1∩X2) < Min(q(X1), q(X2))

(2)Univariate weakening: Min (q(X1), q(X2)) < q(X1∩X2) < Max(q(X1), q(X2))

(3)Bivariate enhancement: q(X1∩X2) > Max(q(X1), q(X2))

(4)Independence: q(X1∩X2) = q(X1) + q(X2)

(5)Nonlinear enhancement: q(X1∩X2) > q(X1) + q(X2)

3. **Risk detector,** used to determine whether there is a statistically significant difference in the mean of the dependent variable Y between different sub-regions (i.e., different categories or partitions). Its statistic is given by Equation (8):

$$t = \frac{\bar{Y}_{h=1} - \bar{Y}_{h=2}}{\left[\frac{V_{ar}(\bar{Y}_{h=1})}{n_{h=1}} + \frac{V_{ar}(\bar{Y}_h = 2)}{n_{h=2}}\right]^{1/2}} \quad (8)$$

where $\bar{Y}_h$ is the mean of sub-region h, n_h is the sample size, and V_{ar} is the variance. This statistic approximately follows a t-distribution. The output results provide significance judgments for pairwise comparisons of sub-region means (e.g., "Y" indicates a significant difference, "N" indicates no significant difference), thereby identifying high-risk or high-value areas.

4. Ecological detector, used to compare whether the impacts of two independent variables X1 and X2 on the spatial distribution of the dependent variable Y are significantly different. The output results are displayed in a matrix format, with rows and columns representing different independent variables. Each cell in the matrix displays "Y" or "N". "Y" indicates that at the 0.05 significance level, the effects of the two independent variables corresponding to that row and column on the spatial distribution of Y are significantly different. "N" indicates no significant difference between the effects of the two independent variables. Its statistic is given by Equation (9):

$$F = \frac{N_{x_1}(N_{x_2} - 1)SSW_{x_1}}{N_{x_2}(N_{x_1} - 1)SSW_{x_2}} \quad (9)$$

where SSW_{X1} and SSW_{X2} are the sums of within-layer variances for the strata formed by x1 and x2, respectively, and N_{X1} and N_{X2} are the sample sizes. If the null hypothesis SSW_{X1}=SSW_{X2} is rejected at a given significance level, it is considered that the effects of the two factors on Y are significantly different. (Wang and Xu, 2017)

IV. RESULTS AND ANALYSIS

4.1 Land Surface Temperature Retrieval and Spatiotemporal Analysis

Based on the LST retrieval results for 2013, 2018, and 2024, a consistent classification scheme was applied to generate heat- and cold-island maps (Figures 3–5). In conjunction with administrative boundary data, the results were analyzed in terms of spatial patterns and temporal evolution to characterize the spatiotemporal dynamics of Wuhan's urban thermal environment.

4.1.1 Spatial Patterns of Heat and Cold Islands

Wuhan's thermal environment exhibited a relatively stable center–periphery pattern. Strong heat-island areas were concentrated in the traditional central urban districts along the Yangtze River and Han River, particularly Hankou, Wuchang, and Hanyang. These areas largely coincided with densely built-up areas and zones of intensive human activity. In contrast, strong cold-island areas were consistently observed near woodland areas in northern Huangpi District, extensive lake systems in southern Jiangxia District, and water bodies within the central urban area, including East Lake. These spatial patterns highlight the cooling role of major ecological land covers in Wuhan's thermal environment.

The main channels of the Yangtze River and Han River also formed prominent linear cooling corridors that spatially separated and moderated heat-island areas along their banks. Together, these urbanized areas, ecological land covers, and major water bodies constituted important structural elements of Wuhan's thermal environment throughout the study period.

4.1.2 Temporal Evolution of Heat and Cold Islands

From 2013 to 2024, heat-island areas expanded outward from the urban core and increased in intensity, whereas cold-island areas decreased overall and became increasingly fragmented.

2013: Strong heat-island areas were concentrated in central urban districts, including Jianghan, Qiaokou, and Wuchang, accounting for 6.1% of the study area. These areas were relatively compact and had clearly defined boundaries. Normal-temperature areas predominated in the suburban zones, while the overall ecological landscape remained relatively intact. In the outer suburbs, particularly Huangpi, Xinzhou, and Caidian, cold-island areas formed relatively extensive and contiguous patches, with clear spatial contrasts between hot and cold zones.

2018: Strong heat-island areas in the central urban area became denser and coalesced into larger patches, with their proportion increasing to 6.7%. Meanwhile, normal-temperature areas declined. Heat-island patches extended beyond the central urban area into nearby suburban districts, including Dongxihu, Hongshan, and Jiangxia. In the outer suburbs, some cold-island areas decreased in extent, and signs of spatial fragmentation became increasingly apparent.

2024: Strong heat-island areas in the central urban area became more spatially continuous, with their proportion increasing markedly to 11.4%. Normal-temperature areas declined substantially. In the near suburbs, individual heat-island patches merged and became increasingly connected to the main urban heat-island belt. Meanwhile, numerous small, localized heat-island patches emerged in built-up areas associated with towns and industrial parks in the outer suburbs, disrupting the previously more contiguous distribution of cold-island areas. The proportion of cold-island areas decreased to 26.6%, accompanied by a marked increase in their spatial dispersion and fragmentation.

Overall, the results indicate that heat-island areas expanded outward from the urban core and intensified between 2013 and 2024, while cold-island areas decreased in extent and became more fragmented. Urban expansion and the associated conversion of natural or semi-natural land covers to artificial surfaces likely contributed to these changes. The spatial evolution of the thermal environment also exhibited a distinct center–periphery gradient: the central urban area was characterized primarily by increasing heat-island intensity, the near suburbs experienced the most pronounced contiguous expansion of heat-island areas, and the outer suburbs showed the

emergence of localized heat-island patches alongside increasing fragmentation of cold-island areas.

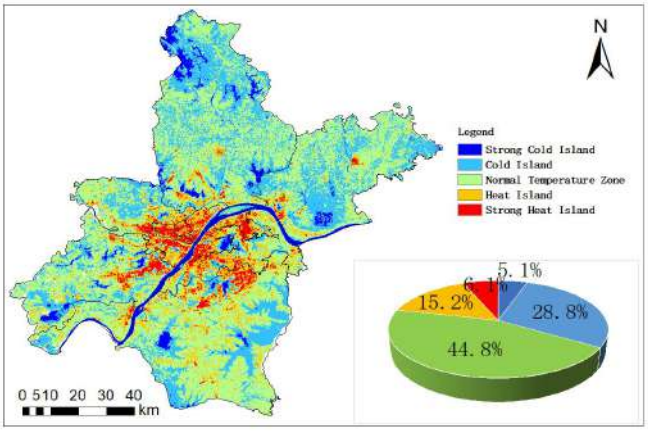


Fig.3 Classification map of heat and cold islands in Wuhan City, 2013

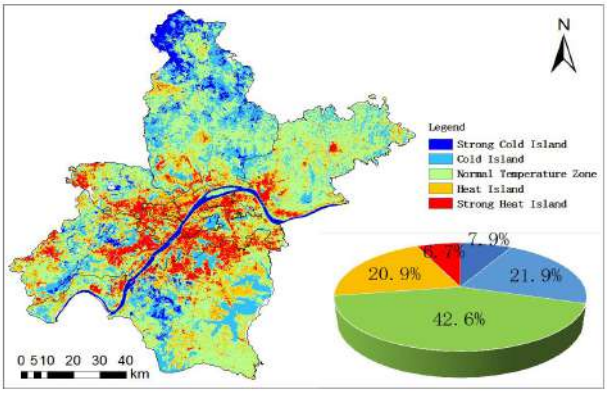


Fig.4 Classification map of heat and cold islands in Wuhan City, 2018

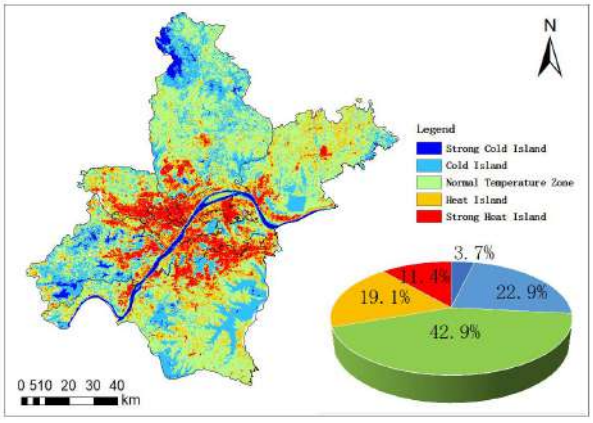


Fig.5 Classification map of heat and cold islands in Wuhan City, 2024

4.1.3 Trends in Heat- and Cold-Island Areas across the Study Region

Based on the LST retrieval results, the proportions of heat-island and cold-island areas were statistically analyzed for each administrative district (Figure 6). The results show that, from 2013 to 2024, the proportion of heat-island areas in Wuhan increased from 43.98% to 54.17%, representing a rise of 10.19 percentage points. Linear regression analysis revealed a strong positive temporal trend ($R^2 = 0.9146$). In contrast, the proportion of cold-island areas decreased from 24.81% to 19.96%, a decline of 4.85 percentage points. This decrease was most pronounced between 2013 and 2018, after which the declining trend became less pronounced. Overall, heat-island areas exhibited a clear increasing trend, whereas cold-island areas showed a decreasing trend ($R^2 = 0.6754$). These findings quantitatively support the observed expansion and increasing aggregation of heat-island areas, alongside the overall contraction and fragmentation of cold-island areas.

This pattern suggests deterioration in Wuhan's urban thermal environment associated with the increasing artificialization of land surfaces. The opposing trends in heat-island and cold-island areas further suggest that the encroachment of urban development on ecological spaces, particularly green spaces and water bodies, may have contributed to the intensification of the urban heat-island effect in Wuhan.

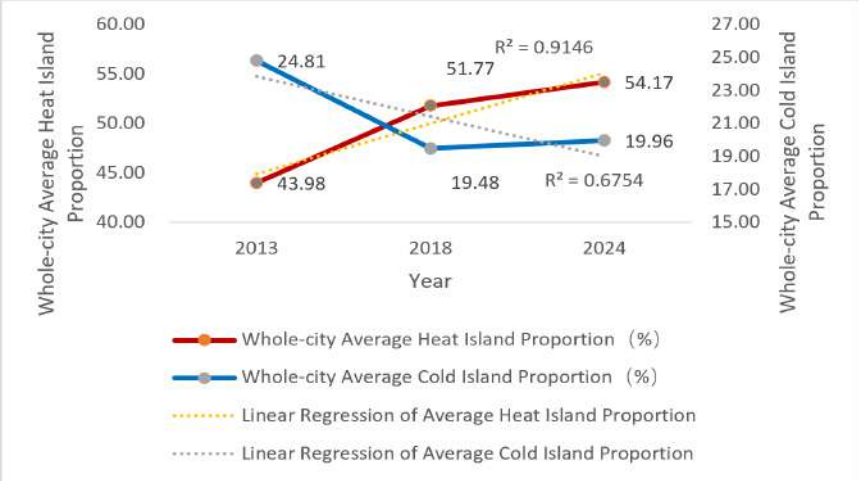


Fig.6 Trends in the areal proportion of heat islands and cold islands, 2013–2024

Pronounced spatial differences in the proportion of heat-island areas were observed among Wuhan's administrative districts, exhibiting a distinct spatial gradient characterized by higher proportions in the central urban area and lower proportions in the outer suburban areas (Figure 7). In 2024, the proportions of heat-island areas in Jianghan and Qiaokou districts both exceeded 90%, indicating that these districts were among the areas most severely affected by the urban heat-island effect. In contrast, the corresponding proportions in Huangpi and Xinzhou districts were below 30%, substantially lower than those in the central urban area.

From 2013 to 2024, the proportion of heat-island areas increased in all administrative districts, although the magnitude of the increase varied considerably across the urban–suburban gradient. Hongshan and Dongxihu districts exhibited the most pronounced increases, suggesting that the near suburbs have become key areas of urban warming associated with outward urban expansion. In the central districts of Jianghan and Qiaokou, where urban development is relatively mature and built-up areas are highly concentrated, the proportions of heat-island areas remained consistently high, with comparatively modest increases over the study period. Extensive commercial and residential development, dense road networks, and impervious surfaces, combined with multiple sources of anthropogenic heat, may contribute to the persistently high heat-island proportions in these districts.

In Qingshan District, the concentration of heavy industry, particularly the Wuhan Iron and Steel Corporation, provides a potential source of sustained anthropogenic heat emissions that may contribute to the gradual intensification of the local heat-island effect. Meanwhile, Hongshan District, particularly the Optics Valley area, and Hanyang District, including the Zhuankou Economic and Technological Development Zone, have experienced continued expansion of industrial parks and residential areas over the past decade. The rapid expansion of impervious surfaces in these areas may have contributed substantially to the increase in the proportion of heat-island areas. In outer suburban districts such as Huangpi and Jiangxia, new-town development and associated land-use changes, including the conversion of farmland and small water bodies to built-up land, may also have contributed to the expansion of heat-island areas. In Caidian District, ecological protection and development restrictions around Houguan Lake may have helped limit the increase in heat-island areas by preserving the lake's cooling function and surrounding ecological spaces.

Overall, the spatial distribution of heat-island areas in Wuhan closely corresponds to the distribution of built-up land. The extensive impervious surfaces and concentrated human activities in the central urban area are likely to be

important factors associated with the prevalence of heat-island conditions, while continued urban expansion in the suburbs may be contributing to the outward spread of heat-island areas.

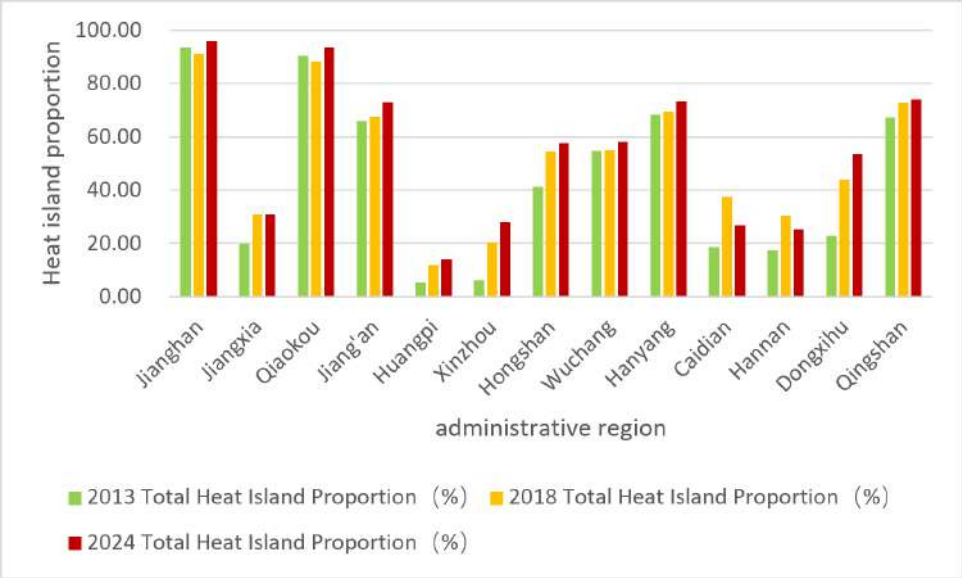


Fig.7 Changes in the proportion of heat islands in each administrative region, 2013–2024

The spatial distribution of cold-island areas in Wuhan exhibits a pattern of concentration in the outer suburbs and scarcity in the central urban area, contrasting markedly with the distribution of heat-island areas (Figure 8). In 2024, the proportions of cold-island areas in Huangpi and Jiangxia districts exceeded 20%, identifying them as major cold-island zones. In contrast, the corresponding proportions in Jianghan and Qiaokou districts were below 5%, indicating a severe scarcity of cooling spaces. In the older inner-city areas, the historical infilling of rivers and lakes, the high proportion of impervious surfaces, and the scarcity of large, contiguous green spaces have limited the availability of cooling areas. Dense street networks may also impede ventilation, while anthropogenic heat from commercial, residential, and industrial activities further intensifies local thermal stress. Moreover, the high degree of built-up development restricts opportunities to establish large-scale blue–green spaces (Li et al., 2026).

From 2013 to 2024, the proportion of cold-island areas declined in most administrative districts, with particularly pronounced decreases in Huangpi and Jiangxia. Despite their extensive natural woodlands, agricultural land, and lakes, including Tangxun Lake, these districts have experienced rapid urbanization. Encroachment on lakeside buffer zones and small suburban water bodies has fragmented contiguous blue–green spaces, contributing to the substantial contraction of cold-island areas (Ren, 2024). These changes suggest that urban expansion has placed considerable pressure on suburban cooling spaces, weakening their thermal-regulation functions. In Hongshan and Hanyang districts, large water bodies such as East Lake and Moshui Lake remain important cooling resources; however, continued encroachment of built-up land on surrounding green spaces may have reduced the extent of their cooling influence, contributing to the gradual decline in cold-island areas. By contrast, ecological conservation and lakeside restoration around Houguan Lake in Caidian District have supported the recovery of ecological land, accompanied by an increase in the proportion of cold-island areas. Overall, the spatial and temporal contraction of cold-island areas broadly coincides with the intensification of the urban heat-island effect, suggesting that the loss of cooling spaces may have contributed to the deterioration of Wuhan's urban thermal environment.

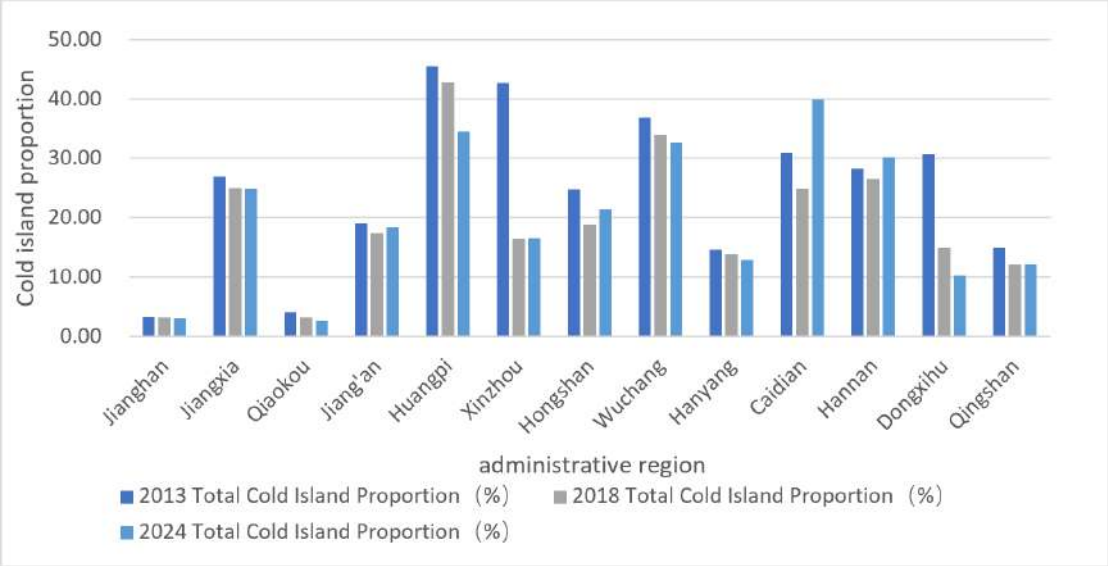


Fig.8 Changes in the proportion of cold islands in each administrative region, 2013–2024

The combined analysis of spatial imagery and administrative-district proportions reveals distinct zonal gradients in the evolution of urban heat and cold islands. Development in the central urban core has largely reached saturation, leaving limited scope for large-scale outward expansion. Consequently, changes in this zone are characterized primarily by increasing heat island intensity and the continued contraction of internal cold-island patches. The overall heat–cold island configuration remains relatively stable, although urban renewal contributes to localized warming. The inner suburbs constitute the principal zone of urban expansion and heat island growth, experiencing the most rapid urbanization and industrialization. The substantial increase in impervious surface coverage has led to a sharp decline in cold islands and the contiguous expansion of heat islands, making this zone the most dynamic in terms of thermal landscape change. In the outer urban districts, cold islands remain the dominant landscape component. However, industrial spillover, transportation infrastructure development, and township expansion have driven the emergence of isolated heat islands and their localized spread, indicating a later stage of thermal landscape transformation. Meanwhile, contiguous cold-island areas have gradually fragmented into scattered patches.

Overall, heat island expansion in Wuhan from 2013 to 2024 followed a clear spatial gradient of inner suburbs > outer urban districts > central urban core, closely corresponding to the city's concentric urban expansion pattern. In contrast, cold-island areas generally exhibited contraction and fragmentation, particularly in the inner and outer suburbs. The persistent loss of cold islands has not only weakened regional ecological regulation capacity but also exacerbated intra-urban thermal environmental disparities. These spatiotemporal patterns provide an empirical basis for further investigating the relationship between urban spatial structure and thermal environmental effects, as well as for developing targeted ecological planning strategies.

4.2 Driving Factors of the Urban Heat Island Effect

4.2.1 Factor Detector Results

The factor detector was used to quantify the independent explanatory power (q-value) of each driving factor for the spatial differentiation of the urban heat island effect. The results showed that, in 2013, the factors ranked in descending order of explanatory power were NDBI > NDVI > population density > land use type > elevation. NDBI exhibited the highest q-value, indicating that it was the dominant independent explanatory factor for the urban heat island effect in that year. This finding suggests that

the expansion of built-up areas played a critical role in shaping the spatial variation in land surface temperature (LST). NDVI ranked second, highlighting the significant role of vegetation cover in regulating LST. Population density and land use type demonstrated moderate explanatory power, whereas elevation had an extremely low q-value, suggesting limited independent explanatory power for the spatial differentiation of the heat island effect (Figure 9).

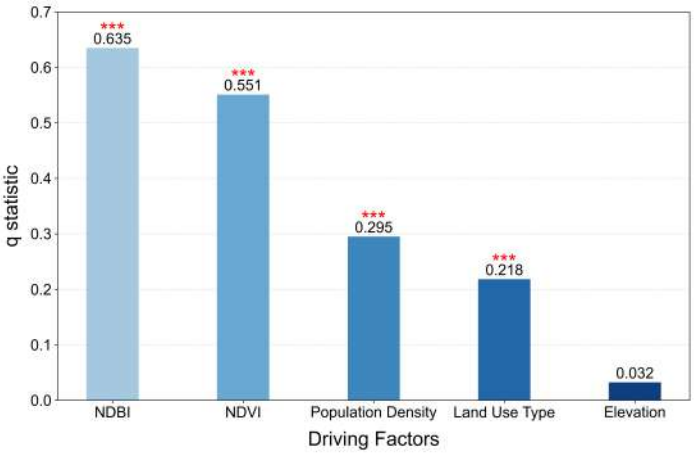


Fig.9 Results of the factor detector in 2013

*** indicates significance at the $p < 0.001$ level

In 2018, the independent explanatory power of all driving factors decreased substantially compared with 2013. The factors ranked in descending order of q-values were NDBI > NDVI > land use type > population density > elevation. NDBI and NDVI remained the two most influential factors in terms of explanatory power, although their q-values decreased by 0.190 and 0.135, respectively, relative to 2013. These declines may reflect, in part, the effects of urban ecological restoration and green space development, which may have altered the relationships between built-up land, vegetation cover, and the spatial differentiation of the heat island effect. The explanatory power of land use type and population density also declined, indicating their limited independent explanatory capacity. The q-value for elevation increased slightly to 0.054 but remained substantially lower than those of the other factors, suggesting that elevation had limited independent explanatory power for the spatial differentiation of the heat island effect (Figure 10)

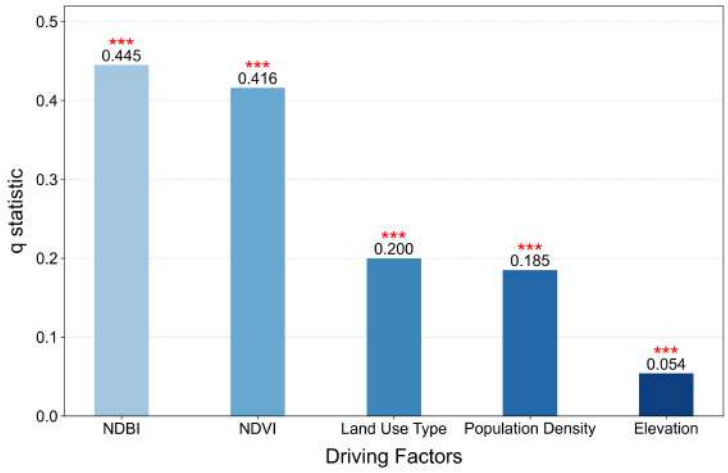


Fig.10 Results of the factor detector in 2018

*** indicates significance at the $p < 0.001$ level

In 2024, the independent explanatory power of the driving factors rebounded compared with 2018. The factors ranked in descending order of q-values were NDBI > NDVI > land use type > population density > elevation. The q-values of NDBI (0.528) and NDVI (0.451) increased markedly relative to 2018, with NDBI exhibiting the greater increase. This suggests that accelerating urban development may have strengthened the independent explanatory power of built-up land expansion for the spatial differentiation of the heat island effect. The q-values of land use type (0.296) and population density (0.248) also increased substantially, indicating a potential strengthening of the associations between human activities, land use patterns, and the heat island effect. In contrast, the q-value of elevation declined to 0.027, the lowest level observed over the three study years, indicating that elevation had consistently limited independent explanatory power for the spatial differentiation of the heat island effect (Figure 11).

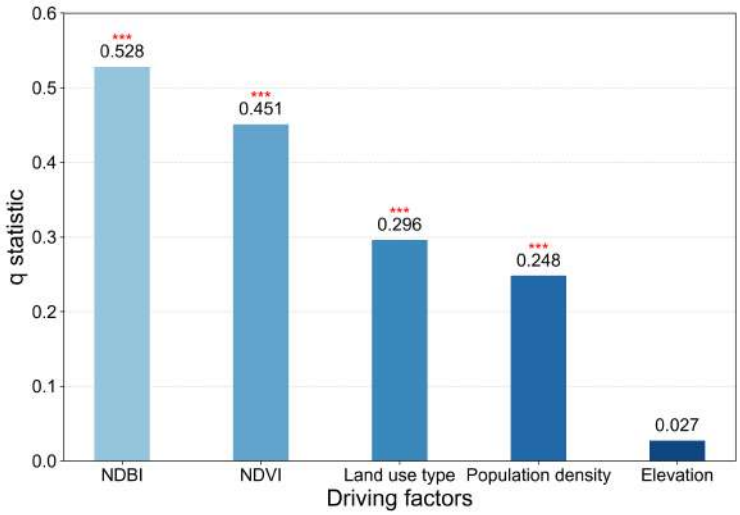


Fig.11 Results of the factor detector in 2024

*** indicates significance at the $p < 0.001$ level

The comprehensive factor detection results indicate that NDBI consistently exhibited the highest explanatory power from 2013 to 2024, followed by NDVI. The q-values of these two factors were substantially higher than those of the other factors, suggesting that built-up land expansion and changes in vegetation cover were the primary independent explanatory factors associated with the urban heat island effect in Wuhan. Overall, the q-values of the driving factors followed a pattern of decline from 2013 to 2018, followed by a rebound in 2024. This temporal variation may reflect the changing influences of urban development and ecological regulation measures across different stages of urbanization. The q-value of elevation remained below 0.06 in all three study years, indicating limited independent explanatory power for the spatial differentiation of the heat island effect. Furthermore, anthropogenic factors, including NDBI, NDVI, population density, and land use type, generally exhibited greater explanatory power than elevation, highlighting the prominent role of human activities in shaping Wuhan's urban heat island

4.2.2 Interaction Detector Results

Interaction detection examines whether the combined effects of two driving factors enhance or weaken their explanatory power for the spatial differentiation of the dependent variable (Chen and Zhong, 2024). The results show that, from 2013 to 2024, all pairs of driving factors exhibited two-factor enhancement, with neither independent nor nonlinear weakening detected. The explanatory power of factor interactions was consistently greater than that of individual factors, highlighting the importance of multifactor interactions in explaining the spatial differentiation of the urban heat island effect. The

interaction patterns varied across the study years, reflecting potential changes associated with different stages of urban development.

In 2013, the q-values of factor interactions ranged from 0.032 to 0.771, representing the highest overall interaction strength among the three study years. The interaction between NDBI and NDVI exhibited the highest explanatory power (q = 0.771), suggesting that the combined effects of built-up land expansion and vegetation cover changes were closely associated with the spatial differentiation of the heat island effect. Furthermore, the interactions between NDBI and population density (q = 0.674), NDBI and land use type (q = 0.679), and NDVI and population density (q = 0.661) all had q-values exceeding 0.65. These results highlight the strong combined explanatory power of urban development intensity, population distribution, and land surface characteristics. By contrast, elevation exhibited relatively low explanatory power both independently and in interaction with other factors, indicating its limited contribution to explaining the spatial differentiation of the heat island effect (Figure 12).

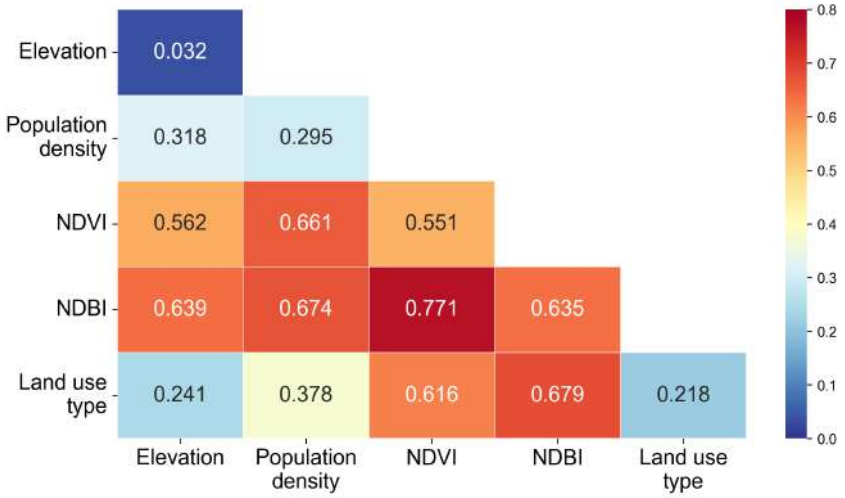


Fig.12 Heatmap of the interaction detector results for LST driving factors in 2013

In 2018, the q-values of factor interactions ranged from 0.054 to 0.593, indicating an overall decline in interaction strength compared with 2013. Although the interaction between NDBI and NDVI remained the strongest (q = 0.593), its q-value decreased by 0.178 relative to 2013. This decline may be associated with the implementation of ecological management measures, including urban green space development, which may have moderated the combined effects of built-up land expansion and vegetation cover changes on the urban heat island effect. Meanwhile, the interactions between NDBI and land use type (q = 0.501) and between NDVI and population density (q = 0.493) continued to exhibit relatively high explanatory power. These results highlight the persistent importance of interactions among urban development, population distribution, and land surface characteristics in explaining the spatial differentiation of the heat island effect. By contrast, elevation-related effects remained relatively weak (Figure 13).

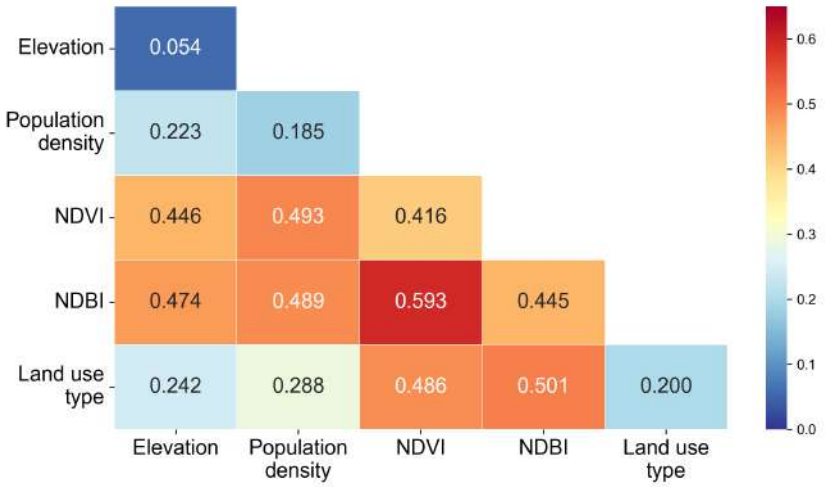


Fig.13 Heatmap of the interaction detector results for LST driving factors in 2018

In 2024, the q-values of factor interactions ranged from 0.027 to 0.674, indicating an overall rebound in interaction strength compared with 2018. The interaction between NDBI and NDVI remained dominant (q = 0.674), increasing by 0.081 relative to 2018. This increase may reflect the renewed intensification of competition between built-up land expansion and vegetation space amid accelerated urban development. Meanwhile, the q-values for the interactions between NDBI and population density (q = 0.594) and between NDBI and land use type (q = 0.613) also increased substantially, highlighting the combined explanatory power of human activity intensity and built-up land expansion. By contrast, the independent explanatory power of elevation reached its lowest level over the three study years, while its interactions with other factors remained relatively weak (Figure 14).

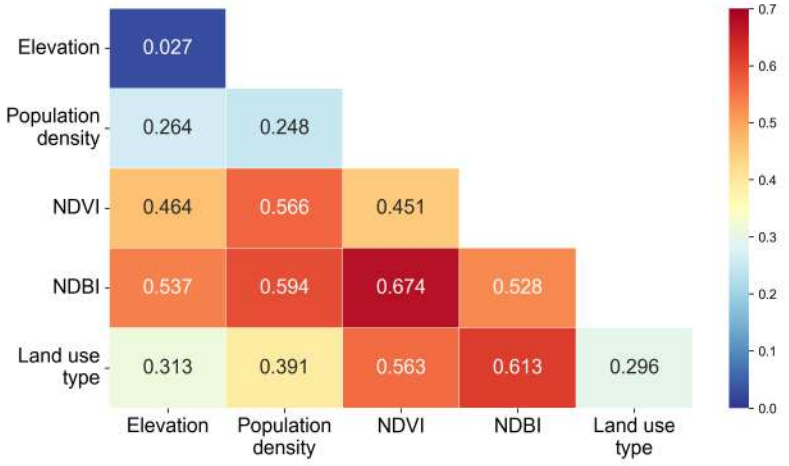


Fig.14 Heatmap of the interaction detector results for LST driving factors in 2024

The comprehensive interaction detection results for the three study years indicate that the interaction between NDBI and NDVI consistently exhibited the highest explanatory power from 2013 to 2024, highlighting the importance of the combined effects of built-up land expansion and vegetation cover changes in shaping Wuhan's urban heat island patterns. The interaction strength followed a pattern of high values in 2013, a decline in 2018, and a rebound in 2024. This temporal variation may be associated with changes in urban development and ecological management measures. All factor pairs exhibited two-factor enhancement, indicating

that the spatial differentiation of the heat island effect is better explained by interactions among multiple factors than by individual factors alone. In contrast, the independent and interactive explanatory power of elevation remained consistently low, suggesting that it was not a dominant factor in explaining the spatial differentiation of Wuhan's urban heat island effect.

4.2.3 Results of the Ecological Detector

The ecological detector was used to assess whether significant differences existed between the effects of different driving factors on the spatial differentiation of the urban heat island effect. The results are summarized as follows.

In 2013, all pairs of driving factors exhibited significant differences (Y), with no nonsignificant pairs identified. This indicates that the effects of elevation, population density, NDVI, NDBI, and land use type differed significantly in their explanatory power for the spatial differentiation of the heat island effect.

In 2018, significant differences persisted for most factor pairs (Y), whereas the pair of population density and land use type showed no significant difference (N). This result suggests that these two factors had statistically indistinguishable effects on the spatial differentiation of the heat island effect during this period. The remaining factor pairs continued to exhibit significant differences, indicating that their relative explanatory effects remained distinguishable.

In 2024, all pairs of driving factors again exhibited significant differences (Y), with no nonsignificant pairs identified. This suggests that the effects of population density and land use type became statistically distinguishable again. Overall, the ecological detector results reveal temporal variation in the differences between the explanatory effects of individual factors, with only population density and land use type showing no significant difference in 2018 (Figure 15).

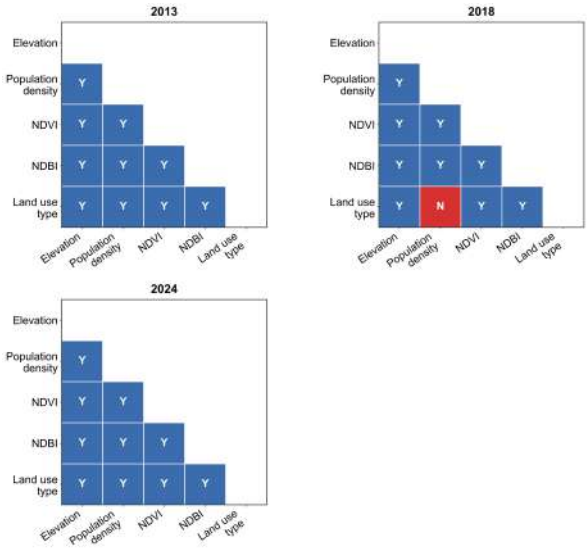


Fig.15 Results of the Ecological Detector for 2013, 2018, and 2024

Overall, from 2013 to 2024, the differences in the effects of most factors were significant, indicating that the driving factors of the urban heat island effect in Wuhan had differentiated influence mechanisms overall, with no universal substitutable relationship. The periodic convergence of population density and land use type in 2018 may be related to the coordinated adjustment of urban population distribution and land use structure during that period. From the perspective of long-term evolution trends, the differences in the effects of various driving factors remained predominantly significant, suggesting that different factors play irreplaceable roles in the formation of the urban heat island effect.

4.2.4 Results of the Risk Detector

The risk detector was used to examine the gradient differentiation in the effects of various driving factors on the UHI effect by comparing LST across different risk levels (Figures 16–18).

NDBI was positively associated with LST. Mean LST increased progressively with increasing NDBI risk levels. The boxplots exhibited a clear stepwise increase, with limited overlap between boxes, indicating pronounced temperature differences across risk levels. The largest temperature increase occurred at high-risk levels, and LST in Level 5 areas in 2024 was notably higher than in the previous two periods. These findings suggest that the association between built-up land and elevated LST was particularly pronounced in high-risk areas and became stronger over time.

NDVI was negatively associated with LST. The boxplots showed a clear downward trend across NDVI levels, indicating the cooling effect associated with greater vegetation cover. LST was lowest in low-risk areas, with a particularly evident cooling pattern in low-to-moderate-risk areas.

Population density was positively associated with LST, which increased with rising risk levels. However, substantial overlap between the boxes at Levels 4 and 5 suggests that temperature differences became less distinct at higher population-density levels. The temperature response was more evident at moderate-to-high risk levels, while LST in high-risk areas was higher in 2024 than in the previous two periods. This pattern indicates a stronger association between population density and elevated LST in high-risk areas.

Land use type was positively associated with LST. Areas dominated by built-up land exhibited the highest temperatures and heat island risk. However, considerable overlap among the boxes indicates substantial within-category heterogeneity, potentially reflecting differences in vegetation cover, building density, and other local characteristics.

Elevation was negatively associated with LST. Mean LST declined progressively across increasing elevation-related risk levels, highlighting the role of topography in spatial variations in the thermal environment. This pattern remained consistent across all three periods, suggesting a persistent association between elevation and lower LST.

Overall, NDBI, population density, and land use type were positively associated with LST, whereas NDVI and elevation were negatively associated with it. The relationships varied across risk levels: positive associations were more pronounced in high-risk areas, while the cooling association of vegetation was particularly evident in low-to-moderate-risk areas. From 2013 to 2024, the association between NDBI and elevated LST strengthened, whereas the cooling association of NDVI remained relatively stable. These findings highlight the importance of managing built-up land expansion and maintaining vegetation cover in mitigating Wuhan's UHI effect.

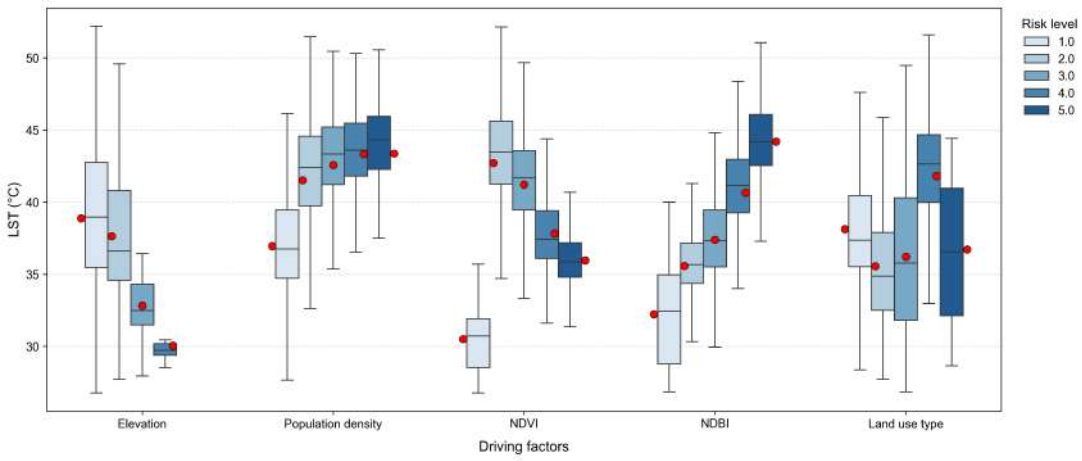


Fig.16 Risk detector results for the factors influencing LST in 2013

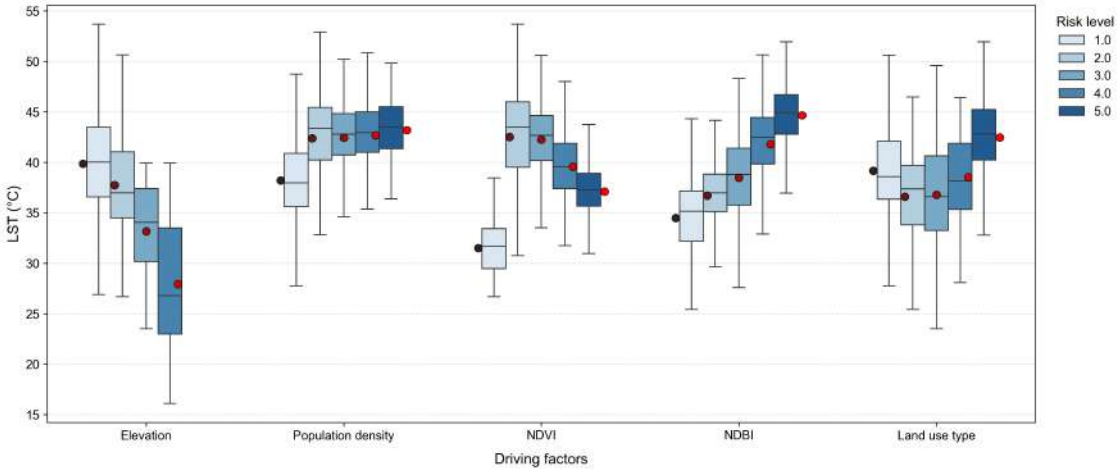


Fig.17 Risk detector results for the factors influencing LST in 2018

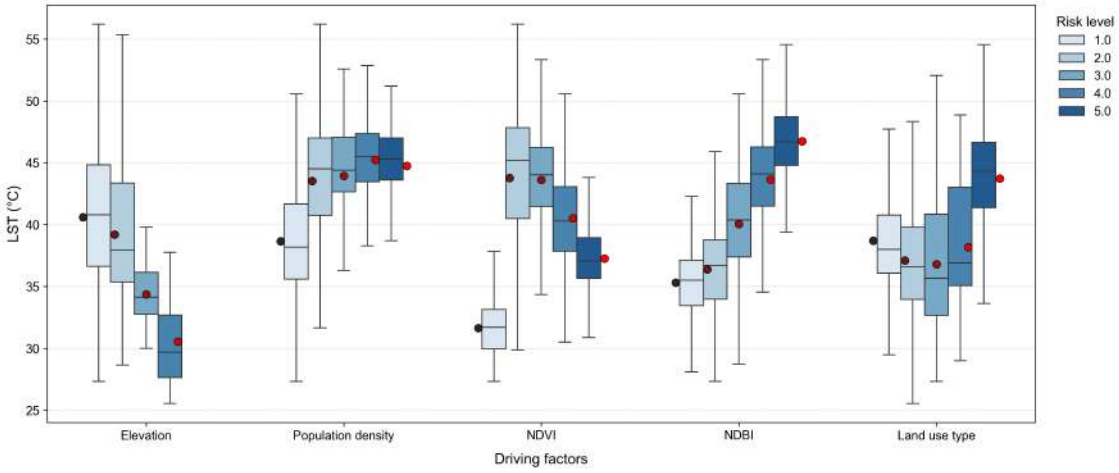


Fig.18 Risk detector results for the factors influencing LST in 2024

The UHI effect in Wuhan reflects the combined influence of human activities and multiple interacting factors. The trade-off between built-up land expansion and vegetation degradation represents a key tension in its long-term evolution. From 2013 to 2024, NDBI and NDVI exhibited the strongest interaction in explaining UHI spatial differentiation. The interaction intensity fluctuated over time, whereas topographic influence remained relatively weak. All factor pairs exhibited two-factor enhancement, with no independent effects detected. Ecological detection revealed significant differences in explanatory power between most factor pairs, except for population density and land use type in 2018. Risk detection further indicated that built-up land expansion and population agglomeration were associated with higher LST, whereas vegetation cover and elevation were associated with lower LST.

Accordingly, the following measures are recommended: (1) control disorderly urban expansion, promote compact development, and limit the warming associated with built-up land; (2) increase urban vegetation cover, establish ventilation corridors and ecological buffer zones, and strengthen vegetation-related cooling; (3) alleviate population pressure in urban cores and improve the equitable distribution of public services; and (4) prioritize high-risk areas through measures such as permeable pavements and green buildings, while protecting ecological resources in low-risk areas.

V. CONCLUSION

This study investigated the spatiotemporal evolution of the UHI effect in Wuhan in 2013, 2018, and 2024 using Landsat imagery and multisource auxiliary data. LST was retrieved and analyzed, and the geographical detector model was employed to examine the factors associated with its spatial differentiation. The main conclusions are as follows.

(1) From 2013 to 2024, the UHI effect in Wuhan intensified, exhibiting a broadly concentric spatial pattern characterized by strong heat islands in the urban core and shrinking cold-island areas toward the periphery. The proportion of heat-island areas increased from 43.98% to 54.17%, while that of cold-island areas declined from 24.81% to 19.96%. Strong heat islands formed contiguous patches in the central urban area, while the most pronounced expansion occurred in the inner suburbs. Cold-island areas in the outer suburbs became increasingly fragmented, indicating outward diffusion of the UHI effect from the urban core toward the inner suburbs.

(2) Underlying surface characteristics were strongly associated with UHI differentiation. NDBI and NDVI consistently exhibited the highest single-factor explanatory power, highlighting the importance of built-up land and vegetation cover. Population density and land use type had comparatively weaker explanatory power, while elevation had the weakest influence. These findings underscore the importance of urban development and vegetation changes in shaping the spatial distribution of LST.

(3) Interactions among all examined factors enhanced their explanatory power, indicating a synergistic pattern of influence involving anthropogenic and natural factors. The NDBI–NDVI interaction had the strongest explanatory power, highlighting the combined relevance of built-up land expansion and vegetation conditions to UHI differentiation. Land use types also exhibited contrasting thermal characteristics: built-up and industrial areas were associated with higher temperatures, whereas forests and water bodies generally provided cooler environments.

(4) UHI evolution was closely associated with urban expansion, industrial development, and changes in ecological land. Extensive impervious surfaces in the central urban area were associated with persistent strong heat islands, while expansion in the outer suburbs may be linked to new-town development, transport infrastructure, and agricultural land conversion. Vegetation cover, urban green spaces, and water bodies played important roles in moderating local temperatures. These findings suggest that UHI mitigation requires an integrated approach, including increasing vegetation cover in built-up areas, protecting wetlands and other ecological spaces, and establishing ecological green corridors between major heat-island clusters to limit their further coalescence (Wang and Gao, 2026).

REFERENCES

[1] Liang, Y., Chen, Z., and Xia, Z. Decadal Evolution and Mechanism of the Urban Heat Island Effect in Wuhan Based on RS and GIS. Resources and Environment in the Yangtze Basin, 2010, 19(08): 914-918.

[2] Li, A. Remote Sensing Analysis of Urban Heat Island Effect in Mianyang City Based on RS. Anhui Agricultural Science Bulletin, 2013, 19(13): 143-148. DOI: 10.16377/j.cnki.issn1007-7731.2013.13.010.

[3] Ma, X., and Ding, H. Study on Spatiotemporal Evolution Characteristics and Driving Mechanism of Thermal Environment in Historical Urban Areas: A Case of Ming City Wall Area in Xi'an. In: China Urban Planning Society, Shenyang Municipal People's Government. Toward Chinese-Style Modernization: Value and Action of Planning—Proceedings of 2025 China Annual Conference on Urban Planning (09 Urban Ecological Planning). School of Architecture, Chang'an University, 2025: 666-680. DOI: 10.26914/c.cnkihy.2025.046698.

[4] Wang, Z. X., and Gao, W. Analysis of Heat Island Effect in Tianjin Based on Surface Temperature Inversion and Geodetector Model. Journal of Atmospheric and Environmental Optics, 2026, 21(02): 330-342.

[5] Zhao, Q., Tan, L., Fang, Q. S., et al. Analysis of Spatiotemporal Evolution and Influencing Factors of Heat Island Effect in Hefei Based on Satellite Data. Journal of Atmospheric and Environmental Optics, 2023, 18(02): 153-167.

[6] Sui, J. M., Jia, G. M., Tian, N., et al. Analysis on Change and Influencing Factors of Urban Heat Island Effect in Baoding Based on Landsat Images. Inner Mongolia Science Technology & Economy, 2024, (13): 101-104+109.

[7] Sheng, L. L., Hao, S., Cui, Y. H., et al. Influence of Urban Development on Surface Heat Island Effect and Its Relationship: A Case of Hefei and Nanchang. Journal of Atmospheric and Environmental Optics, 2023, 18(06): 602-616.

[8] Wang, J. F., and Xu, C. D. Geodetector: Principle and Prospective. Acta Geographica Sinica, 2017, 72(01): 116-134.

[9] Wang, Y. N. Research on Urban Heat Island Effect Analysis Based on Remote Sensing Images. Geomatics & Spatial Information Technology, 2025, 48(05): 75-77.

[10] Zhou, X. S., Zhang, Y. S., and Huang, Q. H. Study on Factors of Urban Local Climate Zone Heat Island Intensity Based on Geodetector. Journal of Hebei Normal University (Natural Science Edition): 1-17. https://doi.org/10.13763/j.cnki.jhebnu.nse.202605001.

[11] Chen, P. H., and Zhong, K. W. The Impact of Urban Land Use Changes on the Urban Heat Island Effect: A Case Study of Nanjing. Science of Surveying and Mapping, 2024, 49(07): 173-183. DOI: 10.16251/j.cnki.1009-2307.2024.07.018.

[12] Li, Q.Q., Li, M., and Liu, H.M. Comparison of Methods for Exploring Spatiotemporal Variations of Urban Heat Island Effect: With Wuhan Metropolitan Development Area as an Example. Chinese Journal of Applied Ecology, vol. 37, no. 3, 2026, pp. 671–682.

[13] Ren, L. Spatiotemporal variation of urban water bodies and its impact on thermal environment in Wuhan, China. Hubei University, 2024. DOI:10.27130/d.cnki.ghubu.2024.000608.

[14] Sobrino, J.A., Jimenez-Munoz, J.C. and Paolini, L. Land Surface Temperature Retrieval from LANDSAT TM 5. Remote Sensing of Environment, 90, 2024, 434-440. http://dx.doi.org/10.1016/j.rse.2004.02.003

International Journal of Environment, Agriculture and Biotechnology
Vol-11, Issue-5; Sep-Oct, 2026
Peer-Reviewed International Journal
Journal Home Page Available: https://ijeab.com/
Journal DOI: 10.22161/ijeab

Phytoremediation of Household Air Pollution: A Critical Review of Pollutant Sources, Health Impacts and Plant-Based Mitigation Strategies

Dr. Hemant Dnyaneshwar Chandore [1*] , Dr. Surnar Laxman Balaji [2]

[1]Head and Associate Professor, Department of Horticulture, Shikshan Maharshi Dnyandeo Mohekar Mahavidyalaya Kalamb, Tal. Kalamb (413507). Dist. Dharashiv, M.S. India
[2]Department of Horticulture, PGI, MPKV Rahuri, M.S. India
Email: hemantflori08@gmail.com[1], surnar23@rediffmail.com [2]

Received: 20 Sep 2026; Received in revised form: 18 Oct 2026; Accepted: 22 Oct 2026; Available online: 29 Oct 2026
©2026 The Author(s). Published by Infogain Publication. This is an open-access article *under* the CC BY license (https://creativecommons.org/licenses/by/4.0/)

Abstract— *Household air pollution (HAP) affects about 2.45 billion people in developing countries. Burning kerosene, coal and biomass releases particulate matter, carbon monoxide, nitrogen dioxide and volatile organic compounds (VOCs), and recent fuel price rises have pushed some families back to these fuels. Paints, cleaning products, furnishings and office equipment add formaldehyde, benzene, toluene and xylene. Exposure links to asthma, COPD, lung cancer, cardiovascular disease and sick building syndrome. This review classifies indoor air quality parameters as physical, chemical and biological, describes major pollutant sources, and examines monitoring approaches, with attention to data gaps in India. It then explains how phytoremediation works through the plant-microbe-soil-air interaction, including enzyme activity, dry deposition and microbial VOC degradation in the rhizosphere and phyllosphere. Experimental studies report 81 to 96% formaldehyde removal by Epipremnum aureum within 24 h, 48 to 53% PM2.5 and PM10 removal by Chlorophytum comosum, and 88% TVOC removal by Areca palm over four months. Most results come from sealed chambers, which limits how far they apply to ventilated homes. Plants work best alongside source control, ventilation and clean cooking fuels.*

Keywords— ***Indoor air quality, Phytoremediation, Household air pollution, Volatile organic compounds, Formaldehyde, Particulate matter, Botanical biofiltration***

I. INTRODUCTION

Indoor air pollution is a growing health concern, and many households are still exposed to it every day. Traditional fuels such as kerosene, coal, wood, charcoal, crop residues and animal manure produce household air pollution, and recent fuel shortages and high LPG and CNG prices are pushing people back to them. Around 2.45 billion people in developing countries are affected (Schraufnagel *et al.,* 2019., Lim *et al.,* 2010)., and household air pollution is linked to millions of premature deaths each year, mostly from stroke, heart disease, lung cancer and chronic obstructive pulmonary disease. Children, women and girls carry a heavy share of this burden. Indoor air also carries particulate matter, combustion gases, volatile organic compounds, aldehydes, radioactive gases and biological aerosols from building materials, furnishings, consumer products and poor ventilation. These pollutants cause headaches, eye and airway irritation, asthma and sick building syndrome. India still lacks enough work on monitoring, modelling and mitigation of indoor pollutants. This review covers the main pollutant sources, how they are monitored and controlled, and how indoor plants can reduce these pollutants through phytoremediation.

II. REVIEW OF LITERATURE

1.1. Household Air Pollution (HAP): Sources and Resurgence of Traditional Fuels

Indoor air pollution has more seriously discussed as people day by day awake of health. Due to modernization various chemicals and biological sources have been used in households which are major sources of indoor air pollution. This indoor air pollutant called as Household Air Pollutant (HAP) which comes from traditional sources of fuel in house like kerosene, coal, biomass sources (Wood, charcoal, crop residues, and animal manure). This use of fuel is now decreasing in some houses due to various alternatives but recent fuel crises and soaring prices or modern fuel such as LPG, CNG etc., raised because of war are again moving common people to use these traditional sources which again caused critical concern of indoor air pollution. Research shows these sources are contributing to global environmental health problems with affecting 2.45 billion people in developing countries. (Schraufnagel *et al.,* 2019., Lim *et al.,* 2010). Near about 2.8 and 4.3 million yearly premature deaths of children with alarming 7.7 % global mortality that surpass combined death of malaria, TB, HIV/AIDS. (Forouzanfar *et al.,* 2016) Report says that among these premature deaths, 3.8 million caused by non-communicable diseases (NCDs). Among those NCDs, HAP is estimated to cause 25% of all stroke deaths, 15% of ischemic heart disease deaths, 17% (280,000) of lung cancer deaths, and more than 33% (800,000) people of all deaths from chronic obstructive pulmonary disease (COPD).4 HAP is the second largest risk factor for women and girls; and for men it is the fifth largest risk factor, after smoking, alcohol use, and high blood pressure. (Naghavi *et al.,* 2013). Among 20 cities of USA found high amount of PM10 (PM ≤ 10 μm) which leads to higher mortality rates due to cardiovascular or respiratory disorders and autism spectrum disorder (ASD) during pregnancy and early life stages of children (Becerra, *et al.,* 2013. Raz *et al.,* 2015, Samet, *et al.,* 2000). AS per WHO reports indoor air pollutation leads sick building syndormes (SBS) having common symptoms such as headaches, eye and respiratory system irritation, dizziness, nausea, fatigue, drowsiness, and general impatience (Orwell *et al.,* 2006; Aydogan and Montoya 2011; Soreanu *et al.,* 2013) and respiratory and cardiovascular diseases are major concerns of inoodr air pollution where VOC are the main cause of SBS (Jafari *et al.,* 2015, Hun *et al.,* 2010).

1.2 Respiratory Effects of Traditional Fuels and Indoor Pollutants:

Lung infection [Bhat *et al.,*2012, Ezzati and Kammen, 2001 Sharma *et al.,* 1998] which correlated with respiratory syndrome and tuberculosis [Öztürk *et al.,* 2014] caused because of traditional biofuels such as kerosene, coal, and firewood. In baltimore (USA) region sudden rise of symptoms of asthma and COPD among 150 preschool-aged children are reported (25) whersas reduction of pulmonary function of school-age children who exposed to indoor PM2.5 particles and do not use inhaled corticosteroids (Koenig *et al.,* 2005). There is correlation of higher concetration of NO2 leads to asthma (Hansel *et al.,* 2008) or allergene effect (Strand *et al.,* 1998), exposure of VOC leads to asthma with non significant cooraltion between them (Kwon *et al.,* 2018, Nurmatov *et al.,* 2015), VOC alongwith other pollutant caused COPD and lung cancer (Kurmi *et al.,* 2010).

1.3 Indoor Air Quality, Exposure Factors and Health Hazards:

In human household environment Indoor air quality (IAQ) is an important component of for his and his lovale pet overall health either mentally or physiobiologically. This environment has three parameters physical, chemical, and biological which not only includes residential buildings but also contains educational institutions, offices, healthcare facilities, and industrial workplaces. The exposure of interior environments with substantial times are affected with indoor pollutant which depends on the building characteristics, ventilation, occupancy, outdoor air infiltration, combustion activities, consumer products, and emissions from construction materials and furnishings (Van Tran *et al.,* 2020; Saini *et al.,* 2020). The effect of indoor pollutant leads to various health hazards like respiratory irritation, allergic reactions, asthma exacerbation, cardiovascular effects, and other adverse health outcomes, depending on the pollutant, concentration, exposure duration, and individual susceptibility. Hence we systematically reviewed the possible pollutant sources, alongwith its monitoring approaches, and control strategies to alongwith valuable indoor plants which reduce this adverse toxic effect on occupant health by phytoremediation (Pillarisetti *et al.,* 2022; Nazli *et al.,* 2024.)

1.4. Research Gaps and Major Indoor Pollutants in the Indian Context

Specially in india we need to identify the gaps in monitoring, modelling, and mitigation, indicating a need for more comprehensive assessments of indoor environments (Thakur *et al.,* 2023). As far as indoor pollutants are reviewed which came form indoor and outdoor soruces we found that particulate matter, combustion gases, volatile organic compounds (VOCs), aldehydes, radioactive gases, biological aerosols, and allergens are the major concerns of occupant health which are need to source identification and integrated management approaches (Pillarisetti *et al.,* 2022; Thakur *et al.,* 2023; Deng *et al.,* 2024).

2. Classification of Indoor Air Quality Parameters (Figure 1.a and 1.b).

Air Quality Index are framed into three parameters such as physical, chemical and biological. Which determines environmental conditions (Saini *et al.,* 2020; Van Tran *et al.,* 2020) and the presence of airborne contaminants. However alone this not completely found to be independent: for example, particulate matter may contain chemical compounds or biological materials, while temperature, humidity, and ventilation influence pollutant concentrations and persistence (Nazli *et al.,* 2024; Chawla *et al.,* 2023).

2.1. Physical Parameters

Physical parameters relevant to indoor environmental assessment include temperature, relative humidity, particulate matter ($PM_{2.5}$ and PM_{10}), air velocity, ventilation rate, and pressure differences between indoor and outdoor spaces. Temperature and humidity influence thermal comfort, chemical emissions, and the conditions that support microbial growth. Particulate matter originates from cooking, combustion, cleaning, resuspension of settled dust, construction activities, and outdoor infiltration. The concentration and distribution of indoor particles are also affected by occupant activities, air exchange, filtration, and deposition processes (Li *et al.,* 2023). Recent research has emphasized the importance of understanding both indoor-generated particles and particles infiltrating from outdoor environments when evaluating exposure and developing mitigation strategies. These review also supllemtary support by various researchers . (Baeza Romero *et al.,* (2022)., Saraga, D. E., *et al.,* (2023).

2.2. Chemical Parameters

Chemical parameters containing of carbon monoxide (CO), carbon dioxide (CO_2), nitrogen dioxide (NO_2), ozone (O_3), volatile organic compounds (VOCs), formaldehyde, and radon. Combustion appliances and traditional fuel use can release CO, CO_2, NO_2, SO_2, PM 2.5, whereas paints, varnishes, adhesives, furnishings, cleaning agents, and solvents alongwith office equipment which cant ignored like photocopiers, printers, and gas cooktops can contribute to VOC (benzene, toluene, ethylbenzene, xylene (BTEX), poly aromatic hydrocarbons (PAHs), and aldehyde emissions (Maisey *et al.,* 2013 , Myers and Maynard, 2005., Gawronski *et al.,* 2017; Wei *et al.,* 2017). Entry of Radon gas in room from soil and geological region either form indoor or outdoor. Use of various cleaning and disinfecting products augmenting release of various volatile compounds and generate secondary pollutants through reactions with other substances in indoor air. Consequently, chemical assessments should consider source-specific emissions, ventilation, chemical transformations, and the intended use of the indoor space (Salonen *et al.,* 2024; Thakur *et al.,* 2023). Saraga *et al.,* (2023) reviewed indoor air pollution source-apportionment methods and emphasized the challenges associated with distinguishing indoor emissions from outdoor contributions and secondary pollutant formation.

2.3 Biological Parameters

Biological parameters which containing various airborne bacteria, fungal spores, viruses carried in respiratory aerosols, pollen, dust-mite allergens, animal-derived allergens, and other biological particles. These contaminants may originate from occupants, pets, plants, outdoor air, damp building materials, contaminated dust, and inadequately maintained ventilation systems. Moisture intrusion and persistent dampness can support microbial growth and contribute to the presence of mould and associated biological components. Chawla *et al.*, (2023) reviewed microbial contamination in indoor environments, addressing its sources, sampling approaches, health risks, and mitigation strategies. Biological assessment requires appropriate sampling and analytical procedures because airborne microbial concentrations vary with occupancy, humidity, ventilation, sampling duration, and environmental conditions.

3. Types and Sources of Indoor Air Pollutants (Figure 2).

Indoor air pollutants can be classified according to their physical state, chemical or biological nature, and source of origin. Based on physical state, they include particulate pollutants (fine and coarse particles, dust, soot, fibres, and airborne biological materials), gaseous pollutants (combustion gases, VOCs, aldehydes, ozone, and radon, organic vapours), and biological aerosols (microorganisms, pollen, allergens, and biological fragments). Unfortunately, some categories are overlap such as fungal spores came in both biological contaminants and airborne particles. The entry of origin of these sources are either generated indoor or entering form outdoor environments. They are formed by chemical or biooogical process within home. Some indoor sources are identified as cooking and heating appliances, tobacco smoke, candles, incense, cleaning products, pesticides, building materials, furnishings, and human activities. Similallrly outdoor sources that includes road traffic, industrial emissions, dust, smoke, and pollen entering through windows, doors, and ventilation systems (Van Tran *et al.,* 2020; Saraga *et al.,* 2023). Source apportionment studies indicate that identifying the contribution of individual sources is challenging because indoor pollutants are influenced by multiple emission sources, chemical transformations, deposition, and exchange with outdoor air (Saraga, D. E., *et al.,* (2023)). Research on cleaning products further demonstrates that indoor chemical pollution may arise from both directly

emitted compounds and products formed through subsequent chemical reactions (Salonen *et al.,* 2024).

The contribution of individual sources varies according to building design, fuel use, occupant behaviour, ventilation, climate, and the surrounding environment. Source identification is therefore a central component of IAQ management. Saraga *et al.,* (2023) demonstrated that indoor source-apportionment studies commonly investigate particulate matter and that the contribution of outdoor sources can vary substantially between buildings and studies. More recent reviews have also examined the use of continuous monitoring and real-time data to identify pollutant sources and support mitigation decisions (Chojer, *et al.,* 2024).

4. Integrated Assessment and Monitoring of Indoor Air Quality

An integrated IAQ assessment should consider physical conditions, chemical contaminants, biological pollutants, ventilation, and potential emission sources. No single parameter can adequately represent all aspects of indoor air quality. For example, carbon dioxide can help assess ventilation in relation to occupancy, but it does not directly quantify particulate matter, VOCs, or biological contaminants. Similarly, particulate matter measurements provide information about airborne particle concentrations but do not, by themselves, establish particle composition or biological origin. Saini *et al.* (2020) reviewed IAQ monitoring systems and the application of sensor-based technologies, while Nazli *et al.,* (2024) examined research trends in indoor air quality through a bibliometric analysis of literature published between 2018 and 2023. Together, these studies support the need for appropriate monitoring strategies and continued research into pollutant measurement and control.

In addition, indoor air quality research has particular relevance to India, where building characteristics, household energy use, urban pollution, and ventilation practices can produce different exposure conditions. Patel *et al.,* (2023) reviewed the status of indoor air quality research in urban India and identified limitations in the availability and scope of measurements compared with research in several developed countries. Further investigations should therefore consider locally relevant sources, building types, seasonal conditions, and occupant activities when designing IAQ monitoring programmes (Thakur *et al.,* 2023; Chawla *et al.,* 2023; Deng *et al.,* 2024). These considerations provide a scientific basis for classifying indoor air quality parameters, identifying pollutant sources, and developing targeted strategies to improve indoor environmental conditions.

5. Research Need and Scope of the Review

Despite advances in indoor air monitoring, the assessment of indoor air pollution remains challenging because multiple pollutants and emission sources interact within enclosed environments. Differences in sampling methods, monitoring duration, building characteristics, and source-identification techniques can also complicate comparisons between studies. A systematic synthesis of physical, chemical, and biological IAQ parameters, together with their major indoor and outdoor sources, is needed to support consistent assessment and effective pollution management. Accordingly, this review focuses on the classification of indoor air quality parameters, the types and sources of indoor pollutants, monitoring approaches, and the implications of pollutant exposure for indoor environmental health.

6. How Phytoremediation Works: Plant–Microbe–Soil–Air Interaction in Indoor Environments

6.1. Mechanism of Pollutant Removal by Indoor Plants

Indoor plant ecosystem can help to prevent or minimize most of the pollutant by phytoremediation process where upper zone of the plant helps to absorbs some of the pollutant and lower part of rhizosphere alongwith microbes helps to degrade or absorbs fallen leaves or scavenging its absorbed pollutant by filtration, metabolism (Nowak *et al.,* 2006, Brack, C.L 2002 , Van Tran Lee *et al.*, 2020; Supreeth 2021 Kim *et al.,* 2020) , sequestration, or excretion methods which detoxify indoor environment. Some of the pollutants are also uptake by plant and utilized for its devlopment while extra are stored in their stomata or other parts which latter fall on and recycled it in soil. This plant-microbes-soil -air interaction acts as a proper cycle of controlling indoor air pollution.

6.2. Role of Plant–Microbe Symbiosis

The symbiotic relationship of microbes alongwith plants are important where microbes help to cop plant in biotic and abiotic stress, assist their host for better nutrient and water uptake , production of plant hormones, siderophores, and suppressing allelopathic effect of chemicals (Bulgarelli, 2013, Weyens 2009).

6.3. Microlevel Processes: Enzymes, Microbial Degradation and Biostimulants

In microlevel studies shows that plant metabolites, such as enzymes (catalase, dehydrogenase), decomposed hazardous air pollutants (Rachmadiarti *et al.,* 2019; Han *et al.,* 2022) while CO2 utilized during photosynthesis , VOC degraded by rhizosphere/phyllosphere microorganisms that caused deportation of PM on plant surface ad dry deposition (Orwell *et al.,* 2006; Gawronska and Bakera 2015; Torpy *et al.,* 2018). Active biotsimulant produced by soil micboes are hlpes to convert that aerial and filtered leached pollutant

in substarte to utlised it carbon source of plant mostly using VOC, CO_2 . In indoor enrionment aerial and root zones of of potted plant are equally important for reducing indoor air pollutant (Pettit *et al.,* 2015, Wang *et al.,* 2014, Xu *et al.,* 2010, Xu *et al.,*2011)

6.4. Aerial (Phyllosphere) and Root Zone Contributions:

On upper zone of the indoor plant where plant leaves and stems are zone of phyllosphere bacteria and endophytic bacteria which detox some pollutant by absorption, degradation, transformation or sequestration process. While during watering process some part of the air pollutant around the plant are drained out on lower zone of the plant (Weyens *et al.,* 2015). Structural representation of this plant-microbes-soil -air interaction (PMSAI) is shown in figure 3

7. Pollutant Removal Efficiency of Indoor Plants: Reported Experimental Studies:

Some Indoor plant (Wolverton *et al.,* 1989) can effectively used for natural water and air-filtration under National Aeronautics and Space Administration (NASA) scientific studies which proves that use two plants in each room of 100 square feet (9.3 m^2) [Klepeis *et al.,* 2001] helps to filter or absorb VOCs (formaldehyde, benzene, and trichloroethylene, ethylbenzene, xylene, styrene, acetaldehyde, and toluene)[Seguel *et al.,* 2016., Wolverton *et al.,* 1984., Orwell *et al.,* 2004., Hong *et al.,* 2017) Some plants like Genus ficus (Hong *et al.,* 2017) reduce VOC, *Nephrolepis Obliterata* reduce formaldehyde (up to 100%) (Teiri *et al.,* 2018) *Hedera helix, Chrysanthemum morifolium, Dieffenbachia compacta, and Epipremnum aureum* formaldehyde (up to 90%) *within 24 hr (Aydogan and Montoya 2011.). Reduction of VOC, CO and CO2 level by indoor plant (Panyametheekul, et al, 2018).*

Scientific studies on 13 different pot but shows different amoujt of formaledyhyde absorption where out of this 13 , *Asplenium nidus* having highest adsorption capacity (5.13 mg/m^2) and *Epipremnum aureum* has the has the lowest adsorption capacity (0.64 mg/m^3) per unit leaf area (HongBo *et al.,* (2010). Su *et al.,* 2019 also reported that when indoor plants are exposed under higher concentration of formaldehyde it affects growth of plant alongwith witling and leaf yellowing like symptoms. He studied that various species under green wall alongwith various kind of growth media which exposed at various concertation of pollutatnt (µg/m^3) and phytoremediation process have ben reported that *Chlorophytum comosum and Epipremnum aureum* removed CO_2 (1,800,000 µg/m^3) by 20% and 8%, respectively exposed pollutant (Torpy *et al.,* 2017); *Chlorophytum comosum* achieved 48.21–53.35% removal of $PM_{2.5}$ and PM_{10} (700 µg/m^3) (Irga *et al.,* 2017); an active green wall containing *Philodendron scandens, Asplenium antiquum*, and *Syngonium podophyllum* removed 56.6 ± 0.86% of methyl ethyl ketone (MEK) (101.63 µg/m^3) within 8 h (Torpy *et al.,* 2018); *Nephrolepis exaltata* achieved 12.8–77.3% removal of total volatile organic compounds (TVOCs) (3,900–6,600 µg/m^3) within 3 h (Suárez-Cáceres *et al.,* 2021); *Epipremnum aureum* in a hydroponic system removed 81–96% of formaldehyde (2,000 µg/m^3) within 24 h (Aydogan & Montoya, 2011), while a botanical indoor air biofilter containing *Epipremnum aureum* achieved removal rates of 54.5% for $PM_{2.5}$, 65.42% for PM_{10}, and 46% for VOCs (18,000–25,000 µg/m^3) within 16 min (Ibrahim *et al.,* 2021).

Studies in the tables (1) report that potted indoor plants remove formaldehyde (CH_2O), benzene (C_6H_6), toluene (C_7H_8), hexane (C_6H_{14}), xylene, particulate matter (PM), TVOCs, CO_2 and CO. In batch (closed chamber) exposure, *Nephrolepis exaltata*, *Chrysanthemum morifolium* and *Phoenix roebelenii* were exposed to CH_2O at 6140 µg/m^3 and removed 1863, 1450 and 1385 µg $plant^{-1}$ h^{-1} (Wolverton and Wolverton 1993). *Howea forsteriana* removed 4032 $mg/m^3/day/m^2$ of C_6H_{14} at 353,000 µg/m^3 (Wood et al. 2002). *Azalea indica* removed 95% of C_7H_8 at 339,000 µg/m^3 in 7 to 76 h (De Kempeneer et al.2004). At 3195 µg/m^3 of C_6H_6, *Spathiphyllum wallisii*, *Syngonium podophyllum*, *Cissus rhombifolia* and *Hedera helix* removed 174.5, 103.4, 50.3 and 102.8 ng m^{-3} h^{-1} cm^{-2} leaf area respectively (Yoo *et al.*, 2006). At 2456 µg/m^3 of CH_2O, *Fatsia japonica* removed 39% (day) and 98% (night), and *Ficus benjamina* 57% (day) and 94% (night) in 5 h (Kim et al. 2008). *Ficus elastica* removed 28 to 91% of C_6H_6 at 15,116 µg/m^3 in 12 h (Chun et al. 2010). At 2000 µg/m^3 of CH_2O, *Hedera helix*, *Chrysanthemum morifolium*, *Dieffenbachia compacta* and *Epipremnum aureum* removed 88, 84, 96 and 94% in 24 h (Aydogan and Montoya 2011). *Dracaena sanderiana* removed 46% (by wax) and 54% (by stomata) of C_6H_6 at 63,894 µg/m^3 in 72 h (Treesubuntorn and Thiravetyan 2012). *Sansevieria trifasciata* removed 10.17 µmol of C_7H_8 at 78,800 to 81,670 µg/m^3 in 72 h (Sriprapat *et al.*, 2014). *Hedera helix* removed 99.99% of CH_2O at 6,140,000 µg/m^3 in 67.6 h (Chen *et al.*, 2017). *Epipremnum aureum*, *Chlorophytum comosum*, *Hedera helix* and *Echinopsis tubiflora* removed 72% of C_6H_6 at 319,470 µg/m^3 in 72 h (Gong et al. 2019). Under continuous exposure, *Chlorophytum comosum*, *Aloe vera* and *Epipremnum aureum* removed 95, 53 and 84% of CH_2O at 4000 µg/m^3 (Xu et al. 2011). *Chlorophytum comosum* removed 13.62 to 19.79 µg m^{-2} leaf of PM in 2 months in a real room environment (Gawrońska and Bakera 2015). At 43.0 (toluene) and 62.3 (xylene) µg/m^3, *Schefflera actinophylla* removed 13.3 and 7.0 µg m^{-3} m^{-2} leaf area, and *Ficus benghalensis* removed 13.0 and 7.3 µg m^{-3} m^{-2} (Kim et al. 2016). *Schefflera arboricola* and *Spathiphyllum*

wallisii removed 91 to 97% of C_6H_6 at 3.6 to 29.5 µg/m³ in 48 h (Parseh *et al.*, 2018). *Nephrolepis obliterata* removed 81 to 100% of CH_2O at 600 to 11,000 µg/m³, and *Chamaedorea elegans* removed 65 to 100% at 660 to 16,400 µg/m³, both in 48 h (Teiri *et al.*, 2018). *Laurus nobilis* removed 360,002 µg/m³/day/m² of CO_2 at 684,003 to 1,800,009 µg/m³ (Salvatori *et al.*, 2020). *Areca palm* removed 88.16% of TVOCs (829.4 µg/m³), 52.33% of CO_2 (1,545,092 µg/m³) and 95.70% of CO (5728 µg/m³) in 4 months (Bhargava *et al.*, 2021).

III. FIGURES AND TABLES

Table 1 . Indoor air pollutants reported in phytoremediation studies

S. No.	Formula	Chemical name
1	CH_2O	Methanal (formaldehyde)
2	C_6H_6	Benzene
3	C_7H_8	Methylbenzene (toluene)
4	$C_6H_5CH_2CH_3$	Ethylbenzene
5	C_8H_{10}	Dimethylbenzene (xylene)
6	C_6H_{14}	Hexane
7	C_3H_6O	Propan-2-one (acetone)
8	CO_2	Carbon dioxide
9	CO	Carbon monoxide
10	PM	Particulate matter
11	TVOCs	Total volatile organic compounds

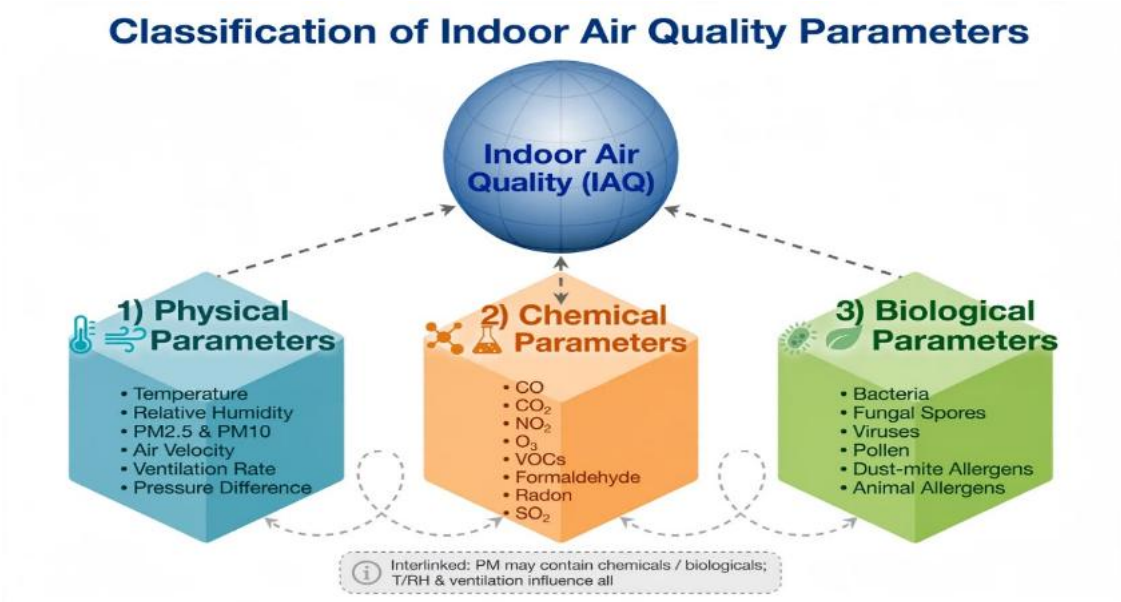


Fig.1a: Classification of Indoor Air Quality Parameters

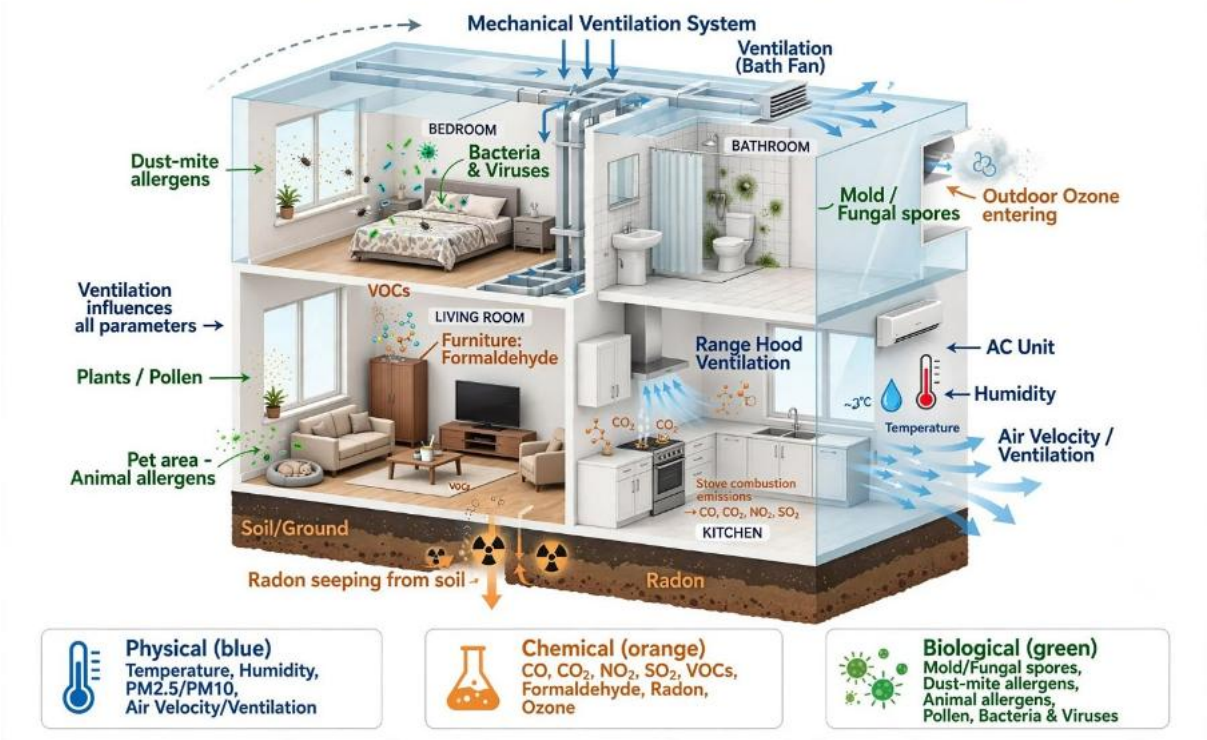


Fig.1b: 3D View of Classification of Indoor Air Quality Parameters



Fig.2: 3 D View of Types and Sources of Indoor Air Pollutants

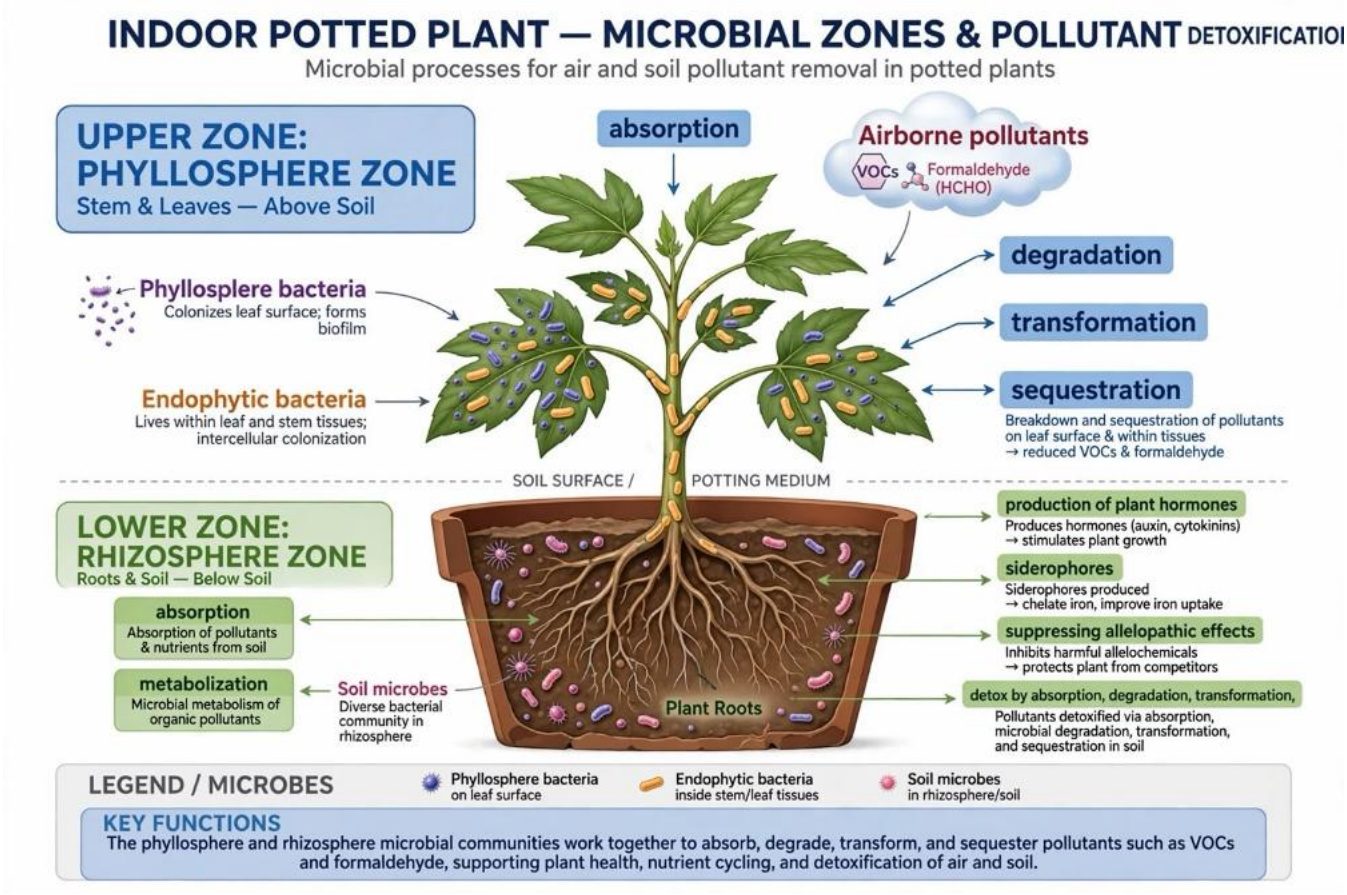


Fig.3: Structural representation of this plant-microbes-soil -air interaction (PMSAI) is shown in

IV. CONCLUSION

The literature reviewed here shows that household air pollution has no single cause and no single indicator. Solid fuel combustion, building materials, cleaning products, furnishings and infiltrating outdoor air all contribute, and the resulting mix of particles, combustion gases, VOCs, aldehydes and bioaerosols varies with fuel use, ventilation and building type. Studies in India remain few and often cover short monitoring periods in a limited range of homes, so exposure estimates for rural and low-income households are the weakest part of the evidence base.

Phytoremediation studies consistently report pollutant reduction by potted plants, active green walls and botanical biofilters. Removal is attributed to leaf and stomatal uptake, cuticular wax adsorption, particle deposition, and degradation by rhizosphere and phyllosphere microbes. Experimental studies show that potted plants, green walls and botanical biofilters can lower indoor pollutant concentrations. Reported removal reached 81 to 96% of formaldehyde by *Epipremnum aureum* in 24 h, 48 to 53% of PM2.5 and PM10 by *Chlorophytum comosum*, and 88% of TVOCs by Areca palm over four months. Removal depends on leaf uptake, stomatal and wax absorption, particle deposition, and degradation by rhizosphere and phyllosphere microbes. Most of these results come from sealed chambers with high pollutant doses and short exposure times, and studies report removal in different units. Direct comparison between species is therefore difficult, and chamber results probably overestimate what a ventilated room with continuous emissions would achieve.

Based on current evidence, plants are best treated as a supplement to source control, clean cooking fuels and ventilation. Future studies should test plants in occupied homes over months, report removal per unit leaf area per hour, include mixed pollutant exposure and PM, and pair plant systems with continuous sensors. Studies on Indian housing and locally available species would also make the findings more applicable.

ACKNOWLEDGEMENTS

SOURCE OF FUNDING: This research received no specific grant or funding from any public, commercial, or not-for-profit funding agency.

CONFLICT OF INTEREST: The authors declare that they have no conflict of interest.

REFERENCES

[1] Aydogan A, Montoya LD (2011) Formaldehyde removal by common indoor plant species, various growing media. *Atmos. Env.* 45(16):2675–2682. https://doi.org/10.1016/j.atmosenv. 2011.02.062

[2] Baeza-Romero, M. T., Dudzińska, M. R., Amouei Torkmahalleh, M., Barros, N., Coggins, A. M., Gazioglu Ruzgar, D., Kildsgaard, I., Naseri, M., Rong, L., Saffell, J., Scutaru, A. M., & Staszowska, A. (2022). A review of critical residential buildings parameters and activities when investigating indoor air quality and pollutants. Indoor Air, 32(11), e13144. DOI: 10.1111/ina.13144

[3] Becerra TA, Wilhelm M, Olsen J, Cockburn M, Ritz B (2013). Ambient air pollution and autism in Los Angeles county, California. Environ Health Perspect. 121(3):380-386. https://doi.org/10.1289/ehp.1205827

[4] Bhat YR, Manjunath N, Sanjay D, Dhanya Y (2012). Association of indoor air pollution with acute lower respiratory tract infections in children under 5 years of age. Paediatr Int Child Health. 32(3):132-135. https://doi.org/10.1179/2046905512Y.0000000027

[5] Brack CL (2002). Pollution mitigation and carbon sequestration by an urban forest. Environ Pollut. 116(Suppl 1):S195-S200. https://doi.org/10.1016/S0269-7491(01)00251-2

[6] Bulgarelli D, Schlaeppi K, Spaepen S, Ver Loren van Themaat E, Schulze-Lefert P (2013). Structure and functions of the bacterial microbiota of plants. Annu Rev Plant Biol. 64:807-838. https://doi.org/10.1146/annurev-arplant-050312-120106

[7] Chawla, H., Anand, P., Garg, K., Bhagat, N., Varmani, S. G., Bansal, T., McBain, A. J., & Marwah, R. G. (2023). A comprehensive review of microbial contamination in the indoor environment: Sources, sampling, health risks, and mitigation strategies. Frontiers in Public Health, 11, 1285393.DOI: 10.3389/fpubh.2023.1285393

[8] Chojer, H., Branco, P. T. B. S., Martins, F. G., Alvim-Ferraz, M., & Sousa, S. I. V. (2024). Source identification and mitigation of indoor air pollution using monitoring data: Current trends. Environmental Technology & Innovation, 33, 103534. DOI: 10.1016/j.eti.2024.103534

[9] Chun SC, Yoo MH, Moon YS, Shin MH, Son KC, Chung IM, Kays SJ (2010) Effect of bacterial population from rhizosphere of various foliage plants on removal of indoor volatile organic compounds. Horticultural Science & Technology 28(3):476–483

[10] De Kempeneer L, Sercu B, Vanbrabant W, Van Langenhove H, Verstraete W (2004) Bioaugmentation of the phyllosphere for the removal of toluene from indoor air. Applied microbiology, biotechnology 64(2):284–288. https://doi.org/10.1007/ s00253-003-1415-3

[11] Deng, Z., Dong, B., Guo, X., & Zhang, J. (2024). Impact of Indoor Air Quality and Multi-domain Factors on Human Productivity and Physiological Responses: A Comprehensive Review. Indoor Air, 2024, 5584960 DOI: 10.1155/2024/5584960

[12] Ezzati M, Kammen DM (2001). Indoor air pollution from biomass combustion and acute respiratory infections in Kenya: an exposure-response study. Lancet. 358(9282):619-624. https://doi.org/10.1016/S0140-6736(01)05777-4

[13] Forouzanfar MH, Afshin A, Alexander LT, Anderson HR, Bhutta ZA, Biryukov S, et al. (2016). Global, regional, and national comparative risk assessment of behavioural, environmental and occupational, and metabolic risks or clusters of risks, 1990-2015: a systematic analysis for the Global Burden of Disease Study 2015. Lancet. 388(10053):1659-1724. https://doi.org/10.1016/S0140-6736(16)31679-8

[14] Gawronska H, Bakera B (2015) Phytoremediation of particulate matter from indoor air by Chlorophytum comosum L. plants. Air Quality, Atmosphere & Health 8(3):265–272. https://doi.org/10.1007/ s11869-014-0285-4

[15] Gawronski SW, Gawronska H, Lomnicki S, Saebo A, Vangronsveld J (2017) Plants in air phytoremediation. In: Advances in botanical research, vol 83. Academic Press, pp 319–346. https://doi.org/ 10.1016/bs.abr.2016.12.008

[16] Gong Y, Zhou T, Wang P, Lin Y, Zheng R, Zhao Y, Xu B (2019) Fundamentals of ornamental plants in removing benzene in indoor air. Atmosphere 10(4):221. https://doi.org/10.3390/atmos10040 221

[17] Han Y, Lee J, Haiping G, Kim KH, Wanxi P, Bhardwaj N, Oh JM, Brown RJ (2022) Plant-based remediation of air pollution: a review. Journal of Environmental Management 301:113860. https://doi.org/10.1016/j.jenvman.2021.113860

[18] Hansel NN, Breysse PN, McCormack MC, Matsui EC, Curtin-Brosnan J, Williams DL, Moore JL, Cuhran JL, Diette GB (2008). A longitudinal study of indoor nitrogen dioxide levels and respiratory symptoms in inner-city children with asthma. Environ Health Perspect. 116(10):1428-1432. https://doi.org/10.1289/ehp.11349

[19] Hong SH, Hong J, Yu J, Lim Y (2017). Study of the removal difference in indoor particulate matter and volatile organic compounds through the application of plants. Environ Health Toxicol. 32:e2017006. https://doi.org/10.5620/eht.e2017006

[20] Hong-Bo S, Li-Ye C, Cheng-Jiang R, Hua L, Dong-Gang G, Wei-Xiang L (2010) Understanding molecular mechanisms for improving phytoremediation of heavy metal-contaminated soils. Critical reviews in biotechnology 30(1):23–30. https://doi.org/10.3109/ 07388550903208057

[21] Hun DE, Corsi RL, Morandi MT, Siegel JA (2010). Formaldehyde in residences: long-term indoor concentrations and influencing factors. Indoor Air. 20(3):196-203. https://doi.org/10.1111/j.1600-0668.2010.00644.x

[22] Ibrahim IZ, Chong WT, Yusoff S, Wang CT, Xiang X, Muzammil WK (2021) Evaluation of common indoor air

pollutant reduction by a botanical indoor air biofilter system. Indoor Built Environ 30:7–21. https://doi.org/10.1177/1420326X19882080

[23] Irga PJ, Paull NJ, Abdo P, Torpy FR (2017) An assessment of the atmospheric particle removal efficiency of an in-room botanical biofilter system. Building, Environment 115:281–290. https:// doi.org/10.1016/j.buildenv.2017.01.035

[24] Jafari MJ, Khajevandi AA, Mousavi Najarkola SA, Yekaninejad MS, Pourhoseingholi MA, Omidi L, Kalantary S (2015). Association of sick building syndrome with indoor air parameters. Tanaffos. 14(1):55-62. PMID: 26221153. https://pmc.ncbi.nlm.nih.gov/articles/PMC4515331/

[25] Kim KJ, Kim HJ, Khalekuzzaman M, Yoo EH, Jung HH, Jang HS (2016) Removal ratio of gaseous toluene, xylene transported from air to root zone via the stem by indoor plants. Environmental Science, Pollution Research 23(7):6149–6158. https://doi.org/ 10.1007/s11356-016-6065-y

[26] Kim KJ, Lee DW (2008) Efficiency of volatile formaldehyde removal of orchids as affected by species and crassulacean acid metabolism (CAM) nature. Horticult Environ Biotechnol 49(2):132–137

[27] Kim KJ, Shagol CC, Torpy FR, Pettit T, Irga PJ (2020) Plant physiological mechanisms of air treatment. In from biofiltration to promising options in gaseous fluxes biotreatment 219-244. Elsevier. https://doi.org/10.1016/B978-0-12-819064-7.00011-X

[28] Klepeis NE, Nelson WC, Ott WR, Robinson JP, Tsang AM, Switzer P, Behar JV, Hern SC, Engelmann WH (2001). The National Human Activity Pattern Survey (NHAPS): a resource for assessing exposure to environmental pollutants. J Expo Anal Environ Epidemiol. 11:231-252. https://doi.org/10.1038/sj.jea.7500165

[29] Koenig JQ, Mar TF, Allen RW, Jansen K, Lumley T, Sullivan JH, Trenga C, Larson T, Liu LJS. (2005). Pulmonary effects of indoor- and outdoor-generated particles in children with asthma. Environ Health Perspect.;113(4):499-503. https://doi.org/10.1289/ehp.7511

[30] Kurmi OP, Semple S, Simkhada P, Smith WC, Ayres JG. (2010) COPD and chronic bronchitis risk of indoor air pollution from solid fuel: a systematic review and meta-analysis. Thorax.;65(3):221-228. https://doi.org/10.1136/thx.2009.124644

[31] Kwon JW, Park HW, Kim WJ, Kim MG, Lee SJ. (2018). Exposure to volatile organic compounds and airway inflammation. Environ Health. 17(1):65. https://doi.org/10.1186/s12940-018-0410-1

[32] Li, J., Fan, G., Ou, Y., & Deng, Q. (2023). Characteristics and control strategies of indoor particles: An updated review. Energy and Buildings, 294, 113232. DOI: 10.1016/j.enbuild.2023.113232

[33] Lim, S. S., Vos, T., Flaxman, A. D., Danaei, G., Shibuya, K., Adair-Rohani, H., AlMazroa, M. A., Amann, M., Anderson, H. R., Andrews, K. G., Aryee, M., Atkinson, C., Bacchus, L. J., Bahalim, A. N., Balakrishnan, K., Balmes, J., Barker-Collo, S., Baxter, A., Bell, M. L., … Memish, Z. A. (2012). A comparative risk assessment of burden of disease and injury attributable to 67 risk factors and risk factor clusters in 21 regions, 1990–2010: A systematic analysis for the Global Burden of Disease Study 2010. The Lancet, 380(9859), 2224–2260. DOI: 10.1016/S0140-6736(12)61766-8

[34] Maisey SJ, Saunders SM, West N, Franklin PJ (2013) An extended baseline examination of indoor VOCs in a city of low ambient pollution: Perth, Western Australia. Atmospheric Environment 81:546–553. https://doi.org/10.1016/j.atmosenv.2013.09.008

[35] Myers, I.; Maynard, R.L. (2005). Polluted air—Outdoors and indoors. *Occup. Med.*, *55*, 432–438.

[36] Naghavi M, Wang H, Lozano R, Davis A, Liang X, Zhou M. (2015). Global Burden of Disease Collaborative Network. Global,regional, and national age–sex specific all-cause and cause specific mortality for 240 causes of death, 1990–2013: a systematic analysis for the global burden of disease study 2013. Lancet.;385(9963):117–171.

[37] Nazli, S. N., Vilcins, D., Sly, P. D., Abd Razak, A., Sabri, N., & Tengku Ibrahim, T. N. B. (2024). Indoor Air Quality: Bibliometric Analysis of the Published Literature Between 2018 and 2023. Environmental Quality Management, 34(1), e22297.DOI: 10.1002/tqem.22297

[38] Nowak, D.J.; Crane, D.E.; Stevens, J.C. (2006). Air pollution removal by urban trees and shrubs in the United States. *Urban For. Urban Green.*, *4*, 115–123.

[39] Nurmatov UB, Tagiyeva N, Semple S, Devereux G, Sheikh A. (2015). Volatile organic compounds and risk of asthma and allergy: a systematic review. Eur Respir Rev. ;24(135):92-101. https://doi.org/10.1183/09059180.00000714

[40] Orwell RL, Wood RA, Burchett MD, Tarran J, Torpy F (2006) The potted-plant microcosm substantially reduces indoor air VOC pollution: II. Laboratory study. Water, air, soil pollution 177(1):59–80. https://doi.org/10.1007/s11270-006-9092-3

[41] Orwell RL, Wood RL, Tarran J, Torpy F, Burchett MD. (2004). Removal of benzene by the indoor plant/substrate microcosm and implications for air quality. Water Air Soil Pollut;157:193–207.

[42] Öztürk AB, Kılıçaslan Z, İşsever H. (2014). Effect of smoking and indoor air pollution on the risk of tuberculosis: smoking, indoor air pollution and tuberculosis. Tuberk Toraks.;62(1):1-6. DOI: verify on the journal site or PubMed, I am not confident of it.

[43] Panyametheekul S, Rattanapun T, Ongwandee M. (2018). Ability of artificial and live houseplants to capture indoor particulate matter. Indoor Built Environ;27:121–8.

[44] Parseh I, Teiri H, Hajizadeh Y, Ebrahimpour K (2018) Phytoremediation of benzene vapors from indoor air by Schefflera arboricola. Spathiphyllum wallisii plants. Atmospheric Pollution Research 9(6):1083–1087. https://doi.org/10.1016/j.apr.2018.04.005

[45] Patel, S., et al. (2023). Indoor Air Quality in Urban India: Current Status, Research Gap, and the Way Forward.

Environmental Science & Technology Letters, 10(12), 1146–1158. DOI: 10.1021/acs.estlett.3c00636

[46] Pettit T, Irga PJ, Torpy FR. (2018). Towards practical indoor air phytoremediation: a review. Chemosphere;208:960–74.

[47] Pillarisetti, A., Ye, W., & Chowdhury, S. (2022). Indoor Air Pollution and Health: Bridging Perspectives from Developing and Developed Countries. Annual Review of Environment and Resources, 47, 197–229. DOI: 10.1146/annurev-environ-012220-010602

[48] Rachmadiarti F, Purnomo T, Azizah DN, Fascavitri A (2019) Syzigium oleina, wedelia trilobata for phytoremediation of lead pollution in the atmosphere. Nat. Environ. Pollut. Technol. 18:157–162

[49] Raz, R.; Roberts, A.L.; Lyall, K.; Hart, J.E.; Just, A.C.; Laden, F.; Weisskopf, M.G(2015). Autism spectrum disorder and particulate matter air pollution before, during, and after pregnancy: A nested case-control analysis within the nurses' health study II cohort. *Environ. Health Perspect.*, *123*, 264–270.

[50] Saini, J., Dutta, M., & Marques, G. (2020). A comprehensive review on indoor air quality monitoring systems for enhanced public health.Sustainable Environment Research, 30, Article 6. DOI: 10.1186/s42834-020-0047-y

[51] Salonen, H., Salthammer, T., Castagnoli, E., Täubel, M., & Morawska, L. (2024). Cleaning products: Their chemistry, effects on indoor air quality, and implications for human health. Environment International, 190, 108836.DOI: 10.1016/j.envint.2024.108836

[52] Salvatori E, Gentile C, Altieri A, Aramini F, Manes F (2020) Naturebased solution for reducing CO2 levels in museum environments: a phytoremediation study for the Leonardo da Vinci's "Last Supper". Sustainability 12(2):565. https://doi.org/10.3390/ su12020565

[53] Samet, J.M.; Dominici, F.; Curriero, F.C.; Coursac, I.; Zeger, S.L. Fine particulate air pollution and mortality in 20 US cities, 1987–1994. *N. Eng. J. Med.* 2000, *343*, 1742–1749.

[54] Saraga, D. E., Querol, X., Duarte, R. M. B. O., Aquilina, N. J., Canha, N., Gómez Alvarez, E., Jovasevic-Stojanovic, M., Bekö, G., Byčenkienė, S., Kovacevic, R., Plauškaitė, K., & Carslaw, N. (2023). Source apportionment for indoor air pollution: Current challenges and future directions. Science of the Total Environment, 900, 165744. https://doi.org/10.1016/j.scitotenv.2023.165744

[55] Schraufnagel, D. E., Balmes, J. R., Cowl, C. T., De Matteis, S., Jung, S.-H., Mortimer, K., Perez-Padilla, R., Rice, M. B., Riojas-Rodriguez, H., Sood, A., Thurston, G. D., To, T., Vanker, A., & Wuebbles, D. J. (2019). Air pollution and noncommunicable diseases: A review by the Forum of International Respiratory Societies' Environmental Committee, Part 1: The damaging effects of air pollution. Chest, 155(2), 409–416. DOI: 10.1016/j.chest.2018.10.042

[56] Seguel JM, Merrill R, Seguel D, Campagna AC. (2016). Indoor Air Quality. Am J Lifestyle Med;11:284–95

[57] Sharma S, Sethi GR, Rohtagi A, Chaudhary A, Shankar R, Bapna JS, Joshi V, Sapir DG. (1998). Indoor air quality and acute lower respiratory infection in Indian urban slums. Environ Health Perspect.;106(5):291-297. https://doi.org/10.1289/ehp.98106291

[58] Soreanu G, Dixon M, Darlington A (2013) Botanical biofiltration of indoor gaseous pollutants–a mini-review. Chemical engineering journal 229:585–594. https://doi.org/10.1016/j.cej.2013.06.074

[59] Sriprapat W, Suksabye P, Areephak S, Klantup P, Waraha A, Sawattan A, Thiravetyan P (2014) Uptake of toluene, ethylbenzene by plants: removal of volatile indoor air contaminants. Ecotoxicology, Environmental Safety 102:147–151. https://doi.org/10. 1016/j.ecoenv.2014.01.032

[60] Strand V, Svartengren M, Rak S, Barck C, Bylin G. (1998). Repeated exposure to an ambient level of NO2 enhances asthmatic response to a nonsymptomatic allergen dose. Eur Respir J.;12(1):6-12. https://doi.org/10.1183/09031936.98.12010006

[61] Su W, Liu C, Hu Q, Zhao S, Sun Y, Wang W, Zhu Y, Liu J, Kim J (2019) Primary, secondary sources of ambient formaldehyde in the Yangtze River Delta based on ozone mapping, profiler suite (OMPS) observations. Atmos. Chem. Phys. 19:6717–6736. https://doi.org/10.5194/acp-19-6717-2019

[62] Suarez-Caceres GP, Fernandez-Canero R, Fernandez-Espinosa AJ, Rossini-Oliva S, Franco-Salas A, Perez-Urrestarazu L (2021) Volatile organic compounds removal by means of a felt-based living wall to improve indoor air quality. Atmospheric Pollution Research 12(3):224–229. https://doi.org/10.1016/j.apr.2020.11. 009

[63] Supreeth M (2021) Enhanced remediation of pollutants by microorganisms–plant combination. International Journal of Environmental Science, Technology 19:1–12. https://doi.org/10.1007/ s13762-021-03354-7

[64] Teiri H, Pourzamani H, Hajizadeh Y (2018) Phytoremediation of VOCs from indoor air by ornamental potted plants: a pilot study using a palm species under the controlled environment. Chemosphere 197:375–381. https://doi.org/10.1016/j.chemosphere.2018.01. 078

[65] Teiri H, Pourzamzni H, Hajizadeh Y. (2018). Phytoremediation of formaldehyde from indoor environment by ornamental plants: an approach to promote occupants health. Int J Prev Med;9:70.

[66] Thakur, A. K., & Patel, S. (2023). Indoor Air Quality in Urban India: Current Status, Research Gap, and the Way Forward. Environmental Science & Technology Letters, 10(12), 1146–1158. DOI: 10.1021/acs.estlett.3c00636

[67] Torpy F, Clements N, Pollinger M, Dengel A, Mulvihill I, He C, Irga P (2018) Testing the single-pass VOC removal efficiency of an active green wall using methyl ethyl ketone (MEK). Air Quality, Atmosphere & Health 11(2):163–170. https://doi.org/10.1007/ s11869-017-0518-4

[68] Torpy F, Clements N, Pollinger M, Dengel A, Mulvihill I, He C, Irga P (2018) Testing the single-pass VOC removal efficiency of an active green wall using methyl ethyl ketone (MEK). Air Quality, Atmosphere & Health 11(2):163–170. https://doi.org/10.1007/ s11869-017-0518-4

[69] Treesubsuntorn C, Thiravetyan P (2012) Removal of benzene from indoor air by Dracaena sanderiana: effect of wax, stomata. Atmospheric Environment 57:317–321. https://doi.org/10.1016/j. atmosenv.2012.04.016

[70] U.S. Environmental Protection Agency. Indoor Air Quality. Report on the Environment. 2017.

[71] U.S. Environmental Protection Agency. The Inside Story: A Guide to Indoor Air Quality. 2014.

[72] U.S. Environmental Protection Agency. What is Indoor Air Quality? Fact Sheet. 2025.

[73] Van Tran, V., Park, D., & Lee, Y.-C. (2020). Indoor Air Pollution, Related Human Diseases, and Recent Trends in the Control and Improvement of Indoor Air Quality. International Journal of Environmental Research and Public Health, 17(8), 2927.DOI: 10.3390/ijerph17082927

[74] Wang Z, Pei J, Zhang JS. (2014). Experimental investigation of the formaldehyde removal mechanisms in a dynamic botanical filtration system for indoor air purification. J Hazard Mater; 280:235–43.

[75] Wei X, Lyu S, Yu Y, Wang Z, Liu H, Pan D, Chen J (2017) Phylloremediation of air pollutants: exploiting the potential of plant leaves, leaf-associated microbes. Front Plant Sci 8:1–23.https://doi.org/10.3389/fpls.2017.01318

[76] Weyens, N., Thijs, S., Popek, R., Witters, N., Przybysz, A., Espenshade, J., Gawronska, H., Vangronsveld, J., & Gawronski, S. W. (2015). The role of plant–microbe interactions and their exploitation for phytoremediation of air pollutants. *International Journal of Molecular Sciences, 16*(10), 25576-25604. https://doi.org/10.3390/ijms161025576

[77] Weyens, N.; van der Lelie, D.; Taghavi, S.; Newman, L.; Vangronsveld, J. (2009). Exploiting plant–microbe partnerships for improving biomass production and remediation. *Trends Biotechnol.*, *27*, 591–598

[78] Wolverton BC, Johnson A, Bounds K. (1989). Interior landscape plants for indoor air pollution abatement. NASA John C. Stennis Space Center Science and Technology Laboratory;. 10–11 pp., Final Report

[79] Wolverton BC, McDonald RC, Watkins EA. (1984) Foliage plants for removing indoor air pollutants from energy-efficient homes. Econ. Bot;38:224–8.

[80] Wolverton BC, Wolverton JD (1993) Plants, soil microorganisms: removal of formaldehyde, xylene, ammonia from the indoor environment. Journal of the Mississippi Academy of Sciences 38(2):11–15

[81] Wood RA, Orwell RL, Tarran J, Torpy F, Burchett M (2002) Potted-plant/growth media interactions, capacities for removal of volatiles from indoor air. Journal of Horticultural Science, Biotechnology 77(1):120–129. https://doi.org/10.1080/14620316. 2002.11511467

[82] Xu Z, Qin N, Wang J, Tong H. (2010). Formaldehyde biofiltration as affected by spider plant. Bioresour Technol 101:6930–4.

[83] Xu Z, Wang L, Hou H (2011) Formaldehyde removal by potted plant– soil systems. Journal of Hazardous Materials 192(1):314–318. https://doi.org/10.1016/j.jhazmat.2011.05.020

[84] Yoo MH, Kwon YJ, Son KC, Kays SJ (2006) Efficacy of indoor plants for the removal of single, mixed volatile organic pollutants, physiological effects of the volatiles on the plants. Journal of the American Society for Horticultural Science 131(4):452–458. https://doi.org/10.21273/JASHS.131.4.452

International Journal of Environment, Agriculture and Biotechnology
Vol-11, Issue-5; Sep-Oct, 2026
Peer-Reviewed International Journal
Journal Home Page Available: https://ijeab.com/
Journal DOI: 10.22161/ijeab

Efficacy of Different Botanicals and Insecticide against Chafer Beetles on Jamun (*Syzygium cumini* L.)

A. P. Khating [1], D. S. Mutkule[2], S. B. Shelke[3], K. M. Tokhendra[4], M. P. Satpute[5] and D. K. Thorat[6]

M.Sc. (Agri.) Research Scholar, Department of Entomology, College of Agriculture, Badnapur, VNMKV, Parbhani, Maharashtra, India.
Professor (CAS), Department of Entomology, NARP, Chh. Sambhajinagar, Maharashtra, India.
Senior Research Fellow, National Agricultural Research Project, Chh. Sambhajinagar, Maharashtra, India.
Ph.D. Research Scholar, Department of Entomology, VNMKV, Parbhani, Maharashtra, India.
M.Sc. (Agri.) Research Scholar, Department of Entomology, College of Agriculture, Badnapur, VNMKV, Parbhani, Maharashtra, India.
M.Sc. (Agri.) Research Scholar, Department of Entomology, College of Agriculture, Badnapur, VNMKV, Parbhani, Maharashtra, India.

Received: 08 Sep 2026; Received in revised form: 05 Oct 2026; Accepted: 07 Oct 2026; Available online: 15 Oct 2026
©2026 The Author(s). Published by Infogain Publication. This is an open-access article *under* the CC BY license (https://creativecommons.org/licenses/by/4.0/).

Abstract— *The present investigation was conducted to evaluate the efficacy of different botanical and chemical treatments against chafer beetles infesting jamun (Syzygium cumini L.). Seven treatments, comprising neem oil (2.0 ml/litre), karanj oil (2.0 ml/litre), mahua oil (2.0 ml/litre), Bacillus thuringiensis (2.0 g/litre), neem seed kernel extract (NSKE) 5% (50 g/litre), lambda-cyhalothrin 5% EC (1.0 ml/litre), and an untreated control, were evaluated through three consecutive sprays. The pooled results revealed considerable variation in treatment efficacy against chafer beetles. Among the treatments, lambda-cyhalothrin 5% EC recorded the lowest pooled mean infestation value of 7.47 (15.86), followed by NSKE 5% at 8.68 (17.13), neem oil at 10.07 (18.50), Bacillus thuringiensis at 10.95 (19.32), karanj oil at 11.57 (19.89), and mahua oil at 12.82 (20.98). The untreated control recorded the highest pooled mean value of 17.63 (24.83). The critical difference at the 5% level was 2.87 for the pooled mean, indicating significant differences among treatments. The results demonstrated that lambda-cyhalothrin 5% EC was the most effective treatment for managing chafer beetles on jamun, followed by NSKE 5% and neem oil. Among the botanical treatments, NSKE 5% showed the greatest efficacy.*

Keywords— ***Jamun, Syzygium cuminii, chafer beetle, botanical pesticides, NSKE, Bacillus thuringiensis, lambda-cyhalothrin, pest management.***

I. INTRODUCTION

Jamun (*Syzygium cumini* L.) is an important fruit crop belonging to the family Myrtaceae and is valued for its edible fruits and nutritional and medicinal properties. Several insect pests are associated with jamun and may affect foliage, flowers and fruits. Chafer beetles feed on plant foliage and can cause visible damage that may affect plant vigour. Effective management of these pests is therefore important for maintaining healthy jamun trees. Botanical products such as neem oil, karanj oil, mahua oil and neem seed kernel extract (NSKE), along with microbial biopesticides such as *Bacillus thuringiensis*, may be considered as components of pest management. Chemical insecticides may also provide suppression when used according to approved label directions. The present investigation evaluated selected botanical, microbial and chemical treatments against chafer beetles on jamun under field conditions.

II. MATERIALS AND METHOD

The field experiment was conducted during 2025–26 in a nine-year-old jamun orchard of the variety ‘Kokan Bahadoli’ at the Research Farm, College of Agriculture, Badnapur, Maharashtra. The orchard spacing was 6 m × 6 m and recommended agronomic practices were followed. The management experiment comprised seven treatments arranged in a Randomized Block Design (RBD) with three replications. Three sprays were applied at 15-day intervals.

Table 1. Experimental details

Sr. No.	Particulars	Details
1	Design	RBD
2	Crop	Jamun (*Syzygium cumini* L.)
3	Variety	Kokan Bahadoli
4	Age of orchard	9 years
5	Treatments	07
6	Replications	03
7	Spacing	6 m × 6 m
8	Experimental year	2025–26
9	Number of sprays	03

Table 2. Treatment details

Tr. No.	Botanical / Chemical	Dose per litre of water
T1	Neem oil	2.0 ml
T2	Karanj oil	2.0 ml
T3	Mahua oil	2.0 ml
T4	*Bacillus thuringiensis*	2.0 g
T5	NSKE 5%	50 g
T6	Lambda-cyhalothrin 5% EC	1.0 ml
T7	Untreated control	—

Imposition of Treatments

The seven treatments were imposed as three consecutive sprays at an interval of 15 days. Each treatment was applied at its specified experimental dose, while T7 was maintained as an untreated control. Observations were recorded before and after spraying.

Method of Observations

Chafer beetle infestation was assessed on the selected jamun trees by recording the infestation values before and after the sprays. The treatment data were analysed using analysis of variance (ANOVA) appropriate for a Randomized Block Design. Treatment means were compared using the critical difference (C.D.) at the 5% level of significance. Figures in parentheses are arcsine-transformed values.

RESULTS AND DISCUSSION

The pooled efficacy of three consecutive sprays of the evaluated treatments against chafer beetles on jamun is presented in Table 3. The treatments showed variation in their recorded infestation values. At the initial observation (1 DBS), treatment differences were non-significant (NS). Following the sprays, lower infestation values were recorded in the treated plots, whereas the untreated control retained comparatively high infestation.

Table 3. Pooled efficacy of three consecutive sprays of different botanical treatments against chafer beetles on jamun.

Tr. No.	Botanical / Pesticide	Dose / litre	1 DBS (First spray)	First spray Mean	Second spray Mean	Third spray Mean	Pooled mean of all sprays
T1	Neem oil	2.0 ml	16.97 (24.33)	11.74 (20.04)	9.94 (18.38)	8.54 (16.99)	10.07 (18.50)
T2	Karanj oil	2.0 ml	18.33 (25.35)	13.41 (21.48)	11.47 (19.80)	9.84 (18.28)	11.57 (19.89)
T3	Mahua oil	2.0 ml	18.00 (25.10)	14.71 (22.55)	12.62 (20.81)	11.13 (19.49)	12.82 (20.98)
T4	*Bacillus thuringiensis*	2.0 gm	17.20 (24.50)	13.40 (21.47)	10.44 (18.85)	9.01 (17.47)	10.95 (19.32)
T5	NSKE 5%	50 gm	16.50 (23.97)	10.31 (18.73)	8.32 (16.76)	7.40 (15.79)	8.68 (17.13)
T6	Lambda-cyhalothrin 5% EC	1.0 ml	15.80 (23.42)	8.98 (17.44)	7.03 (15.38)	6.40 (14.65)	7.47 (15.86)

T7	Untreated control	—	16.03 (23.60)	18.37 (25.38)	17.82 (24.97)	16.69 (24.11)	17.63 (24.83)
S.E. ±			1.35	1.05	0.97	0.78	0.93
C.D. at 5%			NS	3.23	2.99	2.40	2.87
C.V. (%)			13.78	13.99	15.10	13.79	14.29

(Figures in parentheses are arcsine-transformed values.)

First spray application

After the first spray, lambda-cyhalothrin 5% EC @ 1.0 ml/litre (T6) recorded the lowest mean infestation of 8.98 (17.44). It was followed by NSKE 5% @ 50 g/litre (T5) with 10.31 (18.73), neem oil @ 2.0 ml/litre (T1) with 11.74 (20.04), *Bacillus thuringiensis* @ 2.0 g/litre (T4) with 13.40 (21.47), karanj oil @ 2.0 ml/litre (T2) with 13.41 (21.48), and mahua oil @ 2.0 ml/litre (T3) with 14.71 (22.55). The untreated control recorded the highest value of 18.37 (25.38). The C.D. at 5% was 3.23.

Second spray application

Following the second spray, lambda-cyhalothrin 5% EC (T6) continued to record the lowest mean infestation of 7.03 (15.38), followed by NSKE 5% (T5) at 8.32 (16.76), neem oil (T1) at 9.94 (18.38), *Bacillus thuringiensis* (T4) at 10.44 (18.85), karanj oil (T2) at 11.47 (19.80), and mahua oil (T3) at 12.62 (20.81). The untreated control recorded 17.82 (24.97). The C.D. at 5% was 2.99.

Third spray application

After the third spray, T6 recorded the lowest mean infestation of 6.40 (14.65), followed by NSKE 5% (T5) at 7.40 (15.79), neem oil (T1) at 8.54 (16.99), *Bacillus thuringiensis* (T4) at 9.01 (17.47), karanj oil (T2) at 9.84 (18.28), and mahua oil (T3) at 11.13 (19.49). The untreated control recorded the highest infestation value of 16.69 (24.11). The C.D. at 5% was 2.40.

Pooled mean

The pooled mean of the three consecutive sprays demonstrated that lambda-cyhalothrin 5% EC @ 1.0 ml/litre (T6) was the most effective treatment, recording the lowest pooled mean infestation of 7.47 (15.86). It was followed by NSKE 5% @ 50 g/litre (T5) at 8.68 (17.13), neem oil @ 2.0 ml/litre (T1) at 10.07 (18.50), *Bacillus thuringiensis* @ 2.0 g/litre (T4) at 10.95 (19.32), karanj oil @ 2.0 ml/litre (T2) at 11.57 (19.89), and mahua oil @ 2.0 ml/litre (T3) at 12.82 (20.98). The untreated control recorded the highest pooled mean of 17.63 (24.83). The pooled C.D. at 5% was 2.87, S.E. ± was 0.93 and C.V. was 14.29%. Among the botanical treatments, NSKE 5% was the most effective, followed by neem oil. Thus, lambda-cyhalothrin 5% EC gave the strongest overall suppression in this experiment, while NSKE 5% was the best-performing botanical option.

III. CONCLUSION

The field evaluation indicated differences among treatments against chafer beetles on jamun. Lambda-cyhalothrin 5% EC @ 1.0 ml/litre recorded the lowest pooled mean infestation of 7.47 (15.86), followed by NSKE 5% @ 50 g/litre with 8.68 (17.13). Among the botanical treatments, NSKE 5% was the most effective, followed by neem oil. The untreated control recorded the highest pooled mean infestation of 17.63 (24.83).

REFERENCES

[1] Gomez, K. A. and Gomez, A. A. (1984). Statistical Procedures for Agricultural Research. John Wiley & Sons.

[2] Kumar, R., Ramamurthy, V. V. and Sharma, G. (2010). Checklist of insects associated with Jamun (*Syzygium cuminii* L) from India. Biological Forum: An International Journal, 2: 1–5.

[3] Sehwag, S. and Das, M. (2014). Nutritive, therapeutic and processing aspects of Jamun, Syzygium cuminii (L.) —An overview. Indian Journal of Natural Products and Resources, 5(4): 295–307.

[4] Singh, S., Singh, A. K., Singh, H. P., Pagle, B. G. and More, T. A. (2011). Jamun booklet. ICAR, New Delhi, pp. 1–46.

[5] Warrier, P. K. (1993). Indian Medicinal Plants: A Compendium of 500 Species. Vol. 5. Orient Blackswan.

International Journal of Environment, Agriculture and Biotechnology
Vol-11, Issue-5; Sep-Oct, 2026
Peer-Reviewed International Journal
Journal Home Page Available: https://ijeab.com/
Journal DOI: 10.22161/ijeab

Evaluation of Mungbean (*Vigna radiata* L.) genotypes for resistance to Mungbean Yellow Mosaic Virus (MYMV) under natural conditions

Lahari Karumuri[1], V. Satya Priya Lalitha[2] and J. Padmavathi[3]

[1]Scientist (Plant Pathology), Acharya N.G. Ranga Agricultural University, Sugarcane Research Station, Vuyyuru-521165, Andhra Pradesh, India
[2]Principal Scientist (Plant Breeding) & Head, Acharya N.G. Ranga Agricultural University, Sugarcane Research Station, Vuyyuru-521165, Andhra Pradesh, India
[3]Scientist (Agronomy), Acharya N.G. Ranga Agricultural University, Agricultural Research Station, Ghantasala-521133, Andhra Pradesh, India

Received: 18 Sep 2026; Received in revised form: 15 Oct 2026; Accepted: 20 Oct 2026; Available online: 29 Oct 2026
©2026 The Author(s). Published by Infogain Publication. This is an open-access article *under* the CC BY license (https://creativecommons.org/licenses/by/4.0/)

Abstract— *Mungbean (Vigna radiata (L.) R. Wilczek) is an essential grain legume crop valued for its nutritional profile, rich protein content, and soil-enriching nitrogen-fixing capacity. Despite the crop's adaptability and rapid growth cycle, Mungbean Yellow Mosaic Virus (MYMV) remains the most economically devastating biotic threat to commercial mungbean production. Consequently, identifying resistant genotypes is essential to develop sustainable disease management strategies n this study, 64 mungbean genotypes, comprising 62 testing entries and two standard checks were evaluated under natural field conditions during summer 2023 to identify potential sources of genetic resistance. Based on disease severity scores, the genotypes were categorized into distinct resistance categories. The screening revealed that 6 entries (GGG 156, GGG 163, GGG 168, GGG 169, GGG 170, and GGG 171) were completely free/immune to the virus. Additionally, 8 genotypes exhibited a highly resistant (HR) reaction, including the resistant check IPM 2-14, while 15 and 12 genotypes were classified as resistant (R) and moderately resistant (MR), respectively. Conversely, 9 genotypes showed moderate susceptibility (MS), 14 genotypes were found susceptible (S) including the susceptible check LGG-450), and no entries fell under the highly susceptible (HS) category. The identification of these stable resistant sources provides valuable donor material for marker-assisted selection and breeding programs aimed at developing MYMV resistant mungbean cultivars.*

Keywords— ***Mungbean (Vigna radiata), Mungbean Yellow Mosaic Virus (MYMV), screening/, Disease resistance***

I. INTRODUCTION

Mungbean (*Vigna radiata* L. Wilczek) is a fast-growing pulse crop with high nutritional and economic importance, widely cultivated across South and Southeast Asia (Mukhtar, S. and Mohamad, E.A.A, 2022). Its grains contain approximately 51% carbohydrates, 24–26% protein, 4% minerals, and 3% vitamins, making it an important dietary protein source in predominantly cereal-based, subtropical diets (Shilpa *et. al.,* 2024). Beyond nutrition, mungbean fixes atmospheric nitrogen through symbiotic root rhizobia, enriching soil fertility In India alone, it was cultivated over 3.787 million hectares during 2023–24 with a total production of 2.916 million tonnes (Kiranakumara *et. al.,* 2025). Mungbean yellow mosaic virus (MYMV) belongs to the genus *Begomovirus* (family *Geminiviridae*) and cause yellow mosaic disease (YMD) across Asian mungbean-growing regions, with MYMV predominant in southern India and MYMIV in northern, central, and eastern India (Bharsakale *et.al.,* 2024).

Yield losses from MYMV range from 10% to 100% depending on the crop growth stage at infection,

virus strain, mungbean genotype, and environmental interactions (Shilpa *et. al.,* 2024). Chemical management of MYMV relies on reducing whitefly vector populations through insecticide sprays which is economically unsustainable and ecologically harmful. Consequently, identifying and breeding inherently resistant host genotypes is the most viable, eco-friendly, and cost-effective strategy to mitigate these viral diseases. This study aims to evaluate and screen diverse mungbean entries to identify reliable sources of resistance against MYMV.

II. MATERIALS AND METHODS

The experiment was conducted under natural field conditions during the summer, 2023. A total of 62 mungbean genotypes along with resistant check (IPM 2-14) and one susceptible check (LGG-450) were evaluated for resistance to mungbean yellow mosaic virus (MYMV) using an Augmented Completely Randomized Block Design (ACRBD) and an infector-row technique, with no insecticide application to allow natural vector build-up and disease spread.

2.1 Disease rating Scale for Scoring Yellow Mosaic Virus Disease (1-9 scale)

Disease severity is typically scored using 1-9 scale to categorize genotypes reaction based on the extent of yellow mosaic symptoms observed on the foliage. The scoring criteria were as follows.

Table 1: The rating scale for scoring Mungbean Yellow Mosaic Virus disease (Alice and Nadarajan, 2007)

Grade	Description	Reaction
1	No visible symptoms on leaves or very minute yellow specks on leaves	Free
2	Small yellow specks with restricted spread covering 0.1-5% leaf area	Highly Resistant (HR)
3	Mottling of leaves covering 6-10% leaf area	Resistant (R)
4	Yellow mottling covering 11-15% leaf area	Moderately resistant (MR)
5	Yellow mottling and discolouration of 15-20% leaf area	Moderately susceptible (MS)
6	Yellow coloration of 21-30% leaves and yellow pods	Susceptible (S)
7	Pronounced yellow mottling and discoloration of leaves and pods, reduction in leaf size and stunting of plants covering 30-50% 0f foliage	Susceptible (S)
8	Severe yellow discoloration of leaves covering 50-75% of foliage, stunting of plants and reduction in pod size	Highly susceptible (HS)
9	Severe yellowing of leaves covering above of foliage, stunting of plants and no pod formation	Highly susceptible (HS)

III. RESULTS AND DISCUSSION

3.1. Phenotypic Evaluation and Disease Progress

Total 62 mungbean entries along with two checks (IPM 2-14 as the resistant check and LGG-450 as the susceptible check) were evaluated under natural field screening conditions during summer, 2023. Phenotypic reactions against the Mungbean Yellow Mosaic Virus (MYMV) were categorized using the 1–9 modified disease rating scale proposed under AICRP on MULLaRP. Disease scoring commenced when more than 80% of the susceptible plants exhibited clear, systemic visual symptoms, ensuring that the phenotypic expressions captured reflected accurate genetic responses under high disease pressure.

The performance of IPM 2-14 as a resistant check (Score 2) validates the reliability of the screening set, as this line has repeatedly been reported as stably resistant across diverse studies and seasons (Kiranakumara *et al.,* 2025). By contrast, the high score of LGG-450 as a susceptible check aligns with standard MYMV screening protocols, where susceptible controls are intentionally included to ensure adequate disease pressure and to discriminate resistance classes reliably (Ramarao *et al.,* 2021).

The evaluation revealed wide phenotypic variation among the tested material, spanning from complete immunity to high susceptibility. Total 62 genotypes were partitioned into different distinct reaction categories (Table 2).

Table 2. Screening of mungbean entries against viral diseases during Summer, 2023

S. No.	Entry	MYMV score (1-9 scale)	S.No.	Entry	MYMV score (1-9 scale)
1	GGG 95	3	33	GGG 144	5
2	GGG 101	3	34	GGG 145	5
3	GGG106	5	35	GGG 146	6
4	GGG107	3	36	GGG 147	3
5	GGG108	3	37	GGG 148	2
6	GGG109	5	38	GGG 149	2
7	GGG110	4	39	GGG 150	3
8	GGG 113	6	40	GGG 151	3
9	GGG 118	6	41	GGG 152	3
10	GGG 119	6	42	GGG 153	4
11	GGG 116	6	43	GGG 154	4
12	GGG 120	6	44	GGG 155	2
13	GGG 121	6	45	GGG 156	1
14	GGG 123	6	46	GGG 157	2
15	GGG 122	5	47	GGG 158	5
16	GGG 124	6	48	GGG 159	4
17	GGG 127	3	49	GGG 160	4
18	GGG 128	4	50	GGG 161	4
19	GGG 129	4	51	GGG 162	7
20	GGG 130	3	52	GGG 163	1
21	GGG 131	6	53	GGG 164	6
22	GGG 132	4	54	GGG 165	5
23	GGG 133	4	55	GGG 166	4
24	GGG 134	3	56	GGG 167	2
25	GGG 136	2	57	GGG 168	1
26	GGG 137	3	58	GGG 169	1
27	GGG 138	2	59	GGG 170	1
28	GGG 139	3	60	GGG 171	1
29	GGG 140	3	61	LGG-460	5
30	GGG 141	3	62	TM 96-2	6
31	GGG 142	5		LGG-450 (S. Check)	7
32	GGG 143	4		IPM 2-14 (R. Check)	2

3.2. Grouping and Distribution of Genotypes based on MYMV Reaction

Among the 62 test entries, 6 entries (GGG 156, GGG 163, GGG 168, GGG 169, GGG 170, and GGG 171) were found to be completely Free/Immune (Grade 1) from the disease, showing no visible symptoms on their foliage. Exceptional field resistance was noted in 7 test entries along with the resistant check IPM 2-14, which were classified as Highly Resistant (Grade 2) due to highly restricted, minor yellow specks occupying less than 5% of the individual leaf

area (GGG 136, GGG 138, GGG 148, GGG 149, GGG 155, GGG 157, and GGG 167) (Table 3).

The largest segment of the resistant block fell under the Resistant (Grade 3) designation, comprising 15 entries that exhibited mottling of leaves covering 6-10% leaf area. Additionally, 12 entries exhibited Moderately Resistant (Grade 4) profiles with scattered yellow patches covering 11–15% of the leaf surfaces.

Table 3. Grouping of mungbean genotypes based on their reaction to MYMV during summer, 2023 under natural field conditions.

Grade	Disease Severity / Reaction	No. of Entries	Entries
1	Free / Immune	6	GGG 156, GGG 163, GGG 168, GGG 169, GGG 170, GGG 171
2	Highly Resistant (HR)	8	GGG 136, GGG 138, GGG 148, GGG 149, GGG 155, GGG 157, GGG 167, **IPM 2-14 (R. Check)**
3	Resistant (R)	15	GGG 95, GGG 101, GGG 107, GGG 108, GGG 127, GGG 130, GGG 134, GGG 137, GGG 139, GGG 140, GGG 141, GGG 147, GGG 150, GGG 151, GGG 152
4	Moderately Resistant (MR)	12	GGG 110, GGG 128, GGG 129, GGG 132, GGG 133, GGG 143, GGG 153, GGG 154, GGG 159, GGG 160, GGG 161, GGG 166
5	Moderately Susceptible (MS)	9	GGG 106, GGG 109, GGG 122, GGG 144, GGG 142, GGG 145, GGG 158, GGG 165, LGG-460
6	Susceptible (S)	12	GGG 113, GGG 116, GGG 118, GGG 119, GGG 120, GGG 121, GGG 123, GGG 124, GGG 131, GGG 146, GGG 164, TM 96-2,
7	Susceptible (S)	2	GGG 162, **LGG-450 (S. Check)**
8-9	Highly Susceptible (HS)	0	None
	Total	**64**	**(62 Entries + 2 Checks)**

Vulnerability to the virus expanded within the remaining germplasm lines. Eight genotypes including the commercial line LGG-460 manifested moderately susceptible (Grade 5) symptoms, showcasing severe chlorotic patches across 15–20% of their canopy. Definitive, heavy systemic breakdown was verified in 14 genotypes clustered into the Susceptible (Grades 6 and 7) group. Genotypes in Grade 6 suffered from vast chlorosis (21–30% leaf area) alongside distinct yellowing of the pods, whereas GGG 162 and the check LGG-450 (Grade 7) exhibited severe plant stunting and drastic leaf shrinkage. Notably, no genotype advanced into the Highly Susceptible bounds (Grades 8 and 9), indicating the absence of total reproductive failure or absolute biomass collapse among the screened entries.

The identification of a distinct subset of resistant genotypes within a broader population characterized by intermediate and susceptible reactions is a central finding of this study. This pattern aligns with repeated field evaluations demonstrating that natural MYMV resistance is relatively uncommon, with the majority of germplasm tending to cluster into susceptible, highly susceptible, or intermediate categories under natural epiphytotic conditions (Jyothi *et al.,* 2020).

The presence of entries scoring 1 and 2 holds considerable agricultural importance because host resistance remains the most practical and economical strategy for managing MYMV, a begomovirus transmitted by *Bemisia tabaci* that is capable of causing severe yield losses in mungbean. Multiple studies therefore recommend that field-identified resistant lines be advanced as donor parents for breeding programs, quantitative trait locus (QTL) discovery, marker development, and multi-location validation, rather than being judged from a single season alone (Ambarish *et al.,* 2023).

Some genotype-specific disagreements with existing literature are nevertheless expected. For example, LGG-460 has been reported as susceptible in one inheritance study but moderately resistant in another field screening, demonstrating that genotypic reactions can shift with location, season, inoculum load, and vector pressure

(Saable *et al.,* 2024). Similar instability has been documented more broadly, field resistance often weakens under cage inoculation, whitefly-mediated artificial transmission, graft inoculation, or diverse hotspot environments, indicating that symptom-based field resistance typically reflects partial resistance rather than complete immunity (Madhumitha *et al.,* 2020).

Although the biological basis of resistance in the superior entries cannot be inferred directly from the score table alone, prior work suggests that resistant genotypes frequently combine favorable morphological and biochemical traits. These include higher levels of phenolics, tannins, trichome density, and stronger antioxidant responses, coupled with lower sugar content and reduced stomatal density-related susceptibility signals (Kamireddy *et al.,* 2025). Recent marker studies further show that field resistance can be strengthened through molecular confirmation, as phenotypically identified resistant genotypes have been successfully validated using linked markers or resistance gene analogs (Dharajiya *et al.,* 2021).

Finally, inheritance studies explain why stable resistance is difficult to recover consistently. Evidence remains mixed across genetic backgrounds, with reports supporting either two dominant genes or a single recessive gene. This indicates that resistance architecture is genotype-dependent, which likely contributes to variable expression across populations and environments (Mahalingam *et al.,* 2018). This complexity, together with virus variation and quantitative effects, is a key reason why repeated screening across years and locations is necessary before nominating entries as durable MYMV-resistant donors (Saable *et al.,* 2024).

IV. CONCLUSION

In summary, the MYMV screening identified multiple resistant entries, most notably, six entries (GGG 156, GGG 163, GGG 168, GGG 169, GGG 170, and GGG 171) demonstrated complete immunity (Grade 1) with zero visible symptoms under high natural vector pressure while, confirming strong susceptibility in GGG 162 and LGG-450. These elite immune lines, alongside the seven highly resistant genotypes, are prime candidates for direct field deployment and parental selection. Utilizing these genetic resources in upcoming hybridization programs will accelerate the development of high-yielding, climate-resilient mungbean cultivars with durable resistance to MYMV. These preliminary resistant sources that warrant replicated, multi-season, and multi-location validation with phenotypic and molecular confirmation before use in resistance breeding.

REFERENCES

[1] Alice D and Nadarajan N. (2007). Pulses: Screening techniques and assessment for disease resistance. All India Coordinated Research Project on MULLaRP-Tamil NaduAgricultural University. Coimbatore: Kasturi Graphics and Printers; p. 24.

[2] Ambarish, S., Kalleshwaraswamy, C.M. & Venkataravanappa, V. (2023).Identification of source of resistance in greengram germplasm against Mungbean yellow mosaic virus and its vector whitefly, *Bemisia tabaci* (Gennadius). *Indian Phytopathology,* **76**: 1073–1081.

[3] Bharsakale, R.D., Wankhade, D.J., Jadhav, P.K., Gholave, K.K., Deshmukh, A.S., Chavan, R.L. and Hinge, V.R. (2024). Coat protein-based molecular characterization of the mungbean yellow mosaic virus (MYMV) infected cowpea (V. unguiculata (L.) Walp.) in Maharashtra. *International Journal of Advanced Biochemistry Research,* .8(2):431-440.

[4] Dharajiya, D.T., Tiwari, K.K. & Ravindrababu, Y. (2021) Identification of resistant sources of mungbean [*Vigna radiata* (L.) Wilczek] against *mungbean yellow mosaic virus (MYMV)* by field evaluation and linked molecular markers. *Vegetos,* 34:814–821.

[5] Gokidi, Yugandhar, M. Singh, Ashok Singamsetti, and Swathi Lekkala. (2021).Screening of mungbean *(Vigna radiata L. Wilczek)* genotypes for resistance to *Mungbean Yellow Mosaic Virus under* field condition. *International Journal of Plant & Soil Science.* 33(7): 39-45.

[6] Jyothi, N., Patil, B.R., Lokeshkumar, B.M. (2020). Screening of mungbean germplasm against mungbean yellow mosaic virus under natural condition. *International Journal of Chemical Studies,* 8(4):2135-2137.

[7] Kamireddy, R., Lakra, N., Ahlawat, Y. K., Sundaramoorthy, M., Menon, S. V., Manorama, K., Sharma, N., Malik, A., & Upadhyay, S. K. (2025). Integrated morphological, biochemical and molecular screening of mungbean (*Vigna radiata* L.) genotypes for mungbean yellow mosaic virus (MYMV) resistance. *Plant physiology and biochemistry,* 229(C):110596.

[8] Kiranakumara, D. M., Bhat, S., Sridevi, O., Krishnaraj, P. U., & Saable, P. R. (2025). Assessment of mungbean genotypes for durable resistance to mungbean yellow mosaic virus (MYMV). *Journal of Farm Sciences*, 38(04):370-374.

[9] Madhumitha, B., Aiyanathan, K.E.A., Raveendran, M. and Sudha, M. (2022). Identification and Confirmation of Resistance in Mungbean [Vigna radiata (L.)

Wilczek] Derivatives to Mungbean Yellow Mosaic Virus (MYMV). *Legume Research*. 45(1): 122-127.

[10] Mahalingam, A., Satya, V.K.., Manivannan, N., Lakshmi Narayanan, S. and Sathya, P. (2018). Inheritance of Mungbean Yellow Mosaic Virus Disease Resistance in Greengram [*Vigna radiata* (L.) Wilczek]. *International Journal of Current Microbiology and Applied Sciences*, 7(01): 880-885.

[11] Mukhtar, S. and Mohamad, E.A.A. (2022). Perspectives of molecular marker-assisted breeding in mungbean (*Vigna radiata* L.) to develop resistance for mungbean yellow mosaic virus (MYMV) disease. *Phytopathogenomics and Disease Control,* 1(1):1-24.

[12] Ramarao G., Satishbabu J., Harisatyanarayana N., Adinarayana M. (2023). Morpho-physiological and Biochemical Variability in Greengram [*Vigna radiata* (L.) Wilczek] Varieties for Mungbean Yellow Mosaic Virus (MYMV) Resistance under Natural Field Conditions. *Legume Research*, 46(7): 934-939.

[13] Saable, P., Biradar, S., Shinde, P., Manu, B., Kamati, C., Nair, R., Prajapati, U., Pratap, A., Akram, M., & K. (2024). Response of mungbean genotypes for resistance against mungbean yellow mosaic virus. *Journal of Food Legumes*. 37(1): 90-94.

[14] Shilpa, M., B. Manjunath, C.M. Sunil, Devaraja, Gayathri, and N. Nagaraju (2024). Enhancing Mungbean Resistance to Yellow Mosaic Virus: Insights from Biochemical Studies.*Journal of Scientific Research and Reports,* 30 (7):1100-1107.

International Journal of Environment, Agriculture and Biotechnology
Vol-11, Issue-5; Sep-Oct, 2026
Peer-Reviewed International Journal
Journal Home Page Available: https://ijeab.com/
Journal DOI: 10.22161/ijeab

Parcel-Level Land Cover and Soil Fertility Mapping using Multi-Sensor Satellite Imagery, Cadastral Overlays and Soil Health Card Records in a Semi-Arid Taluka of Saurashtra, Gujarat, India

Hardeep Kumar*[1], N. K. Gontia[2], Pritam Das[2] and P. A. Pandya[2]

[1]Gujarat State Watershed Management Agency (GSWMA), Gandhinagar, Gujarat, India
[2]Junagadh Agricultural Univrsity, Junagadh, Gujarat, India
*Corresponding Author Email:- hardeep47@gmail.com

Received: 23 Sep 2026; Received in revised form: 19 Oct 2026; Accepted: 25 Oct 2026; Available online: 31 Oct 2026
©2026 The Author(s). Published by Infogain Publication. This is an open-access article *under* the CC BY license (https://creativecommons.org/licenses/by/4.0/)

Abstract— *Reliable, spatially explicit information on land cover and soil fertility is a prerequisite for micro-level planning of land and water resources in rainfed, groundwater-dependent agricultural regions. This study demonstrates a workflow that links multi-sensor Indian Remote Sensing satellite data, digitised cadastral records and Soil Health Card (SHC) data for Amreli Taluka (83,112 ha), Saurashtra, Gujarat. CARTOSAT-1 panchromatic, IRS-P6 LISS-III and LISS-IV scenes were georeferenced and overlaid with village boundaries and survey-number polygons for seven randomly selected villages. A LISS-III scene of 31 January 2009 was classified with a maximum-likelihood supervised classifier using training signatures derived from a false colour composite, and the result was evaluated with a confusion matrix and the kappa coefficient. Nutrient status (N, P, K, organic carbon) and soil reaction (pH, electrical conductivity) from the SHCs were joined to cadastral polygons and mapped at survey-number level for Sanosara village. Dense, medium and poor agriculture occupied 28.27%, 22.24% and 14.23% of the taluka, respectively, which together with fallow land (16.81%) accounted for 81.55% of the area; habitation covered 12.01%, waste or eroded land 4.73% and water bodies 1.71%. The summary statistics reported with the matrix are an average accuracy of 83.08%, an overall accuracy of 79.32% and a kappa coefficient of 0.754 (standard deviation 0.00165; 95% confidence limit ±0.00324). SHC records showed predominantly medium nitrogen, low phosphorus and high potash, with normal pH (6.5-8.2) and electrical conductivity below 1 dS m^{-1}. The cadastral-level approach converts farm-scale soil data into mappable, plot-specific recommendations, but accuracy reporting, class design and sampling density need strengthening before the maps are used operationally. The workflow is transferable to other talukas where SHC and cadastral data exist.*

Keywords— ***IRS-P6 LISS-III, Maximum likelihood classification, Micro-level planning, Soil fertility mapping***

HIGHLIGHTS

- Cadastral overlays on multi-sensor satellite imagery enable plot-level visibility.
- Cultivated land covers 64.73%, but dense-medium agriculture confusion limits accuracy.
- Soil Health Cards show low phosphorus, medium nitrogen, high potash.

I. INTRODUCTION

Land and water are the two resources on which dryland agriculture in western India depends, and both are under increasing pressure from population growth, variable

monsoon rainfall and declining groundwater tables. Planning for their sustainable use has traditionally been done at the macro level, with district or state aggregates guiding investment. Such aggregates conceal the spatial heterogeneity that determines whether a particular field, village or cluster of villages can sustain a given cropping system. Decentralised, village-level or "micro-level" planning therefore needs information at a resolution fine enough to resolve individual land parcels and to link them to the farmers who manage them. India has a long record of remote-sensing-based resource inventories (Kasturirangan, 1995; Puri, 2007), and local-level planning has been supported by natural-resource databases and decision support systems (Acharya et al., 2011; Gupta et al., 2001; Bariar et al., 2004), by watershed-based resource management (Krishna, 1996) and, through watershed development projects, by programmes whose performance has been formally evaluated (Kerr et al., 2002).

Satellite remote sensing has long been the main source of synoptic land cover information, and the methods used to turn imagery into thematic maps have evolved from visual interpretation and per-pixel supervised and unsupervised classifiers (Lillesand et al., 2015) to ensemble learners and deep neural networks. Reviews of land use and land cover (LULC) classification emphasise that, despite decades of progress, issues of multi-source, multi-temporal and multi-level analysis, robustness, quality and scalability remain open (Macarringue et al., 2022). Deep-learning approaches now dominate the recent literature and offer clear gains in accuracy where large labelled datasets exist, yet they depend on training samples that are scarce for many agricultural regions, and classic algorithms such as maximum likelihood, support vector machines and decision trees remain widely used (Zhao et al., 2023; Digra et al., 2022). For operational work in data-poor districts, where field-verified samples are limited and analysts need transparent, reproducible procedures, the supervised statistical classifier retains practical value, provided its accuracy is reported honestly.

A second strand of work concerns the mapping of soil properties. Digital soil mapping has matured around the idea of using remote sensing and other environmental covariates either as a substitute for analytical measurements or as predictors of soil-forming factors (Richer-de-Forges et al., 2023). A global review of broad-scale digital soil mapping found that most studies targeted soil organic matter or carbon, that texture fractions were comparatively well predicted, and that soil depth and coarse fragments were poorly predicted; the authors called for rescued legacy data, better sampling designs and representative covariates (Chen et al., 2022). These findings are relevant to India, where an unusually dense source of measured soil data already exists in the form of Soil Health Cards. The Soil Health Card scheme, launched nationally in 2015 after earlier state-level initiatives, provides plot-wise nutrient status and fertiliser recommendations; a recent systematic review reports that the scheme has been associated with yield increases of 5-6% and reductions in chemical fertiliser use of 8-10%, while also identifying institutional gaps that limit its impact (Timilsina et al., 2025). The idea of a soil health card as a decision-support tool for balanced fertilisation predates the national scheme (Thiyageshwari et al., 2006). Because each card is tied to a survey number, the data are intrinsically cadastral and can be mapped directly if the cadastral polygons are digitised and georeferenced. Where point observations must instead be converted into continuous surfaces, geostatistical interpolation such as kriging has long been used (Largueche, 2006), but it needs a sample that is dense and representative enough to support the interpolation.

The bridge between parcel-scale records and satellite imagery is the agricultural parcel itself. A comprehensive review of agricultural parcel and boundary delineation notes that the number of studies using very high resolution imagery has grown exponentially since 2019, that satellite imagery supplies the large majority of data sources, and that smallholder systems with small, irregular and fragmented fields remain the hardest setting for automated delineation (Zheng et al., 2026). Cadastral boundaries, where they exist, offer a stable alternative to automatically derived boundaries, but they must be registered precisely to imagery for the combination to be useful. Systematic reviews of crop mapping and crop monitoring similarly stress the value of combining multiple sensors and ancillary information for agricultural applications (Alami Machichi et al., 2023; Joshi et al., 2023; Wu et al., 2023). Remote sensing has also been applied to irrigated agriculture for several decades, with examples ranging from research to practical use (Bastiaanssen et al., 2000).

Against this background, the present study documents and critically evaluates a workflow applied to Amreli Taluka in the Saurashtra region of Gujarat. The objectives were (i) to georeference and overlay CARTOSAT-1, IRS-P6 LISS-III and LISS-IV imagery with cadastral and village boundaries so that individual survey numbers can be located on the images; (ii) to derive a land use/land cover map for the taluka from a LISS-III scene using a supervised maximum-likelihood classifier and to quantify its accuracy; and (iii) to map nutrient status and soil reaction from Soil Health Card records at survey-number level and to summarise the status of seven selected villages. The intention is not only to report the maps but also to examine how reliable they are and what is needed to make such products dependable inputs to village-level planning.

II. MATERIALS AND METHODS

Study area

Amreli Taluka lies in Amreli District in the Saurashtra peninsula of Gujarat, between 21°24′ and 21°43′ N latitude and 70°59′ and 71°24′ E longitude (Fig. 1), with a geographical areas of 83,112 ha. About 80% of the population depends on agriculture as its main occupation and groundwater is the principal irrigation source. The area is predominantly dry-land farmed, with groundnut and sesame as the main kharif crops, wheat and coriander in the rabi season, summer sesame in irrigated pockets, and vegetables and orchards (coconut, mango and sapota) on the remaining cropland. The taluka is crossed by a network of roads and a railway line and contains numerous settlements; Fig. 2 shows the transport network, settlement points and village boundaries on which the cadastral work was based.

Seven villages were selected at random for detailed parcel-level work, *i.e.*, Bhandariya Mota, Sanosara, Vadhera, Rangapur, Navakhijadiya, Bhandariya Nana and Mangvapal (Fig. 3). Sanosara was used as the demonstration village for survey-number-level overlays and nutrient maps.

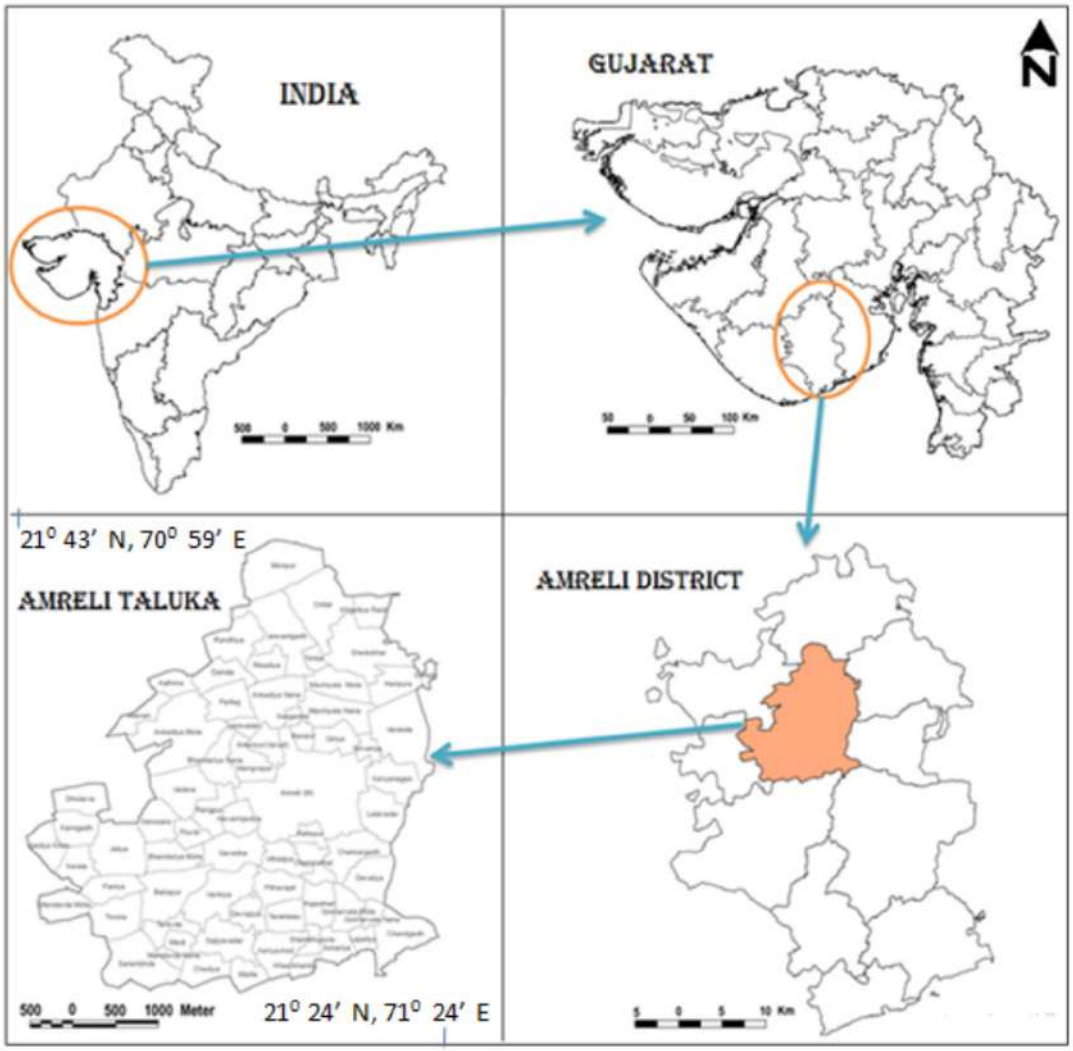


Fig. 1. Location of Amreli Taluka within India, Gujarat state and Amreli District.

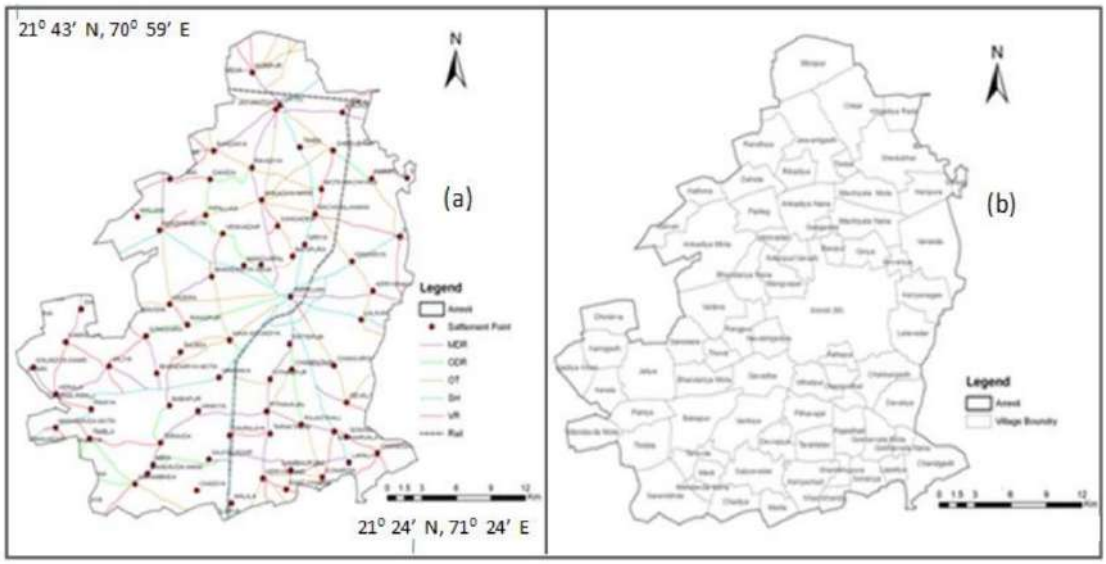


Fig. 2. (a) Roads, railway and settlement points and (b) village boundaries of Amreli Taluka.

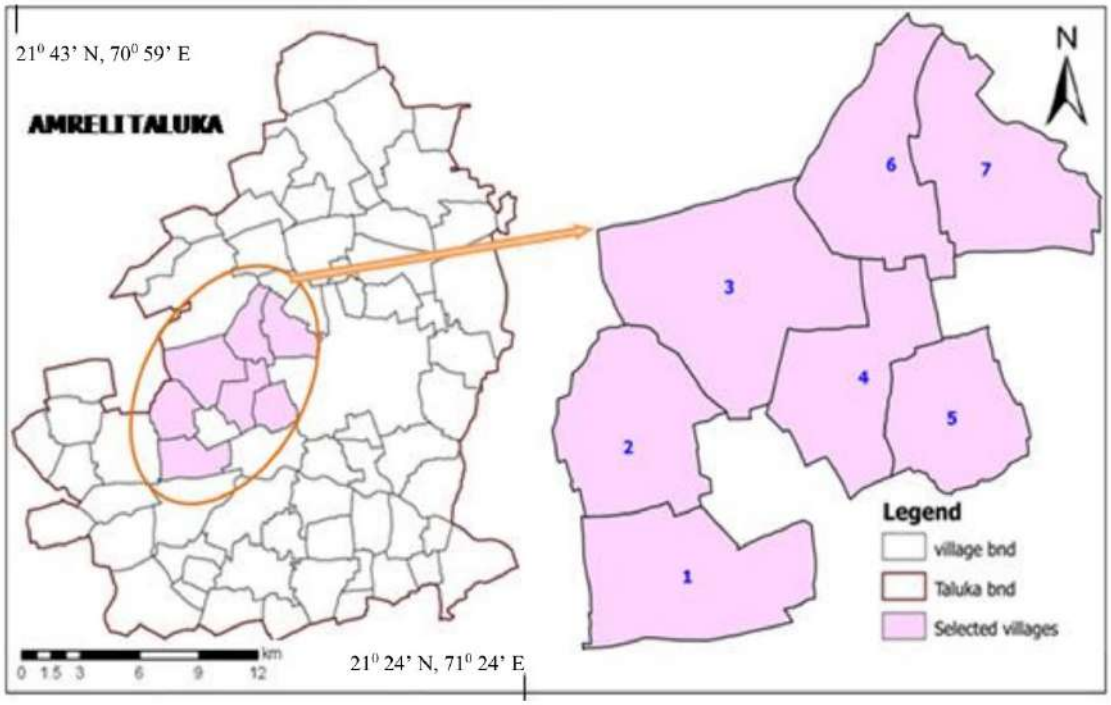


Fig. 3. Layout of the seven selected villages within Amreli Taluka (1. Bhandariya Mota, 2. Sanosara, 3. Vadhera, 4. Rangapur, 5. Navakhijadiya, 6. Bhandariya Nana, 7. Mangvapal).

Satellite and ancillary data

Three Indian Remote Sensing data types were used (Table 1). CARTOSAT-1 panchromatic data (nominal spatial resolution of 2.5 m) supplied the finest geometric detail for locating plot boundaries. IRS-P6 (Resourcesat-1) LISS-IV scenes (nominal 5.8 m multispectral) provided intermediate resolution, and IRS-P6 LISS-III (nominal 23.5 m, four spectral bands) was used for taluka-wide classification. All scenes were procured from the Bhaskaracharya Institute for Space Applications and Geo-informatics (BISAG), Gandhinagar. Google Earth Pro images were consulted as a visual reference. A district map of Amreli provided district, taluka and village boundaries, and scanned cadastral sheets gave village boundaries and survey numbers for the selected villages.

Table 1: Satellite data used in the study.

Sr. no.	Satellite	Sensor	Path/Row	Date of pass
1	CARTOSAT-1	PAN	502/297	17 Feb 2006
2	CARTOSAT-1	PAN	502/298	17 Feb 2006
3	IRS-P6	LISS-III	92/57	31 Jan 2009
4	IRS-P6	LISS-IV	201/102	12 May 2008
5	IRS-P6	LISS-IV	202/80	24 Feb 2009
6	IRS-P6	LISS-IV	202/96	31 Jan 2009
7	IRS-P6	LISS-IV	203/57	30 Mar 2009

Soil Health Card data for the seven villages were downloaded from the Government of Gujarat web site. Each card records the soil type, the fertility status of the plot (nitrogen, phosphorus, potash and organic carbon, in qualitative classes), pH and electrical conductivity, and the name of the farmer who holds the survey number. The scheme was started in 2008-09 on a per-plot basis, so the cards provide a soil record for individual fields.

Georeferencing and cadastral digitisation

Scanned maps were registered to the satellite images and converted to vector data by on-screen digitisation. In ArcGIS 9.2, each scanned sheet was added as a raster, a polygon shapefile was created, and village and survey-number boundaries were traced with the editing tools using edge-snapping to reduce digitising error. Image geometry was handled in PCI Geomatica 10.1, where an affine transformation model was applied to the cadastral sheets and image scenes were clipped to the study area through a vector mask and subset dialogue. After registration, the cadastral vectors were superimposed on each image and checked visually so that every survey-number boundary coincided with a field boundary or road visible on the imagery. Overlays were produced for all three sensors to allow a like-for-like comparison of how well each sensor resolves plot geometry. Integrating spatial databases of this kind with quantitative models is a long-standing theme in land resource assessment (Stehman, 1997).

Image classification

Land cover was derived from the LISS-III scene of 31 January 2009, which falls at the end of the May-January cotton growing season analysed in the companion study. A false colour composite (FCC) was displayed and used to select training polygons for seven information classes: water bodies, dense agriculture, medium agriculture, poor agriculture, fallow land, habitation or establishment, and waste or eroded land. The signature of each class, comprising mean, standard deviation, variance and the covariance matrix of the selected pixels in the five channels held in the signature file, was inspected for separability. Dense agriculture and fallow land were each split into two spectral sub-classes during training so that internal spectral variability was represented. The image was then classified using the maximum-likelihood decision rule, in which each pixel is assigned to the class for which its probability of membership, assuming a multivariate normal distribution, is highest (Lillesand et al., 2015). The methods chapter of the source thesis also describes K-means clustering as a classification option, but the results and abstract report the supervised maximum-likelihood map, which was therefore adopted here. Class areas were extracted from the attribute table of the classified raster using the pixel size of the scene.

Accuracy assessment

Classification accuracy was evaluated with an error (confusion) matrix in which rows represent reference classes and columns the mapped classes, with the percentage of pixels of each reference class falling into each mapped class reported. The diagonal elements give per-class accuracy. Overall measures and the kappa coefficient of agreement with its confidence limits were computed from the matrix. Because the thesis from which the data derive reports different values for “average” and “overall” accuracy, both are reported below and an independent pixel-weighted recalculation from the tabulated row percentages was added as a consistency check. Standard treatments of thematic accuracy recommend reporting the full confusion matrix and per-class accuracy alongside any summary index (Stehman, 1997), and this principle was followed here.

Mapping soil fertility and reaction from Soil Health Cards

For each village, the SHC records were keyed to survey numbers and joined to the digitised survey-number polygons through a common identifier. Nutrient classes

were retained as reported (nitrogen, phosphorus and potash as low, medium or high; organic carbon as low, medium or optimum; pH as normal within 6.5-8.2; electrical conductivity as normal below 1 dS m^{-1}). Polygons with an SHC record were coloured by class and displayed on the CARTOSAT-1 image together with all survey-number boundaries, so that polygons without a card remain visible as unmapped. This produced one map per attribute for Sanosara village. A village-level summary was prepared by recording the dominant class of each nutrient in the seven villages. No spatial interpolation was applied, so unsampled plots remain unmapped instead of being assigned values by methods such as kriging (Largueche, 2006). The overall methodology is presented in Fig. 4.

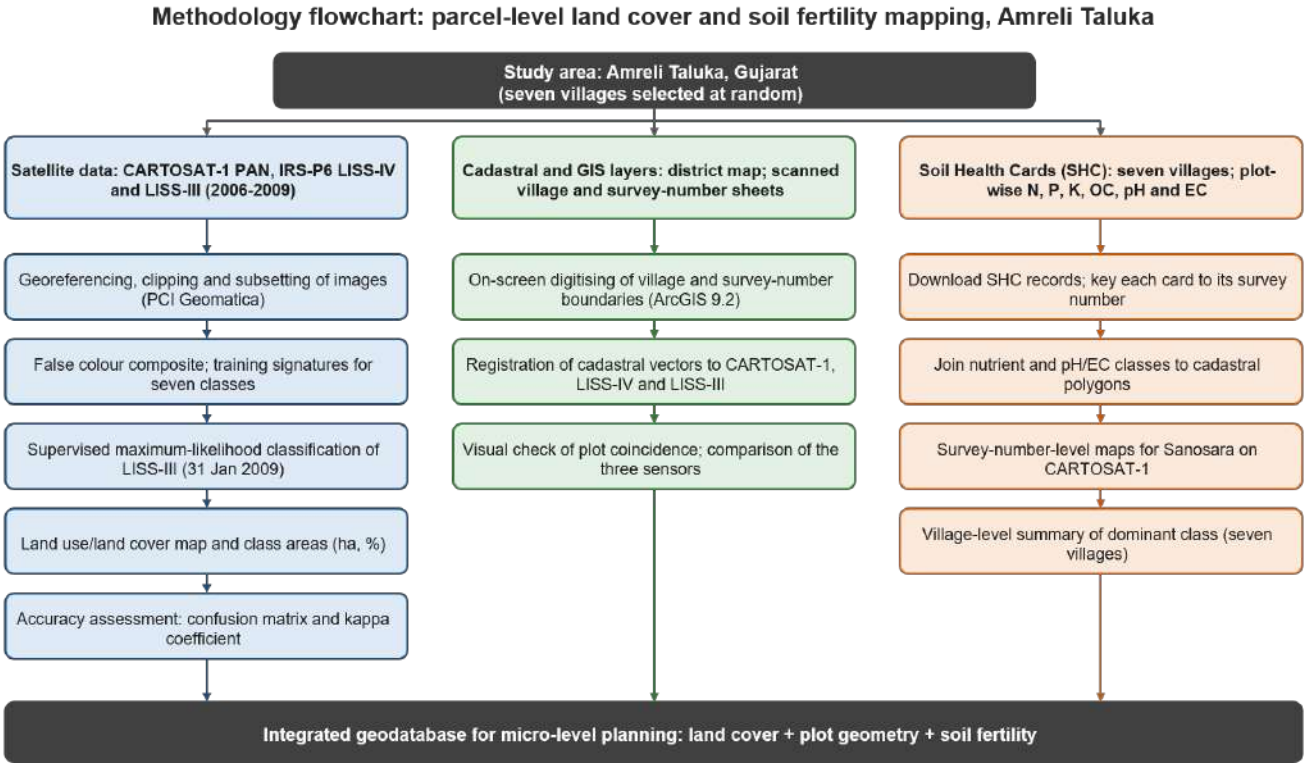


Fig. 4. The overall methodology adopted in this study

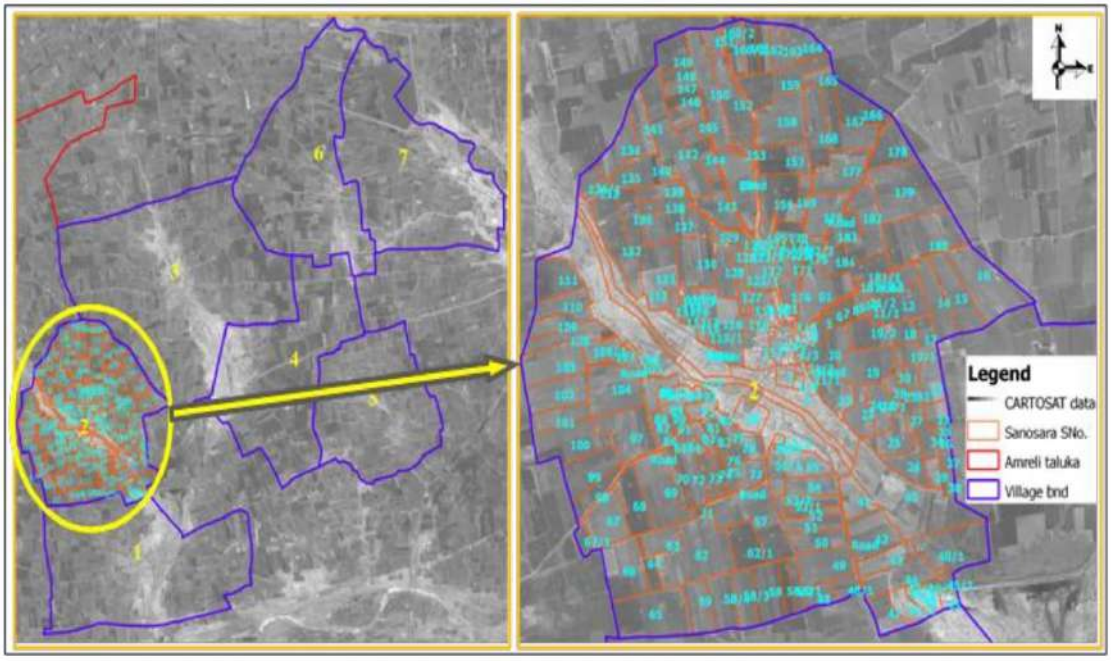


Fig. 5. Cadastral map of Sanosara village with survey numbers superimposed on CARTOSAT-1 data

III. RESULTS AND DISCUSSION

Multi-sensor overlays and plot-level visibility

Overlaying the village boundaries and survey-number polygons on the three sensors showed clear differences in how well plots could be recognised. On CARTOSAT-1 (Fig. 5) the individual field patterns, tracks, the drainage line crossing Sanosara and the village built-up core were easily identified, and each survey-number polygon could be matched to a visible field unit. On LISS-III (Fig. 6) the cadastral grid was much finer than the pixel size, so that a single pixel frequently spanned two or more survey numbers. On LISS-IV (Fig. 7) larger plots were distinguishable, though small plots and narrow strips were mixed.

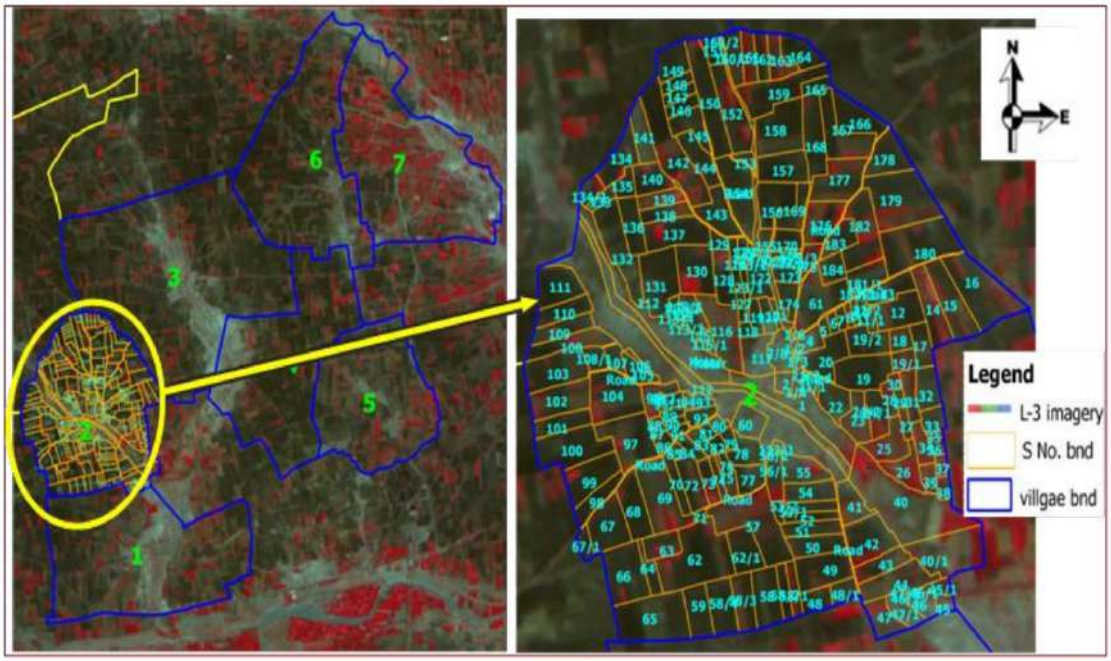


Fig. 6. Cadastral map of Sanosara village with survey numbers superimposed on the LISS-III image

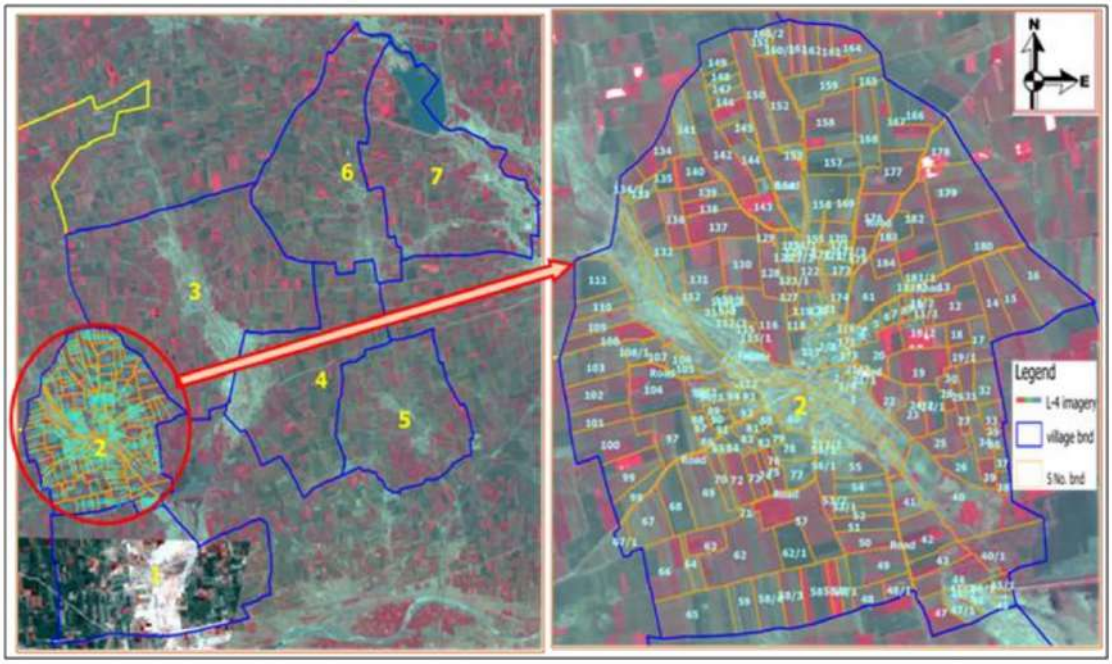


Fig. 7. Cadastral map of Sanosara village with survey numbers superimposed on the LISS-IV image

This ordering is consistent with the nominal resolutions of the sensors and with the general finding of the parcel-delineation literature that spatial resolution is the primary determinant of recoverable geometric information in fragmented smallholder landscapes (Zheng et al., 2026). The practical consequence is a division of labour: LISS-III is adequate for a taluka-wide land cover inventory in which the mapping unit is a class patch, whereas plot-level work needs CARTOSAT-1 or LISS-IV, at least as a visual backdrop. A fused product, in which the multispectral information of LISS-IV or LISS-III is sharpened with the panchromatic CARTOSAT-1 band, would be the logical next step and corresponds to the multi-source data integration that reviews identify as a continuing challenge (Macarringue et al., 2022; Zheng et al., 2026). The present study did not carry out fusion, and the three overlays were interpreted separately.

A caveat applies to all overlays. The CARTOSAT-1 scene dates from February 2006 and the cadastral maps from earlier surveys, whereas the SHC records were collected after 2008. Field amalgamation, subdivision and changes in tracks over a three-year gap can introduce small mismatches between polygons and what is visible on the image. Visual coincidence was verified, but no positional error statistic, such as root-mean-square error against ground control points, is available.

Training signatures and class separability

The signature statistics of the training classes are shown in Fig. 8. The mean digital numbers in the five channels differ markedly between classes. Water bodies and habitation have distinct channel means, and the sub-classes of dense agriculture, fallow land and medium agriculture differ especially in the near-infrared channel, the channel that captures the strong reflectance of healthy vegetation. Standard deviations are small relative to the differences between class means for most classes, which indicates compact training clusters. The two dense-agriculture signatures, trained on 2,935 and 594 sample pixels respectively in the displayed statistics, illustrate how a single information class can contain more than one spectral population; this decision to split the class is revisited when accuracy is discussed.

Land use and land cover of Amreli Taluka

The false colour composite and the supervised classification are shown side by side in Fig. 9. In the FCC, dense healthy vegetation appears in red tones, fallow and bare surfaces in light cyan and white, and water as dark blue to black. The classified map reproduces this pattern, with the drainage network, the larger settlements and the fallow land of the southern part of the taluka clearly delineated.



Fig.8. Training signature statistics (mean and standard deviation by channel) for the land cover classes derived from the LISS-III image

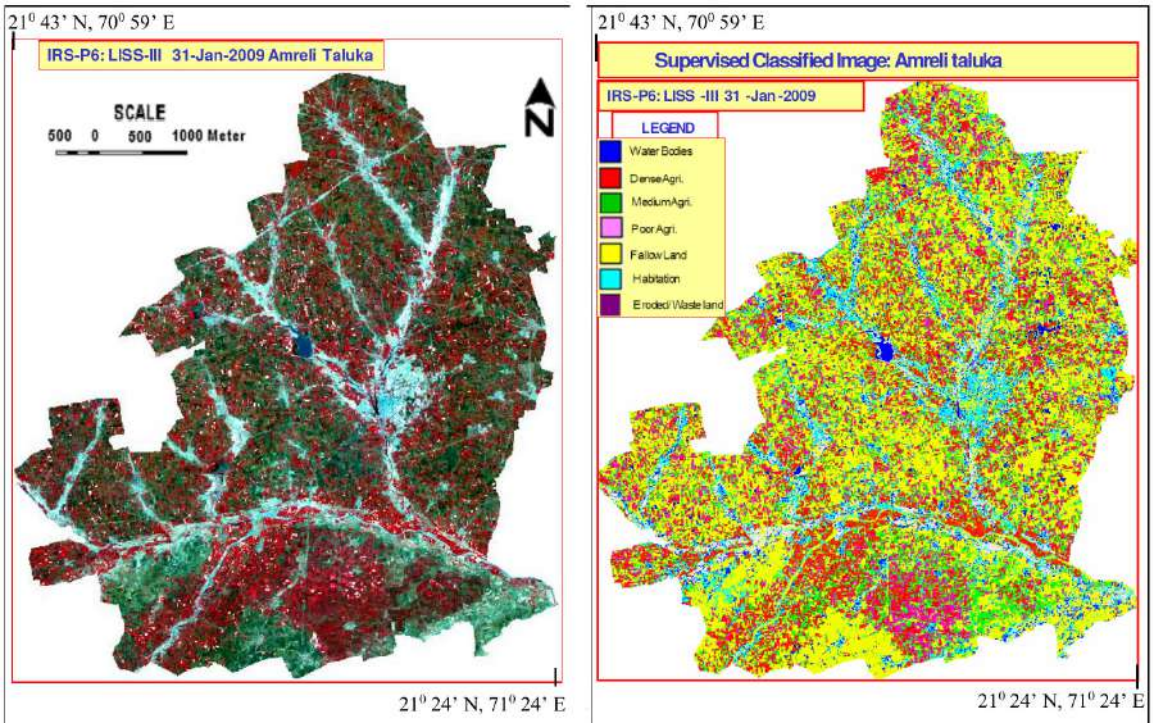


Fig. 9. IRS-P6 LISS-III false colour composite of 31 January 2009 (left) and the supervised land use/land cover classification (right) of Amreli Taluka

Table 2: Land use/land cover classes of Amreli Taluka derived from the LISS-III image of 31 January 2009

Class	Area (ha)	Share of taluka (%)	Share of mapped agricultural and fallow land (%)
Water bodies	1,425	1.71	-
Dense agriculture	23,493	28.27	34.7
Medium agriculture	18,484	22.24	27.3
Poor agriculture	11,825	14.23	17.4
Fallow land	13,974	16.81	20.6
Habitation/establishment	9,980	12.01	-
Waste/eroded land	3,931	4.73	-
Total	83,112	100.00	100.0

Cultivated land, defined as dense, medium and poor agriculture, covered 53,802 ha (64.73% of the taluka), and with fallow land the agricultural land base reached 67,776 ha (81.55%). Habitation, mainly the many small villages and the town of Amreli, occupied 12.01% of the taluka, a share that is high for a rural taluka and that reflects the dense network of settlements visible in Fig. 2. Land-cover maps of this kind can be repeated at later dates to follow land development over time, as has been done for urban expansion elsewhere (Markon, 2003). Waste and eroded land were limited to 4.73%, and water bodies, mostly ponds and submerged areas, to 1.71%.

The sub-division of cultivated land by vegetation density deserves a careful reading. Of the cultivated area, dense agriculture accounts for 43.7%, medium for 34.4% and poor for 22.0%. These shares differ from the 60%, 30% and 10% quoted in the original thesis narrative, which cannot be

reproduced from the tabulated areas; the table values are used here. Because the image was acquired on 31 January, the "dense" class represents fields with high canopy vigour at that date, which may include cotton and other irrigated crops. Vigour classes on a single date should not be read as crop-type areas, and any statement about the area under a particular crop would require time-series data and field verification.

The 16.81% of fallow land recorded in January needs similar caution. Part of it may be fields harvested early, fields awaiting rabi sowing under residual moisture, or land left idle for lack of irrigation. Because rainfed fields in Saurashtra are often sown only once in the monsoon, high January fallow in a dry-land taluka is plausible, but a second date in the rabi or summer season would be needed to distinguish permanent fallow from seasonal fallow.

Classification accuracy

Table 3 condenses the confusion matrix into per-class accuracy. Most classes were correctly classified in 83-91% of reference pixels. Water bodies (87.72%), habitation (85.49%), waste or eroded land (85.94%), medium agriculture (85.76%), poor agriculture (83.36%), fallow land (88.53% and 90.79% for the two sub-classes) and the first dense-agriculture sub-class (88.01%) all met or approached the accuracy thresholds commonly accepted for thematic maps. The principal exception is the second dense-agriculture sub-class, which was correctly assigned in only 35.19% of its 17,202 reference pixels, with 52.49% allocated to medium agriculture. This sub-class holds by far the largest number of pixels of any agricultural class in the matrix, so its confusion has a disproportionate effect on both overall accuracy and the area estimates of the dense and medium agriculture classes.

Table 3: Per-class accuracy from the confusion matrix of the LISS-III classification

Reference class	Pixels	Correctly classified (%)	Main confusion (%)
Dense agriculture-1	2,935	88.01	Unclassified 10.97
Dense agriculture-2	17,202	35.19	Medium agriculture 52.49
Medium agriculture	597	85.76	Poor agriculture 7.71
Poor agriculture	613	83.36	Medium agriculture 9.14
Fallow land-1	13,814	88.53	Unclassified 9.12
Fallow land-2	3,920	90.79	Fallow land-1 3.24
Water body	1,735	87.72	Unclassified 12.28
Habitation	2,823	85.49	Waste/eroded 6.67
Waste/eroded land	8,993	85.94	Habitation 4.47

The summary statistics reported with the matrix are an average accuracy of 83.08%, an overall accuracy of 79.32% and a kappa coefficient of 0.754 (standard deviation 0.00165; 95% confidence limit ±0.00324). The original narrative treats the 83.08% value as the overall accuracy, while the table lists it as the average. As a consistency check, the nine diagonal percentages in Table 3 average 81.2%, and weighting them by the number of reference pixels in each class gives an overall accuracy of about 70.5%. The difference from the reported 79.32% suggests that the reported indices were computed on a different, possibly cleaned, sample or after merging sub-classes. The effect of merging is relevant because combining spectrally confusable classes inflates apparent accuracy, a point emphasised in discussions of thematic map assessment. The only defensible reading is that overall accuracy lies between roughly 70% and 80%, depending on the sample and on whether sub-classes are merged, and that the kappa value of 0.754, which would normally be called substantial agreement, may overstate performance for the two dense-agriculture sub-classes.

Kappa itself is a contested statistic for thematic accuracy, because chance agreement is not clearly relevant to map users and kappa adds little to the information in overall and per-class accuracy; the practical recommendation is to report the confusion matrix, per-class user's and producer's accuracy and area-adjusted estimates (Stehman, 1997). The present matrix gives only reference-row percentages, so producer's accuracy is available but user's accuracy is not. Reference samples were also not described in terms of

design (random, stratified, or purposive), and the matrix includes a very large "outside" count of 22,422 pixels that should not influence accuracy.

The practical reading of the accuracy results is that the map is reliable for settlement, water, waste land and fallow land, and acceptable for the broad cultivated class, but that the split between dense and medium agriculture is uncertain. The cause is probably spectral: both are green vegetation on a January date with a continuum of canopy density, and a hard boundary between them is arbitrary. Two remedies are available. One is to merge the two classes into a single "cropland with vegetation" class for area statistics and to retain density as a continuous index such as NDVI. The other is to add training samples from fields verified on the ground for crop type and canopy cover. Deep-learning classifiers have shown clear gains over classic methods where large labelled samples are available (Zhao et al., 2023; Digra et al., 2022), but in a district where only a few training polygons exist the first remedy is more realistic.

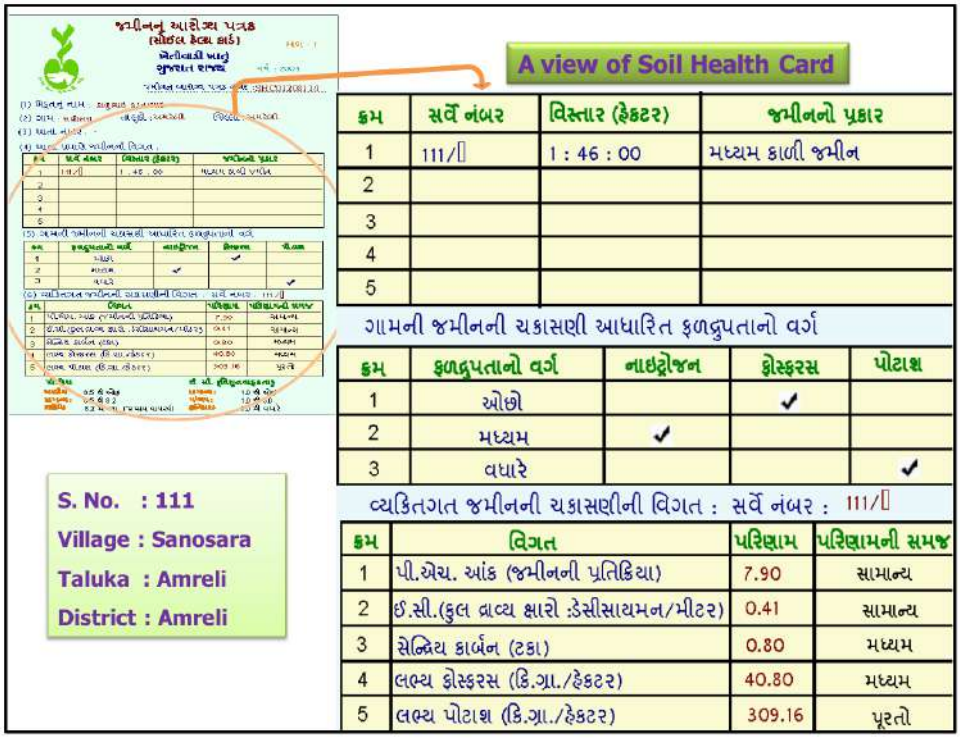
Soil fertility and reaction from Soil Health Cards

Soil Health Cards for the seven villages show a consistent pattern (Table 4). Available nitrogen was medium in six of the seven villages and not in the medium class in Mangvapal. Available phosphorus was low in six villages with the exception of Bhandariya Mota, and available potash was high in every village. Soil reaction was normal (6.5-8.2) and electrical conductivity below 1 dS m^{-1}, indicating no salinity problem at the plots sampled. Organic carbon at the village level was mostly medium to optimum, with only small areas in the low class.

Table 4. Dominant soil health class in the seven selected villages, based on Soil Health Card records

Attribute	Dominant class	Exceptions among the seven villages
Available nitrogen	Medium	Mangvapal (not medium)
Available phosphorus	Low	Bhandariya Mota (not low)
Available potash	High	None
Organic carbon	Medium to optimum	Small low-class area (Sanosara)
pH	Normal (6.5-8.2)	None
Electrical conductivity	Normal (<1 dS m^{-1})	None

The cards themselves are bilingual, with farmer, village, taluka, survey number and nutrient values (Fig. 10). Their regular format is what allows automated joining to cadastral polygons.



ક્રમ	સર્વે નંબર	વિસ્તાર (હેકટર)	જમીનનો પ્રકાર
1	111/	1 : 46 : 00	મધ્યમ કાળી જમીન
2			
3			
4			
5			

ગામની જમીનની ચકાસણી આધારિત ફળદ્રુપતાનો વર્ગ

ક્રમ	ફળદ્રુપતાનો વર્ગ	નાઇટ્રોજન	ફોસ્ફરસ	પોટાશ
1	ઓછો		✓	
2	મધ્યમ	✓		
3	વધારે			✓

વ્યકિતગત જમીનની ચકાસણીની વિગત : સર્વે નંબર : 111/

ક્રમ	વિગત	પરિણામ	પરિણામની સમજ
1	પી.એચ. આંક (જમીનની પ્રતિક્રિયા)	7.90	સામાન્ય
2	ઈ.સી.(કુલ દ્રાવ્ય ક્ષારો :ડેસીસાયમન/મીટર)	0.41	સામાન્ય
3	સેન્દ્રિય કાર્બન (ટકા)	0.80	મધ્યમ
4	લભ્ય ફોસ્ફરસ (કિ.ગ્રા./હેકટર)	40.80	મધ્યમ
5	લભ્ય પોટાશ (કિ.ગ્રા./હેકટર)	309.16	પૂરતો

Fig. 10. Example of a Soil Health Card for a farmer's field in Sanosara village (survey no. 111)

Maps for Sanosara show how these records look when tied to cadastral polygons. Nitrogen was medium and phosphorus low wherever a card was available (Fig. 11). Potash was high on all mapped plots, and organic carbon varied from low through medium to optimum, with optimum plots clustered in the north and east (Fig. 12). pH and electrical conductivity were in the normal class on all mapped plots (Fig. 13).

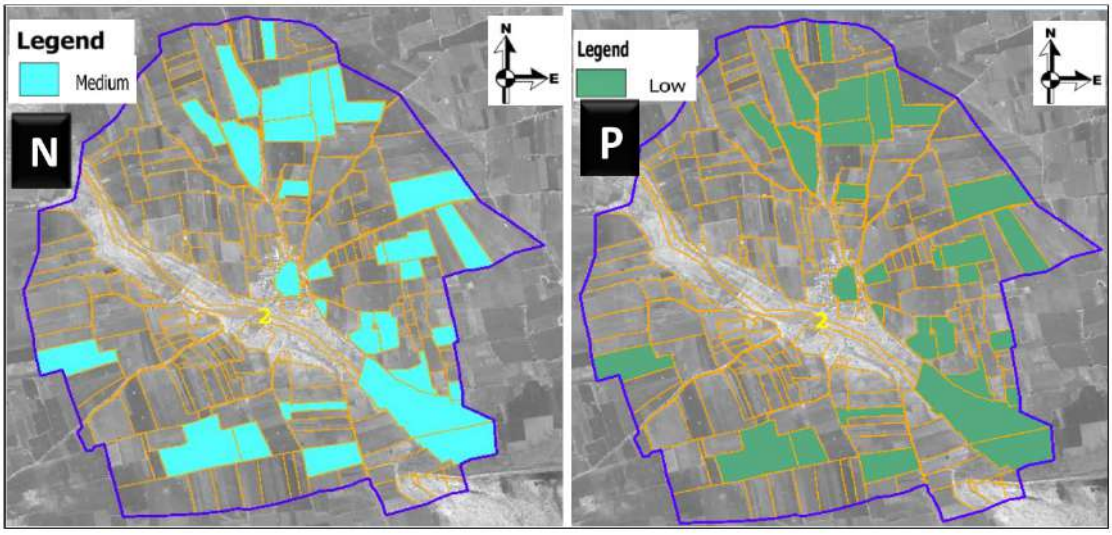


Fig. 11. Nitrogen (left) and phosphorus (right) status of soils in Sanosara village based on Soil Health Cards

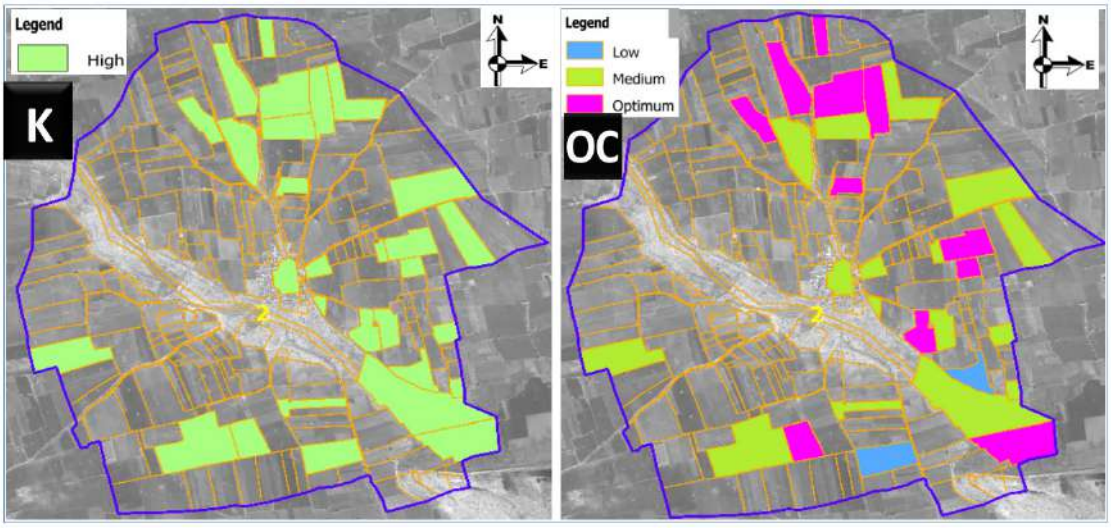


Fig. 12. Potash (left) and organic carbon (right) status of soils in Sanosara village based on Soil Health Cards

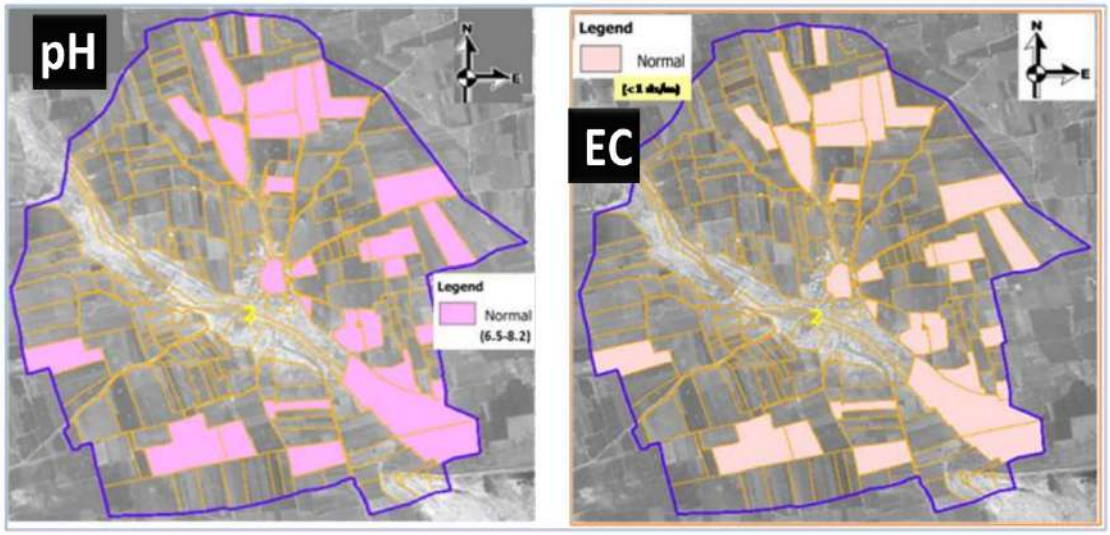


Fig. 13. Cadastral-level pH (left) and electrical conductivity (right) status of Sanosara village

Agronomically, the pattern of medium nitrogen, low phosphorus and high potash implies that fertiliser recommendations should emphasise phosphorus and nitrogen and that potash application can be deferred on most plots. The Soil Health Card scheme was designed for precisely this purpose, and its reported benefits, including yield increases of 5-6% and fertiliser reductions of 8-10% in the reviewed evidence (Timisina et al., 2025), depend on farmers acting on plot-specific advice. Mapping the cards turns a stack of individual documents into a village-level overview that extension staff can use to identify clusters of plots with the same deficiency. In Sanosara, for example, the plots without a mapped card form large contiguous blocks that could be prioritised for sampling. Linking cards to a decision tool in this way follows earlier proposals for balanced fertilisation (Thiyageshwari et al., 2006).

Two features of the maps limit their interpretation. First, only plots with an SHC are coloured, so the maps document where data exist rather than the complete fertility pattern; wherever cards are absent the map is blank. Second, the cards report qualitative classes and not numerical values, so gradients within a class are lost. The review of broad-scale digital soil mapping stresses that models and maps are only as good as the sampling that underlies them and that well-designed sampling schemes are needed (Chen et al., 2022). The cards were collected under an administrative scheme rather than a statistical design, and their spatial coverage is determined by who participated.

The thesis extends the findings from seven villages to the entire taluka by assuming that the pattern holds. That extrapolation is an assumption and is not tested here. Remote sensing covariates, such as terrain attributes, soil colour from imagery and vegetation indices, are used in

digital soil mapping to extend point observations spatially (Richer-de-Forges et al., 2023), and a model of this kind trained on the plot cards, with independent validation on withheld villages, would be the defensible way to produce a taluka-wide fertility surface.

Integration for micro-level planning

The three components of the workflow, parcel-level cadastral overlays, a taluka-wide land cover map and plot-level soil health maps, answer different planning questions. The land cover map shows how much land is under vigorous crop, how much is fallow and where settlements and waste land lie; it is the tool for allocation questions at the taluka or cluster level. The cadastral overlay on high-resolution imagery lets field staff locate any survey number, check field condition and plan visits. The SHC maps support input planning, especially fertiliser recommendations, at village and plot scale. Combined in one geodatabase, the three layers allow queries such as "which survey numbers under dense cropping in January have low phosphorus?" or "which fallow plots have good fertility and could be brought under irrigation?" Such integrated databases follow the logic of earlier GIS-based decision support systems for district and local planning in India (Archarya et al., 2011; Gupta et al., 2001; Bariar et al., 2004) and of watershed-oriented resource mapping (Krishna, 1996; Kerr et al., 2002). Reviews of agricultural remote sensing note that the real value of mapped products lies in their coupling with agronomic and management data and not in the maps alone (Alami Machichi et al., 2023; Joshi et al., 2023; Wu et al., 2023).

Several steps would increase the operational value of the workflow: (i) merging uncertain classes and reporting accuracy with a transparent sample design; (ii) adding a second image date to separate permanent from seasonal fallow and to infer cropping intensity; (iii) automating the extraction of field boundaries from CARTOSAT-1 or LISS-IV, so that cadastral digitisation need not be repeated manually for every village, as work on boundary delineation suggests is feasible (Zheng et al., 2026); and (iv) linking the SHC database through a unique survey-number identifier so that updates after each two-year card cycle flow automatically into the maps.

IV. LIMITATIONS

The study has several limitations that readers should keep in mind. The imagery dates from 2006 to 2009 and the maps describe the land of that period; land use in the taluka, particularly irrigation, has probably changed since. The classification used a per-pixel maximum-likelihood classifier on a 23.5 m image, with no texture or object-based information and no ancillary data, and it has the known tendency of the maximum-likelihood rule to confuse classes with overlapping distributions. The accuracy figures in the source are internally inconsistent, a pixel-weighted recalculation gives lower overall accuracy than the figure reported, the reference sampling design is undocumented, and one dense-agriculture sub-class is poorly separated. Class areas are therefore uncertain by an unknown margin, and no area-adjusted estimates with confidence intervals were produced.

The cadastral work lacks a quantified positional error, and the CARTOSAT-1 scene predates the soil data by several years. The Soil Health Card data are qualitative, restricted to seven villages chosen at random but not stratified by soil or land cover, and mapped for only one village in detail. Organic carbon, nitrogen and phosphorus classes depend on laboratory methods and threshold values that are not given on the cards reproduced here. Joined polygons are limited to plots with a card.

V. CONCLUSION

A workflow combining georeferenced CARTOSAT-1, LISS-IV and LISS-III imagery, digitised cadastral boundaries and Soil Health Card records was applied to Amreli Taluka to provide land cover and soil fertility information at the scale of villages and survey numbers. The LISS-III classification showed that cultivated land with dense, medium or poor vegetation covered 64.73% of the taluka, fallow land 16.81%, habitation 12.01%, waste land 4.73% and water 1.71%. The classification performed well for most classes but separated dense from medium agriculture poorly, and the reported accuracy indices should be treated as an upper bound; overall accuracy was probably between 70 and 80%. Soil Health Card records for seven villages showed medium nitrogen, low phosphorus and high potash, with normal pH and electrical conductivity, a pattern that supports phosphorus-focused fertiliser advice. Mapping the cards at survey-number level for Sanosara demonstrated how farm-scale records can be turned into spatial tools for extension. The approach is transferable and inexpensive, but it should be strengthened by transparent accuracy assessment, multi-date imagery, automated field boundary extraction and a validated spatial model for extending the soil data beyond the sampled plots.

ACKNOWLEDGEMENTS

The satellite data and GIS facilities were provided by the Bhaskaracharya Institute for Space Applications and Geo-informatics (BISAG), Gandhinagar. Meteorological and field information were supplied by Junagadh Agricultural University and the farmers of Amreli Taluka.

REFERENCES

[1] Acharya, P.S., Ghosh, S.K. and De Sarkar, S.C. 2011. Natural resources data management system (NRDMS) a suite of web-accessible geo-spatial data processing tools for e-Governance in India. In *Proceedings of the 2nd International Conference on Computing for Geospatial Research & Applications* (pp. 1-1). https://doi.org/10.1145/1999320.1999380.

[2] Alami Machichi, M., Mansouri, L.E., Imani, Y., Bourja, O., Lahlou, O., Zennayi, Y., Nourzeix, F., Houmma, I.H. and Hadria, R. 2023. Crop mapping using supervised machine learning and deep learning: A systematic literature review. *International Journal of Remote Sensing*, **44**(8): 2717-2753. https://doi.org/10.1080/01431161.2023.2205984.

[3] Bariar, A., Gupta, R.D. and Prasad, S.C. 2004. Development of GIS based spatial data infrastructure for micro-level planning. In *Map World Forum. Hyderabad, India*.

[4] Bastiaanssen, W.G., Molden, D.J. and Makin, I.W. 2000. Remote sensing for irrigated agriculture: examples from research and possible applications. *Agricultural water management*, **46**(2): 137-155. https://doi.org/10.1016/S0378-3774(00)00080-9.

[5] Burrough, P.A. 1989. Matching spatial databases and quantitative models in land resource assessment. *Soil Use and Management*, ***5***(1): 3-8. https://doi.org/10.1111/j.1475-2743.1989.tb00753.x

[6] Chen, S., Arrouays, D., Mulder, V.L., Poggio, L., Minasny, B., Roudier, P., Libohova, Z., Lagacherie, P., Hannam, J., Meersmans, J., Richer-de-Forges, A.C. and Walter, C. 2022. Digital mapping of GlobalSoilMap soil properties at a broad scale: A review. *Geoderma*, **409**: 115567. https://doi.org/10.1016/j.geoderma.2021.115567.

[7] Digra, M., Dhir, R. and Sharma, N. 2022. Land use land cover classification of remote sensing images based on the deep learning approaches: a statistical analysis and review. *Arabian Journal of Geosciences*, **15**(10): 1003. https://doi.org/10.1007/s12517-022-10246-8.

[8] Gupta, R.D., Garg, P.K. and Arora, M. 2001. A GIS Based Decision Support System for Developmental Planning in Dehradun District. *J. Indian Cartogr*, **21**.

[9] Joshi, A., Pradhan, B., Gite, S. and Chakraborty, S. 2023. Remote-sensing data and deep-learning techniques in crop mapping and yield prediction: A systematic review. *Remote Sensing*, **15**(8): 2014. https://doi.org/10.3390/rs15082014.

[10] Kasturirangan, K. 1995. Remote Sensing in India—Present scenario and future thrusts. *Journal of the Indian Society of Remote Sensing*, **23**(1): 1-6. https://doi.org/10.1007/BF02997429.

[11] Kerr, J.M., Pangare, G. and Pangare, V. 2002. *Watershed development projects in India: an evaluation* (Vol. 127). Intl Food Policy Res Inst.

[12] Krishna, A.P. 1996. Remote sensing approach for watershed based resources management in the Sikkim Himalaya: a case study. *Journal of the Indian Society of Remote Sensing*, **24**(2): 71-83. https://doi.org/10.1007/BF03016119.

[13] Largueche, F.Z.B. 2006. Estimating soil contamination with Kriging interpolation method. *American Journal of Applied Sciences*, **3**(6): 1894-1898.

[14] Lillesand, T.M., Kiefer, R.W. and Chipman, J.W. 2015. Remote Sensing and Image Interpretation. John Wiley & Sons, New York.

[15] Macarringue, L.S., Bolfe, É.L. and Pereira, P.R.M. 2022. Developments in land use and land cover classification techniques in remote sensing: A review. *Journal of Geographic Information System*, **14**(1): 1-28. https://doi.org/10.4236/jgis.2022.141001.

[16] Markon, C.J. 2003. A temporal study of urban development for the municipality of Anchorage, Alaska. *GeoCarto International*, **18**(3): 21-33. https://doi.org/10.1080/10106040308542278.

[17] Puri, S.K. 2007. Integrating Scientific with Indigenous Knowledge: Constructing Knowledge Alliances for Land Management in India1. *MIS quarterly*, **31**(2): 355-379. https://doi.org/10.2307/25148795.

[18] Richer-de-Forges, A.C., Chen, Q., Baghdadi, N., Chen, S., Gomez, C., Jacquemoud, S., Martelet, G., Mulder, V.L., Urbina-Salazar, D., Vaudour, E., Weiss, M., Wigneron, J.P. and Arrouays, D. 2023. Remote sensing data for digital soil mapping in French research—a review. *Remote Sensing*, **15**(12): 3070. https://doi.org/10.3390/rs15123070.

[19] Stehman, S.V. 1997. Selecting and interpreting measures of thematic classification accuracy. *Remote sensing of Environment*, **62**(1): 77-89. https://doi.org/10.1016/S0034-4257(97)00083-7.

[20] Thiyageshwari, S., Natesan, R., Boopathi, P.M., Paulraj, C. and Natarajan, S. 2006. Soil health sustenance tools to ensure balanced fertilization-DSSIFER and Soil Health Card.

[21] Timilsina, R.R., Khosla, S., Rahut, D.B., Jena, P.R. and Sonobe, T. 2025. A comprehensive review of the soil health status for enhancing agricultural sustainability. *Frontiers in Environmental Science*, **13**: 1548095. https://doi.org/10.3389/fenvs.2025.1548095.

[22] Wu, B., Zhang, M., Zeng, H., Tian, F., Potgieter, A.B., Qin, X., Yan, N., Chang, S., Zhao, Y., Dong, Q., Boken, V., Plotnikov, D., Guo, H., Wu, F., Zhao, H., Deronde, B., Tits, L. and Loupian, E. 2023. Challenges and opportunities in remote sensing-based crop monitoring: A review. *National Science Review*, **10**(4): nwac290. https://doi.org/10.1093/nsr/nwac290.

[23] Zhao, S., Tu, K., Ye, S., Tang, H., Hu, Y. and Xie, C. 2023. Land use and land cover classification meets deep learning: A review. *Sensors*, *23*(21), 8966. https://doi.org/10.3390/s23218966.

[24] Zheng, J., Ye, Z., Wen, Y., Huang, J., Zhang, Z., Li, Q., Hu, Q., Xu, B., Zhao, L. and Fu, H. 2026. A comprehensive review of agricultural parcel and boundary delineation from remote sensing images: Recent progress and future perspectives. *IEEE Geoscience and Remote Sensing Magazine*. doi: 10.1109/MGRS.2026.3658493.

International Journal of Environment, Agriculture and Biotechnology
Vol-11, Issue-5; Sep-Oct, 2026
Peer-Reviewed International Journal
Journal Home Page Available: https://ijeab.com/
Journal DOI: 10.22161/ijeab

Food Consumption, Digestibility and Conversion Efficiency in Bivoltine Silkworm (*Bombyx mori* L.) Hybrids under Temperate Conditions of Kashmir

Gh. Nabi Mir[1], Aabid Ahmad Bhat[2], Lubna Altaf[2], Misara Jaan[2], Ishfaq Ahmad Malla[2], M. A. Malik[3], H. U. Dar[3]

[1]Additional Director, Sericulture Development Department, Jammu and Kashmir, India
[2]PhD Graduate, College of Temperate Sericulture (CoTS), Sher-e-Kashmir University of Agricultural Sciences and Technology of Kashmir (SKUAST-K), Mirgund, Jammu and Kashmir, India
[3]College of Temperate Sericulture (CoTS), Sher-e-Kashmir University of Agricultural Sciences and Technology of Kashmir (SKUAST-K), Mirgund, Jammu and Kashmir, India
*Corresponding authors: Gh. Nabi Mir (ghnabimirseri@gmail.com) and Ishfaq Ahmad Malla (ishfaqzamaan@gmail.com)

Received: 10 Sep 2026; Received in revised form: 19 Oct 2026; Accepted: 28 Oct 2026; Available online: 31 Oct 2026
©2026 The Author(s). Published by Infogain Publication. This is an open-access article *under* the CC BY license (https://creativecommons.org/licenses/by/4.0/)

Abstract**—** *Feed conversion efficiency is a key physiological criterion for judging silkworm hybrids, yet little is known about how newly introduced CSR hybrids and regional hybrids utilise mulberry leaf under temperate conditions. This study compared food consumption, faecal egestion, growth rate, approximate digestibility (A.D.) and the efficiencies of conversion of ingested (E.C.I.) and digested (E.C.D.) food into body matter in four bivoltine Bombyx mori L. hybrids, NB4D2 × SH6, SKAU-R-1 × SKAU-R-6, CSR2 × CSR4 and CSR2 × CSR5. The hybrids were reared in a randomised complete block design with five replications during spring 2002 at Mirgund, Kashmir, on a single mulberry variety, Ichinose, and utilisation indices for the 4th and 5th instars were computed by the method of Waldbauer (1968). CSR2 × CSR5 recorded the lowest ingesta (18.70 g per larva, against 20.21 g in NB4D2 × SH6; C.D. = 0.984) and faecal egestion (6.87 g against 8.39 g; C.D. = 0.475) and the highest A.D. (63.177% against 58.466%; C.D. = 3.671). Growth rate was highest in CSR2 × CSR4 (0.1682) and CSR2 × CSR5 (0.1680), both significantly above the two conventional hybrids (0.1640–0.1645; C.D. = 0.0009). E.C.I. was numerically highest in CSR2 × CSR5 (24.736%) and E.C.D. in NB4D2 × SH6 (40.668%), but neither differed significantly among hybrids. The CSR hybrids thus achieved comparable conversion efficiency with lower leaf intake, lower egestion and higher digestibility, suggesting a lower leaf requirement per larva in commercial rearing. These indices can complement cocoon yield in breed evaluation for temperate regions.*

Keywords**— Bombyx mori, bivoltine hybrids, food consumption, approximate digestibility, efficiency of conversion of ingested food, efficiency of conversion of digested food, Kashmir**

I. INTRODUCTION

Sericulture is an agro-based industry that suits the socio-economic setting of India well. Silk has symbolised luxury for centuries, and it is the product of the combined efforts of seed producers, silkworm rearers and reelers. India continues to be the world's second-largest silk producer, with total raw silk production reaching 42,033 metric tonnes in 2025–26, Mulberry silk remains the principal component of national production, while India also produces tasar, eri and muga silks . Jammu and Kashmir has a distinctive place in this sector because its temperate agro-climatic conditions are particularly suitable for bivoltine sericulture. The Union Territory produces approximately 800 metric tonnes of bivoltine cocoons annually and the sector supports nearly 27,000 families, making it an important source of rural livelihood (Anonymous.,2026). The production of high-

quality bivoltine silk therefore depends not only on cocoon yield but also on the nutritional performance and efficient utilisation of mulberry leaves by silkworm hybrids. The feasibility of bivoltine hybrids that give better productivity therefore needs to be recognised. Jammu and Kashmir is ideally suited to rearing bivoltine hybrids and is a major bivoltine silk-producing state in India, with silk comparable in quality to the best imported raw silk. Identifying hybrids suited to specific agro-climatic regions and seasons, with emphasis on hardy strains that give good commercial cocoon yields, is therefore one of the central research problems in sericulture. The performance of a hybrid reflects both heredity and environment. Heredity transmits characters that nature has pre-fixed, but nurture is equally important, and *Bombyx mori* L. maintains a fine balance between the two. The expression of a race's useful characteristics depends on its genetic make-up and on prevailing conditions such as climate and soil, with food being the most important contributor; uniform conditions and careful handling of rearing material are therefore essential. Tazima (1957) noted that climatic conditions are the most important factor in improving sericulture. Although silkworms are reared indoors, their food source, mulberry, grows in the open and cannot escape the influence of climate and soil.The alimentation and physiology of the silkworm are closely correlated, and the nutritional demands of the larva have received growing attention in recent years. Supplying quality leaf is the most direct and efficient way to obtain good-quality raw silk, and the aim of rearing is to reduce the leaf–cocoon ratio, which depends on silkworm variety, leaf quality and management. Growth will not be uniform if leaf quality is poor, and leaf quantity directly influences silk production (Ramachandra *et al.*, 1992). The characteristics of a mulberry variety affect the amount ingested, so qualitative under-feeding is always linked with quantitative under-feeding (Legay, 1958). The importance of leaf quality for growth, development and silk production is well documented (Dasgupta, 1961; Yokoyama, 1963; Das and Sikdar, 1970; Krishnaswami, 1971; Radha *et al.*, 1978; Venugopala Pillai *et al.*, 1980; Tayade and Jawale, 1984; Dar *et al.*, 1988, ; Kulbir, 2001). Many mulberry varieties are available in Kashmir, but only a few are popular commercially because significant varietal differences exist and affect rearing performance and cocoon characters in *B. mori* L.

How efficiently a larva turns leaf into body matter is quantified by food utilisation indices: approximate digestibility, the efficiency of conversion of ingested food (E.C.I.) and the efficiency of conversion of digested food (E.C.D.) (Waldbauer, 1968). These indices contribute directly to the cost–benefit ratio of rearing and are regarded as important physiological criteria for judging the superiority of hybrids (Trivedy and Nair, 1998). A larva that uses food to the maximum extent for its own gain is considered more efficient (Remadevi *et al.*, 1992), and the leaf-to-silk conversion rate is treated as an important economic index in breeding programmes (Xu and Wu, 1992). Consumption, utilisation and conversion efficiency differ among breeds (Benchamin and Jolly, 1986; Slansky and Scriber, 1985).Despite extensive evaluation of quantitative cocoon parameters, the nutritional physiology of newly introduced high-yielding CSR combinations and traditional regional hybrids has received little attention under temperate conditions. Conventional breeding trials prioritise final cocoon yield, yet ingesta, approximate digestibility and conversion efficiencies are central to optimising leaf-to-silk conversion. The present study addresses this gap. Its objectives were (i) to quantify ingesta, faecal egestion, growth rate and approximate digestibility, and (ii) to estimate E.C.I. and E.C.D., in four bivoltine hybrids (NB4D2 × SH6, SKAU-R-1 × SKAU-R-6, CSR2 × CSR4 and CSR2 × CSR5) fed on a single exotic mulberry variety, Ichinose, in the spring season. Using one variety isolates hybrid differences from variation in leaf quality, so that the results indicate how far the genotype itself determines how efficiently food is used.

II. MATERIALS AND METHODS

The four hybrids, NB4D2 × SH6, SKAU-R-1 × SKAU-R-6, CSR2 × CSR4 and CSR2 × CSR5, are standard hybrids reared commercially in Jammu and Kashmir. They were procured from the Division of Sericulture, SKUAST-K, Mirgund, and the Central Sericultural Research and Training Institute, Pampore. The experiment was laid out in a randomised complete block design with five replications per treatment and was conducted in spring 2002 (April–May) at the Division of Sericulture, Mirgund, SKUAST-K. Two hundred larvae taken after the third moult formed one replication.

The first three instars were reared following Krishnaswami (1978) and Dar and Singh (1998). A weighed quantity of leaf was given soon after resumption of feeding in the 4th and 5th instars. After each feed, the unconsumed leaf and the faecal matter were weighed, and a control without larvae was kept to estimate moisture loss from the leaf between feeds. Any mortality was compensated from reserve larvae of the same treatment. Larval weight was recorded at the beginning of the 4th instar and at the end of the 5th instar, one day before spinning, to calculate the average weight gain and the maximum weight attained during the feeding period. At the end of the 5th instar, growth rate and the efficiencies of conversion of ingested and digested food into

body matter were computed by the methods of Waldbauer (1968).

2.1 Food utilisation parameters

- **Leaf fed per larva (g):** from the feeding chart prepared separately for each treatment.
- **Ingesta (g):** F = leaf fed − [(leaf fed ÷ leaf in control at the end of feeding) × leftover leaf].
- **Faeces voided per larva (g):** collected separately and weighed at the end of every feed.
- **Moisture loss in leaves per feed (g):** calculated from a single control tray holding the same quantity of weighed leaf without larvae.
- **Growth rate (G.R.):** G ÷ (T × A), where G is the fresh weight gained per larva (g), T the duration of the feeding period (days) and A the mean fresh weight of the larvae (g).
- **Approximate digestibility (A.D., %):** [(weight of food ingested − weight of faeces voided) ÷ weight of food ingested] × 100.
- **Efficiency of conversion of ingested food (E.C.I., %):** (weight gained ÷ weight of food ingested) × 100.
- **Efficiency of conversion of digested food (E.C.D., %):** [weight gained ÷ (weight of food ingested − weight of faeces voided)] × 100.

Data were analysed by analysis of variance for a randomised block design, and means were compared at the 5% level of significance (Gomez and Gomez, 1976). Percentage data were square-root transformed before analysis; transformed values are given in parentheses in Table 2. Results are presented in Tables 1 and 2 and Figures 1–6.

III. RESULTS

The commercial hybrids NB4D2 × SH6 and SKAU-R-1 × SKAU-R-6 and the newly evolved CSR hybrids CSR2 × CSR4 and CSR2 × CSR5 differed in their dietary and nutritional efficiency, as detailed in Tables 1 and 2 and Figures 1–6.

3.1 Food consumption and faecal egestion

Leaf fed per larva was 41.92 g in NB4D2 × SH6 and SKAU-R-1 × SKAU-R-6 and 41.62 g in CSR2 × CSR4 and CSR2 × CSR5; the two CSR hybrids differed significantly ($p < 0.05$) from the other two (Table 1). Ingesta per larva ranged from 18.70 g in CSR2 × CSR5 to 20.21 g in NB4D2 × SH6, with 19.07 g in CSR2 × CSR4 and 20.01 g in SKAU-R-1 × SKAU-R-6. Faeces voided per larva was lowest in CSR2 × CSR5 (6.87 g), followed by CSR2 × CSR4 (7.24 g), SKAU-R-1 × SKAU-R-6 (8.18 g) and NB4D2 × SH6 (8.39 g) (Table 1; Figure 1). Moisture loss in leaves per feed was 31.88 g for NB4D2 × SH6 and SKAU-R-1 × SKAU-R-6 and 32.06 g for the CSR hybrids, a non-significant difference (Table 1).

Table 1. Mean leaf fed, ingesta, faeces voided and moisture loss in leaves per feed during the 4th and 5th instars of Bombyx mori L. larvae fed on the Ichinose variety.

S. No.	Hybrid	Leaf fed / larva (g)	Ingesta / larva (g)	Faeces voided / larva (g)	Moisture loss in leaves / feed (g)
1	NB4D2 × SH6	41.92^{b}	20.21^{c}	8.39^{b}	31.88
2	SKAU-R-1 × SKAU-R-6	41.92^{b}	20.01^{bc}	8.18^{b}	31.88
3	CSR2 × CSR4	41.62^{a}	19.07^{ab}	7.24^{a}	32.06
4	CSR2 × CSR5	41.62^{a}	18.70^{a}	6.87^{a}	32.06
	S.E. diff.	0.109	0.451	0.218	–
	C.D. (p = 0.05)	0.238	0.984	0.475	N.S.

Note: Means followed by the same letter(s) within a column are statistically at par. N.S., non-significant.

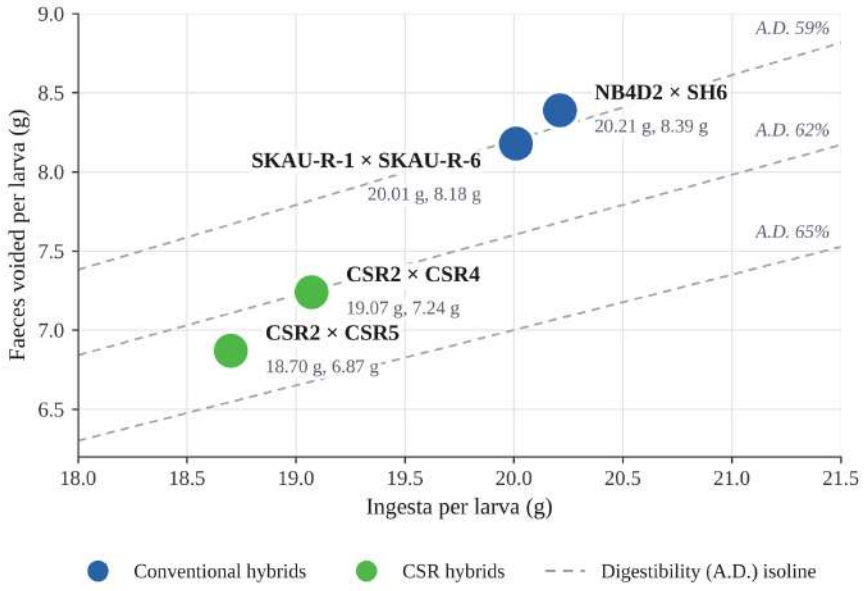


Fig.1. Relationship between ingesta and faeces voided per larva (g) in four bivoltine silkworm hybrids (data from Table 1). Dashed lines are isolines of approximate digestibility: a hybrid lies lower for a given ingesta when more of its food is digested.

3.2 Growth rate, digestibility and conversion efficiency

Growth rate ranged from 0.1640 to 0.1682, in the order CSR2 × CSR4 > CSR2 × CSR5 > NB4D2 × SH6 > SKAU-R-1 × SKAU-R-6 (Table 2; Figu\re 2). Approximate digestibility was highest in CSR2 × CSR5 (63.177%), followed by CSR2 × CSR4 (61.932%), SKAU-R-1 × SKAU-R-6 (59.018%) and NB4D2 × SH6 (58.466%) (Figure 3). E.C.I. was 24.736% in CSR2 × CSR5, 24.684% in CSR2 × CSR4, 23.724% in NB4D2 × SH6 and 23.690% in SKAU-R-1 × SKAU-R-6, whereas E.C.D. was 40.668% in NB4D2 × SH6, 40.358% in SKAU-R-1 × SKAU-R-6, 39.958% in CSR2 × CSR4 and 39.198% in CSR2 × CSR5. Differences in E.C.I. and E.C.D. were not statistically significant (Table 2; Figure 4). Partitioning the Table 2 means (Figure 5), 23.7–24.7% of ingested food was converted to body matter, 34.7–38.4% was digested but metabolised, and 36.8–41.5% was egested; the egested share was smallest in CSR2 × CSR5. Figure 6 summarises all six traits in one view: ingesta and faeces voided are highest in the conventional hybrids, whereas approximate digestibility and growth rate are highest in the CSR hybrids.

Table 2. Mean growth rate, approximate digestibility and efficiency of conversion of ingested (E.C.I.) and digested (E.C.D.) food into body matter in four Bombyx mori L. hybrids during the spring season.

S. No.	Hybrid	Growth rate	Approximate digestibility, A.D. (%)	E.C.I. (%)	E.C.D. (%)
1	NB4D2 × SH6	0.1645^{b}	58.466^{b}	23.724 (4.87)	40.668
2	SKAU-R-1 × SKAU-R-6	0.1640^{b}	59.018^{b}	23.690 (4.86)	40.358
3	CSR2 × CSR4	0.1682^{a}	61.932^{ab}	24.684 (4.96)	39.958
4	CSR2 × CSR5	0.1680^{a}	63.177^{a}	24.736 (4.97)	39.198
	S.E. diff.	0.0004	1.685	–	–
	C.D. (p = 0.05)	0.0009	3.671	N.S.	N.S.

Note: Values in parentheses are transformed data (Gomez and Gomez, 1976). Means followed by the same letter(s) within a column are statistically at par. N.S., non-significant.

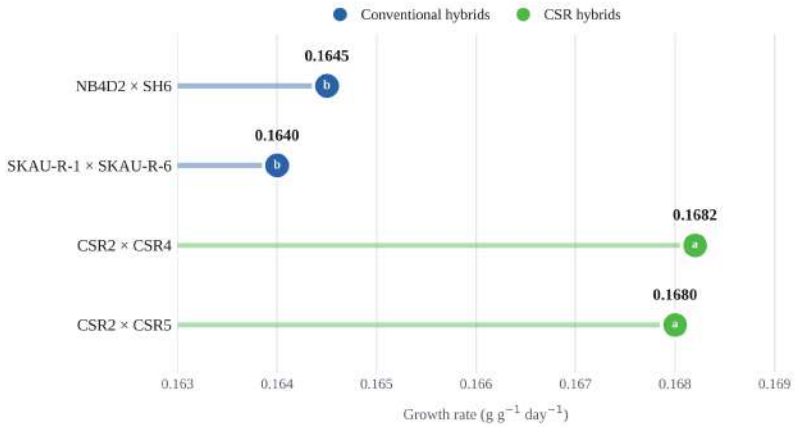


Fig.2. Growth rate of four bivoltine silkworm hybrids. Data from Table 2. Letters inside the markers indicate significance groupings: hybrids sharing a letter are statistically at par (C.D. = 0.0009 at p = 0.05).

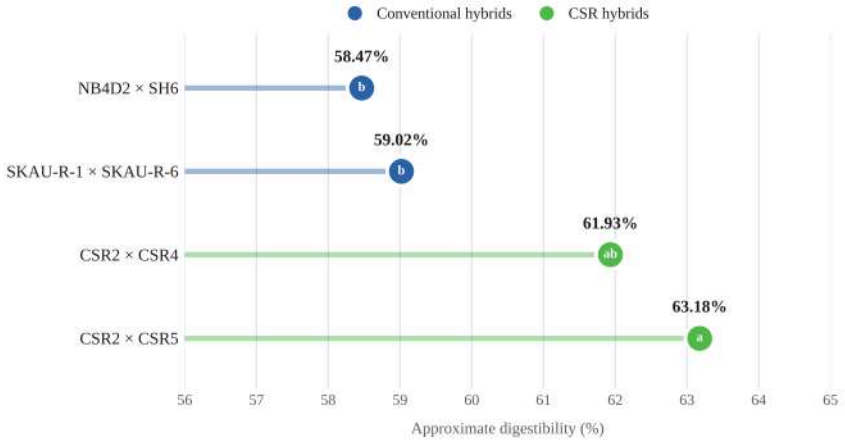


Fig.3. Approximate digestibility (%) of four bivoltine silkworm hybrids (data from Table 2). Letters inside the markers: hybrids sharing a letter are statistically at par (C.D. = 3.671 at p = 0.05).

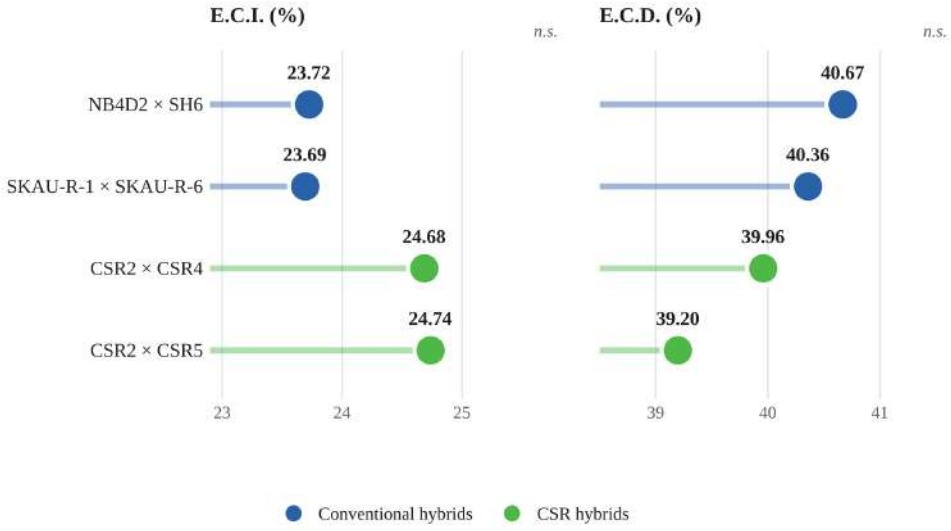


Fig.4. Efficiency of conversion of ingested food (E.C.I., left) and digested food (E.C.D., right) into body matter (data from Table 2). Differences among hybrids were not significant. Note the different x-axis ranges of the two panels.

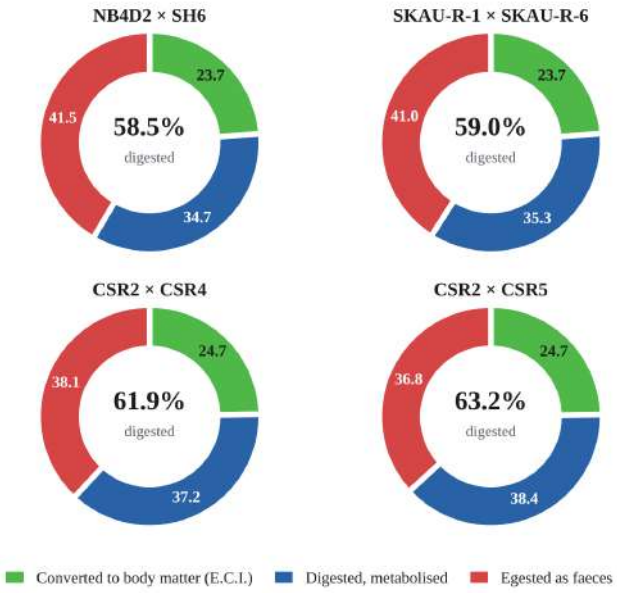


Fig.5. Partitioning of ingested food (%) in each hybrid, with approximate digestibility shown at the centre of each ring; derived from the mean values in Table 2: converted to body matter (E.C.I.), digested but metabolised (A.D. − E.C.I.) and egested (100 − A.D.). Hybrid means were used, so the segments are indicative of the overall budget rather than separately analysed variables.

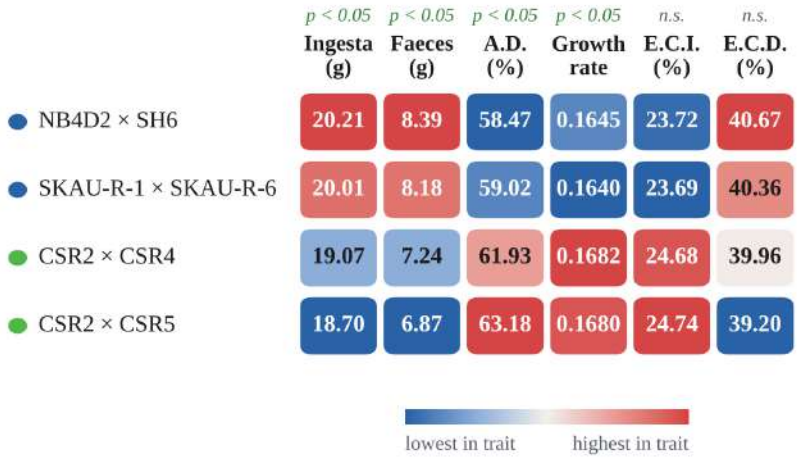


Fig.6. Heat map of the six measured traits in the four hybrids (values from Tables 1 and 2). Colour shows each value relative to the lowest (blue) and highest (red) hybrid within the same trait; red does not necessarily mean worse. Traits marked p < 0.05 differed significantly among hybrids; n.s., non-significant.

IV. DISCUSSION

Rearing success and cocoon crop quality depend on the rearing technique, the quality, quantity and management of leaf, and the silkworm race. Leaf quality strongly influences how much leaf is ingested, and feed conversion efficiency contributes substantially to the cost–benefit ratio of rearing, which makes it an important physiological criterion for judging the superiority of hybrids (Trivedy and Nair, 1998). Larvae take up nutrients from mulberry leaf to build the body, sustain life and spin cocoons, and the capacity to ingest, digest, absorb, assimilate and convert leaf into silk differs among breeds. Because all four hybrids here received the same variety, Ichinose, under the same conditions, the differences described below can be attributed largely to the hybrids themselves.

4.1 Food consumption and faecal egestion

The hybrids differed in ingesta, faeces voided and leaf fed (Table 1; Figure 1). CSR2 × CSR5 had the lowest ingesta

(18.70 g per larva) and CSR2 × CSR4 the next lowest (19.07 g), against 20.01–20.21 g in the two conventional hybrids. A lower leaf requirement per larva is economically advantageous in commercial rearing because it reduces leaf demand and the labour involved in feeding. Overall food consumption influences growth, survival, biomass accumulation and reproductive performance in insects (Slansky and Scriber, 1985), so intake is an informative trait in its own right. Whether the lower intake of CSR2 × CSR5 reflects earlier maturity could not be assessed here, as larval duration was not compared among treatments.

Faecal egestion, an indicator of feed acceptance linked to the nutritive status of the feed and to cocoon productivity, followed the same order: lowest in CSR2 × CSR5 (6.87 g per larva), then CSR2 × CSR4 (7.24 g), then SKAU-R-1 × SKAU-R-6 (8.18 g) and NB4D2 × SH6 (8.39 g). Both CSR hybrids differed significantly from both conventional hybrids in faecal output. This agrees with Mathavan and Pandian (1974), who used faecal weight as an index of food consumption in lepidopterans, and with Benchamin and Jolly (1986), who did the same in *B. mori*.

4.2 Approximate digestibility

Approximate digestibility was highest in CSR2 × CSR5 (63.177%), followed by CSR2 × CSR4 (61.932%) (Table 2; Figure 3). Statistically, NB4D2 × SH6 and SKAU-R-1 × SKAU-R-6 were at par with CSR2 × CSR4 but differed significantly ($p < 0.05$) from CSR2 × CSR5. The pattern of higher digestibility with lower consumption suggests that digestibility varies inversely with consumption. In the two conventional hybrids, higher intake probably speeded the passage of food through the gut and left less time for digestion; in the CSR hybrids, the smaller quantity of food passing through the gut allowed more time for digestion (Figure 5). This agrees with Trivedy and Nair (1999).

4.3 Leaf moisture

Leaf moisture affects palatability, assimilation and food consumption in the silkworm (Parpiev, 1968; Maribashetty *et al.*, 1999). Because a single variety was used and a single control tray was kept, moisture loss per feed was essentially the same across hybrids (Table 1): 31.88 g for NB4D2 × SH6 and SKAU-R-1 × SKAU-R-6 and 32.06 g for the CSR hybrids. Moisture loss therefore cannot explain the differences in intake or digestibility. Kulbir (2001), working on indigenous mulberry varieties of the Kashmir valley, reported a moisture loss of 40.03 g per feed in Ichinose leaves. The difference between the two studies, conducted in different years, may be attributed to the environmental conditions prevailing in each year.

4.4 Growth rate

Growth rate indicates how efficiently nutrients are used for growth and development. It was significantly higher in CSR2 × CSR4 (0.1682) and CSR2 × CSR5 (0.1680) than in NB4D2 × SH6 (0.1645) and SKAU-R-1 × SKAU-R-6 (0.1640) (Table 2; Figure 2). Approximate digestibility and E.C.D. interact to determine growth (Slansky and Scriber, 1985), and Remadevi *et al.* (1991) reported that these components vary significantly among races, in line with the present findings. The CSR hybrids thus grew faster while ingesting less, a combination that points to more efficient use of the leaf they consumed. A larva that uses food to the maximum extent for its own gain is considered more efficient (Remadevi *et al.*, 1992).

4.5 Efficiency of conversion of ingested and digested food

The CSR hybrids had numerically higher E.C.I. than the conventional hybrids (24.684–24.736% against 23.690–23.724%) but numerically lower E.C.D. (39.198–39.958% against 40.358–40.668%), a reverse trend between the two efficiencies (Table 2; Figure 4). Neither difference was statistically significant, so this trend should be interpreted cautiously. Waldbauer (1968) explained that E.C.I. varies both with digestibility and with the proportion of the digested food converted to body substance rather than metabolised for energy. E.C.I. therefore rises and falls with approximate digestibility and E.C.D., and E.C.D. decreases as the proportion of digested food metabolised for energy increases. The partitioning in Figure 5 illustrates this: the CSR hybrids digested a larger share of their intake, and a larger part of that digested share was metabolised, so their higher digestibility did not translate into a significantly higher conversion to body matter. E.C.D. is affected by factors that influence the energy devoted to maintenance, and it is not directly dependent on digestibility but varies with the level of nutrient intake.

4.6 Practical implications and limitations

Taken together, the CSR hybrids reached similar conversion efficiency with less leaf, less faecal output, higher digestibility and faster growth. For commercial rearers this means a lower leaf requirement per larva, which is relevant where leaf supply or labour is limiting, and conversion efficiency is regarded as an important economic index in breeding programmes (Xu and Wu, 1992). The findings are, however, based on one mulberry variety, one season and one rearing year, and E.C.I. and E.C.D. did not differ significantly. Confirmation across seasons and mulberry varieties, together with larval duration and cocoon and silk traits, would show whether the nutritional advantage of the CSR hybrids carries through to leaf-to-silk conversion.

V. CONCLUSION

The newly introduced CSR hybrids (CSR2 × CSR4 and CSR2 × CSR5) showed more favourable nutritional indices than the conventional hybrids (NB4D2 × SH6 and SKAU-R-1 × SKAU-R-6): lower leaf consumption (ingesta), lower faecal egestion, higher approximate digestibility and higher growth rates. Lower ingesta is advantageous to commercial rearers because it reduces leaf requirement and labour in the final larval instars. The inverse relationship between consumption and approximate digestibility suggests that slower gut passage in the CSR hybrids allows more time for nutrient extraction. E.C.I. and E.C.D. did not differ significantly among the hybrids, so the advantage of the CSR hybrids lies in lower intake and higher digestibility rather than in a demonstrably better conversion of food into body matter. Including feed-conversion measures in breed evaluation protocols can help sericulturists select superior genotypes and so improve raw silk productivity and economic returns.

AUTHOR CONTRIBUTIONS

Gh. **Nabi** Mir: Conceptualization, interpretation of findings, writing and reviewing the original draft, critical review and editing of the manuscript. Aabid Ahmad Bhat: Compilation and organization of experimental data, preparation of tables, development of graphical illustrations, literature review and initial drafting of the manuscript. Lubna Altaf: Data compilation, verification of tables, literature search and proofreading. Misara Jaan: Literature compilation, manuscript formatting, reference checking and proofreading. M. A. Malik and H. U. Dar: Formulation of research objectives, supervision, and guidance on experimental design and methodology. Ishfaq Ahmad Malla: Interpretation and verification of results, review of tables and figures, critical reading and proofreading of the manuscript. All authors reviewed the manuscript and approved the final version.

ACKNOWLEDGEMENTS

The authors acknowledge the institutional support provided by the Division of Sericulture, CoTS Mirgund, SKUAST-Kashmir.

FUNDING

The authors received no specific external funding for this study.

CONFLICT OF INTEREST

The authors declare that they have no known competing financial interests or personal relationships that could have appeared to influence the work reported in this paper.

ETHICS APPROVAL

Not applicable. The study involved routine rearing and assessment of silkworm larvae and did not involve human participants or vertebrate animals.

DATA AVAILABILITY

The data supporting the findings of this study are available from the corresponding author upon reasonable request.

CONSENT TO PUBLISH

Not applicable.

REFERENCES

[1] Anonymous 2025.Central Silk Board, Ministry of Textiles. Sericultural Statistics in India: A Glance.https://www.texmin.gov.in/static/uploads/2025/07/d4c598d3053a3bd6586e745bef6fc45c.pdf

[2] Benchamin, K. V., & Jolly, M. S. (1986). Studies on ingestion, digestion and conversion efficiency in polyvoltine and bivoltine silkworm breeds, *Bombyx mori* L. *Proceedings of Oriental Entomology Symposium, 2*, 195–206.

[3] Dar, H. U., & Singh, T. P. (1998). Improved rearing techniques for *Bombyx mori* L. in Jammu & Kashmir. *Oriental Science, 3*(2), 30–46.

[4] Dar, H. U., Singh, T. P., & Aijaz, M. (1997). Evaluation of mulberry varieties by feeding to *Bombyx mori* L. *Oriental Science, 2*(1), 23–28.

[5] Dar, H. U., Singh, T. P., & Das, B. C. (1988). Evaluation of mulberry varieties by feeding to *Bombyx mori* L. *Indian Journal of Sericulture, 27*(1), 16–22.

[6] Das, B. C., & Sikdar, A. K. (1970). Evaluation of some improved strains of mulberry by feeding experiment. *Indian Journal of Sericulture, 9*(1), 26–30.

[7] Dasgupta, K. P. (1961). Feeding mulberry to silkworm: A comparative analytical study on the effect of feeding with different types of mulberry leaves obtained by different methods of cultivation on silkworm, *Bombyx mori* L. *Indian Silk Journal, 1*(4), 14–22.

[8] Gomez, K. A., & Gomez, A. A. (1976). *Statistical procedures for agricultural research* (2nd ed.). John Wiley & Sons.

[9] Krishnaswami, S. (1971). On some aspects of the improved technique of rearing mulberry silkworm. *Indian Silk, 5*(2), 7–9.

[10] Krishnaswami, S. (1978). *New technology of silkworm rearing* (Bulletin No. 2). Central Sericultural Research and Training Institute.

[11] Kulbir, S. (2001). *Bioassay of some indigenous mulberry varieties of Kashmir valley with silkworm Bombyx mori L.* [Master's thesis, Sher-e-Kashmir University of Agricultural Sciences and Technology of Kashmir].

[12] Legay, J. M. (1958). Recent advances in silkworm nutrition. *Annual Review of Entomology, 3*, 75–86.

[13] Maribashetty, V. G., Aftab Ahmad, C. A., Chandrakala, M. V., & Rajanna, G. S. (1999). Consumption and conversion efficiency of food and water in new multivoltine breeds of silkworm, *Bombyx mori* L. *Indian Journal of Sericulture, 38*(2), 140–144.

[14] Mathavan, S., & Pandian, T. J. (1974). Use of fecal weight as an indicator of food consumption in some lepidopteran insects. *Oecologia, 15*, 177–185.

[15] Parpiev, B. A. (1968). Water metabolism in silkworms fed with a different mulberry strain changing diet. *Shelk, 39*(2), 15–17.

[16] Radha, N. V., Letchoumanane, S., Rajeswari, & Obliswami, G. (1978). Effect of feeding with the leaves of different mulberry varieties on the races of silkworm [Conference abstract]. *All India Symposium on Sericultural Sciences*, Bangalore, India.

[17] Remadevi, O. K., Magadum, S. B., Shivashankar, N., Benchamin, K. V., & Datta, R. K. (1991). Studies on the growth rate and growth pattern in the fifth instar larvae of some multivoltine races of silkworm, *Bombyx mori* L. *Indian Journal of Sericulture, 30*(2), 125–130.

[18] Remadevi, O. K., Magadum, S. B., Shivashankar, N., & Benchamin, K. V. (1992). Evaluation of the food utilization efficiency in some breeds of silkworm. *Sericologia, 32*(1), 61–66.

[19] Saratchandra, B., Rajanna, L., Philomena, K. L., Paramesha, C., Ramesh, S. P., Jayappa, T., & Sabitha, M. G. (1992). An evaluation of elite mulberry varieties for yield and quality through bioassay. *Sericologia, 32*(1), 127–134.

[20] Slansky, F., Jr., & Scriber, J. M. (1985). Food consumption and utilization. In G. A. Kerkut & L. I. Gilbert (Eds.), *Comprehensive insect physiology, biochemistry and pharmacology* (Vol. 4, pp. 87–151). Pergamon Press.

[21] Tayade, D. S., & Jawale, M. D. (1984). Studies on the comparative performance of silkworm races against different varieties of mulberry under Marathwada conditions. *Sericologia, 24*(3), 361–364.

[22] Tazima, Y. (1957). *Report on sericulture industry in India*. Central Silk Board.

[23] Trivedy, K., & Nair, K. S. (1998). Dietary efficiency and silk productivity. *Indian Silk, 36*(9), 5–7.

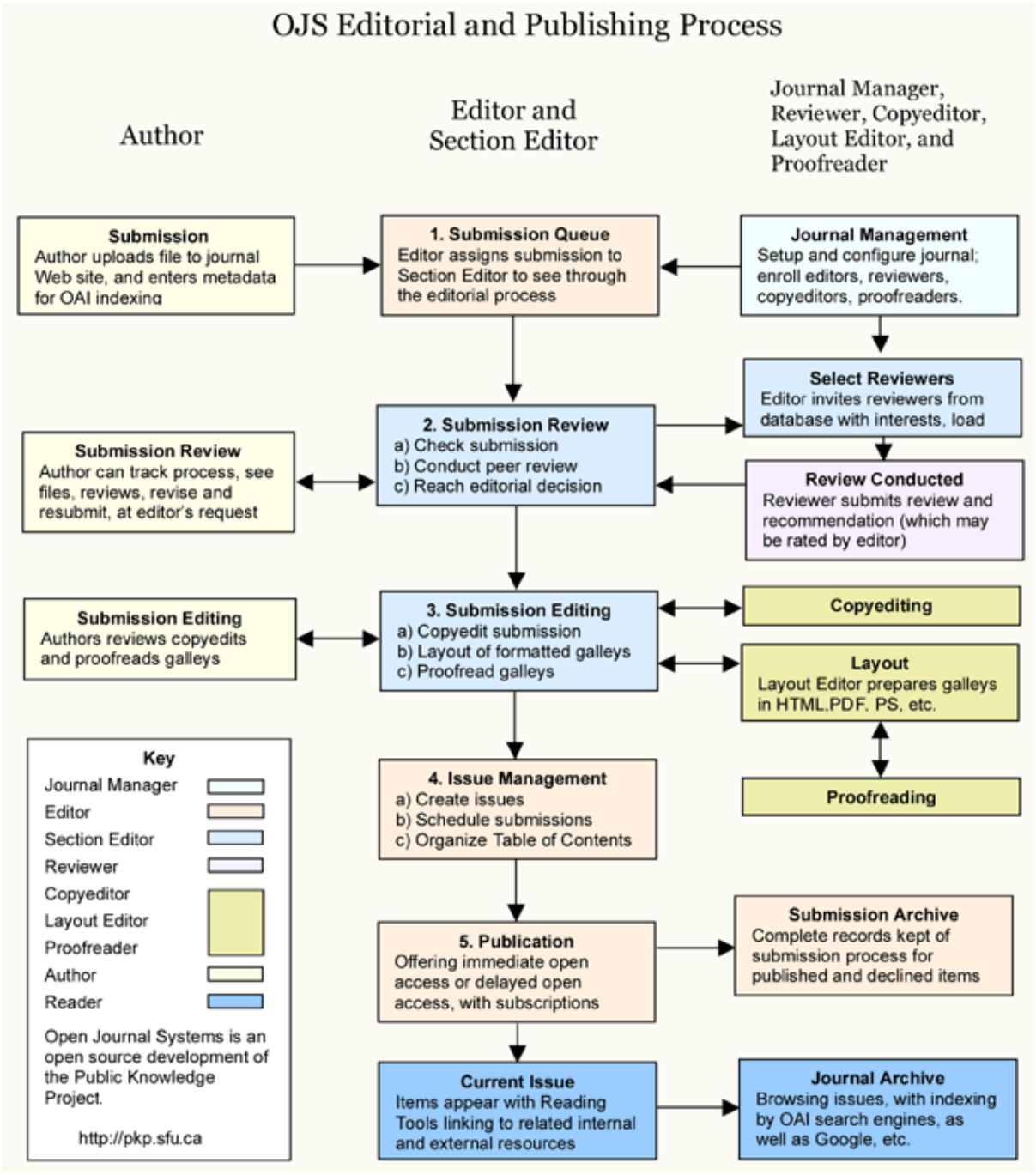
[24] Trivedy, K., & Nair, K. S. (1999). Feed conversion efficiency of improved multi × bivoltine hybrids of silkworm, *Bombyx mori* L. *Indian Journal of Sericulture, 38*(1), 30–34.

[25] Venugopala Pillai, S., Krishnaswami, S., Bhat, D. V., & Ranganath, B. K. (1980). Varietal effect on the development and economic characters of *Bombyx mori* L. In *Proceedings of Sericulture Symposium and Seminar* (pp. 137–140). Tamil Nadu Agricultural University.

[26] Waldbauer, G. P. (1968). The consumption and utilization of food by insects. In J. W. L. Beament, J. E. Treherne, & V. B. Wigglesworth (Eds.), *Advances in insect physiology* (Vol. 5, pp. 229–288). Academic Press.

[27] Xu, J., & Wu, X. (1992). Studies on the leaf-silk conversion rate of the silkworm, *Bombyx mori*. In *Proceedings of the XIX International Congress of Entomology*, Beijing, China.

[28] Yokoyama, T. (1963). Sericulture. *Annual Review of Entomology, 8*, 287–298.



~OJS Workflow~

Important links:

Paper Submission Link:
OJS:
https://ijeab.com/ojs/index.php/ijeab/about/submissions
https://ijeab.com/submit-paper/
Editorial Team:
https://ijeab.com/editorial-board/

Peer Review Process:
https://ijeab.com/peer-review-process/
Publication Ethics:
https://ijeab.com/publication-policies-and-ethics/
Author Guidelines:
https://ijeab.com/author-guidelines/
Join Us a Reviewer:
https://ijeab.com/join-us/

Journal Indexed and Abstracted in:

- Qualis-CAPES -Brazil
- Normatiza (Under Review)
- Bielefeld Academic Search Engine(BASE)
- Aalborg University Library (Denmark)
- WorldCat: The World's Largest Library Catalog
- Semantic Scholar
- J-Gate
- Open J-Gate
- CORE-The world’s largest collection of open access research papers
- JURN
- Microsoft Academic Search
- Google Scholar
- Kopernio - powered by Web of Science
- Pol-Index
- PBN(Polish Scholarly Bibliography)Nauka Polaska
- Scilit, MDPI AG (Basel, Switzerland)
- Tyndale University College & Seminary
- indiana Library WorldCat
- CrossRef DOI-10.22161/ijeab
- Neliti - Indonesia's Research Repository
- Journal TOC
- Dimensions.ai: Re-imagining discovery and access to research
- Citeseerx
- Massachusetts Institute of Technology (USA)
- Simpson University (USA)
- University of Louisville (USA)
- Biola University (USA)
- IE Library (Spain)
- Mount Saint Vincent University Library (Halifax, Nova Scotia Canada)
- University Of Arizona (USA)
- INDIANA UNIVERSITY-PURDUE UNIVERSITY INDIANAPOLIS (USA)
- Roderic Bowen Library and Archives (United Kingdom)
- University Library of Skövde (Sweden)
- Indiana University East (campuslibrary (USA))
- Tilburg University (The Netherlands)
- Williams College (USA)
- University of Connecticut (USA)
- Brandeis University (USA)
- Tufts University (USA)
- Boston University (USA)
- McGill University (Canada)
- Northeastern University (USA)
- BibSonomy-The blue social bookmark and publication sharing system
- Slide Share
- Academia
- Archive
- Scribd
- SJIF-InnoSpace
- ISSUU
- Research Bib
- DRJI
- journal-repository

Platform & workflow by OJS / PKP

Infogain Publication
International Journal of English, Literature and Social Science (IJELS)